BIOMECHANICS OF THE PAEDIATIIC FOOT AND LOWER LIMB: ASSOCIATIONS WITH ADIPOSITY

RYAN MAHAFFEY

A thesis in partial fulfilment of the requirements of the University of East London for a degree of Doctor of Philosophy

April 2013

Declaration

I declare that while registered as a research degree student at UEL, I have not been a registered or enrolled student for another award of this university or of any other academic or professional institution. I declare that no material contained in the thesis has been used in any other submission for an academic award.

Signed

Student Number u0940652

School of Health, Sport and Bioscience

University of East London

April 2013

Abstract

Childhood obesity is a growing problem in the UK and primary schoolchildren are particularly at risk. With this growing concern the associated co-morbidities of obesity are increasingly evident. There has been limited research undertaken to quantify the impact of excessive body fat mass (adiposity) on the function of the child's lower limb and feet. The primary aim of this research was to explore the relationships between adiposity with lower limb and foot biomechanics in boys age 7 to 11 years old.

Fifty five children were recruited to participate in protocols for body composition and three-dimensional gait analysis established in the initial phases of the study. Kinematic and kinetic variables from four lower limb joints (pelvis, hip, knee and ankle) and four foot joints (hindfoot-shank, midfoot-hindfoot, forefoot-midfoot and hallux-first metatarsal) were analysed over the gait cycle. Statistical analysis by principal component analysis was undertaken and allowed the determination of components, constructed of lower limb and foot variables, to be analysed in multiple regression. Multiple regression was also undertaken to assess the relationships between the lower limb and foot variables and body composition whilst accounting for confounding factors including age, anthropometric and spatiotemporal variables. The key findings demonstrated that higher adiposity was associated with greater hip flexion, knee adduction moments and a pronated foot type. These findings indicate that boys with higher fat mass are at risk of future musculoskeletal co-morbidities including concerns of developing flat feet.

This work presents a novel protocol for advanced understanding of lower limb and foot biomechanics and comprehensive data of paediatric lower limb and foot function during gait in normal weight and obese children. The research details, for the first time, that obesity affects the dynamic function of the paediatric foot. This work underpins the need for further longitudinal research looking at the prevention and management of musculoskeletal complications associated with childhood obesity.

Acknowledgments

I would like to thank the children and families who volunteered to participate in this study. I appreciate without their cooperation and enthusiasm this study could not have been completed. Furthermore, I am indebted to the schools and clubs for their participation and support during stages of data collection. I would like to sincerely thank my supervisors, Dr Stewart Morrison, Dr Wendy Drechsler and Dr Mary Cramp for their guidance, advice, encouragement and inspiration during my research. For their professional guidance I wish to thank Mr Paul Bassett, Ms Priya Clarke, Ms Susan Harrison, Mr Duncan Kennedy, Dr David McCarthy and Mr Timothy Pitt.

The study was supported by the Dr William M Scholl Podiatric Research and Development Fund who I would like to thank along with the members of the steering group; Professor Emeritus Oona Scott, Professor Brian Durward and Dr Jill Ferrari. I also acknowledge the financial support of the University of East London. Finally, and most importantly, a special thank you to my partner Hannah and daughter Mia for their support, encouragement and understanding that enabled me to complete this work.

Contents

List of Tables

List of Figures

Abbreviations, Acronyms and Nomenclature

95% Confidence Interval	95%CI
Age	A
Air Displacement Child Specific Body fat mass Estimate	ADP_{child}
Air Displacement Manufacturer Body fat mass Estimate	ADP_{man}
Air Displacement Plethysmography	ADP
Anterior Superior Iliac Spine	ASIS
Between-Subject Mean Square Variance	BMS
Bioelectrical Impedance Analysis	BIA
Bioelectrical Impedance Analysis Child Specific Body fat mass Estimate	BIA_{child}
Bioelectrical Impedance Analysis Manufacturer Body fat mass Estimate	BIA_{man}
Body density	Db
Body height	Ht
Body Mass Index	BMI
Body volume	Vb
Body weight	Wt
Calcaneal Inclination Angle	CIA
Calibration Anatomical System Technique	CAST
Centimetres	cm
Centre for Disease Control	CDC
Centre Of Mass	COM
Coefficient of determination	r^2
Coefficient of Multiple Correlation	CMC
Coefficient of Reliability	*R*
Coefficient of Variation	CV
Computerised Tomography	CT
Contralateral Initial Contact	CIC
Contralateral Toe-Off	CTO
Correlation coefficient	*r*
Cubic Centilitres	Cc
Degrees (Angular)	°
Dual X-Ray Absorptiometry	DEXA
Error Mean Square Variance	EMS
Fat Free Mass	FFM
Fat Mass	FM
First Double Support Phase of Gait Cycle	DS1
First Single Support Phase of Gait Cycle	SS1
Four Component Body Composition Model	4C
Global Coordinate System	GCS
Grams	g
Ground Reaction Force	GRF
Ground Reaction Vector	GRV
Health Survey for England	HSE
Heidelberg Foot Measurement Method	HFMM
International Obesity Task Force	IOTF
International Society of Biomechanics	IBS
Intraclass Correlation Coefficient	ICC (*rxx*)
Ipsilateral Initial Contact	IIC
Ipsilateral Toe-Off	ITO
Joint Coordinate System	JCS
Kilograms	Kg
Knee Alignment Device	KAD
Lambda, Mu, Sigma	LMS
Limits of Agreement	LoA
Litres	L
Local Coordinate System	LCS
Magnetic Resonance Imaging	MRI
Mean	$\bar{x}$
Mean Difference	*d*
Mean Square Error	MSE
Medial Longitudinal Arch	MLA
Metatarsal-Phalangeal Joint	MP
Meters	M
Millimetres	mm
Minimum Levels of Detectable Change	MDC
National Child Measurement Programme	NCMP
Newton Meters	Nm
Newtons	N
Number of participants	*n*
Number of Raters	*k*
Optimised Lower-Limb Gait Analysis	OLGA
Oxford Foot Model	OFM
Percentage Fat Mass Relative To Body Mass	%FM
Plug-in Gait (Conventional) Lower Limb Model	PiG
Pooled Standard Deviation	*Sx*
Posterior Superior Iliac Spine	PSIS

Principle Component Analysis	PCA	Talus-First Metatarsal Angle	TFMA
Probability Statistic	*p*	Tarsal-Metatarsal Joint	TM
Range Of Motion	ROM	Technical Error of Measurement	TEM
Reactance	*X*		
Resistance	Ω	Technical Error of Measurement Percentage of Mean	TEM%
Root Mean Square	RMS		
Root Mean Square Error	RMSE		
Second Double Support Phase of Gait Cycle	DS2	Thoracic Gas Volume	TGV
		Three Component Body Composition Measure	3C
Second Single Support Phase of Gait Cycle (Swing)	SS2		
		Three Dimensional	3D
Skin Surface Artefact	SAA	Total Body Water	TBW
Skinfold Thickness	SKF	Two Dimensional	2D
Slipped Capital Femoral Epiphysis	SCFE	United Kingdom	UK
		United Kingdom Growth Reference Data (1990)	UK90
Soft Tissue Artefact	STA		
Standard Deviation	SD (σ)	United States	US
Standard Deviation Score	SDS	United States National Health Examination Surveys	NHANES
Standard Error of Estimate	SEE		
Standard Error of Measurement	SEM	World Health Organisation	WHO
Stereophotogrammetry	SPG		

1. Thesis Introduction

Childhood obesity, defined as an excess of body fat mass (also referred to as adiposity) that may impair health, is a major public health concern (World Health Organisation, 2000). The aetiology of childhood obesity is multifaceted, but low levels of physical activity have been linked to the prevalence of obesity in school-age children (Hills et al., 2007). Walking is a major mechanical factor for musculoskeletal development in childhood and is recommended to increase physical activity and reduce sedentary behaviours in obese children (Shultz et al., 2011). However, musculoskeletal co-morbidities of the lower limbs and foot joints may predispose obese children to discomfort and pain reducing motivation to partake in walking activities. Therefore, determining altered walking characteristics associated with obesity may lead to clinical interventions to facilitate healthy gait and increase participation in physical activity.

Studies examining the effects of obesity on paediatric gait have found altered spatiotemporal characteristics reported to include a slower walking speed, greater stance phase duration and lower cadence (Hills & Parker 1991; Morrison et al., 2008). With regard to lower limb joint motion, obese children walk with less hip, knee and ankle flexion in the sagittal plane, greater knee adduction and hindfoot eversion in the frontal plane (Hills & Parker 1991; McMillan et al., 2009). Analysis of the forces acting on the lower limb joints revealed that joint moments are higher in obese children at the hip, knee and ankle joint in the sagittal and frontal planes (Shultz et al., 2009; McMillan et al., 2010). These findings indicate that obese children demonstrate greater dynamic instability, higher medial/lateral limb motion, and larger joint forces during gait which may predispose obese children to musculoskeletal co-morbidities (Shultz et al., 2009).

Musculoskeletal co-morbidities associated with childhood obesity include slipped capital femoral epiphysis, Blount's disease (tibia vara), and flatfeet (pes planus) (Skinner 1996; Riddiford-Harland et al., 2000; Zwiauer et al., 2006). These conditions are related to increased stress on the immature musculoskeletal system due to the carriage of excessive body mass. This can lead to malalignment and structural damage of the lower limbs inhibiting movement and impairing mobility (Shultz et al., 2009). However, there is a dearth of information on the dynamic alignment of the lower limb and foot joints during gait of obese children.

Significant differences in foot structure between obese and non-children have been reported using foot print indices, radiographs, anthropometric and morphological measures (Wearing et

al., 2004; Morrison et al., 2007; Mauch et al., 2008; Villarroya et al., 2009). These studies reveal that obese children present a flatter midfoot region, valgus calcaneus, dorsiflexed first metatarsal, relatively lower navicular height and larger foot dimensions. However, static measures of foot structure are not indicative of dynamic foot motion and the relationship between static and dynamic foot structure may be altered by obesity (Taisa Filippin et al., 2008). The impact of obesity on the three-dimensional motion of the foot has not been determined. It is therefore essential that further work be conducted in order to evaluate the full impact of obesity on the biomechanics of the paediatric lower limb and feet.

The novelty and originality of the work can be defined as follows:

1. To provide a thorough analyse of lower limb kinematic and kinetic variables associated with obesity during gait whilst controlling for anthropometric and spatiotemporal confounding factors that impact gait.
2. To define obesity in terms of adiposity, a measure of body fat mass rather than body mass index (a ratio of weight-to-height), which serves as a proxy for body fat mass.
3. Two protocols to improve lower limb marker placement in obese and non-obese children will be tested to increase between-session reliability and better represent skeletal motion.
4. Test between-session reliability of biomechanical foot models in order to present the most appropriate model to understand the relationships between 3D foot segment motion and obesity in children.

1.1 Thesis Aims

The aim of this research was to explore the association between gait biomechanics and adiposity in a cross-sectional sample of boys age 7 to 11 years old. More specifically, to characterise angular motion and external joint moments of the lower limb joints (hip, knee and ankle) and the foot segments (hindfoot, midfoot, forefoot and hallux) whilst walking at a self-selected speed. Furthermore, to relate any kinematic and kinetic findings to the level of body fat mass when controlling for other factors that influence gait biomechanics (age, spatiotemporal or anthropometric factors). The specific aims are related to the experimental chapters of the research which were defined as follows:

Aim 1. Experimental chapter 1 (chapter 5):

Establish protocols and tested between-session reliability of body composition assessment for determining childhood obesity and adiposity, presented in chapter 5.

Aim 2. Experimental chapters 2 and 3 (chapters 6 and 7):

Establish protocols and tested between-session reliability of three dimensional gait analysis of lower limb and foot biomechanics during paediatric gait, presented in chapter 6 and 7.

Aim3. Main study chapter (chapter 8):

Explore the relationship between adiposity and gait biomechanics in a cross-sectional sample of boys age 7 to 11 years old, presented in chapter 8.

1.2 Thesis Structure

The structure of this thesis is presented in Figure 1.1. The first outcome of the first literature chapter on childhood obesity (thesis chapter 2) defined the need to find a reliable and accurate measure of obesity which was examined in experimental chapter 1 (thesis chapter 5). The second outcome of the first literature review chapter on childhood obesity (thesis chapter 2) describes the need to review measures of gait in obese children in literature review chapter 2 (thesis chapter 3). The first outcome of the second literature review on three-dimensional gait analysis (thesis chapter 3) details the need to test between-session reliability of the Plug-in Gait (PiG) lower limb model in obese children in experimental chapter 2 (thesis chapter 6). The second outcome of the second literature review on three-dimensional gait analysis (thesis chapter 3) informs the need to test between-session reliability of available foot models to measure foot motion during gait in experimental chapter 3 (thesis chapter 7). The results of the first experimental chapter (thesis chapter 5) inform the protocols used in the main study (thesis chapter 8) to determine childhood obesity by adiposity measures. The results of experimental chapters 2 and 3 (thesis chapters 6 and 7) will determine the protocols for measuring lower limb and foot biomechanics in obese children. The main study chapter (thesis chapter 8) will explore the relationships between adiposity with lower limb and foot biomechanics during gait using the literature review outcomes and experimental protocols defined in earlier chapters.

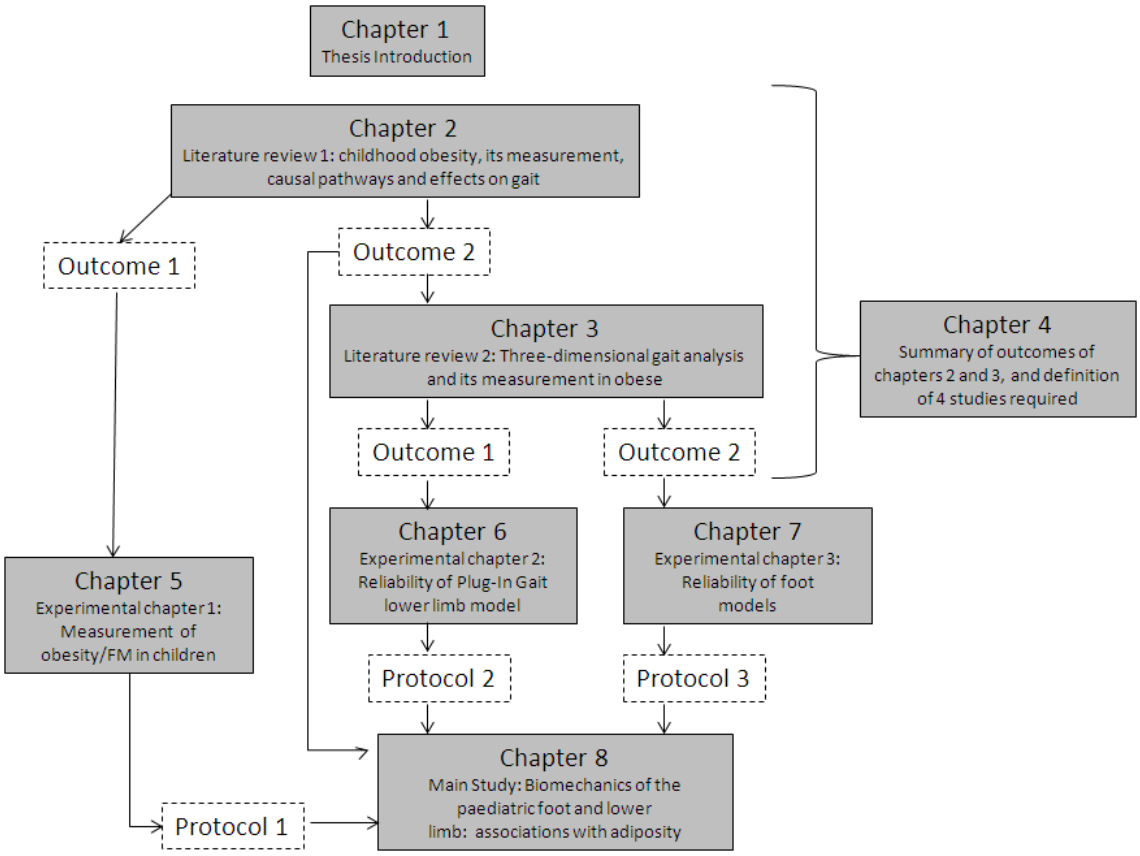

Figure 1.1. Chapter structure in thesis. The outcomes of the literature review chapters inform the measures in experimental chapters (chapters 5, 6 & 7) which define the protocols to be used in the main study (chapter 8)

2. Literature Review Chapter 1: Childhood Obesity

2.1 Introduction to Childhood Obesity

The following chapter will critically explore childhood obesity. The current literature on the assessment of childhood obesity by body mass index, body fat mass (adiposity), bioelectrical impedance analysis, air displacement plethysmography, reference body composition methods and multi-component body composition models are evaluated. The aetiology of childhood obesity will be examined with special attention on the relationship between childhood obesity and physical activity. The health consequences of childhood obesity will be explored with particular relevance to childhood obesity and musculoskeletal co-morbidities. Finally, the results of previous research to investigate lower limb and foot biomechanics during gait in obese and non-obese children are reviewed. The aims of this chapter are to: (1) demonstrate the need to define childhood obesity using accurate and reliable measurement protocols, and (2) demonstrate the need to investigate foot and lower limb biomechanics during gait in obese children.

2.2 Definition of Obesity

Obesity is described as a disease in which excessive body fat mass accumulates to the extent that health may be impaired (World Health Organisation, 2000). Accumulated body fat mass is referred to as adiposity which occurs when energy intake exceeds expenditure (Dehghan et al., 2005). Overweight and obesity can be defined as a body mass index (BMI) higher than a predefined standard or cutoff (Flegal & Ogdan, 2011). Table 2.1 presents the BMI classification system for adults; a BMI between 30 – 39.9kg·m^2 defines obese and a BMI between 25 – 29.9kg·m^2 defines overweight.

Table 2.1. World Health Organisation (WHO) BMI classification system for adults

BMI range (kg/m^2)	Classification
<18.5	Underweight
18.5 – 24.9	Normal weight
25 - 29.9	Overweight
30 – 39.9	Obese
>40	Morbidly obese

In adults, obesity is defined by morbidity and mortality related cutoffs according to measures of adiposity. Childhood obesity has not been related to morbidity and mortality, as there is no consensus on the optimum approach to identify children at risk of future adverse health outcomes due to obesity or overweight (Flegal & Ogden 2011). Furthermore, health studies have routinely used BMI rather than measures of body fat mass to identify disease risk in children (Freedman & Sherry 2009). Whilst the definition of adiposity is clear what constitutes excess adiposity has not reached consensus. However, increasing incidence of health co-morbidities linked to excessive adiposity may be used in the future to define childhood obesity (Styne 2001). Currently childhood obesity is defined by a BMI relative to previous national obesity rates or predicted obesity at the age of 18 years old. The definition of childhood obesity is important to establish in research studies if relationships with potential health co-morbidities are to be explored. For the purpose of this thesis obesity and overweight refers to a BMI over predefined cutoffs and adiposity refers to the level of body fat with no cutoff.

It is important to recognise that a small proportion of obese children have a syndrome or pathology underlying their obesity, termed endogenous obesity. Genetic syndromes, such as Prader-Willi, Bardet-Biedl and Cohen's present with dysmorphic features and delayed development (North et al., 1985; Green et al., 1989; Farooqi & O'Rahilly 2000). Endocrinologic causes of overweight include hypothyroidism and Cushing's syndrome (Barlow & Dietz 1998). The vast majority of obese children do not have an underlying cause and are termed exogenous (simple obesity) and have specific problems and clinical signs. For the purpose of this thesis only exogenous obesity will be considered.

2.3 Prevalence of Obesity

The prevalence of childhood obesity has been estimated on international, national and regional scales with the incidence increasing in most countries over recent decades. According to International Obesity Task Force (IOTF) criteria it was estimated that 10% of children aged 5-17 years old had excessive body fat mass (Lobstein et al., 2004). The IOTF estimates up to 200 million children are overweight, of which 40-50 million are obese (International Obesity Task Force, 2010).

Data from the Health Survey for England (HSE) in 2002 estimated the level of national childhood obesity to be 5.5% and overweight to be 22% in boys age 2- to 15-years (Rennie & Jebb 2005). As seen in Figure 2.1 the latest numbers (for years 2010/11) from the National

Child Measurement Programme (NCMP) highlight the prevalence of obesity and overweight for boys aged 4 – 5 years as 10.1% and 13.8% respectively, increasing to 14.3% and 20.6% at age 10-11 years (NCMP, 2012). Comparing data from 2002 to 2010/11 indicates that the prevalence of overweight among boys in England has remained stable over the last decade, but the incidence of obesity has doubled.

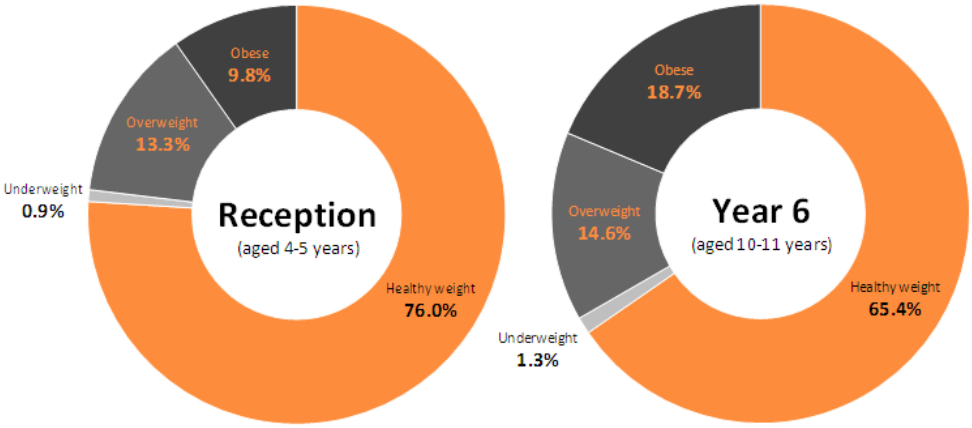

Figure 2.1. Prevalence of obesity, overweight, healthy weight and underweight in England in reception class (4-5 years) and Year 6 (10-11 years) according to the UK90 growth reference for BMI for the years 2010/11 (National Child Measurement Programme 2012).

In the London borough of Newham, levels of obesity and overweight was 11.2% and 12.9% respectively at 5-6 years of age and 15.1% and 24.7% at 10-11 years (NCMP, 2012). The incidence of overweight and obesity among primary school boys is generally higher in Newham than the English average particularly for the prevalence of obesity at age 10-11 years old. Local prevalence rates are of interest to this thesis as the subject sample will be recruited as a representative sample of the local Newham population.

2.4 Assessment of Obesity

The difficulties associated with the assessment of obesity arise from the definition of obesity. Obesity is measured by BMI, an indirect anthropometric measurement, which has been validated against measures of body fat (adiposity) (Lobstein et al., 2004). In large scale population surveys and clinical public health screening BMI is commonly used to infer body fat mass content because of the ease of data collection. The prevalence of adiposity and the links

with future mortality and morbidities are dependent on BMI cutoffs and reference data-set used to define obese and overweight children (Troiano & Flegal 1999; Rolland-Cachera 2011). When obesity is defined in terms of adiposity (level of body fat mass) the measure of body composition is required to be accurate, reliable and valid. Therefore, to understand relationship between lower limb and foot biomechanics and childhood obesity, the methods of determining obesity and adiposity must be tested against reference body composition measures. This section will review the various forms of assessments used to define obesity and adiposity.

2.4.1 Reference Measures of Body Composition

Body composition assessment ranges from cellular, molecular and tissue measures which can determine the level of body fat mass in an individual. Reference measures of body composition provide an estimation of body fat mass which can be used to validate indirect measures of body fat mass. Computerised tomography (CT) uses X-rays to produce cross sectional images of the body allowing body fat mass to be measured. These scans expose participants to high levels of radiation (Duren et al., 2008). This method is highly accurate at measuring intra-abdominal and subcutaneous fat. Magnetic resonance imaging (MRI) records the resonating frequencies of protons in tissues producing an image to measure body composition. This method is accurate for measuring body fat mass and there is no known long-term side effects (Kullberg et al., 2009). Dual-energy X-ray absorptiometry (DEXA) is a scanning technique that measures bone mineral, fat tissue, and fat-free soft tissue. However, the estimates of fat mass can be influenced by several factors including the hydration and level of obesity of the subjects (Freedman & Sherry 2009; Beechy et al., 2012). Finally, isotope dilution is used to measure Total Body Water (TBW) by introducing a known isotope to a participant (relative to their weight) to estimate their total water content. This method relies on assumptions of the hydration of fat-free mass (FFM) of 73% to estimate fat mass which may be altered in obese participants. These reference procedures provide greater accuracy of body fat mass measures compared to indirect measures, but are time consuming and may not be suitable for children (Lobstein et al., 2004).

2.4.2 'Gold standard' Multi-Component Body Composition Models

Multi-component models of body composition account for the fact that the human body is composed of different components including fat mass and fat free mass (water, muscle, protein, bone, minerals). Combinations of two, three, four or more body composition methods are often used in a multi-compartment model. They are considered the 'gold standard' for other body composition methods (Wang et al., 1998). Many single body composition assessments are based on assumptions, like the assumption of standard hydration or FFM density and the assumption of constant hydration in fat-free soft tissues in air displacement plethysmography (ADP) (Plasqui et al., 2009). The most basic two-compartment models are also based on assumptions like the water or potassium constancy in FFM (Wang et al., 1998). A three-compartment model allows for improvement over a two-compartment model, because it does not rely on the assumptions of standard hydration of FFM density (Das et al., 2003). Three compartment models may combine body density and TBW measures to account for hydration assumptions (Das 2005). Four-compartment methods include measurements of fat, water, mineral, and protein, for example combining measurements from body density, TBW, and DEXA to account for body mineral mass (Fuller et al., 1992). However, multi-compartment methods rely on the accuracy of the different measurements that are combined. An error in one of the measurements will result in an inaccurate body composition assessment. Furthermore, the negative aspects of using reference body composition techniques in children reduce their application. These reference and 'gold standard' measures of body composition are referred to throughout this section with regard to validity of measures of obesity.

2.4.3 Assessment of Obesity by Anthropometrics

Anthropometric measures are basic methods for assessing body composition and are used to determine body mass, size, shape and level of body fat mass (Duren et al., 2008). For anthropometric measurements to be accurate and of value, skill and training of the observer (rater) is important (Wang et al., 2007). The most frequent measurements are weight and height, these are usually combined as weight to a power of height to minimise the correlation with height or maximise the correlation with body fat mass. Other measurements of relative adiposity are waist, hip and other girth measurements (Lobstein et al., 2004). This section will

review the definition of childhood obesity by body mass index (BMI) describing the theory, methods, accuracy and issues that surround this measure.

2.4.3.1 Assessment of Childhood Obesity by Body Mass Index

Body weight is related to body fat mass and the adjustment of weight for height (Body Mass Index) provides a sensitive and specific index of adiposity (Cole, 1991, Cole et al 2002). BMI is associated with body composition and health risk factors in childhood so it is accepted as a valid indirect measure of adiposity in children (Kotchen et al., 1980; Must et al., 1992; Gidding et al., 1995).

During childhood fluctuations in growth and development make comparisons of BMI across ages and genders difficult. Therefore, BMI values for children have been transformed into BMI-for-age and -gender Z-scores for comparison against BMI distributions based on national or international representative surveys (Freedman & Sherry, 2009). Centile curves have been constructed from data sets of children's BMI measurements using the lambda, mu, and sigma (LMS) method (Cole et al., 1998). The LMS method describes three smoothed age-specific curves from which a child's centile can be extracted describing their BMI in relation to age and gender specific population (Cole et al., 2000). The advantage of using BMI-for-age and -gender reference charts and Z-scores is that a child can be described as being above or below a certain centile line (i.e. obesity = >95th percentile, overweight = >85th) relative to their age and gender (Lobstein et al., 2004).

Body Mass Index (BMI) is a screening tool and is useful for making comparisons between populations and monitoring population groups (Rolland-Cachera 2011). Several childhood reference population BMI charts have been constructed (Cole et al., 1995; Cole et al., 2000; Kuczmarski et al., 2000; de Onis et al., 2007). The 1990 UK (UK90) growth reference (Cole et al., 1995) contains measurements of weight and height from 37,000 children in the United Kingdom. In the US, the centre for disease control (CDC) growth charts were developed from five nationally representative survey data sets (the National Health Examination Surveys II and III in the 1960s, the NHANES I and II in the 1970s, NHANES III, 1988-1994) (Kuczmarski et al., 2000). The World Health Organisation (WHO) developed growth standards based on the same data from the CDC growth charts (de Onis et al., 2007). International BMI reference curves based on large representative data sets from six countries (Cole et al., 2000) is referred to as the International Obesity Task Force (IOTF) reference shown in Table 2.2. Choosing the

appropriate reference data set to determine if a single child is obese in relation to the population is necessary as age, gender and ethnicity affect the measurement (Reilly et al., 2000).

Table 2.2. IOTF cutoffs for childhood overweight and obesity in males according to BMI score at 18 years old.

Age	Body Mass Index $25kg/m^2$	Body Mass Index $30kg/m^2$
2	18.41	20.09
3	17.89	19.57
4	17.55	19.29
5	17.42	19.30
6	17.55	19.78
7	17.92	20.63
8	18.44	21.60
9	19.10	22.77
10	19.34	24.00
11	20.55	25.10
12	21.22	26.02
13	21.91	26.84
14	22.62	27.63
15	23.29	28.30
16	23.90	28.88
17	24.46	29.41
18	25	30

Once a reference population has been determined a BMI centile or Z-Score relative to age and gender cutoffs are required to define the level of obesity. There are different approaches to define overweight and obesity in childhood. In Britain the UK90 data set cutoffs (Table 2.3) of the 91^{st} and 98^{th} percentiles, based on increments of Z-score of +1.33 and +2.37 respectively represent overweight and obese (Cole et al., 1995). Other BMI-for-age reference charts use cutoffs of 85^{th} and 95^{th} (Kuczmarski et al., 2000) or a standard deviation score (SDS) of +1 and +2 (World Health Organisation, 2006; de Onis et al., 2007) to define overweight and obesity. Table 2.2 presents the IOTF charts with cutoff values representing obesity were chosen as the percentiles that match the adult BMI cutoff values of $25kg/m^2$ and $30kg/m^2$ for women and men respectively at 18 years (Cole et al., 2000). Because little is known about the levels of risk associated with specific BMI levels in children cutoffs are based on arbitrary statistical approaches (Sweeting, 2007) rather than related to incidence of obesity-related co-morbidities.

Table 2.3. UK90 clinical cutoffs for obese, overweight, healthy weight and underweight boys

BMI classification	UK90 Centile range	UK90 Z-Score range
Obese	>=98th	+1.64
Overweight	>=91st	+1.33
Healthy weight	>=2nd	-2.16
Underweight	<=2nd	<-2.16

Studies have examined the ability of BMI reference cutoffs to screen for obesity in children (Barlow & Dietz 1998; Pietrobelli et al., 1998; Reilly et al., 2000). BMI correlated with measures of adiposity in children and adolescents, the correlation coefficient ranges from low to highly correlated (r = 0.39 to 0.90) depending on the method of adiposity measurement, the age and sex of the subjects (Barlow & Dietz 1998). A study of 198 white boys and girls aged 5-19 years found a correlation of 0.85 between BMI and total body fat mass measured with dual energy X-ray absorptiometry (DEXA) (Pietrobelli et al., 1998). Reilly et al., (2000) compared the IOTF and the UK90 cutoffs against measures of body fat mass (by bioelectrical impedance analysis). The UK90 cutoff had a moderately high sensitivity (88% of children who were obese were classified correctly as obese by BMI) and high specificity (94% of children who were not obese were classified correctly as non-obese by BMI). Sensitivity of BMI using the IOTF cutoff for obesity was much lower (46% boys and 72% girls), specificity was high at 99%. Any definition suitable for clinical use must have high specificity in order to avoid unnecessary treatment of non-obese children, the stigma associated with being labelled obese, and potential for consequential harm (Power et al., 1997; Barlow & Dietz 1998). Data from Reilly et al (2000) suggests that the use of the BMI>98th centile with UK90 reference data as an obesity definition has low sensitivity (71%) but high specificity (98%) and therefore may be more appropriate to define childhood obesity.

Although BMI is generally accepted as a reasonable measure of body fat mass there is some evidence that the relationship between BMI and adiposity is not constant throughout a population and may vary greatly between ethnic groups in children (Must et al., 1991). Data from British population studies have consistently shown that, compared with white Europeans, south Asian children had higher percentage body fat mass for a given BMI (Viner et al., 2010). Ehtisham et al., (2005) found south Asian adolescents living in the UK to have significantly higher %FM calculated from skinfold thickness across BMI ranges compared to Caucasians. Freedman et al., (2008) found at equivalent levels of BMI-for-age, black children had less body fat mass (mean 3%) than white children. Variations in relative subcutaneous fat distribution and relative proportions of the trunk and lower extremities to height have been suggested to be potential causes (Deurenberg et al., 1999) as well as physical activity level (Gurrici et al.,

1999). These ethnic differences in the BMI-%FM relationship result in differences in the sensitivity of BMI to identify children with excess adiposity.

In adults BMI cutoffs values correspond to a significant increased risk of mortality and are consistent with the WHO definition (Rolland-Cachera 2011). Presently a BMI of 25kg/m^2 is considered overweight and 30kg/m^2 is considered obese (World Health Organisation, 2000). Children with a BMI over predefined cutoff points do not necessarily have clinical complications or health risks related to adiposity (Flegal & Ogdan 2011). As stated earlier links between high BMI in childhood and health risk factors have been established, but which cutoff is most appropriate for intervention has not been defined. The long duration before adverse outcomes appear makes finding risk related cutoffs difficult (Flegal & Ogdan 2011). However, the use of the 95th BMI-for-age percentile identifies children with a significant likelihood or persistence of obesity into adulthood (Barlow & Dietz 1998). Further examination of the relation between various health measures and adiposity measured as a continuous variable may provide additional valuable information and therefore a cutoff may not be needed (Bell et al., 2007).

Body Mass Index is a simple, low cost tool that incurs little burden to the child, but is dependent on the reliability of the observer to take the measures (Wang et al., 2007). The key limitation for the use of BMI in children is that it is an indirect measure of body composition and thus, fat mass and lean mass cannot be distinguished. Additionally, the measure assumes that height and weight increase linearly during childhood. However, lean mass increases more than fat mass during growth (Maynard et al., 2001) giving misleading information about children's body composition (Wells et al,. 1999). The disagreement between previously published correlations of BMI against measures of fat mass in children means there is a need to assess the relationship between the two measures in the sample population of interest. There is a need to determine the use of BMI to define the level of childhood obesity against measures of obesity from determinants of adiposity (body fat level). Furthermore, the reliability of height and weight measures are required in order to demonstrate the utility of BMI in the research setting.

2.4.4 Assessment of Obesity by Adiposity (Body Fat Mass)

Power et al., (1997) stated that an ideal measure of adiposity should be accurate in its estimate of body fat mass (small measurement error) accessible (low cost, ease of use),

acceptable (comfortable for the subjects), and well-documented (references against 'gold standards'). Health consequences of obesity have been related to excess adipose tissue, therefore the ideal method of classification should be based on direct measurement of body fat mass (Dehghan et al., 2005). However, there is no consensus on the classification for excessive adiposity in children or adults. This section will review indirect methods of estimating body fat mass in children demonstrating their validity with previous references methods.

2.4.4.1 Assessment of Adiposity by Bioelectrical Impedance Analysis

Impedance is the term used to describe the reactance and resistance of the human body to an electrical current (Kyle et al., 2004a). The opposition of the tissues cause the resistance and the additional hindrance due to the capacitance of membranes, tissue interfaces, and non-ionic tissues results in reactance. Impedance measured through different tissues varies with the frequency of the current used (typically 50 kHz, when a single frequency is used). Therefore applications of BIA use multi-frequency measurements (5 to 200 kHz) to evaluate differences in body composition.

In practise electrodes are placed on the wrist and foot with the current passing from the source electrode and measured at the sink electrode. The current magnitude is about 800μA which is small enough so as not to be perceived by the subject, but large enough to produce voltages that are above interfering noise. The conditions for recording impedance should be standardised (body position, previous exercise and dietary intake) to optimise measurements (Kyle et al., 2004b).

Bioelectrical impedance analysis only measures the current across the entire path of the body between the electrodes. Impedance measurements do not provide any direct information with respect to the amount of current travelling through different tissue volumes, body liquids, or in fat versus fat-free mass. Relationships between impedance and TBW, fat-free mass (FFM), or body fat mass (%FM) have been established in statistical regression analysis with impedance for a specific population rather than on a biophysical basis (National Institutes of Health, 1996).

There is no direct relationship between impedance and body fat mass but the resistance of current through the body is related to total body water (TBW). An empirical relationship can be estimated between impedance (height^2/resistance) and the volume of body water which

contains electrolytes that conduct the electrical current through the body. Total body water (TBW) is strongly related to fat-free mass (typically 73% water) and resistance relative to body height. Therefore, predication equations from regression analysis are used in specific subject populations to estimate body fat mass.

Selecting a BIA equation should be based on the specific population under investigation and general prediction equations should be avoided (Kyle et al., 2004a). Most of the validation studies compared TBW, FFM or FM to criterion methods (DEXA or 4 compartment models) so are dependent on the accuracy of the criterion method. Determination of FFM from TBW assumes a constant hydration level of FFM of 73% within and across individuals. These assumptions can differ in populations and therefore population specific regression equations are advised.

Between-session reliability and accuracy of whole-body BIA have been evaluated for estimating body composition in children. Houtkooper et al., (1989) compared fat free mass and %FM against a deuterium dilution (a reference method using chemically labelled water to estimate TBW) in 94 Caucasian children. Impendence measures referenced to body weight had adjusted R^2 values of 0.93 and 0.87 and standard error of the estimate (SEE) values of 2.0kg and 4.2% for FFM and %FM respectively. Houtkooper et al., (1989) concluded that BIA measures of impendence were found to be reliable to estimate body composition in 10-14 year old children.

The use of BIA to measure body fat mass in 77 obese children and adolescents (5-22 years old) was reported by Haroun et al., (2009). Body fat mass was over-estimated by 3.5kg compared to the reference method (three-compartment model) and showed a tendency (not significant) to over-estimate body fat mass in larger children. Obesity alters the hydration of the FFM making predictions of body fat mass based on a fixed value liable to error. The paper concludes that obesity specific regression equations are required to estimate body fat mass.

Techniques have been used to estimate gender- and age-specific percentiles of body fat mass (Lazarus et al., 1996; Mei et al., 2000; Zimmermann et al., 2004) as well as age-specific levels that correspond to the percentage body fat mass of a typical 18 year old with BMI of 30 (Taylor et al., 2002; McCarthy et al., 2006). McCarthy et al., (2006) devised sex-specific centile curves for body fat mass based on reference data from 1985 Caucasian children aged 5 to 18 years. Smoothed centile curves for %FM in boys and girls were constructed and cutoffs, consistent with the IOTF BMI cutoffs (85^{th} and 95^{th} centiles), were applied for overweight and obese. The

benefit of this method was the new curves assess adipose tissue mass, the component of excess weight that is associated with co-morbidities (Fortuno et al., 2003). This therefore, reduces misclassification in large-framed and/or muscular children who are defined as overweight or obese by BMI. Problems with this method relate to other anthropometric reference curves where the study sample needs to be representative of the wider population. Body fat mass cutoffs also share problems with previous BMI charts; namely they lack clinical correlates on which to base such definitions of obesity. Future risk factors and obesity-related ill health from large scale surveys could relate body fat mass to morbidity and mortality.

Bioelectrical Impedance analysis can be taken quickly and inexpensively, it is relatively non-invasive and has high within- and between-rater reliability. It may be a useful tool in longitudinal studies addressing questions of morbidity and/or mortality outcomes according to relative body fat mass in early childhood. However, it requires equations specific to the instrument used and for the population under investigation. The measurements may vary with hydration status affected by obesity and ethnic status (Wabitsch et al., 1996).

2.4.4.2 Assessment of Adiposity by Air Displacement Plethysmography

Air displacement Plethysmographic (ADP) methods to determine body volume involve the use of a volumetric chamber to which a subject is introduced and the change in volume recorded (Dempster & Aitkens, 1995). The Bodpod is a commercially available ADP consisting of the test chamber (for the subject) and a references chamber separating by an oscillating diaphragm (Figure 2.2). Small volume perturbations between the chambers change the pressure equal in magnitude but opposite in sign which are recorded. The ratio of the pressures between the two chambers is a measure of the test chamber's volume.

The presence of a subject in the chamber causes changes to temperature and gas composition with the test chamber creating adiabatic conditions. However, air in the lungs, hair, clothes and close to the skin is held under isothermal conditions (constant temperature). Under isothermal conditions the relationship between pressure and volume is constant, according to Boyle's law. However, under adiabatic conditions air temperature does not remain constant as its volume changes and is instead described by a ratio of pressure to volume at the specific temperature (1.4 for air), according to Poisson's law. This difference in behaviour of gases under isothermal and adiabatic conditions is significant for the accurate measure of volume by ADP.

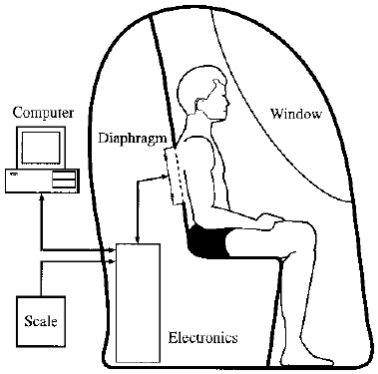

Figure 2.2. Schematic representation of the Bodpod. Dempster & Aitkens, (1995)

To account for isothermal air minimal clothing and a swim cap to compress the hair are worn. Skin surface area artefact is calculated based on regression formula from weight and height (Dubois & Dubois, 1916) although other subject specific formulas are available from the literature. The amount of air in the lungs can be measured at mid-tidal exhalation by occluding the airway while the subject performs 2 or 3 gentle puffs whilst in the ADP chamber. The changes in chamber pressure allow calculation of lung volume via proprietary methods (Fields et al., 2002). However, children may have difficulty performing this procedure (Lockner et al., 2000). Therefore, lung volume can be predicted based on Crapo et al., (1982) equations within the Bodpod software.

Once the raw body volume has been corrected for skin area artefact and lung volume the properties of densitometry are applied. Body density is calculated by dividing body mass by the corrected body volume. Body density is then entered into formulas for estimating body fat mass based on the two-compartment model (fat and fat-free mass). The assumptions of estimating body fat mass according to the two-compartment model is that fat and fat-free mass have constant densities of 0.9 and 1.1kg/l respectively. However, the density of the fat-free mass can differ substantially in the elderly, children and people of black ethnicity (Fields et al., 2002). The Siri, (1961) body fat mass estimation equation based on adult two-compartment densities is integrated into the Bodpod software.

Wells & Fuller, (2001) investigated the precision of estimating %FM by ADP in 28 adults and 30 children. The absolute precision of repeated measurements of %FM was 0.83% (of total body mass) for boys and 0.99% for girls. Precision was shown to be similar to findings in adults (0.99% and 0.76% %FM for men and women respectively) validating its use in participants of varying body sizes.

Fields & Goran, (2000) evaluated Bodpod against a four component (4C) model of Lohman (1989) comprised of individual body density, TBW and DEXA measurements. The age adjusted two component model of Lohman, (1989) was used to calculate %FM to allow for changes in hydration status in children compared to adults. The correlation, measured by R^2 value, was relatively high (0.85) and SEE low (3.2% BF). The Bodpod significantly underestimated %FM by 2.7% compared to the 4C body composition model. However, compared to the individual measures of body composition (body density, TBW and DEXA) the Bodpod was the only method that showed no significant tendency to underestimate %FM at a lower fatness and underestimate %FM at higher fatness. Thus in children the Bodpod emerged as the single best method to evaluate %FM comparison with the gold standard provided by the 4C model.

In obese children (BMI 31.6 ± 5.5), no difference in %FM was found between the Bodpod and the 4C model (Gately et al., 2003). This study used body fat mass prediction equations for ADP in children by Lohman, (1989) finding a non-significant mean difference of -0.04 ± 3.6% (%BF) compared to the 4C model. The authors concluded that the Bodpod accurately accounting for the variation in hydration of the FFM in obese children (Gately et al., 2003).

The tool is highly sensitive to change in body volume, is valuable for trending small changes in body composition, is quick to perform, has low participant burden (Le Carvennec et al., 2007) and is non-invasive (Shafer et al., 2009). However, compared to BIA fewer studies have examined the accuracy of the ADP measured by Bodpod in obese children. Because of its high precision and validity, ADP is now considered to be a criterion method of body composition (Bosy-Westphal et al., 2005). In research studies this method of estimating body density in children is deemed the 'gold standard' for measuring body composition (Pietrobelli et al., 2003).

2.4.5 Summary of Assessment of Obesity by Adiposity (Body Fat Mass)

To determine health related consequences of childhood obesity in a research setting an accurate, reliable and valid method of measuring body fat mass is needed. Although some studies have provided cutoff points in body fat mass for children related to metabolic and cardiovascular health risks these are considered arbitrary. Similar to the use of BMI centile scores as a continuous variable, body fat mass percentage can be considered as a continuous variable, therefore avoiding errors in defining a cutoff for excessive adiposity. Estimates of paediatric body fat mass by BIA provide high correlations with reference methods, but

accuracy is dependent on valid regression equations taking into account participants age and gender. The measure of body density by ADP using the Bodpod has been shown to accurately estimate body fat mass across a wide range of adiposities compared to reference methods and is considered a standard method of determining paediatric body composition. Both BIA and ADP are dependent on the characteristics of the population being tested. Therefore, both should be tested within a study's sample population to insure the tool can accurately and reliably measure adiposity.

2.5 Aetiology of Obesity

Obesity results from an energy imbalance; a disruption between energy consumed and energy expended (Hills et al., 2011). This results from a complex interaction between diet, physical activity, metabolic and genetic factors in an environment that encourages consumption of high-energy food and discourages expenditure of energy (Pietrobelli et al., 2008; Bouchard 2010). The multi-factorial nature of obesity in children includes; genetic (Link et al., 2004), socioeconomic (Saxena et al., 2004; Rennie & Jebb, 2005), psycho-social (Lang & Rayner 2005), the obesogenic environment (Egger & Swinburn, 1997), and diet (Gregory et al., 2000) factors. This section will focus on physical activity. Understanding the relationship between physical activity and childhood obesity is of importance to determine the effects of carrying excessive fat on the biomechanics of the feet and lower limbs. Furthermore, determining the biomechanical differences between obese and non-obese children may lead to interventions to increase physical activity and reduce obesity.

2.5.1 Physical Activity and Obesity

Studies examining the relationships between physical activity and childhood obesity have been limited due to methodological issues regarding measures of adiposity and physical activity. Inconsistent results have been reported with some studies indicating no association between the two variables while others postulating physical activity as a major contributing factor in the increased prevalence of childhood obesity (Riddoch et al., 2009; Owen et al., 2010; Hills et al., 2011, Shultz et al., 2011). Hills et al., (2011) discusses a strong association between physical activity and obesity and defined this as '*reciprocal causality*' such that physical activity enables individuals to control their weight by increasing energy expenditure. In contrast, unsuccessful

weight control reduces aerobic fitness, increases musculoskeletal pain and increases discomfort, which results in physical activity being more challenging.

Owen et al., (2010) examined the associations of physical activity, obesity and cardiovascular risk factors in a cross-sectional study of 2,049 UK children, of multi-ethnic origin, aged 9 and 10 years. Body fat mass was measured by bioelectrical impedance analysis (BIA) and skinfold thickness (SKF). Physical activity was recorded (wearable activity monitor and activity questionnaire) providing activity counts per minute for each child over seven days. The findings demonstrated a strong inverse relationship between physical activity and adiposity. For every increase in 100 counts of physical activity per minute recorded across the sample population, a 12.2% (95%CI 10.2-14.1%) reduction in body fat mass was recorded.

The prospective association between physical activity and adiposity in children between the age of 12 and 14 years was studied by Riddoch et al., (2009). The study recruited 1,964 boys from the UK, measuring fat mass by dual X-ray absorptiometry (DEXA) and physical activity. The study quantified total activity level by activity counts per minute from an accelerometer worn over 10 days. For twelve year old boys, a higher total activity level of 100 counts/mins was associated with a 6.4% lower fat mass. Furthermore, moderate-vigorous physical activity (defined an activity count corresponding to a brisk walking pace) that was 15min/day higher at age 12 was associated with an 11.9% lower fat mass, in boys, at age 14 years. The study confirmed that higher levels of physical activity are strongly and inversely associated with levels of fat mass in twelve year old boys and prospectively at fourteen years old.

Metcalf et al., (2011) examined the relationship over time between physical activity and obesity in 202 UK children aged 7 to 10 years. The study recorded total physical activity and time in moderate-vigorous activity using accelerometry and fat mass, measured by DEXA, at yearly intervals for 3 years. The results indicated that a 10% higher body fat mass percentage at age 7 years was predictive of a decrease in moderate to vigorous activity of 4 mins/day from ages 7 to 10 years old. However, greater physical activity did not predict a decrease in body fat mass percentage between 7 and 10 years old. The authors concluded that percentage body fat mass predicted changes in physical activity over the 3 year period but physical activity did not predict changes in body fat mass percentage over the same period. This leads to the suggestion that encouraging physical activity in children with higher body fat mass at the age of seven may reduce obesity in later years.

Shultz et al., (2011) reviewed childhood obesity and physical activity and highlighted recommendations and challenges daily walking targets. Physical activity targets of 60 minutes of moderate-to-vigorous intensity daily activity were recommended for all children (US Department of Health and Human Services, 2008). However, the review reported lower step counts for obese children compared to non-obese children. Lower physical activity levels recorded in obese children may be due to increased metabolic and biomechanical demands. Increased metabolic demands relate to the increased energy expenditure and reduced economy from carry of extra mass during walking. Obese children preferred to walk at slower velocity and, when walking at a given walking speed, expended more energy compared to non-obese children (Hills et al., 2001, Shultz et al., 2011). Increased biomechanical demands relate to excessive joint loads and instability from the carriage of extra mass during walking. Increased stress across hip, knee and ankle joints were suggested to predispose obese children to injury, trauma and pain and may result in obese children having more difficulty walking (Shultz et al., 2011). This has led to speculation that increased pain and injury in obese children could affect motivation to be physically active and hinder attainment of moderate intensity of physical activity shown to reduce body fat mass in children (Shultz et al., 2009, de Sa Pinto et al., 2006). However, US boys are recommended to accumulate 15,000 steps per day (120-150 minutes) to meet physical activity targets

Hills et al., (2007) reviewed the contribution of physical activity and sedentary behaviours to skeletal health. The authors stated that physical activity represents a major mechanical loading factor for bone growth, modelling and remodelling during childhood, important for long term skeletal health. Children who are overweight or obese may be vulnerable to skeletal health problems as they commonly have marginal nutrition and are sedentary; the more common risk factors for low bone mineral.

2.5.2 Summary of the Aetiology of Childhood Obesity

The results of these studies indicate that obese children performed less physical activity than non-obese children and that higher levels of moderate to vigorous activity was associated with less fat between the ages of 12 and 14 years. Physical inactivity appears to be caused by a higher fat mass rather than the cause in 7 to 10 year old children. Therefore, children with higher fat mass may reduce the chance of becoming obese by participating in physical activity. Musculoskeletal growth and development rely on weight bearing activities, such as walking,

for the mechanics of the lower limbs to develop allowing efficient locomotion. A recommendation for 60-mins of moderate-to-vigorous activity has been made for children to maintain healthy weight and 45mins of moderate activity has been shown to reduce body fat mass. However, moderate-to-vigorous activity, may cause discomfort in obese children and hinder motivation to be physically active. Therefore, it is important to explore the biomechanical alterations of walking with obesity in order to correct for pathological motion and increase the potential for physical activity participation.

2.6 Health Co-morbidities of Obesity

Until recently, co-morbidities of childhood obesity were rarely seen until many years after obesity developed, usually in adulthood. However, with the escalating prevalence of childhood obesity and predisposition to obesity into later life, the health risks and morbidities are no longer the exclusive domain of adulthood (Lobstein et al., 2004). Children as young as 5 years old have been identified as having cardiovascular risk factors (Ebbeling et al., 2002). Examination of the links between obesity and health consequences in childhood (shown in Figure 2.3) reveals; cardiovascular (Freedman et al., 1999; Bell et al., 2007), endocrinology (Weiss et al., 2004), psychosocial (Hills et al., 2011), and respiratory consequences (Young et al., 2002; Speiser et al., 2005). However, for this study particular interest will be paid to musculoskeletal consequences in order to explore the links between excessive adiposity and lower limb biomechanics.

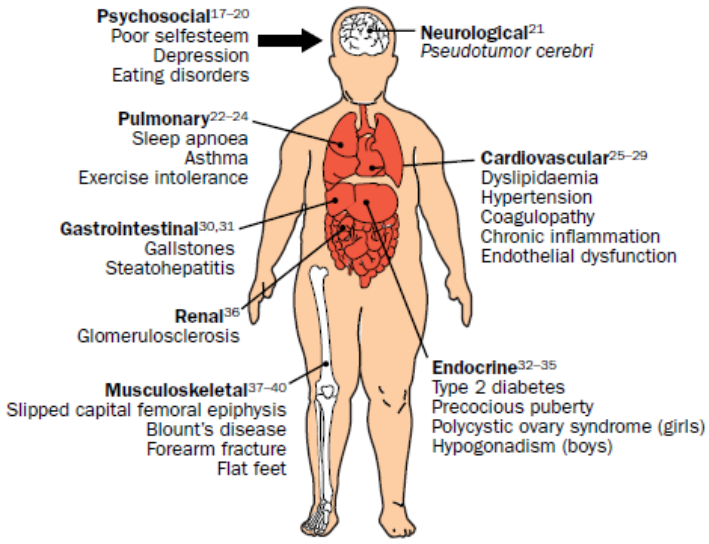

Figure 2.3. Health co-morbidities of childhood obesity. Ebbeling et al., (2002)

2.6.1 Musculoskeletal Consequences of Obesity

The delineation of the effects of childhood obesity on musculoskeletal structure in terms of mass, adiposity, anthropometry, metabolic effects or physical inactivity, or their combination, have not been investigated (Wearing et al., 2006). In the child, the musculoskeletal system develops under appropriate magnitude, direction and duration of load to form the long tubular bones of the lower limbs (Bernhardt 1988). At the ends of bones is an area of cartilage growth plate which is the site for bone formation and growth (Tachdjian, 1985). The formation of bone and articulation of joints depends on the loading patterns across articular cartilage and epiphyseal plates (Watt et al., 2006). Immature cartilage, unfused epiphyseal plates and softer cartilaginous bones of the lower limbs have not evolved to carry substantial body mass and may lead to malalignment and structural damage of the lower extremity joints in obesity. This contributes to orthopaedic complications of slipped capital femoral epiphysis, Blount's disease and flat feet (pes planus) seen in childhood obesity. Reports of persistent obesity in the paediatric population are associated with inhibition of normal movement patterns leading to greater impairment of mobility (Shultz et al., 2009) exacerbating the situation. This section details lower limb and foot musculoskeletal conditions reported in childhood obesity and the methods to measure static skeletal structure. Understanding the effects of childhood obesity on the static musculoskeletal structure of the lower limbs and feet may determine the potential for altered biomechanics during gait.

2.6.2 Lower limb Musculoskeletal Consequences of Obesity

2.6.2.1 Consequences of Obesity on Hip Structure

The hip is the articulation of the concave acetabulum of the pelvis and the convex head of the femur. Torsion of the femur in the transverse plane relative to the femoral head and neck medially rotates the lower limb from an externally rotated position of 25-30^{o} at birth. This anteversion decreases throughout life to 8-16^{o} at maturity (Levangie & Norkin 2005). Femoral anteversion correlates with femoral neck-shaft angles and bicondylar angles. Excessive anteversion has been linked with in-toeing during gait (Carriero et al., 2009). In the transverse plane the normal range of motion of the hip joint is 120-150^{o} (70^{o}+ external, 0-30^{o} internal rotation) at birth, this decreases to 90-120^{o} by 4 years of age and approximately 90^{o} at 6 years of age (45^{o} external, 45^{o} internal rotation) (Yates, 2009).

Galbraith et al., (1987) compared hip alignment using computer axial tomography in 12 obese children (>93rd centile CDC) and 13 non-obese children (<93rd centile CDC). The obese children had significantly less hip anteversion (0.4 ± 13.0^{o}) compared to the non-obese (10.6 ± 8.6^{o}). The authors concluded that greater weight-bearing forces promoted remodelling of the femoral neck resulting in less anteversion. Decreased femoral anteversion has been reported to be a predisposing factor for slipped capital femoral epiphysis in obese children (Esposito et al., 2013).

Slipped capital femoral epiphysis (SCFE) occurs when the epiphysis of the proximal femur slips off the metaphysis posteriorly and medially and there is proximal and anterior migration of the femoral metaphysic (Skinner 1996). The incidence is approximately 3.4 per 100,000 children (Kelsey et al., 1972) but 50-70% of patients with SCFE are obese and two-thirds of patients with bilateral SCFE are obese (Zwiauer et al., 2006).

Further to the findings of less hip anteversion in obese children is the finding of greater hip abduction (Wills, 2004). Greater hip abduction in obese increase shear forces across the capital femoral growth plate resulting in a higher risk of SCFE. These studies indicate that obesity can alter the hip joint in the frontal and transverse planes during skeletal development causing malalignments. Whether obesity induces these malalignments is not fully understood but the excessive compressive and shear forces in obese children may cause failure of the proximal femoral epiphysis and SCFE.

2.6.2.2 Consequences of Obesity on Knee Structure

The two articulation between the tibiofemoral joint and the patellofemoral joint describe the knee (genu refers to the knee joint). Normal genu varum (medial rotation of the shank relative to the thigh) values of 15-20^{o} are measured at birth, but knee alignment moves in the frontal plane with development to; straight at 2-5 years old, genu valgum between 4-6 years, and back to straight around 6-12 years old (Yates, 2009). The femoral bicondylar angle represents the angle between the long axis of the femur and axis between the distal condyles in the femoral plane. The bicondylar angle reaches adult values (8-11^{o}) by the age of 4-8 years. The ultimate effect of femoral bicondylar angle in humans is to adduct the knee, thereby placing the knee under the body's centre of gravity during locomotion (Cowgill et al., 2010).

Childhood obesity has been related to Blount's disease, characterised by tibia vara (medial bowing of the tibia). Tibia vara is formed from irregular growth of the medial aspect of the

proximal tibial epiphysis. It is suggested that the condition results from growth suppression due to increased compressive forces across the medial aspect of the knee (Cook et al., 1983). Previous studies have shown the prevalence of obesity to be 50% to 80% in children with Blount's disease (Skinner, 1996). Younger age of onset and bilateral Blount's disease are particularly related to obesity (Styne 2001).

Incidence of genu valgum has been reported to be higher in obese children compared to non-obese counterparts (Taylor et al., 2006). De Sa Pinto, (2006) found significant associations between genu valgum and obesity (BMI) in 53 children. The authors related genu valgum to the presence of obesity during normal physiologic valgus (at 3-4 years old) while genu varus may be related to obesity during normal varus (18-20 months old).

2.6.2.3 Consequences of Obesity on Foot Structure

Flatfoot (pes planus) is a term describing any condition of the foot in which the medial longitudinal arch (MLA) is lowered or lost (Kim & Weinstein, 2000). It is characterised by eversion of the subtalar joint during weight bearing with dorsiflexion of the talus and calcaneus, an abducted navicular and pronated foot (Gunther, 2004). Paediatric studies have repeatedly found associations between flat feet and increased body weight (Bordin et al., 2001; Riddiford-Harland 2000; Dowling et al., 2001). Excess weight-bearing in overweight children may lead to structural dysfunction and collapse of the longitudinal arch (Hills, 2002).

Riddiford-Harland et al., (2000) used a pedograph (ink imprint of feet on paper) to evaluate the plantar footprint from both feet of 62 obese (BMI>95th percentile) and 62 non-obese (10th percentile <BMI> 90th percentile) children (mean age 8.5 ± 0.5 years). Obese subjects demonstrated a flatter cavity and broader midfoot area of the footprint corresponding to a lower MLA (Cavanagh & Rogers, 1987). These findings are indicative of decreased integrity of the foot as a weight-bearing structure which may hinder participation in physical activity.

Villarroya et al., (2009) examined radiographic parameters in 49 obese children and adolescents between the ages of 9 and 16.5 years of age. The study used footprint assessments together with radiographic measures of talus-first metatarsal head angle (TFMA) and Calcaneal inclination angle (CIA) as indicators of flatfoot deformity. Mean TFMA values showed of the 49 subjects, only three had TFMA less than 4° indicating normal MLA structure. The mean value for the obese subjects was 15°-16° meaning a moderate amount of flatfoot

deformity. Similarly mean CIA were indicative of flatfootedness, with 37 out of the 49 obese subjects demonstrating angles lower than the 18°- 21° described as normal values.

Pfeiffer et al., (2006) conducted a cross-sectional study, examining 835 children (aged 3 to 6 years) for clinical diagnosis of flatfeet based on valgus positioning of the heel. A laser skin surface scanner was employed to create a 3D model of the child's feet from which hindfoot angles (calculated from the Achilles tendon to the distal extension of the hindfoot) were measured to define flat-footedness. The results demonstrated that obese and overweight children had a significantly greater prevalence (62% and 51% respectively) of flatfeet compared to normal weight counterparts (42%). A further finding of the study was that the children tended to have a greater prevalence of flatfeet in the younger age groups which decreased in the older groups. In boys particularly the prevalence of flat-footedness decreased from 71% to 32% between the ages of 3 to 6 years (Pfeiffer et al., 2006).

Difficulty arises from defining how structural changes of the foot leads to pathologies because it is not possible to infer compromised gait dynamics from indirect static measures. Measures of static footprints are expected to respond predictably to variations in the medial longitudinal arch. However, the fact that these are indirect measures of foot structure means they may inconsistently predict dynamic dimensions of the foot (Mathieson 1999).

2.6.3 Summary of Lower Limb Musculoskeletal Consequences of Obesity

The health consequences of childhood obesity are becoming more apparent as the prevalence of obesity rises. Musculoskeletal dysfunction of the lower limbs associated with obesity has been examined in children, with many studies reporting links between orthopaedic conditions such as slipped capital epiphysis and Blount's disease and static measures of flat feet (Taylor et al., 2006; Chan & Chen 2009). Foot structural maladaptations, such as flat feet may arise due to musculoskeletal dysfunction as a result of excessive weight bearing, the consequences of which may lead to deformity, pain and a reluctance for weight bearing activities such a gait. However, little attention in the literature has been paid to effects on dynamic alignment of the lower limb joints during walking. The dynamic nature and forces that act on the lower limb joints during gait can lead to altered alignment and potential structural damage of the lower extremity joints in childhood obesity. There is a need to investigate the dynamic structure of the lower limbs and feet to understand the effects of obesity on joint motion and forces.

2.7 Lower limb and Foot Biomechanics during Gait in Obese Children

The repetitive nature of loading and unloading during ambulation makes significant demands on the musculoskeletal system. Physical activity and in particular walking can be linked to both the aetiology of childhood obesity, with low levels linked to incidence of obesity, and aetiology of musculoskeletal co-morbidities, from excessive joint loads and malalignments. This section will examine findings from gait analysis conducted on obese and overweight children to determine the associations between obesity and gait characteristics in relation to understanding musculoskeletal pathology and promoting physical activity.

2.8.1 Introduction to Gait

Bipedal walking is a process of vaulting over an inverted pendulum of the stance limb while simultaneously swinging the contralateral limb (a compound pendulum) in a synchronised fashion (Ivanenko et al., 2007). Spatiotemporal parameters of gait include stride length (the distance between two successive placements of the same foot), step length (the distance between the placement of one foot with the forward placement of the other foot), step width (the medio-lateral distance between the mid-point of each ankle), cadence (steps per minute), stride time, step time and walking speed (Whittle, 1997).

Perry, (1992) described the gait cycle according to phases distinguished by reciprocal foot contact patterns. The stance phase describes the first ~60% of the gait cycle for one limb and can be divided into; first double support (first ~10%), first single support (~40%) and second double support (~10%), shown in Figure 2.4. Ipsilateral initial contact (IIC) of the heel determines the start of the gait cycle, the first double support phase (DS1) is defined from IIC to contralateral toe-off (CTO). The first single support phase is defined from CTO to contralateral initial contact (CIC). The second double support phase is defined from CIC to ipsilateral toe-off (ITO). The limb then enters the swing phase for the final ~40% of the gait cycle while the other limb is in single limb stance. The second single support phase (the swing phase) is defined from ITO to IIC which determines the end of the gait cycle.

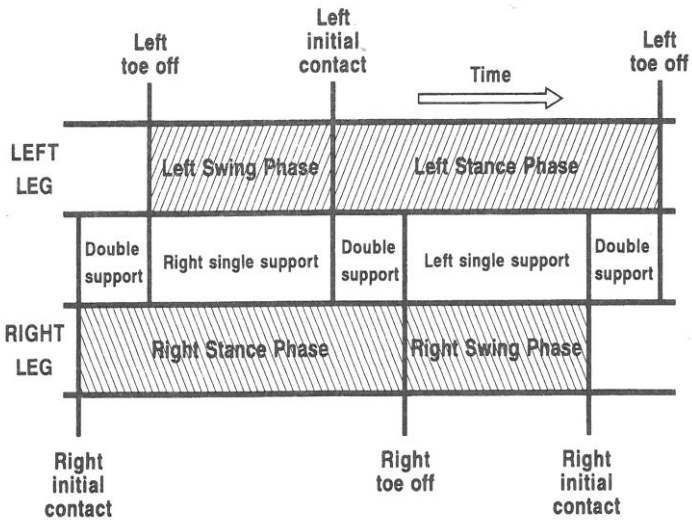

Figure 2.4. Timing of single and double support phases starting from right initial contact (ipsilateral initial contact). Whittle, (1997)

The phases of the gait cycle can be further broken down by the functional characteristics of the foot and lower limbs which are to absorb shock of impact, stabilise the body, and facilitate the goal of gait which is progression. The first task is weight acceptance made up of initial contact (0-2%) and loading response (2-12%). The heel is positioned for initial contact to preserve progression, plantarflexion of the hindfoot occurs as the heel rocks forward (Smith et al., 2008). The ankle is positioned at 90^{o} with the ground reaction vector behind the ankle, the knee is fully extended (5^{o} flexed) and hip slightly flexed (20^{o}). During single limb support, consisting of mid stance (10-30%) and terminal stance (30-50%) one limb supports the entire body weight as it progresses over and beyond the stance foot. The ankle rocker advances the ground reaction vector over the ankle joint axis as the hindfoot gradually dorsiflexes relative to the tibia, eversion of the subtalar joint peaks at 4-6^{o} by early midstance. The knee remains fully extended to maintain stability as the ground reaction vector moves anterior to knee joint axis. The hip extends and the joint centre advances in front of the ground reaction vector. As the heel rises to mark the onset of terminal stance, the subtalar joint inverts (end position 2^{o} eversion) locking the midtarsal joint. Body weight is now supported on the forefoot, the metatarsal heads providing the third rocker, advancing the ground reaction vector for continued progression. The third functional task of gait is limb advancement, constituted of the swing phases; pre-swing (50-60%), initial swing (60-73%), mid swing (73-87%) and terminal swing (87-100%). In pre-swing, the ankle plantarflexes (to 15^{o} plantarflexion) as weight is transferred on to the contralateral limb and the forefoot supinates as toe-off occurs (Smith et al., 2008). The knee passively flexes to 40^{o} which gives adequate toe clearance for the swing phase. The hip begins to accelerate forward from its hyperextended position (from 20^{o} to 10^{o}

hyperextension by end of phase). During the rest of the swing phase the ankle dorsiflexes and the forefoot pronates and abducts to reach approximate neutral for the next heel strike. The knee extends through the swing phase for limb advancement and preparation for stance. The thigh flexes to 15^{o} at the end of initial swing to 25^{o} at end of mid swing but finishes at 20^{o} for heel strike.

2.7.2 Measures of Gait

Gait can be assessed using a variety of techniques from instrumented walkways, accelerometers to two-dimensional (2D) and three-dimensional (3D) motion analysis systems. Three-dimensional gait analysis, the most common method discussed in this section, utilises the motion capture of body segments and the forces that act on them to describe locomotor patterns during the gait cycle. Information on joint kinematics, the forces exchanged, and the loads transmitted across body segments can be quantified and compared to distinguish gait performance (Cappozzo et al., 2005). When applied to three-dimensional gait analysis, motion analysis offers a wealth of information on the gait cycle including temporal and spatial parameters such as speed, cadence, step and stride length, the stability and dynamic control of gait and the efficiency of ambulation (Theologis & Stebbins 2010). A detailed review of the methods of 3D motion analysis and the biomechanical models used are in literature review chapter 2 (chapter 3).

2.7.3 Spatiotemporal Findings of Obese Gait in Children

Table 2.4 shows the findings from studies to compare spatiotemporal characteristics in obese and non-obese children. In one of the first studies to examine spatiotemporal and kinematic characteristic differences between obese and non-obese children, Hills & Parker (1991) identified obese children as having a slow and tentative gait. Using two cameras placed in the sagittal and frontal plane, the authors recorded ambulation of ten obese (26.0 ± 1.6 kg/m^2) and ten normal weight (16.0 ± 0.7 kg/m^2) children (mean age 10.5 years). Walking at a self-selected walking speed obese participants demonstrated greater cycle duration, lower cadence, and velocity. Obese subjects also demonstrated consistently higher mean values for double stance (61.48 and 61.22% for obese and normal weight subjects respectively). Step length differed significantly for obese subject's right and left limbs, but not for normal weight subjects indicating greater asymmetry. The authors concluded that this may be indicative of

greater weight bearing instability during gait in the children with excessive body mass (Winter, 1987). Gait stability refers to the body's reaction to small perturbations whilst maintaining equilibrium, during dynamic conditions (Hamacher et al., 2011).

McGraw et al., (2000) also reported that obese boys (BMI 30.3 ± 7.86 kg/m^2) spent significantly greater amount of time in double support compared to ten non-obese (BMI 17.4 ± 1.14 kg/m^2) boys age 8 to 10years. The study also measured postural sway, employing a force plate to measure static ground reaction force. The findings demonstrated greater sway areas in the medial/lateral direction in the obese boys; this together with more time spent in double support may indicate that instability in obese children is caused by excess weight rather than underlying postural instability.

Nantel et al., (2006) found few spatiotemporal differences between obese (BMI 26.7 ± 7.1kg/m^2) children and non-obese children, aged 8 to 13 years. The only measure significantly different between the two body mass groups in this study was that obese children exhibited less single support phase time during the gait cycle (36.6 ± 3.6% and 39.5 ± 2.0% obese and non-obese respectively). The authors reported that reduced single support time in the obese group maximised stability by keeping the centre of mass within the base of support.

Morrison et al., (2008) found both shorter single support duration and longer double support duration with increased body mass. Forty four children (mean age 9.5 ± 0.6years) were analysed for temporal parameters of gait using the GAITrite®, a pressure sensitive instrumental walkway. Individuals with excessive body mass (BMI Z-Score 2.05 ± 0.14) were described as having experienced disequilibrium during gait compared to those with normal body weight (BMI Z-Score -0.16 ± 0.14). The spatiotemporal findings revealed; increased stance phase time, slower walking speed and lower cadence which may be a strategy employed by obese children to decrease instability.

In summary, the spatiotemporal findings show that obese children present a slower, more tentative gait and greater instability. This has implications for physical activity in the long term as obese children are encouraged to be active including walking more. However, greater instability may be caused by reduced musculoskeletal function and/or structural malalignments. Therefore, the short term goal should focus on improving musculoskeletal function to enable the children to become active and prevent or reduce structural malalignments which can cause problems for life (Morrison et al., 2008). The findings of altered medial/lateral ground reaction force in obese subjects may indicate that frontal plane

biomechanics are affected by excessive body weight. An important consideration is whether spatiotemporal changes in obese subjects lead to or are as result from lower limb malalignments which may be linked to musculoskeletal pathologies.

Table 2.4 Mean ± SD for spatiotemporal findings from studies of childhood obesity

Author	Speed ($m \cdot s^{-1}$)		Cadence (steps·min) *(strides·min)		Stride length (m) *Step length (m)		Stance phase duration (%)		Single support duration (%)		Double support duration (%)	
	obese	Non-obese	obese	Non-obese	obese	Non-obese	obese	Non-obese	obese	Non-obese	obese	Non-obese
Nantel et al., (2006)	0.98±0.22	1.01±0.16	111.6±6.9	110.9±13.4	1.06±0.20	1.08±0.16	62.3±1.4	62.7±2.5	39.5±2.0	36.6±3.6	22.8±3.0	26.0±5.5
Morrison et al., (2008)			129±9.9	123.6±10.7					38.6±3.4	39.7±1.0	22.7±3.2	19.9±2.4
Hills & Parker (1991)	1.29±0.10	1.43±0.04	125±4.6	133±5.3	0.63±0.07*	0.60±0.06*	61.48	61.22				
McGraw et al., (2000)			65.3±8.1*	70.4±6.7*								

2.7.4 Kinematic Findings of Obese Gait in Children

Kinematic analysis of gait involves the measurement of linear and angular displacements, velocities and accelerations of body segments, it is not concerned with the forces that act on the segments but with the movement itself (Richards, 2008). Three-dimensional motion capture techniques have allowed the quantification of segmental movement within the laboratory setting. Table 2.5 shows the significant results of kinematic studies that reported the differences in lower limb joint angles between obese and non-obese children.

Using infrared-emitting diodes, Gushue et al., (2005) tracked the movement of pelvic, hip, knee and ankle motion in ten overweight (mean age 11.9 ± 1.2years) and thirteen normal weight children (mean age 12.2 ± 1.6years). In this study the only kinematic difference between the weight groups was that the overweight children (BMI 29.9 ± 5.4 kg/m^2) walked with a significantly lower peak knee flexion angle (21.1 ± 5.0° versus 14.5 ± 5.5° for normal and overweight subjects respectively) during early stance compared to the normal weight (BMI 18.0 ± 2.2 kg/m^2). Hip and ankle kinematics maintained a similar pattern over the stance phase between the weight groups indicating that overweight children's hip and ankle motion may not be affected by increased adiposity.

Shultz et al., (2009) found that 3D kinematic measures of overweight and healthy weight children (n = 10, mean age 10.4 ± 1.6years) were comparable, with no significant differences

observed for angular displacement of the lower limb. All overweight (BMI 30.47 ± 5.54 kg/m^2) and normal weight (BMI 16.85 ± 1.31 kg/m^2) children exhibited less hip, knee and ankle joint motion during gait when walking at 130% compared to 100% of their self-selected walking cadence. Walking speed is an important factor in gait analysis because of the effect it has on joint kinematics (Stansfield et al., 2001). Spatiotemporal findings, as described in the previous section, present obese children as having a slower gait which may increase frontal plane movement due to greater medial/lateral sway. However, it is necessary to determine whether increased body weight reduces walking speed to maintain stability or whether a slower walking speed is as a result of musculoskeletal malalignments and pathologies.

Frontal plane kinematics of the lower limbs during gait in male children (n = age 10 to 12 years) have been examined in isolation from the other planes (McMillan et al., (2009). The study reported that overweight boys (BMI 40.5 ± 10.0 kg/m^2) produced greater hindfoot eversion, larger range of motion (ROM) and later peak eversion motion (temporal) relative to the healthy weight subjects (BMI 17.0 ± 3.3 kg/m^2). Peak knee abduction motion in early and late stance was of greater amplitude in the obese group. The authors conclude that overweight boys redistribute forces in the medial-lateral direction during gait, this may lead to excessive stress on the joints possibly leading to musculoskeletal injuries. McMillan et al., (2009) study recruited participants with a greater degree of obesity than in many of the other studies; with a mean BMI of 40.5kg/m^2 the subjects were approximately 10kg/m^2 heavier than Gushue et al., (2005) and Shultz et al., (2009). Indeed, the difference between the obese and non-obese group (11.9 kg/m^2) in Gushue et al., (2005) was similar to the difference between the obese groups in Gushue et al., (2005) and McMillan et al., (2009) (10.4kg/m^2). These large differences in obese subject group definitions may mean that comparisons between studies are difficult and possibly lead to inaccurate assertions. The use of obesity measures as a continuous variable may alleviate the issue of group comparisons as the error involved in defining the groups is removed.

McMillan et al., (2010) conducted a study examining lower limb motion during gait on 36 obese (44.6±10.2kg/m^2) and healthy weight (20.3±2.0kg/m^2) male and female adolescents. No significant differences were reported in the magnitude, timing or range of joint motion at the ankle. However significant differences were discovered at the knee and hip in the sagittal and frontal planes; obese subjects demonstrated less knee flexion and more knee valgus at initial contact, the knee remained in valgus positioning throughout stance and the hip joint remained less flexed at initial contact. The larger degree of valgus motion of the knee during the stance

phase and greater joint ROM in the frontal plane may be a result of excessive weight causing structural alteration.

In summary, these studies on the associations between childhood obesity and kinematic changes in the lower limb reveal that; flexion of the hip joint is reduced during stance and adduction is increased; the knee is less flexed and demonstrates more valgus positioning at initial contact; and, no differences have been observed when the foot is considered as one segment articulating at the ankle joint. However, when the hindfoot is considered separate to the distal foot (relative to the shank) it appears to be more everted during the stance phase in obese children. There is no clear definition of how excessive body mass affects lower limb kinematics during gait. In contrast to the significant differences summarised above, one study found no significant difference between obese and non-obese children gait kinematics. The major confounding factor for analysing gait is that there is no consensus on the gold standard for kinematic modelling and how to analysis the gait cycle to determine where differences may occur. As technology and techniques for measurement of gait kinematics become more sophisticated the ability to accurately describe the movements of gait has improved. However, errors due to excessive soft tissue motion in obese participants may hinder the application of marker attachment and tracking to skeletal landmarks and warrants further investigation.

Table 2.5. Mean ± SD of significant joint angle findings in gait studies of obese and non-obese children.

	Hip			Knee			Hindfoot		
Author	Sagittal	Frontal	Transverse	Sagittal	Frontal	Transverse	Sagittal	Frontal	Transverse
McMillan et al., (2009) (°)					Add (1st)				
	N				1.81±5.01				
	O				-11.96±5.74				
					Add (2nd)				
	N				5.19±5.60				
	O				-6.23±4.33				
McMillan et al., (2010) (°)	Flex (IIC)			Flex (IIC)	Abd (IIC)				
	N 30.47±9.62			-7.10±3.41	0.35±2.46				
	O 18.01±10.50			-1.38±7.35	4.12±4.37				
					Add (1st)				
	N				2.99±2.73				
	O				-0.76±4.32				
					Abd (2nd)				
	N				-0.80±3.94				
	O				-9.55±7.62				

O – Obese/overweight and N – Non obese children. (1st) or (2nd) used if there is more than one peak during the gait cycle, (IIC) moments at ipsilateral initial contact. Flex = flexion, abd = abduction, add = adduction

2.7.5 Kinetic Findings of Obese Gait in Children

Kinetic analysis of gait parameters is imperative to explain the causes of joint movement, the mechanisms of locomotion and why differing strategies are employed by specific study populations. All studies referenced in this section reported internal joint moments which, in general, provide information on the joint areas involved and the tension between them (Whittle, 1996). External joint moments are calculated using a combination of ground reaction forces (GRF), anthropometric and 3D joint centre positional data entered into inverse dynamic equations to give the forces, moments and powers about a joint. Kinetic findings have varied considerably between studies due to differences in the equipment and protocols used. This section will highlight the various studies that have looked at hip, knee and ankle joint moments in obese and non-obese children. Table 2.6 is a summary of findings from 3D gait analyses conducted on children who are overweight compared to normal weight controls.

Gushue et al., (2005) reported that increased internal knee abduction moments suggest that overweight children may not adequately compensate for increased loads placed on the knee causing movement in the frontal plane increasing medial compartment joint loads. This study reported internal joint moments both non-normalised and normalised to body weight. When the latter was reported significant differences between weight groups were eliminated. Studies that have examined how obesity affects joint structure found that increases in body mass are not proportional to articulating surface area (Ding et al., 2005) the greater absolute forces acting around the joint will cause relatively greater stress. This increase in stress has been proposed to lead to a number of malalignments and injuries to the lower limbs such as slipped capital femoral epiphysis and genu valgum (Pritchett, 1988; Taylor et al., 2006). This supports the use of absolute joint kinetics to determine differences between obese and non-obese children rather than joint kinetics normalised to body weight.

Shultz et al., (2009) reported greater absolute (not normalised to body weight and/or height) internal joint moments and the hip, knee and ankle in all planes except; hip adduction and internal rotation; knee external rotation; and, ankle dorsiflexion and eversion. The authors reported that greater internal hip moments can cause excessive compressing, shearing and rotational forces at the proximal femoral epiphysis resulting in slipped capital femoral epiphysis (SCFE). Increased internal knee abduction moments may increase the risk of genu valgum, a common condition in obese children. At the ankle joint, increased internal inversion moments may be the consequence of altered hip and knee joint loading, and a greater peak internal ankle dorsiflexor moment may be attributed to a greater braking mechanism in the

overweight subjects aiding them to remain upright. The paper concludes that increased joint forces can impact orthopaedic health and implications for non-weight bearing activity prescription.

McMillan et al., (2009) presented frontal plane hip, knee and hindfoot kinetics (normalised to participant's height and weight) in addition to the kinematic findings discussed above. Significantly greater hip abduction peaks in early and late stance were found between obese and non-obese children. The study explained that greater hip abduction moments were in response to the adducted position of the hip and may relate to slipped capital femoral epiphysis (SCFE).

In a later study, McMillan et al., (2010) also presented hip, knee and hindfoot kinetics (normalised to participants height and weight) in the sagittal and frontal planes. Obese children had significantly less hip extension, knee flexion and hindfoot plantarflexion moments in early stance and higher hip flexion moments during late stance. In the frontal plane, obese children had significantly lower hip abduction, knee abduction and hindfoot inversion moments. The authors reported that increased hip flexion moment was a compensatory mechanism whereby the hip flexors pull rather than the plantarflexors push the limb into the swing phase. It was hypothesised that muscle weaknesses is a potential cause of the movement differences.

In summary, the results of studies examining kinetic differences between obese and non-obese children are dependent on the means of expressing joint moments. Expressing absolute joint moments may provide more insight into the alterations of the lower limbs during gait in obese children. Higher internal joint moments may indicate muscle weakness relative to the force of ambulating the body particularly damaging to lower limb joints in the frontal and transverse planes.

Table 2.6. Mean ± SD of significant joint moment findings in gait studies of obese and non-obese children.

		Hip			Knee			Ankle (hindfoot)		
Author		Sagittal	Frontal	Transverse	Sagittal	Frontal	Transverse	Sagittal	Frontal	Transverse
Gushue et al., (2005) (Nm)						Abd		Flex		
	N					10.8±5.5		67.6±17.0		
	O					22.5±10.5		95.0±27.0		
Shultz et al., (2009) (Nm)		Flex	Abd	Ext rot	Flex	Abd		Flex		Ext rot
	N	25.12±7.88	30.46±10.69	14.15±4.50	10.34±3.66	14.11±4.35		50.93±16.24		7.23±2.36
	O	54.66±27.08	66.30±20.22	33.62±13.68	23.65±13.67	26.24±14.15		96.97±33.81		13.48±5.58
		Ext			Ext	Add	Int rot	Ext	In	Int rot
	N	32.58±5.00			18.28±8.48	2.29±1.41	3.65±1.78	50.93±16.24	2.69±1.83	0.68±0.38
	O	65.36±27.80			51.67±26.75	9.81±7.22	9.46±6.38	96.97±33.81	7.27±4.41	1.99±1.41
McMillan et al., (2009) (Nm·kg*m)			Abd (1st)							
	N		0.24±0.07							
	O		0.50±0.10							
			Abd (2nd)							
	N		0.27±.010							
	O		0.55±0.14							
McMillan et al., (2010) (Nm·kg*m)		Flex (IIC)	Abd (1st)		Flex (IIC)	Abd (1st)		Flex (2nd)		
	N	0.72±0.23	0.55±0.13		0.28±0.11	0.30±0.09		0.88±0.07		
	O	0.43±0.12	0.42±0.12		0.19±0.06	0.16±0.06		0.67±0.13		
		Flex (1st)			Flex (1st)	Abd (2nd)			In (1st)	
	N	0.24±0.08			0.31±0.11	0.27±0.09			0.11±0.02	
	O	0.37±0.16			0.10±0.14	0.14±0.06			0.07±0.03	
						Add (1st)				
	N					0.07±0.06				
	O					0.03±0.03				

O – Obese/overweight and N – Non obese children. Gushue et al., (2005) reported peak absolute internal moments, Shultz et al., (2009) presents mean absolute internal moments over stance phase. McMillan et al., (2009 & 2010) reported peak normalised joint moments at gait cycle peaks and events. (1^{st}) or (2^{nd}) used if there is more than one peak during the gait cycle, (IIC) moments at ipsilateral initial contact. McMillan reported hindfoot moments, Gushue et al., (2005) and Shultz et al., (2009) reported ankle moments. Flex = flexion, Ext = extension, abd = abduction, add = adduction, Int rot = internal rotation, Ext rot = external rotation, In = inversion.

2.7.6 Foot Motion during Gait in Obese Children

Fewer studies have examined the kinematics of the foot in obese and non-obese children compared to the lower limb joints. The foot deals with high forces over multiple joints as it supports, balances and propels the body during gait and is, therefore an area that warrants investigation in relation to childhood obesity. There is a need for studies to examine how alterations in joint motion caused by body mass affect movement of the joints up and down the kinematic chain. However, currently studies have only examined foot structural differences using 2D plantar measures of dynamic footprint and plantar pressure analysis.

2.7.6.1 Dynamic Foot Prints

In one of only a few studies to examine the differences between static footprints and dynamic plantar pressure in obese and non-obese children, Taisa Filippin et al., (2008) found that

obesity may have an effect on relationships between static and dynamic measures. Twenty children aged 9 to 11 were divided into obese and non-obese groups according to BMI percentiles. Obese subjects demonstrated significantly higher arch index (midfoot area relative to the whole foot area), static contact area and dynamic contact area. Non-obese children demonstrated good correlations between static contact area and dynamic contact area (r=0.7), and arch index with dynamic contact area (r=0.8) but obese group did not (r=0.4 and r=0.3 for static and dynamic contact area and arch index and dynamic, respectively). The paper proposed that static footprints taken in isolation were not enough to infer the characteristics of obese children's feet in dynamic conditions.

Wearing et al., (2004) used dynamic electronic footprints in a pilot study to determine the indirect measure of arch height in 24 overweight and obese adult subjects (mean age 39.9±8.1 years) from arch index. Body composition and body mass index (BMI range 26.7kg/m^2 to 38.1 kg/m^2) were both measured and compared by correlation analysis to the plantar surface area of the foot and arch index. Interestingly arch index was significantly correlated with percentage fat mass (r = .67) but not with body weight (r = -.13) or BMI (r = .27). Midfoot area was significantly correlated with fat mass explaining approximately 29% of the variance. Furthermore, ultrasound assessment of the obese paediatric foot has revealed the medial longitudinal arch to be flatter and the plantar fat pad larger than non-obese children (Riddiford-Harland et al., 2000). Excessive fat mass and the distribution of body mass may be related to altered foot structure seen in obese children.

Whilst these studies have found differences in dynamic footprint measures between obese and non-obese children there are methodological limitations to the procedures. Direct measures of medial longitudinal arch height such as navicular height have not been used as frequently in the literature compared to indirect measures such as arch index. While both measures have been found to correlate with each other (r = -0.46) navicular height may be more sensitive to define arch height in children and is not affected by body weight in contrast to measures of arch index (Gilmour & Burns, 2001). This finding may highlight the fact that excessive body weight may predispose the foot to larger amounts of adiposity, on the sole rather than the navicular area, increasing soft tissue on the plantar surface of the foot changing the footprint to appear flatter. Furthermore, the reliability of footprint parameters compared to direct measures of arch height is low with only 4-15% of the variation in arch height explained by variations in footprints (Razeghi & Batt, 2002). Therefore, measuring

dynamic foot structure by tracking bone landmarks such as the navicular, rather than examining the plantar surface, could reveal associations between flat feet and obesity.

2.7.6.2 Plantar Pressures

Foot structure and function can be assessed using plantar pressure measurements, which divide the foot into specific regions from which loading characteristics can then be calculated (Stebbins et al., 2005). Dowling et al., (2001) examined foot plantar pressures during static and dynamic conditions in 13 obese and 13 non-obese children (mean age 8.1 ± 1.2years). Each dynamic pressure footprint was divided into two areas; the forefoot and hindfoot. The obese group demonstrated greater peak force under both forefoot (341.0±93.6 and 227.5±33.9N for obese and non-obese subjects respectively) and hindfoot (446.6±83.9 and 311.0±55.0N for obese and non-obese subjects respectively) areas but this was distributed over a larger surface area (total foot area 97.1±11.9 versus 74.3±9.2cm^2). Therefore, hindfoot peak pressures (force/area) were not significantly different between the obese and non-obese groups but forefoot peak pressures were (39.3±15.7N·cm^{-2} versus 32.3±9.2 N·cm^{-2}). The authors reported that the increased forefoot plantar pressures in obese children may lead to discomfort and hinder participation in physical activity. A limitation of this study is the division of the foot in half to describe the forefoot and hindfoot eliminating important findings that may have been found under the midfoot region.

In a follow-up study Dowling et al., (2004) examined ten obese and non-obese children (mean age 8.8 ± 2.0years) using static and dynamic assessment of pressure, dividing the plantar surface of the feet into ten discrete regions. This study found significant differences in plantar pressures between the weight groups (37.1 ± 9.4Ncm^{-2} versus 26.2 ± 8.5Ncm^{-2} for obese and non-obese subjects respectively, p=.022). The authors conclude that the obese children demonstrated altered distribution of forces over their feet compared to their leaner peers which may be related to structural alterations due to excessive body mass. However, differences may also arise from the technology of the different systems used as type of sensor, number of sensors and sampling frequency vary between systems and will have an effect on the data presented (Taisa Filippin et al., 2008). Dowling et al., (2004) reported that all regions of the foot except the toes demonstrated an increase in plantar force in the obese group, similarly all plantar contact areas apart from the hallux were of greater size compared to the non-obese. Plantar pressures in obese children highlight the midfoot regions as showing the

greatest difference compared to the non-obese children. These are the areas under or adjoining the MLA (including medial and lateral midfoot and metatarsal heads 2 to 5). The authors concluded that the increase in midfoot plantar pressure is likely a consequence of the obese group having flatfeet. However, whether this is soft tissue or a structural change in the MLA is unknown.

Mickle et al., (2006) examined dynamic plantar pressures in a study of 17 obese pre-school age children (mean age 4.4 ± 0.8years). In this study the only foot plantar region to demonstrate significantly higher pressure was the midfoot. Force-time integrals were also significantly higher in the obese group at the midfoot region, possibly predisposing their feet to increased stress upon the navicular and cuneiform during weight-bearing activities. Furthermore trauma to the soft tissues in the obese subjects is likely to cause pain and discomfort, possibly decreasing activity levels without interventions (Mickle et al., 2006).

Studies that have examined plantar pressures in obese and non-obese have reported significant differences between forces, surface area and pressure from the supporting foot during the stance phase of gait. Certainly excessive body mass will cause greater force to be imparted on the ground during ambulation but what affect this has on the joints of the foot cannot be discovered using plantar pressure technology. Obese subjects may develop an altered gait pattern in order to cope with the greater forces thereby reducing the possibility of damage to joints in the lower limbs.

2.7.7 Summary of Lower Limb and Foot Biomechanics in Obese Children

Co-morbidities associated with childhood obesity may affect the position of the foot and lower limb during gait. It has been proposed that these changes lead to musculoskeletal pathology and reduced engagement with physical activity. However, further work is required to understand the kinematic and kinetic differences between obese and non-obese paediatric gait. Analyses of spatiotemporal gait data have found obese children spend longer in double support phase of the gait cycle, possibly as a way of compensating for loss of stability. Kinematic findings of how obesity effects joint motion have reported differing results with some studies finding significant differences between obese and non-obese children while others did not. However, due to the greater amount of forces being transferred across the joints of the lower limbs even a small change in joint motion or position may result in musculoskeletal pathologies. Kinetic analysis, in particular joint moments, can provide an

insight into the true nature of gait disruption from obesity as the combination of greater forces and joint malalignment can cause detrimental affects to joint structures. Footprint and plantar pressure measures show that a greater area of the midfoot region comes into contact with the ground in children with higher fat-mass. Relatively few studies have examined in detail the biomechanical affects of obesity on paediatric gait characteristics. An overall understanding of how adiposity relates to altered walking patterns and how children may employ protective mechanisms to cope with developmental changes is required.

2.8 Clinical Reasoning of Study

Virtually all reviews have indicated that the prevention of obesity is the most realistic and cost effective approach for dealing with childhood obesity (Ebbeling et al., 2002; Lissau et al., 2002). Given the genetic propensity for certain populations to develop obesity in conducive environments, prevention is best targeted at young people (Lobstein et al., 2004). This may be achieved through a variety of interventions targeting the environment, physical activity and diet (Dehghan et al., 2005). Identifying 'anti-obesogenic' environments including walking and cycling networks, parks and recreation facilities can be promoted to the community as a healthier choice. However, sedentary pursuits including television, computers and video games have a greater effect on childhood obesity (Swinburn & Egger, 2002; Tremblay & Willms, 2003) and there is evidence that obese children spend more time in sedentary activities than non-obese children (Marshall et al., 2004). As stated earlier in this chapter (aetiology of childhood obesity), physical inactivity appears to result in reciprocal causality with childhood obesity. Therefore, the prevention of childhood obesity appears to be linked to levels physical activity.

Approaches to the management of childhood obesity are generally designed to bring weight gain under control and to mange and alleviate associated co-morbidities (Lobstein et al., 2004). Interventions that target energy expenditure are more successful when reductions in sedentary behaviour are targeted rather than increases in the level of exercise (Robinson 2001, Epstein et al., 2001). Appropriate levels of physical activity can confer fitness while lowering the risk of obesity and health risks associated with excess adiposity and contributing to greater bone density (Fogelholm, 2010; Hamer & O'Donovan, 2010; Hills et al., 2011). Furthermore, partaking in physical activity may induce musculoskeletal pain, discomfort and impairment of mobility (Shultz et al., 2009). Therefore, for the prevention or management of childhood

obesity physical activity is encouraged and walking is a recommended form of physical activity for obese children (Shultz et al., 2011).

Figure 2.5 presents the potential causal pathways between childhood obesity and altered lower limb and foot biomechanics during gait. Beginning with childhood obesity at the bottom of Figure 2.5 the relationship with physical activity is reciprocal; i.e. obese children perform less physical activity than non-obese children and this may lead to an energy imbalance due to less energy expenditure than energy intake and a build up of fat mass. Being less physically active may result in lower relative muscle strength due to improper development of the musculoskeletal system. This is also true for the skeletal system where lower limb and foot structural development is dependent on mechanical loading. Both lower relative muscle strength and altered structure of the feet and lower limbs in obese children can lead to abnormal gait characteristics. These factors, in turn, can lead to pain and discomfort which results in even lower physical activity and/or joint malalignment from repetitive joint loading. If untreated the effects of childhood obesity could lead to musculoskeletal co-morbidities such as slipped capital femoral epiphysis, Blount's disease and pes planus. The long term affects of childhood obesity could result in osteoarthritis in adulthood from abnormal joint alignment and lower muscle strength (Chan & Chen 2009). This literature review demonstrates the potential causal relationships between childhood obesity, physical activity, muscle strength, lower limb and foot alignment and gait characteristics. However, there is a dearth of information on these relationships indicting the need for future research to explore the causal pathways. The aim of this thesis is to explore the relationships between two factors in Figure 2.5; childhood obesity with lower limb and foot biomechanics during gait. The findings of which will provide a basis for future work to explore the multifaceted pathways between childhood obesity and musculoskeletal co-morbidities.

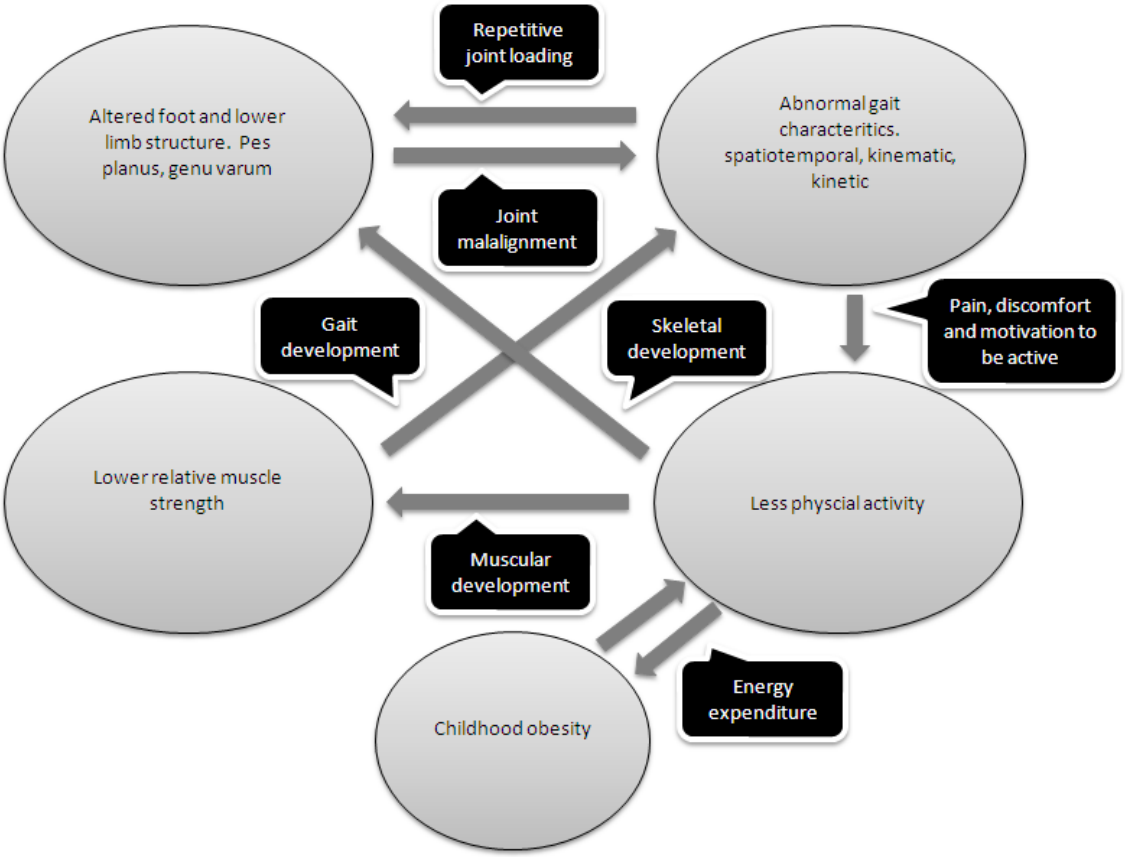

Figure 2.5. Potential causal pathways between childhood obesity and altered lower limb and foot biomechanics during gait

2.9 Chapter Summary

The findings of this literature review demonstrate two needs for the investigation of foot and lower limb biomechanics during gait in obese children. Firstly, there is a risk of obese children to develop musculoskeletal co-morbidities such as slipped capital femoral epiphysis, Blount's disease and flat feet. These co-morbidities are linked to altered alignment and greater forces acting on the lower limb joints caused by carriage of excessive load during gait. Secondly, walking is a form of physical activity recommended for obese children to increase energy expenditure and future incidence of obesity. Reports have demonstrated that obese children walk less and are less motivated to do participate in physical activity. Thus, there is a need to understand the effects of childhood obesity on gait in order to prevent incidence of musculoskeletal co-morbidities and increase physical activity. The methods of measuring lower limb and foot biomechanics are addressed in the second literature review chapter 2 (chapter 3).

In order to understand the effects of obesity on foot and lower limb biomechanics during gait there is a need to determine a measure of obesity. The findings of this literature review demonstrate that body mass index (BMI) Z-Score has been previously used to define obese and non-obese children. The measure is quick, cheap and with little participant burden, but the ability of BMI to act as a proxy for body fat is inconsistent. Measures of body fat in children involve more invasive methods compared to BMI but demonstrate greater accuracy to define obesity. There is no conclusive evidence as to the best measure of childhood obesity, therefore there is a need to compare methods to define obesity.

3. Literature Review Chapter 2: 3D Assessment of Lower Limb and Foot Motion During gait

3.1 Introduction

Human motion and, in particular, gait has been analysed using a variety of techniques from instrumented walkways, accelerometers to three-dimensional (3D) motion analysis systems. Three-dimensional gait analysis utilises the capture of body segment motion and forces to describe musculoskeletal mechanics and locomotor patterns during the gait cycle. Information on joint kinematics and kinetics can be quantified and compared to distinguish motor task performance (Cappozzo et al., 2005). This section will focus on methods of three-dimensional gait analysis; how locomotor patterns are quantified and the validity, variability and reliability of these systems. The aims of this chapter are; (1) to demonstrate the need to understand between-session reliability and the affect of obesity of lower limb biomechanics, and (2) review currently used foot models to determine the most appropriate to determine relationship between adiposity and foot biomechanics based on reliability and segmentisation.

3.1.1 Stereophotogrammetry

Stereophotogrammetry (SPG) is the use of multiple cameras to record the position of markers, usually placed on the skin surface, which represent bone landmarks. From these markers the position and orientation of the segments, comprised of one or more bones, can be estimated. When recorded over many time frames the motion of two segments adjacent to each other can be calculated thus determining the kinematics of a joint. When combined with external force, measuring devices such as ground reaction forces from floor mounted force plates, joint kinetic information can be recorded (Cappozzo et al., 2005).

Optoelectronic SPG captures the 3D position of markers within the laboratory capture volume using the geometrical properties of central projection from multi-camera observation (Braune & Fischer, 1987). At least two cameras must record the marker for its centroid position to be located and digitised from image matching the marker shape (Chiari et al., 2005). Calibration of the SPG cameras is essential and determines the geometric and optical characteristics of the cameras (internal parameters) and the position and orientation of the camera within the laboratory (external parameters) (Chiari et al., 2005). Each camera provides a two dimensional (2D) image from known 3D coordinates of markers placed in the calibration volume. The residuals of the difference between the captured position and the actual position are recorded

as a measure of systematic accuracy. Typical accuracy of 3D coordinates is ±0.1mm for all three planes (Richards, 2008).

The converted coordinate data from SPG capture is raw data; it contains additive noise from sources including the optoelectronic devices themselves which produce electrical noise. It is therefore important to use smoothing and filtering techniques on the raw data (Winter, 2005). Human movement data is usually low frequency with impulsive events associated with impacts (Chiari et al., 2005). Many smoothing algorithms or filters have been applied to marker trajectories and can affect kinematic data; the most common are digital filters and spline techniques. The commonly used plug-in gait (PiG) body model, in Vicon software, uses a quintic spline filter based on code written by Woltring (1986). High frequency noise, associated digitising and skin movement errors, is filtered out by low pass filters.

3.1.2 Three-Dimensional Movement Analysis

Three dimensional (3D) movement analysis requires the reconstruction of the instantaneous position and orientation of a system of axes which rigidly relate to the bones of a body segment within the global coordinate system (GCS). The GCS is the SPG frame which sets the axis in which marker position coordinates are defined (Cappozzo et al., 2005). The usual GCS convention is with the X axis anterior/posterior, Y axis vertical and the Z axis medial/lateral (Winter, 2004). The GCS is aligned by the calibrated matrix of the force plates axes (defining the origin) and positive/negative orientations aligned with the direction of walking.

Skin mounted markers, placed on bony landmarks, represent limb segments and are captured using SPG. These markers provide an axis system defined by a technical local coordinate system (LCS) for each segment. The origin and orientation of this LCS can be specified in the GCS. A second LCS (anatomical) is created in the Cartesian reference system based on the morphology of the segment with points representing the segments centre of mass (COM), joint centre and point of external force application (Winter, 2004). The anatomical LCS provides vector quantities based on the orthogonal set of axes involved for numerical representation of the segment to quantify segment orientation (Cappozzo et al., 2005). A total of two transformations are required to get from the GCS to the technical LCS (marker based axes) and from the technical LCS to the anatomical LCS (morphology based axes).

The first of the two transformations, required to get from the GCS to the technical axes, involves a rotation matrix that is time-varying because the markers continually change relative

to the GCS. To define the technical, marker based, LCS at least three markers must be placed (non-collinearly) on the segment. Markers are placed on bony landmarks which are chosen to provide bone geometry and orientation of the anatomical axis system (Cappozzo et al., 1995). Superficial anatomical landmarks, usually bony prominences, are used and identified by palpation. Internal anatomical landmarks are estimated from the position of superficial anatomical landmarks and predictive biomechanical models (Cappozzo et al., 2005). The anatomical calibration procedure finds the relation between the technical marker axes and the anatomical LCS. For this procedure the subject is required to adopt a well defined position, usually the anatomical position. Anthropometric measures can be recorded to aid the calculation of joint centres by offsets from the external markers. Extra calibration markers can be temporarily attached during the calibration procedure to define the segments anatomical axes and are removed during the motor tasks. The position of these extra markers, termed technical or virtual markers, can be tracked from the remaining markers attached to the limb during the dynamic tasks. The second transformation is required to get from the technical markers to the anatomical axis system. This rotation matrix is assumed to be constant and results from the calibration protocol. The combination of the two rotation matrices gives the final orientation of the anatomical axes directly from the tracking marker's coordinates in the GCS (Winter, 2004).

A comparison of the representative anatomical axes system from two adjacent bony segments allows the estimation of three angular and three linear qualities which effectively describe joint attitude (Grood & Suntay, 1983; Woltring, 1994). Errors between the technical LCS, based on marker position, and actual anatomical LCS affect joint angles and reliability of kinematic outputs. A primary intrinsic issue with marker placement on anatomical landmarks is the fact that bony landmarks tend to be convex or concave areas rather than discrete points (Della Croce et al., 1999). The anatomical LCS is not arbitrary, as the technical LCS is, but is constructed to approximate the sagittal, frontal and transverse anatomical planes of the limbs and therefore, reliably determine segment motion (Coppozzo et al., 2005).

3.1.3 Joint Coordinate Systems

The limb segments are considered non-deformable to adhere to classical mechanics, with each modelled joint having between no or six degrees of motion based on the actual anatomy of the joint (Cappozzo et al., 2005). Angular motion of each joint is calculated in a rotation sequence

which aligns the joint with the final orientation of the actual movement called the Carden/Euler sequences. The commonly used Carden sequence of x-y-z results in the first rotation occurring around the x axis, the second around the y-axis and finally the z-axis (Winter 2004). Euler angles are another commonly used system to describe the angular orientation of a segment in space (Winter, 2004). Euler sequences (z-y-z, z-x-z, y-x-y, etc) have been applied to shoulder movements to aid relatively high ROM in multiple planes (Wu et al., 2005). The joint coordinate system (JCS) described by Grood & Suntay (1983) gives anatomical meaning to the Carden/Euler sequence (Richards 2008).

The conventional lower limb model (PiG) uses the Euler sequence Y-X-Z to define motion of the hip, knee and ankle relating to the medial/lateral, anterior/posterior and vertical axis respectively. This gives the order of rotation of flexion/extension, abduction/adduction and rotation in line with the International Society of Biomechanics (ISB) recommendations for the description of lower limb kinematics, including the use of the JCS (Wu et al., 2002). In the ISB JCS recommendations (Wu et al., 2002) the Cartesian coordinate system is established for two adjacent segments. The common origin of both segments is the point of reference; about which, two body fixed and one orthogonal axis are derived. However, the alignment of the coordinate systems in each segment may not be correctly aligned with the cardinal planes and therefore, cross-talk between the different planes of motion can occur (Richards, 2008).

3.2 Biomechanical Models

In landmark specific marker placement the final kinematic output is reliant on the accuracy of markers to represent their corresponding bony landmarks. The most commonly used example is the Newington Hospital Helen Hayes model (Kadaba et al., 1990; Davis et al., 1991,). This model and associated marker set is referred to by different names; Vicon Clinical Manager (VCM), PiG (Plug-in Gait) and the modified Helen Hays marker-set. There are significant issues relating to the assumptions of this model; firstly, repeatability of marker placement, secondly the underlying geometry of the model is generalised and not subject specific, and finally motion of soft tissue relative to the bone causes errors in the kinematic calculations. This section will highlight these issues with reference to the lower limbs and foot biomechanical models.

3.2.1 Marker Placement

Della Croce et al., (1999) examined the repeatability of marker placement on anatomical landmarks commonly used in lower limb three-dimensional gait analysis. Six observers (raters) and 2 subjects participated in the study. Precision of all lower limb anatomical landmark identification, indicated by RMS, was 6-21mm and 13-25mm for within- and between-rater respectively. Pelvis landmark dispersion was greater than the lower limbs and repeatability of foot landmarks was reasonable with the exception of the calcaneal marker position. Joint angle precision in standing posture was then reported based on marker positing; hip RMS error values were 4^{o}, 2.5^{o} and 6^{o}; knee angles were and 1^{o}, 2^{o}, and 6^{o} for flexion/extension, abduction/adduction and internal/external rotation respectively. The ankle RMS values were 1.5^{o}, 3.5^{o} and 3.9^{o} for flexion/extension, abduction/adduction and internal/external rotation respectively. These finding highlight the imprecision of anatomical landmark identification that could limit accurate 3D motion analysis and the need for detailed protocols.

Henley et al., (2008) determined between-session and between-clinician reliability associated with placing markers on specific landmarks on the foot and ankle of 14 adult feet and 8 paediatric feet. Three clinician across three gait laboratories applied markers to anatomical landmarks of the foot and ankle in two sessions. To ensure the subjects' feet were positioned in the same orientation in the capture volume a plaster of Paris mould was formed around the sole of each foot. Intraclass correlation coefficients (ICCs) for the reliability of the subjects to stand in the same position in the moulds without reapplication of markers ranged from 0.826 for the vertical position of the fifth metatarsal head to 0.997 for the horizontal position of the cuboid. Between-application ICCs ranged from 0.487 for the vertical position of the fifth metatarsal head to 0.958 for the horizontal position of the first metatarsal head. ICCs for between-clinician comparison ranged from -0.098 for the vertical position of the cuboid to 0.497 for the mediolateral position of the hallux. The mean measured differences in marker position ranged from 1.33mm for repositioning the feet, 2.39mm for between-application and 5.10mm for between-clinician. The effects of differences in marker placement on standing joint angles was greatest at the hindfoot, measured to laboratory coordinates, with between-application errors of 0.45^{o}, 8.03^{o} and 4.72^{o} for sagittal, frontal and transverse planes respectively. Between-application errors in the first ray relative to the hindfoot were 2.33^{o} and 5.77^{o} for sagittal and transverse planes. Between-application errors in fifth ray relative to the hindfoot were 3.04^{o} and 5.19^{o} for sagittal and transverse planes respectively. Finally, between-application errors at the hallux relative to the forefoot were 3.95^{o} and 4.02^{o} for

sagittal and transverse planes respectively. The authors summarise that errors in the motion capture system are small, with <1mm of marker position errors for markers placed ≥10mm apart. Subjects were able to stand in the same position, but between-application variability was high indicating limitation in reliably palpating and marking anatomical landmarks of the foot.

3.2.2 Segment and Joint Centre Estimations

Each limb segment of the human body is estimated from an anthropometric model from measurements of cadavers (Dempster, 1959; Braune & Fisher, 1987; Seidel et al., 1995). The geometry of the bones and joint axes are estimated from marker positions forming the LCS in the GCS based on vector algebra and standardised algorithms (Charlton et al., 2004). The hip joint centre position is predicted from an approach requiring regression equations and anthropometric measurements (Della Croce et al., 2005). The most commonly used prediction approaches are those provided by Bell et al., (1990) and Davis et al., (1991). However, these are based on a very specific and limited population of subjects with little published data on the validity of use in children (Baker, 2006). Studies that have examined the error in estimating hip joint centre have reported mean errors of approximately 21-23mm (Leardini et al., 1999). Jenkins et al., (2000) examined the accuracy of hip joint centre location with magnetic resonance imaging (MRI) analysis; finding mean discrepancies of 22mm in children and 17mm in adults. These studies suggested the need for specific regression parameters according to age, gender, anthropometric and pathology.

Baker et al., (1999) proposed an approach to determine the hip rotation profile based on a correction factor from knee varus-valgus artefacts. Malalignment of the thigh segment from thigh marker misplacement causes the knee joint centre to displace which results in cross-talk between knee sagittal and frontal motion occurs. The thigh-marker rotation offset technique was tested on 40 children with cerebral palsy with various levels of walking ability. The results of subjective assessments suggested that the correct factor improved lower limb kinetics in 60% of cases. The authors proposed this technique as an alternative approach to Cappozzo et al., (1995) use of functional techniques to define the lower limb joint centres. Malt et al., (2012) justifies the use of thigh marker rotation off-sets from monitoring of knee valgus-varus motion at the knee. The authors examined between- and within-rater reliability in one adult subject. The results showed that correction of the thigh marker offsets decreased mean and

SD of knee valgus-varus, variability in hip rotation and reduced knee hyperextension in the stance phase.

The knee joint is modelled as a ball-and-socket joint for ease of marker-sets though the substantial movement of the skin over the distal femur during knee flexion may move the knee joint centre several centimetres. The effect of anatomical axis misplacement on joint kinematics has been shown to cause offsets but not affect the waveform patterns through the gait cycle (Kadaba et al., 1990). Piazza & Cavanagh (2000) estimated knee kinematics by controlling the degrees of freedom using custom devices. They found that cross-talk between the angular components was sensitive to incorrect rotation axes and recommended limited use of out-of-sagittal angular data.

The ankle joint centre like the knee joint centre is derived from the position of the proximal joint centre using a chord function (Vicon manual, 2010). The chord is the circumference of a circle on which the proximal joint centre, the lateral segment marker and the distal joint centre lie on. To estimate the knee joint centre, the estimated hip joint centre (from pelvis), the lateral thigh marker and the knee joint marker (with an offset for knee joint width) are used. However, the ankle joint centre is dependent on the placement of seven markers (pelvis, thigh and shank), thus errors in the proximal joints are transferred to the distal joints. This is especially true in subjects where bony landmarks are difficult to identify around the pelvis, e.g. obese or overweight subjects (Prabhakaran Nair, 2010).

3.2.3 Soft Tissue Artefacts

Errors in marker position relative to the underlying bone are referred to as relative and absolute errors (Richard, 2008). Relative errors describe the movement of two markers relative to each other on a rigid segment. Absolute errors are defined as the movement of markers with respect to the bony landmark it represents. Together these errors are referred to as soft-tissue artefacts (STA) (Leardini et al., 2005). Despite numerous solutions to dealing with STA the reliable estimations of skeletal motions has not been achieved satisfactorily.

Peters et al., (2010) systematically reviewed the literature on soft tissue artefacts (STA) in lower limb motion. The review found that greatest STA from landmark tracking at the thigh (>20mm) compared to the shank (>10mm). Reinschmidt et al., (1997) examined STA by comparing differences in knee and ankle motion during walking from skin mounted markers and intra-cortical pins inserted into the femur, tibia and calcaneus of six volunteers. Root

mean squared (RMS) differences at the knee ranged from 1.5-3.2^{o}, 2.1-2.8^{o} and 2.1-5.3^{o} for sagittal, frontal and transverse plane motion respectively. At the ankle RMS differences were 2.5-4.4^{o}, 2.0-4.3^{o} and 2.9-4.4^{o} for sagittal, frontal and transverse plane motion respectively.

The calibrated anatomical system technique (CAST) was proposed for a more rational determinant of anatomical local reference frames (Cappozzo et al., 1995). This technique involves a single static calibration of a number of anatomical landmarks for their identification in the relevant technical LCS. An 'instrumented pointer device' mounted with markers in known locations or temporary skin mounted markers can be used to identify these anatomical landmarks accurately (Leardini et al., 2005). Some anatomical landmarks may not represent good attachment for markers due to many reasons including; marker occlusion from cameras and skin motion artefact. Therefore, some markers may be positioned on the skin giving priority to experimental requirements making the anatomical LCS arbitrary (Cappozzo et al., 1995). The CAST method provides a means for determining the orientation and position of anatomical landmarks in a technical LCS which can be used to determine the anatomical LCS during motion trials. Thus the CAST technique is a method to reduce STA because markers may be placed on the segment where STA is expected to be less significant (Stagni et al., 2005).

3.3 The Effect of Obesity on Biomechanical Modelling of the Lower Limbs.

An important factor to consider when examining the relationship between obesity and lower limb kinematics and kinetics is whether biomechanical models can accurately represent osseous structures in individuals with excessive fat mass. Relatively few studies have examined the effects of obesity on the kinematics and kinetics of lower limb biomechanical modelling. Rash et al., (1999) examined the effects of simulating anterior superior iliac crest (ASIS) marker placement in obese subjects. A single gait trial from three non-obese adults was captured to which the ASIS markers where anteriorly or laterally displaced, simulating abdominal fat mass. The hip joint centre was calculated based on the Davis et al., (1991) method described in the conventional (PiG) lower limb model. Lateral movement of the ASIS markers demonstrated the least amount of change (<3^{o}) in kinematic and kinetic outputs. However, when the ASIS markers were moved anteriorly pelvic tilt reduced by 2-5^{o}, hip flexion by 10-15^{o}, knee flexion by 5-10^{o}, and hip and knee rotation by 10-20^{o}. Hip flexion/extension moments and powers altered by 50-75Nm and 100-150Watts respectively.

Board et al., (2012) tested five lower limb kinematic models on eleven obese adults using skin mounted markers, marker clusters and digitised (virtual) landmarks. The conventional (PiG) lower limb model marker set was applied with 4 alterations; one used virtual ASIS markers based on DEXA derived offsets, another used virtual markers on the ASIS and skin mounted markers on the iliac crests and another two custom built models. Peak knee and hip flexion and extension angles during stance were significantly different between models (by 11% and 14% respectively). Peak hip flexor, knee extensor and knee flexor moments were significantly different between the models. Peak hip and knee powers were also significantly different between all five lower limb models. However, peak ankle plantar-flexor angles, moments and powers were similar between models. The authors conclude that the model used to describe obese data has a substantial effect on kinematic data and future studies should clearly describe marker placement protocols on obese subjects.

Together these two studies highlight the fact that obesity can have an effect on the palpation and tracking of ASIS landmarks due to soft tissue artefact (STA) from greater adiposity. These errors from STA can affect kinematic and kinetic outputs from the lower limb conventional (PiG) model. Protocols employed to identify and track ASIS markers irrespective of greater adipose tissue may help the interpretation of gait parameters between obese and non-obese participants. However, there is a need to examine the effects of obesity on palpation and tracking of the ASIS in children and develop protocols to reduce STA.

3.4 Between-Session Reliability of Lower Limb Models Kinematic and Kinetics Measures

The purpose of the reconstruction of a limb segment in 3D space is the collection of quantitative data from segmental kinematics over the time period of the motor task (Cappozzo et al., 2005). With regard to lower limb biomechanical models, which are used to represent the underlying bony anatomy of the limb, many have been implemented in 3D gait analysis. The reliability of lower limb models with specific interest in the reliability of the conventional lower limb model (PiG) in adults and children is detailed in the section. If a model is unreliable or demonstrates high error conclusions regarding the relationships between gait biomechanics and obesity cannot be made.

3.4.1 Concepts of Reliability and Statistics Analysis

In order to determine the between-session reliability of the conventional (PiG) lower limb model an understanding of the concept of reliability and statistical measures is required. Reliability is the extent to which measurements are consistent and free from error (Portney & Watkins 2000). A reliable lower limb biomechanical model will produce consistent kinematic and kinetic outputs between multiple sessions under the same conditions. However, measures are rarely perfectly reliable; humans demonstrate gait variability, the 3D motion capture is susceptible from reconstruction errors and inconsistent marker placement is common in motion capture. Therefore, an estimate of between-session reliability is required to quantify the extent to which lower limb biomechanics varies. Repeatability refers to the variation in repeated measurements made on the same subject under the same conditions. A test retest assessment can establish the variability from repeated measurement to ascribe the errors to the measurement protocol.

Coefficient of Variation (CV) is calculated as the standard deviation of the data divided by the mean and multiplying by 100. However, the problem with expressing error as a percentage is that smaller scores will differ markedly compared to larger scores (Bruton et al., 2000). Chinn et al., (1991) suggests that the intraclass correlation coefficient (ICC) is preferable to CV because error variation is related to the size of the score in CVs.

Intraclass correlation coefficient (ICC) can measure the level of agreement among different measuring instruments when used on the same set of objects or people. In the case of the conventional (PiG) lower limb model it is the extent to which kinematic and kinetic outputs agree when performing the same test twice. The total variance of the output σ^2_{total} is made up of two components: the variance of the true output, which can be termed σ^2_{output} and the error variance $\sigma^2_{within\ output}$, which depends partly upon differences between the sessions. In simple terms, a larger first component of total variance in relation to the second, the closer the agreement between the sessions.

Reliability can be assessed using one of the six ICC models described by Shrout and Fleiss, (1979) (ICC 1,1; ICC 1,*k*; ICC 2,1; ICC 2,*k*; ICC 3,1; ICC 3,*k*). The first four ICC models describe reliability of multiple raters and can be generalised beyond the limits of the research situation. The last two ICC models can evaluate between-session reliability with one rater of lower limb biomechanical outputs but, only within the specific research setting. The within-rater ICC equations 3, 1 and 3,*k* are differentiated by the number of measurements, 1 refers to a single

measurement and *k* several measurements (re-tests). The equation for ICC 3,*k* can be calculated from a two-way ANOVA:

$$ICC\,(3,k) = \frac{BMS - EMS}{BMS} \quad (1)$$

BMS is the between subject variance and EMS is the error or residual mean square variance. Intraclass correlation coefficient can only give the reliability of a single output, usually the output will be a kinematic or kinetic peak value or value at a specific gait event. Therefore, it is not known whether kinematics or kinetics are reliable over the whole gait cycle.

The output of ICCs is a coefficient that ranges from 0 (no reliability) to 1 (perfectly reliable), but this does not give an idea of the expected error of repeated measurements. The Standard Error of Measurement (SEM) can be calculated to quantify the standard deviation (SD) of measurement errors in the same units as the measurement is given. The SD of repeated measures in expressed relative to its ICC score, thus giving a measure of absolute between-session reliability (Bruton et al., 2000).

Bland & Altman (1986) described a series of statistical methods for assessing agreement between two methods of clinical measurement. Their approach was based on analysis of differences between measurements and they suggest that estimation of the agreement between measures is more appropriate than a reliability coefficient or hypothesis (significance) testing. The differences between two measures are plotted against the average of the two measurements, the mean. From this graph, the size of each difference, the range of differences, their distribution about zero (perfect agreement) and measurement bias can be seen clearly. The mean difference (*d*) and the standard deviation (SD_{diff}) are calculated. The closer *d* is to zero and the smaller the value of SD_{diff} the better the agreement between measures. It is also of interest to estimate the true value of *d* which is a measure of the bias between measures and a 95% confidence interval (95%CI). If zero does not lie within the interval it can be concluded that a bias exists between the two measures. The main disadvantage of Bland & Altman plots is that a sample set of 50 is required otherwise the 95%CI will be very wide making interpretation of the result difficult (Rankin & Stokes, 1998).

Kadaba et al., (1989) described the similarity or variability of waveforms using Coefficient of Multiple Correlation (CMC) to determine the reliability of repeated measurement from kinematic and kinetic outputs. The advantage of CMC is that the whole waveform is assessed

and a single coefficient score is produced. The CMC is calculated as a ratio of the variance about the mean at a particular time point to the total variability about the grand mean for the session. However, CMC are susceptible to small range of motion (ROM) of the waveform which results in lower CMC values. Also waveforms with higher ROM will appear more similar, i.e. higher CMC values. This strong dependency of CMC on ROM implies that comparisons across joint, planes, biomechanical models and participants would not be meaningful (Røislien et al., 2012).

McGinley et al., (2009) performed a systematic review on the reliability of 3D gait analysis measurements. Their paper highlighted evidence for between-session and between-assessor reliability by examining sample selection procedures, procedures, statistical analysis and reliability. The key points of the review found that; most 3D gait analysis studies chose convenience sampling which may be susceptible to bias such as selective sampling of more cooperative subjects; the authors warned against generalising the error associated with repeated measures of healthy adults to children as adult data is generally less variable than children's; measures of gait data variability are population-specific, therefore, between-session reliability testing should be conducted on the population of interest; studies should provide spatiotemporal data concurrent to kinematic data as an indicator of between-session gait stability, and variations due to walking speed effects; and, adequate model description for the comparison of reliability of alternative models is also recommended.

In terms of statistical analysis, McGinley et al., (2009) stated that correlation indices (CMC, ICC), alone do not give enough information on reliability. Studies that have used CMC have shown an influence of ROM on the value, with large ROM resulting in high CMCs and vice versa. The authors recommend expressing gait variability in a measurement that in quantified in the same units (e.g. ^{o}). Furthermore, reporting of reliability should include absolute measurement error such as SD or SEM and consideration for the minimum levels of detectable change (MDC). Other points to consider when examining between-session reliability of 3D gait analysis included justification of session intervals, amount of sessions, amount of trials within a session, blinding assessors. The review concludes that whether 3D gait analysis data is reliable can only be answered in the context of the proposed use. Although, most errors are considered acceptable they are not small enough to be ignored during clinical interpretation. The authors summarise that in most clinical situations, error of 2^{o} or less is considered acceptable, errors between 2^{o} and 5^{o} reasonable and errors $>5^{o}$ should raise concern of misleading clinical interpretation.

3.4.2 Reliability of the Conventional Lower Limb Model (PiG)

Davis et al., (1991) was one of the first studies to describe a protocol for assessment lower limb kinematics using a model known as the conventional lower limb model (PiG). The testing protocol involved anthropometric measures of knee and ankle width, between-ASIS distance and the vertical distance in the sagittal plane between the ASIS and greater tronchanter. Markers were placed on specific bony landmarks or on wands defining the frontal plane of the lower limb. The hip joint centre calculation was based on an algorithm from radiographic examination of 25 hips and was a function of leg length. The knee and ankle joint centres were calculated based on the coronal plane joint width measurements. The limb rotation algorithm was based on the determination of Euler angles with a y-x-z axis. The transformation matrix which defined the orientation of a particular set of coordinate axes was developed and employed to yield the joint angles corresponding to flex/ext, add/abd and int/ext rotation respectively. Trunk and pelvis angles are absolute angles referenced to the inertially fixed laboratory coordinate system. The hip, knee and ankle angles were all relative angles. Foot rotation angle was an absolute angle referenced to the laboratory, which indicates the subject's foot with respect to the direction of progression (Davis et al., 1991). This model was developed using the minimum number of markers possible to determine 3D kinematic and kinetics of the lower limb (Ounpuu et al., 1991) because, at the time, the camera systems were only capable of detecting a small number of markers (Baker, 2006).

Kadaba et al., (1989) tested the reliability of the conventional lower limb model (PiG) in 40 healthy adult subjects. Markers were attached to specific lower limb anatomical landmarks to create the segments described by Davis et al., (1991). In addition two floor plates recorded ground reaction forces and foot switches indicated gait cycle timings during preferred individual gait speed locomotion. Data was captured on three sessions on three different test days. The authors used coefficient of multiple correlation (CMC) statistical analysis to describe the similarities or variability of waveforms. Within-day CMC values ranged from 0.643 ± 0.180 for pelvic tilt to 0.996 ± 0.003 for hip flexion/extension. Between-day CMC values ranged from 0.240 ± 0.180 for pelvis tilt to 0.985 ± 0.009 for knee flexion/extension. The authors noted that within-day reliability was not influenced by marker reapplication errors; low CMC values within-day for pelvic tilt was due to the low range of motion (ROM). Furthermore, between-day reliability was affected by inherent physiological and systematic variability and marker placement errors, significantly affecting pelvic tilt and knee varus/valgus motion. The lower limb joints demonstrated an axis specific rank of variability with sagittal the most reliable,

followed by frontal and transverse. Ground reaction forces demonstrated small variability with most attributed to physiological factors. The reliability of joint moments were similarly ranked between the axis of rotation as the angular motion with the highest order of reliability at sagittal, then frontal and transverse. The ankle demonstrated greater reliability of moment patterns due to less variability in the estimation of the instantaneous position of the joint centre compared to hip and knee. The authors concluded that variability of joint angle motion in the sagittal plane was small compared to the frontal and transverse plane. Between-day reliability of joint motion in these two planes was dramatically affected by errors in the application of lateral wand markers that define rotation along the longitudinal axis. Variability in the patterns of force and moments were minimal.

Ramakrishnan & Kadaba (1991) examined the effects of uncertainties in the definition and construction of embedded segment axes, from local coordinate system (LCS), using representative data from a healthy subject and a subject with cerebral palsy. Using the conventional lower limb model (PiG), embedded reference axes for the pelvis, thigh, shank and foot segments were created. By perturbing the embedded axis system the flexion/extension axis of the hip and knee were displaced in the transverse plane from 15^{o} internal to 15^{o} external. Knee and hip joint motion in the healthy subject showed relatively unaffected flexion/extension angles, while abduction/adduction and rotation angles were significantly affected. Knee abduction/adduction error in the stance phase were small (2-3^{o}) due to relatively small flexion/extension angles (5-12^{o}) but during the early to mid swing phase (60-80% of the gait cycle) errors in abduction/adduction angle increase (8-12^{o}) with greater knee flexion (40-60^{o}). Knee rotation errors were minimal during the stance phase and had a constant offset approximately equal to the error in the imposed flexion/extension axis. Hip abduction/adduction angle errors were relatively larger in the stance phase (5-7^{o}) when hip flexion angle is large (30-35^{o}). Hip rotation angles are also affected by hip flexion but to a smaller degree (1-2^{o}). The authors conclude that the measurement of 3D joint angle motion can be subject to uncertainties in the definition of the embedded axes in the body segments. This highlights the need for accurate marker placement to define the lower limb segments in the transverse plane.

Gorton et al., (2009) assessed the kinematic reliability of 12 motion analysis laboratories using the conventional lower limb model (PiG) on one adult subject walking at a self-selected speed. The range of mean values for each of kinematic variables varied between 5.6^{o} for pelvic obliquity to 28.3^{o} for hip rotation. A follow-up assessment was undertaken after

implementation of a standardised gait analysis protocol. This lead to a 20% decrease in variability although some kinematic measures still demonstrated low reliability; range of mean values for hip rotation 33.8^{o}, hip flexion 17.1^{o} and pelvic tilt 13.9^{o}. Using an instrumented rod, the study also examined systematic accuracy of simulated motion of the lower limb. The average standard deviation across 12 sties was 0.5^{o} and the maximum difference between measurements ranged from 1.4^{o} to 1.9^{o}. Within-session reliability, consisting of changes in a subject's walking patterns, was not a major contributor to overall variance. Between-session reliability included walking pattern differences and marker placement errors. The authors reported that the marker placement errors contributed more to the degree of variance.

Schwartz et al., (2004) estimated errors associated with quantitative gait data by proposing a method for incorporating these errors into the interpretation process. Using the conventional lower limb model (PiG) on two healthy adult subjects a total of 120 trials were recorded; 5 trials from 3 sessions, from 4 observers. Within-subject, within-rater and between-rater errors at each time point for the gait cycle were computed. The reliability of a joint angle was measured by the between-observer error and a ratio of between-trial error to between-observer error. Between-trial error serves as a baseline for comparisons because it is free of methodological error (marker placement errors). The authors determined the error in all lower limb kinematic outputs and gave reasons for the quantified errors. Of the 11 joint angles, pelvis obliquity and pelvis rotation were the most reliable, pelvic tilt contained significantly larger errors. Position of the anterior superior iliac spine (ASIS) markers effects pelvic obliquity more than pelvic rotation and posterior superior iliac spine (PSIS) position causes errors in pelvic tilt. At the hip largest errors were in the transverse plane due to problems aligning the long axis of the thigh. Hip flexion/extension was more reliable but hip abduction/adduction demonstrated high methodological errors possibly due to the regression equations used to calculate hip joint centres. Errors in the knee are caused by the hierarchical biomechanical model (errors in proximal segments are propagated to distal segments), joint centre locations and long axis alignment. The largest between-observer errors were for knee varus/valgus, meaning experimental errors due to axis definition and cross-talk reduce reliability in this plane. Knee flexion/extension and rotation errors are similar to hip errors. Foot progression errors were both high for between-observer and the ratio to between-trial indicating discrepancies in marker placement and methods to achieve this placement. Dorsi/plantarflexion error was small throughout most of the gait cycle and most likely due to inherent variability. The authors state that these results are only valid for the laboratory used but the general magnitudes are likely to be consistent across laboratories. The proposed

assessment of between-trial and between-observer approach gives understanding of intrinsic (inherent) and extrinsic (experimental) factors that cause gait data variability. An unbiased method was proposed for identifying significant deviations during routine gait analysis from which clinical significance may then be subjectively judged. However, the authors also note that deviations in joint angles may be a result of a temporal shift from altered spatiotemporal variables (i.e. walking speed) which is not accounted for in this analysis.

These studies have described the conventional lower limb model (PiG) from the development of the protocol Davis (1991), the within- and between-session reliability testing on adult subjects (Kadaba et al., 1989) as well an assessment of errors in embedded axis, between-rater reliability (Schwartz et al., 2004) and between-laboratory reliability (Gorton et al., 2009). The results of these studies highlight the fact that the model is prone to larger errors in out-of-sagittal plane kinematics at the hip and knee joints. A particular issue for reliability is placement of the thigh marker to determine the transverse rotation of the hip and knee and warrants further investigation (Ramakrishnan & Kadaba., 1991, Schwartz et al., 2004). The conventional (PiG) model has been compared to more recent models to examine reliability of gait data in healthy adult populations, these studies are summarised below.

3.4.3 Reliability of Other Lower Limb Models

Charlton et al., (2004) compared the reliability of the conventional lower limb model (PiG) with an optimised lower-limb gait analysis model (OLGA). The optimised algorithms of OLGA model were designed to correct for marker motion, improve smoothing for STA and knee cross-talk minimisation. A single healthy adult completed 25 walking trials with the Helen Hayes marker set attached by three observers (raters) on one occasion and by one observer (rater) on another occasion (total trials = 100). The SD of local marker coordinates, equating to erroneous marker motion relative to the underlying anatomy, was 0.6 to 27.8mm for the conventional lower limb model (PiG) compared to OLGA with greatest SD at the heel and toe markers. This indicates that the ankle joint centres are least well located. Cross talk at the knee joint between knee flexion and varus/valgus angles resulted in significantly altered varus/valgus and rotation profiles. At the hip, significant differences between the rotation angles were seen due to misalignment of the knee axis (Baker et al., 1999). Significant differences were reported in inversion/eversion and rotation profiles at the ankle joint due to poorly aligned knee axes and cross-talk. Compared to OLGA, between-session kinematic RMS

errors of the conventional lower limb model (PiG) joint rotations were <8^{o} for rotation angles, <4^{o} flex/ext angles and <2^{o} abd/add angles. Between-session kinetic RMS errors of the conventional lower limb model (PiG) were <400Nm/kg flex/ext, <150Nm/kg abd/add and <50Nm/kg abd/add. This paper highlighted the reliability associated with lower body kinematics caused by specific landmark errors which results in joint centre location inaccuracies.

Benedetti et al., (2012) explored between-laboratory consistency of three lower limb biomechanical models; the conventional lower limb model (PiG) protocols; Total3DGait (anatomically based protocol, see Leardini et al., 2007b); and, the CAST protocol, across seven gait laboratories. A single healthy adult subject was examined within each laboratory by one observer (rater) providing 6 gait trials of anthropometrics, spatiotemporal kinematics and kinetics. Anthropometric measurement differences were as large as 2-3cm for the pelvis. Coefficient of variation (CV) of spatiotemporal parameters was generally lower than 6%. Similarity of kinematic curves between the laboratories was measured by coefficient of determination (r^2). Sagittal and frontal plane r^2 values were greater than 0.90 and transverse plane greater than 0.60 (excluding the knee), the worse performance was the transverse plane hip (r^2 0.30). Joint moments demonstrated excellent similarity at the ankle (r^2 0.90), good at the knee (r^2 0.70) and hip (r^2 0.66). The paper concluded that large consistencies were found in joint kinematic curves between the laboratories despite the large spectrum of different techniques utilised. Reliability was accounted for by differences in marker positioning on the thigh, anthropometric measurements and event detection.

Ferrari et al., (2008) compared five body model protocols for gait analysis over exactly the same gait cycles from two adult healthy subjects and a subject with a lower limb prosthesis. The conventional lower limb model (PiG) was compared to Total3DGait (Leardini et al., 2007), CAST (Cappozzo et al., 1995, Benedetti et al., 1998), SAFLo (Frigo et al., 2008) and LAMB (Rabuffetti et al., 2004) for gait data acquisition. A single marker set was designed that incorporated each of the marker sets from the five body models. Neither normalisation nor offset subtraction was performed on the kinematic data. This study protocol allowed the analysis of multiple body models independent of landmark identification, marker attachment, anthropometric measurements and data processing. Within-protocol reliability was high and similar for each protocol, mean absolute variability was less than 7^{o} for all joint rotations and less than 18Nm for joint moments. Between-protocol mean absolute reliability was high, especially for knee internal/external rotation (31^{o}) and ankle dorsi/plantarflexion (27^{o}), and up

to 21Nm for all joint moments. Joint rotations measured for one subject with a prosthesis allowing full knee flexion/extension and internal/external rotation but restricted abduction/adduction demonstrated between-protocol differences. The conventional lower limb model (PiG) demonstrated abduction/adduction ROM of 35^{o} but the other four protocols resulting in ROM <10^{o}. The findings indicate that while sagittal plane kinematics were comparable between body models, frontal and transverse plane were poorly correlated and even biased. It was hypothesised that large variability in knee abd/add was due to bias in axis location and resulted in cross-talk between planes. In the conventional lower limb model (PiG), this is caused by high variability in alignment of wand markers (Gorton et al., 2001 & 2002). The authors concluded that comparisons of gait data between protocols should be made very carefully, especially for knee frontal and transverse plane motion.

In summary, the previous findings indicate that, while most lower limb kinematic variables are reliable, hip and knee transverse plane reliability is less so (Ferrari et al., 2008; Benedetti et al., 2012). Methodological errors of the conventional (PiG) body model have been highlighted and new approaches suggested to improve the reliability of gait data. The methods described utilise some form of mathematical method to determine, marker motion, STA and cross-talk (Charlton et al., 2004). Ferrari et al., (2008) demonstrated the reliability of using different body model protocols on concurrent gait cycle to reduce inherent variability from intrinsic gait variability and marker placement between errors between-protocols. This protocol has been implemented to determine the between-session reliability of concurrent foot models in experimental chapter 3 (chapter 7). The between-session reliability of the conventional (PiG) model has not been extensively examined in paediatric populations as adult populations, but the next papers presents the findings of the few studies available.

3.4.4 Reliability of the Convention Lower Limb Model (PiG) in Children

Ounpuu et al., (1991) developed a paediatric database of gait kinematics and kinetics in healthy children using the conventional lower limb model (PiG). Thirty one healthy children (mean age 9.6 years) were asked to ambulate at a self selected speed for 3 trials with the conventional (PiG) marker-set attached. The study found between-subject reliability to be low, ranging from SD between 2 and 8^{o} for maximum, minimum, ROM and mean joint kinematic data over the gait cycle. The authors reported that the reliability was similar to that

from adult gait data of Kadaba et al., (1990) confirming the use of the convention lower limb model in children.

Within- and between-session reliability of lower limb kinematics and kinetics during gait analysis was examined in 5 healthy children and 5 children with cerebral palsy, mean age 9.6 years (Miller et al., 1996, Quigley et al., 1997). A modified Helen Hays marker set (conventional lower limb model, PiG) was attached to the children's lower limbs to calculate 3D joint kinematics of the hip, knee and ankle. Children were asked to walk at their self-selected walking speed for 3 trials per session over 5 sessions. Intraclass correlation coefficients (ICC) were calculated for each time point of 100 time points over the gait cycle, for within and between-session to determine reliability. Healthy children's within-session reliability of kinematic data was high (ICC averaged 0.856), with highest ICCs for knee rotation and lowest for knee flexion/extension. Between-session ICC for the healthy children was lower, averaging 0.687, highest knee flexion/extension and lowest for hip abd/add. Between-session kinetic data results demonstrated highly reliable joint forces, average ICC of 0.855, highest in the compression force at the knee and lowest in the anterior/posterior force at the knee. Joint moments were also highly reliable, average ICC 0.853, highest at the hip flexion/extension moment and lowest at the hip rotation moment. The authors concluded that the techniques to capture joint kinematics and kinetics during paediatric gait analysis was reproducible both within- and between-sessions.

Further to these two studies, the same research team examined the reliability of gait measurements, from the same captured data, at specific points of the gait cycle (Quigley et al., 1999). Lower limb angles were extracted at initial contact and peaks in the stance and swing phases based on values of clinical interest. For the analysis the authors utilised within- and between-session CV and SD of spatiotemporal, kinematic and kinetic measures. The spatiotemporal parameters demonstrated low reliability both within-session (CV range 0.02-0.19%) and between-session (CV range 0.02-0.17%). Ground reaction force peak also demonstrated low reliability both within-session (CV range 0.03-0.09) and between-session (CV range 0.03-0.09). Kinematics CV range for within-session was 0.02-1.34% and between-session 0.02-0.88%. Kinetics CV range within-session was 0.02-0.17% and between-session 0.02-0.19%. The authors conclude that spatiotemporal, ground reaction forces and joint kinetics are more consistent than joint kinematics. The sources of reliability can be attributed to inherent within-session variability and marker placement error contributing to between-session variability.

Gorton et al., (1997) presented the findings of their study on between-session reliability of the conventional lower limb model (PiG) for gait analysis in 50 children between the ages of five and sixteen. The children were invited to two sessions one week apart. In each session markers were placed on anatomical landmarks by two observers (raters). The children were asked to walk at their self-selected walking speed, three trials were selected to represent session data. The study used within- and between-day CMC to assess the reliability of the kinematic and kinetic waveforms. Within-day CMC ranged from 0.805 for pelvic tilt to 0.994 for hip flexion and between-day CMC 0.791 for pelvic tilt to 0.990 for hip flexion. Within- and between-day CMC for kinetic waveforms were >0.98 for all variables examined. In general, the reliability of gait variables observed in this study were higher than those reported by Kadaba et al., (1989) suggesting improvements in gait analysis technology and methods. The authors summarised that gait patterns were consistent across the age range but reliability was found to increase with age.

More recently, Skaaret et al., (2012) examined between-session reliability of 3D gait kinematics in 10 healthy children age 8 to 14 years using the conventional lower limb protocol/model (PiG). Two observer teams placed markers on two consecutive days, two weeks apart. This study determined reliability from Bland & Altman plots and corresponding Limits of Agreement (LoA) with LoA of $\pm 10^{o}$ considered clinically acceptable. The greatest difference within- and between- observers was in the all knee planes, ankle sagittal plane and hip transverse plane (LoA ranging from ±10 to20^{o}). Pelvic motion, foot progression, hip sagittal and frontal plane motion were all $<\pm 10^{o}$. The greater differences found in some variables confirm marker placement reliability between- and within-observers. Joint kinematic demonstrated higher variability at certain periods of the gait cycle, for example, ankle sagittal during pre-swing and knee sagittal during terminal swing. These periods may have more inherent variability from sensitivity to walking speed or experimental variability from event detection errors.

Steinwender et al., (2000) examined within-subject reliability of gait analysis data in healthy children and children with cerebral palsy. Forty children (20 with cerebral palsy, 20 healthy), age range 7-15 years, took part in three sessions within the period of one week. Marker sets where attached to anatomical landmarks in-line with protocols for the conventional lower limb model (PiG). Data analysis involved the calculation of CV for spatiotemporal parameters and CMC for kinematic and kinetic parameters. Spatiotemporal parameters from the healthy children demonstrated CV values of 3.4-5.2% within-day and 5.7-8.0% between-day. Joint

kinematics of the healthy children ranged from, within-day 0.73 for pelvis rotation to 0.98 for hip and knee flexion/extension, and between-day 0.34 for knee rotation and 0.96 for hip and knee flexion/extension. Joint kinetics of the healthy children ranged from within-day 0.86 for hip frontal plane power to 0.96 for hip sagittal plane moment and between-day 0.73 for hip frontal plane power and 0.91 for ankle sagittal plane moment. The authors concluded that the healthy children had a reliable kinematic gait pattern due to their ability to vary individual joint moments but keeping the overall lower limb moment steady.

Van der Linden et al., (2002) examined kinematic and kinetic characteristics of 36 healthy children (mean age 9 years) at 5 clinically relevant speeds. Walking speed was normalised to body height using the method of Hof (1996), 3 trials at a self-selected walking speed and at four speeds slower were collected. Markers were attached according to the conventional lower limb model (PiG) and a knee alignment device (KAD) was utilised to orientate the knee flexion-extension axis. Dimensionless spatiotemporal, GRFs and moments were calculated (Hof 1996) for comparison across the speed groups. All spatiotemporal parameters; speed, cadence, stride time, percentage of single and double support, step length, stride length were significantly different between groups except step width. Some significant differences in lower limb joint angles and moments were found, especially in the sagittal plane, between the speed groups but not necessarily ordered incrementally. Walking speed had a strong effect on the anterior-posterior and vertical GRF. The anterior GRF peak in the second half of the stance phase and the trough in the vertical GRF were significantly greater at higher speeds. The authors reported that walking speed strongly influenced the kinematics and kinetics characteristics of gait, but its effects were not linear. This study advises caution when examining gait data for abnormalities attributed to pathology but may be due to the effects of walking speed.

Comparisons between these paediatric gait studies are difficult due to the varying statistical analyses used to assess reliability of kinematics and kinetics. In general, spatiotemporal, GRF and joint kinetics are more reliable than kinematics (Quigley et al., 1999) at gait cycle events and peaks. However, the protocols to measure 3D paediatric gait involving the conventional lower limb model (PiG) is reproducible both within- and between-sessions. Marker placement errors are the biggest cause of variability and have greatest effect at points in the gait cycle where large rotations occur, causing cross-talk between planes. Walking speed has a large effect on gait data and may underlie significant differences between subject groups (Van der Linden et al., 2002). Therefore, measures to control walking speed variability should be used

whether during capture (metronome) or post capture (mathematical scaling or regression analysis). There is a need to understand between-session reliability of the lower limb model within a paediatric population to determine the relationships between obesity and lower limb biomechanics during gait.

3.5 Foot Models

The conventional gait model (PiG) represents the foot as a rigid body articulating at the ankle. This over-simplification can lead to errors caused by disregarding relative motion within the foot. Review articles have highlighted the vast number of foot models tested on healthy and pathological adults as well as children (Rankine et al., 2008; Deschamps et al., 2011; Bishop et al., 2012). International standards have been published for the modelling of upper and lower limbs according to joint coordinate systems, anatomical landmarks and axes recommendations (Wu et al., 2002 & 2005). However, no standards exist for modelling the foot. This section will give a brief history of the development of foot models and detail studies that have tested foot model protocols in terms of reliability in adult and child populations.

The conventional lower limb model (PiG) for gait analysis regards the foot as a single rigid segment articulating at the ankle. This was due to limitations in motion capture technology at the time which restricted the complexity of the model (Theologis & Stebbins 2010). This single segment description leads to errors when motion occurs within the foot segment. Early 3D foot models, tested on adults, involved comparing the calcaneus or hindfoot segment to the shank (Kepple et al., 1990; Scott & Winter 1991; Siegel et al., 1995; Moseley et al., 1996; Liu et al., 1997; Cornwall et al., 1999; Woodburn et al., 1999). Difficulty in tracking the talus with surface markers and optoelectronic capture systems led to the talus and calcaneus being considered as one segment (Rankine et al., 2008).

In 1996, Kidder et al. developed a foot model which captured motion of the shank, calcaneus, metatarsals and hallux; this model would later be known as the Milwaukee Foot Model. This foot model used radiographic measures of foot segmental alignment to construct correlation matrices to which segment coordinate systems could be rotated into anatomical positions. In this way offsets were created as a reference to ‘neutral alignment’. Because of the exposure to x-rays, this model may not be appropriate for clinical studies particularly those that involve children. Carson et al., (2001) also developed a 3D foot model describing the shank, hindfoot (calcaneus and talus), forefoot (five metatarsals) and hallux segments. Their protocol was non-

invasive, did not dependent on x-ray information and was later adapted for use in children (Stebbins et al., 2006). Leardini et al., (1999) produced a five segment 3D foot model, describing motion of the tibia/fibula, calcaneus, midfoot (cuboid, three cuneiforms and navicular), first metatarsal and hallux. This study utilised rigid clusters of markers placed and anatomical landmark calibration techniques to define joint rotations. The use of marker clusters to describe foot segments was also utilised by Jenkyn & Nicol (2007) in their foot model which described five segments of the foot; the calcaneus, talus, midfoot (cuboid, three cuneiforms and navicular) , as well as medial and lateral forefoot but no hallux segment. The five marker clusters are composed of three 10mm markers at set angles and distance to each other resulting in a 40mm triad cluster. The use of this marker cluster on paediatric feet may be difficult to track due to markers from adjacent clusters being in close proximity to each other. Leardini et al., (2007) produced a second foot model utilising skin mounted markers to create the tibia/fibula, calcaneus, midfoot (cuboid, three cuneiforms and navicular), and metatarsals with the hallux represented as two projection lines from the first metatarsal in the sagittal and transverse plane. The Heidelberg foot model uses a series of projection lines to define motion between functional foot segments (Simon et al., 2006). Relative motion between segments is represented by vectors along a predetermined axis or rotation which does not necessarily align with the standard planes (Deschamps et al., 2011). A nine-segment foot model proposed by MacWilliams et al., (2003) includes the joints; talocrural, subtalar, calcaneocuboid, medial tarsometatarsal, lateral tarsometatarsal, lateral metatarsophalangeal, medial metatarsophalangeal and first metatarsophalangeal. This model calculated segment position and orientation based on skin mounted markers and estimates based on adjacent segments to provide a database of normal gait in adolescents.

3.5.1 Validity of Foot Models

Few foot model studies have demonstrated the validity of digitally reconstructing foot segment motion to actual motion between the bones of the foot. Some studies have examined the validity of using a SPG system to reconstruct marker sets (Myers et al., 2004). Studies have also examined the kinematic output of their foot models when the foot is placed in known alignments (MacWilliams et al., 2003). Reliability of each foot model has usually been tested for within-session and between-sessions and sometimes between-rater using varying statistical techniques (Carson et al., 2001; Stebbins et al., 2006; Wright et al., 2010; Caravaggi et al., 2010; Deschamps et al., 2011; Bruening et al., 2012; Sarawat et al., 2012).

Studies that have sort to quantify the errors involved in foot model's attempt to record actual bone motion have depended on bone pins or cadaver methodologies which are reliant on assumptions of normal gait patterns under testing conditions. These studies do however, provide evidence for the validity of describing multi-segment foot motion using skin mounted markers.

3.5.2 Invasive Testing of Validity in Foot Models

Nester et al., (2007) compared kinematic data from an experimental foot model that segmented the foot into the heel, navicular and cuboid, medial forefoot and lateral forefoot to measure bone motion from markers mounted on inter cortical pins. Six adult subjects ambulated in three conditions; bone pins, skin mounted markers and plate mounted markers (the plates were stuck directly to the skin and the markers on top). Data were collected from 10 gait trials from each subject to be representative of their gait patterns. The mean and maximal differences between any two of the three protocols during stance was >3° in 35% and 100% respectively and >5° in 3.5% and 73% respectively. The results of the experimental foot model in the three conditions demonstrated that error due to violation of rigid body assumption (within-segment motion within an assumed rigid segment) and skin motion artefacts were minimal. Kinematic differences were greatest for the navicular-cuboid to calcaneus and medial forefoot to navicular-cuboid. The authors concluded that although precise foot kinematics will not be accurately captured with plate or skin mounted markers, foot models are of value in distinguishing gross pathology compared to healthy individuals or changes over time.

Okita et al., (2009) evaluated the fidelity of a three segment foot and ankle model by recording skin mounted against bone mounted marker sets on cadaver's feet during simulated stance phase of gait. Internal/external rotation of the hindfoot segment, based on skin mounted markers, differed significantly from the actual motion of the calcaneus by a mean difference of 0.6^{o}. Larger differences between forefoot segment and underlying bone motion were recorded in adduction/abduction and internal/external rotations by 1.5^{o} and 1.2^{o} respectively. The artefact of skin motion compared to bone motion varied by 3mm to 7mm, but no more than 3mm in one direction, in the foot segments. Segmental kinematics were compared to bone kinematics to examine the rigid body assumption; the shank and hindfoot behaved as rigid bodies however the forefoot violated the rigid body assumption. This finding indicates

that the forefoot segment could be modelled more accurately by subdividing the metatarsals into medial and lateral portions as proposed by MacWilliams et al., (2003) and Buczek et al., (2006). The study reported that, despite errors the segmental foot model appeared to perform reasonably well.

Nester et al., (2010) examined mean and maximal errors due to violation of the rigid body assumption from foot models that divide the bones of the foot into segments for kinematic analysis. The authors used data from a dynamic cadaver model with markers attached to bone pins during simulated stance phase of gait. Kinematic differences between individual motion and segmental motion were calculated with mean errors between 0.8° to 4.4°. Based on the errors reported a three segment mid and forefoot model was proposed consisting of the; (1) navicular and cuboid, (2) cuneiforms and metatarsals 1, 2 and 3 and, (3) metatarsals 4 and 5. The authors stated that the greater the number of bones and articulation within a rigid segment the greater the likely violation of the rigid segment assumption.

These studies using bone pins or cadaver specimens indicate that dividing the foot into segments consisting of multiple bones incurs errors in the kinematic outputs compared to actual bone motion. Errors also occur due to skin movement which causes marker displacement irrespective of the underlying bony landmark. Modelling the hindfoot resulted in the greatest accuracy because of fewer errors from assumptions of rigid body modelling. The midfoot and forefoot segments produce greater errors, though most errors were reported to be <5°.

3.5.3 Validity of Foot Models in Adolescents and Children

MacWilliams et al., (2003) validated their nine-segment foot model in four adult subjects using wedges placed under the foot to give known angles between the forefoot and toes, as well as ankle flexion. Average mean errors between the foot model output and the known angles were 1.4^{o} at the ankle, 1.6^{o} for the hallux, 3.3^{o} for medial toes and 1.8^{o} for lateral toes. The study also compared the kinematic foot angles during the stance phase with radiographic measures of Cavanagh et al., (1997). They found the largest difference between these studies was 4^{o} in first metatarsal inclination angle which the authors note was less than the SD in both studies for this measure.

Myers et al., (2004) reported the development, accuracy, within-session reliability and validation protocol of a four-segment paediatric foot model. The study population consisted

of three children between the ages of 6 and 11 years from which foot kinematic outputs were cross-correlated against the Milwaukee model in adult subjects (Kidder et al., 1996). Validation of the model incorporated static and dynamic linear and angular testing of a dummy segment consisting of markers placed at distances representative of the foot model and repeated on a different day. Computed marker position reconstruction and distances were compared to measurements taken by vernier callipers. Dynamic angular testing involved motion capture of a dummy segment against a Biodex dynamometer rotating at a set angular velocity. The authors stated that system accuracy was 'exceptional' with static linear accuracy >99.9%, dynamic linear accuracy >99.8% and angular accuracy to be >98.9%. Correlation coefficients ranged from 0.988 ± 0.001 to 0.749 ± 0.200 between this paediatric model and the Milwaukee model (Kidder et al., 1996). The static marker reconstruction indicated high accuracy in all 3D orientations. Dynamic testing revealed that resolution increased with decreasing marker distance, but even at the shortest marker distance (39.9mm) resolution was still satisfactory, 0.53 ± 0.31mm at 0.01 significance level. Compared to the Milwaukee foot model used in adults (Kidder et al., 1996) all but one of the segments had positive correlation coefficients, the hallux demonstrated an altered waveform and offset throughout most of the gait cycle (mean correlation coefficients -0.096). The mean correlation coefficients of the other 11 kinematic graphs were 0.961±0.044. The planar order of highest correlation is sagittal, coronal and transverse in segment order of tibia, hindfoot, forefoot and hallux. This is due to the order of Euler rotations and segment expression relative the next proximal segment.

These validity findings indicate that the accuracy of typical SPG motion capture systems is high enough to capture markers in close proximity (40mm) on the foot of a child (Myers et al., 2004). Validating the static angular outputs to measured angles either from wedges or radiography demonstrated errors <5°, although this protocol may result in errors between 2D and 3D comparisons. High between-subjects SD in MacWilliams et al., (2003) study indicates that dividing the foot into nine segments incurs a large amount of variability which could be due to large differences between walking patterns or errors in modelling assumptions.

3.5.4 Reliability of Foot Models

This section reviews six foot models that have been tested for reliability by original studies and where necessary by subsequent studies (a summary of the studies is in Table 3.1). Comparison

of foot model reliability between studies is difficult due to the different populations being tested; adults (Carson et al., 2001; Simon et al., 2006; Jenkyn & Nicol 2007; Leardini et al., 2007), adolescents (MacWilliams et al., 2003) and children (Stebbins et al., 2006); the study design, between-session repeated measures (Carson et al., 2001; Stebbins et al., 2006; Simon et al., 2006; Caravaggi et al., 2010; Deschamps et al., 2011), between-subject measures (MacWilliams et al., 2003; Leardini et al., 2007); and the statistics used to measure reliability, standard deviation (Carson et al., 2003; Stebbins et al., 2006; Leardini et al., 2007; Caravaggi et al., 2010), intraclass correlation coefficient (Curtis et al., 2009; Wright et al., 2011), coefficient of multiple correlation (Deschamps et al., 2011; MacWilliams et al., 2003, Jenkyn & Nicol 2007; Simon et al., 2006). The purpose of this review was to highlight the technical aspects (including segmentation, joint coordinates and testing protocols) and reliability. The outcomes of this review will aid the selection of a foot model to be used to determine the relationships between foot biomechanics and obesity in children.

Table 3.1. Review of foot models; population tested, number of segments, measures of validity and reliability and relevant clinical applications.

Reference	Population	Foot segments (amount)	Validity and reliability	Relevant clinical applications
Carson et al., (2003)	n=2 HS (24 and 29y)	(3) Hindfoot, forefoot and hallux	No validation BR BS BT, n=2 , R=2	Theologis et al., (2003) paed club foot
MacWilliams et al., (2003)	n=18 HS (12.4±2.6y)	(8)Talus/navicular/cuneiform, cuboid, calcaneus, lateral forefoot, medial forefoot, lateral toes, medial toes and hallux	Compared to radiographic data and wedge test BSu BT, n=18, R=1	
Simon et al., (2006)	n=10 HS (19-43y)	(0) No segments, projection angles	Compared to radiographic data and indirect checks BR BS BT, n=1, R=5	Twomey et al., (2010) paed flat feet
Stebbins et al., (2006)	n=15 HS (6-14y)	(3) Hindfoot, forefoot and hallux	No validation BS BT Also Curtis et al., (2009) and Wright et al., (2011)	Alonso-Vazquez et al., (2009) paed forefoot varus. Levinger et al., (2010) normal- and flat-arched adults
Jenkyn & Nicol (2007)	n=12 HS (22-40y)	(4) Hindfoot, midfoot, medial forefoot, lateral forefoot	No validation BSu BT n=18, R=1	
Leardini et al., (2007)	n=10 HS (25±4.0y)	(4) Calcaneus, midfoot, metatarsals, hallux and planar angles	No validation BSu n=2, r=1 also Caravaggi et al., (2010) and Deschmaps et al., (2011)	Powell et al., (2011) high- and low-arched adults

HS = healthy subjects, y = years old, n=number of subjects, R= number of Raters, BR = between-Rater, BS = between-session, BT = between-trial, BSu = between-subject, paed = paediatric

3.5.4.1 Reliability of Carson et al., (2001) Foot Model

Carson et al., (2001) developed the Oxford Foot Model (OFM) and evaluated between-session reliability of the protocol and model in adult subjects. The marker set and anatomical axes

definition were based on knowledge of foot kinematics and tested in healthy and deformed feet in a clinical setting. The model used 17 markers of which three were removed following the static calibration trial (posterior medial heel, medial malleolus and head of 1st metatarsal). A four segment model was constructed for calculation of segmental kinematics. Data were captured using Vicon motion capture system. Between-segment angles were calculated according to Grood & Suntay's (1991) method using Joint Coordinate System (JCS). Reliability of the model was assessed in two healthy subjects, by two observers over four sessions, whilst walking a self-selected speed. Subtle patterns of foot motion was detected using the OFM and qualitatively comparable to existing knowledge of foot kinematics.

Between-trial SD for each inter-segment angle over the stance phase ranged from 0.57° for forefoot to hindfoot abduction/adduction to 0.95° for hallux plantar-/dorsiflexion. Between-session reliability was found to be within ±3.0° for the ankle joint, ±4.3° for the forefoot and ±6.5° for hallux motion. Between-observer results were similar to between-session reliability, with expected differences between-observers no greater than 1° of the between-session result. Marker placement variability is the primary reason for the decrease in reliability compared to between-observer variability or skin movement artefact. The authors conclude that their protocol for non-invasive assessment of the foot demonstrated acceptable reliability for use in research and clinical applications.

3.5.4.2 Reliability of Stebbins et al., (2006) Foot Model

The OFM was adapted by Stebbins et al., (2006) for use in a paediatric population and examined for between-session reliability in 15 healthy children (mean age 9.5 years). The OFM describes hindfoot to tibia motion as flexion/extension about the medio/lateral axis, inversion/eversion about the longitudinal axis and internal/external rotation about the axis orthogonal to the previous two. The forefoot of OFM is described by flexion/extension about the medio/lateral axis, supination/pronation about the longitudinal axis and abduction/adduction about the axis orthogonal to the previous two.

Five variations of the OFM were tested for feasibility and between-session reliability over three trials performed by each child at their self-selected walking speed in three sessions between 2 weeks and 6 months apart. These included using a scaled virtual marker instead of a toe marker between 2nd and 3rd metatarsals, tracking the forefoot segment with only lateral markers, removing the wand marker on the calcaneus, using markers on the tibia rather than the knee joint centre and finally removing the calcaneal wand marker during the static trial. As

shown in Table 3.2, variations in the OFM model presented minimal changes in between-session reliability. The only significant change in between-session reliability came from elimination of the wand marker during the static trial, which reduced between-day variability of the hindfoot in the transverse plane. The study recommended the continuing use of a physical toe marker, elimination of the calcaneal wand marker, to use the conventional knee joint centre to calculate the long axis of the tibia, and to measure forefoot medial arch height compared to lateral markers for estimation of error produced in forefoot supination as a result of rigid body assumptions.

Within-subject SD of maximal values were higher than ROM values which the authors interpreted as good consistency between foot motion patterns, but with offsets affecting absolute values. The sagittal plane was most reliable followed by frontal, then transverse. Table 3.2 reported the model's maximal angles and ROM angular outputs; within subject variation was least in the hindfoot compared to the forefoot, (hallux SD not presented). The authors conclude that awareness of the reliability of inter-segment foot motion in children is of importance for accurate interpretation of results.

Table 3.2. Mean ± SD (within subject) kinematics of the Stebbins et al., (2006) default foot model with model variations.

	Default Model (°)	SD (°)	Variation of Model (°)
Max Forefoot DF	9.8	3.4	9.8 – 10.1
Max Forefoot Sup	6.5	5.3	6.4 – 6.5
Max Forefoot Abd	5.0	7.4	0.6[a] – 4.1
Range Forefoot DF	20.8	2.7	19.2[a] – 20.8
Range Forefoot Sup	8.8	1.6	7.8[a] – 8.6
Range Forefoot Abd	9.9	2.4	8.8[a] – 9.9
Max Hindfoot DF	11.2	3.0	10.7 – 12.2
Max Hindfoot Sup	9.0	5.2	7.6 – 9.3
Max Hindfoot Abd	13.8	8.4	13.9 – 15.6[b]
Range Hindfoot DF	24.2	2.7	20.4[a] – 23.8
Range Hindfoot Sup	10.8	2.2	10.2 – 11.5
Range Hindfoot Abd	12.3	2.7	11.1 – 12.4

[a] indicates significant differences in mean values. [b] indicates significant differences in reliability

Further studies have examined the between-session reliability of the OFM in paediatric and adult populations. Curtis et al., (2009) examined between-session reliability of the OFM in 8

healthy children (mean age 12 ± 3 years) during gait. The children were tested, according to the protocols of Stebbins et al., (2006), on two sessions between 2 and 58 days apart. Maximal, minimal and mean values for each inter-segment angle were presented over the stance phase at each foot roll over process (heel, ankle and metatarsal head rockers). Absolute differences in foot segment kinematics were small ranging from 0.3^{o} to 1.9^{o} and non-significant between sessions. Absolute reliability (measured by typical error of measurement ((SD(retest-test))$\sqrt{2}$) ranged from 0.93^{o} for maximal forefoot dorsiflexion during the ankle rocker to 8.56^{o} for maximal hindfoot internal rotation during the heel rocker. The hindfoot, in particular, demonstrated poor between-session reliability in the frontal and transverse planes due to problems defining hindfoot neutral causing offsets in kinematic waveforms.

Wright et al., (2011) tested the between-session reliability of the OFM defined by Stebbins et al., (2006) on 17 healthy adults during two sessions on the same day by one observer (rater). Ten trials were collected at each session whilst subjects walked at their self-selected speed. The OFM segmental outputs where presented either referenced to neutral stance angles (thereby reducing marker placement error) or non-normalised. Inter-segment angles at initial contact and toe-off gait events were considered for between-session reliability. When foot kinematics were not referenced to neutral stance, ICCs ranged from 0.38 (SEM 5.09^{o}) for frontal plane hindfoot at toe-off to 0.97 (SEM 2.53^{o}) for sagittal plane hindfoot at toe-off. When foot kinematics were referenced to neutral stance variability was decreased, ICC ranged from 0.83 (SEM 2.45^{o}) for sagittal plane forefoot at toe-off to 0.97 (SEM 1.12^{o}) for transverse plane hindfoot at toe-off. This study found highest between-session reliability in the sagittal followed by transverse and frontal when not referencing to neutral standing, but when referencing to neutral standing transverse became less reliable than frontal suggesting that marker placement error for the OFM is greater in the frontal plane than transverse. The authors conclude that referencing foot kinematics to a neutral standing position can minimise error between marker set applications enabling the detection of small angular changes between subject groups.

The development, validation and reliability of the OFM has been described by detail in these studies (Carson et al., 2001, Stebbins et al., 2006, Curtis et al., 2009 and Wright et al., 2011). The model provides good between-session reliability of paediatric hindfoot, forefoot and hallux motion over the gait cycle. Wright et al., (2011) reported the use of kinematic offsets by neutral standing angles to improve reliability of marker placement. However, Stebbins et al., (2006) and Carson et al., (2001) do not implement this protocol as this artificially reduced

between-session variability and reduce clinical application of the model. Another model that does describe foot kinematics relative to neutral standing position is the 3DFoot model (Leardini et al., 2007a). The development of this model is described below as well as reliability in adult populations.

3.5.4.3 Reliability of Leardini et al., (2007) Foot Model

Leardini et al., (2007a) developed an anatomically based protocol for the description of five segments and planar angles over the gait cycle. For all segments, flexion/extension was calculated about the z-axis (medio/lateral axis), abduction/adduction about the y-axis (vertical) and internal/external rotation about the x-axis (orthogonal to previous two). The model used 14 markers five of which were on the shank, three virtual markers were calculated using physical marker mid-points or a calibration procedure. The location of bony landmarks was recorded with the use of an 'instrumented pointer device' to the position of skin mounted markers using CAST procedures. Two markers were designated as defining two landmarks; the base of the 2^{nd} met with the middle cuneiform and the base of the 5^{th} met with the tuberosity of the cuboid.

Data were captured using Vicon motion capture system from ten adult subjects, ambulating at self-selected speed, from which three trials were collected for analysis. Inter-segment angles were calculated according to the International Society of Biomechanics (ISB) recommendations which are based on the Joint Coordinate System (JCS). Static joint angles, captured during standing, were used to offset the dynamic joint rotations. This paper did not report reliability of using 3DFoot model but reported that the information obtained was consistent with previous clinical knowledge on the dynamics of the foot during stance phase of gait.

Caravaggi et al., (2010) analysed the between-trial, between-session and between-rater reliability of 3DFoot model in two healthy adult subjects. Both subjects were tested by four observers (raters), two experienced and two not experienced, in three sessions. For each joint rotation, between-rater reliability was largest followed by between-session and between-trial reliability. Lowest reliability was found in the midfoot to calcaneus motion (Chopart joint) with sagittal plane variability of 1.1^{o}, 7.8^{o} and 11.5^{o} for between-trial, between-session and between-rater respectively. Overall between-session reliability of all the foot joints, over the stance phase was 3.6^{o} and 3.3^{o} for the two experienced observers (raters). The study utilised the statistical method of Schwartz et al., (2004) to test the reliability of 3DFoot model protocol

by presenting between-trial and between-rater SD as well as a ratio between the two. The large observer (rater)-to-trial ratio SD compared to observer (rater) SD at the calcaneus indicates methodological errors in the definition of the segment. The authors discovered, through photographic examination, that significant differences in the placement of the medial and lateral calcaneal markers were present. The close proximity of the markers placed on the calcaneus meant that small alterations in marker position resulted in significant variations in segment motion. In summary, the authors reported that foot kinematic reliability can be increased to that of lower limb models.

Deschamps et al., (2011) also examined the between-session reliability of 3DFoot for joint kinematics in adults, using six healthy volunteers walking at self-selected speed (Table 3.3). Two observers (one experienced, one not experienced) conducted the foot model protocol on each subject over four repeated sessions. Both relative angles (offset to a standing position) and absolute angles were analysed for clinical utility. Between-trial CMCs were >0.82 for both observers for the relative angles, whereas absolute between-trial CMCs were 0.782 to 0.987 and 0.673 to 0.991 for the experienced and inexperienced observer respectively. Between-day relative CMCs ranged between 0.701 to 0.971 and 0.557 to 0.982 for the experienced and inexperienced observers respectively. Between-observer relative CMCs of the 3D rotations ranged from 0.448 to 0.891. Mean trial SD was $<2.0^{o}$ for all angles, mean session relative angles ranged from 0.9 to 4.2^{o} and 1.6 to 5.0^{o} for the experienced and inexperienced observers respectively. Mean observer relative SD ranged between 2.2 to 6.5^{o}. When examining absolute angles, CMCs and SD were consistently lower within-day compared to between-day and between-observer. Eighty percent of the relative parameters had a between-observer between-trial SD ratio of $\leq 4.0^{o}$, while only 35% of the absolute parameters had a ratio $\leq 4.0^{o}$. The authors summarise that measuring reliability as the extent to which gait measurements are consistent or free from variations is critical for clinical application. Clinical utility of the 3DFoot model should be based on absolute rather than relative angles as they are easier to incorporate in to clinical reasoning and decision making. The findings of this study indicate that absolute angles did not have a critical impact on between-session reliability of 3D rotations and therefore, can be reliably used in clinical applications.

The development and reliability of 3DFoot has been examined in these studies (Leardini et al., 2007a; Caravaggi et al., 2010; Deschamps et al., 2011). High within-trial reliability indicates that subjects are able to walk repeatability with the markers attached. Between-session reliability was generally $<5^{o}$ indicating that observers (raters) are able to repeatedly place the

markers on anatomical landmarks. Differences between absolute and relative between-session (relative to static standing pose) angles were minimal in an adult population. Between-observer reliability was higher indicating that practise and training of inexperienced users of 3DFoot is required. However, the reliability findings from 3DFoot are based solely on adult gait data whereas OFM is based on both adult and paediatric samples.

Table 3.3. Mean ± SD range of motion and between-trial, within-day and between-day coefficient of multiple correlation (CMC) for relative and absolute joint angles of Leardini et al (2007) foot model.

			Relative angles		Absolute angles	
Joint	ROM (°)	Mean Between-trial CMC	Within-day CMC	Between day CMC	Within-day CMC	Between day CMC
Hindfoot sag	33.2 ± 5.1	0.968	0.923	0.933	0.911	0.890
Hindfoot fro	22.5 ± 3.1	0.935	0.912	0.899	0.872	0.811
Hindfoot tra	12.9 ± 1.2	0.907	0.877	0.854	0.884	0.840
Midfoot sag	20.8 ± 6.2	0.981	0.952	0.842	0.814	0.733
Midfoot fro	13.0 ± 4.2	0.964	0.933	0.831	0.797	0.712
Midfoot tra	15.9 ± 10.1	0.881	0.782	0.801	0.733	0.699
Forefoot sag	14.9 ± 8.1	0.928	0.837	0.741	0.786	0.819
Forefoot fro	15.9 ± 5.3	0.924	0.867	0.801	0.799	0.686
Forefoot tra	4.3 ± 3.5	0.908	0.851	0.761	0.735	0.652
Hallux sag	40.0 ± 13.6	0.987	0.954	0.851	0.515	0.246
Hallux tra	11.9 ± 3.5	0.920	0.901	0.862	0.681	0.623

ROM: range of motion. Sag: sagittal, fro: frontal, tra: transverse. CMC are based on the senior observers results presented in Deschamps et al., (2011)

3.5.4.4 Reliability of MacWilliams et al., (2003) Foot Model

The MacWilliams model divides the foot in nine segments with the use of 19 markers, three of which lie on the shank and include a marker triad on the hallux. Kinfoot describes joint rotations using the Euler sequence with flexion/extension (medio/lateral axis) first followed by inversion/eversion (longitudinal axis) and internal /external rotation (orthogonal to previous two). As previous noted in this chapter MacWilliams et al., (2003) validated their nine-segment foot model using foot wedges placed and radiographic measures. The study also examined reliability of 3D joint kinematics over the stance phase of gait in 18 adolescent subjects (mean age 12.4 ± 2.6 years) during one session, shown in Table 3.4. Within-subject

sagittal plane variability, measured by SD, ranged from 0.8° at the subtalar and lateral tarsometatarsal joints to 4.0° at the hallux. Within-subject reliability, measured by CMC, ranged from 0.92 at the medial metatarsophalangeal to 0.57 at the subtalar joint. Between-subject variability ranged from 4.7° at the lateral tarsometatarsal to 11.1° at the calcaneocuboid joint. Between-subject reliability ranged from 0.82 at the lateral metatarsophalangeal to 0.11 at the subtalar joint. These findings suggest subtalar and calcaneocuboid joints were the least reliable and lateral tarsometatarsal and lateral metatarsophalangeal joints the most reliable. This may be due to the estimation of the talus, navicular, cuneiform and cuboid segments based on the position of adjacent segments rather than skin mounted marker tracking. The hallux MP joint had the highest intra-subject SD most likely as a result of vibration artefact from the rigid triad used for the hallux segment. This joint also had the second highest intersegment SD reflecting not only the range of walking patterns but also the positioning on the triad on the hallux on individual subjects.

No subsequent study has examined between-session or between-rater reliability of the MacWilliams foot model. Furthermore, no study has utilised the MacWilliams in a clinical population to define foot motion differences between groups. High between-subjects SD in MacWilliams et al., (2003) study indicates that dividing the foot into nine segments incurs a large amount of variability which could be due to large differences between walking patterns or errors in modelling assumptions. However, only the subtalar and calcaneocuboid joints demonstrated low between-subject reliability. The ankle, hallux, medial and lateral forefoot and toe joints of the Kinfoot may provide greater insight into inter-segment foot motion.

Table 3.4. SD and CMC of MacWilliams et al., (2003) Within- and between-subject variability and reliability of sagittal plane kinematics and kinetics

	Angles (°)				Moments (Nm/kg)				Powers (W/kg)			
	Intra		Inter		Intra		Inter		Intra		Inter	
	SD	CMC	SD	CMC	SD	CMC	SD	CMC	SD	CMC	SD	CMC
Talocrural	1.5	0.85	4.8	0.62	0.077	0.92	0.145	0.77	0.168	0.91	0.224	0.80
Subtalar	0.8	0.57	8.1	0.11	0.060	0.87	0.098	0.53	0.035	0.56	0.035	0.33
Calcaneocuboid	1.1	0.61	11.1	0.13	0.024	0.74	0.043	0.61	0.024	0.65	0.027	0.52
Medial TM	1.2	0.93	7.6	0.40	0.034	0.94	0.046	0.88	0.064	0.84	0.092	0.74
Lateral TM	0.8	0.74	4.7	0.43	0.009	0.46	0.016	0.31	0.010	0.67	0.014	0.40
Hallux MP	4.0	0.81	10.7	0.65	0.003	0.74	0.015	0.50	0.035	0.80	0.048	0.72
Medial MP	2.6	0.92	6.6	0.78	0.002	0.85	0.004	0.63	0.008	0.80	0.013	0.65
Lateral MP	2.9	0.91	5.7	0.82	0.001	0.33	0.002	0.22	0.002	0.51	0.002	0.39

3.5.4.5 Reliability of Jenkyn & Nicol (2007) Foot Model

Jenkyn & Nicol (2007) introduced a foot model for use in a clinical gait laboratory. This study digitized bony landmarks on the subject's feet following palpation in neutral standing posture. Three landmarks defined each segment, with the foot split into four segments (hindfoot, midfoot, medial forefoot and lateral forefoot) plus the shank and thigh. Eight clusters were placed in each segment with the midfoot and lower leg containing two each. Segment fixed axes were created with two unit vectors formed from the digitized landmarks, the third vector was calculated orthogonally from the first two. Ankle and subtalar JCSs were constructed (Grood & Suntay 1983), from which the midfoot orientation was determined. Orientation of the hindfoot and forefoot was determined against the midfoot.

The novelty of this model is that it separates the hindfoot into two segments; the calcaneus and the talus. These segments were then used to define movements of the talocrural and subtalar joints. The sagittal axis of rotation for the talocrural joint was calculated from the lateral and medial malleoli, the coronal axis by the lateral malleolus and the talar head. The subtalar joint axis of rotation in the sagittal plane was the same as the talocrural joint, through the malleoli, whilst the coronal axis was defined by the calcaneal tuberosity and the subtalar head. However, the paper only reports data for the talocrural joint in the sagittal and the subtalar joint in the coronal axes.

Jenkyn & Nicol (2007) examined the kinematic outputs from the five segment model on 12 subjects (22-40 years old) during one session consisting of five trials and a self-selected walking speed (shown in Table 3.5). Within and between-subject CMC were reported; within-subject reliability ranged from 0.92 at the ankle, 0.86 subtalar, 0.71 and 0.58 for hindfoot frontal and transverse plane motion respectively, 0.85 at the forefoot and 0.73 for the medial longitudinal arch. The authors commented that, in terms of clinical utility, more segments will provide greater information for determining foot joint motion between populations. However, to record segmental motion more markers are required. For 3D kinematics of segments three markers are required per segment, as more markers are tracked there is more marker trajectory drop-out and cross-over leading to errors. The model devised by Jenkyn & Nicol (2007) attempted to strike a balance between these contrasting points.

The Jenkyn & Nicol (2007) has been further tested for utility during medial turning tasks which demonstrated the benefit of modelling the subtalar joint during a functional activity (Jenkyn et al., 2010). However, no study has examined between-session or between-rater reliability of

the Jenkyn & Nicol foot model. Furthermore, no study has utilised the Jenkyn & Nicol in a clinical population to define foot motion differences between groups.

Table 3.5. ROM, mean ± SD within- and between joint angles of Jenkyn and Nicol (2007) foot model.

Joint Motions °	Range (°) (max, min)	Within-subject mean (°) (SD)	Between-subject (°)
Ankle	15 (5 to -10)	0.92 ± 0.10	0.71
Subtalar	10 (5 to -5)	0.86 ± 0.11	0.51
Hindfoot			
SU/PR	11 (8 to -3)	0.71 ± 0.18	0.31
IN/EX Rot	8 (6 to -2)	0.58 ± 0.20	0.41
Forefoot	12 (15 to 3)	0.85 ± 0.15	0.70
Medial Longitudinal Arch	0.4 (1.3 to 0.9)	0.73 ± 0.21	0.48

3.5.4.6 Reliability of Simon et al., (2006) Foot Model

Simon et al., (2006) developed the Heidelberg foot measurement method (HFMM) to analyse foot and ankle kinematics. The aim of the study was to design a methodology to measure detailed kinematics of the foot in such a way that deformed feet could be included in the same protocol as healthy feet. This study uses no rigorous definition of the foot segments instead 'functional segments' are used to describe the relative motion of projection angles based on proposed clinically relevant angles. Joints are broken down into single hinge joints with one degree of freedom. A heel alignment device was used to ensure each subject's foot was placed in neutral alignment for the malleoli to be accurate marked.

Projection angles have advantages over conventional modelling in that only two markers are needed to define the angle compared to three markers used to define a segment. The authors also infer that it is possible to define rotational angles without defined rigid segments. However, this interpretation of foot movement may limit deeper insights into the biomechanical properties of the foot. Subtalar motion is calculated by the movements of the calcaneal markers due to the difficulty in placing talus markers in vivo. Simon et al., (2006) validates this representation of the subtalar joint because the calcaneal motion can be attributed primarily to subtalar joint action. However, the movement of the ankle and the subtalar joint cannot be separated leading to possible inaccuracies. The paper monitored rigidity of the ankle and subtalar joints by measuring motion of the navicular to the calcaneus.

Angles which are calculated from the navicular marker position showed larger between-rater standard deviation, >5° compared to <5° for most other joint angles.

The HFMM (Simon et al., 2006) presents an alternative method of quantifying foot segmental motion using projection angles. Maximal between-trial and between-session standard deviations were 1.51° and 3.93° respectively indicating low variability, shown in Table 3.6. However offsets related to marker placement differences can cause high sensitivity of the magnitudes from kinematic variables. The model has been show to be suitable for use in a paediatric population demonstrating the ability to find kinematic differences between normal- and low-arched children.

Table 3.6. SD and CMC of between-stride, -day and -rater reliability and ROM ± SD of Simon et al., (2006) foot model

	SD stride	SD Day	SD Rater	ROM ± SD	CMC Stride	CMC Day	CMC Rater
Tibio-talar flexion	0.93	1.34	1.89	22.2 ± 1.8	0.987	0.974	0.939
Medial arch inclination	1.15	2.78	5.64	16.5 ± 1.0	0.958	0.873	0.693
Medial arch	0.65	3.93	6.66	13.2 ± 1.0	0.985	0.675	0.476
Lateral arch	0.68	3.06	4.96	9.2 ± 0.8	0.971	0.661	0.449
Subtalar inversion	0.80	3.38	3.20	10.0 ± 0.3	0.966	0.653	0.702
Forefoot/ankle supination	0.74	1.35	3.30	11.5 ± 0.8	0.974	0.919	0.680
Fore-/midfoot supination	0.53	1.38	7.29	4.5 ± 0.4	0.859	0.520	0.086
Forefoot/ankle abduction	0.67	1.22	3.29	12.0 ± 0.6	0.971	0.912	0.597
Fore-/midfoot abduction	0.55	2.54	3.00	9.0 ± 1.6	0.950	0.518	0.388
Met 1-5 angle	0.74	0.97	2.55	11.0 ± 1.1	0.985	0.975	0.849
Hallux flexion	1.37	1.97	2.80	42.1 ± 1.1	0.993	0.984	0.970
Hallux Abduction	0.45	1.45	2.87	3.2 ± 0.5	0.834	0.383	0.124

3.5.5 Variability of Foot Models Segmental Motion

Comparing reliability between foot models would be inappropriate because each previous study used different protocols and populations. However, comparing standard deviations within the each foot model's segments gives a measure of the most variable foot joints and planes. A comparison of within-subject, between-subject, between-session and between-rater standard deviations (SD) of foot models (Oxford Foot Model, 3DFoot, Jenkyn & Nicol, HFMM and Kinfoot) is presented in Figure 3.1. Within-subject variability range from 0.76° ± 0.22° for HFMM, 1.25° ± 0.01° for 3DFoot, 1.97° ± 1.22° for Kinfoot and 5.45° ± 0.12° for OFM (it should

be noted that OFM was the only study to analysis within-subject reliability in children, from Stebbins et al., 2006, which may have caused higher variability). Between-subject variability was higher than within-subject variability in all models (except OFM which measured between-subject SD in adults, from Wright et al., 2011); 5.76° ± 0.59° for HFMM, 6.89° ± 2.13° for Kinfoot, 5.30° ± 0.06° for OFM, and 1.29° ± 0.27° for Jenkyn & Nicol foot model. Between-session variability was 2.01° ± 0.33° for HFMM, 3.28° ± 0.28° for OFM and 5.06° ± 0.82° for 3DFoot. Finally, between-rater variability was 3.51° ± 1.42° for HFMM and 6.54° ± 2.65° for 3DFoot.

Within-subject SD was the lowest of variability measures in the foot model studies. Within-subject variability is a measure of the ability of a subject to walk through the capture volume under the testing conditions. Also, errors in the motion capture system's ability to reconstruct marker position and errors in the processing of motion data. In general within-subject SD was highest in the transverse plane followed by frontal and sagittal. This may be due to the order of joint rotations used to describe motion around a joint centre (Richards, 2008). Joint angular motion is first considered in the sagittal plane where most motion occurs followed by frontal then transverse. Errors in the orientation of the sagittal plane axis during motion will cascade down to the other axis causes greater errors.

Between-subject SD was generally the highest source of measurement variability in all three planes. Sources of between-subject variability include the biological differences inherent in the sample population. However, marker placement error between subjects may artificially increase variation within groups. The ability to palpate and attach skin mounted markers to certain populations may lead to these sources of between-subject variability. Obese subjects may have more adipose tissue which may make palpating anatomical landmarks difficult and result in soft tissue artefacts causing misrepresentation of bone motion. Between-subject variability was generally higher than within-subject variability. However, if within-subject variability is relatively high compared to between-subject variation the ability of the foot models to determine between group differences is lost. Quantifying expected within- and between-subject variation provides information on the sample size needed to reach statistical significance, if differences exist.

Between-session SD was higher than within- and lower than between-subject SD. A low between-session SD indicates good reliability of the foot models to output kinematic parameters. Sources of variability between repeated sessions include all variability discussed in within- and between-subject variability. By measuring reliability over test-retest sessions

intrinsic sources of variability (natural gait variation) are reduced highlighting the extrinsic sources of variation (marker placement). The sagittal plane demonstrated higher variability than the frontal or transverse planes possibly due to greater ROM at the foot joints in this plane. Between-rater SD was similar to between-session SD indicating that, for experienced users of foot models, variability is similar.

Comparisons of between-session SD between the foot models show that OFM demonstrated greatest variability in the frontal plane at the hindfoot and forefoot between sessions. The 3DFoot model presented greatest variability in the sagittal plane for at the hindfoot and midfoot. Both the 3DFoot and HFMM reported highest variability in the transverse plane at the forefoot. Further examination of the individual segments reveals that the hallux has the highest variability of any foot joints with between-subject variability ranging from 5.5 to 10.7°. This may be due to issues aligned the axis of the hallux with the first metatarsal by using one marker of the phalanx and one on the first metatarsal head. Both boney surfaces are concave meaning the flat surface of the marker can rotate position with little translation movement. Furthermore, the hallux demonstrates large ROM in the sagittal plane over the gait cycle increasing biological variation as a result. The midfoot demonstrated slightly better variability than the hallux with values ranging from 2.1 to 11.1°. This segment consists of many small joints which may move within the assumed rigid body altering marker relative marker position. Furthermore, landmarks including the third metatarsal base and navicular tuberosity, on the midfoot are harder to palpate. The hindfoot and forefoot segments produced similar variability with SD of 1.1 to 7.6° and 1.0 to 8.1° respectively. Both segment's landmarks are readily palpable compared to the midfoot but errors in shank orientation can lead to hindfoot offsets in the frontal plane. Variability of the forefoot segments may arise from motion between the medial and lateral metatarsal which have been shown to demonstrate considerable motion between each other (Nester et al., 2010).

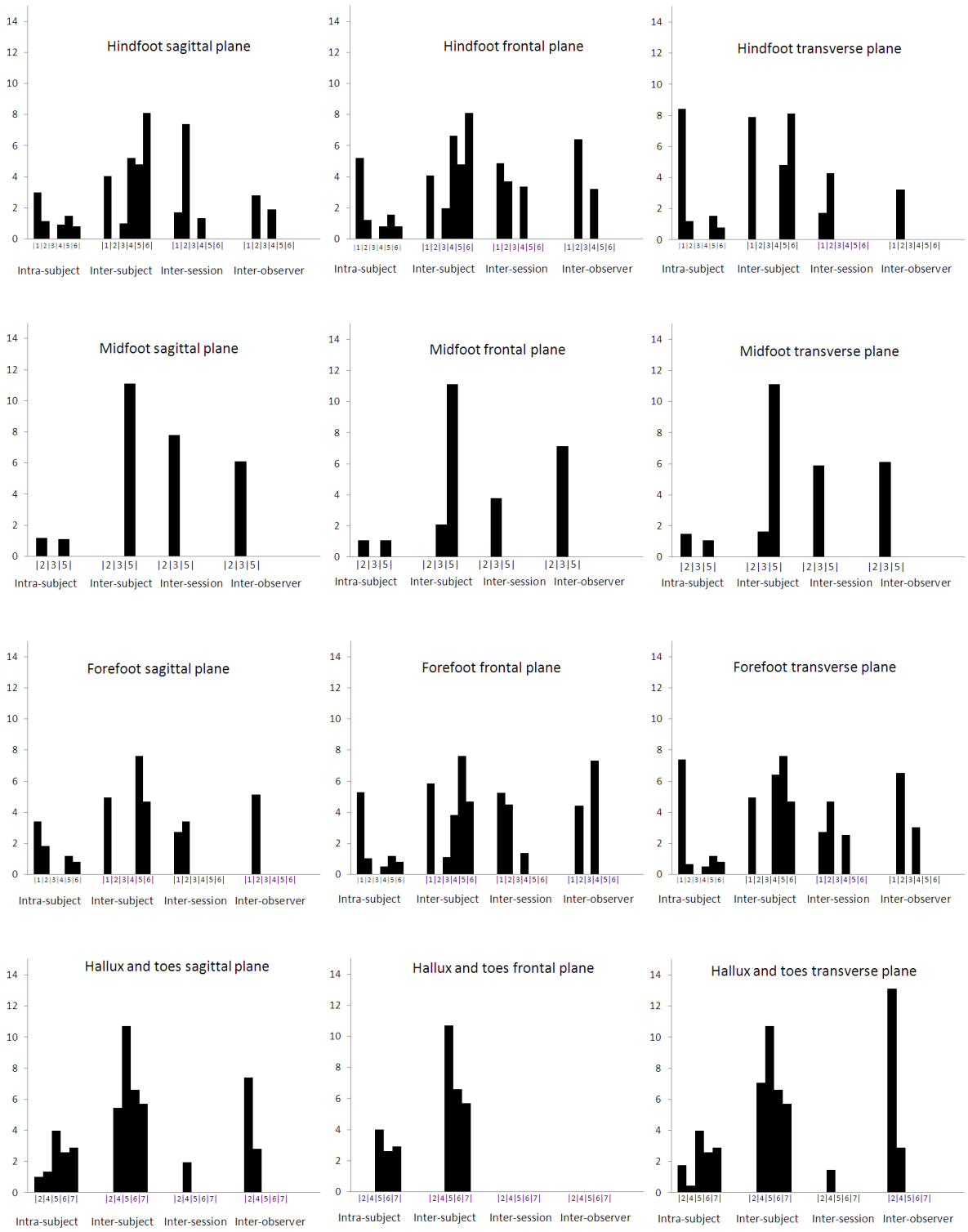

Figure 3.1. Summary of within-subject, between-subject, between-session and between-observer (rater) standard deviations of foot models described by (1) The Oxford foot model (within-subject SD from Stebbins et al., 2006, between-subject and between-session SD from Wright et al., 2011), (2) the 3DFoot model (within-subject and between-session SD from Caravaggi et al., 2010), (3) Jenkyn & Nicol foot model (between-subject SD from Jenkyn & Nicol, 2007), (4) The Heidelberg foot measurement method (within-subject , between-subject, between-session and between-observer from Simon et al., 2006), (5), (6) and (7) the Kinfoot model (within-subject and between-subject SD from MacWilliams et al., 2003)

3.6 Chapter Summary

Lower limb and foot motion analysis involves the use of biomechanical models which are applied to the captured and tracked marker coordinates. It is the application of the biomechanical model that creates the vast majority of the errors in 3D motion capture gait analysis. Standing joint angles are affected by correct marker position on anatomical landmarks with errors up to 6^{o} noted at the hip and knee (Della Croce et al., 1999). The model assumptions based on regression analysis create errors in joint centre locations. The sequence of joint angle rotations significantly alters measured angles and soft tissue artefact causes motion not representative of the bone. The conventional lower limb model (PiG) was tested on adults and found to be reliable, with between-session SD of <4^{o} (Schwartz et al., 2004). In children the conventional lower limb model (PiG) was less reliable between sessions but, it is not clear whether this is due to greater inherent variability in paediatric gait or difficulties attached the markers to smaller landmarks. These findings highlight the need to determine between-session reliability of the conventional lower limb model (PiG) to determine the level of expected error. The effect of soft tissue artefact on the ability of the conventional lower limb model (PiG) to determine joint centres is also required. This will aid the interpretations of relationships between lower limb biomechanics during gait and obesity.

A variety of multi-segmental foot models have been implemented to analyse foot motion during gait. Whether the foot models represent the motion of bony segments sufficiently for clinical utility has not been established, however, mean differences between marker and bone pin motion was <5^{o} (Nester et al., 2007). The between-session reliability of foot models during adult and paediatric gait have been reported to be <7^{o} for OFM (Carson et al., 2003; Stebbins et al., 2006) and <5^{o} for 3DFoot (Deschamps et al., 2011). The range of approaches for segmentalising the foot means a decision on the appropriate foot model to measure foot biomechanics in children should be based on the reliability of the foot segments of interest. One of the aims of this thesis is to explore the relationships between adiposity and foot biomechanics and therefore, selecting and testing foot models is a prerequisite. The first consideration is the amount of foot segments and the second consideration the reliability of each segment during gait.

In conclusion, the between-session reliability of lower limb and foot models must be examined specific to the observer, laboratory, subject group, study design and statistical procedure. Furthermore, the reliability of protocols must be defined before implementation in a clinical study in order to provide a level of error above which clinical relevance can be distinguished.

4. Literature Review Chapter Summary

The purpose of this chapter is to draw together the findings from the two literature review chapters. The literature chapters highlighted what is understood about the relationships between obesity with lower limb and foot biomechanics and what areas need further investigation. This gives the rationale behind the proceeding experimental chapters.

4.1 Aims of Literature Review Chapter 1 (Chapter 2)

The aims of literature review chapter 1 (chapter 2) were to: (1) demonstrate the need to define childhood obesity and adiposity using accurate and reliable measurement protocols, and (2) demonstrate the need to investigate foot and lower limb biomechanics during gait in obese children.

4.1.1 Literature Review Chapter 1 (Chapter 2), Aim 1

Firstly, a definition of obesity is required in order to answer the aims of this thesis. The World Health Organisation (2000) described obesity as a disease in which excessive body fat accumulates to the extent that health may be impaired. The accumulation of body fat is referred to as adiposity which occurs when energy intake exceeds energy expenditure. Whilst the definition of obesity is clear the measurement of obesity is not well defined. Currently childhood obesity is measured by body mass index (BMI), a proxy for body fat mass. This measure is a simple, low cost tool that incurs little burden to the child, but is dependent on the reliability of the observer to take the measures. The key limitation for the use of BMI in children is that it is an indirect measure of body composition and thus, fat mass and lean mass cannot be distinguished. In order to demonstrate the accuracy and reliability of BMI to define childhood obesity a comparison with measures of body fat are required. Two available measures of body fat (adiposity) are bioelectrical impedance analysis (BIA) and air displacement plethysmography (ADP). The high precision and validity of ADP means it is considered to be a criterion measure of body fat against which other measures can be compared. Measures of body fat by BIA offer greater ease-of-use and are less susceptible to changes in environmental conditions. The first experimental chapter (chapter 5) will test the between-session reliability of BMI, ADP and BIA in order to determine the expected error of each measure. Furthermore, the ability of BIA and BMI to define children as obese will be

tested against ADP (considered the criterion measure of body fat). The results will provide the method for determining obesity (BMI) or adiposity (ADP or BIA) in the main study chapter (chapter 8).

4.1.2 Literature Review Chapter 1 (Chapter 2), Aim 2

The need to study the links between childhood obesity with foot and lower limb biomechanics was demonstrated by the literature review sections on the aetiology, musculoskeletal co-morbidities, gait biomechanics and obesity management sections in literature review chapter 1 (chapter 2). Childhood obesity is a growing problem, with the prevalence in England doubling over the previous decade. Of particular interest to this thesis is the higher incidence of obesity in the borough of Newham where participants for the study were to be recruited. Recent data suggests that children in Newham are more likely to be obese compared to the rest of England. This information highlights the need to understand the links between childhood obesity with lower limb and foot biomechanics in Newham.

The aetiology of childhood obesity is multifaceted, but in simple terms it arises from an energy imbalance. Physical activity is a key factor for energy expenditure and low participation in physical activities such as walking has been linked to future incidence of obesity. It has been suggested that to reduce childhood obesity a minimum level of physical activity should be prescribed. However, obese children can find walking painful and discomforting which reduces motivation to be physical active. The precise reasons for this are unclear but may relate to altered musculoskeletal structure which can manifest in orthopaedic conditions such as slipped capital femoral epiphysis, Blount's disease and pes planus.

Musculoskeletal development relies on weight bearing activities such as walking to provide appropriate forces for adaption and growth of lower limb and foot structures. The dynamic nature and forces that act on the lower limb joints during gait can lead to altered alignment and potential structural damage of the lower extremity joints in obese children. Biomechanical analysis of obese children's gait has shown altered spatiotemporal as well as lower limb kinematic and kinetic parameters. However, few studies have examined the relationships between lower limb and foot biomechanics during gait and obesity. Knowledge of these relationships can form a basis to explore interventions to prevent abnormal joint motion or forces during gait. Two such interventions may seek to improve muscular strength or reduce pronation in pes planus. The long term goal is to improve obese children's gait

parameters to reduce pain and discomfort and increase physical activity. The hope is that musculoskeletal maladaptations from the carriage of excessive mass can be corrected and will lead to an increase in physical activity which could reduce body fat and thus the health co-morbidities associated with obesity.

Further research is required to investigate the relationships between childhood obesity and altered gait biomechanics. These relationships may provide a better understanding of the links between childhood obesity, reduced physical activity, abnormal musculoskeletal development and risk orthopaedic conditions. The main study (chapter 8) will examine the relationships between childhood obesity with foot and lower limb biomechanics during gait.

4.2 Aims of Literature Review Chapter 2 (Chapter 3)

In order to measure lower limb and biomechanics a literature review of three-dimensional (3D) motion analysis was carried out in literature review chapter 2 (chapter 3). As well as defining the process of capturing motion and applying biomechanical models to calculate kinematic and kinetics the errors of such techniques are considered. The aims of this chapter were to: (1) to demonstrate the need to understand between-session reliability and the affect of obesity on lower limb biomechanics, and (2) review currently used foot models to determine the most appropriate to determine the relationships between adiposity and foot biomechanics based on reliability and segmentisation.

4.2.1 Literature Review Chapter 2 (Chapter 3), Aim 1

Biomechanical modelling of the human body involves the application of reflective markers to anatomical landmarks to track of body segments which are reconstructed to calculate joint biomechanics. The findings of the literature review showed that biomechanical modelling of obese individuals is affected by palpation and tracking of anatomical landmarks due to soft tissue artefact. Soft tissue artefact describes the motion of markers irrespective of the osseous structures which causes errors in kinematic and kinetic measurements. A particular issue surrounds the anterior superior iliac crest (ASIS) marker positions which can be misplaced by excessive adipose tissue. These findings indicate the need to develop protocols to measure biomechanics of obese children which reduces soft tissue artefact.

A further consideration of biomechanical modelling of the human body is between-session reliability of the kinematic and kinetic measures. Reliability is the extent to which measurements are consistent and free from error (Portney & Watkins, 2000). To determine biomechanical relationships between the lower limb and foot with obesity the assessment of 3D motion capture is required to be reliable. Quantifying reliability and error from repeated tests gives a measure of the expected variance and its sources. A large of source of variance is the application of reflective markers which is subject to human error from the identification and placement of anatomical markers. A key finding from previous studies on the reliability of the conventional lower limb model (PiG) is the placement of the thigh marker to determine hip and knee joint centres and 3D motion. There is a need to determine the use of protocols to reduce marker placement error and improve between-session reliability of the conventional lower limb model (PiG).

In order to determine the relationships between childhood obesity with lower limb biomechanics and gait between-session reliability and validity of the conventional lower limb model (PiG) needs to be tested. Experimental chapter 2 (chapter 6) will test between-session reliability and examine the use of methods to determine ASIS marker and thigh marker placement in obese children. The findings of this experimental chapter will potentially reduce marker placement and soft tissue artefact error.

4.2.2 Literature Review Chapter 2 (Chapter 3), Aim 2

With no conventional biomechanical model to measure foot segment motion many foot models have been designed. The variety of available foot models mean the foot can be segmented according to the area of the foot of interest. Sophisticated foot models can divide the foot into eight segments allowing users to pin-point areas that may be affected by pathology. However, these models suffer from lower reliability due to the amount of markers placed in a relatively small area and the amount of assumptions required to model smaller segments. There is a need to investigate the most appropriate foot model to measure foot biomechanics during gait. The primary emphasis of foot model selection is on extracting the most amount of information on foot motion which comes from greater segmentation of the foot. However, prior to adopting a sophisticated foot model the secondary emphasis is on reliability. By adopting this approach the foot model that provides the most reliable information can be selected in order to determine the relationships between childhood

obesity and foot biomechanics. Experimental chapter 3 (chapter 7) examines the between-session reliability of available foot models with a range of foot segments.

5. Experimental Chapter 1: Measurement of Obesity

5.1 Introduction

In order to investigate the relationships between childhood obesity with lower limb and foot biomechanics an accurate and reliable measure of obesity is required. Ulijaszek & Kerr (1999) defined reliability as between-session variability taking into account measurement error (precision) and biological variation. Precision is the variability of repeated measures due to within-and between-rater measurement differences. Measuring reliability can identify the source of error and improve measuring techniques. Large error in measurement precision can mask true biological differences meaning group differences may be lost. Therefore, it is important to determine the precision of anthropometric (height, body mass and BMI) and percentage body fat mass (%FM) measures in the sample population.

Adiposity is the accumulation of body fat mass which can be measured using two-compartment models (fat mass and fat free mass) validated against 'gold standard' measures of body composition (four-compartment models). Air displacement plethysmography (ADP) and bioelectrical impedance analysis (BIA) are measures of body fat mass percentage which rely on the underlying assumption regarding the hydration status of the lean tissues of the body. Fields & Goran (2000) demonstrated the accuracy of ADP in 25 children (age range 9-14 years) against the 4-C model with r^2 values of 0.97 and standard error the estimate of 1.7kg. Sun et al., (2003) determined the accuracy of BIA in subjects (age range 12-94 years) against the 4-C model with r^2values of 0.90 and root mean squared error (RMSE) values of 3.9kg.

Both ADP and BIA methods of determining adiposity were tested for reliability and agreement for use in the main study (chapter 8). Measures of %FM by ADP were determined to be the standard method in the current study against which BIA measures were compared as they show better agreement with 'gold standard' methods (Azcona et al., 2006). Measures of body fat mass by BIA offered a more mobile method of measuring the participants in the main study (chapter 8) which would reduce testing time. However, if BIA was to be utilised in the main study (chapter 8) it must demonstrate acceptable between-session precision and reliability and also agreement with %FM from ADP.

Previous studies that have examined gait characteristics of obese and non-obese children have defined groups based on BMI Z-Score (Gushue et al., 2005; McMillan et al., 2009 & 2010; Shultz et al., 2009). Children were assigned to an 'obese' or 'non-obese' group according to BMI Z-Score cutoffs referenced to age- and gender-specific curves from which mean

biomechanical data from each group was compared. However, this may lead to a type II error (false negative) because groups defined by BMI Z-Score may mislabel children as non-obese when they are obese due to low sensitivity of BMI Z-Score to identify children with high body fat mass (Reilly et al., 2000).

Furthermore, studies that have examined relationships between health risks and childhood obesity have determined obesity by BMI Z-Score on a continuous scale (Williams et al., 1992; Dwyer & Blizzard, 1996; Higgins et al., 2001; Bell et al., 2007). This removes error in mislabelling a child as obese or non-obese but instead relies on BMI Z-Score being an acceptable indirect measure of body fat mass. However, BMI Z-Score may not be the ideal measure to define obesity in children because previous studies have demonstrated only a moderate correlation between BMI Z-Score and body fat mass in children (Williams et al., 2007).

5.2 Aims

The aims of this experimental chapter were to;

(1) Determine between-session reliability of anthropometric measures (for BMI calculation) and %FM measures in boys
(2) Measure agreement between %FM estimates from ADP and BIA to establish the appropriate method to define adiposity
(3) Demonstrate the sensitivity and specificity of BMI Z-Scores to define obese and overweight groups
(4) Demonstrate the relationship between BMI Z-Score and %FM as continuous variables.

In order to answer aim 1 anthropometric (height, body mass and BMI Z-Score) and %FM (BIA and ADP) measures will be tested for between-session reliability, calculated by total error of the measurement (TEM) and the coefficient of reliability (*R*). Agreement between ADP and BIA %FM measures will be measured by Bland & Altman plots to answer aim 2. Both generic (manufacturers) and child specific ADP and BIA %FM prediction equation will tested for agreement with the selected %FM measure from aim 2. To answer aim 3 the sensitivity and specificity of BMI Z-Scores to categorise boys as overweight and obese will calculated against the number of boys categorised as overweight and obese by %FM. Aim 4 will be answered by

determining the relationship between BMI Z-Score (as a continuous variable) and %FM by linear regression analysis. The strength of the association between BMI Z-Score and %FM will be determined by the coefficient of determination (R^2).

5.3 Methods

5.3.1 Participants

Ethical approval was granted by the University of East London Research Ethics Committee (Ref No. ETH/13/11). Following ethical approval local school, after school clubs and children of university staff were invited to participate in the research. Teachers were approached based on a convenience sample of schools taking part in higher education activities at the University of East London. Two local schools, a football club and 10 children of university staff agreed to participate in the study, of which approximately 90 boys were invited to participate in the research. Consent forms and information documents were distributed for boy's parents/guardians, only boys with completed consent forms being allowed to take part. Informed consent was obtained from each participant's parent/guardians and verbal consent was also ascertained from each child.

The participants recruited for this experimental chapter were selected to represent a range of %FM. In total 82 boys (age 6-13 years old) participated in this study. Not all participants took part in every test during this study. Seventy two boys took part in the regression analysis between BMI Z-Score and body fat mass (measured from ADP) and the BMI Z-Score specificity and sensitivity analysis. Ten participants took part in the between-session reliability analysis of ADP and BIA measures. Twenty boys participated in the between-session reliability of anthropometric measures. The number of participants in each test is presented in (Tables 5.3, 5.5, 5.7 and 5.8).

Bias may have been introduced in the recruitment of boys from the convenience sample. Boys most likely to engage in activity and accept exposing their upper body and legs during testing protocols would potentially be more willing to take part in the research. This may under-sample boys with higher body fat mass compared to the local area. Future work should consider approaching obesity clinics with intention of obtaining a random sample of participants which could be matched (by age and height) to non-obese controls.

5.3.2 Inclusion/Exclusion Criteria

Consenting participants were included in the research if they were typically developing boys between the age of 6 and 13 years old. Exclusion criteria included if the child reported to be unwell or with fever, had surgery or chronic illness. Furthermore, any medical conditions affecting neuromuscular and orthopaedic integrity or any complications contributing to altered foot posture and/or gait disturbance. A copy of the health medial questionnaire and consent forms can be found in appendix II and III.

5.3.3 Testing Protocols

Each participant wore tight fitting swimming shorts with no shoes or socks throughout the procedures. Participants were instructed not to eat or exercise two hours before the measurement and to void their bladder 30 minutes before testing. Each child's height, weight, ADP and BIA were measured shortly after each other to avoid biological variation. Participants were tested in pairs and randomly assigned to be tested by either ADP or BIA first after which they swapped so half the participants were first measured by ADP and then BIA and the other half vice versa. Estimates of body fat mass by ADP and BIA were measured within the same day by the same observer (rater). The repeated test was within 10 minutes of the first in order to avoid biological variation in hydration and temperature. Anthropometric measures of height and mass were measured over repeated sessions across a two week period. The two week retest period was implemented so the observer (rater) would not remember participant height and mass between sessions thereby artificially increasing reliability.

5.3.3.1 Anthropometric Measures

Height was measured to the nearest 0.5cm using a stadiometer (Hadlands Photonics, Australia). Height is the maximum distance from the floor to the highest point of the head with the participant looking straight ahead. The participants were asked to stand straight with back, buttocks and heels against the stadiometer with feet together and flat on the floor. The participants were asked to take and hold a deep breath whilst looking straight ahead. Height was recorded at the end of the participants' deep inward breath.

Weight was recorded using the electronic weighing scales integrated within the Bodpod body composition device (Life Measurement, Inc, Concord, CA, USA) procedure. Participants were

asked to stand on the centre of scales, without support and with their weight distributed evenly on both feet. Body mass index (BMI) was calculated by Quetelet's index (weight in kg/height^2 in m).

Body Mass Index Z-Score (BMI Z-Score) was input into LMSgrowth software (Harlow Healthcare, South Shields, UK). The software calculates the BMI Z-Score and BMI Centile, from height and body mass inputs, based on reference data from the United Kingdom 1990 (UK90) data set (Cole et al., 1995) and International Obesity Task Force data set (Cole et al., 2000).

5.3.3.2 Air Displacement Protocols

Air displacement plethysmography (ADP) was measured using the Bodpod device following manufacturer's protocols (Dempster & Aitkens, 1995). Each participant wore a swim cap to cover and compress head hair. The Bodpod weighing scale was calibrated before each testing session with known 20kg weights; all calibrations were within ±0.01kg (deemed acceptable by the Bodpod manual, 2004). The chamber was calibrated against a known volume cylinder (50.024l) before each testing session. Five repeated measures of cylinder volume were made during the calibration procedure; the average estimated volume was 50.047 ± 0.007l. These are within the accuracy and variability range of repeated measures previously reported for volumetric measures by the Bodpod (Dempster & Aitkens, 1995).

The ADP procedure involved three successive measurements of raw body volume, the total procedure time was less than one minute. If body volume differed by more than 0.015l between the measures the procedure was repeated. The mean of the three raw body volumes (V_b) was corrected for isothermal conditions of air in the lungs and around the skin surface. Two correction methods were applied to the raw V_b for analysis; ADP_{Man} corrected raw V_b based on the manufacturer's equations that were implicit in the procedure (Siri, 1961); ADP_{Child} corrected raw V_b based on gender and age specific equations from the literature (Haycock et al., 1978; Lohman, 1989; Fields et al., 2004). Thoracic gas volumes (TGV) were estimated from gender and child specific equations (Fields et al., 2004) and took the form:

$$0.00056Ht^2 - 0.02442Ht + 8.15194 \quad (2)$$

Where Ht is height measured in centimetres (cm). Skin surface area (SAA) was estimated from child specific equations (Haycock et al., 1978) of the form:

$$(0.024265Wt^{0.5378})(Ht^{0.3964})100 \quad (3)$$

Where Wt is body mass measured in kilograms (kg).

Corrected body volume was converted to percentage body fat mass (%FM) by the gender and age specific equations published by Lohman (1989):

$$100[(\frac{k_1}{D_b}) - k_2] \quad (4)$$

Where D_b is body density (Wt/V_b) and k_1 and K_2 are gender and age specific constants.

5.3.3.3 Bioelectrical Impedance Analysis Protocols

A multi-frequency BIA device (Quantum II, RJL systems, Inc. Clinton Township, Michigan, USA) was used to measure body impedance in the participants. The BIA device was calibrated before each testing session using known resistance and reactance. The device recorded mean resistance figures of 383.6 ± 0.34Ω and reactance of 44.9 ± 1.22*X* which were with the manufacturer's guidelines.

The participants were instructed to lay supine on a portable couch for five minutes prior to testing as per the manufacturer's instructions to allow extracellular water to level out across the body. Figure 5.1 shows electrode's placement on the ipsilateral bony prominences of the wrist and ankle (metacarpal and metatarsal lines) ensuring the electrodes were 5 cm apart.

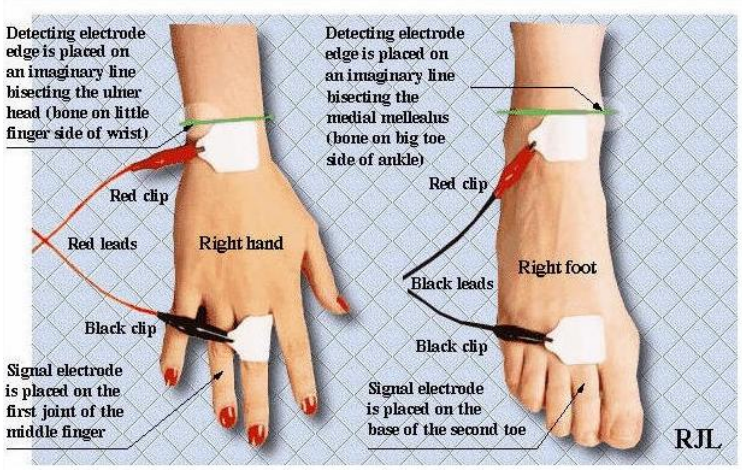

Figure 5.1. Bioelectrical impedance analysis electrode placement. http://www.rjlsystems.com

Reactance (*X*) and resistance (Ω) were outputted for each participant for calculation of %FM based on gender and age specific equations BIA_{child} and the manufacturers equations BIA_{man}. The equation of Horlick et al., (2002) was chosen to estimate %FM based on regression analysis of impedance measures from the same RJL device used in the current study, this equation has the following form:

$$FFM = \frac{(3.474 + 0.459\frac{Ht^2}{\Omega} + 0.140Wt)}{(0.769 - 0.009A - 0.016S)} \quad (5)$$

Where FFM is fat free mass, Ht is height (cm), R is resistance, Wt is body mass (kg), A is age (years) and S is gender (1 for male and 0 for female). To calculate %FM the following formula is used:

$$\%BF = \frac{Wt - FFM}{Wt}100 \quad (6)$$

5.3.4 Statistical Analysis

In order to carry out the parametric test of coefficient of variation the normality and homogeneity of each variable from the sample must be tested. Shapiro-Wilk test compare the distribution of the variables in this study to a normal distribution with the same mean and standard deviation. If the test is non-significant (p>.05) the distribution is not significantly

different from a normal distribution. Homogeneity is the measure of the variance between variables being studied. The variance of one variable should be stable at all levels of the other variables (Fields 2009). This is tested by a Levene's test. If the test is non-significant (p>.05) then the assumption of equal variance is tenable.

5.3.4.1 Between-Session Reliability Analysis

Precision for between-session repeated measures of anthropometric and %FM values were assessed by the technical error of measurement (TEM):

$$TEM = \sqrt{\frac{(\sum d^2)}{2n}} \tag{7}$$

Where d is the difference between measurements and n is the number of individuals measured. This absolute value of precision is given relative to the mean of the variable being analysed:

$$\%TEM = \left(\frac{TEM}{x}\right) 100 \tag{8}$$

This gives a measure of the coefficient of variation (CV) which can be used to compare precision across studies. Another approach to compare precision across studies is to use the coefficient of reliability (R) using the following formula (Ulijaszek & Kerr 1999):

$$R = 1 - \left(\frac{total\ TEM^2}{SD^2}\right) \tag{9}$$

This formula reveals the proportion of between-session variance in the population which is free from measurement error. Measures of R can be used to compare relative precision of different measurements and calculate sample size. An alternative approach is to measure reliability by Intra-class correlation coefficients (ICC) from the proportion of estimated true variance to the measurement error associated with it (Shrout & Fleiss 1979). However, R is the

most widely used measure of reliability in anthropometric studies and is therefore, used in the current study to aid comparison with previous work (Ulijaszek & Kerr 1999).

5.3.4.2 Agreement between %FM Measures of ADP and BIA

Agreement between prediction measures of %FM was analysed using Bland & Altman analysis (Bland & Altman, 1986). Bland & Altman analysis involves the calculation of the mean difference between two methods together with Limits of Agreement (LoA), based on 95% confidence intervals (95%CI), calculated from the SD of the mean difference for each participant (multiplied by 1.96). Bland & Altman plots give a visual assessment of the agreement between two measures; a large mean difference indicates a large bias (over- or under-estimation) and wide LoA refer to large variation between measures. The method of predicting %FM by ADP_{child} was used as the reference to which ADP_{man}, BIA_{child} and BIA_{man} were compared to previous findings of greater reliability and validity (Gately et al., 2003; Vicente-Rodriguez et al., 2012). Measures of %FM by BIA offer a more mobile method of measuring the participants in the main study (chapter 8) which will reduce testing time. However, in order for BIA to be utilised in the main study (chapter 8) it must demonstrate agreement with %FM from ADP.

5.3.4.3 Specificity and Sensitivity of BMI to Identify Childhood Obesity

Sensitivity was defined as the percentage of obese children (from %FM measured by ADP_{child}, based on the %FM reference data set and cutoff of McCarthy et al., 2006) classified as such by BMI Z-Score. Specificity was defined as the percentage of non-obese children (ADP_{child} with data set from McCarthy et al., 2006) classified as non-obese by BMI. Of the 72 children who participated 15 were classified as obese by ADP_{child} and McCarthy et al., (2006) data set and are therefore the true positives. The sensitivity of BMI Z-Scores was calculated by the sum; 100 multiplied by the number of participants defined as obese according to either the UK90 or IOTF data sets, divided by the number of true positives based on ADP_{child} with McCarthy et al., (2006) data set. This was repeated with the definition of obesity replaced by overweight. The specificity of BMI Z-Scores was calculated by the sum; 100 multiplied by the number of participants defined as not obese or overweight by according to either the UK90 or IOTF data sets, divided by the number of true negatives based on ADP_{child} with McCarthy et al., (2006) data set.

5.3.4.4 Linear Regression Analysis of %FM (ADP_{child}) and BMI Z-Score

In order to check the assumptions of random error and homoscedasticity of the model a plot of the standardised predicted values of %FM against the standardised residuals was produced. If the regression model fits the sample data well all data points fall on the regression line and the residuals would be zero (Field, 2009). A histogram of the regression standardised residuals should appear as a normal distribution (bell-shaped curve). Furthermore the normal probability plot shows deviations from normality by plotting the observed residuals against a straight line (representing a normal distribution). All checks on the assumptions of the regression model were compared with published plots in Field (2009)

Linear regression was utilised to determine the relationship between %FM, using the standard measure of this study (ADP_{child}), and BMI Z-Score as a continuous variable. The strength of the association between %FM and BMI Z-Score was determined by the R^2 value. A quadratic term was entered into the linear regression model to assess if the proportion of variability in %FM was increased. The model (linear or quadratic) that represented the best-fit (i.e. highest r^2) was chosen to give the greatest explanatory power between %FM and BMI Z-Score. Significant associations between %FM (ADP_{child}) and BMI Z-Score were reported (p<0.05).

5.4 Results

5.4.1 Normality and Homogeneity

Shapiro-Wilk test for normality, presented in Table 5.1, showed that BMI centile scores were not normally distributed (P<0.05), but all other variables were normally distributed. No parametric tests were conducted with BMI centile. The Levene's test for homogeneity was non-significant (p>0.05) indicating that all variables demonstrated similar variance, shown in Table 5.2.

Table 5.1 Shapiro-Wilk test for normality on anthropometric and body composition variables. Significance $p<.05$

	Shapiro-Wilk		
	Statistic	df	Sig.
Height	.985	71	.741
Weight	.964	71	.054
BMI	.961	71	.054
Z-score	.973	71	.288
Centile	.858	71	.000*
BIA_{man}	.977	70	.402
BIA_{child}	.984	70	.710
ADP_{man}	.955	71	.500
ADP_{child}	.962	71	.093

Table 5.2 Levene's test for homogeneity of variances on anthropometric and body composition variables. Significance $p<.05$

Levene Statistic	df1	df2	Sig.
.394	8	560	.757

5.4.2 Aim 1: Between-Session Reliability Analysis

Precision of four prediction equations for the estimation of %FM by ADP and BIA are presented in Table 5.4. Precision of the estimates of body fat mass by BIA_{man} and BIA_{child} were less than ADP_{man} and ADP_{child} defined by the technical error of measurement (TEM%) and coefficient of reliability (R). Precision (TEM% and R) of the child specific ADP and BIA estimates of body fat mass were higher than the manufacturer's estimates. Estimates of body fat mass by BIA_{man} were higher than ADP_{child}, ADP_{man}, with BIA_{child} the lowest.

Table 5.3. Mean, SD and range of physical characteristics of %FM reliability sample (n=10)

	Age (years)	Height (m)	Mass (kg)	BMI (height/mass^2)	BMI Z-score	BMI centile (%)
Mean	10.00	1.38	33.77	17.07	0.12	52.01
SD	2.55	0.17	10.84	1.87	0.80	23.44
Range	7 – 13	1.16 – 1.67	21.20 - 49.60	13.99 - 20.61	-1.14 – 2.00	12.63 - 97.75

Table 5.4. Mean, SD and within-day test re-test for between-session reliability of %FM measures (n=10)

Method	Mean (%FM)	SD (%FM)	TEM (%FM)	TEM%	R
% BF BIA_{man}	19.68	8.53	0.86	4.37	0.990
% BF BIA_{child}	10.40	8.84	0.75	7.21	0.993
% BF ADP_{man}	12.68	8.70	0.53	4.12	0.996
% BF ADP_{child}	13.70	8.46	0.55	4.01	0.996

All anthropometric measures were highly reliable demonstrating low error values (see Table 5.6). Repeated height measures were more precise (TEM%) than mass and BMI, but between-session reliability was high for all three measures.

Table 5.5. Mean, SD and range of physical characteristic of height, weight and BMI reliability sample (n=20)

	Age (years)	Height (m)	Mass (kg)	BMI (height/mass^2)	BMI Z-score	BMI centile (%)
Mean	9.13	1.34	31.30	16.90	0.24	55.42
SD	2.48	0.15	9.00	1.84	0.94	25.79
Range	6 - 13	1.15 - 1.67	21.00 - 49.60	13.99 - 20.85	-1.69 - 2.34	4.57 - 99.04

Table 5.6. Mean, SD and between-day between-session reliability of anthropometric measures (n=20)

Anthropometric measures	Mean	SD	TEM	TEM%	R
Height (m)	1.34	0.15	0.002	0.15	0.999
Mass (kg)	31.30	9.00	0.094	0.30	0.999
BMI (kg·m^2)	16.90	1.84	0.085	0.50	0.998

5.4.3 Aim 2: Agreement between %FM Measures of ADP and BIA

Agreement between ADP and BIA measures was explored to determine the appropriate measure of %FM to be utilised in the main study (chapter 8) of the research. Figure 5.2 presents Bland & Altman plots for BIA_{man}, BIA_{child} and ADP_{man} against the 'standard' measure of %FM for this study, ADP_{child}. Mean difference against ADP_{child} between methods of determining %FM (± limits of agreement) was -0.56 ± 1.26%, -2.54 ± 6.61% and 3.77 ± 6.26% for ADP_{man}, BIA_{man} and BIA_{child} respectively. These findings indicate that ADP_{man} and BIA_{man} overestimate %FM in this sample, but limits of agreement are wider for BIA_{man}. In contrast

BIA_{child} underestimates %FM but demonstrates wider limits of agreement of similar value to BIA_{man}.

Table 5.7. Mean, SD and range of physical characteristics of sample for agreement between %FM and BMI measures (n=71)

	Age (years)	BIA_{man} (%FM)	BIA_{child} (%FM)	ADP_{man} (%FM)	ADP_{child} (%FM)	BMI (height/mass^2)	BMI Z-score	BMI centile (%)
Mean	10.01	24.26	17.96	22.29	21.73	18.71	0.63	63.19
SD	1.67	8.74	9.19	9.17	9.00	3.67	1.45	33.96
Range	7 - 13	6.67 - 49.65	-1.04 - 40.96	9.46 - 42.79	7.69 - 42.89	12.34 - 29.63	-2.87 - 3.54	0.21 - 99.98

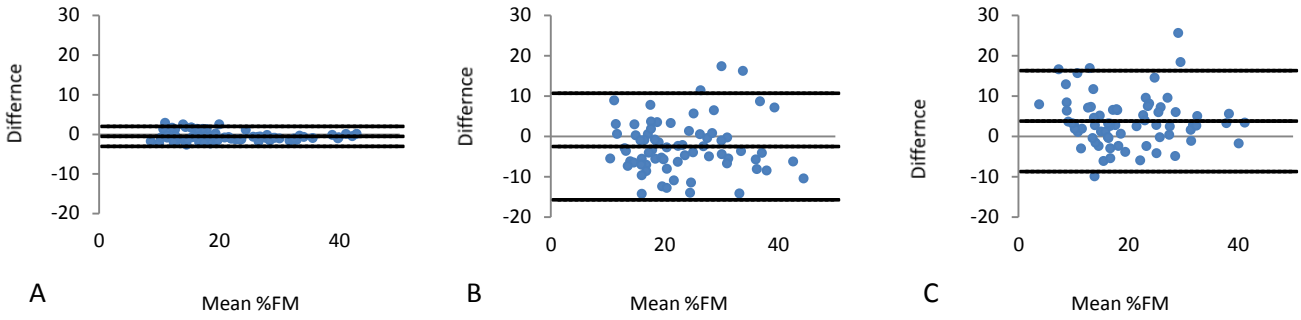

Figure 5.2. Bland & Altman plots comparing %FM determined by ADP_{child} with (A) %FM by ADP_{man}, (B) %FM by BIA_{man} and (C) %FM by BIA_{child}.

5.4.4 Aim 3: Demonstrate the Specificity and Sensitivity of BMI to Identify Obesity against the Standard Measure of %FM

The specificity and sensitivity analysis of BMI demonstrated greater sensitivity of UK90 obesity and overweight definition compared to the IOTF definition. However, specificity of the IOTF definition is greater than the UK90 definition as can be seen in Table 5.9. This means that more obese boys (measured by ADP_{child} %FM) were correctly identified as obese by BMI Z-Score according to UK90 the definition. However, more non-obese boys (measured by ADP_{child} %FM) were correctly identified as non-obese by BMI according to the IOTF definition. The results show that if participants were grouped by obesity defined by either IOTF or UK90 cutoffs 53.33% and 27.67% of boys who are obese will be classified as non-obese compared to obesity defined by measures of body fat mass (ADP_{child}).

Table 5.8. Mean, SD and range of physical characteristics of sample for specificity and sensitivity of BMI analysis and linear regression analysis of %FM *(ADP_{child})* and BMI Z-Score (n=72)

	Age (years)	Height (m)	Mass (kg)	BMI (height/mass^2)	BMI Z-score	BMI centile (%)	%FM	%FM Z-score	%FM centile
Mean	10.06	1.43	39.37	18.69	0.63	63.32	22.34	0.34	60.86
SD	1.69	0.11	11.15	3.65	1.44	33.74	9.12	1.75	37.37
Range	7 - 13	1.20 – 1.73	22.3 - 68.6	12.34 - 29.63	-2.87 - 3.54	0.21 - 99.98	9.46 - 42.79	-5.06 - 2.57	0 - 99.5

Table 5.9. Sensitivity and specificity (expressed as a percentage) of obesity by IOTF and UK90 reference data against %FM measured by ADP_{child} and McCarthy et al., (2006) references curves.

	Sensitivity (%)	Specificity (%)
IOTF		
Obesity	46.67 (7/15)	96.49 (55/57)
Overweight	69.57 (16/23)	81.63 (40/49)
UK90		
Obesity	73.33 (11/15)	84.21 (48/57)
Overweight	78.26 (18/23)	73.47 (36/49)

5.4.5 Aim 4: Demonstration of the Relationship of %FM (ADP_{child}) and BMI Z-Score by Linear Regression Analysis.

Physical characteristics of participants in this study are reported in Table 5.8. Figure 5.3 shows the histogram of the standardised residuals, the distribution appears to form a bell-shaped curve. The normal probability plot represents normal distribution as all points a close to the line. The scatter plot of standardised residuals against standardised predictor value shows a random dispersion of points demonstrating homoscedasticity.

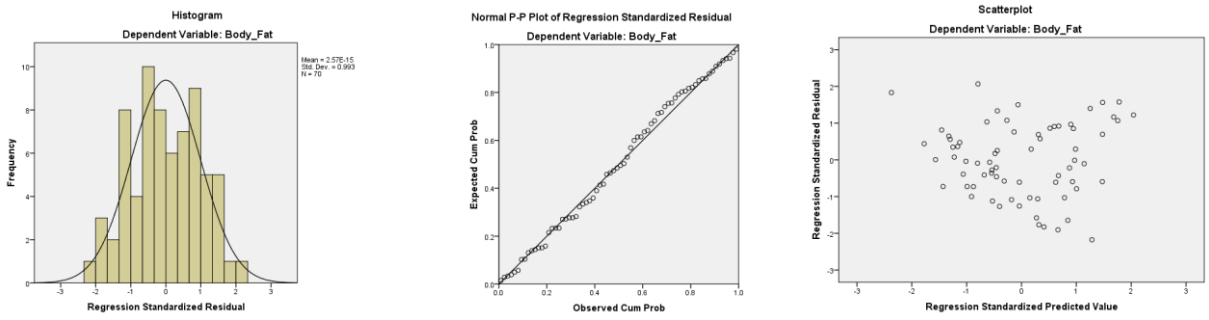

Figure 5.3. Histogram of standardised regression residual, normal probability plot and plot of standardised predicted values against standard residuals for %FM (ADP_{child}) and BMI Z-Score regression model.

Table 5.10 shows that the quadratic term for BMI Z-Score explained more the variance with %FM in this sample population (r^2 = 0.45 and 0.34 for BMI Z-Score^2 and BMI Z-Score respectively). Linear regression analysis reveals a curvilinear relationship between %FM (derived from ADP_{child}) and BMI Z-Score, shown in Figure 5.4. BMI Z-Score explained 42% (r^2 0.45) of the variance in body fat mass (p<0.001, Table 5.11).

Table 5.10. BMI Z-Score Linear and quadratic terms for regression model with %FM. a. Predictors: (Constant), BMI Z-Score^2. b. Predictors: (Constant), BMI Z-score

Model	r	r Square	Adjusted r Square	Std. Error of the Estimate
1	.673[a]	.453	.446	7.02
2	.583[b]	.340	.330	7.36

Table 5.11. Regression model of BMI Z-Score^2 and %FM. Significance p<0.05

Model		Unstandardised Coefficients		Standardized Coefficients		
		B	Std. Error	Beta	t	Sig.
1	(Constant)	17.07	1.05		16.19	.000
	BMI Z-Score^2	2.03	.282	.657	7.18	.000

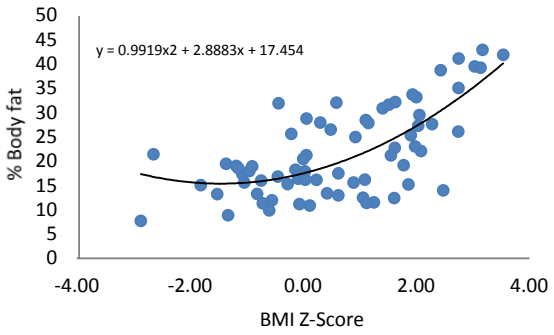

Figure 5.4. Scatter plot and regression line of %FM ADP_{child} and BMI Z-Score

5.5 Discussion

The aims of this phase were to; (1) measure between-session reliability of anthropometric measures (for BMI calculation) and %FM measures in boys, (2) determine the appropriate method (ADP or BIA) and prediction equation (generic or child specific) for measuring %FM, (3) demonstrate the sensitivity and specificity of BMI Z-Scores to define obese and overweight children groups, and (4) demonstrate the agreement between BMI Z-Score and %FM as continuous variables. The findings of these analyses are compared to previous studies.

5.5.1 Between-Session Reliability Analysis

To compare precision and reliability of ADP and BIA a between-session, within-rater study design was implemented with the aim to examine methodological error and minimise biological and environmental variation. In order to minimise instructor memory of height and mass measurements anthropometric measures were taken between-days. The findings of this study indicate that %FM measured by ADP is a more reliable method for estimating %FM compared to BIA. Of the two ADP equations to estimate %FM both demonstrated similar precision as measured by the technical error of the measurement (TEM) (Ulijaszek & Kerr 1999).

In comparison to other studies examining the between-session reliability of ADP in children, the results of this current study present consistent findings. Wells & Fuller (2001) measured %FM in thirteen boys age 5 to 14 years old by ADP in a within-day repeated measures design study. The authors presented precision as $[(SD/n)/d^{-1/2}]$ (where n is the sample size and d the number of repeated measures). They found absolute precision of 0.83% or 6.6% (relative to mean %FM), concluding that this indicates good precision of body composition by ADP. The current study's estimation of %FM by ADP_{child} resulted in greater precision compare to Wells & Fuller (2001); with slightly lower absolute (0.69%) and relative precision (5.0%).

The difference in precision (TEM and %TEM) and between-session reliability (R) between ADP_{child} and ADP_{man} were relatively small because each prediction equation relied on the exact same raw body volume measures to estimated %FM. The small differences that were found were most likely due to the use of height and weight measures in the calculation steps for thoracic gas volume (TGV) and skin area artefact (SAA). Variation in height and weight measures between sessions will alter the results of between-sessions TGV and SAA formulas producing slight deviations between ADP_{child} and ADP_{man}.

Vicente-Rodriguez et al., (2012) measured between-session, within-rater reliability of ADP measures of %FM in 84 adolescents (13-17 years old), finding TEM of 1.07% FM and an R value of 0.989. The current study found greater precision (TEM of 0.55% FM) and greater reliability (R of 0.996) using ADP_{child}. Better precision in the current study may be due to greater participant homogeneity because Vicente-Rodriguez et al., (2012) measured %FM in males as well as females across a broader range of body fat mass levels. Higher between-session reliability in the current study is related to a smaller variation in measures (SD = 8.46%) compared to Vicente-Rodriguez et al., (2012) (SD = 9.96%).

Vicente-Rodriguez et al., (2012) also measured between-session, within-rater reliability of %FM estimation by BIA (BIA device = RJL/Akern, model 101) in the same sample population as described above. This study found within-rater TEM to be 0.74% FM and a R value 0.993 which are very similar to the current study's findings (TEM = 0.75% FM and R = 0.993). Both the current study and Vicente-Rodriguez et al., (2012) found BIA to be less precise and reliable compared to ADP. Vicente-Rodriguez et al., (2012) attributed this to the time difference (10 minutes) between repeated sessions. However, the authors acknowledge that changes in impedance would be small.

The between-session reliability of body fat mass measures from ADP and BIA are dependent on environmental conditions, instructor competence, and participant adherence to the procedures. Environmental variation included; pressure changes within the laboratory (from opening doors or drafts) during the procedure that can affect ADP reliability and; temperature changes in the 10 minutes between repeated measures that can affect BIA reliability. In order to maximise between-session reliability of ADP and BIA %FM measures environmental conditions were strictly monitored throughout testing procedures.

The instructor (RM) received prior training on all BIA and ADP protocols before testing procedures commenced. However, correct electrode placement on the ipsilateral bony prominences of the wrist and ankle (the metacarpal and metatarsal lines) (Akern BIA manual, 2010) can be subjective. Electrode placement variability can alter impedance readings by 4% (Houtkooper et al., 1996) and would have reduced precision and reliability in this study.

Variability due to procedural adherence includes movement of the participant in the Bodpod chamber or irregular breathing. These can cause pressure changes within the Bodpod influencing raw body volumes (Fields et al., 2002). For this reason ADP measures from Bodpod are taken in duplicate and if the raw body volumes differ by >150ml a third measure is taken.

Only if two measures are in agreement of <150ml is the mean of the two taken otherwise the procedure is started again.

For BIA testing protocols participants were asked not to eat 2 hours before testing, because eating prior to testing induces changes in hydration which can alter impedance reading by 0.6% (Fogelholm et al., 1993). This point is potentially the hardest to control for in this study because prior eating or exercise could not be accounted for before arrival for testing. BIA reliance on a controlled hydration state between repeated measures and greater instructor input could be the reason why precision and reliability of BIA was lower than ADP in this study.

Height and body mass are requirements not only for calculations of BMI Z-Scores but are also input into BIA and ADP regression equations for calculation of %FM. Furthermore, height and mass are requirements for the lower limb biomechanical model (PiG). Therefore an understanding of the between-session precision and reliability of these measures is important because anthropometric measures not only define the level of participant adiposity, but also affect the biomechanical measures being compared.

The between-session precision and reliability indices (TEM and R) of height and weight were within the range presented in a review by Ulijaszek & Kerr (1999). The review presented TEM from five paediatric weight measurement studies as 0.1-0.3kg and four height measurement studies as 0.001-0.013m. The R for repeated weight measures from seven weight measurement studies was 0.95-1.00 and height from three studies 0.93-0.99. Ulijaszek & Lourie (1997) provided anthropometric precision and reliability reference values based on age of subjects. Maximal acceptable TEM values for children were 0.04-1.19kg for weight and 0.0046-0.0076m for height. The current study's findings of height TEM = 0.002m and R = 0.999, also weight TEM = 0.094 and R = 0.999 are within these recommendations.

No acceptable values for BMI precision have been recommended, but because BMI is a composite measure, based on height and weight, precision is dependent on these two variables. Mueller & Kaplowitz (1994) reported that anthropometric measures with R values less than 0.99 will result in low R values for composite measures (i.e. BMI). High weight and height R values in the current study resulted in high R for BMI (>0.99) therefore BMI is reliable in this sample population.

5.5.2 Agreement between %FM Measures

The ability to determine %FM in participants is dependent on the validity of ADP and BIA measures. The validity of ADP and BIA has been previously reported in relation to Dual Energy X-ray Absorptiometry (DEXA), Computerised Tomography (CT), Magnetic Resonance Imaging (MRI) or multi compartment models of body composition (Kyle et al., 2004a, Fields et al., 2002). In the current study, access to these 'gold standard' methods was not available and not appropriate for the age of the participants. Therefore, ADP was reported to be the 'standard' measure of %FM in children in the current study because of previous findings of high validity with 'gold standard' measures (Azcona et al., 2006).

To validate the use of ADP in children, Wells et al., (2003) measured %FM in 28 children age 5 to 7 years old against a 'gold standard' three compartment (3C) body composition model. The study found mean difference and limits of agreement (LoA) between %FM from ADP and 3C of 0.4 ± 1.9%. The authors concluded that accuracy and LoA of ADP were high compared to 'gold standard' measures in children validating the use of ADP in a paediatric population.

Further to the validity of ADP against 'gold standard' procedures reported in Wells et al., (2003), was the use of child- and gender-specific regression equations to calculate %FM from the raw body volume measures. Gately et al., (2003) measured %FM in 30 overweight and obese children and adolescents (11 to 17 years old) by ADP_{child} and ADP_{man} against a 'gold standard' four compartment (4C) body composition model. Mean difference and LoA for %FM measured by ADP_{man} was 1.8 ± 3.5% and by ADP_{child} -0.04 ± 3.6% compared to the 4C model. This finding indicates an overestimation of %FM using adult derived manufacturer's regression equations (ADP_{man}) and a slight underestimation using child and gender specific regression equations (ADP_{child}). This study concluded that ADP_{child} equations presented better agreement with the 4C model in overweight and obese children. Therefore, ADP_{child} was considered the reference 'standard' for the current study against which agreement of %FM by ADP_{man}, BIA_{child} and BIA_{man} were compared.

In the current study, body fat mass estimates from ADP_{man} were overestimated by 0.56% with LoA of 1.26% compared to the ADP_{child} 'standard'. This overestimation has been previously found in a study on 258 children and adolescents between the age of 5 and 18 years old (Bosy-Westphal et al., 2005). In the previous study a greater overestimation of %FM from ADP_{man} was found (9.45%) with wider LoA values (4.91%) compared to the current study. This may be

a result of greater sampling variation in the study by Bosy-Westphal et al., (2005) because their participants included males and females, across and wider age range than the current study.

Bosy-Westphal et al., (2005) demonstrated the reason for overestimation of %FM using ADP_{man} by reporting estimated skin area artefact (SAA) and thoracic gas volume (TGV) values compared to ADP_{child} measures. The raw body volume from ADP are corrected for isothermal air by SAA and TGV using either predication equations based on adult values (SAA from Dubois and Dubois, 1916; TGV from Crapo et al., 1982; and %FM from Siri, 1961) or age and gender specific equations (SAA from Haycock et al., 1978; TGV from Zapletal et al., 1976; Rosenthal et al., 1993; Fields et al., 2004; and, %FM from Lohman 1989). Bosy-Westphal et al., (2005) reported that measures of SAA were underestimated (resulting in overestimation of %FM ~2.97%) from the adult based equation of Dubois and Dubois (1916) compared to Haycocks et al., (1978) equation. Furthermore, that adult prediction equations of Crapo et al., (1982) overestimated TGV in children (resulting in overestimation of %FM of ~1.86%) compared to the Zapletal et al., (1976) and Rosenthal et al., (1993) child specific equations. This resulted in and overestimation of %FM (mean 8.5%) using the adult based prediction equations compared the child age and gender specific equation in boys.

These studies established ADP_{child} as the valid reference measure for %FM in this paediatric sample and the results of the current study show that ADP_{man} should not be used to measure %FM in the main study (chapter 8). The current study's ADP_{child} estimates of %FM were used as the 'standard' to determine if BIA from manufacturers (BIA_{man}) or child specific (BIA_{child}) equations can be used to measure %FM in the main study (chapter 8). The benefits of using BIA rather than ADP to measure %FM is greater mobility allowing participants to measured in the gait laboratory (following gait biomechanical assessment) potentially reducing protocol time.

In order to examine the agreement between ADP_{child} with BIA_{man} and BIA_{child} regression equations for %FM the mean difference and limits of agreement (LoA) were presented in Figure 5.2. Body fat mass estimated from BIA_{man} was overestimated by 2.54% with LoA of 6.61%. This is in line with Azcona et al., (2006) who examined the level of agreement between ADP and BIA measures of %FM in obese (n=64) and non-obese (n=123) children and adults between the age of 5 and 22 years old. The results of Azcona et al., (2006) demonstrated a mean underestimation of -3.39% body fat mass with limits of agreement of 10.31%. This disparity between agreement of %FM from BIA and ADP between the current study (overestimation) and Azcona et al., (2006) (underestimation) is likely to be due to the ADP

regression equation used. Their study protocol used ADP_{man}, rather than ADP_{child} (used in the current study) as the reference %FM value and also an alternative BIA_{man} prediction equation (details not given). To this author's knowledge, no previous study has compared agreement between BIA_{man} and ADP_{child}. The results of the current study demonstrate that BIA_{man} regression equation cannot be used as a measure of %FM in boys due to bias and large limits of agreement.

The agreement between BIA_{child} and ADP_{child} were also assessed in the current study because previous studies have recommended the use of paediatric population-specific BIA equations to estimate %FM (Williams et al., 2007). The agreement between BIA_{child} and ADP_{child} in the current study was 3.77% (resulting in an underestimation in BIA_{child}) with LoA of 6.26%. To the authors knowledge no previous study has examined agreement between BIA_{child} and ADP_{child} estimates of body fat mass therefore, no direct comparison can be made in the literature. However, Williams et al., (2007) tested the BIA_{child} equation (same as the current study) against three other %FM equations and found that the equation underestimated %FM in 341 five year old children (mean boys %FM = 11.7%). Therefore, the results of the current and previous studies show that the BIA_{child} equation underestimates %FM.

The BIA_{child} equation used in the current and William et al., (2007) study was originally produced from refitted paediatric fat-free mass equations using BIA (RJL BIA device) and validated against DEXA (Horlick et al., 2002). This equation was tested for accuracy in children (n= 1291) across a wide range of ages (4-18 years old), ethnicities, and disease states (HIV infections). The authors of the BIA_{child} equation present the limits of agreement as high (~11%) for fat free mass (FFM) with significant errors in subgroups (i.e. 4-8 year old children). This suggests that the equation is not suitable for individual assessment of FFM in this population. The BIA_{child} (Horlick et al., 2002) equation was chosen for the current study because the regression equation was based on the same BIA device (RJL) as the current study. Variation in body composition measures between devices has been demonstrated to be the greatest factor affecting agreement with reference methods of determining body composition (Heywood, 1992). The findings of considerably lower %FM values when using the Horlick equation in Williams et al., (2007) and the current study could be result of the significant error in the equation for children between the age of 4 and 8 years. The results of the current study show that the BIA_{child} presented a bias in body fat mass estimation and large LoA in this sample of participants indicating it's inappropriateness for use in the main study (chapter 8).

5.5.3 Specificity and Sensitivity of BMI

Previous studies to compare gait biomechanics between obese and non-obese children have determined groups based on BMI Z-Score (Gushue et al., 2005; McMillan et al., 2009 & 2010; Shultz et al., 2009). This protocol may result in children being allocated to the incorrect 'obese' or 'non-obese' group due to the insensitivity of BMI Z-Score as a proxy measure of body fat mass (Freedman & Sherry, 2009). In order to show why estimates of %FM (from ADP_{child}) should be used to define the main study participants, the sensitivity and specificity of BMI Z-Score was demonstrated in the current sample of boys.

In order to calculate sensitivity and specificity of BMI Z-Score (referenced IOTF or UK90 reference data sets) to define obesity in childhood it is necessary to define obesity by %FM. McCarthy et al., (2006) produced %FM reference data-sets and cutoffs for boys and girls between the ages of 5 and 18 years old. The study sample consisted of 1985 children from the UK, measured for %FM by BIA (Tanita BIA device) using gender and age specific regression equations. Centile curves were constructed using the LMS method with the 95^{th} centile representing obesity and the 85^{th} centile overweight. In the current study %FM measures from ADP_{child} were used to define obesity in the sample. The allocation of children to obese and overweight according to %FM was compared to the allocation from BMI Z-Score from IOTF and UK90. The results of the current study were in-line with previous studies to assess the sensitivity and specificity of BMI Z-Score against %FM in children (Reilly et al., 2000; Marques-Vidal et al., 2008).

Reilly et al., (2000) measured BMI in a representative sample of 4175 seven year olds with obesity defined by two cutoffs; $\geq 95^{th}$ centile UK90 reference and the IOTFs reference equivalent to adult defined obesity of $30kg/m^2$. To measure %FM a BIA (device = Bodystat) was utilised with the use of Houtkooper et al., (1992) prediction equations for children. The top 5% of %FM in the sample population were determined to have 'excessive fatness' from which sensitivity and specificity of BMI were calculated. In the UK90 definition of BMI Z-Score obesity ($\geq 95^{th}$ centile) sensitivity was 88% and specificity was 94%. This means 173 out of 197 children that were defined as obese according to BIA (top 5% cutoff) measures were correctly identified as obese and 3526 out of 3751 children that were not obese were classified correctly. The current study found lower sensitivity (73%) and specificity (84%) than Reilly et al., (2000). This difference between the studies could be the result of different devices to measure %FM; ADP was used in the current study and BIA in Reilly et al., (2000).

In Reilly et al., (2000) the IOTF definition of obesity resulted in 46% sensitivity and 99% for boys. Marques-Vidal et al., (2008) also used McCarthy et al., (2006) %FM reference curves to examine the sensitivity and specificity of BMI (IOTF) in 2494 boys (ages 10-18 years old). This study found IOTF sensitivity and specificity values of 47.5% and 96.8% respectively compared to %FM measured by BIA (Omron device, manufacturer %FM prediction formula). The results of the IOTF BMI Z-Score definition in the current study resulted in similar sensitivity and specificity to the two previous studies, 47% and 96%.

Regardless of the reference data set and cutoff (UK90 or IOTF) all studies found high specificity and lower sensitivity. High specificity of BMI Z-Score is required as a screening tool for paediatric obesity in clinical practise so as to avoid unnecessary treatment of non-obese children. Low sensitivity has been regarded as acceptable for clinical practise as long as specificity is high Reilly et al., (2000). However, this results in some obese children (high %FM) being classified as non-obese due to lower sensitivity. Low sensitivity is a problem for the current study because the prevalence of obesity in the main study (chapter 8) would be substantially underestimated using BMI Z-Score. Reilly et al., (2000) concluded that obesity defined by BMI cannot distinguish changes in lean body mass from changes in fat mass and that %FM (adiposity) measures might provide greater confidence for future studies.

5.5.4 Relationship between %FM and BMI

The final analysis of this chapter demonstrated the potential use of BMI Z-Score as a continuous variable for use in the main study (chapter 8). This protocol removes the error from allocating participants to obese or non-obese groups but still relies on strong relationship between BMI Z-Score and %FM. A strong relationship would mean that fat mass increases proportionally to the ratio of weight to height^2 and can, therefore, be used as a proxy to infer %FM in the main study (chapter 8). However, a weak or null relationship would mean that increases in body fat mass are independent from BMI Z-Score and, therefore, inferences of body fat mass in the main study (chapter 8) cannot be made.

Bell et al., (2007) examined relationships between health complications (including reported musculoskeletal pain) with BMI Z-Scores (IOTF reference) as a continuous variable. Using regression analysis a number of co-morbidities were shown to be related to childhood BMI Z-Score. The authors noted that the majority of published work on childhood obesity and health complications have examined relationships using categorical data ('obese' and 'non-obese'

groups), based on arbitrary threshold cutoffs. Categorical-based health risks are clinically useful, but many co-morbidity risks are not defined by a simple BMI Z-Score threshold effect and may in fact demonstrate a linear or curvilinear relationship. The authors concluded that, instead of using BMI Z-Score to define obesity by category the use of BMI Z-Scores themselves should be implemented, using national data-sets. The use of national rather than international data-sets for determination of BMI-Z Scores has been recommended by Reilly (2002) as they have better biological validity (e.g. screening ability and relationship to morbidity). Therefore, the current study determined the relationship between BMI Z-Score based on the UK90 reference data set and %FM from ADP_{child}.

The results of the current study reveal that 42% of the variance in %FM is explained by BMI Z-Score in the sample. This finding is in line with Williams et al., (2007) who measured BMI Z-Score and %FM from four BIA_{child} equations in a sample of 341 five year old children. Williams et al., (2007) used Spearman's rank correlation (non-parametric linear regression) rather than linear regression to examine the links between %FM and BMI Z-Scores. The correlation from the four %FM equations ranged from 0.290 to 0.624 with BMI Z-Score (Horlick's equation presented the highest correlation). The authors concluded that in 5 year old children BMI Z-Score had little association with %FM and, therefore, cannot be used to infer differences in %FM between participants. Furthermore, Williams et al., (2007) noted a decreasing or stable relationship between %FM and BMI up to a Z-Score of 0, after which the association increased steadily. This suggests that BMI Z-Score was a good indicator of %FM for overweight and obese children, but not for healthy and underweight children.

A further study examined the relationship between BMI Z-Score and %FM using linear regression analysis. Federico et al., (2011) examined the relationship between BMI Z -Score with %FM in a sample of 361 children between the age of 6 and 12 years. The study measured %FM by skinfold thickness (SKF) using four gender and age specific prediction equations and BMI Z-Scores from CDC (US data set) reference values. A curvilinear relationship between BMI Z-Score and %FM measured by the four predication equations was reported. The curvilinear regression model resulted in R^2 ranging from 0.60 to 0.72 with stronger correlations between BMI Z-Score and %FM by SKF in the overweight/obese children. The current study presented the relationship between %FM measured from ADP using gender and age specific equations and BMI Z-Score based on UK90 (UK data set) reference values. In line with Federico et al., (2011), the current study also found a curvilinear relationship between BMI Z-Score and %FM. However, the R^2 in the current study was 0.43 which is lower than values presented by

Federico et al., (2011). This could be due to the method of determining %FM (SKF v ADP) or the reference datasets to determine BMI Z-Score (CDC, US v UK90, UK).

5.6 Limitations

Limitations of this study relate to the estimation of %FM by ADP and BIA based on assumptions of body water content and fat-free density. As children develop through childhood their body's water content decreases (from 79.0% at one year old to 74.2% at 16 years old) and bone mineral content increases (from 3.7% at one year old to 6.5% at 16 years old). This changes the density of the fat-free mass (from 1.068g/cc at one year old to 1.096g/cc at 16 years old). The child specific regression equations for %FM from body volume (ADP) attempt to control for this by including average values from children at bi-yearly intervals (Lohman, 1989). Horlick et al., (2002) also attempt to control for changes in water content by including age and gender in their BIA regression equation. However, as Lohman (1989) states various paediatric populations (defined by activity level, physique, ethnicity or disease) will have altered fat-free body density and water content, which may lead to an under- or overestimation of %FM.

Furthermore, no regression equation for %FM by BIA or ADP could be found from the literature that represents obese children whilst also accounting for age and gender while using the same BIA and ADP devices available to this current study. Studies have demonstrated that estimates of %FM in obese participants are less accurate than in non-obese (Deurenberg, 1996). This is also due to changes in the water content of the fat-free mass in obese children which are not accounted for in prediction equations. The choice of %FM regression equations used in the current study was based on published device-, gender- and age-specific equations.

Limitations relating to the specific protocols of the current study include the use of estimated thoracic lung volumes for correction of body volume using ADP. Previous ADP protocols have described the use of pulmonary plethysmography at midtidal exhalation to measure thoracic lung volume rather than use estimated values (Dempster & Aitkens, 1995). The reason for estimated lung volume over actual measurement is the high disparities between repeated measures suggesting that many children are unable to comply with the pulmonary plethysmography protocol. Bosy-Westphal et al., (2005) reported a failure in 30% of their sample to obtain measured TGV after 3 trials. Furthermore, using age specific equations for

TGV in children has resulted in negligible differences in body composition measures (Dewit et al., 2000).

A further limitation of the current study is the use of %FM estimated from ADP rather than BIA to define obese and overweight groups because measures of %FM by BIA and ADP have been shown to be significantly different (Azcona et al., 2006). The %FM reference curves and cutoffs provided by McCarthy et al., (2006) were based on BIA estimates of %FM. However, in order to examine the ability of BMI measured in the current sample of children to define groups for in the main study (chapter 8) the ADP_{child} method was used due to its ability to accurately measure %FM in boys. Lazzer et al., (2008) showed that ADP (Lohman's child specific prediction equation) measures of %FM compare better (mean bias -2.8 ± 2.9%) to reference measures (DEXA) than BIA (mean bias -6.1 ± 4.2%) in obese boys. Therefore, taking into account that compared to ADP, BIA underestimates %FM in children by a mean bias of -3.39% (Azcona et al., 2006). Sensitivity could increase to 100% (10 out of 10) for UK90 and 70% (7 out of 10) for IOTF, but specificity would decrease to 77.42% (48 out of 62) for UK90 and 88.71% (55 out of 62) for IOTF definition. This result would mean fewer children who are not obese (from %FM measures) would be classified as obese (from BMI measures). However more children who are obese would be classified as not being obese. Although the use of BIA or ADP to define obesity changes the measures of BMI Z-Score sensitivity and specificity the result is the same. Using BMI Z-Score to define obese and non-obese groups would result in the incorrect allocation of some participants.

5.7 Summary

The results of the between-session reliability tests reveal that %FM estimates from ADP are more precise and reliable than from BIA and that this finding in consistent with the literature. The use of manufacture's or child specific regression equations did not alter precision or reliability of ADP and BIA. Anthropometric measurements of height, mass and BMI were all highly precise and reliable in this sample of boys. This indicates that these results are reproducible and, therefore, %FM and anthropometric measures taken in the main study (chapter 8) would consistently define the participants.

Estimates of %FM using ADP manufacturer's regression equation were compared to age- and gender-specific regression equations of ADP, defined as the 'standard' measures of %FM for this study. The results demonstrated that the manufacturer's regression equations

overestimated %FM in this sample of boys. Furthermore, manufacturer's or child specific regression equations for BIA demonstrated an over- and underestimation of %FM. This result indicates that measures of %FM by ADP and BIA using manufacturers and gender and age specific prediction equations could not be used interchangeably in this sample of boys. Therefore the 'standard' measure of %FM (ADP_{child}) will be used to define %FM in the main study (chapter 8).

To demonstrate the issues with defining participant groups according to BMI Z-Score values sensitivity and specificity of BMI Z-Score was calculated in reference to %FM. Using either the UK90 or IOTF reference data sets for BMI Z-Score reference and cutoffs resulted in the incorrect allocation of participants into obese and overweight groups. This finding means that if participants in the main study (chapter 8) were defined by BMI Z-Score groups, the likelihood of a type II error (false negative) would increase compared to groups defined by %FM.

To further explore the use of BMI Z-Score to define participants in the main study (chapter 8), its relationship with %FM was assessed. In this sample of participants BMI Z-Score as a continuous variable explained only 42% of the variance in %FM. This result indicates that the sample of participants should not be defined according to BMI Z-Score but instead by %FM (adiposity) as a continuous variable.

6. Experimental Chapter 2: Between-Session Reliability of the Lower Limb Model in Children Age 6 to 11 Years Old

6.1 Introduction

In order to determine the relationships between childhood obesity with lower limb biomechanics and gait between-session reliability and validity of the conventional lower limb model (PiG) needed to be tested. Previous studies have quantified the reliability of paediatric gait biomechanics (Miller et al., 1996; Gorton et al., 1997; Quigley et al., 1997; Steinwender et al., 2000, Leardini et al., 2007b, Skaaret et al., 2012). The results of these studies relate to specific testing conditions and explicit study design and cannot be used to demonstrate between-session reliability in the current study. Measures of gait data reliability are intrinsically linked to the variability of the study group (McGinley et al., 2009). Therefore, the participants of this between-session reliability study should consist of paediatric participants across a range of adiposity levels. The results of the between-session reliability analysis will aid interpretation of any relationships discovered between lower limb biomechanics and childhood obesity in Chapter 8.

As well as testing between-session reliability of the conventional lower limb model (PiG) two protocols to reduce marker placement and soft tissue artefact error were be tested. A previous study by Baker et al (1999) described a protocol to reduce thigh marker placement error using a post-capture process to remove excessive frontal plane motion of the knee. Reducing marker placement errors may improve the test re-test reliability of the conventional lower limb model (PiG). Improving the reliability could, therefore, increase the likelihood of finding associations between adiposity and lower limb biomechanics if they exist. Significant differences between methods of measuring lower limb biomechanics in obese adults have been reported due to the propagation of errors from excessive soft tissue artefact. Board et al., (2012) found variability in kinematics and kinetics of the hip joint during gait using five variations of lower limb modelling. Therefore, it is important to examine measures to reduce errors due to soft tissue artefact and marker positioning.

6.2 Aims

The aims of this experimental chapter were to:

(1) Examine between-session reliability of the conventional plug-in gait (PiG) lower limb model for use in children across a range of BMI Z-Score values. These results will determine the expected error in measuring paediatric lower limb biomechanics.

(2) Test a protocol with the potential to increase PiG between-session reliability based on thigh marker placement across a range of BMI Z-Score values. Improving between-session reliability by testing marker placement protocols will give greater statistical power to detect associations between adiposity and lower limb biomechanics in the main study (chapter 8).

(3) Assess an alternative method for identifying the anterior superior iliac spine (ASIS) in obese and non-obese children. The palpation and identification of the ASIS can be difficult in obese individuals due to excessive adipose tissue. Therefore, the use of alternative marker placement and virtual markers will be tested against the conventional lower limb model (PiG) protocols

To investigate between-session reliability of the conventional (PiG) model intraclass correlation coefficients (ICCs) and standard error of measurement (SEM) will be calculated for each lower limb joint (hip, knee and ankle). Calculation of ICC and SEM will be taken over the gait cycle events (initial contact and toe off) and from peak values during the stance and swing phases. To determine the use of the thigh rotation offset protocol to improve between-session reliability of the conventional (PiG) lower limb model ICC and SEM will be calculated. A comparison between ICC and SEM before and after application of the thigh marker rotation offset will be made. To assess the alternative method for identifying the ASIS in obese children 3D hip joint motion will be extracted at gait cycle events (initial contact and toe off) and peak values during the stance and swing phase. Angular values of hip motion will be compared using the conventional and new method for identifying the ASIS between obese and non-obese children.

6.3 Methods

6.3.1 Participants

Seventeen participants (age range 6-13 years) were recruited from a convenience sample of children from university staff and an after-school club to take part in the lower limb reliability study. Ten participants, 5 obese and 5 non-obese (age range 8-11 years), were recruited from local primary schools to take part in the protocols to identify the ASIS. All participants were typically developing children and excluded if any medical conditions affecting neuromuscular and orthopaedic integrity or any complications contributing to altered foot posture and/or gait disturbance were identified. Consent was obtained from children's parents. Ethical approval was granted by University Research Ethics Committee (Ref No. ETH/13/11).

In the reliability study participants were selected to be representative of a range of weights from underweight to obese so as to demonstrate between-session reliability of the lower limb model in the expected sample population recruited in the main study (chapter 8). The participants of the ASIS protocol study were selected based on the level of adiposity. Five obese and five non-obese participants were selected to demonstrate the effects of soft tissue artefact on ASIS identification and tracking.

6.3.2 Testing Protocols

6.3.2.1 Stereophotogrammetry

A ten camera Vicon 612 (Vicon Motion Systems Ltd, Oxford, UK) system was used to capture reflective marker coordinates (sampling rate 100Hz) within the capture volume. Six cameras were mounted to the laboratory walls and four on tripods in closer proximity to the capture volume. Pilot testing of the camera positions was carried out to define the best position for the tripod cameras to capture all markers during the gait cycle in contact with the force plates. Cameras were positioned with enough proximity to collect data from many markers in a small area but not be visible to each other.

Cameras were calibrated in accordance with manufacturer's guidelines which required the capture and reconstruction of markers attached to an 'L frame' placed on the corner of one force plate to define the origin of the global coordinate system. A dynamic calibration was carried out using a 'T' frame with markers of known distances which was moved through the capture volume for a period of 10,000 frames. A successful calibration was made if residuals

from marker position and inter-distances standard deviation were less than 1mm and wand visibility exceeded 65%. The volume area calibrated was 1.5m high, 2m long (direction of walking) and 2m wide.

6.3.2.2 Force Plates

Two force plates (Bertec, Model MIE Ltd, Leeds, UK) mounted within the laboratory floor recorded ground reaction forces (1000Hz). Each force plate was switched on 30 minutes before testing and zeroed prior to calibration. Calibration was conducted with known calibration weights of 50kg placed within the centre of the force plate. Vertical ground reaction force was recorded and a correction factor applied to align the force plate reading with the correct acceleration due to gravity calculated to be -445.5N.

6.3.2.3 Anthropometrics

Anthropometric measurements were recorded including leg length, ankle width, knee width, height and mass. Leg length was measured by tape measure from a straight line between the medial malleolus and the anterior superior iliac spine. Knee and ankle width were recorded by bicondylar callipers with the participant standing. Knee width is the distance between the lateral and medial femoral epicondyles and ankle width is the distance between the malleoli (Vicon manual, 2010).

Height was measured to the nearest 0.5cm using a stadiometer (Hadlands Photonics, Australia). Height is the maximum distance from the floor to the highest point of the head with the participant looking straight ahead. The participants were asked to stand straight with back, buttocks and heels against the stadiometer with feet together and flat on the floor. The participants were asked to take and hold a deep breath whilst looking straight ahead. Height was recorded at the end of the participants' deep inward breath.

Weight was recorded using the electronic weighing scales integrated within the Bodpod body composition device (Life Measurement, Inc, Concord, CA, USA) procedure. Participants were asked to stand on the centre of scales, without support and with their weight distributed evenly on both feet. Body mass index (BMI) was calculated by Quetelet's index (weight in kg/height^2 in m).

Body Mass Index Z-Score (BMI Z-Score) was input into LMSgrowth software (Harlow Healthcare, South Shields, UK). The software calculates the BMI Z-Score and BMI Centile, from height and body mass inputs, based on reference data from the United Kingdom 1990 (UK90) data set (Cole et al., 1995).

6.3.2.4 Lower Limb Model

The marker set for PiG was attached, with the participants in a comfortable standing position, in accordance with Vicon software using the protocol established by Davis et al., (1991). Figure 6.1 shows one side of the body for placement of the fifteen retro-reflective 9mm markers attached to the lower limbs. The pelvis was defined by three markers; the sacral marker, placed at the level of second sacral vertebrae and a marker on each anterior superior iliac spine. Thigh markers were placed bilaterally on the lateral aspect of the thighs to define long axis of rotation. To facilitate placement of the thigh markers, the subjects are asked to internally rotate their lower limbs by placing their feet on a straight line. The marker was placed in a straight line between the lateral epicondlye of the femur and the greater tronchanter. The lateral epicondyles of the femurs were palpated, being slightly superior to the knee joint line. The knee markers were placed at the midpoint between anterior and posterior borders of the knee joint. Tibia markers were placed on the lateral shank with the participant standing in comfortable stance (feet returned to slight external rotation) to define the longitudinal axis of the shank. The foot was defined by markers on the lateral malleolus, posterior calcaneus and between the second and third metatarsal heads. The calcaneal and metatarsal markers were placed so that they were equal vertical distance from the floor.

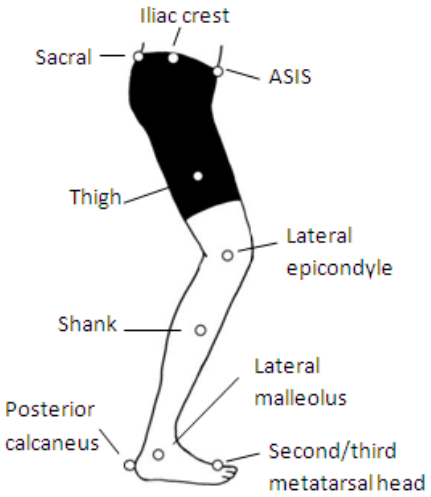

Figure 6.1. Marker placement for the Plug-In Gait lower limb model.

Two variations of the PiG marker set were tested. The first involved the use of an 'instrumented pointer device' to determine the position of virtual ASIS markers based on offsets from lateral iliac crest markers. This procedure may facilitate the palpation of the ASIS in obese participants whose excessive abdominal adipose tissue may hinder proper placement and tracking of skin mounted markers. The 'instrumented pointer device' is fitted with markers of known relative position and a spring which brings the distal markers into closer proximity ('plunged') to the proximal markers on the pointer shaft. When the pointer tip is placed on to the ASIS location and plunged a virtual marker is created by calculated offsets from the iliac crest and sacral markers. Fukuchi et al., (2010) used iliac crest markers as an alternative to ASIS markers to define the pelvis. This study found dynamic pelvis angles to be more reliable and accurate compared to functional and predictive methods to define the pelvis when soft tissue artefact may be a problem. The method of creating virtual markers has been previously used in the calibrated anatomical system technique (CAST) to define the anterior superior iliac crests Cappozzo et al., (1995). The reliability of anatomical calibration has been shown to be improved using this technique with lower limb joint angles errors in the range of 0.9-2.9^{o} (Donati et al., 2008). The second variation on the PiG marker set was to apply a thigh marker rotation offset post data capture using a Bodybuilder script created by Baker et al., (1999). Defining the long axis of the thigh can be problematic; a slight anterior or posterior misplacement of the thigh marker can rotate the thigh segment and cause cross talk between the sagittal and frontal knee joint planes. The Bodybuilder script calculates the necessary offsets needed to be applied to the thigh markers based on varus/valgus curves of the original data to correct the alignment of the thigh segment.

6.3.3 Procedure

Children were asked to ambulate barefoot at a self-selected walking speed for a minimum of three steps before entering and three steps upon exiting the capture volume (7.5m walkway length). This gave the children enough time to accelerate up to normal walking speed and decelerate after the force plates. To avoid artificially increasing effect size and violating assumptions of independence only right limb kinematic and kinetic variables were extracted for analyses (Menz, 2005). Six gait cycles were captured from heel-strike to heel-strike of the right limb. Reliability could be improved with a higher number of trials captured for each participant (Monaghan et al., (2007). However, in order to achieve 6 'clean' (i.e. participants hit the force plates, did not appear to aim, walked in a straight line, all markers stayed attached) it was necessary to record approximately 30 trials. After approximately 30 trials testing was concluded to prevent participant fatigue.

A test retest interval of four weeks was implemented and 14 participants returned within the timeframe. An ideal interval between test-retest protocols required consideration of practical and methodological issues. The interval should be long enough that skin marks from marker attachment or assessor memory of anthropometric measurement will not artificially improve between-session reliability. However, the interval should be short enough that actual changes (i.e. growth, weight gain) do not artificially reduce between-session reliability (McGinley et al., 2009). Three participants were unable to return until more than four weeks after their first testing session and were excluded from the analysis.

In order to examine the difference in hip motion between two protocols to track the ASIS using skin mounted and virtual markers five obese children and five non-obese children were tested. One static calibration was taken of each participant with skin mounted ASIS markers and another static calibration with the plunger device indicating the position of the virtual ASIS markers.

6.3.4 Data Analysis

3D marker trajectories were reconstructed using reconstruction parameters in Vicon software to ensure markers were visible during one whole gait cycle. Pilot testing of the reconstruction parameters that led to the best set-up for marker visibility set; predictor radius at 20mm, acceleration 50m·s^{-2}, noise factor of 2, intersection limit of 6 and a residual factor of 0.5. Trajectories were gap filled to a maximum of 5 frames using a cubic-spline technique. Only

trials where subsequent trajectories were visible over the whole gait cycle were used for analysis. Following the reconstruction of marker trajectories using the parameters described above the raw trajectories were filtered using the Woltring filter routine available in the Vicon software. A recommended mean square error (MSE) value for filtering of gait data is 20 (Vicon Manual, 2010).

Perry (1992) described the phases of the gait cycle according to reciprocal foot contact with the ground. Gait events were determined by onset and conclusion of vertical force by the right foot on the force plates. Vertical ground reaction force above a threshold of 20N was used to indentify initial contact of the right foot, the next frame under 20N was determined as right foot off. Contact with a second force plate above the 20N threshold determined the next right initial contact and the end of the gait cycle. Ipsilateral Initial contact (IIC) and ipsilateral toe-off (ITO) determined the stance and swing phases of the gait cycle in which peak maximum and minimum values were extracted.

In order to analyse between-session reliability of the lower limb model and compare the reliability of the three foot models; (1) specific events; and, (2) peaks were chosen. Between-session reliability of angular and moment outputs during gait analysis has been previously assessed in this way (Maynard et al., 2003; Monaghan et al., 2007; Klejman et al., 2010). This method of analysing specific points of interest has been used previously to examine kinematic differences between obese and non-obese children (see literature review chapter 2, chapter 3). Differences in peak knee flexion angle during stance (Gushue et al., 2005), knee flexion at initial contact (McMillan et al., 2010), peak knee abduction angle (McMillan et al., 2009 & 2010) and hip extension angle at initial contact (McMillan et al., 2010) were reported. Kinetic differences have been found for the hip, knee and ankle both in peaks (Shultz et al., 2009) and at specific events (McMillan et al., 2009 & 2010). Therefore, 3D kinematic and kinetic values of the hip, knee and ankle will be reported at initial contact and toe off as well as joint peaks in the stance and swing phases to assess between-session reliability. This gives 108 parameters for each participants from which lower limb between-session reliability was determined.

To analyse the difference between skin mounted and virtual ASIS markers hip joint centre position and 3D dynamic motion of the hip joint was extracted for each of the five obese and five non-obese participants. From each static trial global ASIS and hip joint centre position were extracted and referenced to the sacral marker position to control for altered standing positioning between subjects. The effects of skin mounted and virtual markers on gait patterns were assessed by examining the same gait cycle, therefore, removing intrinsic

variability. Each child completed 3 gait trials from which 3D hip joint motion was extracted at four gait events. The group means of hip joint angles at each event were then used to compare ASIS marker conditions and between obese and non-obese boys. In total, 6 static measures of ASIS and HJC position and eighteen 3D hip joint motion variables were extracted to determine the difference between ASIS protocols

6.3.5 Statistical Analysis

6.3.5.1 Normality and Homogeneity

In order to carry out the parametric tests of Intraclass correlation coefficients (ICC) the normality and homoscedasticity of each variable from the sample must be tested. Shapiro-Wilk tests compared the distribution of the variables in this study to a normal distribution with the same mean and standard deviation. If the test is non-significant (p>.05) the distribution is not significantly different from a normal distribution. The Shapiro-Wilk test was applied to age, spatiotemporal and anthropometric data. However, the Shapiro-Wilk test are limited with large sample sizes (n>100) because it is easy to deviate from normality or homogeneity. Therefore, significance testing does not necessarily indicate bias in the data (Field, 2009).

In order to check the assumptions of random error and homoscedasticity of the models plots of the standardised predicted values of kinematic and kinetic values against the standardised residuals were produced. If the regression models fit the sample data well all data points fall on the regression line and the residuals would be zero (Field, 2009). A histogram of the regression standardised residuals should appear as a normal distribution (bell-shaped curve). Furthermore the normal probability plot shows deviations from normality by plotting the observed residuals against a straight line (representing a normal distribution). All checks on the assumptions of the regression model were compared with published plots in Field (2009). An example of the plots is in Appendix IV.

6.3.5.2 Anthropometric and Spatiotemporal Measures

Anthropometric and spatiotemporal gait measures were averaged across 6 within-session trials and means tested for significant differences between sessions by paired t-test (significance set at p<0.05). Where variables are not normally distributed a Wilcoxon non-parametric rank test was performed.

6.3.5.3 Lower Limb Model Between-Session Reliability

Between-session reliability was determined by error calculations of joint angles and moments at selected points of the gait cycle. Intraclass correlation coefficients (ICC) are considered the 'gold standard for assessment of the reliability of numerical parameters (Fleiss, 1986). Therefore, ICC (3,k) were calculated for all variables which is appropriate for within-rater, between-session reliability (Shrout & Fleiss, 1979). The confidence intervals (CI) of the ICCs were calculated using one-way analysis of variance (Rankin & Stokes, 1998). All individual trials from session one and session two, rather than subject means, were used to calculate ICCs. This reduces the ICC value because within-subject variability is included in correlation. However, data in the main study (chapter 8) will be analysed based on all individual gait cycles rather than subject means. Therefore, it is appropriate to express between-session reliability and expected error in this study according to all individual trials and is calculated:

$$ICC\,(3,k) = \frac{BMS - EMS}{BMS} \quad (1)$$

Where BMS is the between-subjects variance, EMS is the error or residual mean square variance and k is the number of measurements (Shrout & Fleiss, 1979). To interpret ICCs the scale of Katz et al., (1992) was used; ICC-values > 0.80 represent very high, 0.60–0.79 moderately high, 0.40–0.59 moderate and < 0.40 low reliability. In order to report the mean of multiple ICCs it is necessary to transform the *r* value by Fisher r-to-z transformation, take the average, and transform this back to an ICC value (*r*). This transformation means that the variance of *z* is approximately constant for all correlation coefficient (r) values. Without the Fisher transformation, the variance of *r* grows smaller as *r* gets closer to 1 (Field, 2009). Bland and Altman 95% limits of agreement were considered as an alternative measure of reliability as they indicate the range of error (Bland & Altman, 1986). However, a sample set of 50 is required otherwise limits of agreement can be very wide (Rankin & Stokes, 1998). Where variables violated assumptions of normality a Spearman's rank correlation coefficient was calculated to determine the between-session reliability of repeated measures.

Expressing reliability of gait data in terms of a coefficient by itself makes comparison difficult because the units are hard to interpret (McGinley et al., 2009). Therefore, absolute measures of error were calculated based on the ICC and pooled standard deviation. This gives units in

degrees which can be interpreted as the expected amount of intrinsic and extrinsic error in repeated sessions. The equation for calculating SEM:

$$SEM = Sx\sqrt{1 - rxx}$$

(10)

Where S*x* is the pooled standard deviation (^{o}) and r*xx* refers to intraclass correlation coefficient (ICC 3,*k*) (Portney & Watkins, 2009).

6.3.5.4 Lower Limb Model Differences Following Thigh Marker Rotation Offsets and ASIS Protocols

To assess whether the thigh marker offset protocol significantly altered PiG joint angles and moments at initial contact and toe off paired-means t-tests were performed on individual's data. To examine the differences between skin mounted and virtual ASIS markers root mean square (RMS) together with mean and standard deviations (SD) were extracted. Mean and SD hip angles at ipsilateral initial contact (IIC) and ipsilateral toe-off (ITO) were extracted and compared via paired-means t tests. For all tests significance was set to $p<0.05$.

6.4 Results

6.4.1 Normality and Homogeneity

Shapiro-Wilk test for normality, presented in Table 6.1, showed that age, knee width, ankle width and cadence were not normally distributed ($P<0.05$), but all other variables were normally distributed. Parametric ICC test for between-session reliability was conducted on all normally distributed variables. Spearman's rank correlation was implemented to test between-session reliability of non-parametric variables. Wilcoxon non-parametric test was used to test for significantly different outputs between the sessions. No parametric tests were conducted on age. A visual examination of the plots (an example is shown in Appendix IV) for each lower limb output indicated that all variables were normally distributed and therefore ICC parametric tests for between-session reliability could be undertaken.

Table 6.1 Shapiro-Wilk tests of normality on age, spatiotemporal and anthropometric variables. Significance p<0.5

	Statistic	df	Sig.
Age (years)	.830	27	.012*
Height (cm)	.975	27	.939
Body mass (kg)	.889	27	.079
BMI (kg/m^2)	.909	27	.154
BMI Z-Score	.959	27	.702
Leg length (cm)	.953	27	.239
Knee width (cm)	.912	27	.022*
Ankle width (cm)	.912	27	.023*
Cadence (steps/min)	.901	27	.017*
Stance phase (% of gait cycle)	.967	27	.545
Step length (m)	.976	27	.785
Step width (m)	.931	27	.082
Walking speed (m·s-1)	.951	27	.249

6.4.2 Anthropometrics and Spatiotemporal

Eight boys and six girls took part in the reliability test-retest protocol with a mean duration between repeated sessions of 21.57 ± 5.56 days. Based on BMI Z-Scores (UK90) for each child on each session; one child was classified as obese, five as overweight, 16 as ideal weight, five as underweight and one as very underweight. Two participants changed classification between sessions; one girl from overweight to obese, BMI Z-Score change of 2.24 to 2.38 (obese Z-Score cutoff 2.25), and one girl from underweight to very underweight, BMI Z-Score change of -1.91 to -2.11 (very underweight BMI Z-Score cutoff -2.0).

Table 6.2 shows the mean anthropometric and spatiotemporal characteristics of each session. Between-session reliability of anthropometric measures was between ICC values of .872 and .999. Spatiotemporal measurement between-session reliability demonstrated lower ICCs, between .421 and .885. There were no significant differences in anthropometric or spatiotemporal parameters between session 1 and session 2. However, the subjects height increased by 0.37 ± 0.10cm which was close to reaching significance (p= .062).

Table 6.2. Mean anthropometrics and spatiotemporal measures taken from each subject at session one and session two and the difference between sessions. *p* represents the output of paired t-test or Wilcoxon non-parametric rank, significance set at <0.05. Reliability determined by Intra-class correlation coefficient (ICC) or Spearman rank correlation coefficient for non-parametric measures.

	Session 1	Session 2	Difference	Range	ICC (3,K)	*P* value between sessions
Age (years)	8.50 ± 2.79	8.64 ± 2.84	0.14 ± 0.35	6 - 11		.165
Height (cm)	117.09 ± 50.17	117.46 ± 50.37	0.37 ± 0.10	123.0 – 154.5	.999	.062
Body mass (kg)	31.00 ± 8.52	31.29 ± 8.73	0.29 ± 1.30	21.0 – 48.0	.999	.104
BMI (kg/m^2)	16.81 ± 4.92	16.87 ± 5.01	0.05 ± 0.36	13.57 – 21.43	.993	.111
BMI Z-Score	0.15 ± 1.22	0.12 ± 1.26	0.030 ± 0.24	-2.11 – 2.38	.991	.655
Leg length (cm)	70.07 ± 8.13	70.46 ± 8.33	0.39 ± 1.10	56 – 83	.998	.097
Knee width (cm)	8.46 ± 0.63	8.53 ± 0.61	0.13 ± 0.68	6.4 – 9.6	.872 (Spearman)	.248 (Wilcoxon)
Ankle width (cm)	5.95 ± 0.48	6.01 ± 0.45	0.06 ± 0.22	5.3 – 6.7	.925 (Spearman)	.347 (Wilcoxon)
Cadence (steps/min)	131.82 ± 8.7	133.38 ± 11.4	1.56 ± 9.06	104.8 - 199.2	.732 (Spearman)	.530 (Wilcoxon)
Stance phase (% of gait cycle)	57.54 ± 1.39	57.15 ± 1.28	0.39 ± 1.61	55.2 – 59.8	.421	.420
Step length (m)	0.85 ± 0.24	0.93 ± 0.38	0.08 ± 0.20	1.15 – 2.21	.818	.165
Step width (m)	0.15 ± 0.03	0.14 ± 0.03	0.0 ± 0.04	0.10 – 0.22	.885	.825
Walking speed ($m \cdot s^{-1}$)	1.21 ± 0.15	1.23 ± 0.14	0.02 ± 0.14	0.93 – 1.55	.470	.393

6.4.3 Aim 1 Lower Limb Model

6.4.3.1 Between-Session Reliability of Joint Angles

Between-session test-retest ICC and SEM values for reliability assessment of lower limb kinematics are presented in Table 6.3. Overall, PiG lower limb model demonstrated moderately high ICCs (ICC 0.60 95%CI 0.27 to 0.82) and reasonable SEM values (mean SEM $3.98^{o} \pm 1.89^{o}$). The PiG lower limb kinematic ICCs were moderately high at the hip (ICC 0.66, 95%CI 0.34 to 0.84) and knee (ICC 0.60, 95%CI 0.25 to 0.81), but only moderate at the ankle joint (ICC 0.55, 95%CI 0.21 to 0.79). All lower limb joints demonstrated reasonable error (SEM) from repeated sessions. The knee demonstrated the least error (SEM 3.60° ± 1.43°) from repeated sessions followed by the hip (SEM 3.90° ± 1.85°) and ankle (SEM 4.44° ± 2.57°). The PiG lower limb model showed moderately high ICCs in the transverse (ICC 0.70 95%CI 0.37 to 0.67), but moderate in the frontal (ICC 0.56 95%CI 0.20 to 0.63) and sagittal planes (ICC 0.45 95%CI 0.08 to 0.60). Reasonable errors (SEM) were found in the frontal (SEM 2.32° ± 0.51°)

and sagittal planes (SEM 3.23° ± 0.83°), but unacceptable errors in the transverse plane (SEM 6.39° ± 1.35°). Extracting lower limb kinematics at gait cycle events (initial contact and toe off) (ICC 0.62, 95%CI 0.26 to 0.67), peak maximal (during stance and swing phase) values (ICC 0.60, 95%CI 0.24 to 0.66), and peak minimal (during stance and swing phase) values (ICC 0.59, 95%CI 0.21 to 0.65) demonstrated moderate ICCs. Errors from extracting lower limb variables at peak minimal values (SEM 3.77° ± 1.78°) were lower than peak maximal (SEM 3.95° ± 2.06°) and values at events (SEM 4.22° ± 2.22°), all errors were reasonable.

Hip, knee and ankle 3D joint motion over the gait cycle are shown in Figure 6.2. At the hip joint very high ICC values were found in the transverse plane (ICC 0.87 95%CI 0.72 to 0.94), but only moderate ICCs the sagittal plane (ICC 0.53 95%CI 0.16 to 0.78) and frontal planes (ICC 0.40 95%CI 0.01 to 0.71). Hip SEM values were reasonable in the frontal plane (mean SEM 2.28° ± 0.26°) and sagittal planes (mean SEM 2.90° ± 0.58°), but unacceptable in the transverse plane (mean SEM 6.31° ± 0.74°). Between-session reliability (ICCs) of the hip joint was moderate at gait events (ICC 0.68 95%CI 0.37 to 0.85), peak maximal values (ICC 0.67 95%CI 0.37 to 0.85) and peak minimal values (ICC 0.62 95%CI 0.28 to 0.82). Lowest SEM values were found for repeated peak minimal hip values (mean SEM 3.44° ± 1.72°) followed by peak maximal values (mean SEM 4.07° ± 2.18°) and values at events (mean SEM 4.18° ± 1.88°), all errors were reasonable.

The knee presented moderately high ICCs in the frontal plane (ICC 0.74 95%CI 0.48 to 0.88), but only moderate ICCS the transverse (ICC 0.55 95%CI 0.17 to 0.78) and sagittal planes (ICC 0.46 95%CI 0.07 to 0.74). Knee SEM values were reasonable in the frontal (mean SEM 2.77° ± 0.76°) and sagittal planes (mean SEM 2.97° ± 0.54°), but unacceptable in the transverse plane (mean SEM 5.44° ± 1.01°). Knee joint between-session reliability (ICCs) was moderately high at peak minimal values (ICC 0.62 95%CI 0.29 to 0.82), but only moderate at events (ICC 0.58 95%CI 0.23 to 0.81) and peak maximal values (ICC 0.58 95%CI 0.22 to 0.80). Repeated peak minimal knee values demonstrated the lowest SEM (3.31° ± 1.28°) followed by values at events (3.69° ± 1.62°) and peak maximal values (3.80° ± 1.58°), all errors were reasonable.

Ankle transverse plane motion demonstrated moderately high ICCs (ICC 0.66 95%CI 0.37 to 0.85), but only moderate ICCs in the frontal (ICC 0.55 95%CI 0.21 to 0.79) and sagittal planes (ICC 0.42 95%CI 0.03 to 0.72). The frontal plane demonstrated reasonable SEM values at the ankle (mean SEM 2.07° ± 0.17°) and sagittal planes (mean SEM 3.82° ± 1.15°), but unacceptable in the transverse plane (mean SEM 7.26° ± 1.15°). Between-session reliability of the ankle over the gait cycle showed moderate reliability (ICCs) at events (ICC 0.58 95%CI 0.27

to 0.82), peak maximal values (ICC 0.56 95%CI 0.21 to 0.79) and peak minimal values (ICC 0.52 95%CI 0.14 to 0.77). Repeated peak minimal values showed the lowest SEM values (mean SEM 3.97° ± 2.67°) followed by peak maximal values (mean SEM 4.56° ± 2.24°) and values at events (mean SEM 4.56° ± 3.14°)°), all errors were reasonable.

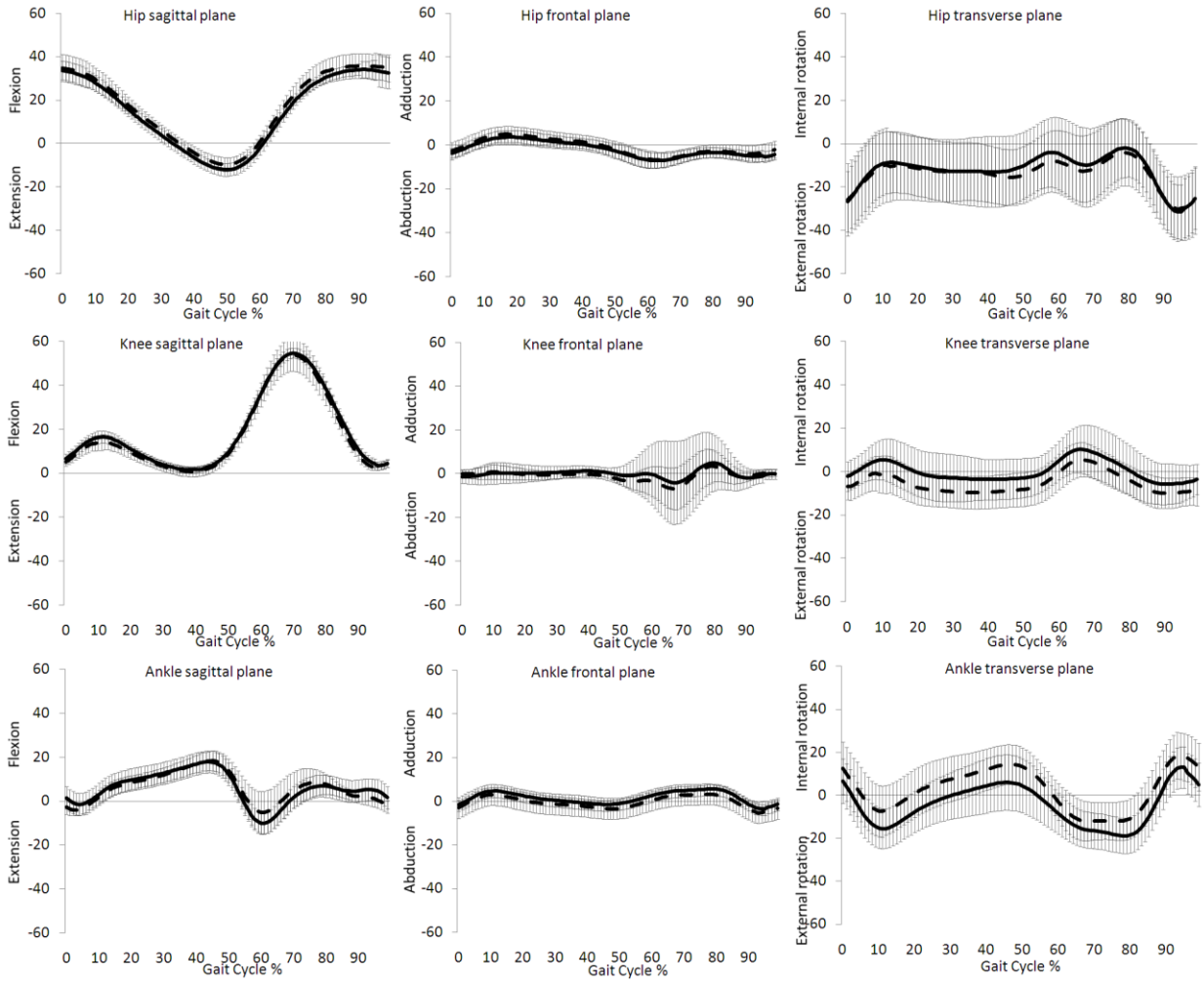

Figure 6.2. Mean ± SD of angular output of Plug-in Gait test-retest. Session 1 black line, session 2 dash line

To summarise the findings of lower limb joint motion between-session reliability the scale of Katz et al., (1992) was used (ICC-values > 0.80 = very high, 0.60–0.79 = moderately high, 0.40–0.59 = moderate and < 0.40 = low reliability). Of the 54 lower limb variables extracted over the gait cycle nine (16.7%) demonstrated low reliability, 24 (44.4%) demonstrated moderate reliability, 12 (22.2%) demonstrated moderately high reliability and nine (16.7%) demonstrated very high reliability. The nine lower limb variables that demonstrated low reliability were (number of variables over the gait cycle in brackets):

- Hip frontal plane stance and swing peak minimal value (2)
- Knee sagittal plane value at ipsilateral initial contact, stance phase peak minimal and swing phase peak maximal values (3)
- Knee transverse plane peak minimal value (1)
- Ankle sagittal plane stance peak maximal value and value at ipsilateral toe-off (2)
- Ankle frontal plane swing peak maximal value (1)

To interpret error values from within-rater repeated sessions the recommendations from McGinley et al., (2009) were used as a guide (<2° = acceptable, 2-5° = reasonable and >5° = unacceptable). Sixteen (29.6%) of the lower limb variables demonstrated unacceptable SEM values, 33 (61.1%) demonstrated reasonable SEM and five demonstrated acceptable SEM values. The 16 lower limb variables to demonstrate (number of variables over the gait cycle in brackets):

- All six hip transverse plane values (6)
- Knee transverse plane values at ipsilateral toe-off and swing maximal and minimal peak values (3)
- Ankle sagittal plane swing peak minimal value (1)
- All six ankle transverse plane values (6)

Table 6.3. ICC (95%Confidence intervals) and SEM of PiG lower limb angular outputs at gait cycle events and peaks

		Gait Cycle					
Segment	Plane	IIC	Stance min	Stance max	ITO	Swing min	Swing max
Hip ICC (CI)	sag	0.45 (0.05 to 0.73)	0.57 (0.21 to 0.80)	0.50 (0.11 to 0.76)	0.56 (0.20 to 0.79)	0.52 (0.13 to 0.77)	0.59 (0.23 to 0.80)
SEM		4.05	2.79	3.53	2.91	2.52	2.75
Hip	fro	0.47 (0.07 to 0.74)	0.20 (-0.23 to 0.56)	0.56 (0.19 to 0.79)	0.58 (0.22 to 0.80)	0.14 (-0.29 to 0.52)	0.49 (0.10 to 0.75)
		2.41	1.93	2.35	2.72	2.16	2.26
Hip	tra	0.88 (0.73 to 0.95)	0.89 (0.75 to 0.95)	0.82 (0.62 to 0.92)	0.87 (0.70 to 0.94)	0.88 (0.74 to 0.95)	0.88 (0.74 to 0.95)
		6.21	5.69	7.52	6.76	5.57	5.99
Knee	sag	0.36 (-0.06 to 0.67)	0.37 (-0.04 to 0.68)	0.55 (0.18 to 0.79)	0.51 (0.12 to 0.76)	0.65 (0.33 to 0.84)	0.28 (-0.15 to 0.62)
		2.61	2.44	3.15	3.80	2.39	3.08
Knee	fro	0.52 (0.14 to 0.77)	0.83 (0.63 to 0.92)	0.54 (0.17 to 0.78)	0.86 (0.69 to 0.94)	0.73 (0.45 to 0.88)	0.83 (0.63 to 0.92)
		1.89	1.90	2.07	3.00	3.55	3.35
Knee	tra	0.55 (0.17 to 0.78)	0.66 (0.33 to 0.84)	0.66 (0.34 to 0.84)	0.58 (0.21 to 0.80)	0.36 (-0.06 to 0.67)	0.43 (0.02 to 0.71)
		4.35	4.46	4.59	6.47	5.11	6.58
Ankle	sag	0.51 (0.13 to 0.76)	0.41 (0.00 to 0.71)	0.38 (-0.04 to 0.69)	0.38 (-0.04 to 0.68)	0.44 (0.03 to 0.72)	0.49 (0.1 to 0.75)
		3.01	4.20	2.61	4.84	5.02	2.42
Ankle	fro	0.50 (0.11 to 0.76)	0.51 (0.13 to 0.76)	0.64 (0.31 to 0.83)	0.77 (0.53 to 0.90)	0.50 (0.12 to 0.76)	0.39 (-0.02 to 0.69)
		1.78	2.05	1.88	2.03	2.27	2.13
Ankle	tra	0.60 (0.24 to 0.81)	0.64 (0.32 to 0.83)	0.76 (0.51 to 0.89)	0.78 (0.54 to 0.90)	0.60 (0.25 to 0.81)	0.66 (0.34 to 0.84)
		9.35	7.94	6.97	7.73	5.88	7.79

6.4.3.2 Between-Session Reliability of Joint Moments

Between-session test-retest ICC and SEM values for reliability assessment of lower limb moments are presented in Table 6.3. Overall, PiG lower limb joint moments showed moderate ICCs (ICC 0.48 95%CI 0.11 to 0.75) and SEM values of 2.32Nm ± 2.04Nm. The PiG lower limb moment variables demonstrated moderate ICCs, highest at the ankle (ICC 0.55, 95%CI 0.19 to 0.79) followed by the knee (ICC 0.47, 95%CI 0.13 to 0.74) and hip joint (ICC 0.40, 95%CI 0.01 to 0.71). The knee demonstrated the least error (SEM 1.60Nm ± 1.53Nm) from repeated sessions followed by the ankle (SEM 1.78Nm ± 4.06Nm) and hip (SEM 3.60Nm ± 3.38Nm). In general, PiG lower limb moments were moderately reliable (ICCs) in the frontal (ICC 0.50 95%CI 0.13 to 0.76) sagittal (ICC 0.48 95%CI 0.13 to 0.75) and transverse planes (ICC 0.45 95%CI 0.07 to 0.74). The smallest errors were found in the transverse plane (SEM 0.69Nm ± 0.70Nm), followed by frontal (SEM 2.08Nm ± 2.85Nm) and sagittal planes (SEM 4.21Nm ± 4.17Nm). Extracting lower limb moments at peak minimal values demonstrated moderately high between-session reliability (ICC 0.72, 95%CI 0.48 to 0.89), but only moderate at peak maximal values (ICC 0.44, 95%CI 0.03 to 0.72) and low at gait cycle events (initial contact and toe off) (ICC 0.33, 95%CI -0.06 to 0.66). Errors from extracting lower limb variables at gait events (SEM 1.12Nm ± 1.33Nm) were lower than peak minimal (SEM 2.09Nm ± 2.04Nm) and peak maximal values (SEM 5.27Nm ± 4.71Nm).

Hip, knee and ankle 3D joint moments over the stance phase are shown in Figure 6.3. Hip joint moments demonstrated moderately high ICCs in the frontal plane (ICC 0.55, 95%CI 0.19 to 0.79), but low ICCs in the sagittal plane (ICC 0.39, 95%CI -0.00 to 0.71) and transverse planes (ICC 0.25, 95%CI -0.17 to 0.60). Repeated measures of hip moment error values were greatest in the sagittal plane (mean SEM 5.83Nm ± 3.03Nm), followed by the frontal (mean SEM 4.25Nm ± 3.78Nm) and transverse planes (mean SEM 0.72Nm ± 0.59Nm). Between-session reliability of hip moments was moderately high at peak minimal values (ICC 0.55 95%CI 0.21 to 0.80), but low at peak maximal values (ICC 0.38 95%CI -0.03 to 0.69) and values at events (ICC 0.34 95%CI -0.78 to 0.66). Errors in hip moment repeated values over the gait cycle showed that maximal peak values demonstrated highest SEM (mean SEM 6.87Nm ± 4.72Nm) followed by minimal peak values (mean SEM 3.28Nm ± 3.06Nm) and values at events (mean SEM 2.12Nm± 1.85Nm).

At the knee, all planes demonstrated moderate ICCs; sagittal (ICC 0.45, 95%CI 0.16 to 0.73), frontal (ICC 0.50, 95%CI 0.12 to 0.76) and transverse planes (ICC 0.44, 95%CI 0.10 to 0.75). Knee transverse plane moments SEM values were the lowest (0.69Nm ± 0.90Nm) followed by

frontal (1.75Nm ± 2.16Nm) and sagittal (2.36Nm ± 1.08Nm). Peak minimal values had moderately high ICCs at the knee joint (ICC 0.71 95%CI 0.48 to 0.88), but peak maximal values were moderate (ICC 0.46 95%CI 0.05 to 0.72) and gait events ICCs were low (ICC 0.31 95%CI -0.03 to 0.64). Knee joint 3D moments were lowest at gait events (mean SEM 0.82 ± 0.77Nm) followed by peak minimal (mean SEM 2.18Nm ± 1.23Nm) and peak maximal (mean SEM 4.62Nm ± 4.37Nm) values.

The ankle demonstrated moderately high ICCs in the transverse plane (ICC 0.62, 95%CI 0.29 to 0.82), but only moderate in the sagittal (ICC 0.58, 95%CI 0.21 to 0.80) and frontal planes (ICC 0.44, 95%CI 0.08 to 0.74). Joint moment error values at the ankle were lowest in the frontal plane (mean SEM 0.24Nm ± 0.25Nm) then transverse plane (mean SEM 0.66Nm ± 0.79Nm) and sagittal plane (mean SEM 4.44Nm ± 6.73Nm). Very high ICCs for ankle moment were found at peak minimal values (ICC 0.84 95%CI 0.69 to 0.94), moderate ICCs at peak maximal values (ICC 0.48 95%CI 0.08 to 0.75) and low ICCs at event values (ICC 0.35 95%CI -0.07 to 0.67). Gait events demonstrated higher SEM values for 3D ankle moments (0.42Nm ± 0.33Nm) followed by peak minimal values (1.81Nm ± 1.25Nm) and peak maximal values (4.71Nm ± 3.57Nm).

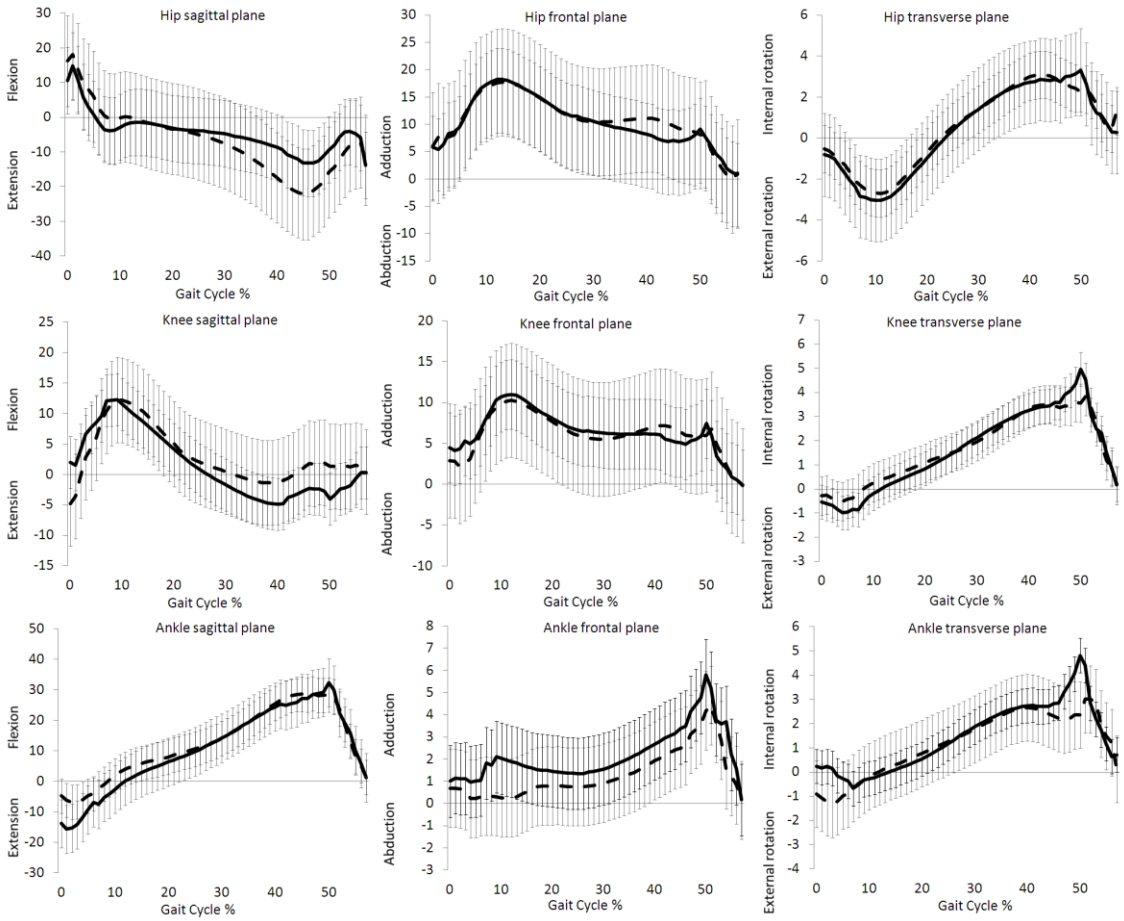

Figure 6.3. Mean ± SD of PiG moments test retest. Session 1 black line, session 2 dash line

In summary, the findings of lower limb joint moment between-session reliability, indicated that of the 36 lower limb variables extracted over the gait cycle 14 (38.9%) demonstrated low reliability, 12 (33.3%) demonstrated moderate reliability, two (5.6%) demonstrated moderately high reliability and eight (22.2%) demonstrated very high reliability. The 14 lower limb variables that demonstrated low reliability were (number of variables over the gait cycle in brackets):

- Hip sagittal plane value at ipsilateral initial contact, stance peak maximal value and value at ipsilateral toe-off (3)
- Hip frontal plane value at stance peak maximal value (1)
- Hip transverse plane value at ipsilateral initial contact and at ipsilateral toe-off (2)
- Knee sagittal plane value at ipsilateral initial contact (1)
- Knee frontal plane value at ipsilateral initial contact (1)
- Knee transverse plane value at ipsilateral initial contact and at ipsilateral toe-off (2)
- Ankle sagittal plane value at ipsilateral toe-off (1)
- Ankle frontal plane value at ipsilateral initial contact and at ipsilateral toe-off (2)
- Ankle transverse plane value at ipsilateral initial contact and at ipsilateral toe-off (2)

No interpretation of the error from repeated session lower limb joint moments has been recommended in the literature. Therefore, the SEM values obtained in the current study cannot be assessed as being acceptable or unacceptable.

Table 6.4. ICC (95% confidence intervals) and SEM of PiG lower limb moment outputs at stance phase events and peaks

PiG kinetics		Gait Cycle			
Segment	Plane	IIC	Stance min	Stance max	ITO
Hip (ICC)	sag	0.43 (0.02 to 0.72)	0.58 (0.22 to 0.80)	0.37 (-0.05 to 0.68)	0.23 (-0.20 to 0.59)
(SEM)		4.32	6.76	9.60	2.63
Hip	fro	0.40 (-0.01 to 0.70)	0.68 (0.37 to 0.85)	0.37 (-0.05 to 0.68)	0.69 (0.40 to 0.86)
		4.10	2.09	9.60	1.21
Hip	tra	0.11 (-0.31 to 0.50)	0.43 (0.02 to 0.72)	0.41 (0.00 to 0.70)	0.03 (-0.38 to 0.44)
		0.28	0.99	1.42	0.17
Knee	sag	0.20 (-0.23 to 0.56)	0.52 (0.13 to 0.77)	0.54 (0.16 to 0.78)	0.52 (0.13 to 0.77)
		2.23	3.45	2.84	0.92
Knee	fro	0.29 (-0.14 to 0.62)	0.76 (0.51 to 0.89)	0.46 (0.05 to 0.73)	0.40 (-0.01 to 0.70)
		0.96	0.71	4.96	0.35
Knee	tra	0.09 (-0.28 to 0.51)	0.86 (0.70 to 0.94)	0.36 (-0.06 to 0.67)	0.31 (-0.11 to 0.64)
		0.25	0.29	2.04	0.18
Ankle	sag	0.70 (0.40 to 0.86)	0.74 (0.47 to 0.88)	0.38 (-0.04 to 0.69)	0.39 (-0.03 to 0.69)
		0.99	1.92	14.49	0.34
Ankle	fro	0.14 (-0.29 to 0.52)	0.77 (0.53 to 0.90)	0.54 (0.17 to 0.78)	0.29 (-0.14 to 0.63)
		0.61	0.10	0.13	0.11
Ankle	tra	0.35 (-0.07 to 0.67)	0.95 (0.89 to 0.98)	0.51 (0.12 to 0.76)	0.14 (-0.29 to 0.52)
		0.23	0.34	1.84	0.22

6.4.4 Aim 2 Lower limb Model – Thigh Marker Rotation Offset

6.4.4.1 Joint Angle Differences Following Thigh Marker Rotation Offset

Table 6.5 shows the difference in lower limb joint angles at ipsilateral initial contact and ipsilateral toe off when the thigh marker rotation offset is applied. The hip was less flexed, less abducted and significantly more internally rotated at initial contact. At toe-off the hip was more extended, significantly less abducted and significantly more internally rotated.

The thigh marker rotation offset had the effect of reducing knee flexion, increasing varus (abduction) and significantly increasing external rotation at initial contact. At toe-off the knee was less flexed, in significantly more valgus (adduction) and less internally rotated.

At the ankle joint, the application of the thigh marker offset significantly increased extension, reduced abduction and reduced external rotation at initial contact. At toe-off the ankle was more extended, less adducted and less externally rotated.

Table 6.5. Mean ± SD of PiG lower limb angular outputs at gait cycle events before and after thigh marker rotation offset. Significance * = p<.05, ** = p<.01, *** = p<.001

PiG		Average joint angle		
		Pre-offset	Post offset	Pre- post-offset
Segment	plane	IIC	IIC	Difference
Hip	sag	32.51 ± 5.45	32.23 ± 5.20	0.28 ± 3.31
Hip	fro	-3.03 ± 3.32	-2.88 ± 3.67	-0.15 ± 1.98
Hip	tra	-23.18 ± 17.87	-19.94 ± 14.38	-3.24 ± 14.36*
Knee	sag	6.11 ± 3.27	6.10 ± 3.07	0.01 ± 2.60
Knee	fro	0.43 ± 2.73	-0.09 ± 2.79	0.52 ± 1.80
Knee	tra	-4.45 ± 6.45	-5.73 ± 9.3	1.28 ± 5.22*
Ankle	sag	0.13 ± 4.32	-1.40 ± 3.85	1.53 ± 3.87***
Ankle	fro	-2.60 ± 2.51	-2.21 ± 4.48	-0.38 ± 3.28
Ankle	tra	17.07 ± 14.7	13.97 ± 13.29	3.11 ± 13.01
		ITO	ITO	
Hip	sag	-5.93 ± 4.4	-6.77 ± 4.5	0.85 ± 2.39
Hip	fro	-5.7 ± 4.21	-5.58 ± 4.45	-0.12 ± 1.38*
Hip	tra	-5.38 ± 18.43	2.82 ± 5.88	-8.20 ± 15.36*
Knee	sag	27.66 ± 5.42	27.28 ± 5.06	0.38 ± 4.02
Knee	fro	-1.22 ± 8.02	1.31 ± 3.07	-2.53 ± 6.62*
Knee	tra	2.13 ± 9.94	2.11 ± 10.17	0.02 ± 6.26
Ankle	sag	-7.27 ± 6.14	-8.03 ± 6.71	0.76 ± 4.65
Ankle	fro	1.23 ± 4.24	0.88 ± 3.49	0.35 ± 2.51
Ankle	tra	-1.11 ± 16.36	-0.35 ± 14.18	-0.77 ± 9.56

6.4.4.2 Between-Session Reliability of Joint Angles Following Thigh Marker Rotation Offset

The application of the thigh marker rotation offset increased mean ICC values for PiG lower limb model (ICC 0.63 95%CI 0.33 to 0.84 after offset) and reduced SEM values (mean SEM 3.56^{o} ± 1.77^{o} after offset). Lower limb joint ICC and SEM values after thigh marker rotation offset are presented in Table 6.6. Hip (ICC 0.62 95%CI 0.30 to 0.83 after offset) and knee (ICC 0.56 95%CI 0.21 to 0.79 after offset) ICCs were lower, but ankle ICCs were higher (ICC 0.71 95%CI 0.45 to 0.88 after offset) following thigh marker rotation offset. Hip (mean SEM 3.22^{o} ± 1.16^{o}) and ankle SEM values (mean SEM 3.66^{o} ± 2.07^{o}) reduced, but knee SEM values increased (mean SEM 3.79^{o} ± 2.11^{o}) following thigh marker rotation offset. Overall, sagittal plane ICCs increased (ICC 0.49 95%CI 0.13 to 0.74 after offset), frontal plane ICCs increased (ICC 0.63 95%CI 0.35 to 0.73 after offset), but transverse plane ICCs reduced (ICC 0.69 95%CI 0.44 to 0.86 after offset). Sagittal plane errors increased (mean SEM 3.30^{o} ± 0.58^{o} after offset), but frontal (mean SEM 1.78^{o} ± 0.47^{o} after offset) and transverse plane errors reduced (mean SEM 5.60^{o} ± 1.36^{o} after offset). All PiG lower limb ICCs for angular motion values increased following thigh marker rotation offset; at events (ICC 0.62 95%CI 0.28 to 0.84 after offset), peak minimal values (ICC 0.59 95%CI 0.32 to 0.85 after offset) and peak maximal values (ICC 0.60 95%CI 0.27 to 0.83 after offset). Error values all reduced following thigh marker rotation offset; at events (mean SEM 3.63^{o} ± 1.99^{o} after offset), peak minimal values (mean SEM 3.58^{o} ± 1.78^{o} after offset) and peak maximal values (mean SEM 3.47^{o} ± 1.76^{o} after offset). However, the changes in between-session reliability and error were not consistent within all lower limb joints.

Hip, knee and ankle 3D joint motion over the gait cycle, following thigh marker rotation offset, are shown in Figure 6.4. Between-session reliability of the hip decreased in the sagittal plane (ICC 0.72, 95%CI 0.48 to 0.89) and transverse planes (ICC 0.78, 95%CI 0.57 to 0.90), but increased in the frontal plane (ICC 0.52, 95%CI 0.14 to 0.77) when the thigh marker rotation offset was applied. Sagittal error values at the hip increased (SEM 3.24^{o} ± 0.63^{o}) after thigh marker rotation offset, but frontal plane (SEM 2.06^{o} ± 0.33^{o}) and transverse plane (SEM 4.37^{o} ± 1.17^{o}) were reduced.

Following thigh marker rotation offset knee transverse plane between-session reliability improved (ICC 0.60, 95%CI 0.26 to 0.82), remained the same in the sagittal plane (ICC 0.46, 95%CI 0.07 to 0.73) and reduced in the frontal plane (ICC 0.60, 95%CI 0.30 to 0.81). Sagittal (SEM 3.25^{o} ± 0.50^{o}) and transverse plane (SEM 6.17^{o} ± 1.10^{o}) error values increased but frontal plane reduced (SEM 1.94^{o} ± 0.36^{o}) after thigh marker rotation offset respectively.

The ankle demonstrated increased between-session reliability in all three planes; sagittal (ICC 0.56, 95%CI 0.22 to 0.80), frontal (ICC 0.80, 95%CI 0.60 to 0.80) and transverse (ICC 0.74, 95%CI 0.51 to 0.89) following thigh marker rotation offset. Ankle error values were reduced in all three planes; sagittal (SEM 3.40^{o} ± 0.67^{o}), frontal (SEM 1.32^{o} ± 0.17^{o}) and transverse plane (SEM 6.28^{o} ± 0.74^{o}).

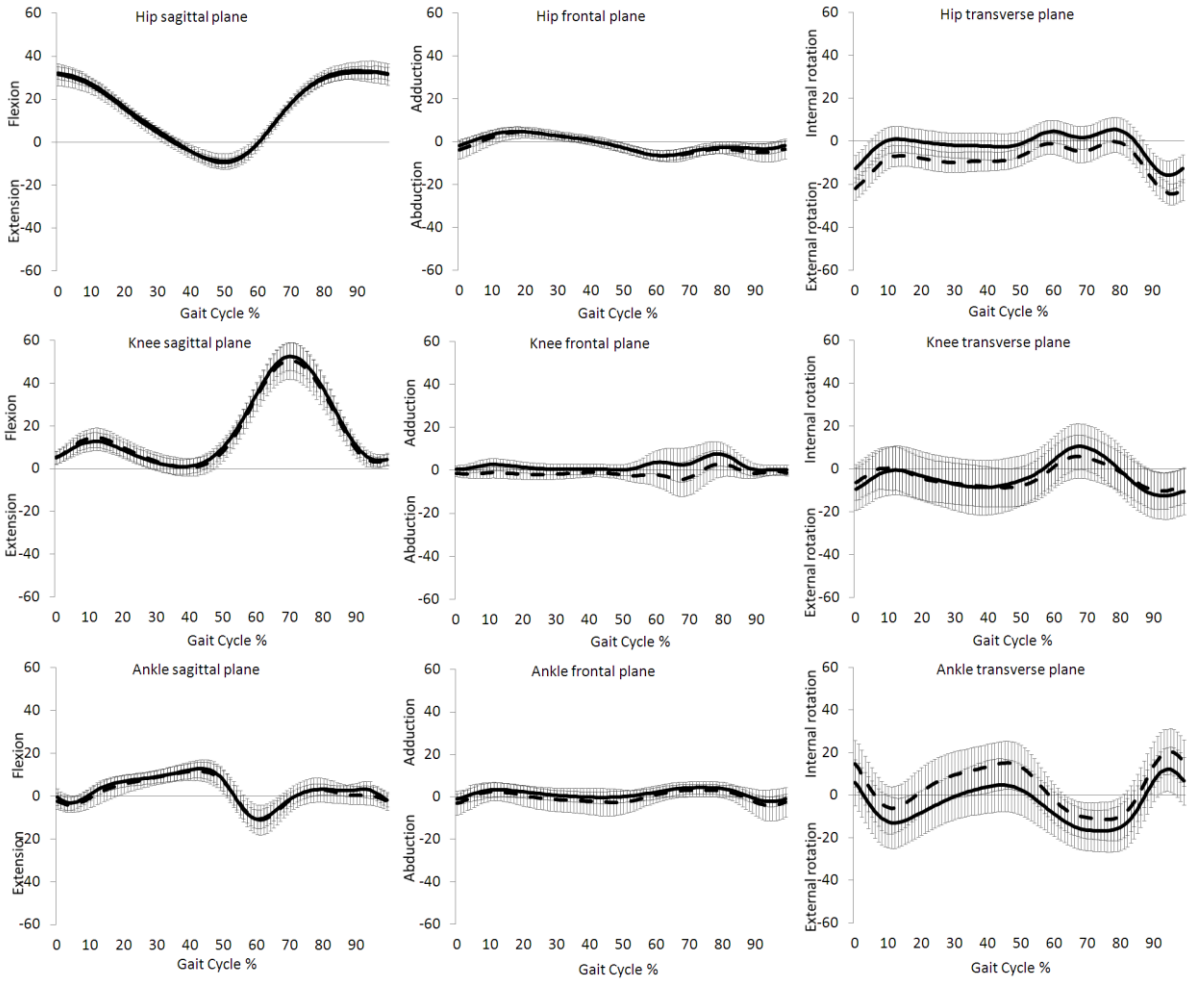

Figure 6.4. Mean ± SD of Plug-in gait test-retest following thigh rotation offset. Session 1 black line, session 2 dash line

In summary, of the 54 lower limb variables extracted over the gait cycle eight (16.7%) demonstrated low reliability, 14 (25.9%) demonstrated moderate reliability, 24 (44.4%) demonstrated moderately high reliability and eight (14.8%) demonstrated very high reliability, following thigh marker rotation offset. The eight lower limb variables that demonstrated low reliability (number of variables over the gait cycle in brackets):

- Hip sagittal plane value at ipsilateral initial contact and at ipsilateral toe-off (2)
- Hip frontal plane value at ipsilateral initial contact stance and swing phase peak minimal value (3)
- Knee sagittal plane value at ipsilateral initial contact, stance phase peak maximal (2)
- Ankle sagittal plane value at ipsilateral initial contact (1)

Following thigh marker rotation offset, 13 (20.3%) of the lower limb variables demonstrated unacceptable SEM values, 30 (55.6%) demonstrated reasonable SEM and 11 demonstrated acceptable SEM values. The 13 lower limb variables to demonstrate (number of variables over the gait cycle in brackets):

- Hip transverse plane stance and swing phase minimal peak values (2)
- All six knee transverse plane values (6)
- Ankle transverse plane stance maximal and minimal peak values, value at ipsilateral toe-off and swing maximal and minimal peak values (5)

Table 6.6. ICC (95% Confidence intervals) and SEM of PiG lower limb angular outputs at gait cycle events and peaks following thigh marker rotation offset

		Gait Cycle					
Segment	Plane	IIC	Stance min	Stance max	ITO	Swing min	Swing max
Hip (ICC)	sag	0.29 (-0.14 to 0.62)	0.77 (0.52 to 0.90)	0.43 (0.02 to 0.71)	0.19 (-0.24 to 0.56)	0.65 (0.33 to 0.84)	0.58 (0.23 to 0.80)
(SEM)		4.14	2.93	3.76	3.95	2.87	2.71
Hip	fro	0.37 (-0.05 to 0.68)	0.24 (-0.19 to 0.59)	0.65 (0.33 to 0.84)	0.80 (0.58 to 0.91)	0.31 (-0.12 to 0.64)	0.57 (0.21 to 0.80)
		2.76	2.18	2.11	1.74	2.17	2.10
Hip	tra	0.93 (0.83 to 0.97)	0.80 (0.58 to 0.91)	0.77 (0.52 to 0.90)	0.56 (0.19 to 0.79)	0.82 (0.62 to 0.92)	0.76 (0.50 to 0.89)
		3.92	5.53	3.76	3.43	5.98	3.14
Knee	sag	0.34 (-0.09 to 0.66)	0.64 (0.30 to 0.83)	0.35 (-0.07 to 0.67)	0.53 (0.14 to 0.77)	0.51 (0.13 to 0.76)	0.41 (0.00 to 0.70)
		2.50	3.14	3.93	3.38	2.77	3.03
Knee	fro	0.74 (0.47 to 0.88)	0.62 (0.29 to 0.82)	0.60 (0.25 to 0.81)	0.66 (0.33 to 0.84)	0.58 (0.22 to 0.80)	0.57 (0.20 to 0.79)
		1.50	1.41	1.93	1.84	2.27	2.25
Knee	tra	0.40 (-0.02 to 0.70)	0.73 (0.45 to 0.88)	0.61 (0.26 to 0.82)	0.55 (0.18 to 0.79)	0.73 (0.45 to 0.88)	0.53 (0.16 to 0.78)
		7.92	5.53	5.67	7.09	5.29	7.26
Ankle	sag	0.33 (-0.10 to 0.65)	0.62 (0.28 to 0.82)	0.59 (0.23 to 0.81)	0.68 (0.37 to 0.85)	0.58 (0.22 to 0.80)	0.61 (0.27 to 0.82)
		3.28	3.61	2.35	3.60	4.37	3.07
Ankle	fro	0.92 (0.82 to 0.97)	0.77 (0.52 to 0.90)	0.83 (0.63 to 0.92)	0.82 (0.61 to 0.92)	0.70 (0.40 to 0.86)	0.77 (0.52 to 0.90)
		1.18	1.14	1.54	1.38	1.13	1.39
Ankle	tra	0.87 (0.72 to 0.94)	0.79 (0.56 to 0.91)	0.65 (0.33 to 0.84)	0.76 (0.50 to 0.89)	0.74 (0.47 to 0.88)	0.70 (0.40 to 0.86)
		4.83	6.60	6.18	6.82	5.51	6.28

6.4.4.3 Joint Moment Differences Following Thigh Marker Rotation Offset

Table 6.7 shows the effects of applying the thigh marker rotation offset to lower limb joint moments on peak maximal and minimal values during the stance phase. The hip joint demonstrated greater peak extension, no change in peak abduction, and lower peak external rotation moments during the stance phase. Higher peak hip flexion, lower peak adduction and lower peak internal rotation moments were found after thigh marker rotation offset.

Following thigh marker rotation offset peak knee joint extension moments were lower, peak varus (abduction) moments were significantly higher and peak external rotation moments were higher. Maximal peak moment values after thigh marker rotation offset showed a significantly lower flexion moment, a higher valgus (adduction) moment and lower internal rotation moment.

Table 6.7 shows that all ankle joint moments were significantly altered following thigh marker offset. Greater peak extension, abduction and external rotation moments were found through the stance phase. Also, greater flexion, adduction and internal rotation moments were found following thigh marker rotation offset.

Table 6.7. Mean ± SD of PiG lower limb moment outputs at gait cycle peaks before and after thigh marker rotation offset. Significance * = p<.05, ** = p<.01, *** = p<.001

PiG kinetics		Average joint angle		
		Pre-offset	Post-offset	Pre post-offset
Segment	Plane	Min	Min	Difference
Hip	sag	-16.8 ± 10.45	-26.31 ± 9.46	9.52 ± 0.15
Hip	fro	0.00 ± 3.68	0.00 ± 4.68	0.00 ± 0.15
Hip	tra	-2.69 ± 1.32	-2.44 ± 1.52	-0.25 ± 0.01
Knee	sag	-0.23 ± 4.97	-1.13 ± 5.01	0.90 ± 0.08
Knee	fro	-0.13 ± 1.46	-0.23 ± 2.43	0.10 ± 0.06***
Knee	tra	-0.22 ± 0.77	-0.88 ± 0.68	0.66 ± 0.01
Ankle	sag	-1.94 ± 3.76	-2.38 ± 2.17	0.44 ± 0.05***
Ankle	fro	-0.08 ± 0.22	-0.26 ± 0.54	0.18 ± 0.02***
Ankle	tra	-0.04 ± 1.58	-3.60 ± 1.53	3.56 ± 0.01***
		Max	Max	
Hip	sag	14.8 ± 12.09	16.93 ± 12.37	-2.13 ± 0.07
Hip	fro	6.77 ± 12.07	5.76 ± 10.27	1.01 ± 0.08
Hip	tra	2.05 ± 1.85	1.61 ± 2.16	0.44 ± 0.01
Knee	sag	2.77 ± 4.17	2.48 ± 5.32	0.30 ± 0.03*
Knee	fro	1.73 ± 6.73	1.87 ± 7.09	-0.14 ± 0.01
Knee	tra	1.11 ± 2.55	0.66 ± 2.14	0.44 ± 0.01
Ankle	sag	4.90 ± 18.41	10.17 ± 16.23	-5.27 ± 0.01*
Ankle	fro	0.15 ± 0.19	0.15 ± 1.84	0.01 ± 0.01***
Ankle	tra	3.96 ± 2.63	7.53 ± 3.17	-3.57 ± 0.01***

6.4.4.4 Between-Session Reliability of Joint Moments after Thigh Marker Rotation Offset

Overall, between-session reliability of lower limb joint moments during the stance phase of gait remained the same (ICC 0.48 95%CI 0.08 to 0.74 after offset) and SEM increased (mean SEM 2.38Nm ± 1.89Nm after offset) following the application of the thigh marker rotation offset. Lower limb joint moment ICC and SEM values after thigh marker rotation offset are presented in Table 6.8. Hip (ICC 0.44 95%CI 0.04 to 0.72 after offset) and ankle ICCs increased (ICC 0.57 95%CI 0.21 to 0.79 after offset), but knee ICCs decreased (ICC 0.41 95%CI -0.00 to 0.70 after offset) following thigh marker rotation offset. Hip SEM values reduced (mean SEM 3.37Nm ± 2.24Nm after offset), but knee (mean SEM 1.88Nm ± 2.03Nm after offset) and ankle SEM values increased (mean SEM 1.88Nm ± 4.06Nm after offset) following thigh marker rotation offset. Mean sagittal (ICC 0.48 95%CI 0.10 to 0.75 after offset) and frontal plane ICCs increased (ICC 0.52 95%CI 0.14 to 0.77 after offset) but transverse plane ICCs reduced (ICC 0.41 95%CI 0.02 to 0.70 after offset). Sagittal (mean SEM 4.36Nm ± 4.45Nm after offset) and transverse plane SEM increased (mean SEM 0.79Nm ± 0.77Nm after offset) but frontal plane SEM reduced (mean SEM 1.99Nm ± 2.43Nm after offset). Lower limb moment ICCs extracted at gait cycle events were higher after thigh rotation marker offset (ICC 0.43 95%CI 0.03 to 0.71 after offset) but peak minimal (ICC 0.65 95%CI 0.33 to 0.84 after offset) and peak maximal values ICCs were lower (ICC 0.35 95%CI -0.07 to 0.67 after offset). Lower limb joint moment errors at gait events were lower (mean SEM 0.91Nm ± 1.05Nm after offset), but peak minimal (mean SEM 2.24Nm ± 2.09Nm after offset) and peak maximal values ICCs were higher (mean SEM 5.59Nm ± 4.50Nm after offset). However, the changes in between-session reliability and error were not consistent across all lower limb joints.

Hip, knee and ankle 3D joint moments over the stance phase, following thigh marker rotation offset, are shown in Figure 6.5. Between-session reliability of hip moment increased in the sagittal (ICC 0.42, 95%CI -0.00 to 0.71) and transverse planes (ICC 0.33, 95%CI -0.17 to 0.60) and remained the same in the frontal plane (ICC 0.55, 95%CI -0.19 to 0.79). Error measures increased in the sagittal (SEM 5.99Nm ± 3.48Nm) and transverse plane (SEM 0.79Nm ± 0.69Nm) and reduced in the frontal plane (SEM 3.35Nm ± 2.81Nm).

Knee joint moment between-session reliability was reduced in the sagittal (ICC 0.32, 95%CI -0.10 to 0.65) and transverse planes (ICC 0.35, 95%CI -0.07 to 0.67), but increased in the frontal plane (ICC 0.53, 95%CI -0.15 to 0.78). Error values increased in the sagittal (SEM 2.88Nm ± 1.69Nm) and frontal planes (SEM 2.06Nm ± 2.86Nm) and remained the same in the transverse plane (SEM 0.69Nm ± 0.84Nm).

Following thigh rotation offset, between-session reliability of ankle joint moments increased in the sagittal (ICC 0.68, 95%CI 0.37 to 0.85) and frontal planes (ICC 0.47, 95%CI 0.08 to 0.74), but reduced in the transverse plane (ICC 0.53, 95%CI 0.16 to 0.76). Ankle error values were lower in the sagittal plane (SEM 4.21Nm ± 7.16Nm) but higher in the frontal (SEM 0.56Nm ± 0.56Nm) and transverse planes (0.88Nm ± 0.97Nm) following thigh rotation offset.

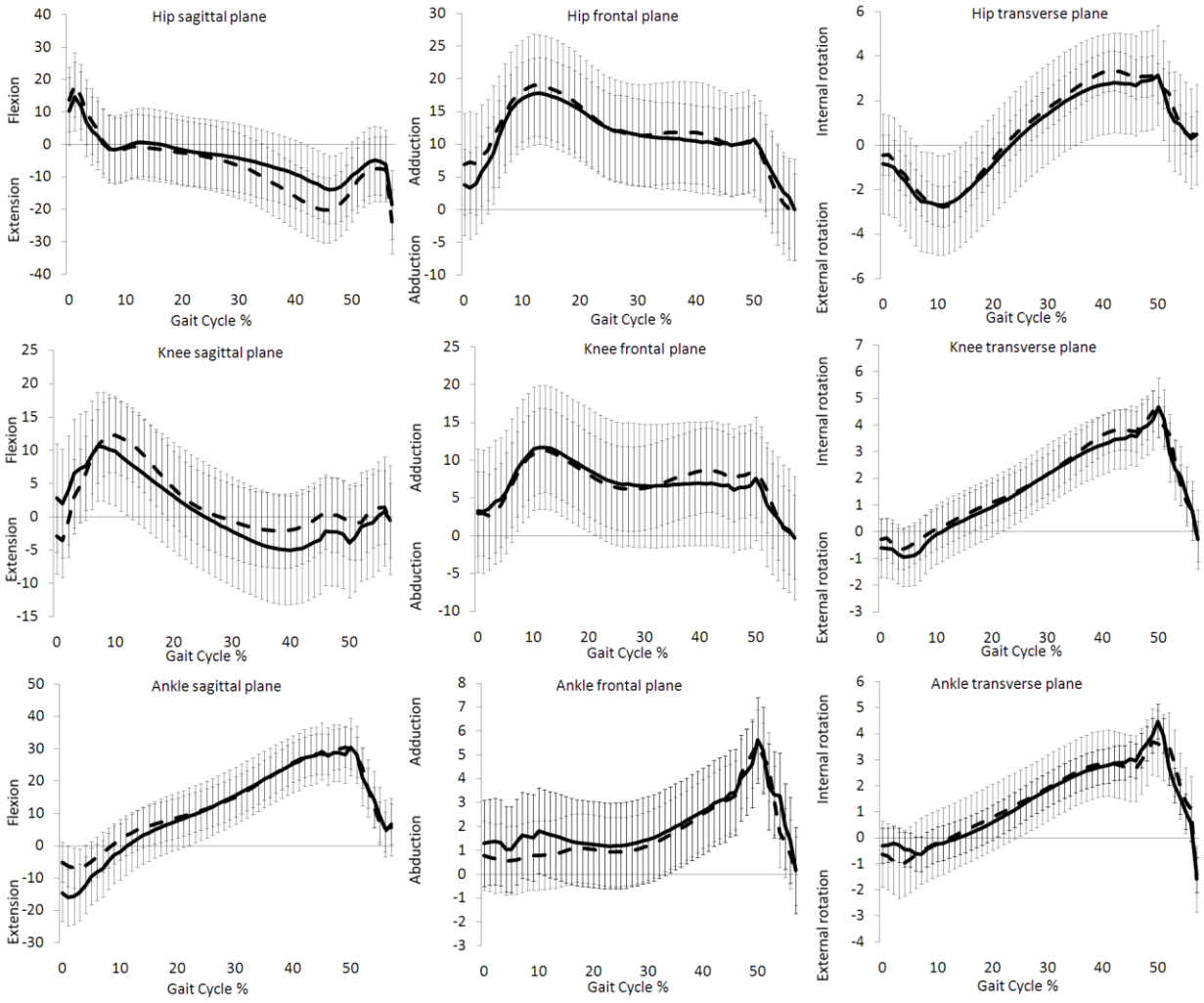

Figure 6.5. Mean ± SD of PiG kinetic test retest following thigh marker rotation offset. Session 1 black line, session 2 dash line

In summary, the findings of lower limb joint moment between-session reliability following thigh marker rotation offset, indicated that of the 36 lower limb variables extracted over the gait cycle 11 (30.6%) demonstrated low reliability, 15 (51.7%) demonstrated moderate reliability, two (5.6%) demonstrated moderately high reliability and eight (22.2%)

demonstrated very high reliability. The 11 lower limb moment variables that demonstrated low reliability were (number of variables over the gait cycle in brackets):

- Hip sagittal plane stance peak maximal value and value at ipsilateral toe-off (2)
- Hip transverse plane stance peak minimal value and value at ipsilateral toe-off (1)
- Knee sagittal plane value at ipsilateral initial contact, stance peak minimal and maximal values (3)
- Knee frontal plane value at stance peak maximal value and value at ipsilateral toe-off (2)
- Knee transverse plane value at ipsilateral initial contact, stance peak maximal value and value at ipsilateral toe-off (3)
- Ankle sagittal plane stance peak maximal value (1)
- Ankle frontal plane value at ipsilateral initial contact (1)
- Ankle transverse plane value at ipsilateral toe-off (1)

Table 6.8. ICC (95% confidence intervals) and SEM of PiG lower limb moment outputs at stance phase events and peaks following thigh marker rotation offset

		Gait Cycle			
Segment	Plane	IIC	Stance min	Stance max	ITO
Hip (ICC)	sag	0.44 (0.03 to 0.72)	0.38 (-0.03 to 0.69)	0.33 (-0.10 to 0.65)	0.53 (0.15 to 0.77)
(SEM)		3.96	7.43	10.14	2.41
Hip	fro	0.53 (0.16 to 0.78)	0.71 (0.42 to 0.87)	0.47 (0.07 to 0.74)	0.47 (0.07 to 0.74)
		2.07	2.52	7.49	1.30
Hip	tra	0.40 (-0.01 to 0.70)	0.38 (-0.04 to 0.69)	0.49 (0.09 to 0.75)	0.03 (-0.39 to 0.44)
		0.25	1.20	1.55	0.16
Knee	sag	0.27 (-0.16 to 0.61)	0.22 (-0.21 to 0.58)	0.38 (-0.04 to 0.68)	0.40 (-0.01 to 0.70)
		1.91	4.41	4.20	1.00
Knee	fro	0.47 (0.07 to 0.74)	0.86 (0.69 to 0.94)	0.20 (-0.23 to 0.57)	0.36 (-0.06 to 0.67)
		0.64	0.92	6.34	0.35
Knee	tra	0.24 (-0.19 to 0.59)	0.69 (0.39 to 0.86)	0.16 (-0.27 to 0.54)	0.22 (-0.21 to 0.58)
		0.24	0.38	1.95	0.17
Ankle	sag	0.80 (0.57 to 0.91)	0.82 (0.61 to 0.92)	0.15 (-0.28 to 0.53)	0.73 (0.45 to 0.88)
		0.79	0.93	14.93	0.18
Ankle	fro	0.16 (-0.27 to 0.53)	0.73 (0.46 to 0.88)	0.45 (0.05 to 0.73)	0.44 (0.04 to 0.72)
		0.48	0.28	1.36	0.10
Ankle	tra	0.51 (0.12 to 0.76)	0.70 (0.41 to 0.86)	0.49 (0.09 to 0.75)	0.38 (-0.03 to 0.69)
		0.25	0.84	2.27	0.17

6.4.4.5 Summary of Lower limb Between-Session Reliability

Table 6.9 reports mean ICCs and SEMs for extracted lower limb angular motion and moments at events and peaks of the gait cycle. Lower limb angular motion between-session reliability was moderately high (ICC scale of Katz et al., 1992) before and after thigh marker rotation

offset. Lower limb moment between-session reliability was moderate before and after thigh marker rotation offset. The mean error values for lower limb angular motion between-session reliability were less than 5°, indicating reasonable errors. Mean lower limb motion ICCs increased following thigh marker rotation offset but the number of motion variables to show low reliability (ICC <0.4) remained the same. Mean lower limb moment ICCs remained the same following thigh marker rotation offset but the number of moment variables to show unacceptable reliability (ICC <0.4) decreased. Mean lower limb motion errors were reduced following thigh marker rotation offset and the number of motion variables to show unacceptable SEM values (>5°) decreased.

Table 6.9. Summary of ICC and SEM values of PiG angular and moment outputs before and after thigh marker rotation offset

Lower limb model	Mean ICC (95%CI)	Percentage of variables with low ICC	Mean SEM (kinematics °, kinetic Nm)	Percentage of variables with unacceptable SEM
Kinematics	0.60 (0.27 to 0.82)	16.7	3.98 ± 1.89	29.6
Kinematics (thigh marker rotation offset)	0.63 (0.33 to 0.84)	16.7	3.56 ± 1.77	20.3
Kinetics	0.48 (0.11 to 0.75)	38.9	2.32 ± 2.04	-
Kinetics (thigh marker rotation offset)	0.48 (0.08 to 0.74)	30.6	2.38 ± 1.89	-

6.4.5 Aim 3 Changes in Lower Limb Joint Parameters Following ASIS 'Instrumented Pointer Device' Protocol

The subject's information is detailed in Table 6.10. Only body mass, percentage of body and BMI Z-Score were significantly different between the obese and non-obese boys.

Table 6.10. Mean ± SD of anthropometric and spatiotemporal measures for five obese and five non-obese boys testing ASIS marker protocols. *p* represents the output from paired t-tests, (significance <.05)

	Obese (n=5)	Non-obese (n=5)	P value between groups
Age (years)	9.60 ± 1.34	10.00 ± 1.22	.621
Height (cm)	145.40 ± 8.91	136.80 ± 6.13	.065
Body Mass (kg)	54.60 ± 13.01	29.20 ± 3.27	.012*
BMI Z-Score	2.77 ± 0.72	-0.70 ± 0.48	.001*
Fat Mass (% Body mass)	38.4 ± 3.97	14.47 ± 3.65	.001*
Cadence (steps/min	132.13 ± 17.60	134.89 ± 11.82	.742
Stance phase (% gait cycle)	59.19 ± 2.61	57.35 ± 1.21	.096
Step Length (m)	1.13 ± 0.11	1.23 ± 0.06	.106
Step Width (m)	0.17 ± 0.02	0.16 ± 0.01	.434
Walking Speed ($m \cdot s^{-1}$)	1.28 ± 0.25	1.38 ± 0.17	.268

Root Mean Square (RMS) differences between skin mounted and virtual ASIS marker position were 19.57, 7.36 and 10.48mm for anterior/posterior, medial/lateral and inferior/superior axis position. The RMS differences in hip joint centre position were 8.70, 6.03 and 7.20mm for anterior/posterior, medial/lateral and inferior/superior axis position. The mean difference in the position of the ASIS and hip joint centre is presented in Table 6.11. Compared to skin mounted ASIS markers the virtual ASIS markers were more posterior, medial and inferior in the obese participants and posterior, lateral and superior in the non-obese participants. The difference in ASIS position moved the hip joint centre posteriorly, medially and inferiorly in the obese participants and anteriorly, laterally and superiorly in non-obese participants. The hip joint centre of the obese boys was positioned significantly more medially when virtual ASIS markers were applied compared to skin mounted ASIS markers. In general, the virtual ASIS markers and hip joint centres of obese boys were positioned more medially, posteriorly and inferiorly compared to healthy weight boys, though not significantly.

Table 6.11. Mean ± SD of Virtual and skin mounted ASIS markers position and difference. * denotes significant difference between virtual and skin mounted position (p<0.05), ** (p<0.01), *** (p<0.001)

	Obese	Non-obese	Obese Non-obese difference
ASIS (mm)			
X axis (anterior +, posterior -)	-16.43 ± 15.62	-6.19 ± 21.40	10.24 ± 16.99
Y axis (lateral +, medial -)	-6.41 ± 6.40	0.18 ± 7.12	6.59 ± 6.78
Z axis (superior +, inferior -)	-3.13 ± 7.77	1.75 ± 15.23	4.88 ± 10.83
Hip Joint Centre (mm)			
X axis	-2.42 ± 7.39	1.97 ± 12.34	4.40 ± 9.07
Y axis	-5.27 ± 1.95**	0.05 ± 7.26	5.32 ± 5.37
Z axis	-1.40 ± 5.63	1.40 ± 10.66	2.80 ± 7.50

At gait cycle events and peaks both the non-obese and obese boy's hip joint motions were altered using virtual compared to skin mounted ASIS markers, shown in Tables 6.12, 6.13 and 6.14. The non-obese boy's hip motion waveform was shifted towards flexion, adduction and internal rotation when virtual ASIS markers are used. The obese boy's hip motion waveform was shifted towards flexion, abduction and internal rotation. The non-obese boys presented significantly greater internal rotation in stance and swing phase maximal peaks and significantly less external rotation in stance and swing phase minimal peaks. The obese boys presented significantly greater hip flexion during stance and swing phase peaks, a significantly greater adduction peak in the stance and swing phases and significantly more internal rotation/less external rotation in stance and swing peaks.

When the obese and non-obese participant's hip joint kinematics are compared using skin mounted ASIS markers significant differences were found in the sagittal and transverse planes. The obese group demonstrated significantly more hip flexion at maximal and minimal peaks in the stance phase, minimal peaks in the swing phase and at ipsilateral toe-off. The obese group also demonstrated significantly less external rotation at ipsilateral initial contact.

When using the virtual ASIS markers the difference between obese and non-obese participant's hip joint kinematics were significant in the sagittal, frontal and transverse planes. The obese group demonstrated significantly more hip flexion at ipsilateral initial contact, ipsilateral toe-off, and maximal and minimal peaks in the stance and swing phases. The obese group's hip was significantly more abducted at ipsilateral initial contact and peak minimal in the swing phase. The obese group also demonstrated significantly less external rotation at ipsilateral initial contact.

Table 6.12. Mean ± SD of PiG sagittal hip angular outputs at gait cycle events and peaks between virtual and skin mounted ASIS markers. * denotes significant difference between virtual and skin mounted ASIS markers. † denotes significant difference between obese and non-obese groups when using skin mounted markers. ‡ denotes significant difference between obese and non-obese groups when using virtual markers

	IIC	Stance min	Stance max	ITO	Swing min	Swing max
Non-obese boys						
Skin ASIS	34.35 ± 6.89	-13.71 ± 7.63†	35.32 ± 6.68†	-9.59 ± 6.81†	-9.66 ± 7.11†	35.42 ± 7.59
Virtual ASIS	35.44 ± 8.47‡	-13.65 ± 9.00‡	36.13 ± 7.80‡	-8.78 ± 7.96‡	-9.23 ± 8.22‡	36.46 ± 8.87‡
Mean difference	1.09 ± 3.26	0.06 ± 2.78	0.78 ± 2.76	0.81 ± 2.59	0.43 ± 2.44	1.04 ± 2.94
Obese boys						
Skin ASIS	40.86 ± 5.13	2.13 ± 4.86†	41.88 ± 5.37†	7.55 ± 4.97†	7.70 ± 5.20†	43.64 ± 4.85
Virtual ASIS	43.55 ± 5.46‡	4.14 ± 5.31‡	44.22 ± 5.71‡	9.43 ± 5.63‡	9.66 ± 5.98‡	46.64 ± 4.68‡
Mean difference	2.69 ± 0.73	2.01 ± 1.87*	2.34 ± 1.38*	1.88 ± 1.97	1.96 ± 2.22	3.00 ± 0.67*

Table 6.13. Mean ± SD of PiG frontal hip angular outputs at gait cycle events and peaks between virtual and skin mounted ASIS markers. * denotes significant difference between virtual and skin mounted ASIS markers. † denotes significant difference between obese and non-obese groups when using skin mounted markers. ‡ denotes significant difference between obese and non-obese groups when using virtual markers

	IIC	Stance min	Stance max	ITO	Swing min	Swing max
Non-obese boys						
Skin ASIS	-3.49 ± 2.70	-4.84 ± 2.14	6.63 ± 2.77	-4.81 ± 1.87	-7.83 ± 1.85	-2.30 ± 1.94
Virtual ASIS	-2.87 ± 3.83‡	-4.76 ± 2.87‡	5.89 ± 3.70	-4.53 ± 2.54	-7.79 ± 1.53	-1.41 ± 3.37
Mean difference	0.62 ± 1.88	0.08 ± 1.61	-0.74 ± 2.06	0.28 ± 1.30	0.05 ± 1.46	0.89 ± 2.01
Obese boys						
Skin ASIS	-4.41 ± 5.68	-8.19 ± 5.21	4.54 ± 4.89	-7.39 ± 4.56	-11.67 ± 4.68	-3.47 ± 4.70
Virtual ASIS	-8.73 ± 5.68‡	-9.46 ± 5.49‡	2.50 ± 4.16	-8.03 ± 4.56	-13.51 ± 3.33	-5.83 ± 4.11
Mean difference	-4.32 ± 2.10	-1.27 ± 1.82	-2.04 ± 1.48*	-0.64 ± 1.69	-1.83 ± 2.05	-2.35 ± 1.81*

Table 6.14. Mean ± SD of PiG transverse hip angular outputs at gait cycle events and peaks between virtual and skin mounted ASIS markers. * denotes significant difference between virtual and skin mounted ASIS markers. † denotes significant difference between obese and non-obese groups when using skin mounted markers. ‡ denotes significant difference between obese and non-obese groups when using virtual markers

	IIC	Stance min	Stance max	ITO	Swing min	Swing max
Non-obese boys						
Skin ASIS	-12.6 ± 10.99†	-15.54 ± 11.38	3.8 ± 10.94	1.52 ± 13.21	-23.56 ± 9.34	14.67 ± 7.28
Virtual ASIS	-9.37 ± 10.62‡	-11.33 ± 11.55	9.48 ± 11.82	5.42 ± 12.57	-20.57 ± 9.60	19.50 ± 4.94
Mean difference	3.22 ± 2.17	4.21 ± 3.50*	5.68 ± 4.42*	3.90 ± 3.55	3.06 ± 2.47*	4.82 ± 5.33*
Obese boys						
Skin ASIS	-1.13 ± 6.54†	-9.52 ± 6.65	7.45 ± 3.79	3.23 ± 5.98	-16.41 ± 5.27	15.85 ± 4.57
Virtual ASIS	3.38 ± 7.96‡	-3.68 ± 5.00	12.49 ± 4.51	4.05 ± 5.53	-10.63 ± 5.27	19.05 ± 3.16
Mean difference	4.51 ± 4.15	5.84 ± 6.37*	5.04 ± 4.86*	0.82 ± 5.48	5.78 ± 3.41*	3.20 ± 6.58

6.5 Discussion

The aims of this experimental chapter of the thesis were to; (1) examine between-session reliability of the conventional plug-in gait (PiG) lower limb model for use in children across a range of BMI values; (2) test a protocol with the potential to increase between-session PiG reliability based on thigh marker placement across a range of BMI Z-Score values; and, (3) assess an alternative method to identify the ASIS on the pelvis of obese and non-obese children. In order to test these aims a within-rater repeated measures (test re-test) study design was implemented to measure between-session reliability (ICC) and error (SEM) of the lower limb model. To assess an alternative protocol to identify the pelvis children participated in a single session in which the conventional (PiG) model and alternative protocol were examined concurrently.

6.5.1 Anthropometrics & Spatiotemporal

The participants of this experimental chapter were recruited to represent the potential participants of the main study (chapter 8). Measures of gait data reliability are intrinsically related to the variability within the studied group (McGinley et al., 2009). Therefore, the results of this experimental chapter aid interpretation of significant findings in the main study (chapter 8) above the error associated with gait analysis.

Anthropometric and spatiotemporal parameters were used to analyse gait consistency between sessions so differences due to growth, weight gain or changes in walking patterns would not affect between-session reliability assessment. Anthropometric repeated measures were highly reliable with all parameters exceeding an ICC of 0.9. This indicates that the measurement protocols were acceptable for the children and furthermore, the test re-test interval (4 weeks) was short enough so only minimal growth or change body mass took place. Spatiotemporal parameters were less reliable than anthropometric measures with ICCs ranging from 0.421 to 0.885. The between-session reliability of spatiotemporal parameters was comparable to previous studies. Stolze et al., (1998) found between-session reliability of gait velocity and stance phase duration to be low (ICC 0.35 and 0.30 respectively) but step length and step width to be high (ICC 0.72 and 0.70 respectively). This finding is comparable to the current study in which gait velocity and stance phase ICCs were lower (0.47 and 0.42 respectively) than step length and step width ICCs (0.82 and 0.89 respectively).

Lower between-session reliability of stance phase duration in the current study may be the result of greater gait velocity in the second session possibly due to familiarity with the testing environment and protocols (McGinley et al., 2009). The slightly faster mean gait velocity could have resulted in reduced stance duration in the second session. A previous study to examine the effect of walking speed on children's gait spatiotemporal parameters found that, as children walked faster the stance phase duration of the gait cycle was reduced (van der Linden et al., 2002). This finding indicates that spatiotemporal measures and potentially kinematic and kinetic variables are greatly affected by walking speed. Therefore, walking speed variability should be accounted for when examining associations between obesity and gait biomechanics. Relationships between obesity and gait biomechanics may arise from differences in walking speed mediated through level of obesity and not obesity *per se*.

Non-significant anthropometric or spatiotemporal differences were found between the two testing sessions in the current study (Table 6.2). This indicates that between-session reliability

and error were due to intrinsic variability (assumed to be equal across both testing sessions) and extrinsic variability due to systematic errors (marker placement and motion capture system marker reconstruction). Participant's height showed a trend of increasing between the sessions though non-significant (p = .062). This may indicate that a shorter test re-test interval may be more appropriate so growth is minimised. The height increase may have contributed to variability of gait parameters between sessions.

6.5.2 Aim 1. Between-Session Reliability of PiG Lower Limb Joint Angles

Between-session reliability of the lower limb (PiG) biomechanical model was moderately high with reasonable levels of error from within-rater repeated sessions. If the lower limb model presented low reliability this would decrease statistical power and potentially lead to type II errors (false-negative) due to too much variability. The results can be used to indicate the expected error for each lower limb joint (hip, knee and ankle) in each plane (sagittal, frontal and transverse) at selected points of the gait cycle (events and peaks). Knowledge of the expected error will reduce over-interpretation of small joint angular motions associated with obesity which may not exceed measurement error (McGinley et al., 2009).

Between-session reliability of hip joint motion was greater than knee and ankle, although all joints were considered to show moderately high reliability. Hip joint errors from repeated sessions were lowest in the frontal plane, followed by the sagittal and transverse. This planar order of errors from lowest to highest was also found by Schwartz et al., (2004) who quantified lower limb errors in repeated gait sessions adult participants. Errors in transverse plane hip motion were caused by problems aligning the thigh marker to determine the orientation of the thigh in the transverse plane. In the current study all transverse plane hip values demonstrated error greater than 5^{o} indicating that the repeatable placement of the thigh marker placement was an issue.

The knee also demonstrated greatest repeated session errors in the transverse plane. These knee errors, like hip joint errors, are due to misalignment of the thigh marker with the addition of shank marker misplacement errors. Knee joint errors in the frontal plane are the result of cross-talk from misalignment of the technical reference frame with the anatomical reference frame of the thigh segment. An examination of Figure 6.2 shows that around ipsilateral toe-off increased variability of frontal plane knee joint motion was found. At this point in the gait cycle the knee is maximally flexing in the sagittal plane, but the misalignment of the thigh

segments attributes some of this flexion to frontal plane motion. This is highlighted in Table 6.3 where unacceptable SEM values are found only at the end of stance and swing when knee flexion was greatest.

The ankle demonstrated the greatest error values from repeated sessions compared to the hip and knee joints. This finding is likely due to the hierarchical nature of the lower limb (PiG) model where errors propagate down the kinematic chain from the pelvis to the foot (Schwartz et al., 2004). The effects of pelvis marker misplacement can offset the position of the calculated hip joint centre. The hip joint centre and thigh marker location are used to calculate the position and orientation of the knee joint centre. Therefore, the knee joint centre becomes misplaced, which together with the shank and foot markers defines the position and orientation of the ankle joint centre. Like the hip joint, all ankle transverse plane errors were higher than 5^{o} indicating that the marker placement error is an issue. This finding illustrates the need to accurately define the pelvis according to marker placement to reduce errors in all lower limb joints.

Miller et al., (1996) recorded lower limb motion of children during repeated sessions, finding ICCs ranging from 0.45 to 0.75 compared to ICCs of 0.42 to 0.87 in the current study. The mean lower limb ICC from Miller et al., (1996) study was 0.69 which is higher than the current study (mean ICC = 0.60). Furthermore, Miller et al., (1996) found greater between-session reliability at the knee joint compared to the hip and ankle. Conversely, the current study found greatest between-session reliability at the hip followed by the knee and ankle. However, while comparing the results of the current study to previous research provides a gauge with which to assess the between-session reliability of the participants sampled, comparison between the two studies should be made with caution. The differences in lower limb between-session reliability between the two studies are well within the ICC confidence limits for each 3D lower limb joint in the current study. Therefore, any differences in between-session reliability between the two studies may arise from chance due to the variable nature of gait analysis. The high confidence limits in the present study are the result of the relatively small sample size giving rise to uncertainty of the true level between-session reliability.

6.5.3 Aim 1. Between-Session Reliability of PiG Lower Limb Joint Moments

Between-session reliability of lower limb (PiG) joint moments for the hip, knee and ankle joints were all moderate. The ICC values of the hip, knee and ankle joint moments in the sagittal,

frontal and transverse plane were consistently above 0.4, indicating moderate reliability. However, this consistency was not found across lower limb moment values extracted at events or stance phase peaks. Extracting lower limb joint moments at peak minimal values resulted in moderately high ICCs, moderate ICCs at peak maximal values and low ICCs at gait events. Low joint moment ICC at gait events was a result of less within-session variability which reduces ICC value. In simple terms, the ICC is a ratio of within-session variance to within-subject variance plus error variance (Rankin & Stokes 1998). In the current study, mean within-session standard deviations (SD) were ±0.13Nm at peak minimal and maximal values, but only ±0.04Nm at gait events. Therefore, peak moments demonstrated a wider range of values compared to moments at events and result in a higher ICC. It is for this reason that standard error of measurement (SEM) was also calculated which relates the ICC to within-session variation. When SEM was calculated, moment values at gait events demonstrated lower errors (SEM 1.12Nm) compared to peak minimal (SEM 2.09Nm) and peak maximal values (SEM 5.27Nm). Greater SEM values at peak maximal values are the result of greater SD for peak maximal values compared to peak minimal and gait event values. In general, positive peak (maximal) lower limb joint moments are greater than negative peak (minimal) moments over the stance phase. This is because positive moment values relate to flexion, adduction and internal rotation moments of the lower limbs which are caused by the anterior and medial position of the ground reaction vector relative to the joint centres. Figure 6.3 shows lower limb joint moments during the stance phase, positive peaks are greater than negative peaks at all 3D joints except the hip in the sagittal plane.

The ankle demonstrated greater between-session reliability of joint moments compared to the knee and hip joints. Kadaba et al., (1989) also found greater between-session reliability of the lower limb (PiG) model at the ankle from repeated gait sessions in adults. The authors attributed this finding to greater errors in hip and knee joint centre position estimations compared to the ankle joint. Greater ankle moment ICCs compared to hip and knee were also found in a between-session paediatric gait reliability study (Quigley et al., 1997). However, Quigley et al., (1997) reported overall higher lower limb joint moment ICCs (mean ICC 0.85) compared to the current study (mean ICC 0.48). This difference between between-session reliability scores could result from the protocol for calculating ICCs. Quigley et al., (1997) analysed ICCs by dilating the gait cycle to 100 data points and calculating an ICC at each point, whereas the present study calculated ICCs at gait events and peak values during the stance phase. However, it is not clear how these two methods to derive ICCs return different results.

Mean SEM values were greatest in the sagittal planes compared to the frontal and transverse due the larger moments acting in the sagittal plane during gait. Few previous studies have reported SEM values for absolute lower limb joint moment. One study reported lower limb kinetic SEM values from repeated measures in adolescents with idiopathic scoliosis (Fortan et al., 2008). In Fortan et al., (2008) hip moment SEM values were 5.90Nm and 3.33Nm in the sagittal and frontal planes respectively compared to 5.83Nm and 4.25Nm in the current study. Knee sagittal and frontal SEM values were 3.50Nm and 1.75Nm in Fortan's study compared to 2.36Nm and 1.75Nm in the current study. Ankle sagittal plane moment SEM values were 2.65Nm in Fortan's study and 4.44Nm in the current study. Whilst comparison across age and pathologic groups should be made with caution, the values show consistency across lower limb joints and planes.

In summary, the lower limb (PiG) model demonstrated moderately high between-session reliability (ICC) indicating that the angular outputs were consistent across repeated sessions. Lower limb angular error values (SEM) were reasonable under the current protocols and population sampled. However, lower limb angular error values were not consistent across three planes; unacceptable errors were found in the transverse plane at the hip, knee and ankle joint. Lower limb joint moments demonstrated moderate between-session reliability (ICC) indicating that the outputs were less consistent than angular outputs across repeated sessions. Low joint moment between-session reliability was found at all joints and all planes, but was particularly evident at gait cycle events. Error values were dependent on moment magnitudes of the lower limb which vary considerable across joint and planes, therefore, no common SEM value can be proposed to determine reasonable SEM values. Between-session reliability and error values of lower limb (PiG) model for each joint, plane and value during the gait cycle can be used as a baseline for expected error when examining biomechanical differences of populations. Caution should be made when interpreting transverse plane joint motion and all joint moments at gait events due to high error or low reliability.

6.5.4 Aim 2 Lower Limb Model Joint Angle Differences and Between-Session Reliability Following Thigh Marker Rotation Offset

The mean value of thigh rotation offset applied to all subjects was $2.22^{o} \pm 5.69^{o}$; this internally rotated the thigh segment causing PiG hip outputs to be more internally rotated and knee externally rotated. The most significant effects of the thigh marker rotation offset caused to

lower limb joint angles at initial contact was to internally rotate the hip, externally rotate the knee and extend the ankle. At the end of the stance phase (toe off) the hips were abducted and more internally rotated, and the knees were more adducted. These alterations bring the lower limb joint motion in line with previous studies on lower limb paediatric gait (Ounpuu et al., 1991; van der Linden et al., 2002). This is particularly true of the hip joint in the transverse plane at ipsilateral toe-off which was internally rotated by approximately 8^{o} after thigh rotation offset. Previous analyses of child and adult hip transverse plane motion demonstrated more internal rotation through the gait cycle (Kadaba et al., 1989, van der Linden 2002). The range of motion was not altered at the hip, knee and ankle following thigh marker rotation offset but, SDs were reduced from 6.58^{o} to 5.90^{o} indicating a reduction in within-session variability. Within-session variability of hip and ankle angles at initial contact and toe off were reduced in the transverse plane. Knee frontal plane angle variability at toe off was reduced but transverse plane variability increased. These findings indicate that by rotating the thigh marker according to knee varus/valgus motion joint angle, between-session reliability due to marker misplacement was improved.

Application of the thigh marker rotation offset improved hip sagittal and frontal, knee sagittal and transverse and ankle sagittal and transverse plane ICCs of joint outputs. Hip transverse, knee and ankle frontal plane ICCs were reduced, but overall between-session reliability of the PiG lower limb was improved. Error in repeated joint angles of the hip, knee and ankle also improved (from a mean SEM of 3.98^{o} to 3.56^{o} after thigh rotation offset); largest improvements in SEM values were seen in the hip and ankle transverse plane and knee frontal plane angles. This finding is in line with Malt et al., (2012) who found that by correcting thigh rotation a significant reduction in hip transverse and knee frontal plane variability was made.

6.5.5 Lower Limb Model joint Moment Differences and Between-Session Reliability Following Thigh Marker Rotation Offset

Rotating the thigh markers significantly altered knee moments in the sagittal plane at peak maximal and minimal values. However, ankle moments were the most affected by the thigh marker offset. Ankle moments at peak values in all three planes were significantly altered by offsetting the thigh marker. Exploration of Figure 6.5 demonstrates that the pattern of ankle joint moments over the stance phase is not altered, but the magnitude of the peaks was. This may be caused by alterations in the ankle joint centre position from changes in position of the

knee joint centre following thigh marker repositioning. The mean thigh internal rotation of ~2^{o} applied to the group moves the knee joint posteriorly (Baker et al., 1999). The shank segment axis system is based on the knee joint centre, the lateral shank marker and the lateral malleolus marker. The posterior repositioning of the knee joint centre repositioned the ankle joint posteriorly, further away from the ground reaction vector at toe off. This increased the moment arm of the ankle joint and caused higher joint flexor moments during toe off.

Using paired t-tests to test the significance of joint moments pre- and post-offset did provide information on within-subject variation between the two conditions. However, the results may mislead interpretation of the effects from the thigh marker rotation offset. Examining lower limb joint moment differences after offset in relation to the range of moment over the stance phase aids meaningful interpretation. Using this strategy, large (>10% of range of moment) differences were seen at all 3D lower limb joint moments except the knee in the frontal plane. This finding suggests that the thigh marker rotation offset protocol has a large effect on all lower limb joint moments. This is due to the change in position of the lower limb joint centres compared to the ground reaction vector, which alters moment arm length.

Comparing lower limb joint moments with previous reliability studies is difficult as all have normalised joint moments to body weight and/or height. Normalising joint moments, in this way, eliminates variation in body weight and height across participants allowing a comparison of gait kinetics across groups (Moisio et al., 2003). However, the association between obesity and joint structure is not linear, joints of obese individuals are not proportionally larger (Browning & Kram, 2007). Therefore, non-normalised moments are assessed in the current study to explore the associations between absolute joint moments and adiposity. While the absolute magnitude of joint moment is different the waveform pattern in similar to previous findings (Chester et al., 2006).

Between-session reliability of lower limb joint moments following thigh marker rotation offset did not change as much as joint angles. The mean absolute difference in ICC values after thigh marker rotation offset was 0.00 ± 0.04 (ICC = 0.44 before and after thigh marker rotation offset) indicating that between-session reliability was not altered to a great extent. Error values between repeated sessions demonstrated an increase in SEM following thigh marker correction but by only 0.04 ± 0.37Nm (from 2.32Nm to 2.38Nm before and after thigh marker rotation offset). These results show that changing the position of the lower limb joint centres can alter joint motion, but joint moments may be more influenced by ground reaction forces.

In summary, the use of a thigh marker rotation offset applied to the same lower limb model trials described in aim 1 significantly altered motion of the hip, knee and ankle at ipsilateral initial contact and ipsilateral toe-off. The mean offset applied to participant's thigh was ~2^{o} of internal rotation affecting lower limb motion values at initial contact and toe-off. The biggest effect of the thigh offset was on hip transverse plane motion, where the hip was internally rotated approximately 8^{o} at toe-off. Overall between-session reliability of the lower limb (PiG) model improved and errors from repeated session decreased. However, some lower limb angular values still showed unacceptable SEM values; knee and ankle transverse plane motion. Joint moments were significantly altered across all lower limb 3D joints following thigh marker rotation offset. However, between-session reliability of lower limb joint moments were not altered after the offset. The aim of this section was to test the thigh marker rotation protocol to potentially improve between-session reliability and reduce error of the lower limb (PiG) model. The results show that joint angular values were more reliable and demonstrated less error and joint moments were relatively unchanged following the thigh marker rotation offset. Therefore, this protocol will be used to assess the relationships between adiposity and lower limb biomechanics. The specific joint and plane SEM outputs at peak and events can be used as a bench mark to determine if differences across adiposities are greater than the expected error. This will aid interpretation of significant findings by reducing the chance of a type II error (false positive).

6.5.6 Aim 3 Changes in Lower Limb Joint Parameters Following ASIS 'Instrumented Pointer Device' Protocol

The study population for this section was composed of different participants to the sections on lower limb between-session reliability. This was due to the fact that participants with higher fat mass were required in order to assess an alternative method for identifying the ASIS across a range of adiposities. The effect of excessive adiposity has been found to effect hip joint motion over the gait cycle (Rash et al., 1999; Board et al., 2012) because of Soft Tissue Artefact (STA) over the ASIS landmarks. However, no previous study has assessed an alternative method for identifying the ASIS in children. The results from the obese children were compared to the non-obese children as it was expected that STA would not be as great in children with lower adiposity.

No significant differences were found between the obese and non-obese boy's spatiotemporal gait parameters. This indicates that differences in hip motion were not due, for example, to increased walking speed which has been showed to significantly increase hip flexion (Stansfield et al., 2001). Therefore, differences between obese and non-obese boys were predominately due to alterations in gait parameters due to increased body mass, BMI Z-Score and body fat mass.

The posterior reconstruction of the ASIS markers and subsequent posterior reconstruction of the hip joint centre resulted in significantly greater hip flexion across the gait cycle. This finding is in-line with Rash et al., (1999) who found reduced hip flexion (2-5°) from anterior displacement of the ASIS markers (5-10cm) in simulated obese gait. The virtual ASIS markers on the obese boys in the present study were 1.64cm posterior to the skin mounted ASIS markers and hip flexion was increased by 4.61°. Rash et al., (1999) also found slight differences in hip frontal plane motion from lateral displacement of the ASIS markers (2-10cm). This was also found in the current study (0.07° less hip abduction) from the medial movement of the reconstructed virtual ASIS marker position (0.64cm) compared to the skin mounted position. Less hip flexion in Rash et al., (1999) could be the result of simulating anterior and lateral repositioning separately and not in combination as in the current study.

The results of the current study indicate that frontal plane hip motion is greatly affected by misplacement of the ASIS markers due to soft tissue artefact. This is due to Plug-In Gait lower limb model's calculation of the hip joint centre from ASIS marker positions (Plug-In Gait manual, 1999). The PiG model calculates hip joint centre in the anterior/posterior (X) and superior/posterior (Z) axis based on an ASIS-greater tronchanter regression equation (Davis et al., 1991):

$$X = C*\cos(\text{theta})*\sin(\text{beta}) - (\text{ASIS-Tronchanter distance} + \text{marker diameter}) * \cos(\text{beta}) \quad (1)$$

$$Z = -C*\cos(\text{theta})*\cos(\text{beta}) - (\text{ASIS-Tronchanter distance} + \text{marker diameter}) * \sin(\text{beta}) \quad (2)$$

Whereas, the medial/lateral position of the hip joint centre is based on the between-ASIS distance and is therefore sensitive to the medial position of the ASIS using virtual ASIS markers.

$$Y = -(C*\sin(theta) - \text{inter-ASIS distance}) \quad (3)$$

The magnitude of the difference between skin mounted and virtual markers position was up to 2cm (RMS) and the effect on the hip joint centre position was up to 0.9cm (RMS). Significantly greater medial position of the hip joint centre from the use of virtual ASIS markers compared to skin mounted ASIS markers is due to the medial reconstruction of the ASIS markers. A medially located hip joint centre increased hip abduction as the thigh becomes more laterally rotated compared to the pelvis

The use of alternative ASIS tracking methods presented in the current study and previous studies (Rash et al., 1999; Board et al., 2012) demonstrate the difficulty in measuring hip joint motion in obese subjects. The validity of using markers to represent the ASIS was not tested in the current study and so it is not known whether virtual markers identify bone landmarks better than skin mounted markers. However, the results of the current study suggest that virtual markers alter obese boy's hip joint position and 3D hip motion more than non-obese boys compared to skin mounted markers. Intuitively, this finding would suggest that excessive adipose tissue displaces skin mounted markers preventing the accurate palpation of the ASIS markers. Therefore, the use of an 'instrumented pointer device' to create virtual markers, with the position referenced to markers placed on the iliac crest, can be used to track ASIS position and calculate lower limb joint angular motion over the gait cycle in obese children.

6.6 Chapter Summary

The findings of this study indicate that children are able to walk consistently both within- and between-sessions with markers attached to their lower limbs. The lower limb model demonstrated moderate between-session reliability (ICCs) in the hip frontal plane as well as knee and ankle sagittal plane. Measurement error from repeated sessions was greater than 5^{o} for the hip, knee and ankle in the transverse which may affect the sensitivity of the model to detect differences across populations. Lower limb joint kinetic measures over the stance phase were less reliable than joint angles, low ICC were found in the transverse plane hip moments and moderate in most other joints.

Overall between-session reliability of the lower limb model (PiG) was improved following the application of the thigh marker offset though hip frontal and knee sagittal plane values

remained lower than other joints. The thigh marker rotation offset reduced angular hip transverse plane errors, but knee and ankle transverse plane error remained higher than 5°. Between-session reliability of joint moments were not affect, but hip transverse plane, knee sagittal and transverse plane demonstrated low reliability. Overall SEM values were not altered to a large degree by the thigh marker rotation offset, the largest improvement in SEM was in transverse hip moments and the largest deterioration was in sagittal plane knee moments. Therefore, the thigh marker rotation offset protocol will be used in the main study (chapter 8) of this thesis to explore associations between lower limb angular motion and moments and body fat mass.

To assess an alternative method to identify the ASIS landmarks in obese and non-obese children a protocol utilising virtual markers was tested. The use of an 'instrumented pointer device' to create virtual markers on the ASIS, tracked by markers of the iliac crest, resulted in a medial and posterior ASIS position and a medial hip joint centre position. However, the differences in hip joint centre position were only significant for the obese boys. This indicates that excessive adiposity mislocates skin mounted markers over the ASIS more in obese boys. A medial hip joint centre significantly flexed, abducted and internally rotated the obese participant's hip joint over the gait cycle. This lead to larger differences in hip joint motion between obese and non-obese boys when using virtual, compared to skin mounted ASIS markers. The use of the 'instrumented pointer device' may remove displacement of the ASIS marker from adipose tissue, thus representing the position and motion of the hip joint and is recommended for assessing lower limb motion in obese and non-obese children.

5.7 Limitations

A key limitation of this study was the use of Intraclass correlation coefficient (ICC) as a measure of lower limb between-session reliability. The ICC equation gives a ratio of within and between session variability (SD), the closer between-session SD was to within-session SD the higher ICC and better between-session reliability. However, ICCs are affected by the range of measurement across the participants, with higher between-participant SD resulting in larger ICCs and vice versa. Standard error of measurement (SEM) accounts for between-participant SD, thus giving a measure of absolute reliability (Bruton, 2000). However, other methods to determine variability from repeated measures of limb motion during gait may provide an unbiased measure of reliability (Schwartz et al., 2004).

While the main focus of this study was to assess the between-session reliability of lower limb biomechanics during gait, the question of validity was not fully addressed. The application of virtual markers on the ASIS and a thigh rotation offset protocol potentially improved the validity of orientating the pelvis and thigh segments. However, both theses protocols rely on assumptions; the ASIS virtual markers are assumed to provide better identification of the pelvis by removing skin mounted marker misplacement due to soft tissue; and, the thigh marker rotation offset protocol reduces cross-talk errors by assuming that frontal place knee joint motion is minimal. It was not possible to test these assumptions against 'gold standards' for bone motion analysis such as in-vivo or in-vitro bone pin protocols. Therefore, while the assumptions are based on logical reasoning for improving analysis of lower limb biomechanics based on known marker placement errors the full extent of validity is not tested.

7. Experimental Chapter 3: Between-Session Reliability of Foot Models in Children Age 6 to 11 Years Old

7.1 Introduction

In order to determine the relationships between childhood obesity and foot segment biomechanics during gait an appropriate method to model the foot is required. The findings from the second literature review (chapter 3: *3D Assessment of lower limb and foot motion during gait*) revealed a number of different foot models of varying number of segments tested for between-session reliability under different testing conditions. In order to determine the foot model to be used in the main study (chapter 8) three foot models were selected for between-session reliability analysis; the Oxford foot model (Stebbins et al., 2006), 3DFoot (Leardini et al., 2007) and Kinfoot (MacWilliams et al., 2003). These foot models represent a range of approaches for dividing the foot into segments; from eight (MacWilliams et al., 2003) to three segments (Stebbins et al., 2006). The Jenkyn & Nicol (2007) and Simon et al., (2006) foot models discussed in literature review chapter 2 (chapter 3) could not be examined due to the inaccessibility of software (Matlab) needed to run these models in the current study.

The choice of foot model for examining associations with adiposity in the main study (chapter 8) is based on the amount of information (foot segments) that can be gathered, with more information on foot motion beneficial for conclusions to be drawn in chapter 8. However, the foot model must also demonstrate acceptable reliability determined across repeated sessions. Therefore, the choice of greater foot segmentation takes preference over reliability in the first instance. However, an acceptable level of reliability (determined in the study) must be reached for the foot model with the greatest segmentation to be of use in the main study (chapter 8). Using previous findings to determine the between-session reliability in this study would be inappropriate due to the different participant ages, gait variable under investigation and statistical methods used. The preference of foot models prior to testing of between-session reliability was Kinfoot (nine segments), 3DFoot (five segments) and OFM (four segments).

7.2 Aims

1. To compare joint angular motion between three foot models with previous findings in the literature. This will provide a conceptual understanding of each foot model's segments, the anatomy they represent and their motion over the gait cycle.
2. To determine between-session reliability of three foot models to describe foot motion over the gait cycle. The potential for discovering associations between adiposity and foot biomechanics is greater in a foot model that provides more information on foot motion. However, the foot model with higher reliability will give greater statistical power to detect associations between adiposity and foot motion in the main study (chapter 8).

Comparison of three foot model's segmental angular motion will be made qualitatively using kinematic waveforms. To investigate the use of foot models in a paediatric population between-session reliability of each segment of each foot model will be assessed by ICC and SEM. Calculation of ICC and SEM will be taken over the gait cycle events (initial contact and toe off) and from peak values during the stance and swing phase.

7.3 Methods

7.3.1 Participants

Seventeen participants (age range 6-13 years) were recruited from a convenience sample of children from university staff and an after-school club. Participants were typically developing children and excluded if any medical conditions affecting neuromuscular and orthopaedic integrity or any complications contributing to altered foot posture and/or gait disturbance were identified. Consent was obtained from children's parents. Ethical approval was granted by University Research Ethics Committee (Ref No. ETH/13/11).

Participants were selected to be representative of a range of obesity levels to demonstrate the reliability of foot models in the expected sample population of the main study (chapter 8). No estimate of body fat mass was available during this study so BMI Z-Score was calculated. Girls and boys were recruited to this study to increase participant numbers for statistical power. It is not clear whether gender differences will affect reliability and therefore the applicability of the results to the main study (chapter 8) on boys only. However, between-session reliability of

biomechanical models has been previously tested in girls and boys combined (Stebbins et al., 2006).

7.3.2 Testing Protocols

7.3.2.1 Stereophotogrammetry

A ten camera Vicon 612 (Vicon Motion Systems Ltd, Oxford, UK) system was used to capture reflective marker coordinates (sampling rate 100Hz) within the capture volume. Six cameras were mounted to the laboratory walls and four on tripods in closer proximity to the capture volume. Pilot testing of the camera positions was carried out to define the best position for the tripod cameras to capture all markers during the gait cycle in contact with the force plates. Cameras were positioned with enough proximity to collect data from many markers in a small area but not be visible to each.

Cameras were calibrated in accordance with manufacturer's guidelines which required the capture and reconstruction of markers attached to an 'L frame' placed on the corner of one force plate to define the origin of the global coordinate system. A dynamic calibration was carried out using a 'T' frame with markers of known distances which was moved through the capture volume for a period of 10,000 frames. A successful calibration was made if residuals from marker position and inter-distances standard deviation were less than 1mm and wand visibility exceeded 65%. The volume area calibrated was 1.5m high, 2m long (direction of walking) and 2m wide.

7.3.2.2 Force Plates

Two force plates (Bertec, Model MIE Ltd, Leeds, UK) mounted within the laboratory floor recorded ground reaction forces (1000Hz). Each force plate was switched on 30 minutes before testing and zeroed prior to calibration. Calibration was conducted with known calibration weights of 50kg placed within the centre of the force plate. Vertical ground reaction force was recorded and a correction factor applied to align the force plate reading with the correct acceleration due to gravity calculated to be -445.5N.

7.3.2.3 Anthropometrics

Foot models did not require anthropometric measurements in order to calculate the biomechanical model. Only height and weight were measured.

Height was measured to the nearest 0.5cm using a stadiometer (Hadlands Photonics, Australia). Height is the maximum distance from the floor to the highest point of the head with the participant looking straight ahead. The participants were asked to stand straight with back, buttocks and heels against the stadiometer with feet together and flat on the floor. The participants were asked to take and hold a deep breath whilst looking straight ahead. Height was recorded at the end of the participants' deep inward breath.

Weight was recorded using the electronic weighing scales integrated within the Bodpod body composition device (Life Measurement, Inc, Concord, CA, USA) procedure. Participants were asked to stand on the centre of scales, without support and with their weight distributed evenly on both feet. Body mass index (BMI) was calculated by Quetelet's index (weight in $kg/height^2$ in m).

Body Mass Index Z-Score (BMI Z-Score) was input into LMSgrowth software (Harlow Healthcare, South Shields, UK). The software calculates the BMI Z-Score and BMI Centile, from height and body mass inputs, based on reference data from the United Kingdom 1990 (UK90) data set (Cole et al., 1995).

7.3.2.4 Foot Models

A single maker set was created as an amalgamation of three foot model's marker sets (Table 7.1): OFM (Stebbins et al., 2006), 3DFoot (Leardini et al., 2007) and Kinfoot (MacWilliams et al., 2003). Previously, this method has been used to compare kinematic results of five whole body models (Ferrari et al., 2008) and benefits from reducing individual variability between trials and sessions. Twenty eight markers (9 mm), mounted on rigid bases, were attached to each participant's right shank and foot. Where anatomical landmarks, used to define each marker placement, were in closer proximity (<40mm) a compromise was met. This was only necessary for the markers on the second metatarsal head (3DFoot), between the second and third head (OFM) and third metatarsal (Kinfoot). The middle position between the second and third metatarsal heads was chosen to represent a compromise between the foot models. Forefoot kinematics of 3DFoot and Kinfoot was compared to previous findings with this offset in mind.

Table 7.1. Amalgamated marker set from three foot models; OFM, 3DFoot and Kinfoot

Segment	Marker number	Foot model		
		OFM	3DFoot	Kinfoot
Shank	1	Femoral condyle		Medial tibial condyle
	2			Lateral tibial condyle
	3	Tibial tuberosity	Tibial tuberosity	
	4	Head of fibular	Head of fibular	
	5	Lateral malleolus	Lateral malleolus	Lateral malleolus
	6	*Medial malleolus*	*Medial malleolus*	Medial malleolus
	7	Anterior aspect of the shin		
	8			Anterior tibia
Hindfoot	*9*	*Posterior distal heel*		
	10	Posterior medial heel		
	11	Posterior calcaneus	Posterior calcaneus	Calcaneal tuberosity
	12	Lateral calcaneus	Peroneal tubercle	Anterior tubercle calcaneus
	13	Sustentaculum tali	Sustentaculum tali	Medial calcaneus
Talus	14			Lateral malleolus
	15			Medial malleolus
				Ankle joint centre (virtual)
				Second metatarsal centre (virtual)
Midfoot	16		Navicular tuberosity	
	17		Base of second metatarsal	
	18		Base of fifth metatarsal	
Cuboid				Calcaneus centre (virtual)
				Third metatarsal centre (virtual)
				Fifth metatarsal centre (virtual)
Forefoot	19	Base of first metatarsal	Base of first metatarsal	Base of first metatarsal (medial)
	20		Base of second metatarsal	Base of third metatarsal (Medial + lateral)
	21	Base of fifth metatarsal	Base of fifth metatarsal	Base of fifth metatarsal (lateral)
	22	*Head of first metatarsal*	Head of first metatarsal	Head of first metatarsal (medial)
	23	Between second and third metatarsal heads	Head of second metatarsal	Head of third metatarsal (Medial + lateral)
	24	Head of fifth metatarsal	Head of fifth metatarsal	Head of fifth metatarsal (lateral)
Hallux	25	Base of hallux	Proximal phalanx of hallux	
	26			Origin of hallux triad on hallux nail
	27			Anterior of hallux triad
	28			Posterior of hallux triad
Toes	29			Origin of triad, hallux nail (medial)
	30			Head of first metatarsal (medial)
	31			Third metatarsal head (medial + lateral)
	32			Fifth metatarsal head (lateral)
	33			Third phalange nail (medial + lateral)
	34			Fifth phalange nail (lateral)

The segments, bones and joints represented by the three foot models used in this study are described in Table 7.2. The OFM model, described by Stebbins et al., (2006) used 17 markers of which three were removed following the static calibration trial (posterior med heel, medial malleolus and head of first metatarsal). A four segment model was constructed for calculation of segmental kinematics shown in Figure 7.2. All segments were represented by three or four markers except the hallux which defined motion about the z-axis (flexion/extension) only. For compatibility with PiG lower limb model the OFM bases the longitudinal axis of the shank on the knee joint centre.

Table 7.2. Description of the three foot model's defined segments, the bones which the segments represent and the anatomical joint about which the bones articulate.

Model	Segments	Bones	Joint
OFM & 3DFoot	Shank & Hindfoot	Tibia/fibula & Calcaneus	Ankle
Kinfoot	Shank & Hindfoot	Tibia/fibula & Calcaneus	Talocrural
Kinfoot	Shank & Hindfoot	Tibia/fibula & Talus/Navicular/Cuneiform	Subtalar
3DFoot	Hindfoot & Midfoot	Calcaneus & Navicular/Cuboid/Cuneiform	Chopart
Kinfoot	Hindfoot & Midfoot	Calcaneus & Cuboid	Calcaneocuboid
OFM	Hindfoot & Forefoot	Calcaneus & first – fifth Metatarsals	Midfoot
Kinfoot	Midfoot & Lateral forefoot	Cuboid & third - fifth Metatarsals	Lateral Tarsometatarsal (TM)
Kinfoot	Midfoot & Medial forefoot	Talus/Navicular/Cuneiform & first – third Metatarsals	Medial Tarsometatarsal (TM)
3DFoot	Midfoot & Forefoot	Navicular/Cuboid/Cuneiform & first – fifth Metatarsals	Lisfranc
Kinfoot	Lateral Forefoot & Lateral toes	third - fifth Metatarsals & third – fifth distal Phalanges	Lateral Metatarsophalangeal (MP)
Kinfoot	Medial Forefoot & Medial toes	first – third Metatarsals & first – third distal Phalanges	Medial Metatarsophalangeal (MP)
OFM & 3DFoot	Forefoot & Hallux	first – fifth Metatarsals & proximal Phalanx of Hallux	Hallux Metatarsal
Kinfoot	Forefoot & Hallux	first – third Metatarsals & distal Phalanx of Hallux	Hallux Metatarsal

The 3DFoot model, described by Leardini et al., (2007) used 14 markers five of which were on the shank, three virtual markers were calculated using physical marker mid-points or a calibration procedure. Two markers were designated as defining two landmarks; the base of the second metatarsal with the middle cuneiform and the base of the fifth metatarsal with the tuberosity of the cuboid. A five segment model is constructed for calculation of segmental kinematics shown in Figure 7.2. All segments were represented by three or four markers except the hallux which defined motion about the z-axis and y-axis (flexion/extension and abduction/adduction) but not the x-axis (eversion/inversion). The 3DFoot model allows dynamic joint angles to be normalised to static standing angles which reduces variability in marker placement.

The Kinfoot model, described by MacWilliams et al., (2003) constructs the foot in nine segments (shown in Figure 7.2) with the use of 19 markers, three of which lie on the shank and includes a marker triad on the hallux. The toes and forefoot segments are represented by markers on the first, third and fifth metatarsal heads and bases as well as the phalanges. The talus/navicular/cuneiform segment is represented by the medio/lateral axis through the medial and lateral malleolus markers and the vertical axis aligned with the ankle joint centre. The talar head virtual marker is in alignment with the second metatarsal centre and an offset based on the second metatarsal length. The cuboid is represented by the anterior/posterior axis through the posterior calcaneus marker and the fourth metatarsal joint centre and the medial/lateral axis through the third and fifth metatarsal bases. Therefore the hindfoot of the Kinfoot model is defined as a combination of three segments; the talus/navicular/cuneiform, the calcaneus and the cuboid. Motion of the talus/navicular/cuneiform motion with respect to the tibia/fibula represents the talocrural joint axis, motion of the calcaneus with respect to the talus/navicular/cuneiform represents the subtalar joint axis and motion of the calcaneus with respect to the cuboid represents the calcaneocuboid axis.

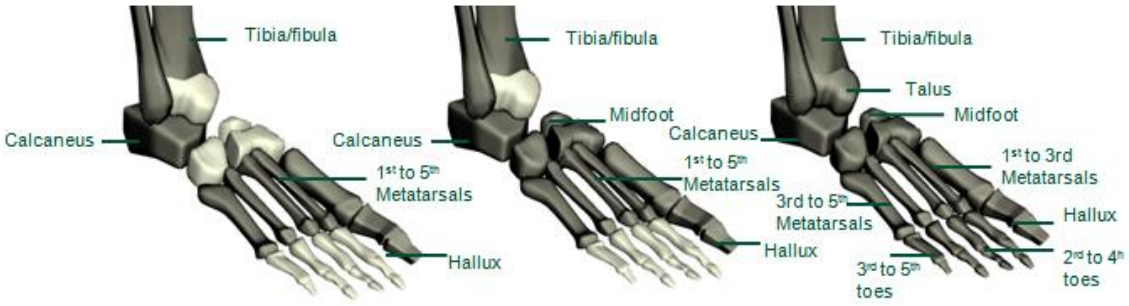

Figure 7.1. Segments of the OFM, 3DFoot model and Kinfoot (from left to right).

7.3.3 Procedure

Children were asked to ambulate barefoot at self-selected walking speed for a minimum of three steps before entering and three steps upon exiting the capture volume (7.5m walkway length). This gave the children enough time to accelerate up to normal walking speed and decelerate after the force plates. To avoid artificially increasing effect size and violating assumptions of independence only right limb kinematic and kinetic variables were extracted for analyses (Menz, 2005). Six gait cycles were captured from heel-strike to heel-strike of the right limb. Between-session reliability could be improved with a higher number of trials captured for each participant (Monaghan et al., (2007). However, in order to achieve 6 'clean' (i.e. participants hit the force plates, did not appear to aim, walked in a straight line, all markers stayed attached) it was necessary to record approximately 30 trials. After approximately 30 trials testing was concluded to prevent participant fatigue.

A test retest interval of four weeks was implemented and 14 participants returned within the timeframe. An ideal interval between test-retest protocols required consideration of practical and methodological issues. The interval should be long enough that skin marks from marker attachment or assessor memory of anthropometric measurement will not artificially improve between-session reliability. However, the interval should be short enough that actual changes (i.e. growth, weight gain) do not artificially reduce between-session reliability (McGinley et al., 2009). Three participants were unable to return until more than four weeks after their first testing session and were excluded from the analysis.

7.3.4 Data Analysis

3D marker trajectories were reconstructed using reconstruction parameters in Vicon software to ensure markers were visible during one whole gait cycle. Pilot testing of the reconstruction parameters, that led to the best set-up for marker visibility, set predictor radius at 20mm, acceleration 50m·s^{-2}, noise factor of 2, intersection limit of 6 and a residual factor of 0.5. Trajectories were gap filled to a maximum of 5 frames using a cubic-spline technique. Only trials where subsequent trajectories were visible over the whole gait cycle were used for analysis. Each trial was copied to make three identical trials for processing according to each model's protocol. Following the reconstruction of marker trajectories using the parameters described above the raw trajectories were filtered using the Woltring filter routine available in

the Vicon software. A recommended mean square error (MSE) value for filtering of gait data is 20 (Vicon Manual, 2010).

Perry (1992) described the phases of the gait cycle according to reciprocal foot contact with the ground. Gait events were determined by onset and conclusion of vertical force by the right foot on the force plates. Vertical ground reaction force above a threshold of 20N was used to indentify initial contact of the right foot, the next frame under 20N was determined as right foot off. Contact with a second force plate above the 20N threshold determined the next right initial contact and the end of the gait cycle. Ipsilateral Initial contact (IIC) and ipsilateral toe-off (ITO) determined the stance and swing phases of the gait cycle in which peak maximum and minimum values were extracted.

In order to analyse between-session reliability of the three foot models; (1) specific events; and, (2) peaks were chosen. To the author's knowledge, the foot has not been examined using kinematic models to examine differences between obese and non-obese individuals. However, studies have used other measures of dynamic and static assessments of foot structure between obese and non-obese children finding differences in; the medial longitudinal arch (Riddiford-Harland et al., 2000; Villarroya et al., 2007), calcaneal inclination angle/heel valgus (Pfeiffer et al., 2006; Villarroya et al., 2009), navicular height (Morrison et al., 2007), hallux (Mickle et al., 2006) and lateral metatarsal heads (Dowling et al., 2004). Particularly relevant is the finding of flat feet in obese children (Riddiford-Harland 2000; Dowling et al., 2001) indicative of a pronated foot structure. This would infer excessive position (and potentially motion) of the hindfoot and midfoot foot segments during gait. However, differences in foot segment position and motion over the gait cycle have not been assessed. Therefore, 3D kinematic values of each foot models segments will be reported at gait cycle events (initial contact and toe off) and peaks during the stance and swing phase. The total number of variables extracted over the gait cycle was: 42 for OFM (seven segmental angles extracted at four peaks and two gait cycle events); 66 for 3DFoot (11 segmental angles extracted at four peaks and two gait cycle events); and 144 for Kinfoot (24 segmental angles extracted at four peaks and two gait events).

7.3.5 Statistical Analysis

7.3.5.1 Normality and Homogeneity

In order to carry out the parametric tests of Intraclass correlation coefficients (ICC) the normality and homoscedasticity of each variable from the sample must be tested. Shapiro-Wilk tests compared the distribution of the variables in this study to a normal distribution with the same mean and standard deviation. If the test is non-significant (p>.05) the distribution is not significantly different from a normal distribution. The Shapiro-Wilk test was applied to age, spatiotemporal and anthropometric data. However, the Shapiro-Wilk test are limited with large sample sizes (n>100) because it is easy to deviate from normality or homogeneity. Therefore, significance testing does not necessarily indicate bias in the data (Field, 2009).

In order to check the assumptions of random error and homoscedasticity of the models plots of the standardised predicted values of kinematic values against the standardised residuals were produced. If the regression models fit the sample data well all data points fall on the regression line and the residuals would be zero (Field, 2009). A histogram of the regression standardised residuals should appear as a normal distribution (bell-shaped curve). Furthermore the normal probability plot shows deviations from normality by plotting the observed residuals against a straight line (representing a normal distribution). All checks on the assumptions of the regression model were compared with published plots in Field (2009). An example of the plots is in Appendix IV.

7.3.5.2 Foot Models Between-Session Reliability

Between-session reliability was determined by error calculations of joint angles at selected points of the gait cycle. Intraclass correlation coefficients (ICC) are considered the 'gold standard for assessment of the reliability of numerical parameters (Fleiss, 1986). Therefore ICC (3,*k*) were calculated for all variables which is appropriate for within-rater, between-session reliability (Shrout & Fleiss, 1979) and the confidence interval (CI) of the ICC, using one-way analysis of variance (Rankin & Stokes, 1998). All individual trials from session one and session two, rather than subject means, were used to calculate ICCs. This reduces the ICC value because within-subject variability is included in correlation. However, data in the main study (chapter 8) will be analysed based on all individual gait cycles rather than subject means. Therefore, it is appropriate to express between-session reliability and expected error in this study according to all individual trials.

$$ICC\,(3,k) = \frac{BMS - EMS}{BMS}$$

(1)

Where BMS is the between-subjects variance, EMS is the Error or residual mean square variance and k is the number of measurements (Shrout & Fleiss, 1979). To interpret ICCs the scale of Katz et al., (1992) was used; ICC-values > 0.80 represent very high, 0.60–0.79 moderately high, 0.40–0.59 moderate and < 0.40 low reliability. In order to report the mean of multiple ICCs it is necessary to transform the *r* value by Fisher r-to-z transformation, take the average, and transform this back to an ICC value (*r*). This transformation means that the variance of *z* is approximately constant for all correlation coefficient (r) values. Without the Fisher transformation, the variance of *r* grows smaller as *r* gets closer to 1 (Field, 2009). Bland and Altman 95% limits of agreement were considered as an alternative measure of reliability as they indicate a range of error (Bland & Altman, 1986). However, a sample set of 50 is required otherwise limits of agreement can be very wide (Rankin & Stokes, 1998). Where variables violated assumptions of normality a Spearman's rank correlation coefficient was calculated to determine the between-session reliability of repeated measures.

Expressing between-session reliability of gait data in terms of a coefficient by itself makes comparison difficult because the units are hard to interpret (McGinley et al., 2009). Therefore, absolute measures of error were calculated based on the ICC and pooled standard deviation. This gives units in degrees which can be interpreted as the expected amount of intrinsic and extrinsic error in repeated sessions. The equation for calculating SEM:

$$SEM = Sx\sqrt{1 - rxx}$$

(10)

Where S*x* is the pooled standard deviation (°) and r*xx* refers to intraclass correlation coefficient (ICC 3,*k*) (Portney & Watkins, 2009).

7.3.5.3 Foot Models Differences Following Thigh Marker Rotation Offset and Normalisation to Static Angles

The OFM is affected by the thigh marker rotation offset protocol because the shank segment is based on the knee joint centre which can be altered by thigh marker position. The 3DFoot

model protocol has to option to normalise joint angles to a standing position. This reduces error from marker placement, but may also remove actual within-session differences. To assess whether the thigh marker offset protocol significantly altered OFM joint angles and moments at initial contact and toe off paired-means t tests were performed on individual's data. Following the normalisation to standing procedure of 3DFoot, joint angles were also compared before and after by paired-means t tests. For both foot model tests significance was set to $p<0.05$. Between-session reliability (ICC and SEM) of both OFM and 3DFoot was tested and compared before and after thigh marker rotation offset and normalisation to static angles.

7.4 Results

7.4.1 Normality and Homogeneity

Shapiro-Wilk test for normality, presented in Table 7.3, showed that age, knee width, ankle width and cadence were not normally distributed ($P<0.05$), but all other variables were normally distributed. Parametric ICC test for between-session reliability was conducted on all normally distributed variables. Spearman's rank correlation was implemented to test between-session reliability of non-parametric variables. Wilcoxon non-parametric test was used to test for significantly different outputs between the sessions. No parametric tests were conducted on age. A visual examination of the plots (an example is shown in Appendix IV) for each lower limb output indicated that all variables were normally distributed and therefore ICC parametric tests for between-session reliability could be undertaken.

Table 7.3 Shapiro-Wilk tests of normality on age, spatiotemporal and anthropometric variables. Significance p<0.5

	Statistic	df	Sig.
Age (years)	.830	27	.012*
Height (cm)	.975	27	.939
Body mass (kg)	.889	27	.079
BMI (kg/m^2)	.909	27	.154
BMI Z-Score	.959	27	.702
Leg length (cm)	.953	27	.239
Knee width (cm)	.912	27	.022*
Ankle width (cm)	.912	27	.023*
Cadence (steps/min)	.901	27	.017*
Stance phase (% of gait cycle)	.967	27	.545
Step length (m)	.976	27	.785
Step width (m)	.931	27	.082
Walking speed (m·s-1)	.951	27	.249

7.4.2 Anthropometrics

Eight boys and six girls took part in the test-retest protocol with a mean duration between repeated sessions of 21.57 ± 5.56days. The mean age of the participants was 8.50 ± 2.79 years. Based on BMI Z-Scores (UK90) for each child on each session, one was classified as obese, five as overweight, 16 as ideal weight, five as underweight and one as very underweight. Two participants changed classification between sessions; one girl from overweight to obese, BMI Z-Score change of 2.24 to 2.38 (obese Z-Score cutoff 2.25), and one girl from underweight to very underweight, BMI Z-Score change of -1.91 to -2.11 (very underweight BMI Z-Score cutoff -2.0).

7.4.3 Aim 1: Comparison of Foot Models

This section will highlight the major differences in patterns of motion of each foot model and refer differences back to the foot model's segment definition of the anatomy it represents. An important difference between the foot models is the definition of planar motion with reference to positive and negative angular displacements. All foot models define dorsiflexion as positive and plantarflexion as negative. However, frontal plane motion is described by 3DFoot and OFM as inversion (supination described by OFM forefoot) being positive and eversion (pronation described by OFM forefoot) negative, but Kinfoot describes eversion as positive and inversion and negative. In the transverse plane 3Dfoot and Kinfoot describe external rotation (abduction described by 3DFoot) as positive and internal rotation (adduction described by 3DFoot) as negative, but the OFM describes external rotation (adduction described by OFM forefoot) as negative and internal rotation (abduction described by OFM forefoot) as positive. These descriptions of positive and negative motion in the cardinal planes are described in Table 7.4. This should be considered when comparing the waveforms from each foot model in Figures 5.8, 5.9, 5.10, 5.11, 5.12a and 5.12b. The consensus of motion and position between the three foot models will be described and compared by assessments of kinematic waveforms (Rankine et al., 2008).

Table 7.4. descriptions of positive and negative foot joint motion in the sagittal, frontal and transverse planes

	Sagittal Plane		Frontal Plane		Transverse Plane	
	Positive	Negative	Positive	Negative	Positive	Negative
Foot Model						
3DFoot	Dorsiflexion	Plantarflexion	Eversion	Inversion	Abduction	Adduction
OFM	Dorsiflexion	Plantarflexion	Supination/ Inversion	Pronation/ Eversion	External rotation/ Adduction	Internal rotation/ Abduction
Kinfoot	Dorsiflexion	Plantarflexion	Inversion	Eversion	Internal rotation	External rotation

7.4.3.1 Comparison of Hindfoot Motion between Three Foot Models

At the hindfoot all three foot models demonstrated a plantarflexion peak following initial contact followed by dorsiflexion motion peaking at contralateral toe-off. The OFM is the only model that reached dorsiflexion during the stance phase. During the swing phase the hindfoot segments of each foot model demonstrated peak plantarflexion at toe-off then dorsiflexion in early and plantarflexion in late stance. At initial contact the hindfoot in the frontal plane was in a neutral position in OFM and 3DFoot but an everted position for Kinfoot. All three foot models (Kinfoot subtalar joint) demonstrated eversion through the stance phase followed by peak inversion around toe-off and inversion through the swing phase. The OFM hindfoot segment presented greater range of motion than 3DFoot and Kinfoot in the transverse plane. The OFM's hindfoot and Kinfoot's ankle joint demonstrated peak external rotation after initial contact followed by peak internal rotation around toe-off. The 3DFoot demonstrated abduction (internal rotation) through the stance phase and a smaller abduction peak around toe-off. During the swing phase OFM's hindfoot demonstrated external and internal rotation peaks, 3DFoot's hindfoot and Kinfoot's ankle joint were internally rotated. Kinfoot's representation of the subtalar joint demonstrated opposing joint waveforms to the ankle (talocrural) joint with more dorsiflexion, eversion and external rotation during the gait cycle.

7.4.3.2 Comparison of Midfoot Motion between Three Foot Models

The 3DFoot model presents the midfoot, consisting of all the midtarsal bones (cuboid, navicular and cuneiforms) comprising the Chopart joint rotating about the calcaneus (Leardini et al., 2007a). However, Kinfoot models the calcaneocuboid joint distinctly from the medial midtarsal bones thus dividing the midfoot into medial and lateral segments. Both 3Dfoot and Kinfoot demonstrated dorsiflexion through the stance phase. However, Kinfoot showed peak dorsiflexion only after toe-off while 3DFoot showed peak dorsiflexion and plantarflexion at the

beginning of the swing phase. The frontal plane motions of both models presented inversion which peaks at toe-off and reduces in the swing phase. However, in the transverse plane motion of the models were opposite, 3DFoot presented adduction (internal rotation) and Kinfoot external rotation.

7.4.3.3 Comparison of Forefoot Motion between Three Foot Models

The angular waveform of all three forefoot segments (Kinfoot's medial forefoot) demonstrated a neutral position at initial contact followed by flexion through the stance phase to a dorsiflexion peak prior to toe off and plantarflexion peak following toe off. The forefoot segments of OFM and 3DFoot were inverted (described as supination in OFM) through the gate cycle but Kinfoot was everted. At toe-off OFM's and Kinfoot forefoot segments showed peak supination (inversion for Kinfoot), but 3DFoot remained inverted (no peak). In the transverse plane OFM and Kinfoot were externally rotated, but 3DFoot internally rotated (adducted). All three foot models demonstrated peak adduction (internal rotation for Kinfoot) around toe-off. The lateral forefoot on the Kinfoot model was in extension, inverted and internally rotated and peaks in extension, eversion and external rotation after toe-off.

7.4.3.4 Comparison of Hallux and Toe Motion between Three Foot Models

Motion of all three foot models' hallux segment showed a reduction in dorsiflexion after initial contact followed by peak dorsiflexion at toe-off. Kinfoot's hallux frontal plane motion was from inversion in the stance phase to peak eversion at toe-off. Both 3DFoot and Kinfoot hallux demonstrated external rotation (abduction) throughout the stance phase. Kinfoot's hallux increased external rotation through the swing phase while 3DFoot remains the same.

In the sagittal plane both medial and lateral toes demonstrated flexion at initial contact followed by neutral in the stance phase and peak flexion at toe-off. The medial toes were more inverted and the lateral toes were everted through the gait cycle. Kinfoot's medial and lateral toes exhibited opposing motion in the transverse plane from external and internal rotation respectively with peak external rotation and internal rotation occurred at toe-off

7.4.4 Aim 2: Between-Session Reliability of Foot Models

7.4.4.1 Within-Subject and Between-Session Variance of Foot Models

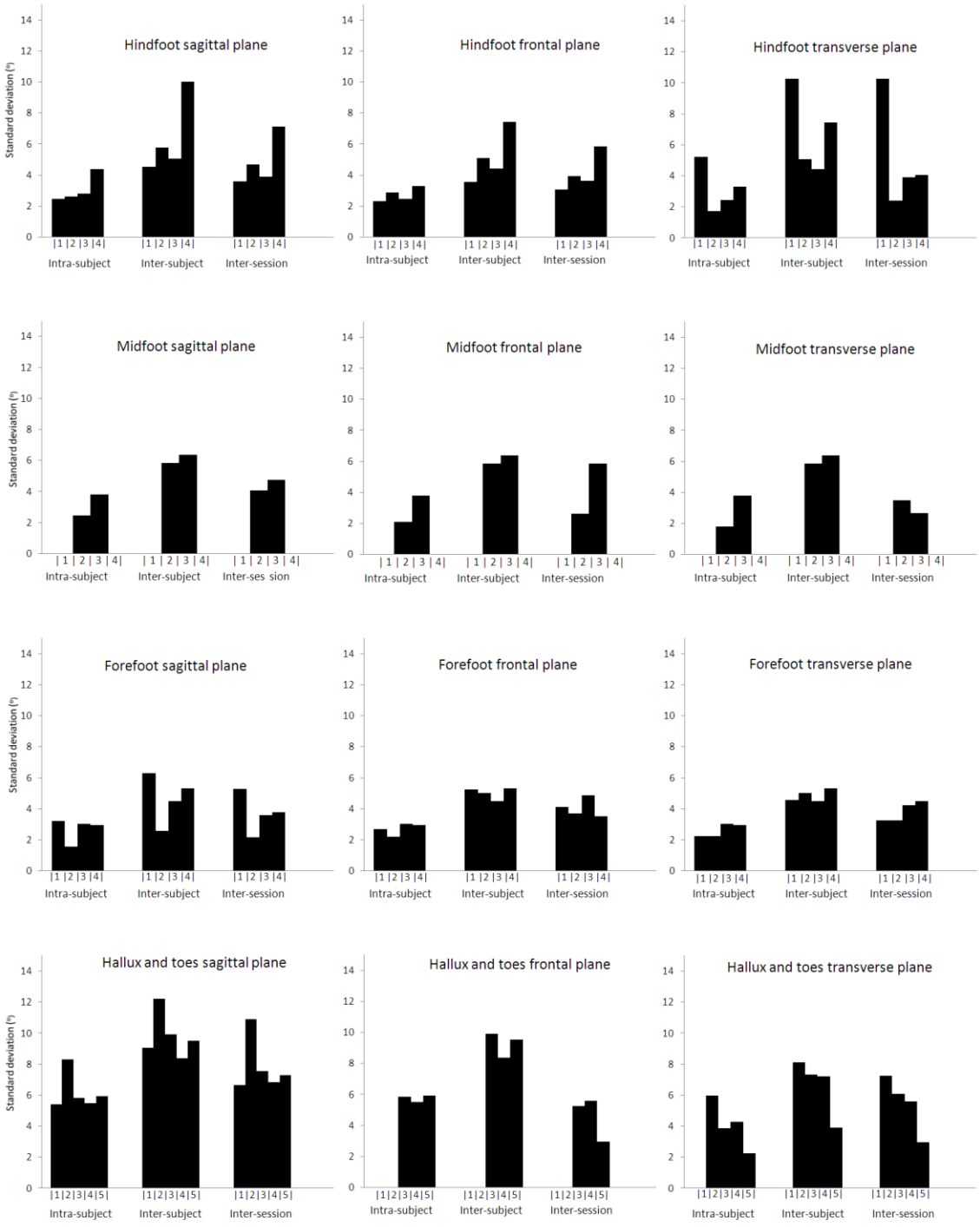

Figure 7.2. Mean within-subject, between-subject, between-session standard deviations of foot models examined. (1) The Oxford foot model, (2) 3DFoot, (3), (4) and (5) Kinfoot

Figure 7.2 presents an overview of variability for each foot model tested in this paediatric population. Mean within-subject SD were lowest for 3DFoot (3.42° ± 2.11°) and highest for OFM (3.82° ± 1.37°) with Kinfoot SD at (3.54° ± 1.11°). Mean within-subject SD were higher than between-subject for all foot models; 3DFoot presented lowest mean between-subject SD (5.87° ± 2.74°), followed by Kinfoot (6.51° ± 1.99°) and OFM (7.43° ± 4.17°). Between-session SD were lower than between-subject and higher than within-subject; 3DFoot demonstrated lowest mean SD (4.80° ± 2.55°) then Kinfoot (4.85° ± 1.44°) and OFM (5.53° ± 2.67°).

7.4.4.2 Between-Session Reliability of OFM

Between-session ICC and SEM values for reliability assessment of OFM are presented in Table 7.5. Overall OFM demonstrated moderate ICCs 0.55 (95%CI 0.16 to 0.77) and reasonable SEM values of 4.61°± 2.86°. The OFM demonstrated moderate ICCs at the hindfoot (ICC 0.58 95%CI 0.22 to 0.79) and forefoot (ICC 0.55 95%CI 0.20 to 0.78), but low ICCs at the hallux segment (ICC 0.35 95%CI -0.15 to 0.63). The forefoot (mean SEM 3.55° ± 1.00°) and hindfoot (mean SEM 4.70° ± 2.56°) demonstrated reasonable SEM values, but the hallux demonstrated unacceptable SEM values (mean SEM 7.52° ± 5.23°). Across all OFM segments, ICCs were moderately high in the transverse plane (ICC 0.65 95%CI 0.15 to 0.76), and moderate in the sagittal (ICC 0.50 95%CI 0.09 to 0.74) and frontal planes (ICC 0.51 95%CI 0.10 to 0.70). Errors were reasonable in the frontal plane (mean SEM 3.07° ± 1.09°), but unacceptable in the sagittal (mean SEM 5.00° ± 3.45°) and transverse planes (mean SEM 5.56° ± 2.57°). Moderate ICCs were found across gait events (ICC 0.53 95%CI 0.15 to 0.77), peak minimal (ICC 0.55 95%CI 0.15 to 0.76) and peak maximal values (ICC 0.57 95%CI 0.18 to 0.77). The OFM presented reasonable SEM values at peak minimal values (mean SEM 3.38° ± 1.74°), but unacceptable SEM values at peak maximal values (mean SEM 5.41° ± 3.51°) and values at events (mean SEM 5.03° ± 2.83°).

The hindfoot showed moderately high between-session reliability (ICCs) in the transverse plane (ICC 0.75 95%CI 0.50 to 0.87) and moderate ICCs in the sagittal (ICC 0.51 95%CI 0.13 to 0.76) and frontal planes (ICC 0.43 95%CI -0.01 to 0.69). Mean SEM values were reasonable in the frontal (mean SEM 2.86° ± 0.49°) and sagittal planes (mean SEM 3.31° ± 0.49°), but unacceptable in the transverse plane (mean SEM 7.93° ± 1.36°).

The forefoot demonstrated moderate between-session reliability (ICCs) in all planes, highest in the sagittal plane (ICC 0.62 95%CI 0.27 to 0.81), frontal (ICC 0.58 95%CI 0.20 to 0.78) and

transverse plane (ICC 0.52 95%CI 0.12 to 0.75). Mean error values for repeated joint angles were lowest in the transverse plane (mean SEM 3.18° ± 0.51°) then frontal (mean SEM 3.29° ± 1.49°) and sagittal (mean SEM 4.16° ± 0.49°), all were reasonable.

The hallux segment demonstrated low ICC value of 0.35 (95%CI -0.15 to 0.64) and an unacceptable SEM value of 7.52° ± 5.23°.

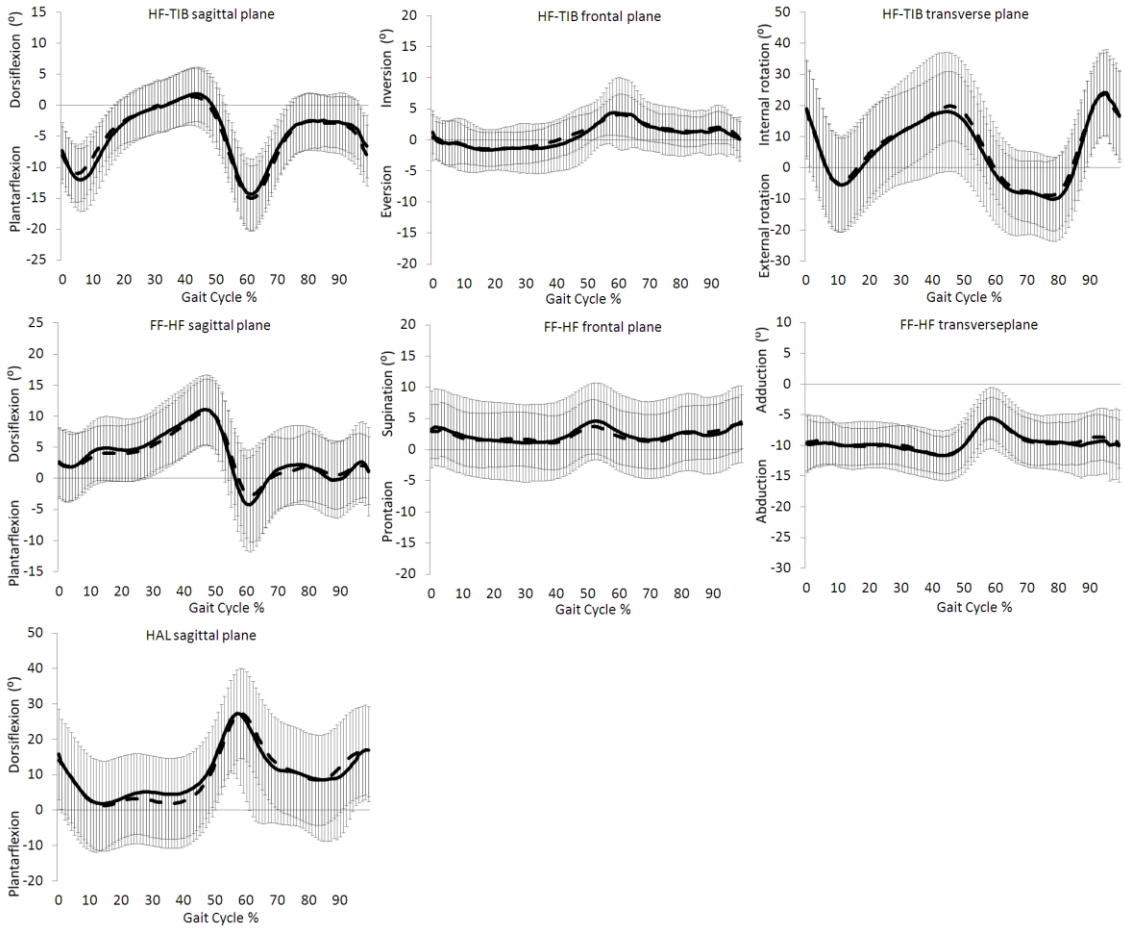

Figure 7.3. Mean ± SD of OFM test-retest. Session 1 black line, session 2 dash line

In summary, of the 42 OFM variables extracted over the gait cycle six (14.3%) demonstrated low reliability, 14 (33.3%) demonstrated moderate reliability, 13 (31.0%) demonstrated moderately high reliability and nine (21.4%) demonstrated very high reliability. The six OFM variables that demonstrated low reliability (number of variables at points of the gait cycle in brackets):

- Hindfoot sagittal plane stance phase peak minimal value (1)
- Hindfoot frontal plane value at ipsilateral toe-off and swing phase peak minimal value (2)
- Hallux sagittal plane value at ipsilateral initial contact, ipsilateral toe-off, swing phase peak minimal and maximal values (4)

Of the 42 OFM variables extracted over the gait cycle 11 (26.2%) of the variables demonstrated unacceptable SEM values, 29 (69.0%) demonstrated reasonable SEM and two (6.8%) demonstrated acceptable SEM values. The 11 OFM variables to demonstrate unacceptable SEM (number of variables at points of the gait cycle in brackets):

- Hindfoot sagittal plane value at ipsilateral initial contact (1)
- All six hindfoot transverse plane values (6)
- Forefoot sagittal plane value at ipsilateral initial contact (1)
- Hallux values at ipsilateral initial contact, stance and swing phase peak maximal value (3)

Table 7.5. ICC (95% confidence interval) and SEM of OFM angular outputs at gait cycle events and peaks

OFM		Gait Cycle					
Segment	Plane	IIC	Stance min	Stance max	ITO	Swing min	Swing max
HF-TIB (ICC)	sag	0.46 (0.06 to 0.73)	0.38 (-0.05 to 0.68)	0.67 (0.36 to 0.84)	0.47 (0.07 to 0.74)	0.41 (-0.02 to 0.69)	0.64 (0.31 to 0.82)
(SEM)		5.00	1.79	2.99	2.92	3.07	4.09
HF-TIB	fro	0.62 (0.28 to 0.82)	0.47 (0.04 to 0.72)	0.51 (0.10 to 0.74)	0.14 (-0.29 to 0.52)	0.35 (-0.14 to 0.64)	0.43 (-0.03 to 0.69)
		2.18	2.92	2.46	3.18	2.83	3.56
HF-TIB	tra	0.75 (0.48 to 0.89)	0.68 (0.37 to 0.84)	0.76 (0.50 to 0.88)	0.8 (0.58 to 0.91)	0.83 (0.64 to 0.92)	0.69 (0.38 to 0.84)
		9.77	7.74	6.90	8.81	6.00	8.38
FF-HF	sag	0.65 (0.32 to 0.84)	0.54 (0.14 to 0.76)	0.68 (0.37 to 0.83)	0.54 (0.17 to 0.78)	0.65 (0.31 to 0.81)	0.65 (0.32 to 0.82)
		4.42	4.13	3.35	4.24	4.12	4.72
FF-HF	fro	0.46 (0.05 to 0.73)	0.57 (0.18 to 0.77)	0.62 (0.26 to 0.79)	0.61 (0.26 to 0.82)	0.60 (0.23 to 0.78)	0.61 (0.24 to 0.79)
		5.18	3.12	2.80	3.82	2.75	4.06
FF-HF	tra	0.45 (0.05 to 0.73)	0.70 (0.41 to 0.84)	0.51 (0.08 to 0.73)	0.49 (0.10 to 0.75)	0.54 (0.13 to 0.75)	0.41 (-0.08 to 0.67)
		3.66	2.32	3.36	2.99	3.09	3.68
HAL	sag	0.29 (-0.14 to 0.63)	0.45 (-0.03 to 0.69)	0.40 (-0.13 to 0.65)	0.34 (-0.08 to 0.66)	0.32 (-0.25 to 0.61)	0.29 (-0.29 to 0.59)
		11.25	2.39	11.77	3.05	2.99	13.67

7.4.4.3 OFM Joint Angle Differences Following Thigh Marker Rotation Offset

Changing the position of the knee joint centre has the effect of altering the shank segment to which foot segmental motion of the OFM is compared. Therefore, a comparison before and after thigh marker rotation offset is made. Table 7.6 shows the mean joint angles at the beginning and end of the stance phase.

The hindfoot was significantly more flexed, less adducted and significantly less internally rotated following thigh marker rotation offset.

All forefoot joint angle changes following thigh marker rotation offset were significant. The forefoot was more plantarflexed, less abducted and more internally rotated after thigh marker rotation offset.

Hallux motion was more flexed.

Table 7.6. Mean ± SD of OFM angular output at initial contact and toe-off before and after thigh marker rotation output. Significance * = p<.05, ** = p<.01, *** = p<.001

		Average joint angle		
		Pre-offset	Post-offset	Pre- and post-
Segment	Plane	IIC	IIC	offset Difference
HF-TIB	sag	-7.02 ± 6.79	21.20 ± 7.19	-28.23 ± 8.18***
HF-TIB	fro	-1.04 ± 3.52	1.28 ± 10.79	-2.32 ± 9.80
HF-TIB	tra	17.55 ± 19.4	17.17 ± 16.01	0.38 ± 11.58
FF-HF	sag	1.39 ± 7.47	-22.61 ± 4.11	24.00 ± 5.94***
FF-HF	fro	7.15 ± 7.02	9.75 ± 7.76	-2.60 ± 5.31***
FF-HF	tra	-10.31 ± 4.95	-8.15 ± 4.54	-2.17 ± 2.91***
HAL	sag	61.72 ± 13.33	62.19 ± 13.54	-0.47 ± 17.90
		ITO	ITO	
HF-TIB	sag	-10.94 ± 4.00	14.8 ± 6.21	-25.74 ± 5.88***
HF-TIB	fro	4.21 ± 3.43	-0.24 ± 5.64	4.45 ± 5.73***
HF-TIB	tra	0.04 ± 19.71	0.63 ± 16.10	-0.59 ± 8.61
FF-HF	sag	-3.20 ± 6.28	-26.85 ± 6.21	23.65 ± 6.23***
FF-HF	fro	7.01 ± 6.12	10.84 ± 5.53	-3.83 ± 5.04***
FF-HF	tra	-5.92 ± 4.19	-2.94 ± 4.29	-2.97 ± 2.45***
HAL	sag	17.29 ± 3.75	17.58 ± 3.95	-0.30 ± 6.23

7.4.4.4 Between-Session Reliability of OFM after Thigh Marker Rotation Offset

The effect of correcting thigh marker misplacement by accounting for excessive frontal plane motion at the knee will affect the angular outputs from OFM because the orientation of the shank segment is based on the PiG knee joint centre. Between-session reliability and error of the OFM after thigh rotation offset is presented in Table 7.7. Between-session reliability of the OFM following thigh marker rotation marker correction was examined and compared to between-session reliability before the offset was applied. Overall ICC values slightly increased to 0.56 (95%CI 0.18 to 0.78 after offset) and mean SEM values reduced to 4.56^{o} ± 2.49^{o} after the offset. Hindfoot (ICC 0.62 95%CI 0.28 to 0.82 after offset) and hallux ICCs increased (ICC 0.39 95%CI -0.09 to 0.66 after offset), but forefoot ICCs decreased (ICC 0.55 95%CI 0.18 to 0.77

after offset) following thigh marker rotation offset. Hindfoot SEM increased (mean SEM 5.04° ± 1.60° after offset), but forefoot (mean SEM 3.49° ± 1.00° after offset) and hallux SEM values reduced. Lower ICCs were found in the sagittal plane (ICC 0.46 95%CI 0.03 to 0.72 after offset), but higher ICCs were found in the transverse (ICC 0.70 95%CI 0.40 to 0.85 after offset) and frontal planes (ICC 0.54 95%CI 0.18 to 0.77 after offset). Mean SEM values reduced in the sagittal (mean SEM 4.88° ± 3.18° after offset) and transverse planes (mean SEM 4.70° ± 2.20° after offset), but increased in the frontal plane (mean SEM 4.38° ± 1.09° after offset). Between-session reliability (ICCs) reduced for values extracted at gait cycle events (ICC 0.49 95%CI 0.10 to 0.75 after offset), but ICCs increased at peak minimal values (ICC 0.62 95%CI 0.25 to 0.80 after offset) and peak maximal values (ICC 0.58 95%CI 0.20 to 0.78 after offset). Error (SEM) from repeated sessions was increased in the sagittal (mean SEM 5.48° ± 2.48° after offset) and frontal planes (mean SEM 3.51° ± 1.05° after offset), but reduced in the transverse plane (mean SEM 5.07° ± 2.98° after offset)

Hindfoot ICCs increased in the transverse (ICC 0.77 95%CI 0.53 to 0.89 after offset) and frontal (ICC 0.55 95%CI 0.18 to 0.77 after offset) planes but decreased in the sagittal plane (ICC 0.49 95%CI 0.09 to 0.75 after offset). Mean SEM values increased in the sagittal (mean SEM 3.86° ± 1.20° after offset) and frontal planes (mean SEM 4.61° ± 1.03° after offset), but reduced in the transverse plane (5.82° ± 2.69° after offset).

Higher ICCs were found in the transverse plane (ICC 0.62 95%CI 0.26 to 0.80 after offset), but lower ICCs in the sagittal (ICC 0.49 95%CI 0.08 to 0.73 after offset) and frontal plane (ICC 0.54 95%CI 0.18 to 0.76 after offset). Error values were reduced in the sagittal (3.55° ± 0.68° after offset) and transverse planes (2.74° ± 0.55° after offset) but frontal plane SEM values increased (4.15° ± 1.19° after offset).

At the hallux, sagittal plane ICC were increased to 0.39 (95%CI -0.09 to 0.66) and SEM reduced to 7.22° ± 4.47° following thigh marker rotation offset.

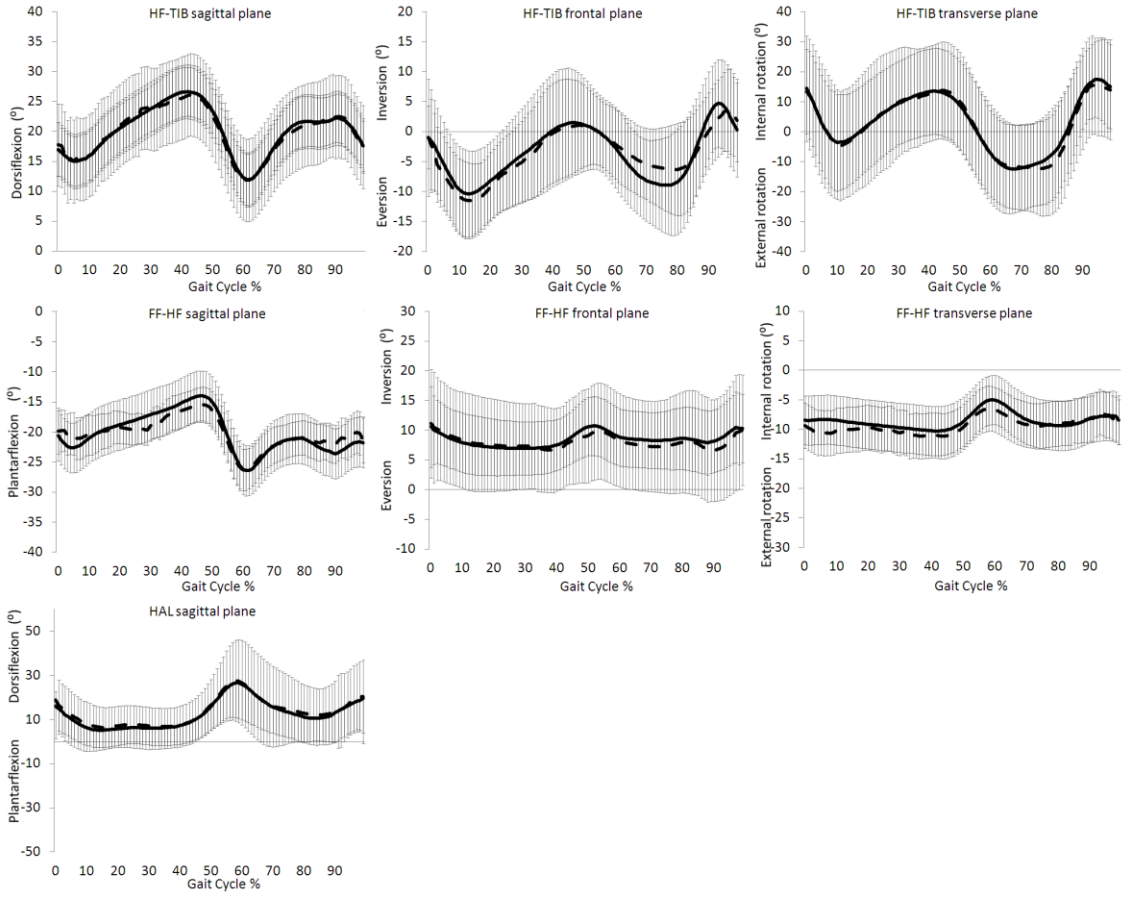

Figure 7.4. Mean ± SD of OFM test-retest following thigh marker rotation offset. Session 1 black line, session 2 dash line

In summary, following thigh marker rotation offset seven (16.7%) demonstrated low reliability, 12 (28.6%) demonstrated moderate reliability, 12 (28.6%) demonstrated moderately high reliability and 11 (26.2%) demonstrated very high reliability. The six OFM variables that demonstrated low reliability following thigh marker rotation offset were (number of variables at points of the gait cycle in brackets):

- Hindfoot sagittal plane value at ipsilateral initial contact (1)
- Hindfoot frontal plane value at ipsilateral toe-off (1)
- Forefoot sagittal plane value at ipsilateral initial contact (1)
- forefoot frontal plane value at ipsilateral initial contact (1)
- Hallux sagittal plane value at ipsilateral initial contact, ipsilateral toe-off and swing phase peak minimal value (3)

Of the 42 OFM variables extracted over the gait cycle, following thigh marker rotation offset, 12 (28.6%) demonstrated unacceptable SEM values, 30 (71.4%) demonstrated reasonable SEM and none demonstrated acceptable SEM values. The 12 OFM variables to demonstrate unacceptable SEM (number of variables at points of the gait cycle in brackets):

- Hindfoot sagittal plane value at ipsilateral initial contact (1)
- All six hindfoot transverse plane values (6)
- Hindfoot frontal plane value at ipsilateral initial contact (1)
- Forefoot sagittal plane value at ipsilateral initial contact (1)
- Hallux values at ipsilateral initial contact, stance and swing phase peak maximal value (3)

Table 7.7. ICC (95% confidence interval) and SEM of OFM at gait events and peaks after thigh marker rotation output.

OFM thigh rotation offset		Gait Cycle					
Segment	Plane	IIC	Stance min	Stance max	ITO	Swing min	Swing max
HF-TIB (ICC)	sag	0.26 (-0.17 to 0.61)	0.56 (0.19 to 0.79)	0.56 (0.18 to 0.78)	0.57 (0.21 to 0.80)	0.45 (0.04 to 0.72)	0.5 (0.10 to 0.74)
(SEM)		6.20	3.18	3.41	4.07	3.15	3.12
HF-TIB	fro	0.64 (0.30 to 0.83)	0.61 (0.26 to 0.80)	0.63 (0.28 to 0.81)	0.25 (-0.18 to 0.60)	0.68 (0.37 to 0.84)	0.45 (0.00 to 0.70)
		6.50	4.00	4.29	4.89	3.51	4.49
HF-TIB	tra	0.74 (0.48 to 0.89)	0.8 (0.58 to 0.91)	0.79 (0.56 to 0.90)	0.81 (0.60 to 0.92)	0.82 (0.62 to 0.91)	0.62 (0.27 to 0.81)
		8.10	5.71	6.07	6.98	5.43	7.64
FF-HF	sag	0.36 (-0.07 to 0.67)	0.49 (0.06 to 0.72)	0.54 (0.13 to 0.75)	0.43 (0.03 to 0.72)	0.60 (0.23 to 0.79)	0.52 (0.10 to 0.74)
		3.30	3.41	2.76	4.68	4.00	3.16
FF-HF	fro	0.30 (-0.12 to 0.64)	0.75 (0.49 to 0.87)	0.69 (0.38 to 0.83)	0.47 (0.08 to 0.74)	0.42 (-0.07 to 0.67)	0.48 (0.02 to 0.71)
		6.47	3.07	3.59	4.01	3.65	4.12
FF-HF	tra	0.44 (0.04 to 0.72)	0.68 (0.36 to 0.83)	0.69 (0.39 to 0.84)	0.53 (0.15 to 0.77)	0.74 (0.46 to 0.86)	0.56 (0.15 to 0.76)
		3.39	2.20	2.33	2.95	2.24	3.31
HAL	sag	0.22 (-0.21 to 0.58)	0.45 (-0.04 to 0.69)	0.45 (-0.03 to 0.69)	0.33 (-0.09 to 0.66)	0.29 (-0.30 to 0.59)	0.56 (0.14 to 0.75)
		11.98	2.33	11.59	3.22	3.21	11.03

7.4.4.5 Between-Session Reliability of 3DFoot

Between-session ICC and SEM values for reliability assessment of 3DFoot is presented in Table 7.8. Overall, moderate ICCs were demonstrated by 3DFoot of 0.47 (95%CI 0.15 to 0.64) and reasonable SEM value of $3.88^{o} \pm 2.18^{o}$. The hindfoot (ICC 0.49 95%CI 0.17 to 0.65), midfoot (ICC 0.51 95%CI 0.23 to 0.66) and forefoot segments (ICC 0.50 95%CI 0.20 to 0.66) demonstrated moderate ICC values, but the hallux demonstrated low ICC values (ICC 0.31 95%CI -0.07 to 0.57). The hindfoot (mean SEM $3.39^{o} \pm 0.85^{o}$), midfoot (mean SEM $2.94^{o} \pm 0.79^{o}$) and forefoot segments (mean SEM $2.74^{o} \pm 0.86^{o}$) demonstrated reasonable SEM values,

but the hallux revealed unacceptable SEM values (mean SEM 7.72° ± 3.18°). Across all 3DFoot segments between-session reliability was moderate; highest in the sagittal plane (ICC 0.51 95%CI 0.22 to 0.66) followed by the frontal (ICC 0.45 95%CI 0.10 to 0.63) and transverse planes (ICC 0.45 95%CI 0.12 to 0.63). Errors from repeated session were all reasonable with highest SEM in the sagittal plane (mean SEM 4.83° ± 3.35°), then transverse (mean SEM 3.75° ± 0.67°) and frontal plane (mean SEM 3.16° ± 1.59°). Between-session reliability (ICCs) was moderate across gait cycle events (ICC 0.45 95%CI 0.15 to 0.63), peak minimal (ICC 0.50 95%CI 0.19 to 0.65) and peak maximal values (ICC 0.47 95%CI 0.15 to 0.64). SEM values were reasonable at peak minimal values (mean SEM 3.53° ± 2.31°), peak maximal values (mean SEM 3.65° ± 1.47°) and values at gait events (mean SEM 4.45° ± 3.07°).

For the hindfoot joint ICC values were moderately high in the sagittal plane (ICC 0.60 95%CI 0.34 to 0.69) and moderate in the frontal (ICC 0.43 95%CI 0.06 to 0.62) and transverse planes (ICC 0.43 95%CI 0.07 to 0.63). Mean SEM values were lowest in the transverse plane (2.54° ± 0.60°) then frontal (3.73° ± 0.52°) and sagittal (3.83° ± 0.74°), all SEM values were reasonable.

The midfoot showed moderately high ICCs in the transverse (ICC 0.63 95%CI 0.44 to 0.71), moderate ICCs in the sagittal plane (ICC 0.55 95%CI 0.29 to 0.68) and low ICCs in the frontal plane (ICC 0.34 95%CI -0.06 to 0.58). Error measures were lowest in the transverse (2.44°± 0.30°), followed by frontal (2.60° ± 0.36°) and sagittal plane (3.77° ± 0.79°), all SEM values were reasonable.

Forefoot ICC were all moderate; highest in the frontal (ICC 0.56 95%CI 0.30 to 0.68) then transverse (ICC 0.48 95%CI 0.14 to 0.65) and sagittal planes (ICC 0.47 95%CI 0.14 to 0.64). Mean SEM values were lowest for the sagittal plane (2.00° ± 1.03°), transverse (3.02° ± 0.41°) and frontal (3.18° ± 0.30°), all SEM values were reasonable

The 3DFoot's hallux showed moderate ICC in the sagittal plane (ICC 0.40 95%CI 0.6 to 0.61), but low ICCs in the transverse plane (ICC 0.22 95%CI -0.20 to 0.52). Mean SEM values were lower in the transverse plane (5.72° ± 1.38°) compared to the sagittal plane (9.71° ± 3.29°), both SEMs were unacceptable.

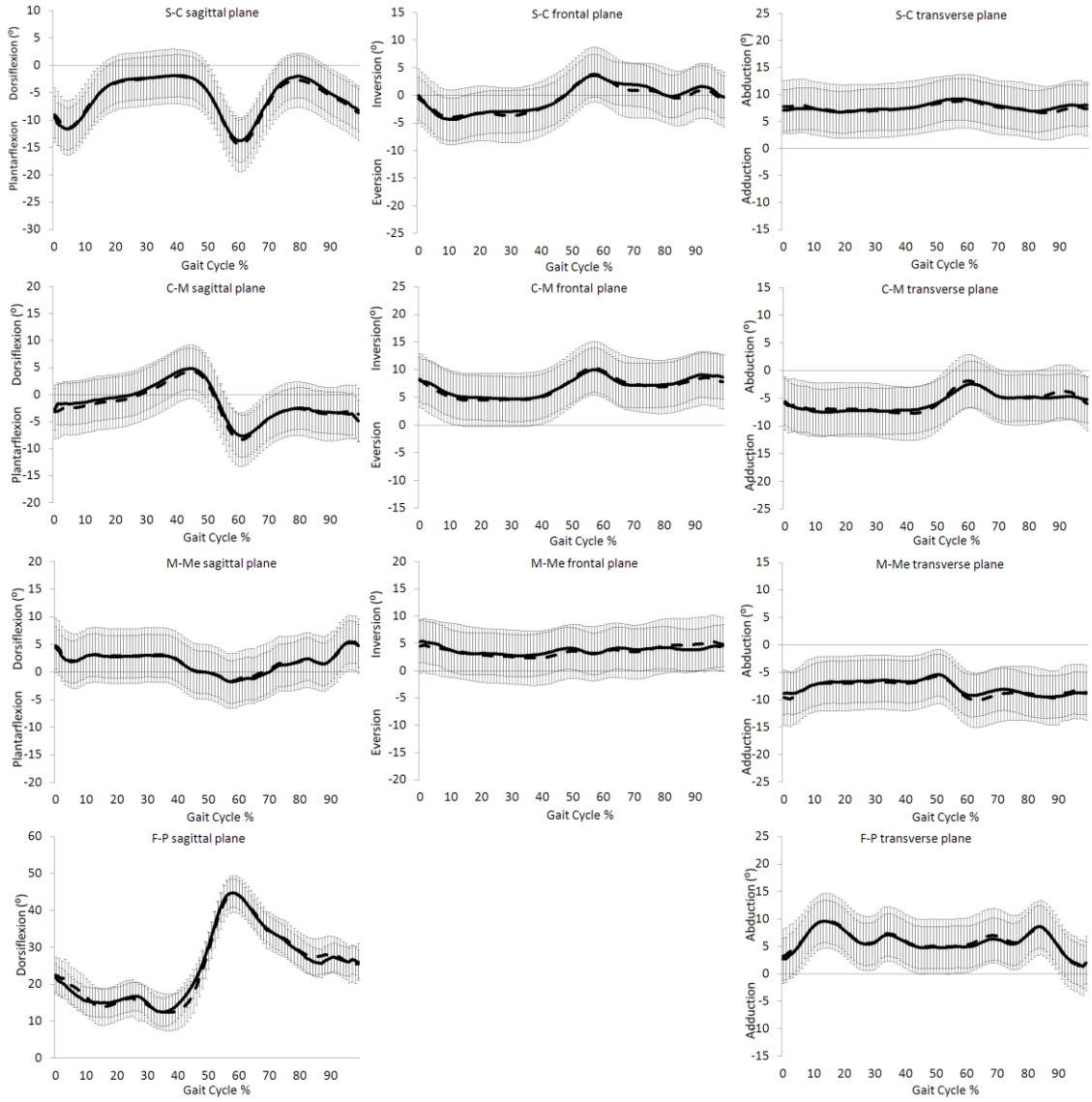

Figure 7.5. Mean ± SD of 3DFoot test-retest. Session 1 black line, Session 2 dash line

In summary, of the 66 3DFoot variables extracted over the gait cycle 15 (22.7%) demonstrated low reliability, 28 (42.4%) demonstrated moderate reliability, 20 (30.3%) demonstrated moderately high reliability and three (4.5%) demonstrated very high reliability. The 15 3Dfoot variables that demonstrated low reliability (number of variables at points of the gait cycle in brackets):

- Hindfoot frontal plane stance phase peak maximal value (1)
- Hindfoot transverse plane stance phase peak minimal value (1)
- Midfoot frontal plane stance phase peak maximal value, value at ipsilateral toe-off, swing phase peak minimal and maximal values (4)

- Forefoot sagittal plane value at ipsilateral initial contact (1)
- Hallux sagittal plane value at ipsilateral toe-off and swing phase peak minimal value (2)
- Hallux transverse plane value at all six values (6)

Of the 66 3DFoot variables extracted over the gait cycle ten (15.2%) of the variables demonstrated unacceptable SEM values, 53 (80.3%) demonstrated reasonable SEM and three (4.5%) demonstrated acceptable SEM values. The ten 3DFoot variables to demonstrate unacceptable SEM (number of variables at points of the gait cycle in brackets):

- All six Hallux sagittal plane values (6)
- Hallux transverse plane value at ipsilateral initial contact, stance peak maximal and minimal values, value at ipsilateral toe-off and swing peak maximal value (5)

Table 7.8. ICC (95% confidence intervals) and SEM of 3DFoot at gait events and peaks

3DFoot		Gait Cycle					
Segment	Plane	IIC	Stance min	Stance max	ITO	Swing min	Swing max
S-C (ICC)	sag	0.81 (0.59 to 0.92)	0.66 (0.34 to 0.84)	0.74 (0.48 to 0.88)	0.74 (0.46 to 0.88)	0.58 (0.22 to 0.80)	0.55 (0.17 to 0.78)
(SEM)		2.65	3.63	3.55	4.12	4.25	4.80
S-C	fro	0.41 (0.00 to 0.70)	0.65 (0.33 to 0.84)	0.32 (-0.11 to 0.65)	0.43 (0.02 to 0.71)	0.50 (0.11 to 0.76)	0.45 (0.04 to 0.73)
		4.56	3.10	3.36	4.01	4.00	3.73
S-C	tra	0.42 (0.01 to 0.71)	0.38 (-0.04 to 0.69)	0.54 (0.16 to 0.78)	0.58 (0.22 to 0.80)	0.40 (-0.01 to 0.70)	0.47 (0.08 to 0.74)
		3.56	2.47	2.10	2.95	2.13	2.07
C-M	sag	0.64 (0.31 to 0.83)	0.56 (0.19 to 0.79)	0.77 (0.52 to 0.90)	0.58 (0.22 to 0.8)	0.59 (0.24 to 0.81)	0.64 (0.32 to 0.84)
		3.10	4.50	3.33	2.82	4.14	4.74
C-M	fro	0.45 (0.05 to 0.73)	0.51 (0.12 to 0.76)	0.38 (-0.04 to 0.68)	0.24 (-0.19 to 0.59)	0.24 (-0.19 to 0.60)	0.31 (-0.12 to 0.64)
		3.31	2.45	2.36	2.40	2.43	2.62
C-M	tra	0.66 (0.34 to 0.84)	0.83 (0.64 to 0.93)	0.73 (0.46 to 0.88)	0.65 (0.33 to 0.84)	0.79 (0.57 to 0.91)	0.75 (0.49 to 0.89)
		2.69	1.93	2.56	2.68	2.25	2.54
M-M	sag	0.23 (-0.20 to 0.59)	0.68 (0.38 to 0.86)	0.43 (0.02 to 0.72)	0.60 (0.24 to 0.81)	0.66 (0.35 to 0.85)	0.46 (0.06 to 0.74)
		2.79	0.62	2.65	2.33	0.76	2.87
M-M	fro	0.40 (-0.02 to 0.69)	0.82 (0.61 to 0.92)	0.60 (0.25 to 0.81)	0.62 (0.27 to 0.82)	0.68 (0.38 to 0.86)	0.67 (0.36 to 0.85)
		3.57	2.53	2.40	3.53	3.50	3.56
M-M	tra	0.45 (0.05 to 0.73)	0.59 (0.23 to 0.80)	0.63 (0.29 to 0.83)	0.55 (0.17 to 0.78)	0.42 (0.01 to 0.71)	0.50 (0.11 to 0.76)
		2.67	2.61	2.87	3.53	2.95	3.54
F-P	sag	0.40 (-0.02 to 0.69)	0.59 (0.23 to 0.81)	0.47 (0.07 to 0.74)	0.32 (-0.11 to 0.65)	0.36 (-0.06 to 0.67)	0.43 (0.02 to 0.71)
		12.01	6.61	7.68	13.86	11.96	6.14
F-P	tra	0.22 (-0.21 to 0.58)	0.21 (-0.22 to 0.57)	0.35 (-0.07 to 0.67)	0.24 (-0.19 to 0.59)	0.24 (-0.19 to 0.59)	0.08 (-0.34 to 0.48)
		6.94	4.21	5.11	7.73	4.58	5.76

7.4.4.6 3DFoot Joint Angle Differences Following Normalisation to Standing Position

In the 3DFoot model's software is the option to normalise joint angles to a standing position. This has the effect of reducing marker placement error within-session, but also removes actual differences in foot segment motion. This section compared joint angles at initial contact and toe-off as an indication of alterations in joint motion, within-session range of joint angles at the two events to see if group differences are reduced, and mean ROM to ascertain if motion

has been reduced or just offset. All joint angles were significantly altered following the normalisation procedure except the metatarsal-midfoot joint in the sagittal plane, shown in Table 7.9.

The calcaneus became less plantarflexed, more everted and less abducted after normalising to standing position. Range of motion (ROM) values decreased in all sagittal and frontal planes and increased in the transverse plane. Within-session range at gait events was reduced for sagittal, frontal and transverse plane angles.

The midfoot demonstrated less plantarflexion, less inversion and more abduction at initial contact and toe off after normalising to standing. Sagittal, frontal and transverse plane ROM values all decreased. Within-session variability, measured by the range of joint angles at gait events between the subjects decreased in the sagittal, frontal and transverse planes.

After zeroing joint angles to standing position the forefoot segment presented less dorsiflexion, less inversion and less adduction. Values of ROM reduced in the sagittal and frontal planes and transverse plane ROM increased. All 3D within-session forefoot angles were reduced for the sagittal, frontal and transverse plane.

Dorsiflexion of the hallux was reduced as was hallux abduction. Joint ROM values were reduced in the sagittal plane and increased in the transverse. Within-session range of hallux joint angles at initial contact and toe off reduced in the sagittal and transverse planes.

Table 7.9. Mean ± SD of 3DFoot angular outputs at initial contact and toe off following normalisation to standing. Significance * = p<.05, ** = p<.01, *** = p<.001

3DFoot		Average joint angle		
		Non-normalised	normalised	Non-normalised-normalised
Segment	Plane	IIC	IIC	Difference
S-C	sag	-13.67 ± 6.05	-3.00 ± 2.84	-10.67 ± 6.31***
S-C	fro	-0.57 ± 5.94	2.73 ± 4.25	-3.30 ± 7.44***
S-C	tra	8.75 ± 4.69	-0.41 ± 1.90	9.16 ± 4.79***
C-M	sag	-2.20 ± 5.18	-0.65 ± 2.44	-1.55 ± 5.77**
C-M	fro	9.08 ± 4.47	2.76 ± 2.80	6.33 ± 5.02***
C-M	tra	-6.99 ± 4.64	1.54 ± 2.05	-8.53 ± 5.16***
M-M	sag	1.16 ± 3.18	0.11 ± 1.65	1.04 ± 3.49
M-M	fro	6.64 ± 4.59	-0.36 ± 3.04	7.00 ± 5.44***
M-M	tra	-9.93 ± 3.61	-1.51 ± 2.86	-8.42 ± 3.68***
F-P	sag	26.75 ± 15.45	13.03 ± 12.71	13.73 ± 21.36***
F-P	tra	4.02 ± 7.87	-1.82 ± 6.46	5.84 ± 10.38***
		ITO	ITO	
S-C	sag	-17.68 ± 8.01	-6.80 ± 4.22	-10.88 ± 9.1***
S-C	fro	4.22 ± 5.29	7.67 ± 5.62	-3.45 ± 8.41***
S-C	tra	10.03 ± 4.54	0.82 ± 2.34	9.21 ± 5.05***
C-M	sag	-5.50 ± 4.35	-3.87 ± 3.87	-1.63 ± 6.12*
C-M	fro	11.68 ± 2.75	5.49 ± 2.35	6.19 ± 3.25***
C-M	tra	-4.06 ± 4.53	4.29 ± 2.84	-8.35 ± 5.03***
M-M	sag	-0.05 ± 3.66	-0.35 ± 3.02	0.31 ± 4.41
M-M	fro	4.14 ± 5.70	-1.07 ± 1.80	5.21 ± 5.48***
M-M	tra	-8.91 ± 5.24	-1.07 ± 2.72	-7.84 ± 5.59***
F-P	sag	46.43 ± 16.79	38.19 ± 8.38	8.24 ± 17.54***
F-P	tra	6.87 ± 8.86	-0.08 ± 4.52	6.95 ± 10.34***

7.4.4.7 Between-Session Reliability of 3DFoot Joint Angle Following Normalisation to Standing Position

The normalisation of 3DFoot joint angles to the subject's standing position reduced ICC values for repeated measures over gait cycle events and peaks to 0.39 (95%CI 0.02 to 0.60). However, SEM values were reduced to 3.29^{o} ± 2.02^{o} when normalised to standing. Between-session reliability and error of 3DFoot following normalisation to standing position are presented in Table 7.10. Hindfoot (ICC 0.43 95%CI 0.07 to 0.62 after normalisation), midfoot (ICC 0.37 95%CI -0.02 to 0.59 after normalisation) and forefoot ICCs decreased (ICC 0.39 95%CI 0.01 to 0.61 after normalisation), but hallux ICCs increased (ICC 0.37 95%CI 0.03 to 0.59 after normalisation) following normalisation to standing. All 3DFoot segments showed decreased SEM values following normalisation to standing; hindfoot (mean SEM 2.80^{o} ± 1.06^{o} after normalisation), midfoot (mean SEM 2.52^{o} ± 0.98^{o} after normalisation), forefoot (mean SEM 3.29 ^{o} ± 2.02^{o} after normalisation) and hallux (mean SEM 6.93^{o} ± 2.29^{o} after normalisation). Across all three planes between-session reliability reduced after thigh marker rotation offset; sagittal (ICC 0.38 95%CI 0.15 to 0.60 after normalisation), frontal (ICC 0.39 95%CI 0.01 to 0.60

after normalisation) and transverse plane (ICC 0.40 95%CI 0.04 to 0.61 after normalisation). However, SEM values reduced across all three planes; sagittal (mean SEM 3.92^{o} ± 2.92^{o} after normalisation), frontal (mean SEM 3.16^{o} ± 1.59^{o} after normalisation) and transverse plane (mean SEM 2.95^{o} ± 0.64^{o} after normalisation). Values extracted at gait cycle events (ICC 0.33 95%CI -0.06 to 0.57 after normalisation), peak minimal values (ICC 0.43 95%CI 0.07 to 0.62 after normalisation) and peak maximal values (ICC 0.47 95%CI 0.06 to 0.61 after normalisation) all demonstrated lower ICC following normalisation to standing. Joint motion values at event (mean SEM 3.07^{o} ± 2.00^{o} after normalisation) and peak maximal value (mean SEM 3.25^{o} ± 1.77^{o} after normalisation) SEMs were lower, but peak minimal value SEMs were higher (mean SEM 3.55 ^{o} ± 2.66^{o} after normalisation).

Mean ICC values were reduced at the hindfoot in the sagittal plane (ICC 0.41 95%CI 0.04 to 0.61 after offset) and transverse plane (ICC 0.41 95%CI 0.04 to 0.61 after offset) but, increased in the frontal (ICC 0.46 95%CI 0.11 to 0.64 after offset). Mean SEM values reduced in the sagittal (mean SEM 3.09^{o} ± 0.52^{o} after offset) and transverse planes (mean SEM 1.68^{o} ± 0.48^{o} after offset) but increased in the frontal plane (mean SEM 3.88^{o} ± 1.08^{o} after offset).

Between-session reliability decreased in all three planes after normalising to standing; sagittal (ICC 0.35 95%CI -0.03 to 0.58 after offset), frontal (ICC 0.33 95%CI -0.07 to 0.58 after offset) and transverse plane (ICC 0.42 95%CI 0.04 to 0.62 after offset). Sagittal (mean SEM 2.55^{o} ± 0.64^{o} after offset) and transverse plane (mean SEM 2.13^{o} ± 0.18^{o} after offset) SEM values reduced, but frontal plane SEM values increased (2.92^{o} ± 0.55^{o} after offset).

Between-session reliability decreased in all three planes after normalising to standing; sagittal (ICC 0.43 95%CI 0.06 to 0.62 after offset), frontal (ICC 0.36 95%CI -0.03 to 0.59 after offset) and transverse plane (ICC 0.38 95%CI -0.00 to 0.60 after offset). However, SEM values reduced for all three planes; sagittal (mean SEM 1.65^{o} ± 0.62^{o} after offset), frontal (mean SEM 1.92^{o} ± 1.02^{o} after offset) and transverse (mean SEM 2.51^{o} ± 0.87^{o} after offset).

Sagittal plane hallux ICCs decreased (ICC 0.34 95%CI -0.01 to 0.57 after offset) and transverse plane ICCs increased (ICC 0.40 95%CI 0.08 to 0.61 after offset). Mean SEM values reduced in the sagittal (mean SEM plane 8.39^{o} ± 2.25^{o} after offset) and transverse from (mean SEM plane 5.48^{o} ± 1.20^{o} after offset).

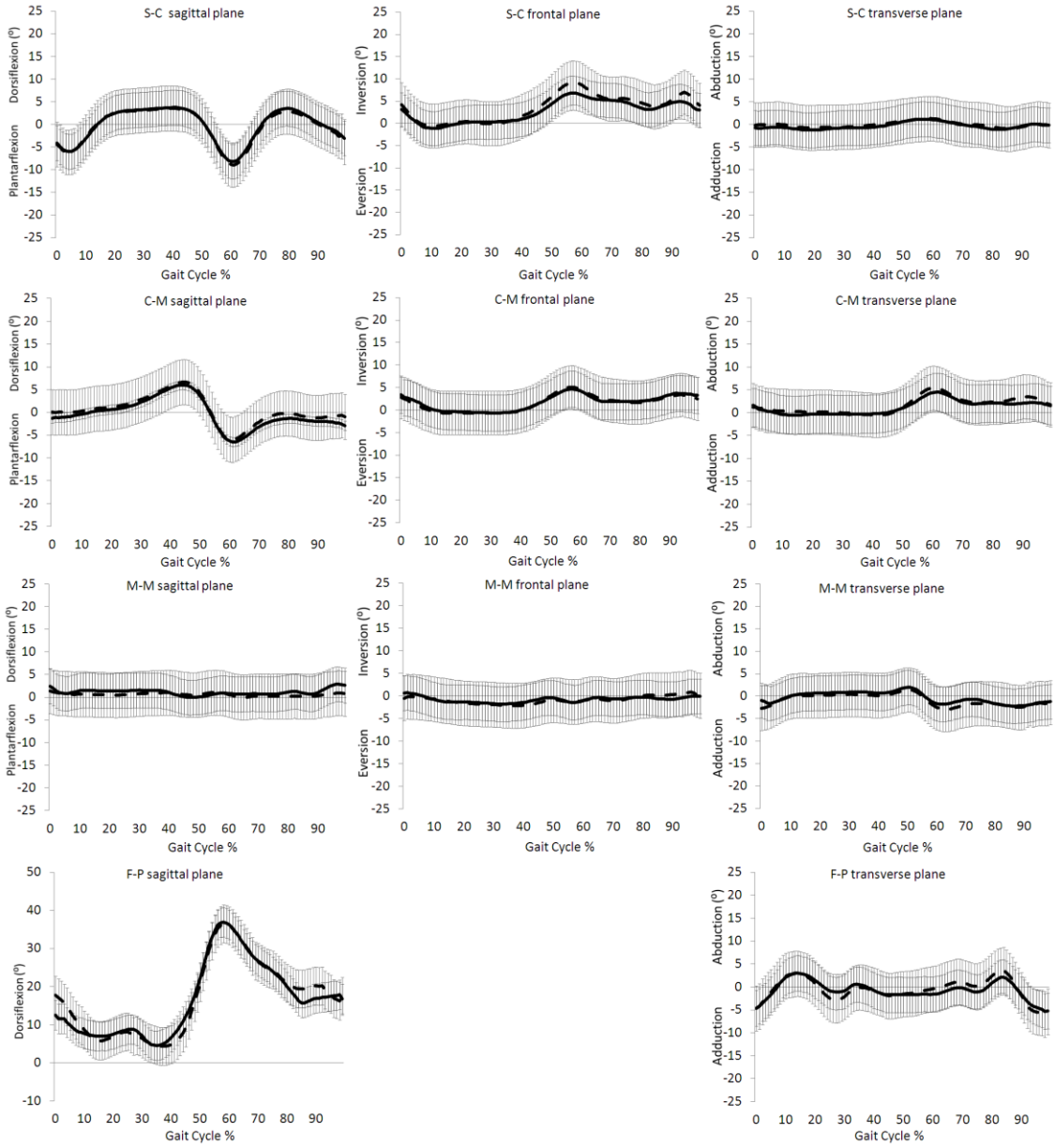

Figure 7.6. Mean ± SD of 3DFoot normalised to standing position. Session 1 black line, session 2 dash line

In summary, after normalising 3DFoot to standing 29 (43.9%) variables demonstrated low reliability, 29 (43.9%) demonstrated moderate reliability, eight (12.1%) demonstrated moderately high reliability and none demonstrated very high reliability. The 29 3Dfoot variables that demonstrated low reliability following normalisation to standing (number of variables at points of the gait cycle in brackets):

- Hindfoot sagittal plane value at ipsilateral initial contact and at ipsilateral toe-off (2)
- Hindfoot frontal plane stance phase peak minimal value (1)

- Hindfoot transverse plane value at ipsilateral initial contact, swing phase peak minimal and maximal values (3)
- Midfoot sagittal plane stance phase peak minimal value, value at ipsilateral toe-off and swing phase peak maximal value (3)
- Midfoot frontal plane value at ipsilateral initial contact, at ipsilateral toe-off, and swing phase peak maximal value (3)
- Midfoot transverse plane value at ipsilateral initial contact (1)
- Forefoot sagittal plane value at ipsilateral initial contact and stance phase peak maximal value (2)
- Forefoot frontal plane value at ipsilateral initial contact, stance phase peak minimal value and value at ipsilateral toe-off (3)
- Forefoot transverse plane value at ipsilateral initial contact, stance phase peak maximal value, and swing phase peak minimal and maximal values (4)
- Hallux sagittal plane value at ipsilateral initial contact, stance phase peak maximal value, value at ipsilateral toe-off and swing phase peak minimal value (5)
- Hallux transverse plane value at ipsilateral toe-off and swing phase peak maximal value (2)

Following normalisation to standing ten (15.2%) of the variables demonstrated unacceptable SEM values, 41 (62.1%) demonstrated reasonable SEM and 15 (22.7%) demonstrated acceptable SEM values. The ten 3DFoot variables to demonstrate unacceptable SEM (number of variables at points of the gait cycle in brackets):

- Hindfoot sagittal plane stance phase peak minimal value (1)
- All six Hallux sagittal plane values (6)
- Hallux transverse plane stance phase peak minimal value, swing phase peak maximal and minimal values (3)

Table 7.10. ICC (95% confidence intervals) and SEM of OFM at gait events and peaks after normalisation to standing

3Dfoot normalised	Gait Cycle					
Segment	Plane	IIC	Stance min	Stance max	ITO	Swing min	Swing max
S-C	sag	0.22 (-0.21 to 0.58)	0.52 (0.14 to 0.77)	0.58 (0.23 to 0.80)	0.39 (-0.03 to 0.69)	0.40 (-0.02 to 0.69)	0.50 (0.12 to 0.76)
		2.51	3.54	2.42	3.30	3.65	3.12
S-C	fro	0.44 (0.04 to 0.72)	0.48 (0.08 to 0.74)	0.62 (0.27 to 0.82)	0.54 (0.16 to 0.78)	0.31 (-0.12 to 0.64)	0.60 (0.26 to 0.81)
		3.18	5.30	3.86	3.83	2.30	4.81
S-C	tra	0.29 (-0.14 to 0.63)	0.60 (0.24 to 0.81)	0.64 (0.31 to 0.83)	0.46 (0.06 to 0.74)	0.36 (-0.06 to 0.68)	0.29 (-0.14 to 0.63)
		1.60	1.76	2.49	1.71	1.00	1.52
C-M	sag	0.46 (0.05 to 0.73)	0.37 (-0.05 to 0.68)	0.72 (0.44 to 0.87)	0.22 (-0.21 to 0.58)	0.41 (0.00 to 0.71)	0.03 (-0.39 to 0.44)
		1.80	2.53	2.30	3.41	2.03	3.21
C-M	fro	0.16 (-0.27 to 0.54)	0.40 (-0.01 to 0.70)	0.45 (0.05 to 0.73)	0.21 (-0.22 to 0.57)	0.47 (0.08 to 0.74)	0.37 (-0.05 to 0.68)
		2.57	2.83	3.20	2.09	3.18	3.66
C-M	tra	0.25 (-0.18 to 0.60)	0.43 (0.02 to 0.71)	0.46 (0.06 to 0.73)	0.44 (0.03 to 0.72)	0.56 (0.19 to 0.79)	0.52 (0.13 to 0.76)
		1.78	2.19	2.33	2.12	2.21	2.16
M-M	sag	0.34 (-0.09 to 0.66)	0.48 (0.09 to 0.75)	0.39 (-0.02 to 0.69)	0.59 (0.24 to 0.81)	0.55 (0.18 to 0.78)	0.40 (-0.02 to 0.70)
		1.35	1.02	2.17	1.93	0.98	2.45
M-M	fro	0.20 (-0.23 to 0.57)	0.27 (-0.16 to 0.62)	0.56 (0.20 to 0.79)	0.30 (-0.13 to 0.63)	0.46 (0.06 to 0.73)	0.49 (0.10 to 0.75)
		2.72	2.10	2.05	1.51	2.75	2.37
M-M	tra	0.28 (-0.15 to 0.62)	0.61 (0.27 to 0.82)	0.56 (0.19 to 0.79)	0.36 (-0.06 to 0.68)	0.32 (-0.10 to 0.65)	0.27 (-0.16 to 0.61)
		2.42	4.23	1.92	2.17	1.97	2.34
F-P	sag	0.39 (-0.03 to 0.69)	0.64 (0.31 to 0.83)	0.35 (-0.08 to 0.66)	0.31 (-0.12 to 0.64)	0.28 (-0.15 to 0.62)	0.18 (-0.25 to 0.55)
		9.92	8.41	7.09	6.95	12.02	5.92
F-P	tra	0.46 (0.06 to 0.73)	0.76 (0.5 to 0.89)	0.41 (0.00 to 0.70)	0.23 (-0.2 to 0.59)	0.41 (-0.01 to 0.7)	0.3 (-0.13 to 0.63)
		4.75	6.51	4.92	3.97	5.52	7.23

7.4.4.8 Between-Session Reliability of Kinfoot

Between-session ICC and SEM values for reliability assessment of Kinfoot are presented in Table 7.11. Overall, moderate ICC values were demonstrated by Kinfoot model of 0.43 (95%CI -0.03 to 0.59), but with unacceptable SEM values of 5.08^{o}± 1.53^{o}. The ankle (ICC 0.45 95%CI 0.10 to 0.63), subtalar (ICC 0.54 95%CI 0.26 to 0.67), medial forefoot (ICC 0.42 95%CI 0.05 to 0.62), lateral forefoot (ICC 0.41 95%CI 0.03 to 0.61), hallux (ICC 0.40 95%CI 0.04 to 0.61), medial toes (ICC 0.41 95%CI 0.04 to 0.61) and lateral toes (ICC 0.40 95%CI 0.02 to 0.61) presented moderate ICCs, but the midfoot (ICC 0.36 95%CI -0.03 to 0.59) presented low ICCs. The ankle (mean SEM 3.65^{o} ± 0.64^{o}), medial forefoot (mean SEM 4.08^{o} ± 0.84^{o}) and lateral forefoot (mean SEM 4.51^{o} ± 2.58^{o}) demonstrated reasonable SEM values but, subtalar (mean SEM 5.29^{o} ± 1.69^{o}), midfoot (mean SEM 5.08^{o} ± 2.83^{o}), hallux (mean SEM 6.09^{o} ± 1.89^{o}), medial toes (mean SEM 5.99^{o} ± 1.50^{o}), and lateral toes (mean SEM 5.99^{o} ± 2.52^{o}) demonstrated unacceptable error. Kinfoot ICCs were moderate in the frontal (ICC 0.45 95%CI 0.10 to 0.63) and transverse planes (ICC 0.44 95%CI 0.09 to 0.63), but low in the sagittal plane (ICC 0.38 95%CI -0.01 to 0.60). Error (SEM) values were unacceptable in the sagittal plane (mean SEM 5.93^{o} ± 1.81^{o}), but reasonable in the frontal (mean SEM 4.59^{o} ± 1.29^{o}) and transverse planes (mean SEM 4.74^{o} ± 2.24^{o}). Between-session reliability was consistent across

gait cycle events (ICC 0.41 95%CI 0.04 to 0.61), peak minimal (ICC 0.43 95%CI 0.08 to 0.63) and peak maximal values (ICC 0.43 95%CI 0.07 to 0.62), all ICCs were moderate. Kinfoot SEM values were reasonable at peak minimal (mean SEM 4.70^{o} ± 2.17^{o}) and at peak maximal values (mean SEM 4.97^{o} ± 1.90^{o}), but unacceptable at gait cycle events (mean SEM 5.58^{o} ± 2.02^{o}).

The ankle joint demonstrated moderate ICC in all three planes; highest in the frontal (ICC 0.48 95%CI 0.14 to 0.64) then sagittal (ICC 0.44 95%CI 0.08 to 0.63) a finally transverse plane (ICC 0.43 95%CI 0.06 to 0.62). Mean SEM values were lowest in the frontal plane (3.13^{o}± 0.59^{o}) followed by sagittal (3.75^{o} ± 0.60^{o}) and transverse (4.05^{o} ± 0.39^{o}).

Between-session reliability of the subtalar joint, measured by ICCs was moderate in all three planes; highest in the frontal (ICC 0.59 95%CI 0.35 to 0.69) followed by sagittal (ICC 0.55 95%CI 0.27 to 0.68) and transverse (ICC 0.49 95%CI 0.15 to 0.65). Lowest SEM values were found in the transverse plane (4.08^{o} ± 0.59^{o}), then frontal (4.55^{o} ± 1.24^{o}) and sagittal plane (7.25^{o} ± 0.89^{o}).

The calcaneocuboid joint demonstrated low ICC in all three planes; highest ICCs in the frontal (ICC 0.38 95%CI -0.01 to 0.60) and transverse planes (ICC 0.38 95%CI -0.02 to 0.60) and lowest in the sagittal plane (ICC 0.33 95%CI -0.08 to 0.58). Transverse plane SEM values were reasonable (2.84^{o} ± 1.76^{o}) but sagittal (5.39^{o} ± 1.80^{o}) and frontal plane SEM values were unacceptable (7.00^{o} ± 3.44^{o})

Medial forefoot ICC values were moderate in the frontal (ICC 0.50 95%CI 0.17 to 0.65) and transverse planes (ICC 0.46 95%CI 0.14 to 0.64) but, low in the sagittal plane (ICC 0.28 95%CI -0.14 to 0.55). Repeat measures error values were lowest in the sagittal plane (3.86^{o} ± 1.02^{o}) then frontal (3.98^{o} ± 0.45^{o}) and transverse planes (4.39^{o}± 1.01^{o}), all SEM values were reasonable.

Lateral forefoot ICC values were moderate in the frontal (ICC 0.43 95%CI 0.07 to 0.62) and transverse planes (ICC 0.43 95%CI 0.06 to 0.62) but, low in the sagittal plane (ICC 0.36 95%CI -0.04 to 0.59). The sagittal plane recorded the lowest mean SEM values (4.28^{o} ± 1.47^{o}) then frontal (4.29^{o} ± 3.53^{o}) and transverse plane (4.96^{o} ± 3.53^{o}), all SEM values were reasonable.

The hallux presented moderate ICC values in the transverse plane (ICC 0.51 95%CI 0.22 to 0.66) but low ICCS in the sagittal (ICC 0.38 95%CI -0.01 to 0.60) and frontal planes (ICC 0.30 95%CI -0.06 to 0.56). The SEM values were reasonable in the transverse plane (4.79^{o} ± 0.75^{o}), but unacceptable in the sagittal (7.85^{o} ± 2.04^{o}) and frontal planes (5.64^{o} ± 1.21^{o}).

Mean ICC values for the medial toes were moderate in the frontal plane (ICC 0.50 95%CI 0.18 to 0.65) but low in the transverse (ICC 0.39 95%CI 0.00 to 0.61) and sagittal (ICC 0.34 95%CI -0.06 to 0.58). Mean SEM values were reasonable in the frontal plane ($4.95^{o} \pm 0.72^{o}$), but unacceptable in the transverse ($5.93^{o} \pm 1.09^{o}$) and sagittal planes ($7.10^{o} \pm 1.76^{o}$)

The lateral toes demonstrated moderate ICCs in the transverse plane (ICC 0.48 95%CI 0.14 to 0.64) but, low ICCS in the frontal (ICC 0.39 95%CI 0.00 to 0.61) and sagittal planes (ICC 0.33 95%CI -0.08 to 0.58). Mean SEM values were reasonable in the frontal plane ($3.13^{o} \pm 0.29^{o}$), but unacceptable in the transverse ($6.91^{o} \pm 1.42^{o}$) and sagittal planes ($7.94^{o} \pm 2.02^{o}$).

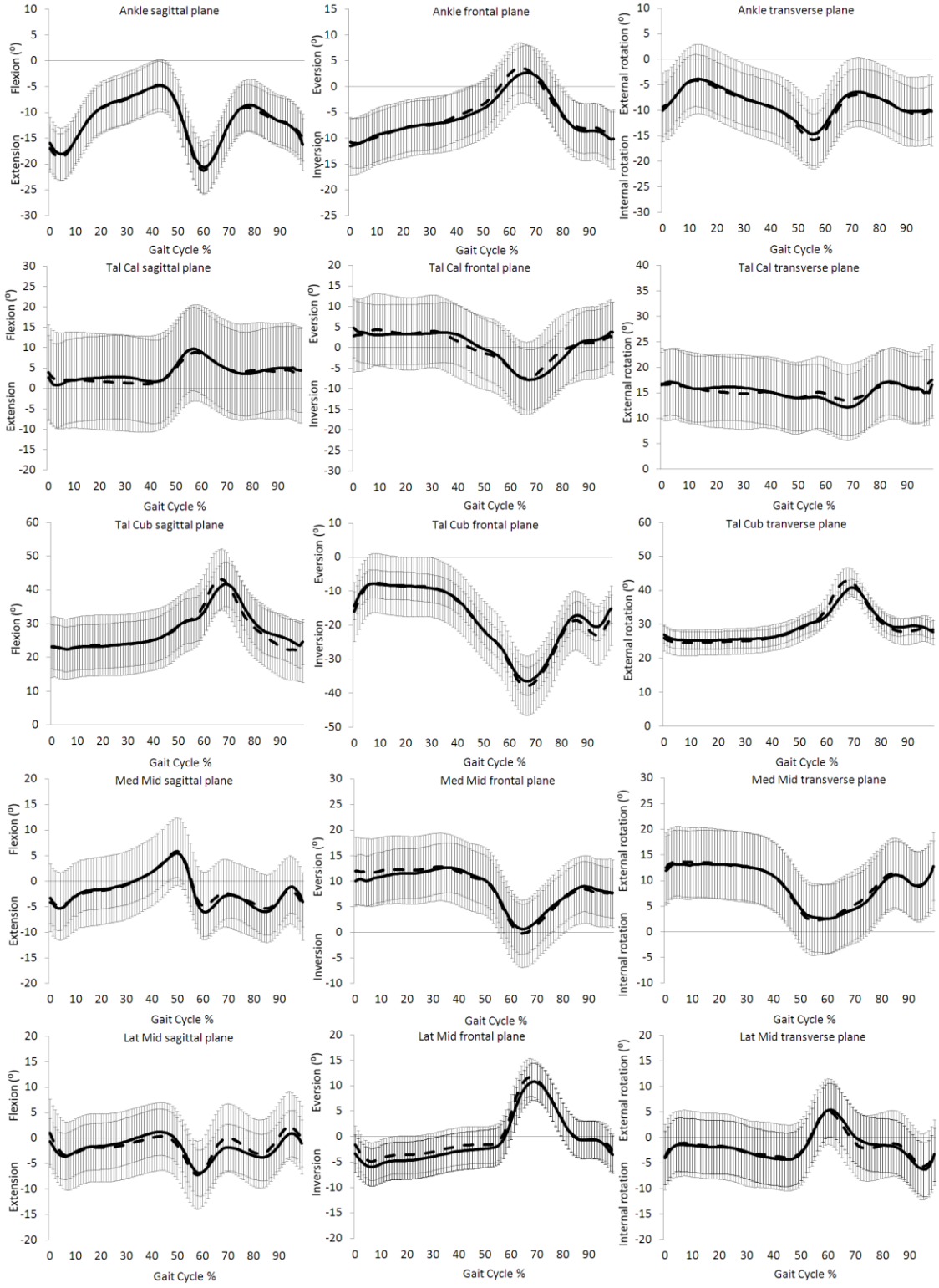

Figure 7.7a . Mean ± SD of Kinfoot hindfoot, midfoot and forefoot test retest. Session 1 black line, session 2 dash line

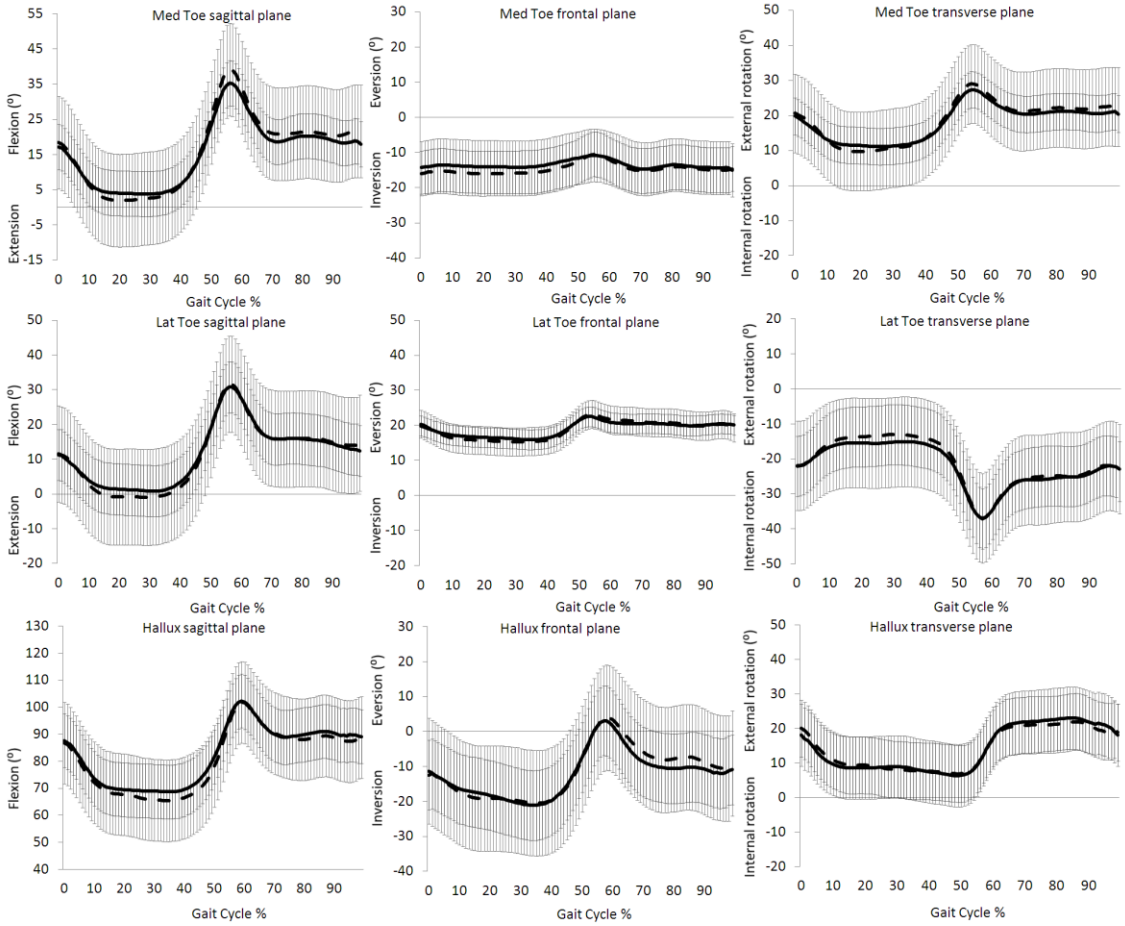

Figure 7.7b. Mean ± SD of Kinfoot toes and hallux test retest. Session 1 black line, session 2 dash line

In summary, of the 144 Kinfoot variables extracted over the gait cycle 47 (37.6%) demonstrated low reliability, 77 (53.5%) demonstrated moderate reliability, 19 (13.2%) demonstrated moderately high reliability and one (0.7%) demonstrated very high reliability. The 47 Kinfoot variables that demonstrated low reliability (number of variables at points of the gait cycle in brackets):

- Ankle frontal plane value at ipsilateral initial contact (1)
- Ankle transverse plane swing phase peak maximal value (1)
- Midfoot sagittal plane value at ipsilateral initial contact, stance phase peak minimal and maximal values, value at ipsilateral toe-off and swing phase peak minimal value (5)
- Midfoot frontal plane value ipsilateral initial contact, stance phase peak maximal value, value at ipsilateral toe-off and swing phase peak maximal value (4)
- Midfoot transverse plane value at ipsilateral initial contact and stance phase peak maximal value (2)

- Medial forefoot sagittal plane all values (6)
- Lateral forefoot sagittal plane value at ipsilateral initial contact, stance phase peak maximal value, and value at ipsilateral toe-off (3)
- Lateral forefoot frontal plane value at ipsilateral toe-off and swing phase peak minimal value (2)
- Lateral forefoot transverse plane at ipsilateral initial contact (1)
- Hallux sagittal plane value at ipsilateral initial contact, stance phase peak maximal value, value at ipsilateral toe-off, swing phase peak minimal and maximal values (5)
- Hallux frontal plane at ipsilateral initial contact, stance phase peak maximal value and value at ipsilateral toe-off (3)
- Medial toes sagittal plane value at ipsilateral initial contact, ipsilateral toe-off, swing phase peak minimal and maximal values (4)
- Medial toes transverse plane value at ipsilateral toe-off and swing phase peak maximal value (2)
- Lateral toes sagittal plane stance phase peak maximal value, value at ipsilateral toe-off, swing phase peak minimal and maximal values (4)
- Lateral toes frontal plane at ipsilateral initial contact, stance phase peak minimal value and swing phase peak minimal value (3)

Of the 144 Kinfoot variables extracted over the gait cycle 63 (43.8%) of the variables demonstrated unacceptable SEM values, 80 (55.6%) demonstrated reasonable SEM and one (0.7%) demonstrated acceptable SEM values. The 63 Kinfoot variables to demonstrate unacceptable SEM (number of variables at points of the gait cycle in brackets):

- All six subtalar sagittal plane values (6)
- Subtalar frontal plane values at ipsilateral initial contact, stance phase peak maximal value, and swing phase peak maximal value (3)
- Subtalar transverse plane values at ipsilateral initial contact (1)
- Midfoot sagittal plane value at ipsilateral initial contact and swing phase peak maximal value (2)
- Midfoot frontal plane value at ipsilateral initial contact, stance phase peak minimal value, value at ipsilateral toe-off, swing phase peak minimal and maximal values (5)
- Midfoot transverse plane swing phase peak maximal value (1)
- Medial forefoot transverse plane value at ipsilateral toe-off and swing phase peak maximal value (2)

- Lateral forefoot sagittal plane swing phase peak maximal value (1)
- Lateral forefoot frontal plane at ipsilateral toe-off and swing phase peak maximal value (2)
- Lateral forefoot transverse plane values at ipsilateral initial contact, ipsilateral toe-off and swing phase peak maximal value (3)
- All six hallux sagittal plane values (6)
- Hallux frontal plane value at ipsilateral initial contact, ipsilateral toe-off, swing phase peak minimal and maximal values (4)
- Hallux transverse plane value at ipsilateral initial contact and at ipsilateral toe-off (2)
- Medial toes sagittal plane value at ipsilateral initial contact, stance phase peak maximal value, value at ipsilateral toe-off, swing phase peak minimal and maximal values (5)
- Medial toes frontal plane stance phase peak maximal value, value at ipsilateral toe-off, swing phase peak minimal and maximal values (4)
- Medial toes transverse plane value at ipsilateral initial contact, stance phase peak maximal value, value at ipsilateral toe-off, swing phase peak minimal and maximal values (5)
- Lateral toes sagittal plane value at ipsilateral initial contact, stance phase peak maximal value, value at ipsilateral toe-off, swing phase peak minimal and maximal values (5)
- All six lateral toes transverse plane values (6)

Table 7.11. ICC (95% confidence intervals) and SEM of Kinfoot at gait events and peaks.

Kinfoot		Gait Cycle					
Segment	Plane	IIC	Stance min	Stance max	ITO	Swing min	Swing max
Ankle(ICC)	sag	0.48 (0.08 to 0.74)	0.49 (0.10 to 0.75)	0.49 (0.09 to 0.75)	0.42 (0.01 to 0.71)	0.42 (0.01 to 0.71)	0.58 (0.22 to 0.80)
(SEM)		3.69	3.62	2.91	4.36	4.5	3.39
Ankle	fro	0.37 (-0.05 to 0.68)	0.47 (0.07 to 0.74)	0.54 (0.17 to 0.78)	0.65 (0.33 to 0.84)	0.49 (0.09 to 0.75)	0.6 (0.25 to 0.81)
		3.60	2.60	2.56	3.27	2.79	4.00
Ankle	tra	0.51 (0.13 to 0.76)	0.41 (-0.01 to 0.70)	0.60 (0.25 to 0.81)	0.46 (0.06 to 0.73)	0.45 (0.05 to 0.73)	0.31 (-0.12 to 0.64)
		4.13	3.39	3.86	4.50	4.09	4.35
Tal Cal	sag	0.60 (0.26 to 0.81)	0.68 (0.37 to 0.85)	0.64 (0.31 to 0.83)	0.68 (0.37 to 0.85)	0.54 (0.16 to 0.78)	0.58 (0.22 to 0.80)
		7.30	6.79	6.58	6.70	8.98	7.12
Tal Cal	fro	0.54 (0.17 to 0.78)	0.74 (0.46 to 0.88)	0.61 (0.26 to 0.81)	0.81 (0.60 to 0.92)	0.79 (0.55 to 0.91)	0.54 (0.17 to 0.78)
		5.62	3.11	5.73	3.33	3.89	5.64
Tal Cal	tra	0.46 (0.05 to 0.73)	0.46 (0.06 to 0.74)	0.52 (0.13 to 0.77)	0.65 (0.32 to 0.84)	0.60 (0.24 to 0.81)	0.49 (0.10 to 0.75)
		5.01	3.85	4.36	3.52	3.45	4.28
Tal Cub	sag	0.37 (-0.04 to 0.68)	0.26 (-0.17 to 0.61)	0.33 (-0.09 to 0.65)	0.32 (-0.11 to 0.65)	0.30 (-0.13 to 0.63)	0.48 (0.08 to 0.74)
		6.28	4.29	3.78	4.77	4.57	8.64
Tal Cub	fro	0.39 (-0.03 to 0.69)	0.49 (0.09 to 0.75)	0.31 (-0.11 to 0.64)	0.36 (-0.06 to 0.67)	0.52 (0.14 to 0.77)	0.34 (-0.09 to 0.66)
		5.54	5.97	3.44	8.43	13.21	5.41
Tal Cub	tra	0.23 (-0.20 to 0.59)	0.45 (0.04 to 0.72)	0.34 (-0.08 to 0.66)	0.46 (0.06 to 0.73)	0.40 (-0.02 to 0.70)	0.49 (0.10 to 0.75)
		2.98	1.48	2.13	2.82	2.45	5.18
Med Mid	sag	0.20 (-0.23 to 0.57)	0.34 (-0.09 to 0.66)	0.14 (-0.29 to 0.53)	0.34 (-0.08 to 0.66)	0.34 (-0.09 to 0.66)	0.34 (-0.09 to 0.66)
		4.92	3.59	2.65	4.90	2.75	4.37
Med Mid	fro	0.62 (0.28 to 0.82)	0.52 (0.14 to 0.77)	0.5 (0.11 to 0.76)	0.62 (0.27 to 0.82)	0.46 (0.07 to 0.74)	0.54 (0.17 to 0.78)
		3.98	3.79	3.34	4.68	4.21	3.87
Med Mid	tra	0.52 (0.14 to 0.77)	0.51 (0.13 to 0.76)	0.58 (0.22 to 0.8)	0.53 (0.15 to 0.77)	0.56 (0.19 to 0.79)	0.40 (-0.01 to 0.70)
		4.61	4.83	3.76	5.45	5.01	2.67
Lat Mid	sag	0.32 (-0.10 to 0.65)	0.40 (-0.02 to 0.70)	0.34 (-0.08 to 0.66)	0.29 (-0.14 to 0.63)	0.44 (0.04 to 0.72)	0.48 (0.08 to 0.74)
		4.67	3.08	2.83	3.99	4.14	6.95
Lat Mid	fro	0.51 (0.12 to 0.76)	0.55 (0.18 to 0.78)	0.43 (0.02 to 0.71)	0.33 (-0.09 to 0.65)	0.34 (-0.08 to 0.66)	0.61 (0.26 to 0.82)
		2.12	2.12	2.40	5.27	2.76	11.08
Lat Mid	tra	0.30 (-0.13 to 0.63)	0.51 (0.12 to 0.76)	0.52 (0.14 to 0.77)	0.42 (0.01 to 0.71)	0.43 (0.02 to 0.72)	0.55 (0.18 to 0.78)
		5.01	3.38	4.93	6.46	4.26	5.71
Hallux	sag	0.36 (-0.06 to 0.67)	0.59 (0.23 to 0.80)	0.37 (-0.05 to 0.68)	0.34 (-0.08 to 0.66)	0.39 (-0.03 to 0.69)	0.36 (-0.06 to 0.67)
		10.23	5.99	5.85	8.68	10.01	6.35
Hallux	fro	0.22 (-0.22 to 0.58)	0.43 (0.02 to 0.71)	0.23 (-0.20 to 0.59)	0.33 (-0.10 to 0.65)	0.48 (0.09 to 0.75)	0.19 (-0.24 to 0.56)
		7.37	4.30	4.23	5.62	6.01	6.29
Hallux	tra	0.58 (0.23 to 0.80)	0.58 (0.21 to 0.8)	0.69 (0.38 to 0.86)	0.43 (0.02 to 0.72)	0.44 (0.03 to 0.72)	0.76 (0.50 to 0.89)
		5.76	4.15	4.89	5.6	4.15	4.16
Med Toe	sag	0.34 (-0.09 to 0.66)	0.57 (0.21 to 0.80)	0.42 (0.01 to 0.71)	0.34 (-0.08 to 0.66)	0.08 (-0.34 to 0.48)	0.36 (-0.06 to 0.67)
		8.79	4.08	6.90	8.93	6.71	7.19
Med Toe	fro	0.58 (0.22 to 0.80)	0.70 (0.41 to 0.86)	0.53 (0.15 to 0.77)	0.49 (0.10 to 0.75)	0.49 (0.10 to 0.75)	0.52 (0.14 to 0.77)
		4.61	3.65	5.26	5.67	5.31	5.21
Med Toe	tra	0.52 (0.13 to 0.77)	0.41 (-0.01 to 0.70)	0.4 (-0.02 to 0.70)	0.29 (-0.14 to 0.63)	0.45 (0.05 to 0.73)	0.37 (-0.05 to 0.68)
		6.46	4.51	5.23	6.32	7.60	5.44
Lat Toe	sag	0.40 (-0.01 to 0.70)	0.44 (0.04 to 0.72)	0.32 (-0.11 to 0.65)	0.28 (-0.15 to 0.62)	0.27 (-0.16 to 0.62)	0.32 (-0.11 to 0.65)
		8.82	4.88	8.89	10.31	6.12	8.63
Lat Toe	fro	0.31 (-0.12 to 0.64)	0.39 (-0.03 to 0.69)	0.49 (0.09 to 0.75)	0.50 (0.11 to 0.76)	0.36 (-0.07 to 0.67)	0.44 (0.04 to 0.72)
		2.94	3.48	2.95	3.49	2.82	3.11
Lat Toe	tra	0.47 (0.07 to 0.74)	0.51 (0.12 to 0.76)	0.71 (0.42 to 0.87)	0.47 (0.07 to 0.74)	0.5 (0.11 to 0.76)	0.44 (0.03 to 0.72)
		7.90	7.60	5.12	8.23	7.50	5.10

7.4.4.9 Comparison of Between-Session Reliability from Three Foot Models

In order to compare between-session reliability of the three foot models Table 7.12 highlights mean ICCs and SEMs for extracted segment motion at events and peaks of the gait cycle. All foot models demonstrated moderate between-session reliability (according to the ICC scale of Katz et al., 1992) except 3DFoot following normalisation to standing (which demonstrated low between-session reliability). The OFM and 3DFoot demonstrated errors less than 5°, indicating reasonable errors from repeated sessions. However, Kinfoot demonstrated unacceptably high errors, higher than 5°. The amount of between-session reliable segmental motion variables decreased with increasing number of segments comprised in the foot models. The OFM demonstrated low between-session reliability in less than half the variables (relative to total variables) of Kinfoot. However, error values did not show this trend with number of foot model segments. The 3DFoot model demonstrated less than half the variables with unacceptable error of OFM and nearly a third of Kinfoot.

Table 7.12. Summary of ICC and SEM of OFM, 3DFoot and Kinfoot.

Foot Model	Number of foot segments	Mean ICC (95%CI)	Percentage of variables with low ICC	Mean SEM (kinematics °, kinetic Nm)	Percentage of variables with unacceptable SEM
OFM	3	0.55 (0.16 to 0.77)	14.3	4.61 ± 2.86	26.2
OFM (thigh marker rotation offset)	3	0.56 (0.18 to 0.78)	16.7	4.56 ± 2.49	28.6
3DFoot	4	0.47 (0.15 to 0.64)	22.7	3.88 ± 2.18	15.2
3DFoot (normalised to standing)	4	0.39 (0.02 to 0.60)	43.9	3.29 ± 2.02	15.2
Kinfoot	8	0.43 (-0.03 to 0.59)	37.6	5.08 ± 1.53	43.8

7.5 Discussion

The aims of this chapter were to; (1) compare angular motion and, (2) determine the between-session reliability of three foot models over the gait cycle. In order to test these aims a within-rater repeated measures (test re-test) study design was implemented to measure the between-session reliability (ICC) and error (SEM) of the three foot models. The basis of selecting a foot model for use in the main study (chapter 8) was based firstly, on the most information on foot motion (most foot segments) and secondly, that the information was reliable.

7.5.1 Aim 1 Comparison of Foot Models

7.5.1.1 Comparison of Foot Models

A comparison of foot model's angular outputs was made to demonstrate the similarities and differences between the methods of segmenting the foot. Comparison of the three foot models tested in this study was made by qualitative assessment of the kinematic waveforms for each joint (Rankine et al., 2008). Comparison of each foot model's joint angular motion through statistical methods was not appropriate because the models measure different segments, which are defined in alternative ways and contain an array of different anatomical joints and bones. With no 'gold standard' to measure bone motion available in this current study the results are compared to cadaver and bone pin studies of foot bone motion. The aim of this section was not to address the issues of foot model validity, but to demonstrate how errors relate to anatomical reference frames and rigid body assumptions. These errors can reduce foot model reliability and so form part of the comparison of the three foot models tested in this chapter.

7.5.1.2 Comparison of Hindfoot Motion

Three-dimensional motion of OFM, 3DFoot and Kinfoot hindfoot segment was comparable to calcaneal-tibia motion measured previously by bone pins (Nester et al., 2007). However, OFM's hindfoot transverse plane motion demonstrated a significantly altered angular pattern. This difference between hindfoot motion of OFM compared to the other foot models in the current study and previous work is due to the definition of the shank segment. The OFM's shank segment is defined to be compatible with the anatomical definitions of the lower limb joints of the PiG model. The motion of OFM's hindfoot segment in the transverse plane is comparable to the ankle joint of PiG. However, the SD of the OFM is greater than PiG. Variation in the orientation of the shank segment due to the lateral tibial marker is likely to be the cause of the higher SD. Variation in placement of the heel marker to define the transverse axis of the hindfoot has previously been described in the OFM (Stebbins et al., 2006, Curtis et al., 2009). The 3DFoot and Kinfoot models define the shank as the most proximal segment against which hindfoot motion is reported relative to. The shank of the OFM may be affected by thigh marker placement error which externally rotated the thigh and internally rotated the shank. A measure of tibial torsion can be entered as a correction factor, in the same way as the thigh angle offset correction, to rotate the shank segment to account for marker

placement error. A measure of tibial torsion using a goniometer was unavailable for the current study, but future studies should include this when using the OFM.

7.5.1.3 Comparison of Midfoot Motion

In order to define midfoot motion a definition and alignment of the hindfoot is necessary. The hindfoot segment of Kinfoot in divided into calcaneus and the talus/navicular/cuneiform segments. However, due to the small size of navicular/cuneiform bones and the lack of skin marker placements on the talus tracking of this segment is calculated by offsets from adjacent segments. Furthermore Kinfoot's midfoot segment is also based on adjacent segments due the small bone size of the cuboid. The talar/navicular/cuneiform and the cuboid segments are both oriented based on metatarsal segment position. The talar/navicular/cuneiform segment is represented by a virtual marker defining the vertical axis from the second metatarsal joint centre. The second metatarsal joint centre is calculated as the midpoint between the first and third metatarsal. The anterior axis of the cuboid segment is based on the position of the fourth metatarsal joint centre which itself in calculated as half way between the third and fifth metatarsal joint centres. This definition of the hindfoot segments is based on alignment assumption across multiple foot joints. Lundgren et al., (2008) found ROM of 18^{o}, 10^{o} and 15^{o} in the sagittal, frontal and transverse planes respectively between the talus and first metatarsal. These ranges of motions between the metatarsal and the talus may give rise to the high variability in Kinfoot's subtalar joint motion. Motion of the fifth metatarsal relative to the cuboid has been reported to be $>12^{o}$ in the sagittal and frontal planes (Nester et al., 2007). This amount of potential motion of the fourth metatarsal joint centre may explain the seemingly excessive and variable sagittal and frontal plane motion of the calcaneocuboid joint in the Kinfoot model.

7.5.1.4 Comparison of Forefoot Motion

The forefoot segment of the OFM is described relative to the hindfoot (calcaneus) segment thus the midfoot is not represented in this model. Motion of the OFM forefoot is from a supinated and abducted position through the stance phase with peak supination and adduction motion at toe-off. The 3DFoot forefoot relative to midfoot segment shows the inverted (supinated) but abducted position through stance and no peak inversion at toe off. Instead 3DFoot's midfoot inverts on the hindfoot at toe-off while the forefoot remains

inverted. This demonstrates that considerable frontal motion that occurs at the midfoot which could be incorrectly attributed to the forefoot during gait. It is unclear whether 3DFoot forefoot segment motion is representative of actual metatarsal bone motion. This is because bone pin studies do not consider the forefoot as one segment due to considerable differences in motion between the first and fifth metatarsals (Nester et al., 2009). However, range of motion (ROM) of the Lisfranc joint (forefoot to midfoot which is described by 3DFoot) has been reported to be 10^{o} Lundberg et al., (1989). Therefore considering motion only between the hindfoot and forefoot segments would diminish all Lisfranc joint motion by not considering a midfoot segment.

7.5.1.5 Comparison of Hallux Motion

Kinfoot is the only model to present hallux motion in 3D by the use of a marker triad. The OFM and 3DFoot models use markers mounted on the medial hallux to define sagittal and in the case of 3DFoot transverse plane motion. The use of marker triads has been used in other foot models (Jenkyn & Nicol, 2007) to describe all foot segment motion. The benefits are that one anatomical location for marker attachment is required meaning small segments can be tracked. However, the triad itself maybe susceptible to vibration artefact during heel strike, though these may be filtered out of the kinematic signal (Leardini et al., 2005).

7.5.1.6 Comparison of segmental motion summary

The comparison of three foot models during concurrent gait cycles in a paediatric population revealed that joint motion is comparable at the hindfoot to shank between all three models, forefoot to midfoot between 3DFoot and Kinfoot and at the hallux to first metatarsal for all three foot models. However, differences in the orientation of the shank segment in the transverse plane caused cross-talk between the sagittal and frontal planes in the OFM resulting in a different output of angular motion. All three foot models used skin mounted markers to define each segment's orientation and axis with rotations being given relative to the proximal segment using Carden or Euler systems. However, Kinfoot's use of virtual markers on the talus/navicular/cuneiform and cuboid segments based on offsets from metatarsal joint centres meant subtalar and calcaneocuboid motion could be measured.

7.5.2 Aim 2. Between-Session Reliability of Foot Models

7.5.2.1 Within- and Between-Session Variance of Foot Models

Standard deviations provide a method of determining variation within each session, between subjects and between sessions. Across all three foot models within-subject SD were greater than between-session SD indicating that the children were able to walk consistently through the gait laboratory with the amalgamated marker set. Within-subject standard deviations (SD) were higher in the sagittal plane where most ROM occurs except for OFM which presented highest SD in the transverse plane. Compared to the use of the OFM in a paediatric sample in Stebbins et al., (2006), within-subject variability was less in the current study by approximately 2°. This could be the result of the use of different gait cycle parameters to measure SD. Stebbins et al., (2006) measured one peak angle in each plane whereas the current study measured four peaks and two event angles. Furthermore, Stebbins et al., (2006) collected data from each subject over three sessions spaced between 2 weeks and 6 months apart. This longer interval between test re-test sessions could have led to growth or weight gain leading to greater within-subject variation compared to the current study.

Within-session variability of Kinfoot was comparable with the previous use in a population of adolescents (MacWilliams et al., 2003). Mean within-session SD were 7.50° in the current study compared to 7.41° in MacWilliams et al., (2003). However, between-session reliability of Kinfoot in a test re-test protocol has not previously been measured. Therefore, the results of the current study will, for the first time reveal between-session reliability of Kinfoot in a paediatric population. Between-session SD gives a measure of the variability in repeated tests and a measure of the ability of the foot model protocol to provide consistent angular outputs. The 3DFoot and Kinfoot models presented similar between-session SD indicating that marker placement is consistent across these two models. The OFM presented higher between-session variability indicating more error in repeated marker placement. A comparison of 3DFoot with previous between-session use in adults demonstrates that the findings of the current study are comparable. Caravaggi et al., (2010) found mean SD of the shank-calcaneus, calcaneus-midfoot and midfoot-metatarsal to be 3.92°, 4.20° and 3.33° respectively. Variability of the same 3DFoot joints in the current study were 3.67°, 4.42° and 3.05° respectively. Comparing within-subject, within-session and between-session SD of the current study with previous findings justifies the implementation of the foot models within the concurrent protocol established for this chapter. This allows the reliability of each foot model to be compared in the current study and with previous reliability studies.

7.5.2.2 Between-Session Reliability of OFM

The hindfoot, forefoot and hallux segments demonstrated moderate between-session reliability of repeated joint angles during paediatric gait. Between-session reliability was highest in the transverse plane (ICC 0.65) and similar in the sagittal and frontal planes (ICC of 0.50 and 0.51 respectively). This however, was not an indication that the transverse plane demonstrates better agreement than the other two planes but that within-session variation was higher. Bland & Altman (1990) stated that ICCs are dependent on the range of measurement, with higher within-session standard deviation (SD) resulting in a larger ICCs. The within-session range of the OFM was greatest in the transverse, particularly at the hindfoot where the within-session range of joint angles was 76.68^{o} at initial contact. This large amount of within-session variation is due to the misplacement of the thigh segment and the lateral shank marker to define the shank segment orientation. For comparison, sagittal and frontal plane within-session range were 26.25^{o} and 13.70^{o} respectively. For this reason, SEM was utilised to calculate the expected error of repeated sessions because the equation for SEM includes within-sessions (pooled) SD. The pooled SD of OFMs hindfoot segment in the transverse plane at initial contact was 19.40^{o} which resulted in a SEM of 7.93^{o}. The pooled SD of the sagittal and frontal hindfoot segment at initial contact was 6.79^{o} and 3.52^{o}. This resulted in sagittal and frontal plane SEM values that were more than half that for frontal plane (SEM = 3.31^{o} and 2.86^{o} for sagittal and frontal plane respectively). It has been recommended that ICC values alone should not be used to assess the reliability of gait parameters (McGinley et al., 2009).

The within-subject SD of OFM's maximal hindfoot motion in Stebbins et al., (2006) was highest in the transverse plane (8.4^{o}) compared to the frontal (5.2^{o}) and sagittal plane (3.0^{o}). This order was also found in the current study; transverse plane (8.8^{o}), frontal (2.9^{o}) and sagittal (1.9^{o}). Another previous study to examine the within-rater reliability of the OFM have reported lowest error values in the sagittal plane followed by the frontal and transverse planes (Curtis et al., 2009). Curtis et al., (2009) recorded Typical Error of the Measurement (TEM) of the OFM at specific gait cycle events (heel, ankle and toe rockers). The authors found hindfoot error values of 0.93^{o}-2.47^{o} in the sagittal plane, 2.22^{o}-2.64^{o} in the frontal plane and 2.65^{o}-3.45^{o} in the transverse plane. The same values in the current study at specific gait events (ipsilateral initial contact and ipsilateral toe-off) resulted in errors of 2.92^{o} - 5.00^{o} in the sagittal plane, 2.18^{o}-3.18^{o} in the frontal plane and 8.81^{o}- 9.77^{o} in the transverse plane. Greater error values in the current may arise from the use of SEM rather than TEM as SEM

gives SD relative to the ICC values and TEM gives SD relative to the between sessions difference. Curtis et al., (2009) describes the poor reliability of the hindfoot in the frontal and transverse planes on difficulty defining and identifying neutral position of the hindfoot. Wright et al., (2011) reported ICCs and SEM of the OFM at initial contact and toe-off in adult participants. Their results showed that the OFM demonstrated lower between-session reliability and greater error in the frontal compared to the sagittal and transverse planes. Wright et al., (2011) reported SEM values of 1.37°-1.61° in the sagittal plane, 5.09°-5.69° in the frontal plane and 1.86°-2.53° in the transverse plane. The authors suggest that greater frontal plane errors are the results of marker placement error. This finding is likely due to the switching of frontal and transverse planes when extracting angular data in Vicon.

7.5.2.3 OFM Joint Angle Differences and Between-Session Reliability Following Thigh Marker Rotation Offset

Following rotational correction of the thigh marker OFM's hindfoot segment appeared significantly more flexed and significantly less internally rotated. The excessive flexion of the hindfoot is caused by the posterior displacement of the knee joint centre, placing the hindfoot in a flexed position. The forefoot segment then becomes plantarflexed to a similar degree to which the hindfoot was dorsiflexed. Using the thigh marker rotation offset resulted in hindfoot and forefoot motion that was less consistent with previous studies to use the OFM. A comparison of the hindfoot and forefoot sagittal waveforms of the current study with the corresponding waveforms presented in Stebbins et al., (2006) shows a considerable offset caused by the posterior displacement of the knee joint centre. This finding indicates that the use of the thigh marker offset resulted in inappropriate angular offsets of OFM. An approach to solve this would be to calculate the necessary shank marker rotation offset (tibial torsion) to realign the shank with the thigh.

Overall between-session reliability of the OFM following thigh marker rotation offset was not greatly affected, ICC were increased from 0.55 to 0.56 and SEM reduced from 4.61° to 4.57°. However, transverse plane hindfoot between-session reliability improved and SEM decreased by approximately 2° due to the correction of lower limb segments transverse rotation offsets. This finding was due to the reduced variation in knee joint centre position and thigh rotation from correction following thigh marker rotation offset. However, lateral shank marker misplacement is still an issue and causes an offset between the orientation of the shank and

hindfoot. Marker placement on the shank may require protocols to obtain longitudinal alignment potentially with the use of knee alignment device.

In summary, the OFM demonstrated moderate between-session reliability (ICC) and reasonable errors (SEM) from repeated sessions. The transverse plane hindfoot motion produced the greater error from repeated sessions which was due to the high variability of joint motion which is due to inconsistent marker placement. The position of the knee joint centre is sensitive to thigh marker placement and may have lead to deviations in the shank orientation between sessions. Furthermore, the lateral shank marker, like the thigh marker defines the longitudinal axis of the shank, therefore small misplacements will lead to rotational offsets and cross-talk at the hindfoot. Between-session reliability of the OFM was lower than previous paediatric studies (Stebbins et al., 2006; Curtis et al., 2009) caused by marker placement error meaning that the protocols of the current study require attention. Following thigh marker rotation offset, between-session reliability (ICC) and repeated session error (SEM) from OFM were not greatly affected. Therefore, interpreting the findings of frontal plane hindfoot motion between populations would be difficult because measurement error may mask any differences.

7.5.2.4 Between-Session Reliability of 3DFoot

The hindfoot, midfoot, forefoot and hallux segments of the 3DFoot model demonstrated moderate between-session reliability (ICC = 0.47) of repeated joint angles during paediatric gait. In general, between-session reliability was highest in the sagittal plane (ICC = 0.51), followed by the same values in the frontal (ICC = 0.45) and transverse (ICC = 0.45) planes. This planar order of reliability was in agreement with Deschamps et al., (2011) who measured the reliability of 3DFoot absolute joint angles in adult subjects. This study found highest coefficient of multiple correlation (CMCs) in the sagittal plane (0.62-0.89), compared to the frontal plane (0.18-0.81) and the transverse plane (0.53-0.84). In the current study, reliability of the hallux projection angles in the sagittal and transverse planes (mean ICC 0.31) were considerably lower than the 3D hindfoot (mean ICC 0.49), midfoot (mean ICC 0.51) and forefoot segments (mean ICC 0.50). This is in line with Deschamps et al., (2011) who found lower reliability (measured by CMC) of the hallux sagittal and transverse plane projection angles compared to the 3D hindfoot, midfoot and forefoot segments. Error in repeated session joint angles was similar between the hindfoot (mean SEM 3.39^{o}), midfoot (mean SEM

2.94°) and forefoot (mean SEM 2.74°), but hallux errors were higher and deemed unacceptable (mean SEM 7.72°). This finding was due to issues with marker placement on the proximal phalanx of the hallux which, in children's feet, is close to the first metatarsal head marker. These markers in close proximity lead to marker trajectory cross-over and drop out which may have lead to higher variability. No previous study to examine the reliability of 3DFoot measured the expected error (standard error of measurement) from between-session measures.

7.5.2.5 3DFoot Joint Angle Differences and Between-Session Reliability Following Normalisation to Standing

All segments of 3DFoot model demonstrated a significant change in angular outputs following normalisation to standing at initial contact and toe off except the midfoot-metatarsal joint. This finding is due to the results of pilot studies conducted on the 3DFoot to practise marker placement protocols. In pilot studies it was found that the calcaneal-midfoot and midfoot-metatarsal joints exhibited excessive dorsiflexion and plantarflexion respectively. This was due to x-axis mislocation from a superior positioning of the calcaneal marker with respect to the sustentaculum tali and lateral calcaneus markers. Efforts were made to correct for this misplacement and consistently align the calcaneal marker with the anterior-posterior axis of the calcaneus. A visual inspection of the angular plots showed that the overall pattern of motion was not altered due to normalising, but that absolute values were. Range of motion values were similar before (mean ROM 12.71 ± 10.00°) and after (12.07 ± 10.07°) normalising to standing.

Normalising joint angles to standing position decreased mean ICCs from 0.52 to 0.43 but SEMs were reduced from 3.88° to 3.29°. Error values were improved most in the sagittal plane indicating that marker placement errors are highest in this plane. The reduction in ICC is due to the large reduction in the within-session range of joint angles caused by normalisation to standing. The mean reduction in joint angles at gait events was 8.01° ± 5.84°. The largest ICC reductions were found in sagittal plane calcaneal-shank, transverse calcaneal-midfoot and frontal midfoot-metatarsal motion. Normalisation to standing reduced variability due to marker placement errors, but within-session SD reduced by relatively greater amounts than within-subject SD. The reduction in within-session variation by the normalisation procedure does not justify the improvements in between-session reliability. This is because removing the

absolute angular peak maximum and minimum values may increase the chances of a type II error (false negative). Any possible associations between foot segment motion and adiposity may not show up as significant if within-session variability was reduced.

The results of the reliability study on 3DFoot show that the model is moderately reliable between-sessions in this study population with reasonable errors from repeated sessions. Between-session reliability and errors were consistent across the hindfoot, midfoot and forefoot segments. However, the hallux demonstrated considerably lower between-session reliability and greater error. Hindfoot, midfoot and forefoot segments could provide reliable information on paediatric foot motion over the gait cycle. Hallux variability would make interpretation of population differences difficult.

7.5.2.6 Between-Session Reliability of Kinfoot

The hindfoot, midfoot, forefoot, toe and hallux of the Kinfoot model demonstrated moderate between-session reliability (ICC = 0.46) of repeated joint angles during paediatric gait. The sagittal plane demonstrated the least between-session reliability (ICC = 0.40) and the frontal and transverse planes being higher (both ICC = 0.48). The previous study to examine the reliability (CMC values) of Kinfoot reported only sagittal plane within-session, from a single session (MacWilliams et al., 2003). A comparison of reliability across segments between MacWilliams et al., (2003) and the current study reveals that the segments distal of the midfoot revealed moderate to high reliability in both studies, but low reliability at the calcaneocuboid and subtalar joints. This finding is due to the use of virtual markers created by offsets from adjacent segments to infer motion of small and difficult to track bones (talus and cuboid). Low between-session reliability is caused by motion between the talus and cuboid and the adjacent segments which represent them (metatarsals) which increases between-session variability. Further comparison of reliability between the current study and MacWilliams et al., (2003) should, however be made with caution because of the differences in study design, statistics and populations tested. MacWilliams et al., (2003) tested reliability of Kinfoot in adolescents, during one session using coefficient of multiple correlation statistic compared to the children tested over two repeated sessions by intraclass correlation coefficient in the present study. The reliability results of one study cannot be assumed to be consistent in an alternative study design using different statistical measures of reliability and in a younger population. This highlights the need to examine the between-session reliability of all

three foot models in this chapter because determining the most appropriate foot model for use in the main study (chapter 8) from previous literature alone may lead to misinterpretation of relative reliability.

The Kinfoot provided great insights into foot segmental motion at eight joints during the gait cycle. However, between-session reliability (ICCs) was low and errors from repeated sessions (SEM) high across most segments and especially at the subtalar, calcaneocuboid and hallux segments. While the potential of this model to extract large amounts of data on paediatric foot motion is preferable, low between-session reliability and high errors mean finding differences (if they truly exist) between populations may not be possible due to high variability.

7.5.2.7 Comparison of Foot Model Between-Session Reliability Summary

The aim of this chapter was to determine the between-session reliability of three available foot models to describe foot motion over the gait cycle. The results can inform the decision as to the most appropriate foot model to determine relationships between foot segmental motion and adiposity. All three foot models provide pros and cons for use. Between-session reliability of the OFM has been previously tested in a paediatric population (Stebbins et al., 2006) and it has been used extensively in clinical paediatric studies (Theologis & Stebbins, 2010) thus demonstrating utility in the population of interest to the current study. However, between-session reliability of the OFM during the protocols implemented in this chapter demonstrated that hindfoot transverse plane motion is sensitive to marker placement errors to define the shank segment. This lack of reliability and the large error values can only be described in terms of this study under the current testing conditions. The findings are no reflection of the foot model itself but of the reliability of the user to implement it in the protocols. The 3DFoot model does not suffer from variability in shank orientation and, therefore between-session reliability and errors were smaller than OFM. The addition of a midfoot segment may provide insights into associations between flat feet and obesity (Leardini et al., 2007a). However, 3DFoot's hallux segment demonstrated particularly low between-session reliability and high errors which have been found previously in reliability studies in adults. Kinfoot offers an abundance of information on inter-segmental foot joint motion and has been previously validated against radiographic measures (MacWilliams et al., 2003). The reasonable errors at the medial and lateral forefoot segments demonstrate the potential to

divide the forefoot into the two sections as recommended by Nester et al., (2010). However, the majority of segments demonstrated errors from repeated sessions greater than 5^{o}, which were deemed unacceptable in the current study. High variability from assumptions of coupled motion between adjacent segments (subtalar and midfoot joints) and high variability from marker misplacement on the hallux and toes are the causes of unacceptable error. Therefore, the findings of this section indicate that 3DFoot offers the best balance between information of foot segmental motion (particularly at the midfoot) and between-session reliability. The error values determined at gait cycle events and minimal and maximal peaks during the stance and swing phase can be used as a baseline to aid interpretation of differences between populations.

7.6 Chapter Summary

Between-session reliability of each model was moderate at the hindfoot, low in the midfoot (3DFoot and Kinfoot only), moderate in the forefoot, low in the hallux and moderate in the toe segments (Kinfoot only). Measurement errors were greatest in OFM and lowest in 3DFoot where all SEM values, except for the hallux, were under 5^{o}. The choice of foot models for use in a paediatric population was based on the reliable capture of the maximum amount of information that can be gained from the segmentisation of the foot. Kinfoot presents information on eight joints of the foot and would provide detailed angular displacements of for exploring the association between adiposity and foot motion during the gait. However, lower between-session reliability and greater measurement error of Kinfoot means associations may be missed. Issues defining the shank segment orientation in the current protocol lead to low between-session reliability and high errors in the hindfoot segment of the OFM. Therefore, 3DFoot will be used in the main study (chapter 8), the model benefits from the tracking of a midfoot segment which will provide information on potential altered foot structure expected in obese children (i.e. pronatory foot type associated with flat feet). The 3DFoot model will not be normalised to a standing position for zeroing of joint angles because vital information about maximal angular displacements is lost. The SEM values reported in this experimental chapter will be used to assess the relevance of significant findings of the main study (chapter 8).

7.7 Limitations

A limitation of the protocol to examine the between-session reliability of three foot models during concurrent application was the compromise of marker placement on the forefoot segment. The 3DFoot model required a marker on the second metatarsal head, the OFM required a marker between the second and third metatarsal head and Kinfoot required a marker on the third metatarsal head. These locations were in too close proximity for three separate 9mm markers to be attached to the skin. Therefore, the centre location, in-line with OFM, was chosen as a compromise. This may have induced errors in the orientation of 3DFoot and Kinfoot's forefoot segments due to differences between the technical and anatomical local coordinate systems. However, the compromised marker position did not appear to generate greater errors in the forefoot errors compared to other foot segments. Indeed, the amount of error in 3Dfoot and Kinfoot's forefoot segments was consistent with previous findings. It is possible that the compromised marker position was within the variability of marker placement found in the current study. Della Croce (1999) found within-rater RMS differences of 9.0mm when identifying the second metatarsal head which is the width of a marker used in the current study. Future work should consider examining the between-session reliability of these foot models in isolation.

8. Main study: Biomechanics of the Paediatric Foot and Lower Limb: Associations with Adiposity.

8.1 Introduction

This chapter presents a cross-sectional study of the associations between lower limb and foot biomechanics and adiposity in boys age 7 to 11 years old. Previous studies have found altered spatiotemporal, kinematic and kinetic gait parameters between obese and non-obese children (Hills & Parker 1991; Morrison et al., 2008; McMillan et al., 2009 & 2010; Shultz et al., 2009). However, few studies have accounted for age, anthropometric and spatiotemporal confounding factors relating to gait parameters.

Measures of body fat mass outlined in experimental chapter 1 (chapter 5) will be utilised to measure adiposity in this study sample. Previous studies have reported childhood obesity according to BMI values relative to national reference curves (Z-Score) with cutoffs for obesity and overweight. There are two issues with defining groups in this way; firstly, BMI is not a direct measure of obesity but a proxy for body fat mass, and secondly, cutoffs for defining obesity and overweight in children have not been related to health co-morbidities. Therefore, children could be mislabelled as obese when they are not and vice versa, increasing type II errors (false negative) and so there is potential to neglect associations with obesity (measured by BMI Z-Score). Defining participants in terms of adiposity measured as a continuous variable may remove these issues.

In order to measure lower limb and foot biomechanics a reliable method of determining human motion is required. In experimental chapter 2 (chapter 6), between-session reliability and expected error of lower limb joint angular and moment outputs was reported in a group of children across a range of BMI Z-Scores. The findings indicated that mean errors (SEM) across 3D lower limb joint angles was 3.98^{o} and moments 2.32Nm. However, angular output errors were improved following thigh marker rotation offset (3.56^{o}) while moment errors were remained approximately equal (2.38Nm). A further amendment to the lower limb biomechanical model (PiG) was the use of an 'instrumented pointer device' to track the anterior pelvis (ASIS) using virtual rather than skin mounted markers. Pelvis anterior markers (ASIS) and hip joint centres were significantly misplaced using skin mounted markers compared to virtual markers by up to 16mm. Hip flexion, abduction and internal rotation were significantly greater (by up to 3.00^{o}, 4.32^{o} and 5.84^{o} in non-obese, respectively) when using virtual markers, indicating the effects of soft tissue artefact when measuring hip joint motion.

To the author's knowledge, no previous study has reported associations between dynamic three-dimensional foot motion during the gait cycle and obesity or adiposity. Previous findings in static foot posture and 2D dynamic plantar assessments have revealed changes at the hindfoot, midfoot and forefoot were indicative of a flatter foot in obese children. Therefore, a biomechanical foot model that can provide reliable data on foot segmental motion was explored in experimental chapter 3 (chapter 7). The 3DFoot model (Leardini et al., 2007a) presented mean errors in repeated sessions of 3.88^{o} in four segments of the foot. Therefore, 3DFoot was determined to be most appropriate to measure foot segmental motion associations with adiposity.

8.2 Aims

The aims of this study were to:

1. Identify relationships between spatiotemporal, kinematic and kinetic lower limb and foot biomechanics with adiposity (body fat mass) in a cross-sectional sample of boys age 7 to 11 years old.
2. A secondary aim was to account for confounding variables of age, anthropometrics and spatiotemporal characteristics of the participants.

To answer aim 1 spatiotemporal, kinematic and kinetic lower limb and foot variables taken at discrete points of the gait cycle were recorded for each participant. The relationships between these variables and body fat were tested using linear regression analysis. Multiple linear regression was used to account for the confounding influence of participant's age, anthropometric and spatiotemporal characteristics on the relationships with body fat to answer aim 2.

8.3 Methodology

8.3.1 Participants

The study was designed to select a representative population of children residing in the borough of Newham, East London. Teachers were approached based on a convenience sample of schools taking part in higher education activities at the University of East London. Two schools agreed to participate in the study of which approximately 90 boys were invited to participate in the research. Consent forms and information documents were distributed for boy's parents/guardians, only boys with completed consent forms being allowed to take part. Ethical approval was obtained from the University of East London (Ref No. ETH/13/11). A sample size of 66 boys was required for sufficient statistical power based on the results of the reliability studies in experimental chapters 2 and 3 (chapters 6 and 7; the sample size calculation is in appendix VI). A total of 55 boys took part in all protocols from which data sets were extracted and analysed.

The sample population from this study was drawn from a convenience sample of boys from local school pupils in Newham. The latest figure for the rates of overweight and obesity in Newham show that overweight prevalence is between 11.2% and 15.1% and obesity between 12.9% and 24.7% among boys age 5 to 11 years old (National Child Measurement Programme 2012). The prevalence of overweight in the current study was lower than the borough of Newham (9.1%) and obesity levels were higher (30.9%). There may have been bias in sampling more obese participants to represent the full range of body fat mass levels thus over sampling obese boys compared to the local prevalence rate. Bias may have also been introduced in the recruitment of boys from the convenience sample. Boys most likely to engage in activity and accept exposing their upper body and legs during testing protocols would potentially be more willing to take part in the research. This may under-sample boys with higher body fat mass compared to local area (Newham, UK).

8.3.2 Inclusion and Exclusion Criteria

Consenting participants were included in the research if they were typically developing boys between the age of 7 and 11 years old. Exclusion criteria included any medical conditions affecting neuromuscular and orthopaedic integrity or any complications contributing to altered foot posture and/or gait disturbance. A copy of the health medial questionnaire can be found in appendix II.

8.3.3 Protocols

8.3.3.1 Demographical Information

Information on the age and ethnicity of the boys was provided by the primary schools according to their records. All data was anonymised for confidentiality. Ethnicity was provided to ensure the sample was representative of the local population in the London borough of Newham.

A recent school census found the ethnical groups of Newham's school age children to be 42.2% 'Asian', 23.9% 'black', 15.7% 'white' and 4.7% 'other' (Pupil Level Annual School Census, 2009). The ethnical groups in the current study were 34.5% 'white', 32.7% 'Asian', 29.1% 'black' and 3.6% 'other'. In the current study sample 'white' and 'black' participants were over sampled, and 'Asian' under sampled, compared to the local demographic data. This bias may have been the result of convenience sampling of local primary schools

8.3.3.2 Body Composition

Protocols for body composition were developed and established in experimental chapter 1 (chapter 5). This section provides an overview of the protocols used in this study, more details can be found in experimental chapter 1 (chapter 5). Subjects were measured barefoot in swimming shorts. Weight was measured to the nearest 0.1 kg using Bodpod scales (Life Measurement, Inc, Concord, CA, USA). Height was measured barefoot to the nearest 0.5cm using a portable Leicester stadiometer (Seca Leicester portable stadiometer; Seca Vogel, Hamburg, Germany). All measures were taken by one researcher, following strict protocols based on manufactures recommendations. Each child's BMI score was calculated as height/weight^2 and expressed as an age and sex specific z-score (standard deviation score). This was based on the distribution of BMI in the UK90 growth reference (Cole et al., 1995) using a Microsoft Excel macro developed for use with this growth reference (Child Growth Foundation, Chiswick, UK).

Air displacement plethysmography was measured using the Bodpod device with protocols determined in experimental chapter 1 (chapter 5). Each participant wore swimming shorts and a swimming cap, jewellery was removed prior to entering the Bodpod. The procedure involved each child entering the Bodpod's chamber for a period of 40 seconds for three successive trials. In each trial small amounts of air (350ml) were forced in and out of the

chamber creating pressures changes that were measured in the Bodpod prior to the child entering the device. These pressure changes were then repeated with the child in the Bodpod chamber from which changes in the pressure signal amplitudes were compared and the volume of the child calculated (Dempster & Aitkens, 1995). These raw body volumes were corrected from isothermal air in the lungs and close to the skin surface using child specific equations (Haycock et al., 1978; Fields et al., 2004). The corrected body volumes were converted to body percentages using age and gender specific equations (Lohman, 1989).

8.3.3.3 Three-Dimensional Gait Analysis

Protocols for three-dimensional gait analysis were established and developed in experimental chapter 2 and 3 (chapters 6 and 7). This section provides an overview of the protocols used in the current study, for more detail please refer to experimental chapter 2 and 3 (chapter 6 and 7). An eight-camera Vicon Nexus (Vicon Motion Systems Ltd, Oxford, UK) captured the motion of reflective markers attached to each subject's lower limbs at 200Hz. Two floor mounted force plates (Bertec, Model MIE Ltd, Leeds, UK) recorded ground reaction forces during gait trials at 1000Hz. Both the cameras and force plates were calibrated before each testing session according the Vicon manual (Vicon Manual, 2010). In addition to height and weight recorded as part of the body composition protocol; leg length, ankle width and knee width were measured using callipers.

The lower limb model was applied with the marker set described in the Plug-In Gait (PiG) manual based on the Helen Hayes marker set first described by Davis et al., (1991). Each child was asked to adopt a comfortable standing position while 9mm markers were attached using double sided tape. Two alterations to the standard PiG protocol were used. Firstly, an 'instrumented pointer device' was used to create virtual markers representing the ASIS landmarks, the location of the ASIS markers was tracked using markers attached to each iliac crest; and secondly, a thigh marker rotation offset was applied to each trial based on the protocol of Baker et al., (1999).

The 3DFoot model was attached to the right foot of each participant following the attachment of the PiG lower limb marker set. The PiG and 3DFoot share the same anatomical landmarks; the second metatarsal head, the posterior calcaneus (same height as the second metatarsal head marker) and lateral malleolus markers.

Each child performed 20 to 30 gait trials through the 7.5m walkway in the gait laboratory with the aim of achieving 10 gait for analysis. Gait trials were accepted for further analysis if the force plate was contacted cleanly, no markers were unattached and the participant walked consistently through the trial (i.e. didn't increase or decrease walking speed, aim for the force plates or adopt an alternative walking style).

The selected trials were cropped to contain, on average, two gait cycles within the capture volume giving 20 trials from each participant for further processing. Marker trajectories were reconstructed and labelled according to the procedures outlined in experimental chapter 2 and 3 (chapters 6 and 7). During post-capture processing some trials were unable to be used for analysis due to excessive marker drop out. This was especially relevant for 3DFoot model markers which were also found to cross-over. In this case the trial was rejected and where possible another trial selected. For kinetic analysis, only the gait cycles where contact was made with one of the force plates were selected. The total number of gait cycles collected was 967 (approximately 18 per participant) for lower limb joint angles, 386 for lower limb joint moments (approximately 7 per participant) and 821 for foot angles (approximately 15 per participant).

8.3.4 Data Analysis

8.3.4.1 Selection of Predictor Variables

Each participant's estimate of body fat mass was entered as the primary predictor variable for all lower limb and foot joint angular motion and moments. The confounding predictor variables; age, anthropometric and spatiotemporal gait variables were included in the analysis in order to account for the variation in lower limb and foot biomechanics. These included; age, height, BMI Z-Score, step length, walking speed, step width, stance phase duration and total support time. The reasons for including these predictor variables was their influence on paediatric gait previously reported:

Age and height were included as predictor variables because changes in lower limb kinetics have been reported up to the age of 9 years old due to the development of gait maturation (Chester et al., 2006). Furthermore, it is not clear at which age gait is fully matured because the age at which gait matures is dependent on the gait measure, though most gait parameters reach adult-like figures by the age of 7 years old (Sutherland et al., 1980; Stansfield et al., 2001; Ganley & Powers 2005). However, Beck et al., (1981) concluded that changes after the

age of 5 years were more attributable to height than age. Therefore, to account for variation in lower limb biomechanics due to age and height, these were included as predictor variables in the analysis.

Ideally body weight would be included as a predictor variable to account for the variation in lower limb biomechanics due to body weight (and height) having a large effect on absolute lower kinetics (Hof et al,. 1996). However, as shown in Table A7.1 body weight cannot be placed in the regression models due to collinearity with the other predictor variables, mainly %FM (this is explained further in *Collinearity and confounding variables* section under *statistical analysis*). However, BMI Z-Score does not cause excessive collinearity between the predictor variables and so can be included in regression analysis as a measure of body weight (relative to height). Furthermore, previous studies have grouped obese and non-obese children according to BMI Z-Score (McMillan et al., 2009 & 2010; Shultz et al., 2009 & 2010). These studies have reported kinematic and kinetic lower limb differences due to excessive forces from the carriage of a greater mass. Therefore, BMI Z-Score is included as a predictor variable in order to distinguish findings that related to adiposity (%FM) and the findings that were related to body weight-for-height (BMI Z-Score). Disparity between adiposity and obesity with lower limb and foot biomechanical findings could indicate that; either, fat mass and weight-for-height affect gait biomechanics in different ways (i.e. distribution of body fat mass and relative limb and trunk sizes); BMI Z-Score is not a suitable measure for obesity in this sample of boys (because actual relationships between obesity and biomechanics are lost due to mislabelling of boys); or finally, methodological differences (i.e. relating to greater soft tissue artefact in boys with higher fat mass compared to boys with higher BMI Z-Score).

Gait spatiotemporal differences have been reported between obese and non-obese children (measured by BMI Z-Scores), these include; a slower walking speed, lower cadence and a greater stance phase (Hills & Parker, 1991; Morrison et al., 2008). These studies have related the findings to the need for greater stability in obese children's gait. This means there is a requirement to account for variation in lower limb and foot biomechanics that may be due to altered spatiotemporal parameters due to a need for greater stability in obese participants. Therefore, step length, walking speed, cadence, step width, stance phase duration and total support time were included as predictor variables. These predictor variables were entered into regression analysis in order to determine the relationships between foot and lower limb angles and moments with adiposity and the influence of confounding factors.

8.3.4.2 Selection of Gait Variables for Extraction

In order to assess the association between the predictor variables with lower limb and foot biomechanics, joint angle and moment data needed to be extracted over the gait cycle. A review of the gait cycle parameters of significance in previous obesity studies informed the choice of gait cycle events and peaks to be explored in this study. Previous studies on the effects of obesity on gait parameters in children and adults have shown altered joint angles and moments throughout the gait cycle. Table 8.1 presents the significant findings from previous obesity studies on biomechanical differences at events and peaks. Studies have typically found differences at ipsilateral initial contact, contralateral toe off, contralateral initial contact and ipsilateral toe off as well as peaks in sub-phases of the stance phase and swing phase.

Table 8.1 A review of previous literature on significant differences between obese and non-obese lower limb angle and moment measures at gait cycle events and phases

Study	Gait cycle			
	Initial contact	Stance	Toe off	Swing
Gushue et al., (2005) Paediatric		Peak ankle flexion moment Peak knee flexion angle Peak knee abduction moment		
McMillan et al., (2009) Paediatric		Peak knee abduction angle Peak hip abduction moment		
McMillan et al., (2010) Paediatric	Knee flexion angle Hip extension angle Hip extension moment	Peak Hindfoot inversion moment Peak ankle extension moment Peak knee flexion moment Peak knee abduction moment Peak hip flexion moment Peak hip abduction moment		
Spyropoulos et al., (1991) Adult		Ankle flexion angle[a] Hip abduction angle [a]	Hip abduction angle	
Lai et al., (2008) Adult		Ankle eversion angle [a] Ankle extension moment Ankle inversion moment Knee adduction angle Hip adduction [a]		Knee adduction
Meissier et al., (1994)	Hindfoot eversion angle			

[a] signifies significant findings at peaks and events throughout the stance phase.

With regard to differences in foot motion over the gait cycle between obese and non-obese subjects, no study has examined the dynamic 3D angular rotations of foot segments. Previous studies have examined dynamic plantar pressure assessment, static and dynamic footprint indices and static structural and morphological differences. Areas of the foot to demonstrate altered position and motion between obese and non-obese children were; the medial longitudinal arch (Riddiford-Harland et al., 2000; Villarroya et al., 2007), calcaneal inclination angle/heel valgus (Pfeiffer et al., 2006; Villarroya et al., 2009), navicular height (Morrison et al., 2007) and the hallux (Mickle et al., 2006). These structural alterations of the foot in obese children can be related to the segments described in the 3DFoot model (Leardini et al., 2007a); the calcaneus, midfoot, metatarsals and hallux. Therefore, the exploration of areas of the foot that have shown to be significantly different between obese and non-obese subjects will be examined at all events and angular peaks during the gait cycle.

Lower limb and foot joint angles and moments were extracted at ipsilateral initial contact, contralateral toe off, contralateral initial contact and ipsilateral toe off for every gait cycle of each participant. Table 8.2 defines the selected peak gait cycle parameters at which lower limb and foot angular displacements and moments were extracted from each participant. Any peaks that coincide with gait events were excluded. The timing of gait events was not significantly associated across the level of adiposity ($p>0.05$). Therefore, kinematic and kinetic differences at events were due to changes in joint angle and moments and not due to the differences in the timing of events. The angular and moment events and peaks were used in principle component analysis (PCA) in the first step of statistical analysis.

8.3.4.3 Gait Variables Extraction Protocol

Perry (1992) described the phases of the gait cycle according to reciprocal foot contact with the ground. Foot contact is measured by the increase in vertical force (Fz) above the threshold of 20N in two forces embedded in the gait laboratory floor. This gives the gait events which can distinguish the phases of the gait cycle according to the first double support phase (ipsilateral initial contact to contralateral toe off), the first single support phase (contralateral toe-off to contralateral initial contact), the second double support phase (contralateral initial contact to ipsilateral toe-off) and the second single support phase (ipsilateral toe-off to ipsilateral initial contact). Values at gait cycle events and peaks during the phases were extracted for analysis. Two factors contribute to the angular and moment values extracted;

the first is temporal normalisation of the gait cycle, and the second is averaging multiple values within and between participants.

In order to compare gait, the common practise in gait analysis is to normalise the gait cycle in the time domain to 100 data points, temporally aligning multiple gait cycles (Morris & Hsiao-Wecksler, 2010). This aids comparison between subjects and interpretation of healthy and pathological gait (Sadeghi et al., 2000), but differences in the timing of gait events within the cycle (contralateral toe-off, contralateral initial contact and ipsilateral toe-off) may still exist. Therefore, differences in joint angle and moment peaks and values at events may be reduced and larger standard deviations will result from between- and within-cycle variability in timing (Forner-Cordero et al., 2006). To eliminate this the current study did not normalise individual gait cycles to 100 data points but instead extracted lower limb and foot angle and moment values at absolute gait events and peaks.

Previous studies to examine the differences in lower limb biomechanics between obese and non-obese children have compared averaged data from two groups (McMillan et al., 2009 & 2010; Shultz et al., 2009 & 2010). Because of the variable nature of gait, extracting the average of gait variables at events and peaks may not completely inform of the differences between groups. Therefore, when averaging trials of several participants, techniques are available to reduce between-subject variability include curve registration, image normalisation or time warping techniques (Sadeghi et al., 2000). These temporally align different gait trials to reduce between-subject variability so biomechanical differences can be explored. However, an alternative method, used in the current study, utilised individual trials from all subjects in the analysis thus removing the need to average individual or group gait cycles. Sutherland et al., (1980) noted that representative gait cycles in a child demonstrated minor variations in the amount of angular rotation from other cycles. Since joint angular displacements (and moments) are interdependent, both, across the gait cycle and between gait cycles averaging gait cycles for each participant would reduce discreet differences. Therefore, including all trials in the statistical analysis maintains angular and moment variability without the need to normalise the gait cycle in the time domain because individual or group means are not being extracted.

In order to highlight the differences between temporally non-normalised and normalised gait data the motion of 10 participant's hip joint angles was extracted and compared. Table A5.1 demonstrates the differences between hip joint angular data that has not been normalised (captured at 200Hz) with data normalised to 100Hz and 50Hz. Both the timing of gait events

and the values at events and peaks were significantly different depending on the amount of normalisation.

Previous studies have used PCA to determine the points of the gait cycle which demonstrate greatest variance across the subject population being testing (Chester et al., 2008). To undertake this form of statistical analysis the gait parameter was normalised to a number of data points over the gait cycle. To perform PCA the total number of data points is required to be at least one less than the number of subjects (Field, 2009). For a sample of 55 participants, 54 data points (or 50 for convenience) would be selected for PCA analysis. However, the process of reducing each gait variable to a data point can result in lost data. Normalising the gait variable to 100 data points would remove approximately 100 data points if the gait data is captured at 200Hz and the subject walks at 1 stride per second. A further 50 data points are removed to meet the requirements of at least one less data points than subjects. The whole normalising process removes 75% (three out of every four capture frames) of the gait parameter data available. Using PCA on waveform data over the gait cycle in this way removes the need to pre-define the gait cycle points based on prior assumptions. However, important peaks and potential differences between subjects maybe lost as the waveform were in-effect filtered.

Instead of analysing normalised peaks in PCA, the protocol of this study extracted peak data from every frame of each gait cycle captured at 200Hz. Angular and moment peaks and values at events were extracted using ParamCalc (Vaquita Software, UK). Peak and event values were identified to describe the amplitude of each joint angle over the gait cycle (Chao et al., 1983). The key angular peaks presented by Bendetti et al., (1998) were derived in addition to peaks occurring in the gait cycle sub-phases (Table 8.2). These values were used to determine the foot and lower limb angle and moment parameters which were be entered into regression analysis

Table 8.2. Lower limb and foot angle and moment peaks over the gait cycle where values were extracted. Flex = flexion, Ext = extension, Abd = abduction, Add = adduction, Ev = eversion, In = inversion, Int Rot = internal rotation, Ext Rot = external rotation. S-C=Shank-Calcaneus, C-M=Calcaneus-Midfoot, M-M=Midfoot-Metatarsal, F-P=First Metatarsal-Phalanx

	Peak in DS 1			Peak in SS 1			Peak DS 2			Peak in SS 2		
	Sag	Fro	Tra	Sag	Fro	Tra	Sag	Fro	Tra	Sag	Fro	Tra
Angles												
Hip					Add	Int Rot					Add	Int Rot
										Ext	Abd	Ext Rot
Knee				Flex	Add	Int Rot				Flex	Add	Int Rot
				Ext	Abd	Ext Rot				Ext	Abd	Ext Rot
Ankle				Flex							Add	Int Rot
	Ext									Ext	Abd	Ext Rot
Moments												
Hip	Flex	Add	Int Rot	Flex	Add	Int Rot						
					Abd	Ext Rot						
Knee			Int Rot	Flex	Add	Int Rot						
	Ext	Abd		Ext	Abd	Ext Rot						
Ankle	Flex	Add	Int Rot	Flex		Int Rot		Add				
					Abd							
Angles												
S-C				Flex						Flex	Ev	
	Ext				In	Add				Ext	In	Add
C-M		Ev				Ev				Flex	Ev	Abd
	Ext		Add	Ext						Ext	In	Add
M-M		Ev		Flex	Ev	Abd	Flex		Abd		Ev	
	Ext		Add		In	Add		In				Add
F-P						Abd	Flex					Abd
	Ext									Ext		Add

8.3.5 Statistical Analysis

8.3.5.1 Statistical Power

Fifty-five boys took part in the body composition and gait analysis protocols. The sample size calculation from the reliability studies in experimental chapters 2 and 3 (chapters 6 and 7) estimated a sample of 66 boys (Appendix VI) was required based on the most variable segment (the hallux). Post-hoc power calculations identified peak calcaneus-midfoot eversion during the first double support phase to have the lowest effect size (0.44). This was a medium effect size according to Cohen (1992), lower effect sizes increase the probability of a type II error (false negative) or not finding an association if one exists. Using the variable with the lowest effect size gives a conservative estimate of statistical power. The statistical power of the sample collected based on the effect size of 0.44 is 93.4% which is above the minimal power which was aimed for (80%). Therefore, the sample of 55 boys recruited to explore the associations between adiposity and gait biomechanics is of suitable statistical power.

8.3.5.2 Collinearity and Confounding Variables

In order to assess the associations between kinematic and kinetic variables with %FM a number of variables that may affect the result must first be explored. These include age, anthropometric and spatiotemporal variables shown in Figure 8.1 with correlations between the included and excluded variables highlighted. Table A7.1 presents the results of collinearity statistic on the selected variables. The variance inflation factor and its tolerance statistic are measures of how much the variance of the estimated regression coefficient is "inflated" by the existence of correlation among the predictor variables in the model. The variance inflation factor should ideally be below 10 and the tolerance statistic above 0.2 (Field, 2009). The variables which were removed to reduce collinearity were; weight, stride time, step time, percentage of gait cycle when contralateral toe-off occurred, percentage of gait cycle when contralateral initial contact occurred, stride distance, and cadence. Therefore, the final predictor variables carried forward to analyse associations with adiposity (shown in Figure 8.1 and Table A7.2) are; age, height, BMI Z-score, %FM, second double support phase time, total single support duration, step distance, velocity and step width.

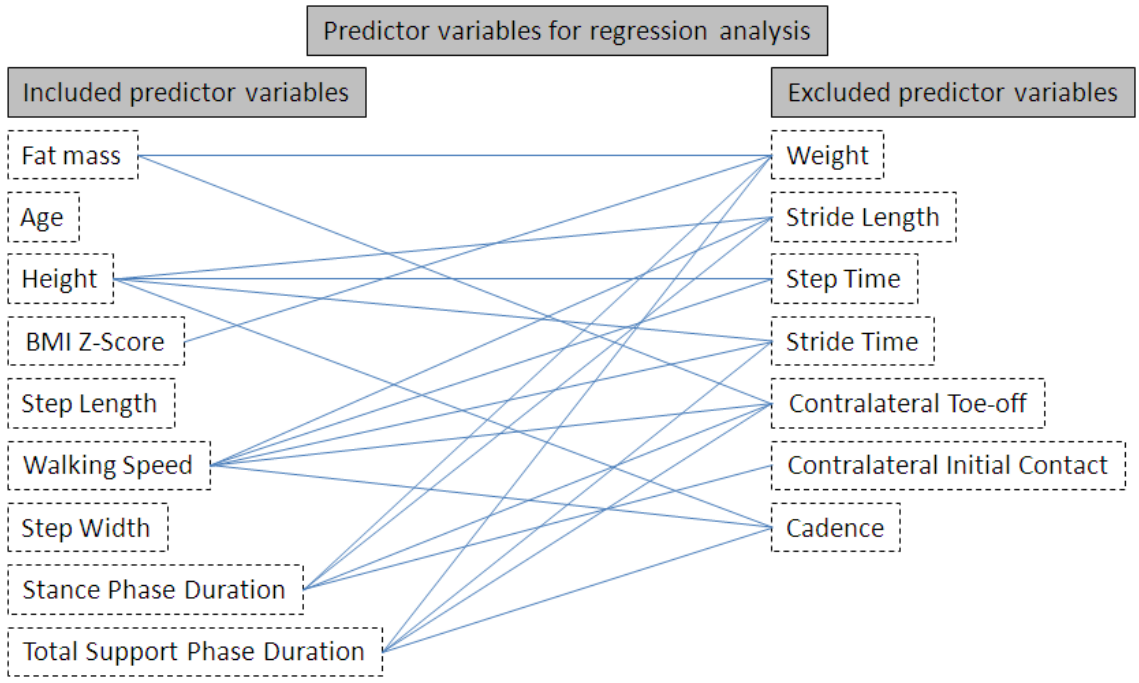

Figure 8.1. Diagram of all predictor variables for regression analysis. Excluded predictor variables removed due to significant correlation with included predictor variables highlighted by adjoining lines.

8.3.5.3 Principle Component Analysis of Lower Limb and Foot Angular and Moment Variables

Once the predictor variables were defined the extracted gait variables required a reduction technique in order to reduce the analysis of 205 lower limb and foot variables. Of the 205 variables selected for analysis in PCA, 62 were joint angular measures from PiG lower limb model, 60 were joint moment measures from PiG lower limb model and 83 were joint angular measures from 3DFoot, shown in Table 8.2. In order to reduce the number of variables principle component analysis (PCA) was selected to produce a component score for variables that demonstrate similar variation across the subject population. Lower limb and foot 3D angles were placed into separate PCAs according to each joint. To aid interpretation, lower limb joint moments were placed into PCAs according to each joint and each 3D plane. In total 16 PCAs were undertaken on the data, an example of one full PCA and multiple regression analysis is given in Appendix VIII. Each variable was entered into PCA in SPSS version 20

In order to select components for further investigation the importance of the relative variance within each component was measured by eigenvalues. Eigenvalues can be used to calculate the percentage of the total variation in the data that is explained by each component. A scree plot was used to identify the number of components for further investigation, shown in Figure A8.1. The cutoff point is determined by taking the components above the inflexion point of the scree curve (Field, 2009).

Once components have been extracted, the degree to which the gait variables load onto the components is calculated. A transformation matrix of components is created and factor rotation used to maximally apply the variables to each component (Field, 2009). A varimax rotation was applied on lower limb angles, lower limb moments and foot angles.

The contribution of each variable to the components was identified by the size of the rotated loadings ranging from -1 to 1. Variables with a loading magnitude greater than 0.722 or less than -0.722 were considered as contributing to that component (Field, 2002). The variables were saved as a regression score for each component and taken forward to multiple linear regression analysis.

8.3.5.4 Multiple Linear Regression

The components obtained from PCA became the outcome variables for the first stage of multiple linear regression analysis; these were measured on a continuous scale. The large amount of multiple observations for each subject means that it is highly likely that the outcome variables are not independent from each other. That is, the angular and moment data values from the same participant will be more similar than those from different participants. Standard statistical methods do not account for this lack of independence in the data. Therefore, regression analysis was conducted over four stages shown in Figure8.2. The first stage was multiple linear regression of the regression score from PCA; the second was mixed model linear regression on the regression score from PCA; the third stage was multiple linear regression on the individual angle and moment values that composed the regression score; and, the fourth stage was mixed model linear regression on the individual angle and moment values that composed the regression score.

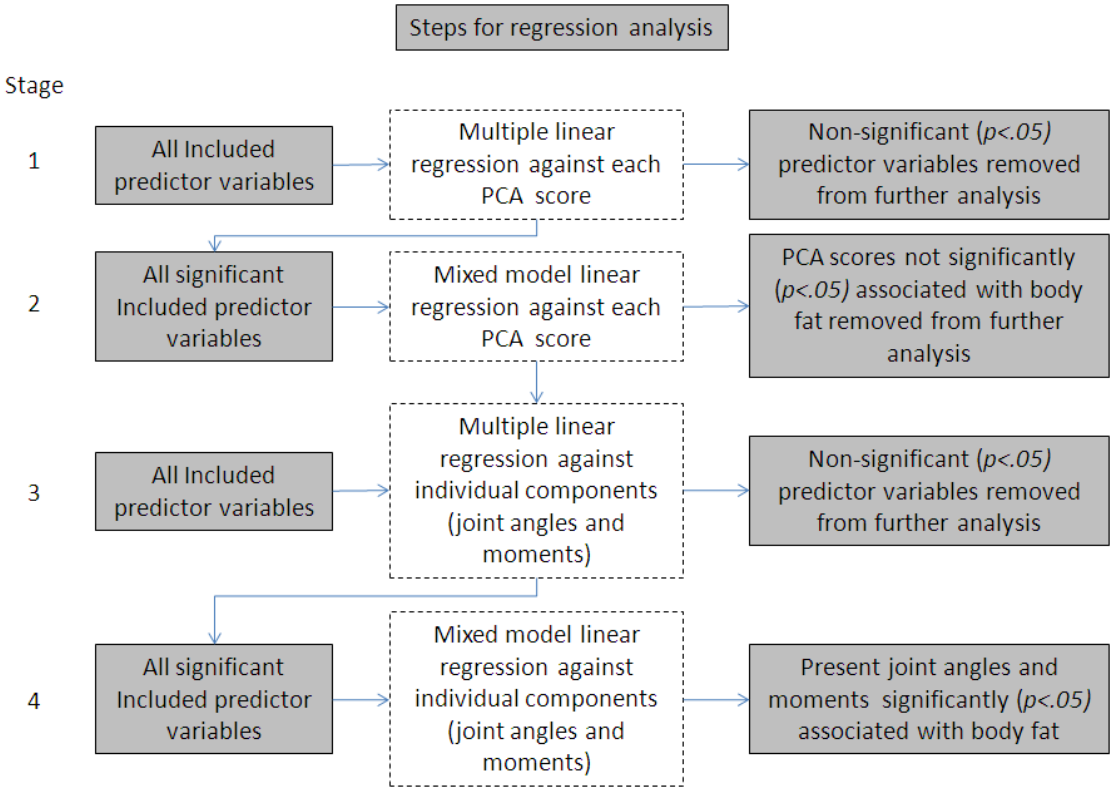

Figure 8.2. Flow chart of multiple regression sequence

8.3.5.5 Multiple Linear Regression on Regression Scores from PCA

Initially a series of univariable analyses were preformed to examine the association between each outcome variable and the selected predictor variables. Subsequently the joint effects were examined in a multivariable analysis using a mixed model for linear regression. The advantage of such an analysis is that the effect of each predictor variable upon the outcome is adjusted for the other predictor variables in the analysis. Thus, this analysis gives a better measure of the underlying effects of each predictor variable (Fields 2009). To reduce the number of predictor variables in this analysis, only those predictor variables that were found to be significant in the univariable analyses were included in this stage of the analysis.

8.3.5.6 Multiple Linear Regression on Gait Cycle Events and Peaks

At this point in the analysis the significant associations between the predictor variables and the component scores, composed of multiple gait cycle events and peaks, were assessed further. Each component from PCA contained gait parameters from one or two planes of motion. The variance between single planar joint motion at different stages of the gait cycle could not be extracted using PCA. In order to explore the associations between adiposity and joint angles/moments over the whole gait cycle multiple linear regression was conducted again. Only component scores that were significantly associated with body fat mass (adiposity) were taken forward into the next stage.

A series of univariable analysis were performed on the gait cycle parameters of each selected component with all predictor variables. Those predictor variables that were significantly associated with the gait cycle parameters were included in the mixed model regression analysis. The significant linear relationships with body fat mass following mixed model regression analysis were extracted.

8.3.5.7 Assumptions for Regression Analysis

In order to check the assumptions of random error and homoscedasticity of the model, a plot of the standardised predicted values of %FM against the standardised residuals was produced. If the regression model fits the sample data well all data points fall on the regression line and the residuals would be zero (Field, 2009). A histogram of the regression standardised residuals should appear as a normal distribution (bell-shaped curve). Furthermore the normal

probability plot shows deviations from normality by plotting the observed residuals against a straight line (representing a normal distribution). All checks on the assumptions of the regression model were compared with published plots in Field (2009).

8.3.5.8 Interpretation of Regression Outputs

The final stage of the analysis was to interpret the associations between body fat mass and the significant gait parameters. A scatter plot of each data point (gait cycle) from the significant gait parameters and the corresponding (%FM) for that participant were constructed. The regression line and regression equation between the data points were used to calculate the regression range of those gait parameters across the participant's (%FM) scores. If the range was below the SEM values from the between-session reliability studies in experimental chapters 2 and 3 (chapters 6 and 7), the association was excluded. This was done on the basis that the angular or moment range across the subject population was less than the expected error.

8.4 Results

8.4.1 Age, Anthropometric and Spatiotemporal

Age, anthropometric and spatiotemporal characteristics are presented in Tables 8.3. BMI Z-Score classification is presented in Table 8.4. The ethnical make-up of the sample is presented in Table 8.5.

Table 8.3. Mean, SD and range of age, anthropometric and spatiotemporal characteristics of sample population (n=55)

	Mean	SD	Range
Age (years)	9.55	1.18	7 - 11
Height (m)	1.40	8.14	119.5 - 159.5
Weight (kg)	37.69	10.67	22.3 – 68.6
BMI (kg/m^2)	18.41	4.00	12.34 - 29.62
Z score	0.55	1.58	-2.87 - 3.54
Centile (%)	59.99	36.08	0.21 - 99.98
Body fat mass (%)	23.78	9.33	9.46 – 42.06
Walking velocity ($m \cdot s^{-1}$)	1.33	0.19	0.95 – 1.81
Cadence (steps/min)	131.69	15.66	105.77 – 171.52
Stance Phase duration (%)	57.29	2.32	52.60 - 65.16
Total single support duration (%)	49.86	1.85	41.59 – 56.70
Step Width (mm)	88.59	28.18	36.47 – 163.38
Step length (m)	0.60	0.06	0.41 – 0.79

Table 8.4. BMI Z-Score classification according to the UK90 reference data set of the sample population (n=55)

BMI Classification	Severely obese	Obese	Overweight	Ideal weight	Underweight	Very underweight
UK90 (clinical)	1	7	12	29	4	2

Table 8.5. Ethnicity classification of the sample population (n=55)

	Black	Caucasian	South Asian	Other
Ethnicity (n)	16	19	18	2

8.4.2 Multiple Regression Analysis of Confounding Variables with %FM

Multiple regression analysis revealed height, BMI Z-Score, stance phase duration and total support duration to be significantly associated with %FM ($P<.05$) in this sample of boys. Table 8.6 shows the amount of variation in %FM explained by each model (predictor variables) and Table 8.7 shows the significance of the explained %FM variance. Figure 8.3 shows that height and BMI Z-Score were positively associated with %FM; meaning taller and heavier (relative to height) participants had higher %FM. Figure 8.4 shows that the duration of stance phase was positively associated with %FM; participants who spent a longer proportion of the gait cycle in the stance phase had higher %FM. Figure 8.4 also shows the total single support duration was negatively associated with %FM; participants who spent less time in the single support phase (SS1) had higher %FM.

Table 8.6. Regression models individual summaries for: Age, height, BMI Z-Score, stance phase duration, step length, velocity, step width and total single support duration, with %FM

Model	r	r Square	Adjusted r Square	Std. Error of the Estimate
Age	.093	.009	-0.11	8.86
Height	.296	.088	.069	8.50
BMI Z-Score	.789	.623	.615	5.47
Stance phase duration	.499	.249	.234	7.71
Step Length	.201	.041	.021	8.72
Velocity	.183	.033	.014	8.75
Step Width	.208	.043	.024	8.71
Total Single Support duration	.472	.222	.207	7.85

Table 8.7 Regression models coefficients for individual predictor variables and %FM. Significance (p<.05)

	Unstandardised Coefficients		Standardized Coefficients		
Model	B	Std. Error	Beta	t	Sig.
age	.738	1.123	.093	.658	.514
Height	.320	.146	.296	2.192	.033*
BMI Z-score	4.377	.482	.789	9.085	.000*
Stance Phase Duration	3.132	.769	.499	4.072	.000*
Step Length	-.037	.025	-.201	-1.453	.152
Velocity	-0.11	.009	-.183	.-1.315	.195
Step Width	.090	.060	.208	1.501	.140
Total Single Support duration	-2.874	.760	-.472	-3.781	.000*

* represents significant association with %FM (p<0.5).

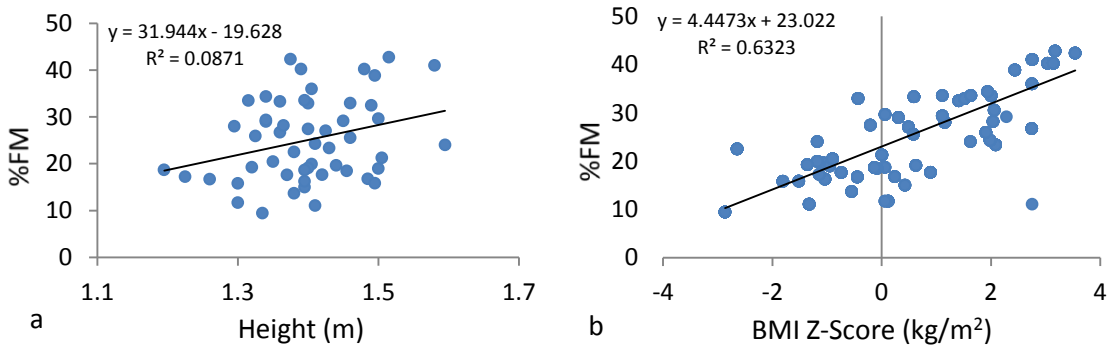

Figure 8.3. Scatter plots of; (a) body fat mass (%FM) with height, and (b) body fat mass (%FM) with BMI Z-Score

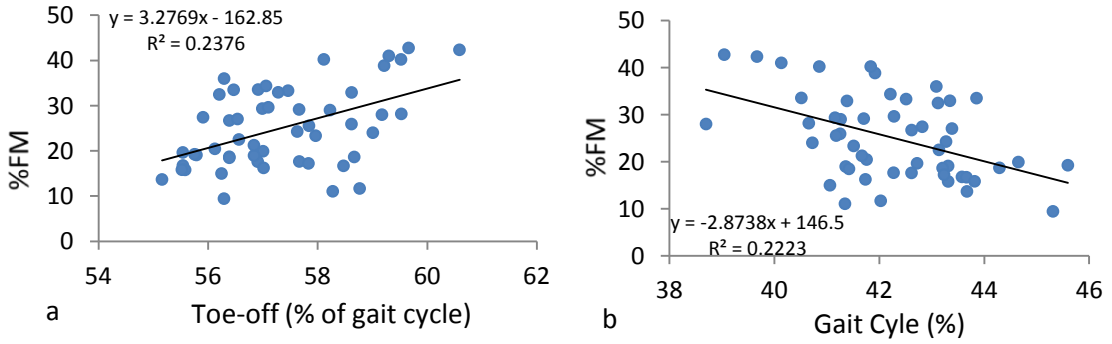

Figure 8.4. Scatter plots of; (a) body fat mass (%FM) with stance phase duration, and (b) body fat mass (%FM) with total single support duration

Height, BMI Z-Score, stance phase duration and total single support duration were modelled in multiple regression to determine their combined influence on %FM. Table 8.8 shows that the model explained 64% of the variance in %FM in this sample of boys. However, only BMI Z-Score remained significantly associated with %FM (p<.001, Table 8.9).

Table 8.8. Model summary for predictor variables: Height, BMI Z-Score, stance phase duration and total single support duration

Model	r	r Square	Adjusted r Square	Std. Error of the Estimate
1	.799	.639	.608	5.51

Table 8.9. Regression models coefficients for predictor variable %FM. Significance (p<.05)

Model		Unstandardised Coefficients		Standardized Coefficients	t	Sig.
		B	Std. Error	Beta		
1	(Constant)	-37.436	70.821		-.529	.600
	Height	.124	.101	.115	1.226	.226
	BMI Z-score	3.984	.623	.718	6.392	.000*
	Stance Phase Duration	.633	.769	.101	.823	.414
	Total Single Support duration	.155	.757	.025	.204	.839

* represents significant association with %FM (p<0.5).

8.4.3 Significant Associations between Gait Parameters and Adiposity

8.4.3.1 Lower Limb Joint Angles - Hip

Three principle components, with Eigenvalues greater than one, accounting for 80.26% of the variance in 3D hip joint motion were identified, shown in Table 8.10. The first component consisted of transverse plane hip motion variables explaining 32.30% of the variance in 3D hip joint motion. The second component consisted of sagittal plane hip motion variables explaining 24.02% of the variance in 3D hip joint motion. The third component consisted of frontal plane hip motion variables explaining 23.96% of the variance in 3D hip joint motion.

Table 8.10. Principle component analysis of Hip angle. Variables >0.722 and <0.722 considered as contributing to each component and denoted by *

	Component (variance explained)		
	1 (32.30%)	2 (24.02%)	3 (23.96%)
SS 2 sag Max (deg.)	-.040	.943*	-.075
SS 1 fro Max (deg.)	.047	.130	.755*
SS 2 fro Min (deg.)	-.197	-.235	.774*
SS 2 fro Max (deg.)	-.017	-.221	.834*
SS 1 tra Min (deg.)	.957*	-.170	-.003
SS 2 tra Min (deg.)	.899*	-.055	-.195
SS 2 tra Max (deg.)	.919*	-.022	.095
Sag IIC (deg.)	-.078	.946*	-.051
Sag CTO (deg.)	-.047	.906*	-.082
Sag CIC (deg.)	-.159	.909*	-.027
Sag ITO (deg.)	-.160	.887*	-.017
Fro IIC (deg.)	.117	-.221	.810*
Fro CTO (deg.)	.073	-.030	.826*
Fro CIC (deg.)	.028	.256	.751*
Fro ITO (deg.)	-.159	-.037	.815*
Tra IIC (deg.)	.903*	.014	-.184
Tra CTO (deg.)	.947*	-.006	.003
Tra CIC (deg.)	.934*	-.214	.048
Tra ITO (deg.)	.914*	-.167	.148

From each principle component three regression score were calculated based on the variables contributing to the amount variance explained. The three regression scores were entered into three separate regression models with the predictor variables; age, height, BMI Z-Score, stance phase duration, step length, velocity, step width and total single support duration. The model summary for each principle component regression score is shown in Table 8.11. The predictor variables explained only 9% of the variation in regression score model 1, 43% of model 2, and 13% of model 3.

Table 8.11. Model summary of principle component Hip angle regression scores with predictors; Predictors: (Constant), age, height, BMI Z-Score, stance phase duration, step length, velocity, step width and total single support duration

Regression Score Model	r	r Square	Adjusted r Square	Std. Error of the Estimate
1	.312	.088	.088	0.96
2	.654	.428	.422	0.76
3	.360	.129	.120	0.94

The linear regression coefficients for the three principle components (models) of 3D hip angles are shown in Table A10.1. In model 1; height, age, BMI Z-Score, %FM, stance phase duration, step width and total single support duration were significantly associated with the regression score model. In model 2; height, age, BMI Z-Score, %FM, stance phase duration, velocity and step width were significantly associated with the regression model. In model 3; height, age and BMI Z-Score were significantly associated with the regression model.

Following linear regression analysis on the regression scores models, from the three principle components of 3D hip angles, mixed model regression was then applied to determine the effects of the predictor variables on the model. Table A10.2 shows the outputs for the three models. In model 1 BMI Z-Score was significantly associated the regression score. In model 2, height and %FM were significantly associated with the regression score. In model 3, BMI Z-Score were significantly associated with the regression score.

Only the second regression score (model) was significantly associated with %FM and was analysed further. Table 8.12 shows the hip sagittal plane variables that regression score (model) 2 was composed of; hip sagittal angle at ipsilateral initial contact (predictor variables explained 35% of variance), contralateral toe-off (predictor variables explained 28% of variance), contralateral initial contact (predictor variables explained 51% of variance), ipsilateral toe-off (predictor variables explained 47% of variance) and maximal peak during SS2 (swing phase) (predictor variables explained 36% of variance). These were entered into their individual regression models to examine the amount variance explained by the predictor variables.

Table 8.12. Model summary of sagittal hip angles at gait cycle events and peaks with predictors; Predictors: (Constant), age, height, BMI Z-Score, stance phase duration, step length, velocity, step width and total single support duration

Regression Score Model	r	r Square	Adjusted r Square	Std. Error of the Estimate
SS 2 sag Max (deg.)	.601	.361	.354	7.33
Sag IIC (deg.)	.589	.346	.339	7.51
Sag CTO (deg.)	.530	.281	.273	7.74
Sag CIC (deg.)	.714	.510	.505	6.80
Sag ITO (deg.)	.685	.470	.464	7.25

Linear regression coefficients for each model of hip sagittal plane angle are shown in Table A10.3. Percentage fat mass (%FM) was significantly associated with each model for hip sagittal plane angle. Therefore, each model was assessed in mixed model regression analysis to determine the combined effects of the predictor variables.

Table A10.4 shows the results of mixed model regression analysis on the hip sagittal plane angle models. The %FM was significantly associated with hip sagittal plane angle at ipsilateral initial contact, contralateral initial contact and ipsilateral toe-off. Walking velocity and height were also significantly associated with hip sagittal plane motion, particularly at contralateral toe-off.

Table 8.13 and Figure 8.5 report the linear regression of %FM with the significantly associated hip sagittal plane variables. The results demonstrated that boys with a higher %FM showed more hip flexion at ipsilateral initial contact, contralateral initial contact and ipsilateral toe off.

Table 8.13. Mean (95% confidence intervals) of Hip sagittal plane variables significantly associated with %FM, range over the sample population

Hip	Joint motion	Gait parameter (% of gait cycle)	Highest %FM (95%CI)	Lowest %FM (95%CI)
Sagittal	Flexion	Ipsilateral Initial contact (0%)	43.85° (1.15°)	27.83° (1.31°)
	Flexion	Contralateral initial contact (49.80 ± 1.96%)	0.76° (1.11°)	-19.95° (1.27°)
	Flexion	Ipsilateral toe off (57.47 ± 2.20%)	5.04° (1.14°)	-15.97° (1.30°)

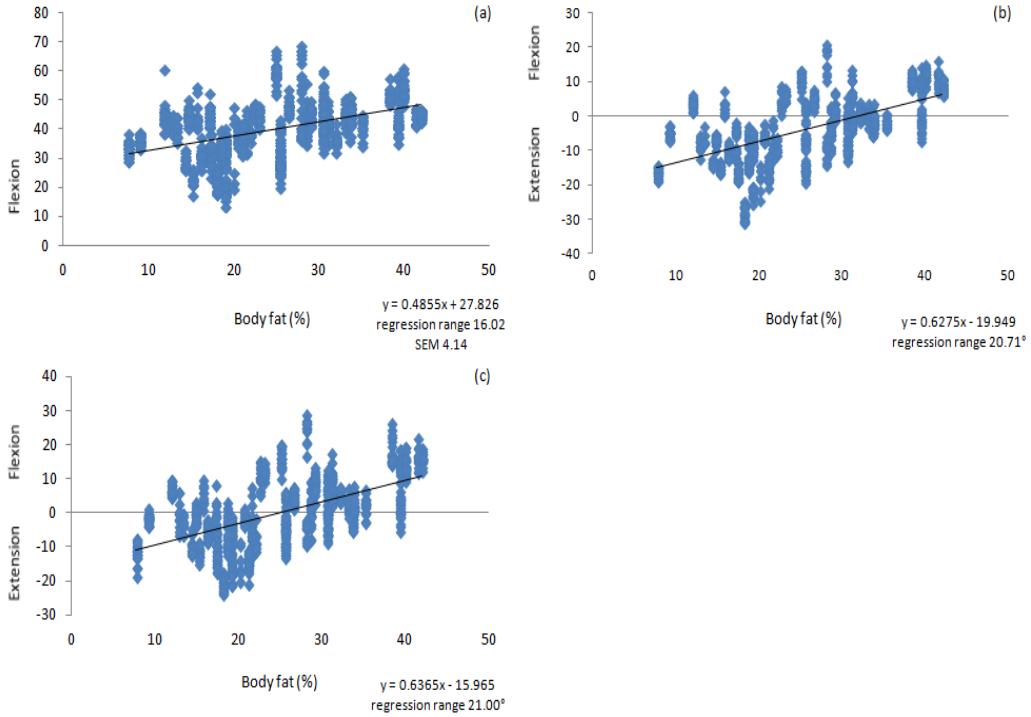

Figure 8.5. Scatter plot of significant associations between body fat mass and hip; (a) flexion at IIC, (b) flexion at CIC, and (c) flexion at ITO.

The association between hip angular motion and %FM is shown in Figure 8.6. The five participants with the highest and five participants with lowest %FM are reported to represent the association across the range of %FM.

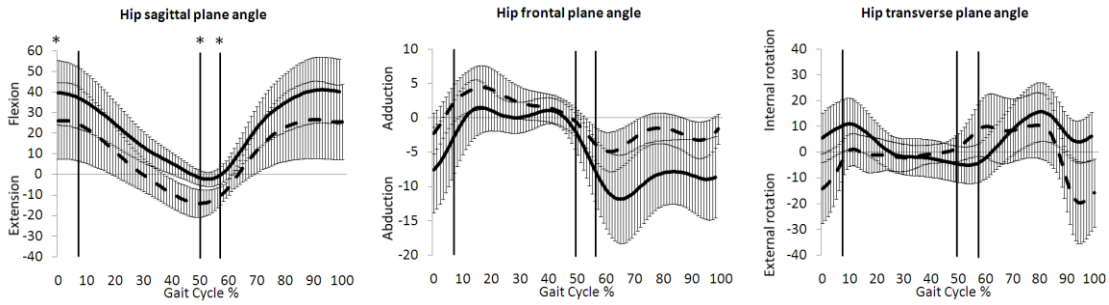

Figure 8.6. Mean ± SD of Hip angular motion in the sagittal, frontal and transverse planes in the five participants with the higher %FM (black line) and the five participants with the lowest %FM (dash line) to represent the association between hip angle and %FM over the gait cycle. * denotes points of the gait where significant association between %FM and hip angle was found

8.4.3.2 Lower Limb Joint Angles - Knee

Four principle components, with Eigenvalues greater than one, accounting for 80.70% of the variance in 3D knee joint motion were identified, shown in Table 8.14. The first component consisted of transverse plane knee motion variables explaining 26.93% of the variance in 3D knee joint motion. The second component consisted of frontal plane knee motion variables explaining 24.38% of the variance in 3D knee joint motion. The third component consisted of sagittal plane knee motion variables during early stance explaining 17.20% of the variance in 3D knee joint motion. The fourth component consisted of sagittal plane knee motion during late stance explaining 7.15% of the variance in knee joint motion.

Table 8.14. Principle component analysis of Knee angle. Variables >0.722 and <0.722 considered as contributing to each component and denoted by *

	Component (variance explained)			
	1 (26.93%)	2 (24.38%)	3 (17.20%)	4 (7.15%)
DS 1 sag Min (deg.)	.081	-.132	.867*	.077
DS 1 sag Max (deg.)	.102	-.043	.902*	.120
SS 1 fro Min (deg.)	.015	.901*	-.131	-.116
SS 1 fro Max (deg.)	-.061	.903*	.119	-.080
SS 2 fro Max (deg.)	-.147	.790*	-.180	-.018
SS 2 fro Min (deg.)	-.087	.753*	-.168	-.003
SS 1 tra Min (deg.)	.904*	-.132	.015	.175
SS 1 tra Max (deg.)	.931*	-.037	.141	-.009
SS 2 tra Min (deg.)	.846*	-.147	.145	-.023
SS 2 tra Max (deg.)	.826*	.095	.105	.028
Sag IIC (deg.)	.106	-.102	.855*	.070
Sag CTO (deg.)	.115	-.049	.896*	.120
Sag CIC (deg.)	.230	-.048	.230	.756*
Sag ITO (deg.)	.102	-.219	.226	.827*
Fro IIC (deg.)	.042	.844*	-.021	.059
Fro CTO (deg.)	-.193	.859*	.163	-.008
Fro CIC (deg.)	-.014	.859*	-.140	-.186
Fro ITO (deg.)	-.208	.797*	-.236	-.125
Tra IIC (deg.)	.854*	-.198	.246	-.062
Tra CTO (deg.)	.909*	-.060	.219	-.017
Tra CIC (deg.)	.893*	-.100	-.074	.258
Tra ITO (deg.)	.860*	-.110	.003	.303

The model summary for each principle component regression score from knee angular motion is shown in Table 8.15. The predictor variables explained 19% of the variation in regression score model 1, 7% of model 2, 27% of model 3 and 18% of model 4.

Table 8.15. Model Summary of principle component regression scores for knee angle with predictors; Predictors: (Constant), age, height, BMI Z-Score, stance phase duration, step length, velocity, step width and total single support duration

Regression Score Model	r	r Square	Adjusted r Square	Std. Error of the Estimate
1	.435	.189	.181	0.90
2	.267	.071	.061	0.96
3	.522	.272	.264	0.86
4	.429	.184	.176	0.91

The linear regression coefficients for the three principle components (models) of 3D knee angles are shown in Table A10.5. In model 1; height, age, BMI Z-Score, step length, step width and total single support duration were significantly associated with the regression score model. In model 2; BMI Z-Score, %FM and velocity were significantly associated with the regression model. In model 3; age, height, BMI Z-Score, stance phase duration, step length,

velocity, step width and total single support duration were significantly associated with the regression model. In model 4; height, %FM, stance phase duration, step length and total single support duration were significantly associated with the regression model.

Table A10.6 shows the outputs of mixed model regression analysis for the four models. In model 1, 2 and 3 no predictor variables were significantly associated with the regression score. In model 4 %FM was significantly associated with the regression score.

Only the fourth regression score (model) was significantly associated with %FM and was analysed further. Table 8.16 shows the knee sagittal plane variables that regression score (model) 4 was composed of; knee sagittal angle at contralateral initial contact (predictor variables explained 6% of variance) and ipsilateral toe-off (predictor variables explained 18% of variance). These were entered into their individual regression models to examine the amount variance explained by the predictor variables.

Table 8.16. Model Summary of sagittal Knee angles at gait cycle events and peaks with predictors; Predictors: (Constant), age, height, BMI Z-Score, stance phase duration, step length, velocity, step width and total single support duration

Regression Score Model	r	r Square	Adjusted r Square	Std. Error of the Estimate
Sag CIC (deg.)	.247	.061	.051	5.69
Sag ITO (deg.)	.424	.180	.171	6.68

Linear regression coefficients for each model of knee sagittal plane angle are shown in Table A10.7. Percentage fat mass (%FM) was significantly associated with both models for knee sagittal plane angle. Therefore, each model was assessed in mixed model regression analysis to determine the combined effects of the predictor variables.

Table A10.8 shows the results of mixed model regression analysis on the knee sagittal plane angle models. Percentage body fat mass (%FM) was significantly associated with knee sagittal plane angle at ipsilateral toe-off. The length of stance phase duration was also associated with knee sagittal plane angle at ipsilateral toe-off.

Table 8.17 and Figure 8.7 report the linear regression of %FM with the significantly associated knee sagittal plane variables. The results demonstrated that boys with higher %FM were associated with greater knee flexion at ipsilateral toe off.

Table 8.17. Mean (95% confidence intervals) of Knee sagittal plane variables significantly associated with %FM, range over the sample population

Knee	Joint motion	Gait parameter (% of gait cycle)	Highest %FM (95%CI)	Lowest %FM (95%CI)
Sagittal	Flexion	Ipsilateral toe off (57.47 ± 2.20%)	27.53° (1.06°)	18.60° (1.20°)

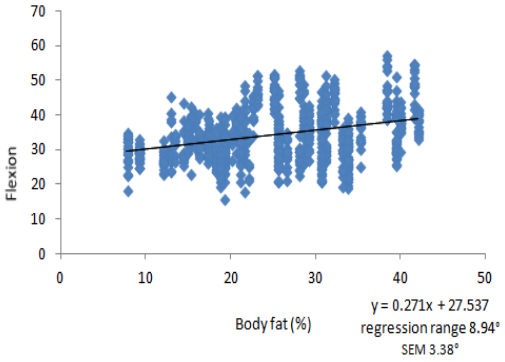

Figure 8.7. Scatter plot of significant associations between body fat mass and knee flexion at ITO.

The association between knee angular motion and %FM is shown in Figure 8.8. The five participants with the highest and five participants with lowest %FM are reported to represent the association across the range of %FM.

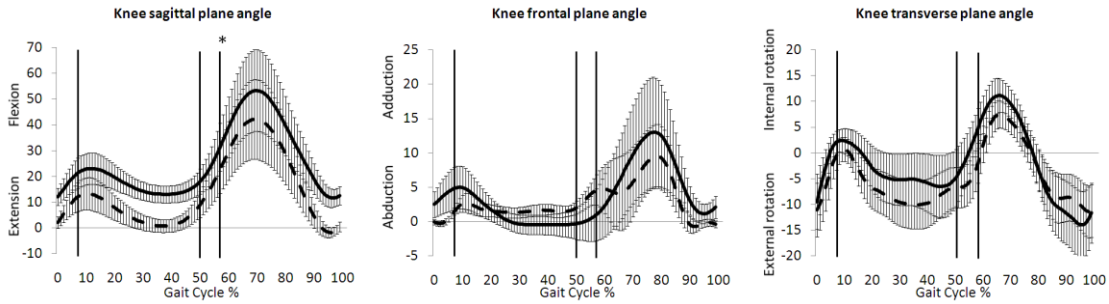

Figure 8.8. Mean ± SD of Knee angular motion in the sagittal, frontal and transverse planes in the five participants with the higher %FM (black line) and the five participants with the lowest %FM (dash line) to represent the association between knee angle and %FM over the gait cycle. * denotes points of the gait where significant association between %FM and knee angle was found

8.4.3.3 Lower Limb Joint Angles - Ankle

Three principle components, with eigenvalues greater than one, accounting for 72.22% of the variance in 3D ankle joint motion were identified, shown in Table 8.18. The first component consisted of frontal and transverse plane ankle motion variables explaining 45.81% of the variance in 3D ankle joint motion. The second component consisted of sagittal plane ankle motion variables in early stance explaining 15.87% of the variance in 3D ankle joint motion. The third component consisted of sagittal plane ankle motion variables during late stance and swing explaining 15.11% of the variance in 3D ankle joint motion.

Table 8.18. Principle component analysis of Ankle angle. Variables >0.722 and <0.722 considered as contributing to each component and denoted by *

	Component (variance explained)		
	1 (45.81%)	2 (15.87%)	3 (15.11%)
DS 1 sag Min (deg.)	.100	.804*	.287
SS 1 sag Max (deg.)	-.169	.470	.676
SS 2 sag Min (deg.)	.165	.180	.772*
SS 2 sag Max (deg.)	.029	.683	.491
SS 2 fro Min (deg.)	.906*	.033	.038
SS 2 fro Max (deg.)	.737*	.067	-.108
SS 2 tra Min (deg.)	-.805*	-.110	.023
SS 2 tra Max (deg.)	-.888*	-.104	-.122
Sag IIC (deg.)	-.008	.760*	.341
Sag CTO (deg.)	.113	.843*	.016
Sag CIC (deg.)	-.109	.202	.831*
Sag ITO (deg.)	.149	.117	.866*
Fro IIC (deg.)	.889*	.159	-.039
Fro CTO (deg.)	.880*	.214	-.097
Fro CIC (deg.)	.876*	-.181	.052
Fro ITO (deg.)	.875*	-.203	.071
tra IIC (deg.)	-.878*	-.234	-.053
tra CTO (deg.)	-.897*	-.254	.023
tra CIC (deg.)	-.910*	.158	-.106
tra ITO (deg.)	-.865*	.174	-.161

The model summary for each principle component regression score from ankle angular motion is shown in Table 8.19. The predictor variables explained 8% of the variation in regression score model 1, 23% of model 2, and 24% of model 3.

Table 8.19. Model Summary of principle component ankle angle regression scores with predictors; Predictors: (Constant), age, height, BMI Z-Score, stance phase duration, step length, velocity, step width and total single support duration

Regression Score Model	r	r Square	Adjusted r Square	Std. Error of the Estimate
1	.281	.079	.069	0.97
2	.482	.232	.225	0.88
3	.490	.240	.233	0.88

The linear regression coefficients for the three principle components (models) of 3D ankle angles are shown in Table A10.9. In model 1; BMI Z-Score, %FM, velocity and step width were significantly associated with the regression score model. In model 2; age, %FM, stance phase duration, step length and velocity were significantly associated with the regression model. In model 3; age, height, BMI Z-Score, stance phase duration, step length, velocity and total single support duration were significantly associated with the regression model.

Table A10.10 shows the outputs of mixed model regression analysis for the four models. In model 1 %FM was significantly associated with the regression score. In model 2 height and %FM were significantly associated with the regression score. In model 3 age, height and %FM were associated with the regression score.

All three regression scores (models) from ankle 3D motion were significantly associated with %FM and were analysed further. Table 8.20 shows the ankle frontal plane variables that regression score (model) 1 was composed of; peak minimum angle in SS2 (swing phase) (predictor variables explained 11% of variance), peak maximum angles in SS2 (predictor variables explained 18% of variance), angle at ipsilateral initial contact (predictor variables explained 11% of variance), contralateral toe-off (predictor variables explained 10% of variance), contralateral initial contact (predictor variables explained 5% of variance) and ipsilateral toe-off (predictor variables explained 10% of variance). Model 1 was also composed of ankle transverse plane variables of; peak minimum angle in SS2 (swing phase) (predictor variables explained 12% of variance), peak maximum angle in SS2 (predictor variables explained 15% of variance), angle at ipsilateral initial contact (predictor variables explained 15% of variance), contralateral toe-off (predictor variables explained 10% of variance), contralateral initial contact (predictor variables explained 8% of variance) and ipsilateral toe-off (predictor variables explained 11% of variance). Regression score 2 (model) was composed of ankle sagittal plane variables of; peak minimum angle in DS1 (double support phase 1) (predictor variables explained 20% of variance), angle at ipsilateral initial contact (predictor variables explained 20% of variance) and contralateral toe-off (predictor variables explained 19% of variance). Regression score 3 (model) was composed of ankle sagittal plane variables

of; peak minimum value during SS2 (swing phase) (predictor variables explained 21% of variance), angle at contralateral initial contact (predictor variables explained 35% of variance) and ipsilateral toe-off (predictor variables explained 20% of variance). These were entered into their individual regression models to examine the amount variance explained by the predictor variables.

Table 8.20. Model Summary of 3D Ankle angles at gait cycle events and peaks with predictors; Predictors: (Constant), age, height, BMI Z-Score, stance phase duration, step length, velocity, step width and total single support duration

Regression Score Model	r	r Square	Adjusted r Square	Std. Error of the Estimate
SS 2 fro Min (deg.)	.331	.109	.100	2.67
SS 2 fro Max (deg.)	.424	.180	.171	2.11
SS 2 tra Min (deg.)	.352	.124	.114	10.98
SS 2 tra Max (deg.)	.383	.147	.138	12.58
Fro IIC (deg.)	.333	.111	.101	2.77
Fro CTO (deg.)	.315	.100	.090	2.46
Fro CIC (deg.)	.232	.054	.043	3.12
Fro ITO (deg.)	.318	.101	.092	2.45
tra IIC (deg.)	.388	.150	.141	13.51
tra CTO (deg.)	.308	.095	.085	13.05
tra CIC (deg.)	.286	.082	.072	14.29
tra ITO (deg.)	.330	.109	.099	12.97
DS 1 sag Min (deg.)	.443	.196	.187	3.65
Sag IIC (deg.)	.442	.196	.188	4.30
Sag CTO (deg.)	.431	.186	.178	3.51
SS 2 sag Min (deg.)	.461	.212	.204	6.94
Sag CIC (deg.)	.590	.348	.342	6.29
Sag ITO (deg.)	.442	.195	.187	6.62

Linear regression coefficients for 3D ankle angles are shown in Table A10.11. Percentage fat mass (%FM) was significantly associated with ankle; peak minimum angle in SS2 (swing phase), peak maximum angles in SS2, angle at ipsilateral initial contact, contralateral toe-off and ipsilateral toe-off in the frontal plane. Percentage fat mass (%FM) was significantly associated with ankle; peak minimum angle in SS2 (swing phase), peak maximum angle in SS2, angle at ipsilateral initial contact, contralateral toe-off and contralateral initial contact in the transverse plane. Percentage fat mass (%FM) was significantly associated with ankle; peak minimum angle in DS1 (double support phase 1), peak minimum value during SS2 (swing phase), angle at ipsilateral initial contact, contralateral toe-off, contralateral initial contact and ipsilateral toe-off in the sagittal plane. Each individual model was assessed in mixed model regression analysis to determine the combined effects of the predictor variables.

Table A10.12 shows the results of mixed model regression analysis on the 3D ankle angle models. In the frontal plane, percentage body fat mass (%FM) was significantly associated with peak ankle angle in SS2 (swing phase) and angle at ipsilateral initial contact. In the transverse plane percentage body fat mass (%FM) was significantly associated with peak ankle

angle in SS2 (swing phase) and angle at ipsilateral initial contact. In the sagittal plane, percentage body fat mass (%FM) was significantly associated with peak ankle angle in DS1 (double support phase 1), at contralateral initial contact and ipsilateral toe-off. Age and height were also associated with sagittal ankle angle at ipsilateral toe-off. Step length and walking velocity were also associated with sagittal ankle angle at contralateral initial contact.

Table 8.21 and Figure 8.9, 8.10 and 8.11 report the linear regression of %FM with the significantly associated 3D ankle angle variables. The results demonstrated that the ankles of boys with a higher %FM demonstrated lower abduction peaks and lower internal rotation peaks prior to initial contact. At initial contact, boys with higher %FM were less abducted and less internally rotated than lower %FM boys. Boy's with higher %FM demonstrated less peak plantarflexion shortly after initial contact and greater dorsiflexion at contralateral initial contact and ipsilateral toe off.

Table 8.21. Mean (95% confidence intervals) of 3D Ankle variables significantly associated with %FM, range over the sample population

Ankle	Joint motion	Gait parameter (% of gait cycle)	Highest %FM (95%CI)	Lowest %FM (95%CI)
Sagittal	Peak Plantarflexion	DS 1 (3.16 ± 2.16%)	-1.59^{o} (3.46^{o})	-5.06^{o} (0.55^{o})
	Dorsiflexion	Contralateral initial contact (49.80 ± 1.96%)	4.69^{o} (2.76^{o})	-1.59^{o} (3.46^{o})
	Plantarflexion	Ipsilateral toe off (57.47 ± 2.20%)	9.85^{o} (3.03^{o})	-18.34^{o} (2.41^{o})
Frontal	Abduction	Ipsilateral Initial contact (0%)	-0.82^{o} (1.27^{o})	-2.44^{o} (1.60^{o})
	Peak abduction	SS 2 (89.49 ± 13.94%)	-3.71^{o} (0.39^{o})	-4.57^{o} (0.45^{o})
Transverse	Internal rotation	Ipsilateral Initial contact (0%)	4.45^{o} (5.08^{o})	17.44^{o} (6.38^{o})
	Peak internal rotation	SS 2 (89.41 ± 14.01%)	12.20^{o} (1.84^{o})	25.34^{o} (2.10^{o})

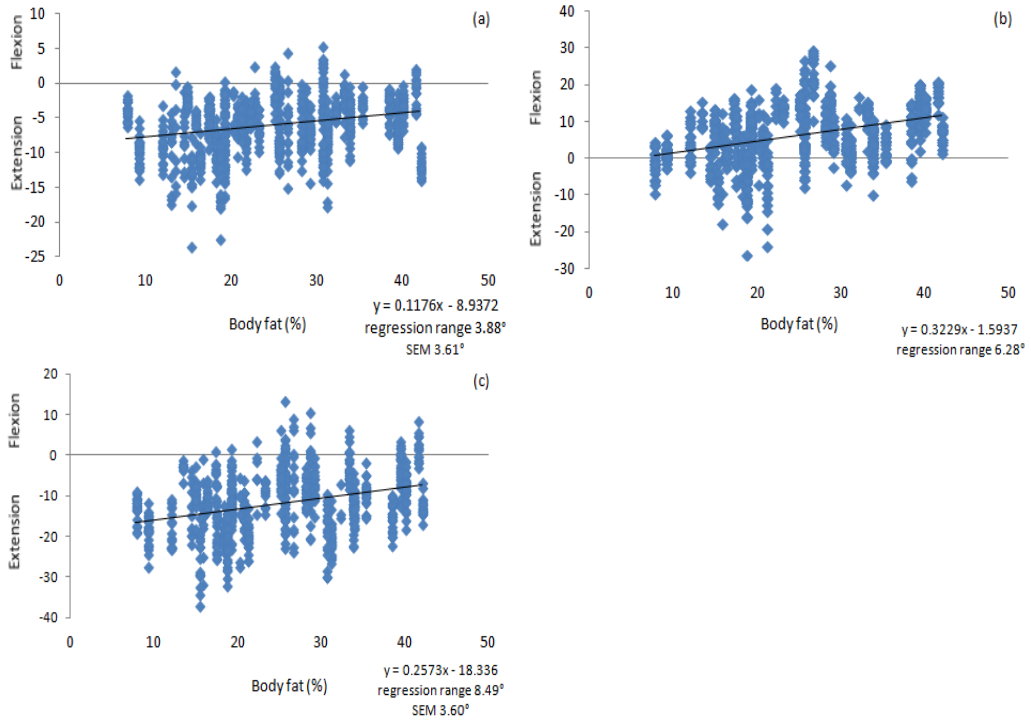

Figure 8.9. Scatter plot of significant association between body fat mass and ankle; (a) peak plantarflexion during DS1, (b) dorsiflexion at CIC and (c) plantarflexion at ITO.

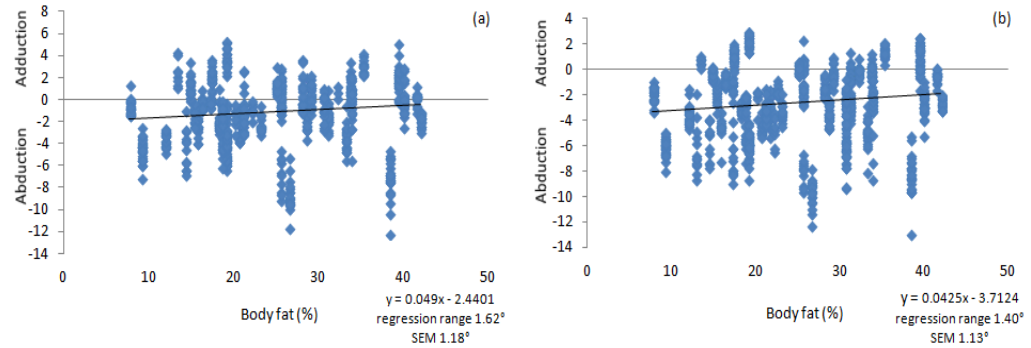

Figure 8.10. Scatter plot of significant association between body fat mass and ankle; (a) abduction at IIC, (b) peak abduction during SS2.

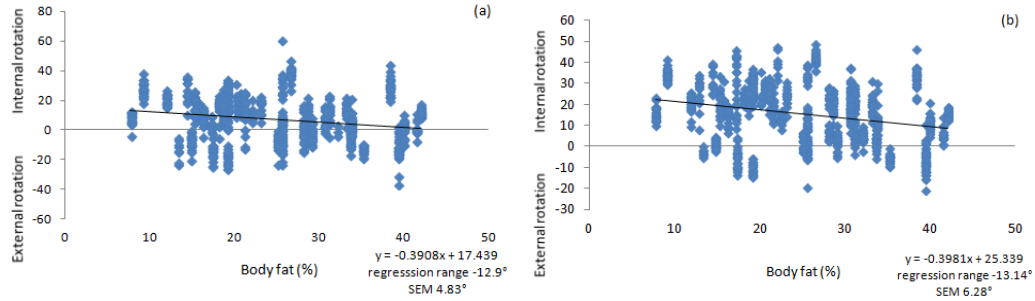

Figure 8.11. Scatter plot of significant associations between body fat mass and ankle; (a) internal rotation at IIC, (b) peak internal rotation during SS2.

The association between ankle angular motion and %FM is shown in Figure 8.12. The five participants with the highest and five participants with lowest %FM are reported to represent the association across the range of %FM.

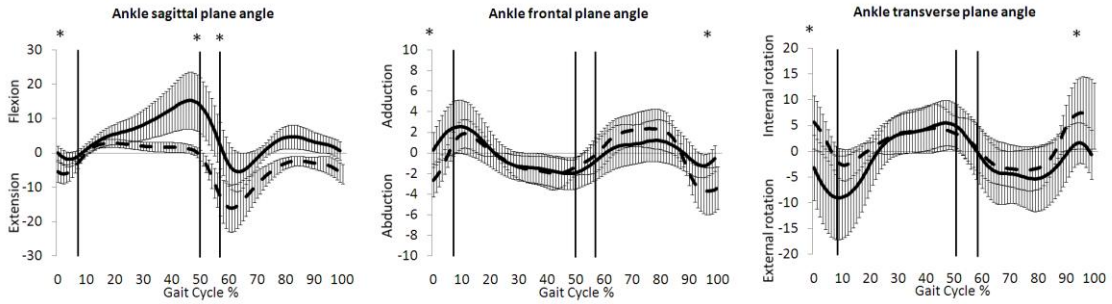

Figure 8.12. Mean ± SD of Ankle angular motion in the sagittal, frontal and transverse planes in the five participants with the higher %FM (black line) and the five participants with the lowest %FM (dash line) to represent the association between ankle angle and %FM over the gait cycle. * denotes points of the gait where significant association between %FM and ankle angle was found

8.4.4.1 Lower Limb Joint Moments - Hip

To interpret lower limb kinetics principle component analysis was carried out on joints and planes separately. Three principle components, with eigenvalues greater than one, accounting for 67.37% of the variance in hip joint sagittal moments were identified, shown in Table 8.22. The first component consisted of hip sagittal moments during the stance phase. The second component of hip sagittal moments consisted of moments at contralateral initial contact. The third component of hip sagittal moments consisted of moments at ipsilateral initial contact.

Three principle components with eigenvalues greater than one, accounting for 68.18% of the variance in hip joint frontal moments were identified, shown in Table 8.22. The first component of hip frontal moments consisted of peak moments in DS1 (double support phase 1). The second component consisted of frontal moments at contralateral toe-off. The third component consisted of peak moments in SS1 (single support phase 1).

Three principle components with eigenvalues greater than one, accounting for 70.31% of the variance in hip transverse moments were identified, shown in Table 8.22. The first component of hip transverse moments consisted of peak moments during mid-stance. The second component consisted of peak transverse moments during SS1. The third component consisted of moments in early stance.

Table 8.22. Principle component analysis of Hip moments. Variables >0.722 and <0.722 considered as contributing to each component and denoted by *

	Component (variance explained)								
	Sagittal			Frontal			Transverse		
	1 (31.86%)	2 (18.82%)	3 (16.69%)	1 (30.04%	2 (20.51%)	3 (17.63%)	1 (30.95%)	2 (22.60%)	3 (16.86%)
DS1 sag Max (Nm)	.834*	-.008	.110						
SS1 sag Max (Nm)	.886*	-.025	-.101						
Sag IIC (Nm)	-.122	.008	.887*						
Sag CTO (Nm)	.779*	.125	-.273						
Sag CIC (Nm)	.116	.727*	.316						
Sag ITO (Nm)	-.050	.770	-.273						
DS 1 fro Min (Nm)				-.832*	.053	.190			
SS 1 fro Min (Nm)				-.238	.063	.901*			
SS 1 fro Max (Nm)				.634	.602	-.081			
Fro IIC (Nm)				.622	.046	.243			
Fro CTO (Nm)				.192	.793*	.180			
Fro CIC (Nm)				.460	-.013	.715			
Fro ITO (Nm)				.166	-.705	.065			
DS1 tra Max (Nm)							.204	-.128	.766*
SS1 tra Min (Nm)							-.108	.940*	-.060
SS1 tra Max (Nm)							.910*	-.180	.038
Tra IIC (Nm)							-.060	.168	.786*
Tra CTO (Nm)							-.029	.919	.105
Tra CIC (Nm)							.922*	.002	-.058
Tra ITO (Nm)							.949*	-.004	.203

The model summary for each principle component regression score is shown in Table 8.23. For sagittal hip moments, the predictor variables explain 28% of the variation in regression score (model) 1, 11% of model 2 and 14% of model 3. For frontal hip moments, the predictor variables explain 22% of the variation in regression score (model) 1, 16% of model 2 and 32% of model 3. For transverse hip moments, the predictor variables explain 24% of the variation in regression score (model) 1, 33% of model 2 and 23% of model 3.

Table 8.23. Model Summary of principle component of hip moments regression scores with predictors; Predictors: (Constant), age, height, BMI Z-Score, stance phase duration, step length, velocity, step width and total single support duration

Regression Score Model	r	r Square	Adjusted r Square	Std. Error of the Estimate
Sagittal				
1	.519	.279	.259	0.86
2	.326	.106	.082	0.96
3	.377	.142	.118	0.94
Frontal				
1	.474	.224	.203	0.89
2	.394	.155	.132	0.93
3	.561	.315	.296	0.84
Transverse				
1	.494	.244	.223	0.88
2	.570	.325	.306	0.83
3	.353	.125	.101	0.95

The linear regression coefficients for the three principle components (models) of hip sagittal moments are shown in Table A10.13. In model 1; height, %FM, step length and velocity were significantly associated with the regression score model. In model 2; BMI Z-Score and height, were significantly associated with the regression model. In model 3; age, BMI Z-Score, height, and velocity were significantly associated with the regression model.

The three principle components (models) of hip frontal moments are shown in Table A10.13. In model 1; height, age and BMI Z-Score and %FM were significantly associated with the regression score model. In model 2; BMI Z-Score, height, %FM, step length and velocity were significantly associated with the regression score model. In model 3; age, BMI Z-Score, %FM, step length, velocity and step width were significantly associated with the regression score model.

The three principle components (models) of hip transverse moments are shown in Table A10.13. In model 1; BMI Z-Score, height and step length were significantly associated with the regression score model. In model 2; Age, BMI Z-Score, stance phase duration, step length and velocity were significantly associated with the regression score model. In model 3; Age, BMI Z-Score, height and velocity were significantly associated with the regression score model.

Table A10.14 shows the outputs for hip sagittal, frontal and transverse components. For sagittal moments, model 1 showed height and %FM were significantly associated with the regression score; model 2 showed BMI Z-Score and height were significantly associated with the regression score; model 3 showed age, height and velocity were significantly associated with the regression score.

For frontal moments, model 1 showed height to be significantly associated with the regression score; model 2 showed BMI Z-Score, height and velocity were significantly associated with the regression score; model 3 showed age, BMI Z-Score, velocity and step width were significantly associated with the regression score.

For transverse moments; model 1 showed height and %FM were significantly associated with the regression score; model 2 showed BMI Z-Score and step width were significantly associated with the regression score; model 3 showed age and height were significantly associated with the regression score.

Only model 1 of sagittal and model 1 of transverse moment were significantly associated with %FM and analysed further. Table 8.24 shows hip moments that comprised sagittal model 1; peak maximal hip moment in DS1 (double support phase 1) (predictor variables explained 30%

of variance), peak maximal hip moment in SS1 (single support 1) (predictor variables explained 21% of variance), and hip moment at contralateral toe-off (predictor variables explained 19% of variance). The hip moments that comprised transverse model 1; peak maximal hip moment in SS1 (predictor variables explained 30% of variance), hip moment at contralateral initial contact (predictor variables explained 14% of variance) and hip moment at ipsilateral tote-off (predictor variables explained 14% of variance).

Table 8.24. Model Summary of sagittal and transverse plane hip moments at gait cycle events and peaks with predictors; Predictors: (Constant), age, height, BMI Z-Score, stance phase duration, step length, velocity, step width and total single support duration

Regression Score Model	r	r Square	Adjusted r Square	Std. Error of the Estimate
DS1 sag Max (Nm)	.551	.303	.284	39.18
SS1 sag Max (Nm)	.462	.213	.191	34.15
Sag CTO (Nm)	.431	.186	.178	3.51
SS1 tra Max (Nm)	.549	.301	.282	1.35
Tra CIC (Nm)	.380	.144	.121	1.37
Tra ITO (Nm)	.367	.135	.111	1.85

Linear regression coefficients for each model of 3D hip moments are shown in Table A10.15. Percentage fat mass (%FM) was significantly associated with hip sagittal moment at contralateral toe-off and hip transverse moment at ipsilateral toe-off. Therefore, each model was assessed in mixed model regression analysis to determine the combined effects of the predictor variables.

Table A10.16 shows the results of mixed model regression analysis on the 3D hip moment models. Percentage body fat mass was significantly associated with hip sagittal moment at contralateral toe-off and hip transverse moment at ipsilateral toe-off. BMI Z-Score was also significantly associated hip transverse moment at ipsilateral toe-off.

Table 8.25 and Figures 8.13 and 8.14 report the linear regression of %FM with the significantly associated sagittal and transverse hip moment variables. The results demonstrated; in the sagittal plane boys with higher %FM were associated with greater hip flexion moments at ipsilateral toe off; in the transverse plane boys with higher %FM demonstrated greater peak hip internal moments at ipsilateral toe off.

Table 8.25. Mean (95% confidence intervals) of Hip moment variables significantly associated with %FM, range over the sample population

Hip	Joint moment	Gait parameter (% of gait cycle)	Highest %FM (95%CI)	Lowest %FM (95%CI)
Sagittal Transverse	Flexion Internal rotation	Contralateral toe off (7.63% ± 2.27%) Ipsilateral toe off (57.47 ± 2.20%)	23.47Nm (8.86Nm) 1.30Nm (0.44Nm)	3.03Nm (9.36Nm) -0.97Nm (0.46Nm)

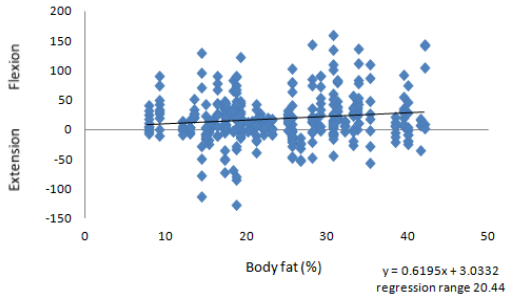

Figure 8.13. Scatter plot of significant associations between body fat mass and hip flexion moment at CTO

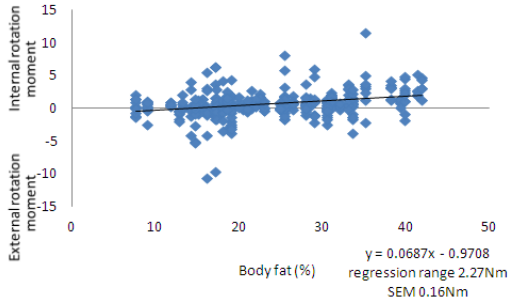

Figure 8.14. Scatter plot of significant associations between body fat mass and hip internal rotation moments at ITO

The association between hip moments and %FM is shown in Figure 8.15. The five participants with the highest and five participants with lowest %FM are reported to represent the association across the range of %FM.

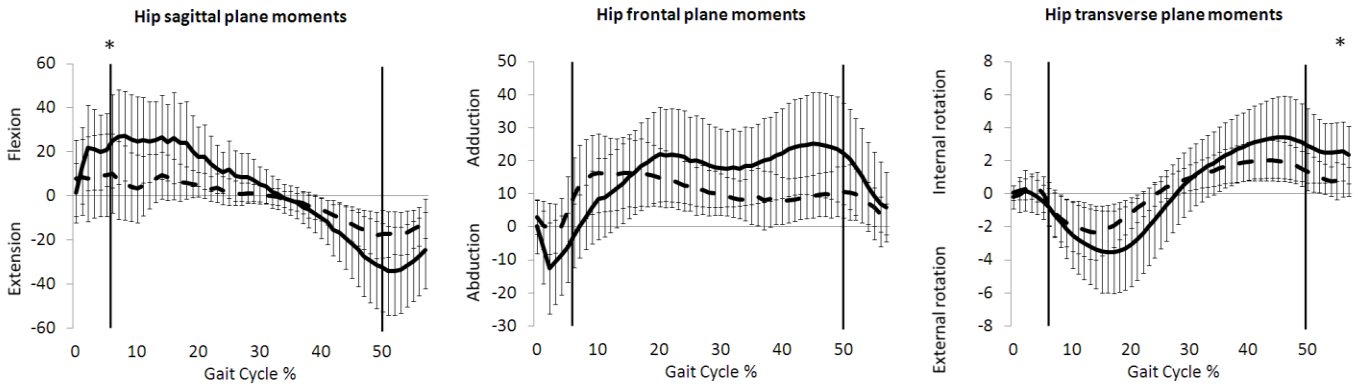

Figure 8.15. Mean ± SD of Hip moments in the sagittal, frontal and transverse planes in the five participants with the higher %FM (black line) and the five participants with the lowest %FM (dash line) to represent the association between hip moment and %FM over the gait cycle. * denotes points of the gait where significant association between %FM and hip moment was found

8.4.4.2 Lower Limb Joint Moments -Knee

Three principle components, with eigenvalues greater than one, accounting for 66.52% of the variance in knee joint sagittal moments were identified, shown in Table 8.26. The first component consisted of knee sagittal moments in mid stance. The second component of knee sagittal moments consisted of moments in early stance. The third component consisted of knee sagittal moments at ipsilateral toe-off.

Three principle components with eigenvalues greater than one, accounting for 69.73% of the variance in knee joint frontal moments were identified, shown in Table 8.26. The first component consisted of knee frontal moments in midstance. The second component consisted of peak knee frontal moments in DS1 (double support phase 1). The third component consisted of knee frontal moments at ipsilateral toe-off.

Three principle components with eigenvalues greater than one, accounting for 69.80% of the variance in hip transverse moments were identified, shown in Table 8.26. The first component consisted of knee transverse moments during mid-stance. The second component consisted of knee transverse moments during early stance. No rotation loading was considered great enough (>0.722) to contribute to the third component therefore, this component was not analysed further.

Table 8.26. Principle component analysis of knee moment. Variables >0.722 and <0.722 considered as contributing to each component and denoted by *

	Component (variance explained)								
	Sagittal			Frontal			Transverse		
	1 (31.25%)	2 (20.80%)	3 (14.47%)	1 (37.98%	2 (17.43%)	3 (14.32%)	1 (30.44%)	2 (24.10%)	3 (15.26%)
DS1 sag Min (Nm)	-.040	.833*	-.080						
SS1 sag Min (Nm)	.383	.795*	-.049						
SS1 sag Max (Nm)	.858*	-.293	-.030						
Sag IIC (Nm)	.083	-.394	-.082						
Sag CTO (Nm)	.834*	.186	.020						
Sag CIC (Nm)	.481	.454	.245						
Sag ITO (Nm)	.031	.012	.976*						
DS1 fro Min (Nm)				-.082	.897*	.090			
SS1 fro Min (Nm)				.594	.610	-.192			
SS1 fro Max (Nm)				.902*	-.091	-.012			
Fro IIC (Nm)				-.080	.087	.623			
Fro CTO (Nm)				.881*	-.039	.078			
Fro CIC (Nm)				.705	.385	-.245			
Fro ITO (Nm)				.032	-.102	.760*			
DS1 tra Max (Nm)							.260	.447	.539
SS1 tra Min (Nm)							.137	.815*	-.200
SS1 tra Max (Nm)							.951*	.076	.095
Tra IIC (Nm)							-.106	-.018	.715
Tra CTO (Nm)							-.029	.886*	.123
Tra CIC (Nm)							.947*	.023	-.017
Tra ITO (Nm)							-.214	.393	-.514

The model summary for each principle component regression score is shown in Table 8.27. For sagittal knee moments, the predictor variables explain 20% of the variation in regression score (model) 1, 23% of model 2 and 7% of model 3. For frontal knee moments, the predictor variables explain 32% of the variation in regression score (model) 1, 17% of model 2 and 9% of model 3. For transverse hip moments, the predictor variables explain 38% of the variation in regression score (model) 1 and 9% of model 2.

Table 8.27. Model Summary of principle component knee moments regression scores with predictors; Predictors: (Constant), age, height, BMI Z-Score, stance phase duration, step length, velocity, step width and total single support duration

Regression Score Model	r	r Square	Adjusted r Square	Std. Error of the Estimate
Sagittal				
1	.450	.203	.181	0.91
2	.474	.225	.204	0.89
3	.256	.065	.040	0.98
Frontal				
1	.566	.321	.302	0.84
2	.408	.166	.143	0.93
3	.297	.088	.063	0.97
Transverse				
1	.617	.381	.364	0.80
2	.294	.086	.061	0.97

The linear regression coefficients for the three principle components (models) of knee sagittal moments are shown in Table A10.17. In model 1; BMI Z-Score, height, step length and step width were significantly associated with the regression score model. In model 2; height, step length and velocity were significantly associated with the regression model. In model 3; height, step length and velocity were significantly associated with the regression model.

The three principle components (models) of knee frontal moments are shown in Table A10.17. In model 1; BMI Z-Score, height, %FM, step length and step width were significantly associated with the regression score model. In model 2; height, age, BMI Z-Score, and %FM were significantly associated with the regression score model. In model 3; height and velocity were significantly associated with the regression score model.

The two principle components (models) of knee transverse moments are shown in Table A10.17. In model 1; age, BMI Z-Score, velocity, step width and total single support duration were significantly associated with the regression score model. In model 2; stance phase duration, step length and velocity were significantly associated with the regression score model.

Table A10.18 shows the outputs for knee moment sagittal, frontal and transverse components. For sagittal moments, model 1 showed step length and height were associated with the regression score; model 2 showed height was significantly associated with the regression score; model 3 height, step length and velocity were significantly associated with the regression score.

For knee frontal moments, model 1 showed height, %FM and step length to be significantly associated with the regression score; model 2 showed BMI Z-Score, height was significantly associated with the regression score; model 3 showed no predictor variables were significantly associated with the regression score.

For transverse moments; model 1 showed BMI Z-Score was significantly associated with the regression score; model 2 showed no predictor variables were significantly associated with the regression score.

Only model 1 of frontal knee moments was significantly associated with %FM and so were analysed further. Table 8.28 shows the variables that comprised model 1; knee moments that knee peak maximum frontal moment in SS1 (double support phase 1) (predictor variables explained 36% of variance) and knee frontal moments at contralateral toe-off (predictor variables explained 29% of variance).

Table 8.28. Model Summary of knee moments at gait cycle events and peaks with predictors; Predictors: (Constant), age, height, BMI Z-Score, stance phase duration, step length, velocity, step width and total single support duration

Regression Score Model	r	r Square	Adjusted r Square	Std. Error of the Estimate
SS1 fro Max (Nm)	.602	.362	.345	8.45
Fro CTO (Nm)	.539	.290	.270	8.37

Linear regression coefficients for knee frontal moments maximum peak in SS1 (single support phase 1) and at contralateral toe-off are shown in Table A10.19. Height, age, BMI Z-Score, %FM, stance phase duration, step length, step width and total single support duration were significantly associated peak maximum frontal knee moment in SS1. BMI Z-Score, step length and step width were significantly associated with frontal knee moments at contralateral toe-off.

Table A10.20 shows the results of mixed model regression analysis on knee frontal moment models. Percentage body fat mass was significantly associated with peak knee frontal moment during SS1. Height and stance phase duration were also significantly associated with peak knee frontal moment during SS1.

Table 8.29 and Figure 8.16 report the linear regression of %FM with peak frontal knee moment during SS1 (single support phase 1). The results demonstrated that boys with a higher %FM showed significantly greater peak knee adduction moments in SS1.

Table 8.29.Mean (95% confidence intervals) of Knee frontal plane variables significantly associated with %FM, range over the sample population

Knee	Joint moment	Gait parameter (% of gait cycle)	Highest %FM (95%CI)	Lowest %FM (95%CI)
Frontal	Peak Adduction	SS 1 (15.14 ± 10.65%)	1.30Nm (0.44Nm)	-0.97Nm (0.46Nm)

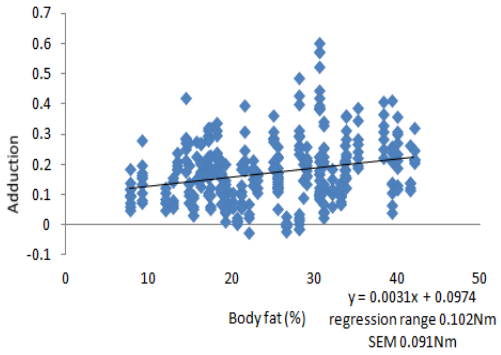

Figure 8.16. Scatter plot of significant associations between body fat mass and peak knee adduction moment during SS1

The association between knee moments and %FM is shown in Figure 8.17. The five participants with the highest and five participants with lowest %FM are reported to represent the association across the range of %FM.

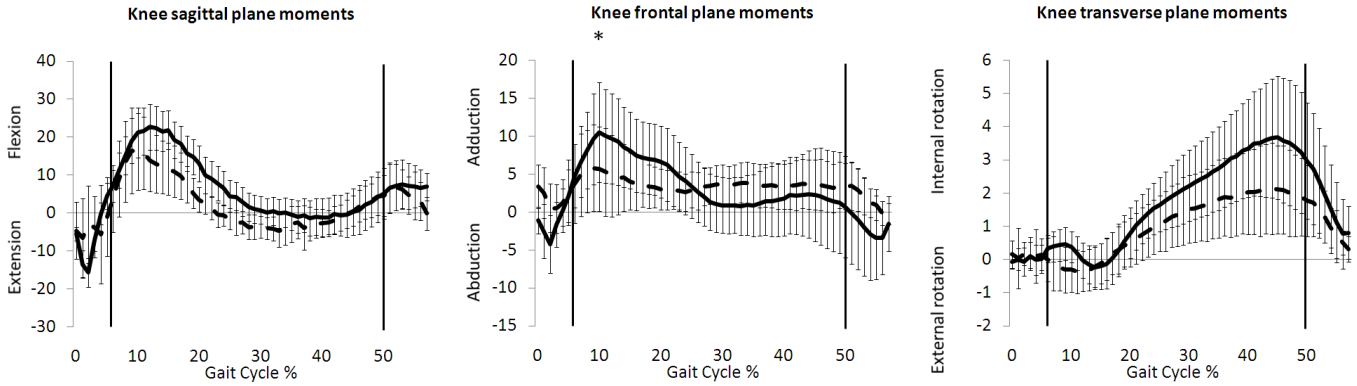

Figure 8.17. Mean ± SD of Knee moments in the sagittal, frontal and transverse planes in the five participants with the higher %FM (black line) and the five participants with the lowest %FM (dash line) to represent the association between knee moment and %FM over the gait cycle. * denotes points of the gait where significant association between %FM and knee moment was found

8.4.4.3 Lower Limb Joint Moments -Ankle

Two principle components, with eigenvalues greater than one, accounting for 67.54% of the variance in ankle joint sagittal moments were identified, shown in Table 8.30. The first component consisted of ankle sagittal moments in midstance. The second component consisted of ankle sagittal moments in early stance.

Two principle components with eigenvalues greater than one, accounting for 69.16% of the variance in ankle joint frontal moments were identified, shown in Table 8.30. The first component consisted of ankle frontal moments in midstance. The second component consisted of ankle frontal moments in early and late stance.

Three principle components with eigenvalues greater than one, accounting for 70.79% of the variance in ankle transverse moments were identified, shown in Table 8.30. The first component consisted of ankle transverse moments during mid-stance. The second component consisted of ankle transverse moments during early stance. The third component of ankle transverse moments consisted of moments at ipsilateral initial contact.

Table 8.30. Principle component analysis of ankle moments. Variables >0.722 and <0.722 considered as contributing to each component and denoted by *

	Component (variance explained)						
	Sagittal		Frontal		Transverse		
	1 (37.14%)	2 (30.40%)	1 (49.60%)	2 (19.56%)	1 (32.87%)	2 (21.06%)	3 (16.86%)
DS1 sag Min (Nm)	-.276	.800*					
SS1 sag Max (Nm)	.964*	-.038					
Sag IIC (Nm)	-.118	.662					
Sag CTO (Nm)	.119	.854*					
Sag CIC (Nm)	.950*	-.115					
Sag ITO (Nm)	-.335	-.426					
DS1 fro Max (Nm)			.557	.518			
SS1 fro Min (Nm)			.827*	.281			
DS2 fro Max (Nm)			.798*	-.005			
Fro IIC (Nm)			.032	.907*			
Fro CTO (Nm)			.711	.393			
Fro CIC (Nm)			.899*	-.017			
Fro ITO (Nm)			.123	.746*			
DS1 tra Max (Nm)					.164	.734*	.048
SS1 tra Max (Nm)					.951*	.074	.015
Tra IIC (Nm)					-.086	.163	.899*
Tra CTO (Nm)					-.063	.787*	-.012
Tra CIC (Nm)					.933*	.058	.041
Tra ITO (Nm)					-.352	.280	-.476

The model summary for each principle component regression score is shown in Table 8.31. For sagittal ankle moments, the predictor variables explained 76% of the variation in regression score (model) 1 and 8% of model 2. For frontal ankle moments, the predictor variables explained 5% of the variation in regression score (model) 1 and 12% of model 2. For transverse ankle moments, the predictor variables explained 34% of the variation in regression score (model) 1, 13% of model 2 and 6% of model 3.

Table 8.31. Model Summary of principle component ankle moments regression scores with predictors; Predictors: (Constant), age, height, BMI Z-Score, stance phase duration, step length, velocity, step width and total single support duration

Regression Score Model	r	r Square	Adjusted r Square	Std. Error of the Estimate
Sagittal				
1	.873	.763	.756	0.49
2	.287	.082	.057	0.97
Frontal				
1	.218	.047	.021	0.99
2	.344	.118	.094	0.95
Transverse				
1	.582	.338	.320	0.82
2	.364	.133	.109	0.94
3	.241	.058	.032	0.98

The linear regression coefficients for the two principle components (models) of ankle sagittal moments are shown in Table A10.21. In model 1; BMI Z-Score, height, stance phase duration and total single support duration were significantly associated with the regression score model. In model 2; height, %FM, and stance phase duration were significantly associated with the regression model.

The two principle components (models) of ankle frontal moments are shown in Table A10.21. In model 1; only age was significantly associated with the regression score model. In model 2; height, age, BMI Z-Score, and stance phase duration were significantly associated with the regression score model.

The three principle components (models) of ankle transverse moments are shown in Table A10.21. In model 1; height, age and BMI Z-Score were significantly associated with the regression score model. In model 2; %FM, step length and velocity were significantly associated with the regression score model. In model 3; BMI Z-Score and step width were significantly associated with the regression score model.

Table A10.22 shows the outputs for ankle moment sagittal, frontal and transverse components. For sagittal moments, model 1 showed BMI Z-Score and height were associated with the regression score; model 2 showed stance phase duration was significantly associated with the regression score.

For ankle frontal moments, model 1 showed no predictor variables were significantly associated with the regression score; model 2 showed age, BMI Z-Score, height and stance phase duration were significantly associated with the regression score.

For transverse moments; model 1 showed BMI Z-Score was significantly associated with the regression score; model 2 showed velocity was significantly associated with the regression score; model 3 showed BMI Z-Score and step width were significantly associated with the regression score.

No model for 3D ankle moments was significantly associated with %FM and so no further analysis was carried out. Figure 8.18 reports 3D ankle moments of the five participants with the highest and five participants with lowest %FM are reported to represent the association across the range of %FM.

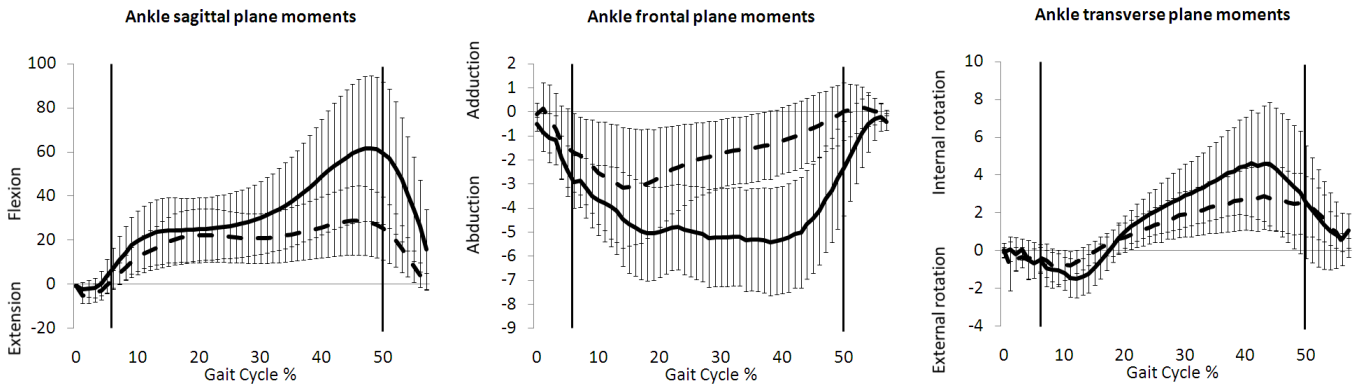

Figure 8.18. Mean ± SD of Ankle moments in the sagittal, frontal and transverse planes in the five participants with the higher %FM (black line) and the five participants with the lowest %FM (dash line) to represent the association between ankle moment and %FM over the gait cycle.

8.4.5.1 Foot Joint Angles - Shank-Calcaneus

Three principle components, with Eigenvalues greater than one, accounting for 92.36% of the variance in 3D shank-calcaneus joint motion were identified, shown in Table 8.32. The first component consisted of sagittal plane shank-calcaneus motion variables explaining 41.42% of the variance in 3D shank-calcaneus joint motion. The second component consisted of frontal plane shank-calcaneus motion variables explaining 30.16% of the variance in 3D shank-calcaneus joint motion. The third component consisted of transverse plane shank-calcaneus motion variables explaining 20.79% of the variance in 3D shank-calcaneus joint motion.

Table 8.32. Principle component analysis of shank-calcaneus angle. Variables >0.722 and <0.722 considered as contributing to each component and denoted by *

	Component (variance explained)		
	1 (41.42%)	2 (30.16%)	3 (20.79%)
DS 1 sag Min (deg.)	.924*	-.093	-.062
SS 1 sag Max (deg.)	.961*	-.028	-.106
DS 2 sag Min (deg.)	.939*	-.013	-.094
DS 2 sag Max (deg.)	.945*	.001	-.091
DS 1 fro Min (deg.)	-.027	.984*	.094
SS 2 fro Min (deg.)	-.029	.983*	.133
SS 2 fro Max (deg.)	-.045	.980*	.121
SS 1 tra Min (deg.)	-.091	.103	.961*
SS 2 tra Min (deg.)	-.032	.147	.941*
Sag IIC (deg.)	.921*	-.076	-.067
Sag CTO (deg.)	.909*	-.097	-.051
Sag CIC (deg.)	.945*	.001	-.092
Sag ITO (deg.)	.939*	-.013	-.094
Fro IIC (deg.)	-.034	.981*	.124
Fro CTO (deg.)	-.031	.982*	.088
Fro CIC (deg.)	-.093	.978*	.108
Fro ITO (deg.)	-.046	.976*	.125
Tra IIC (deg.)	-.057	.121	.946*
Tra CTO (deg.)	-.095	.117	.956*
Tra CIC (deg.)	-.158	.068	.934*
Tra ITO (deg.)	-.129	.149	.913*

The model summary for each principle component regression score is shown in Table 8.33. The predictor variables explain only 12% of the variation in regression score model 1, 17% of model 2 and 35% of model 3.

Table 8.33. Model Summary of principle component regression scores of shank-calcaneus angle with predictors; Predictors: (Constant), age, height, BMI Z-Score, stance phase duration, step length, velocity, step width and total single support duration

Regression Score Model	r	r Square	Adjusted r Square	Std. Error of the Estimate
1	.343	.117	.106	0.95
2	.409	.167	.156	0.92
3	.595	.353	.345	0.81

The linear regression coefficients for the three principle components (models) of 3D shank-calcaneus angles are shown in Table A10.23. In model 1; BMI Z-Score, %FM, stance phase duration, step length, step width and total single support duration were significantly associated with the regression score model. In model 2; height, age, BMI Z-Score, %FM, step length and velocity were significantly associated with the regression model. In model 3; height, age, BMI Z-Score, %FM, step length, velocity and total single support duration were significantly associated with the regression model.

Following linear regression analysis on the regression scores models from the three principle components of 3D shank-calcaneus angles mixed model regression was then applied to determine the effects of the predictor variables on the model. Table A10.24 shows the outputs for the three models. In model 1 no predictor variables were significantly associated the regression score. In model 2, BMI Z-Score was significantly associated with the regression score. In model 3, BMI Z-Score and %FM were significantly associated with the regression score.

Only the third regression score (model) was significantly associated with %FM and was analysed further. Table 8.34 shows the shank-calcaneus transverse plane variables that regression score (model) 3 was composed of; shank-calcaneus transverse peak minimum angle during SS1 (single support phase 1) (predictor variables explained 21% of variance), peak minimum angle during SS2 (swing phase) (predictor variables explained 22% of variance), angle at ipsilateral initial contact (predictor variables explained 36% of variance), contralateral toe-off (predictor variables explained 30% of variance), contralateral initial contact (predictor variables explained 34% of variance), ipsilateral toe-off (predictor variables explained 33% of variance). These were entered into their individual regression models to examine the amount variance explained by the predictor variables.

Table 8.34. Model Summary of shank-calcaneus angles at gait cycle events and peaks with predictors; Predictors: (Constant), age, height, BMI Z-Score, stance phase duration, step length, velocity, step width and total single support duration

Regression Score Model	r	r Square	Adjusted r Square	Std. Error of the Estimate
SS 1 tra Min (deg.)	.457	.209	.200	6.24
SS 2 tra Min (deg.)	.463	.215	.206	6.15
Tra IIC (deg.)	.598	.357	.349	6.00
Tra CTO (deg.)	.548	.300	.291	5.97
Tra CIC (deg.)	.583	.340	.332	5.97
Tra ITO (deg.)	.574	.330	.321	6.41

Linear regression coefficients for each model of shank-calcaneus transverse plane angle are shown in Table A10.25. Percentage fat mass (%FM) was significantly associated with; peak minimum angle during SS1, angle at ipsilateral initial contact, contralateral toe-off, contralateral initial contact, ipsilateral toe-off. Therefore, each model was assessed in mixed model regression analysis to determine the combined effects of the predictor variables.

Table A10.26 shows the results of mixed model regression analysis on the shank-calcaneus transverse plane angle models. Percentage fat mass (%FM) was significantly associated with

shank-calcaneus transverse plane angle at ipsilateral initial contact, contralateral toe-off, contralateral initial contact and ipsilateral toe-off. Stance phase duration was also significantly associated with shank-calcaneus transverse at ipsilateral initial contact. BMI Z-Score was also significantly associated with shank-calcaneus transverse at ipsilateral toe-off.

Table 8.35 and Figure 8.19 report the linear regression of %FM with the significantly associated shank-calcaneus transverse plane variables. The results demonstrated that boys with higher %FM have; a lower adduction angle at ipsilateral initial contact and contralateral toe-off; and greater abduction at contralateral initial contact and ipsilateral toe off.

Table 8.35. Mean (95% confidence intervals) of Shank-calcaneus transverse plane variables significantly associated with %FM, range over the sample population

S-C	Joint motion	Gait parameter (% of gait cycle)	Highest %FM (95%CI)	Lowest %FM (95%CI)
Transverse	Adduction	Ipsilateral Initial contact (0%)	-4.58° (1.07°)	-12.81° (1.31°)
	Adduction	Contralateral toe off (7.63% ± 2.27%)	-7.29° (1.03°)	-14.76° (1.25°)
	Abduction	Contralateral initial contact (49.80 ± 1.96%)	0.88° (1.04°)	-7.80° (1.28°)
	Abduction	Ipsilateral toe off (57.47 ± 2.20%)	0.98° (1.13°)	-6.62° (1.38°)

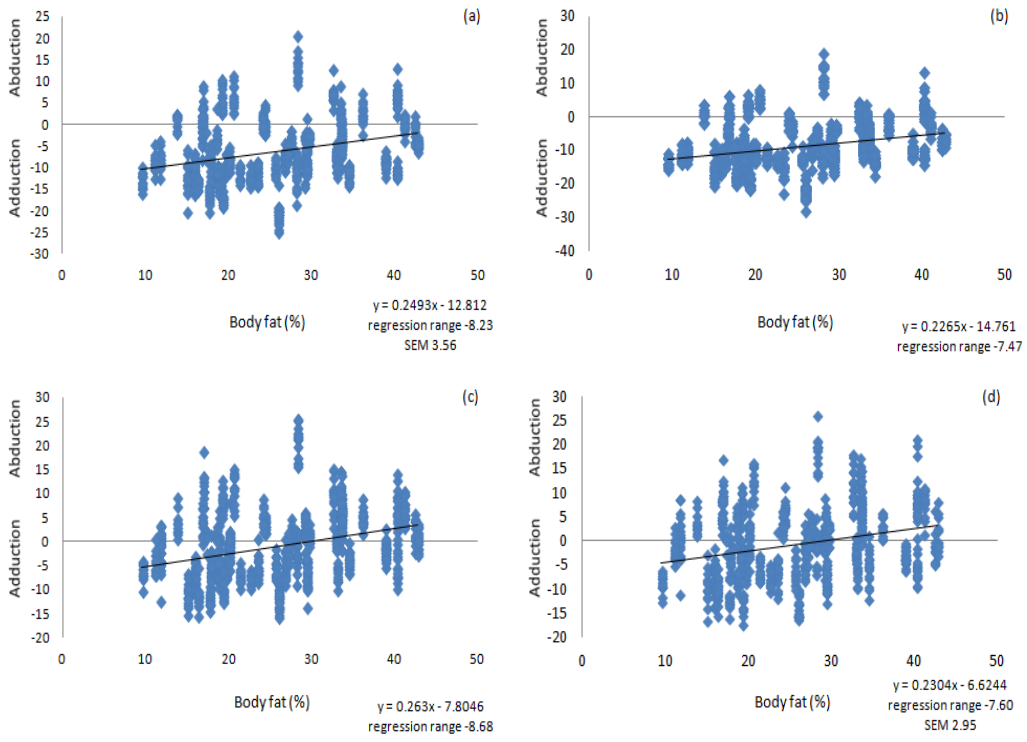

Figure 8.19. Scatter plot of significant association between body fat mass and shank-calcaneus; (a) adduction at IIC, (b) adduction at CTO, (c) abduction at CIC, and (d) abduction at ITO

The association between shank-calcaneus motion and %FM is shown in Figure 8.20. The five participants with the highest and five participants with lowest %FM are reported to represent the association across the range of %FM.

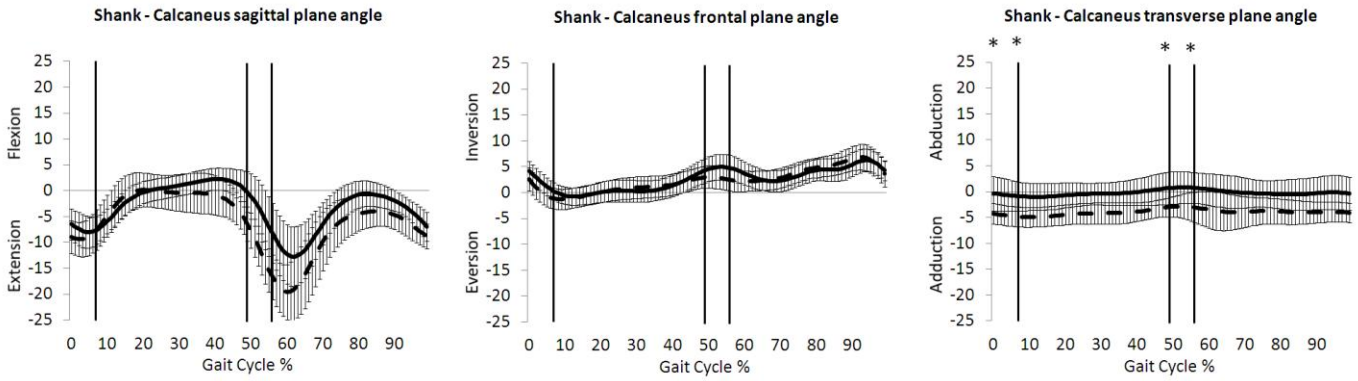

Figure 8.20. Mean ± SD of Shank-calcaneus angular motion in the sagittal, frontal and transverse planes in the five participants with the higher %FM (black line) and the five participants with the lowest %FM (dash line) to represent the association between shank-calcaneus angle and %FM over the gait cycle. * denotes points of the gait where significant association between %FM and shank-calcaneus angle was found

8.4.5.2 Foot Joint Angles - Calcaneus-Midfoot

Three principle components, with eigenvalues greater than one, accounting for 91.19% of the variance in 3D calcaneus-midfoot joint motion were identified, shown in Table 8.36. The first component consisted of transverse plane calcaneus-midfoot motion variables explaining 41.69% of the variance in 3D calcaneus-midfoot joint motion. The second component consisted of sagittal plane calcaneus-midfoot motion variables explaining 31.63% of the variance in 3D calcaneus-midfoot joint motion. The third component consisted of frontal plane calcaneus-midfoot motion variables explaining 17.87% of the variance in 3D calcaneus-midfoot joint motion.

Table 8.36. Principle component analysis of calcaneus-midfoot angle. Variables >0.722 and <0.722 considered as contributing to each component and denoted by *

	Component (variance explained)		
	1 (41.69%)	2 (31.63%)	3 (17.87%)
DS 1 sag Min (deg.)	-.030	.948*	-.114
SS 1 sag Min (deg.)	-.065	.935*	-.100
SS 2 sag Min (deg.)	-.036	.912*	-.058
SS 2 sag Max (deg.)	.077	.912*	-.121
DS 1 fro Max (deg.)	.190	-.147	.932*
SS 2 fro Min (deg.)	.182	-.061	.940*
SS 2 fro Max (deg.)	.197	-.140	.932*
DS 1 tra Min (deg.)	.961*	.003	.159
SS 1 tra Max (deg.)	.965*	-.021	.126
SS 2 tra Min (deg.)	.946*	.018	.192
SS 2 tra Max (deg.)	.928*	.022	.223
Sag IIC (deg.)	.002	.938*	-.137
Sag CTO (deg.)	.005	.941*	-.152
Sag CIC (deg.)	.094	.928*	-.121
Sag ITO (deg.)	.095	.895*	-.048
Fro IIC (deg.)	.143	-.114	.944*
Fro CTO (deg.)	.124	-.112	.939*
Fro CIC (deg.)	.129	-.141	.951*
Fro ITO (deg.)	.165	-.120	.939*
Tra IIC (deg.)	.962*	.038	.129
Tra CTO (deg.)	.965*	.033	.144
Tra CIC (deg.)	.963*	.013	.130
Tra ITO (deg.)	.952*	.045	.111

The model summary for each principle component regression score is shown in Table 8.37. The predictor variables explain only 17% of the variation in regression score model 1, 33% of model 2 and 18% of model 3.

Table 8.37. Model Summary of principle component regression scores of calcaneus-midfoot angle with predictors; Predictors: (Constant), age, height, BMI Z-Score, stance phase duration, step length, velocity, step width and total single support duration

Regression Score Model	r	r Square	Adjusted r Square	Std. Error of the Estimate
1	.411	.169	.158	0.92
2	.570	.325	.317	0.83
3	.428	.183	.173	0.91

The linear regression coefficients for the three principle components (models) of 3D calcaneus-midfoot angles are shown in Table A10.27. In model 1; age, BMI Z-Score, %FM, step length, step width and were significantly associated with the regression score model. In model 2; age, BMI Z-Score, %FM, step length and velocity were significantly associated with the regression model. In model 3; height, age, BMI Z-Score, %FM, stance phase duration and velocity were significantly associated with the regression model.

Following linear regression analysis on the regression scores models from the three principle components of 3D calcaneus-midfoot angles mixed model regression was then applied to determine the effects of the predictor variables on the model. Table A10.28 shows the outputs for the three models. In model 1 no predictor variables were significantly associated the regression score. In model 2, BMI Z-Score and %FM were significantly associated with the regression score. In model 3, BMI Z-Score and %FM were significantly associated with the regression score.

The second and third regression scores (models) were significantly associated with %FM and were analysed further. Table 8.38 shows the calcaneus-midfoot sagittal plane variables that regression score (model) 2 was composed of; calcaneus-midfoot sagittal peak minimum angle during DS1 (double support phase 1) (predictor variables explained 32% of variance), peak minimum angle during SS1 (single support 1) (predictor variables explained 30% of variance), peak minimum angle during SS2 (swing phase) (predictor variables explained 28% of variance), peak maximum angle during SS2 (swing phase) (predictor variables explained 26% of variance), angle at ipsilateral initial contact (predictor variables explained 29% of variance), contralateral toe-off (predictor variables explained 28% of variance), contralateral initial contact (predictor variables explained 31% of variance), ipsilateral toe-off (predictor variables explained 31% of variance).

Table 8.38 also shows calcaneus-midfoot frontal plane variables that regression score (model) 3 was composed of; calcaneus-midfoot frontal peak maximum angle during DS1 (double support phase 1) (predictor variables explained 23% of variance), peak minimum angle during SS2 (swing phase) (predictor variables explained 23% of variance), peak maximum angle during SS2 (swing phase) (predictor variables explained 19% of variance), angle at ipsilateral initial contact (predictor variables explained 22% of variance), contralateral toe-off (predictor variables explained 24% of variance), contralateral initial contact (predictor variables explained 25% of variance), ipsilateral toe-off (predictor variables explained 22% of variance). All calcaneus-midfoot sagittal and frontal plane variables were entered into their individual regression models to examine the amount variance explained by the predictor variables.

Table 8.38. Model Summary of calcaneus-midfoot angles at gait cycle events and peaks with predictors; Predictors: (Constant), age, height, BMI Z-Score, stance phase duration, step length, velocity, step width and total single support duration

Regression Score Model	r	r Square	Adjusted r Square	Std. Error of the Estimate
DS 1 sag Min (deg.)	.568	.323	.306	6.25
SS 1 sag Min (deg.)	.544	.296	.287	6.33
SS 2 sag Min (deg.)	.533	.284	.274	6.60
SS 2 sag Max (deg.)	.512	.263	.253	6.00
Sag IIC (deg.)	.541	.293	.284	5.77
Sag CTO (deg.)	.532	.283	.274	5.82
Sag CIC (deg.)	.558	.311	.302	6.42
Sag ITO (deg.)	.552	.305	.296	6.13
DS 1 fro Max (deg.)	.476	.227	.217	6.01
SS 2 fro Min (deg.)	.481	.232	.222	6.03
SS 2 fro Max (deg.)	.433	.187	.177	6.48
Fro IIC (deg.)	.471	.222	.212	6.37
Fro CTO (deg.)	.489	.239	.229	5.95
Fro CIC (deg.)	.504	.254	.245	6.03
Fro ITO (deg.)	.472	.223	.213	6.48

Linear regression coefficients for each model of calcaneus-midfoot sagittal and frontal plane angle are shown in Table A10.29. Percentage fat mass (%FM) was significantly associated with; sagittal peak minimum angle during SS2 (swing phase), peak maximum angle during SS2 (swing phase), contralateral initial contact and ipsilateral toe-off in the sagittal plane.

Percentage fat mass (%FM) was significantly associated with; frontal peak maximum angle during DS1, peak minimum angle during SS2 (swing phase), angle at ipsilateral initial contact, contralateral toe-off, contralateral initial contact, ipsilateral toe-off in the frontal plane. All calcaneus-midfoot sagittal and frontal plane variables, associated with %FM, were assessed in mixed model regression analysis to determine the combined effects of the predictor variables.

Table A10.30 shows the results of mixed model regression analysis on the calcaneus-midfoot sagittal and frontal plane angle models. Percentage fat mass (%FM) was significantly associated with calcaneus-midfoot sagittal plane peak maximal angle during SS2 (swing phase), contralateral initial contact and ipsilateral toe-off. Velocity was also significantly associated with calcaneus-midfoot sagittal plane peak maximal angle during SS2 (swing phase). BMI Z-Score was also significantly associated calcaneus-midfoot sagittal angle at ipsilateral toe-off.

Percentage fat mass (%FM) was significantly associated with calcaneus-midfoot frontal plane peak maximum angle during DS1 (double support 1). Age and BMI Z-Score were also significantly associated calcaneus-midfoot frontal plane peak maximum angle during DS1 (double support 1).

Table 8.39 and Figures 8.21 and 8.22 report the linear regression of %FM with the significantly associated calcaneus-midfoot sagittal and frontal plane variables. The results demonstrated

that boys with higher %FM have; greater dorsiflexion at contralateral initial contact and ipsilateral toe off and greater peak dorsiflexion during SS2 in the sagittal plane. In the frontal plane greater peak eversion angle during DS1 was found in boys with greater %FM.

Table 8.39. Mean (95% confidence intervals) of Calcaneus-midfoot sagittal and frontal plane variables significantly associated with %FM, range over the sample population

C-M	Joint motion	Gait parameter (% of gait cycle)	Highest %FM (95%CI)	Lowest %FM (95%CI)
Sagittal	Dorsiflexion	Contralateral initial contact (49.80 ± 1.96%)	19.86° (1.02°)	-6.06° (1.24°)
	Plantarflexion	Ipsilateral toe off (57.47 ± 2.20%)	0.39° (0.97°)	-12.40° (1.19°)
	Peak dorsiflexion	SS2 (89.41± 13.31%	4.72° (0.94°)	-6.67° (1.15°)
Frontal	Peak eversion	DS1 2.18 ± 2.75%	-2.19° (1.01°)	1.66° (1.24°)

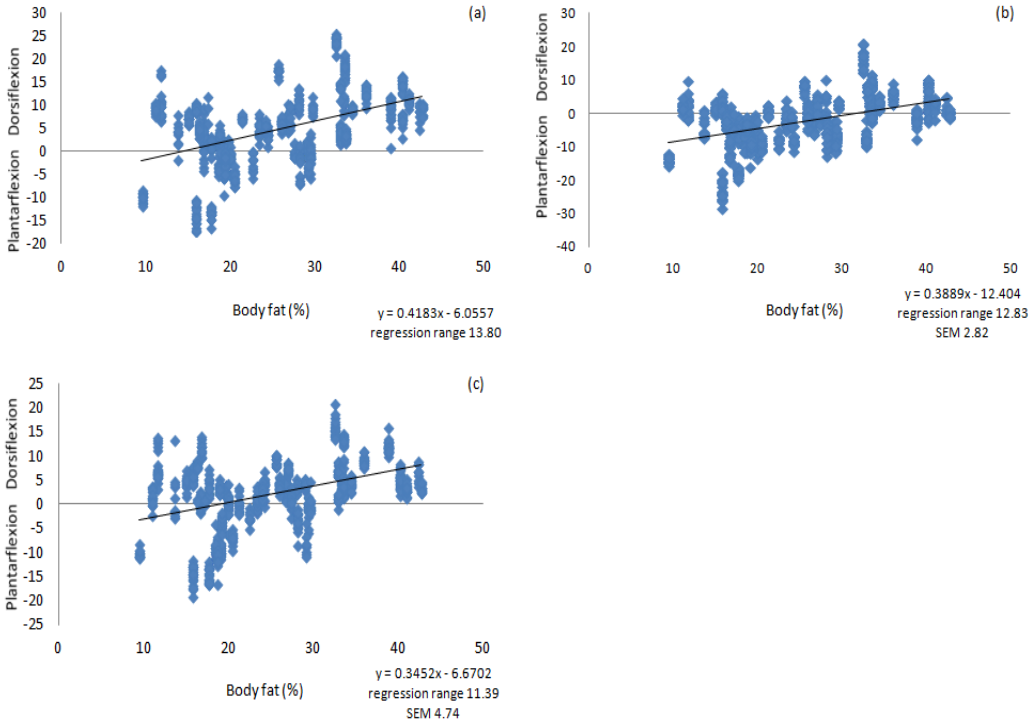

Figure 8.21. Scatter plot of significant association between body fat mass and calcaneus-midfoot; (a) dorsiflexion at CIC, (b) plantarflexion at ITO, (c) peak dorsiflexion during SS2,

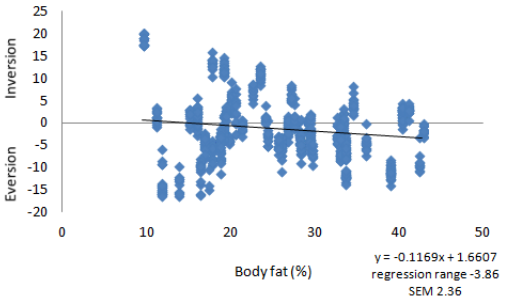

Figure 8.22. Scatter plot of significant association between body fat mass and calcaneus-midfoot peak eversion during DS1

The association between calcaneus-midfoot motion and %FM is shown in Figure 8.23. The five participants with the highest and five participants with lowest %FM are reported to represent the association across the range of %FM.

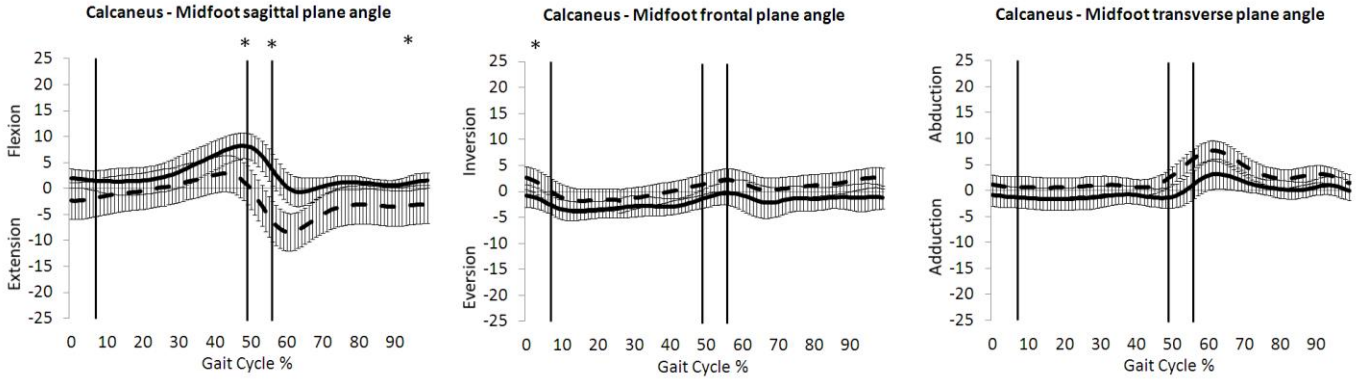

Figure 8.23. Mean ± SD of Calcaneus-midfoot angular motion in the sagittal, frontal and transverse planes in the five participants with the higher %FM (black line) and the five participants with the lowest %FM (dash line) to represent the association between calcaneus-midfoot angle and %FM over the gait cycle. * denotes points of the gait where significant association between %FM and calcaneus-midfoot angle was found

8.4.5.3 Foot Joint Angles - Midfoot-Metatarsals

Three principle components, with eigenvalues greater than one, accounting for 96.75% of the variance in 3D midfoot-metatarsals joint motion were identified, shown in Table 8.40. The first component consisted of frontal plane midfoot-metatarsals motion variables explaining 43.96% of the variance in 3D midfoot-metatarsals joint motion. The second component consisted of transverse plane midfoot-metatarsals motion variables explaining 33.06% of the variance in 3D midfoot-metatarsals joint motion. The third component consisted of sagittal plane midfoot-metatarsals motion variables explaining 19.72% of the variance in 3D midfoot-metatarsals joint motion.

Table 8.40. Principle component analysis of midfoot-metatarsals angle. Variables >0.722 and <0.722 considered as contributing to each component and denoted by *

	Component (variance explained)		
	1 (43.96%)	2 (33.06%)	3 (19.72%)
DS 1 sag Min (deg.)	-.187	-.014	.976*
SS 1 sag Max (deg.)	-.166	.004	.980*
DS 2 sag Max (deg.)	-.151	-.006	.978*
DS 1 fro Max (deg.)	.970*	-.085	-.134
SS 1 fro Min (deg.)	.965*	-.118	-.161
SS 1 fro Max (deg.)	.969*	-.106	-.153
DS 2 fro Min (deg.)	.967*	-.036	-.188
SS 2 fro Max (deg.)	.964*	-.100	-.126
DS 1 tra Min (deg.)	-.049	.985*	.014
SS 1 tra Min (deg.)	-.050	.983*	-.009
SS 1 tra Max (deg.)	-.080	.983*	-.045
DS 2 tra Max (deg.)	-.111	.966*	-.047
SS 2 tra Min (deg.)	-.074	.977*	.058
Sag IIC (deg.)	-.196	-.018	.972*
Sag CTO (deg.)	-.174	-.008	.976*
Sag CIC (deg.)	-.160	.003	.980*
Sag ITO (deg.)	-.165	-.010	.963*
Fro IIC (deg.)	.966*	-.089	-.139
Fro CTO (deg.)	.964*	-.093	-.138
Fro CIC (deg.)	.962*	-.084	-.185
Fro ITO (deg.)	.961*	-.004	-.181
Tra IIC (deg.)	-.047	.982*	.016
Tra CTO (deg.)	-.058	.980*	-.015
Tra CIC (deg.)	-.097	.973*	-.051
Tra ITO (deg.)	-.122	.957*	.036

The model summary for each principle component regression score is shown in Table 8.41. The predictor variables explain only 20% of the variation in regression score model 1, 14% of model 2 and 12% of model 3.

Table 8.41. Model Summary of principle component regression scores of midfoot-metatarsals angle with predictors; Predictors: (Constant), age, height, BMI Z-Score, stance phase duration, step length, velocity, step width and total single support duration

Regression Score Model	r	r Square	Adjusted r Square	Std. Error of the Estimate
1	.448	.201	.191	0.90
2	.372	.138	.127	0.93
3	.345	.119	.108	0.94

The linear regression coefficients for the three principle components (models) of 3D midfoot-metatarsals angles are shown in Table A10.31. In model 1; age, BMI Z-Score, %FM, stance phase duration, step length, velocity and step width were significantly associated with the regression score model. In model 2; height, age, BMI Z-Score, %FM, and step width were

significantly associated with the regression model. In model 3; height, BMI Z-Score, %FM, step length and velocity were significantly associated with the regression model.

Following linear regression analysis on the regression scores models, from the three principle components of 3D midfoot-metatarsals angles, mixed model regression was the applied to determine the effects of the predictor variables on the model. Table A10.32 shows the outputs for the three models. In model 1 no predictor variables were significantly associated the regression score. In model 2, BMI Z-Score was significantly associated with the regression score. In model 3, height was significantly associated with the regression score.

No model for 3D midfoot-metatarsals moments was significantly associated with %FM and so no further analysis was carried out. Figure 8.24 reports 3D midfoot-metatarsals moments of the five participants with the highest and five participants with lowest %FM are reported to represent the association across the range of %FM.

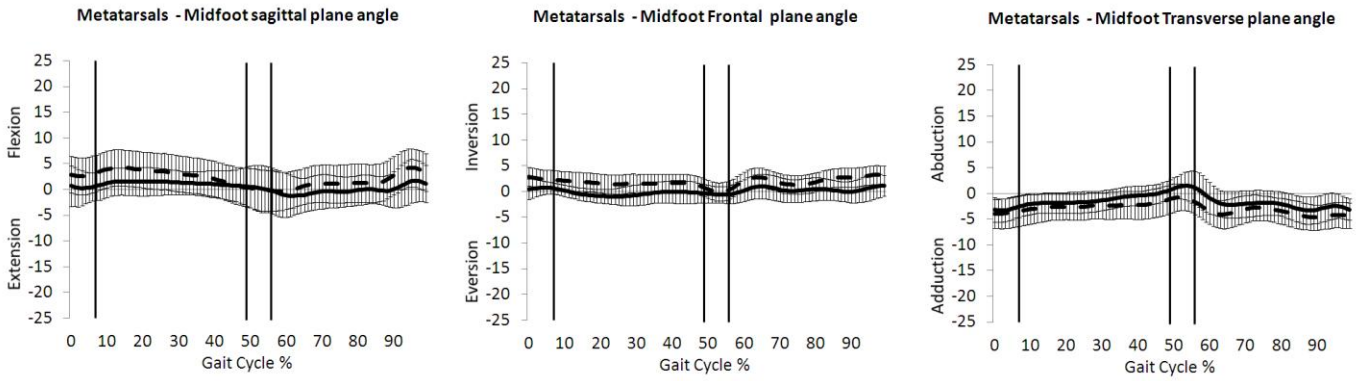

Figure 8.24. Mean ± SD of Midfoot-metatarsals angular motion in the sagittal, frontal and transverse planes in the five participants with the higher %FM (black line) and the five participants with the lowest %FM (dash line) to represent the association between midfoot-metatarsals angle and %FM over the gait cycle. * denotes points of the gait where significant association between %FM and midfoot-metatarsals angle was found

8.4.5.4 Foot Joint Angles - First Metatarsal-Phalanx

Two principle components, with eigenvalues greater than one, accounting for 80.65% of the variance in 3D first metatarsal-phalanx joint motion were identified, shown in Table 8.42. The first component consisted of sagittal plane first metatarsal-phalanx motion variables explaining 52.32% of the variance in 3D first metatarsal-phalanx joint motion. The second component consisted of transverse plane first metatarsal-phalanx motion variables explaining 28.34% of the variance in 3D first metatarsal-phalanx joint motion.

Table 8.42. Principle component analysis of first metatarsal-phalanx angle. Variables >0.722 and <0.722 considered as contributing to each component and denoted by *

	Component (variance explained)	
	1 (52.32%)	2 (28.34%)
SS 1 sag Min (deg.)	.907*	.190
DS 2 sag Max (deg.)	.933*	.013
SS 2 sag Min (deg.)	.895*	.149
SS 1 tra Max (deg.)	.175	.925*
DS 2 tra Min (deg.)	.117	.958*
SS 2 tra Min (deg.)	.552	.524
SS 2 tra Max (deg.)	.628	.404
Sag IIC (deg.)	.892*	.069
Sag CTO (deg.)	.900*	.139
Sag CIC (deg.)	.815*	.092
Sag ITO (deg.)	.929*	.013
Tra IIC (deg.)	.036	.878*
Tra CTO (deg.)	.102	.914*
Tra CIC (deg.)	.117	.943*
Tra ITO (deg.)	.125	.942*

The model summary for each principle component regression score is shown in Table 8.43. The predictor variables explain only 21% of the variation in regression score model 1, and 17% of model 2.

Table 8.43. Model Summary of principle component regression scores of first metatarsal-phalanx angle with predictors; Predictors: (Constant), age, height, BMI Z-Score, stance phase duration, step length, velocity, step width and total single support duration

Regression Score Model	r	r Square	Adjusted r Square	Std. Error of the Estimate
1	.456	.208	.198	0.90
2	.406	.165	.154	0.92

The linear regression coefficients for the two principle components (models) of sagittal and transverse plane first metatarsal-phalanx angles are shown in Table A10.33. In model 1; BMI Z-Score, %FM, stance phase duration, step length, velocity and step width were significantly associated with the regression score model. In model 2; height, age, BMI Z-Score and %FM, were significantly associated with the regression model.

Following linear regression analysis on the regression scores models from the two principle components of sagittal and transverse plane first metatarsal-phalanx angles mixed model regression was the applied to determine the effects of the predictor variables on the model. Table A10.34 shows the outputs for the two models. In model 1 BMI Z-Score was significantly associated the regression score. In model 2, no predictor variables were associated with the regression score.

No model for sagittal and transverse first metatarsal-phalanx angles were significantly associated with %FM and so no further analysis was carried out. Figure 8.25 reports sagittal and transverse plane first metatarsal-phalanx angles of the five participants with the highest and five participants with lowest %FM are reported to represent the association across the range of %FM.

Figure 8.25. Mean ± SD of First metatarsal-phalanx angular motion in the sagittal, frontal and transverse planes in the five participants with the higher %FM (black line) and the five participants with the lowest %FM (dash line) to represent the association between first metatarsal-phalanx angle and %FM over the gait cycle. * denotes points of the gait where significant association between %FM and first metatarsal-phalanx angle was found

8.5 Discussion

The aim of this study was to examine the association between adiposity with lower limb and foot biomechanics during the gait cycle in boys 7 to 11 years old. Few studies have examined the relationships between lower limb and foot biomechanics during the gait cycle with body fat mass (%FM). Previous studies to assess obesity and gait biomechanics found altered spatiotemporal characteristics which may confound the biomechanical effects of obesity on gait. The current study found associations between hip, knee, ankle, hindfoot and midfoot angular motion at gait cycle events and %FM. Furthermore, associations between hip and knee moments with %FM where also determined. The protocol utilised in the current study accounted for confounding affects of age, anthropometric and spatiotemporal characteristics on paediatric gait. The relationships between adiposity (%FM) with lower limb and foot biomechanics in the current study can be used to understand the impact of obesity on the musculoskeletal system in childhood.

8.5.1 Association between %FM with Age, Anthropometric and Spatiotemporal Confounding Variables

Obesity (BMI Z-score) was significantly associated with adiposity (%FM) in this sample of boys shown in Table 8.8. The r^2 of the linear relationship between %FM and BMI Z-Score was 0.63. This correlation was stronger than in the reliability study in experimental chapter 1 (chapter 5) (r^2 0.43), but is in line with previous findings (Federico et al., 2011). Previous studies have shown that fat mass and BMI demonstrate a higher correlation at higher %FM among children (Freedman et al., 2005). The relation of BMI to skinfold thickness has been shown to be very low in relatively thin boys (r=0.1) and moderate among fatter boys (r=0.58) (Schafer et al., 1998). The linear, rather than curvilinear, relationship between body fat mass and BMI Z-Score in this study can be explained by the relatively high mean %FM in this study (23.78%) compared to the reliability study in experimental chapter 1 (chapter 5) (21.73%). In the current study 62% of boys had a BMI Z-Score in excess of zero (zero indicates the mean BMI Z-Score in the reference population) which may explain the high correlation between BMI and Z-Score. Williams et al., (2007) found no relationship between BMI Z-Score and %FM (measured by BIA) in boys up to a BMI Z-Score of zero, but after zero the relationship increased steadily. BMI Z-Score remained significantly associated with %FM after adjustment for confounding predictor variables of height, stance phase duration and total single support phase.

The participants of the current study demonstrated a significant relationship between height and %FM, with taller participants having greater %FM. Figure 8.3 demonstrates the linear relationship between height and %FM in this sample with an r^2 value of 0.09, indicating that 9% of the variation in %FM is explained by height. Dietz (1998) reported that obese children are usually above average height for age. During childhood accelerations in height usually follow excessive weight gain (Burt Solorzano & McCartney, 2010). Height did not remain significantly associated with %FM when entered into mixed regression with BMI Z-Score, stance phase duration and total single support duration. This is because a tall stature is usually accompanied by increased lean body mass: increased skeletal size, muscle mass and advanced bone growth (Dietz, 1998). This highlighted why in the current study, the relationship between height and %FM was weak, although significant. The relationship between height and %FM may have been mediated through lean mass measured in BMI Z-Score. Therefore, when height was adjusted for BMI Z-Score the relationship was no longer significant, shown in Table 8.9.

Figure 8.4 shows that stance phase duration and total support phase duration were significantly associated with %FM in this sample population. Participants with higher %FM demonstrated longer stance phase duration, with approximately 24% of the variance in %FM explained by stance phase duration. Participants with higher %FM also demonstrated less total single support duration, with approximately 22% of the variation in %FM explained by total single support duration. Previous studies on childhood obesity and spatiotemporal characteristics of gait have also shown an increase in stance phase and reduction in single support phase (Hills & Parker 1991; Nantel et al., 2006; Morrison et al., 2008). DeVita and Hortobagyi (2003) reported no significant differences in step length and cadence when obese adults walked at the same speed as non-obese adults. However, swing time was significantly shorter and stance time remained significantly longer compared to the non-obese adults. This finding compares with the current study because there was no significant relationship between walking speed and step length with %FM, but significant relationships between stance phase duration and %FM. Stance phase duration is dependent on walking speed, with increases in walking speed reducing the amount of time spent in stance (Perry, 1992). However, because walking speed was not associated with %FM, participants with higher %FM may achieve similar walking speed to participants with lower %FM by altering limb progression in the swing phase.

Hills & Parker (1991) determined that the greater amount of time spent in double support was indicative of a safer and more tentative gait pattern increasing the capacity to stabilise the body. The relationship between stance phase duration and total single support duration may relate to kinematic and kinetic findings of the current study. Spryropoulos et al., (1991) attributed greater stance phase duration in obese adults to inadequate push-off due to decreased ankle plantar flexion of the ankle. Therefore, including stance phase duration and total single support time as predictor variables in the analysis may determine if altered lower limb biomechanics were related to %FM directly or mediated through the influence of %FM on the support phases of gait.

8.5.2 Lower Limb Kinematic and Kinetic Findings

8.5.2.1 Hip

Significantly greater hip flexion was found at the start and end of the stance phase in boys with greater adiposity, as shown in Table 8.13. Linear regression over the range of %FM showed

that participants with higher %FM demonstrated approximately 16^{o} more hip flexion at ipsilateral initial contact and 20^{o} more hip flexion at the end of the stance phase. This finding is in contrast to previous studies to examine hip motion in obese children (Hills & Parker, 1991; McMillan et al., 2010) and adults (Spyropoulos et al., 1991). McMillan et al., (2010) found that obese adolescents (defined as >95th BMI centile CDC) demonstrated less hip flexion at initial contact (18.01° ± 10.50° and 30.47° ± 9.62° for obese and healthy weight respectively). However, this study based hip joint centres on markers attached to the greater tronchanter which have been shown to be 1-2cm displaced in obese adults due to soft tissue mass (Hortobagyi et al., 2011). The misplacement of greater tronchanter markers in obese participants can orientate the thigh segment relative to the pelvis resulting in altered sagittal plane motion.

Other studies on obese gait have modelled the hip using a functional hip joint centre calculation (Shultz et al., 2009) or virtual ASIS markers (Board et al., 2012). Shultz et al., (2009) used ASIS markers and posterior superior iliac spine calibration markers to define the pelvis and rigid marker clusters to define the thigh segment. This study found that obese children (defined as >95th BMI centile CDC) walked with greater mean hip flexion at slow (30.86° ± 5.00° and 27.65° ± 5.91° for obese and healthy weight children respectively) and fast (130% normal cadence) walking speeds (34.54° ± 6.65° v 29.00° ± 5.87° for obese and healthy weight children respectively). These findings are in-line with the current study, which found hip flexion of 43.85° (95%CI 1.15°) for the highest and 27.83° (95%CI 1.31°) for the lowest adiposity at ipsilateral initial contact. It should be noted that Shultz et al., (2009) reported mean joint angles over the stance and swing phases rather than angles at events and peaks reported in the current study. By averaging joint angles the values will be smaller than the event and peak values reported in the current study meaning absolute joint angle values cannot be readily compared between the two studies. Board et al., (2012) found hip peak flexion and extension angles during the stance phase of gait to be altered by 11% from using virtual or skin mounted ASIS markers in obese adults. However, it is not clear whether the authors found increased hip flexion concurrent with the present study. The effects of soft tissue on correct marker placement appear to affect hip joint kinematics and may lead to different results when comparing obese and non-obese gait. The protocol of the current study used virtual markers which may have reduced soft tissue artefact meaning associations between adiposity and hip flexion could be revealed.

Large hip flexion at initial contact may relate to the significant finding of greater external hip flexor moments at contralateral toe-off in the boys with higher %FM. Sheehan & Gormley (2011) reported greater hip flexion at ipsilateral initial contact in overweight adults (BMI>25kg/m^2). The authors attributed hip flexion to hip extensor weakness reducing their role as anti-gravity muscles. In the current study, weaker hip extensors may contribute to greater external hip flexion moments in early stance due to more hip flexion placing the centre of mass anterior to the hip joint centre. After ipsilateral initial contact the impact of the heel with the ground creates a ground reaction vector anterior to the hip joint centre creating an external hip flexion moment, seen in Figure 8.15. By the end of the first double support phase, the participants with lower %FM demonstrated external hip extensor moments as the ground reaction vector passed posterior to the hip joint centre. However, in participants with greater %FM, external hip flexion moment continued through to midstance. At ipsilateral toe-off (7.63% ± 2.27% of gait cycle) the hip flexor moment was significantly greater in boys with higher %FM (23.47Nm 95%CI 8.86Nm) compared to boys with lower %FM (3.03Nm 95%CI 9.36Nm) possibly due to hip extensor weakness. Shultz et al., (2009) also found significantly higher absolute hip flexor moments in overweight compared to healthy weight children. This study related greater hip sagittal plane moments to increased compressive forces on the capital femoral growth plate possibly leading to slipped capital femoral epiphysis (SCFE).

Internal rotation moments of the hip were significantly higher in boys with greater body fat mass (1.30Nm and -0.97Nm for the highest %FM and lowest %FM respectively). As seen in Figure 8.15, the participants with higher %FM in the current study were more externally rotated at ipsilateral toe off. Towards the end of the stance phase, as the hip internally rotated to bring the leg into the midline of the body, a larger internal rotation moment was required to rotate the limb in participants with higher adiposity. Greater internal joint moments may relate to the externally rotated position of the hip and the greater inertia of the lower limb in participants with higher %FM. This finding is in-line with Shultz et al., (2009), who found significantly higher mean internal (reported as net internal external rotation moments) rotation moments of the hip in obese children. Shultz et al., (2009) reported that greater rotational forces acting on the hip together with larger compression forces from excessive body mass may further predispose obese children to slipped capital femoral epiphysis (SCFE). In cases of SCFE, the femoral head slips inferior and posterior to the femoral neck and the entire limb externally rotates (Wills, 2004). This excessive femoral retroversion in obese children may relate to the higher internal hip internal rotation joint moments at the end of stance phase found in the current study. The sample of boys in the current study was free

from orthopaedic pathologies as indicated in the health screening questionnaire indicating that SCFE was not diagnosed. However, altered hip biomechanics during gait could indicate a trend towards development of SCFE symptoms in the boys with higher adiposity.

8.5.2.2 Knee

The knee joint of boys with higher body fat mass demonstrated greater flexion at ipsilateral toe off. The range of knee flexion across %FM was 27.53^{o} (95%CI 1.06^{o}) in participants with higher %FM to 18.60^{o} (95%CI 1.20^{o}) in participants with lower %FM. This was also found in a study of obese adolescents during the stance phase of gait (McMillan et al., 2010). In the previous study obese adolescents demonstrated 40.82° ± 7.90° of knee flexion at ipsilateral toe off compared to 37.28° ± 5.28° in healthy weight adolescents. The reason for disparity between values of knee flexion at ipsilateral toe-off between McMillan et al., (2010) and the current study is not clear. However, an examination of normative values for paediatric knee flexion at ipsilateral toe-off demonstrates approximate values of 20° to 30° (van der Linden et al., 2002; Ganley & Power 2005; Chester et al., 2006). The slightly higher knee flexion values reported by MacMillan et al., (2010) even for healthy weight children may be due to marker placement differences between the studies.

Also associated with greater knee flexion at ipsilateral toe off was the time spent in stance phase of gait, shown in Table A10.8. Participants who spent longer in the stance phase of gait showed significantly more knee flexion at ipsilateral toe off. At ipsilateral toe-off the ground reaction vector is posterior to the knee joint aiding knee flexion as the hip flexes to propel the thigh forward. Whittle (1996) described the lower limb as a double jointed pendulum so as the hip flexes the shank is 'left behind' due its inertia. The potentially larger shank inertia of participants with higher %FM could result in the toe remaining in contact with the ground for longer. This may indicate that boys with higher %FM exhibited greater instability during gait requiring more time in the double support phase (Winter, 1987).

Boys with higher %FM also demonstrated greater external peak knee adduction moments early in the stance phase. The range of regression values was from 1.30Nm (95%CI 0.44Nm) in participants with higher %FM to -0.97Nm (95%CI 0.46Nm) in participants with lower %FM. The frontal knee joint angle of the participants with higher %FM was in varus (adduction) alignment in early stance compare to a valgus alignment in participants with lower %FM. Greater external knee adduction moments are due to the medial placement of the ground

reaction vector relative to the knee joint. Browning & Kram (2007) reported greater external knee adduction moments in obese adult gait at a range of walking speeds. The authors summarised that external knee adduction moments distribute larger compressive forces across the medial compartment of the tibiofemoral joint. Furthermore, external knee adduction moments have been positively correlated with osteoarthritis severity and progression (Miyazaki et al., 2002). However, greater knee adduction moments do not necessarily result in greater medial knee compartment forces. An external rotation of the lower limb, seen in the current study at the ankle joint in Figure 8.12, would reduce external knee adduction moments by placing the centre of pressure more lateral. This may be a strategy employed to reduce potentially injurious loads (Browning & Kram 2007).

Studies on frontal plane moments in obese paediatric gait have also shown greater peak external knee adduction moments, reported as internal knee abduction moments (Gushue et al., 2005). These authors attributed greater external knee adduction moments to increased adipose tissue between the thighs of obese children. However, a later study examined the effects of altering thigh girth (using neoprene wrapped round the thigh) on knee biomechanics in adults (Westlake et al., 2013). Peak external knee adduction moment was not altered by the addition of the neoprene wrap to thigh girth, but step width significantly increased. The authors concluded that a greater step width with no change in knee adduction moments suggests that greater external knee adduction moments seen in obese gait may be due to greater body mass and not the physical constraints of the thigh. The results of the current study suggest contrary to Westlake et al., (2013) because while %FM was significantly related to greater peak external knee adduction moments, BMI Z-Score was not. This indicates that variance in peak external knee adduction moments was not significantly explained by body mass (relative to height). Therefore, suggesting that other factors other than BMI Z-Score increase peak knee external adduction moments. It is evident that the cause of greater external knee adduction moments in participants with higher %FM is not clear. However, there is a clear link between greater external knee adduction moments and Blount's disease (tibia vara) in obese children and medial knee osteoarthritis in obese adults (Skinner, 1996; Miyazaki et al., 2002).

8.5.2.3 Ankle

Ankle kinematics were significantly associated with %FM in all three planes of motion, as shown in Figures 8.9, 8.10 and 8.11. In the sagittal plane boys with higher adiposity demonstrated approximately 4^{o} less plantarflexion shortly after ipsilateral initial contact, 5^{o} more dorsiflexion at contralateral initial contact and 30^{o} more dorsiflexion at ipsilateral toe-off. This finding is in-line with Spryropoulos et al., (1991) who found greater ankle dorsiflexion throughout the stance phase. Spyropoulos et al., (1991) attributed this to reduced hip flexion and reduced stride length as a mechanism to bring the body mass vector over the flat foot as soon as possible. Furthermore, the study explained that reduced plantarflexion during the push-off period of the gait cycle in the obese adults was due to diminished push-off force, a reduced swing period and subsequently smaller stride lengths. This is in-line with the finding of a significant relationship between stance phase duration and %FM in the current study. Furthermore, dorsiflexion at contralateral toe-off was also significantly associated with step length. Reductions in step length were significantly associated with greater dorsiflexion in the current sample population. Therefore, greater dorsiflexion in participants with higher %FM may be a result of weaker plantarflexors relative to the greater inertia of the lower limb segments resulting in diminished push-off and subsequent reduced step length and swing time.

Prior to and at ipsilateral initial contact, the ankle of boys with higher %FM demonstrated less abduction motion. The difference across the range of %FM was small, approximately 1.5^{o}, which may have little clinical significance. At ipsilateral initial contact the foot begins abducting (everting) in the frontal plane at the subtalar rather than the ankle (talocrural) joint (Perry 1992). As the PiG lower limb model only describes whole foot motion with regard to the shank, the separate motion of the foot joints cannot be established. Shultz et al., (2009) reported greater ankle inversion (adduction) values of approximately 1^{o}, averaged across the gait cycle, in obese children. This finding is in-line with the findings from the current study of less abduction moment in participants with higher %FM. However, McMillan et al., (2009) measured hindfoot frontal plane motion in overweight and healthy weight boys and adolescents, finding greater eversion (abduction) in the stance phase in the overweight boys. The authors reported that greater ankle abduction at ipsilateral initial contact may be a result of calcaneal valgus motion. Measuring ankle joint motion (motion of the foot relative to the shank) appears to give different motion values than when hindfoot motion (relative to the shank) is reported separate from the rest of the foot. It is possible that opposing frontal plane

motion between the hindfoot, midfoot and forefoot reduce the validity of representing the foot as a single segment. The use of a multi segmental foot model can determine which segments of the foot frontal plane motion can be attributed to.

The ankle joint of participants with higher %FM was significantly less internally rotated by approximately 13^{o} at peak internal rotation and ipsilateral initial contact. Peak internal rotation occurs at approximately the same time as peak abduction; prior to ipsilateral initial contact (approximately 89% of the gait cycle). Less internal rotation and less abduction of the ankle are significantly associated with %FM at ipsilateral toe-off. These findings suggest that the frontal and transverse plane motions of the foot are linked in this sample population. Indeed, the frontal and transverse plane gait parameters of the ankle showed enough shared variance to be considered as one principal component. Messier et al., (1994) measured 2D footprint angles from obese and non-obese adults. While the accuracy of using 2D measures of the 3D structures of the foot may be reduced the study did find increased hindfoot inversion (adduction) and out-toeing (forefoot external rotation) at ipsilateral initial contact. These findings match the current studies results of reduced abduction (inversion) and reduced internal rotation of the foot in obese children. Messier et al., (1994) described the abnormally inverted hindfoot motion as the cause of greater eversion during the stance phase to place the first metatarsal head into a weight bearing position. Less internal rotation of the foot about the ankle at the start of the stance phase may reduce lateral body motion enhancing dynamic stability during gait.

8.5.3 Foot Kinematic Findings

The current study shows that hindfoot motion relative to the shank segment in boys with higher %FM were less adducted (internally rotated) during early stance phase and more abducted (externally rotated) during late stance phase. The participants with greater %FM demonstrated approximately 7^{o} more abduction (external rotation) of the hindfoot compared to the participants with lower %FM. This is consistent with the findings of less ankle internal rotation from the PiG lower limb model. This finding may highlight a pronated foot type in boys with higher fat mass giving rise to a flat foot. The findings of greater hip internal rotation hip and adduction knee moments may indicate that the boys with higher fat mass distribute forces more medially through their lower limb joints. This will cause the body's centre of pressure to move medially, potentially inducing pronatory changes in the foot. Teichtahl et al.,

(2006) measured the association between foot rotation (foot modelled a one rigid segment), thigh rotation and external knee adduction moment in non-obese adults. The study found external foot rotation was related to reduced external knee adduction moments during the later part of the stance. The reason for this finding was the medial positioning of the ground reaction vector, closer to the knee joint centre thus reducing the lever arm when the foot is externally rotated. Therefore, the externally rotated position may be a compensatory mechanism the participants with greater %FM employ to reduce knee adduction moments.

The current study found greater midfoot dorsiflexion at the beginning and end of the stance phase and the end of the swing phase in boys with greater adiposity. The difference between the highest %FM participants at the lowest %FM participants was approximately 20^{o} at contralateral toe-off and 12^{o} at ipsilateral toe off. This finding can be linked to radiographic findings of flat feet and a pronatory foot type. In flat foot deformity the medial longitudinal arch collapses and the talus plantarflexes resulting in a plantar position of the metatarsals compared to the hindfoot complex (van Boerum et al., 2003). Villarroya et al., (2009) found talus-first metatarsal sagittal plane angles to be high (greater dorsiflexion) in obese children and adolescents compared to published normal values. While comparisons between static foot alignments from radiographic measures may not compare directly with dynamic motion of the foot, both the talus-first metatarsal and midfoot sagittal plane orientation reveal the presence of a pronatory foot type (Villarroya et al., 2009). This can occur at any midtarsal joint giving the appearance of midfoot dorsiflexion in relation to the hindfoot as seen in current study's participants with higher body fat mass. This finding, along with hindfoot abduction gives more evidence to a pronated foot and lowering of the medial longitudinal arch with excessive fat mass.

The midfoot of participants with greater %FM showed a greater eversion peak after ipsilateral initial contact. The range was small; 2.19^{o} (95%CI 1.01^{o}) of eversion in the participants with higher %FM and 1.66^{o} (95%CI 1.24^{o}) in participants with lower %FM. Midfoot eversion in early stance found in the current study could also indicate a lowering of the medial longitudinal arch in participants with higher %FM. This finding is consistent with previous studies on dynamic plantar pressure in obese children. Mickle et al., (2006) found higher peak pressures under the midfoot segment of obese children compared to non-obese counterparts. This finding is not only due to extra adipose tissue in the plantar pad as ultrasonography confirmed obese children to have fatter and flatter feet (Riddiford-Harland et al., 2011). Weakening or laxity of the arch supporting structures, due to excessive force incurred by the carriage of greater loads,

will flatten the arch. This can happen at the talo-navicular, navicular-cuneiform or tarsal-metatarsal joints (van Boerum et al., 2003). The 3DFoot models the midfoot from the navicular to the first metatarsal so eversion at this segment indicates that the medial longitudinal arch is lowering at the navicular-cuneiform joint. The timing of the peak eversion occurs when greater body mass is transferring through the foot after heel strike predisposing the arch to higher forces. Both excessive fat and total mass where significantly associated with greater peak eversion early in the stance phase in the current study. This indicates that the carriage of excessive load (body mass) from greater adiposity may cause greater midfoot eversion in participants with higher %FM. The finding of greater midfoot eversion from the 3DFoot model was opposite to the finding of greater adduction (inversion) of the ankle joint in the PiG model. By modelling the foot as a single rigid segment the forefoot may appear inverted due to eversion of the midfoot. This highlights the need to present foot motion as a number of segments so motion can be attributed to the correct joint.

8.5.4 Comparisons with Reliability Study

In order to interpret the results of the current study the range of findings across %FM range need to be referred to between-session reliability estimated in experimental chapters 2 and 3 (chapters 6 and 7) to determine if the associations are greater than measurement error. The subjects of the experimental study, on average, were younger and had a lower BMI Z-Score than the subjects of the main study. However, the age range of the participants in the reliability study was inclusive the age range of the participants in the main study. The range of BMI Z-Scores was less than that of the main study meaning the reliability of gait analysis in children with lower and higher BMI Z-Scores has not been confirmed. Therefore, when considering significant associations between gait variables and BMI Z-Score a conservative assessment above standard error measurement values will be made. Body fat mass (%FM) was not measured in the participants of the reliability study due to body composition protocols not being in place when the reliability study took place

All significant associations between lower limb and foot biomechanics at all gait cycle events and peaks were higher than the corresponding standard error of measurement (SEM) values calculated in experimental chapters 2 and 3 (chapters 6 and 7). However, caution should be taken when interpreting frontal plane ankle and midfoot angular associations with body fat mass. The regression range from the lowest to the highest adiposity at the ankle joint in the

frontal plane was 1.62^{o} at ipsilateral initial contact and 1.40^{o} at initial peak abduction in the swing phase. These values are only slightly higher than the SEM values calculated in experimental chapter 2 (chapter 6) (1.18^{o} and 1.13^{o} for ankle angle at ipsilateral initial contact and initial peak abduction in the swing phase respectively). Similar findings were found in knee joint frontal plane moments; the regression range across the spread of body fat mass levels in the sample of boys was 0.102Nm and the SEM from the reliability study in experimental chapter 2 (chapter 6) was 0.091Nm. The frontal plane findings in the main study may be significant, but the small difference in regression between high and low adiposity could mean the associations lack clinical relevance. Previous studies also found small frontal plane differences in motion between obese and non-obese children of 1-2^{o} at the ankle and hindfoot (Shultz et al., 2009, McMillan et al., 2010). It is possible that even small changes in frontal plane motion and forces may predispose children to musculoskeletal pathology (Shultz et al., 2011).

8.6 Summary

The results of the present study show that an association exists between lower limb and foot motion and amount of adiposity in a cross-sectional sample of boys age 7 to 11 years old. At the hip joint, significantly greater flexion throughout the gait cycle may relate to hip extensor muscle weakness resulting in an anterior position of the centre of mass. This anterior displacement of the centre of mass may lead to greater external hip flexion moments which were seen at the start of the gait cycle. Significantly higher internal hip rotation at the end of the stance phase maybe the result of an externally rotated lower limb and greater thigh segmental inertia. Greater rotation forces acting on the hip joint may predispose boys with higher fat mass to orthopaedic conditions such as slipped capital femoral epiphysis. Greater knee flexion at the end of the stance phase in boys with higher %FM was significantly associated with stance phase duration. This finding may indicate the necessity to increase stability by prolonging the stance phase. Boys with higher fat mass demonstrated greater external knee adduction moments, a potential precursor to Blount's disease and medial knee joint osteoarthritis in later life. Fat mass was significantly associated with ankle joint motion over the gait cycle in all three planes. The ankle was more; dorsiflexed, indicting a possible weakness of the plantarflexors; also, adducted and externally rotated, signifying altered foot mechanics. The foot of boys with higher adiposity demonstrated a pronated foot type indicating a lowering of the medial longitudinal arch and a flatter foot. The hindfoot was more

abducted (externally rotated) throughout the gait cycle possibly relating to structural changes to the calcaneal and talus due to excessive forces on the medial lower limbs. The midfoot of higher adiposity boys was more dorsiflexed during the later part of stance indicating a lowering of the medial longitudinal arch. The midfoot was also everted at the beginning of stance also resulting in a greater lowering of medial longitudinal arch possibly due to laxity caused by the carriage of excess fat mass.

8.7 Limitations

The first limitations of this chapter of the thesis was the protocol to determine at which point in the gait cycle to extract lower limb and foot joint angle and moment values for analysis. While previous research informed the choice of values at events and peaks through the gait cycle subphases, this was not a comprehensive assessment. In order to fully explore the gait cycle information at every data point should be considered. This can be achieved by principle component analysis (PCA) to combine areas of the gait which demonstrate shared variance into components for analysis. In this way the, somewhat arbitrary, choice of gait events and peaks is removed. Therefore, further relationships between adiposity with lower limb and foot biomechanics could be explored. Previous work has employed PCA to identify age related kinetic variables to determine gait maturation (Chester et al., 2008). Furthermore, the relationships between adiposity with lower limb and foot biomechanics maybe non-linear rather than assumed linear in the current study. To date little work has been presented on possible curvilinear relationships between body fat (%FM) and joint biomechanics during gait. Future work should consider analysing all %FM-joint biomechanics plots for the potential for curvilinear relationships.

A further limitation of the study was the inability to measure foot joint kinetics using the 3DFoot model. Presenting foot joint kinetics could provide more information on the relationship between adiposity and foot biomechanics. The Kinfoot model tested in experimental chapter 3 (chapter 7) provides foot joint moment and powers (MacWilliams et al., 2003). However, some of inverse dynamic calculations used in Kinfoot have been questioned (Buczek et al., 2006). Recently, a foot model has been developed to measure moments and powers of the hindfoot, forefoot and hallux segments (Bruening et al., 2012). Future research should incorporate foot segment kinetic analysis when analysing relationships with obesity during gait.

Marker placement error was previously described in experimental chapters 2 and 3 (chapters 6 and 7) which can reduce the between-session reliability of the PiG biomechanical model. The 'instrumented pointer device' protocol attempted to reduce errors in the marker placement by removing the effect of soft tissue artefact on skin mounted ASIS markers. However, other marker locations may be also affected by soft tissue artefact misrepresenting angular and moment data in obese participants. Kirtley (2002) presented the effects of altering the position of many marker locations from the modified Helen Hayes marker set (utilised by PiG). The effect of superiorly locating the sacral marker caused anterior tilt of the pelvis which would have the effect of increasing hip flexion. Kirtley (2002) commented that locating the position of the sacral marker on S2 vertebrae is not easy in obese individuals. Therefore, the finding of significantly greater hip flexion in participants with higher %FM may be related to misplacement of the sacral marker and warrants further investigation.

9. Thesis summary

The aims of this study were; firstly, to establish protocols and test between-session reliability of methods for determining body composition for determining obesity (body mass index) and adiposity (body fat); secondly, to establish protocols and test between-session reliability of three dimensional gait analysis to measure lower limb and foot biomechanics in children; and finally, to identify gait characteristics associated with adiposity in a cross-sectional sample of boys age 7 to 11 years old.

Previous research has indicated that obese children demonstrated musculoskeletal co-morbidities that affect the hip, knee and foot and alter gait characteristics. Incidence of slipped capital femoral epiphysis, tibia vara and flatfeet are reported to be higher in obese compared to non-obese children. Each of these co-morbidities has been linked to high body mass causing excessive and misplaced forces across the lower limb joints resulting in remodelling of the musculoskeletal system. Remodelling of lower limb joints in children with higher fat mass may alter gait characteristics before musculoskeletal co-morbidities are diagnosed. Therefore, detecting lower limb gait characteristics associated with higher fat mass could prevent future incidence of musculoskeletal co-morbidities.

Previous studies examining the effects of obesity on paediatric gait have defined obesity according BMI Z-Score. This however, measures weight as a ratio to height matched to age and gender reference values and not body fat mass. This may mislabel children of a short-compact build as overweight or obese even if they do not have excessive adipose tissue (body fat mass). Few previous studies have examined the health implications of childhood obesity by using measures of body fat mass to define obesity. Therefore, the first aim of this study was to examine the effects of adiposity on gait characteristics to assess if excessive adipose tissue is associated with altered joint motion.

Obese children have been previously reported to walk; slower with a greater stance phase of gait; with reduced lower limb flexion throughout the gait cycle; and greater lower limb sagittal and frontal plane moments throughout the stance phase. Specific gait differences between obese and non-obese children were found at gait events (initial contact and toe off) as well as angular and moment peaks. Few studies have examined three-dimensional biomechanics whilst controlling for age, anthropometric and spatiotemporal confounding variables. Therefore, in order to explore the effects of adiposity on lower limb biomechanics a

comprehensive assessment of lower limb biomechanics was required over the entire gait cycle whilst controlling for confounding variables.

Reports on dynamic foot motion differences between obese and non-obese children have shown that the midfoot demonstrated greater plantar surface area and increased plantar pressures. These dynamic measures of foot structure indicate that the feet of obese children are flatter during gait predisposing the midfoot to greater stresses during the stance phase. However, these studies examined the foot in two-dimensions analysing the plantar surface only. Few studies have examined relationships between obesity and three-dimensional motion of the foot in children.

9.1 Aim1: Establish Protocols and Test Between-Session Reliability of Methods for Determining Body Composition for Determining Obesity and Adiposity

In order to define obesity an accurate measure of body fat mass (adiposity) is required. However, in large scale population studies Body Mass Index (BMI) is used to infer body fat mass based on the correlation between them, r values ranging from 0.39 to 0.90 (Barlow & Dietz, 1998). The two key limitations of using BMI as a measure of obesity in paediatric research are; (1) the assumption of an linear increase in fat and lean mass through childhood, when the ratio of fat-to-lean mass changes throughout development; and (2) the poor correlation between BMI and fat mass (%FM) in certain populations (children with low %FM, ethnicity, high physical activity levels). Therefore, obesity defined by adiposity (measure of body fat mass) may be more appropriate in a cross-sectional sample of primary school-aged boys.

Methods to assess adiposity were established in this study by comparing techniques to measure body fat mass. For research purposes a measure of paediatric body fat mass should be accurate, precise and cause little discomfort or potential harm to the participant. Therefore, this study aimed to test between-session reliability of two devices of body fat mass measurement; the air displacement plethysmography (ADP) and bioelectrical impedance analysis (BIA). Previous studies have found equations to estimate body fat mass to be age, gender, ethnicity and level of obesity specific. Therefore, this study also examined subject specific equations to estimate body fat mass in each body composition device.

The results of experimental chapter 1 (chapter 5) indicated that anthropometric and body fat mass measures were reliable in a cross-sectional sample of boys (R>0.99). Measures of body

fat mass by ADP demonstrated greater between-session reliability and lower error compared to BIA (TEM = 0.54%FM and 0.81%FM relative to total body mass, for ADP and BIA respectively). Low agreement between body fat mass estimates based on manufacturers or age- and gender-specific equations indicate that these equations cannot be used interchangeably. As no method of validating body composition measures against 'gold standard' techniques (three or four compartment models) was available the results were compared to the literature. Previous studies have reported that using age- and gender-specific body composition equations present better agreement than manufacturer's equations. Therefore the age- and gender-specific equations of ADP for measuring body composition were to be used in the main study to determine body fat mass in the sample. Furthermore, no clear cutoff for determining the main study (chapter 8) groups based on excessive or healthy levels of adiposity in children has been estimated. Therefore, the level of adiposity in the main study (chapter 8) sample of boys was related to gait characteristics as a continuous variable removing errors in incorrect assignment of body fat mass groups.

9.2 Aim 2: Establish Protocols and Test Between-Session Reliability of Three Dimensional Gait Analysis to Measure Lower Limb and Foot Biomechanics in Children.

Quantifying lower limb motion involves the application of a biomechanical model to the recorded marker motion to determine limb orientation, and relative motion between limbs about a joint centre. Reliability of the conventional lower limb model (PiG) to determine motion and forces has been found to vary between studies with large errors found in the transverse plane (Gorton et al., 2009). Furthermore, marker placement errors may be greater in obese adults due to excessive adipose tissue (Rash et al., 1999). Marker placement errors have been reduced by using a correction factor for transverse plane thigh motion (Baker et al., 1999, Malt et al., 2012) and virtual pelvic markers (Board et al., 2012). However, the reliability before and after such marker placement protocols have not been tested in children across a range of adiposity levels. Therefore, the first aim of experimental chapter 2 (chapter 6) was to establish a reliable protocol for measuring lower limb motion in children. To achieve this, a test re-test protocol was implemented to examin the kinematic and kinetic outputs from the lower limb model (PiG) in a group of children.

Anthropometric measures, required to estimate joint and limb centres, were highly reliable between sessions (ICC >0.93). Cadence, step width and step length were reliable between

sessions (ICC >0.81), but stance phase duration and walking speed were less reliable (ICC >0.42). However, no significant differences between sessions were found between anthropometric and spatiotemporal measures indicating that differences between kinematic and kinetic outputs were due to extrinsic (methodological variability) rather than intrinsic errors (inherent variability). The PiG lower limb model demonstrated moderate between-session reliability for joint angular (ICC 0.58) and joint moment outputs (ICC 0 .44). Errors between repeated sessions were 3.98^{o} ± 1.89^{o} for joint angular and 2.38Nm ± 2.06Nm for joint moment outputs. The application of the thigh rotation protocol improved between-session reliability of lower limb joint angles (ICC 0.62) but did not change joint moments (ICC 0.44). Errors between sessions were reduced to 3.56^{o} ± 1.77^{o} for joint angles but remained the same at 2.38Nm ± 1.89Nm for joint moments. These findings indicate that using the thigh marker rotation offset increased lower limb model between-session reliability and reduced errors; therefore, it was used in the main study (chapter 8). An experimental protocol was developed to track the anterior pelvis by virtual rather than skin mounted markers which are susceptible to soft tissue artefact in obese subjects. Using virtual markers significantly altered in the position of the ASIS and hip joint centre and resulted in greater hip flexion over the gait cycle. The ASIS virtual marker protocol was used to track anterior pelvis position in the main study (chapter 8).

The aim of the third experimental chapter (chapter 7) was to establish protocols and test between-session reliability of measuring foot motion in children. No consensus has been reached on the appropriate method to model the foot and, therefore many foot models are available to determine foot segment motion. Between-session reliability of foot models has varied between studies depending on the segmentation of the foot and population sampled. Foot models that describe motion of many foot segments may provide more information on foot biomechanics during gait but are generally less reliable. Therefore, there was a need to measure the between-session reliability of a variety of foot models in children of varying adiposities.

Three foot models were examined for between-session reliability of kinematic outputs during paediatric gait assessment. The choice of foot model for the main study (chapter 8) was based on the model that can provide the greatest reliable information on foot segmental motion during gait. The three segment, OFM demonstrated highest joint angle between-session reliability (ICC 0.53) followed by the four segment, 3DFoot (ICC 0.52) and the eight segment, Kinfoot (ICC 0.46). However, 3DFoot demonstrated the least joint angle errors (SEM 3.88^{o} ±

2.18°) compared to OFM (4.61° ± 2.17°) and Kinfoot (5.08° ± 1.53°). Therefore, 3DFoot was determined to be the most appropriate for use in this study sample population in the main study (chapter 8). Normalising 3DFoot to a standing position reduced between-session reliability (ICC 0.43) but in also reduced errors (3.29° ± 2.02°). This reduced marker placement errors, but also removed actual differences between subjects. Therefore, 3DFoot model joint angle outputs were analysed without reference to standing position.

9.3 Aim 3: Identify Gait Characteristics Associated with Adiposity in a Cross-Sectional Sample of Boys Age 7 to 11 Years Old

The aim of the main study (chapter 8) was to measure angular motion and joint moments of the lower limb joints (hip, knee and ankle) and the foot segments (hindfoot, midfoot, forefoot and hallux) during paediatric gait. Furthermore, to relate any kinematic and kinetic findings to the level of body fat mass when controlling for other factors that influence gait biomechanics (spatiotemporal, anthropometric or age related factors).

The findings of the main study (chapter 8) can be explored with reference to the functional characteristics of gait which are to absorb the shock of impact, stabilise the body and facilitate forward progression (Perry, 1992). The first double support phase (DS1) of the gait cycle involves the abrupt transfer of body weight onto the ipsilateral limb. During the loading response phase hip stability is maintained by activity of the hip extensors (Perry 1992). Participants with greater %FM demonstrated greater external hip joint flexion moments during the loading response phase (0-10% of the gait cycle). This finding may be linked to greater hip flexion found in boys with higher %FM which could displace the centre of mass anteriorly. This could be a result of weak hip extensors relative to greater forces from the carriage of greater load.

The midtarsal joint facilitates shock-absorption during the loading response phase. This is caused by subtalar joint eversion 'unlocking' the talonavicular and calcaneocuboid joints allowing greater mobility (Perry, 1992). This allows the medial longitudinal arch to act as a spring during weight bearing supporting body weight (Watt, 2006). Participants with greater %FM demonstrated greater midfoot eversion during the loading response phase (approximately 2% of the gait cycle). This finding may indicate greater laxity of midtarsal joint in participants with greater %FM. Greater midfoot eversion was also related to a higher BMI Z-

Score indicating that the carriage of excess adipose tissue may cause excessive compressive forces on the immature osseous structures of the medial longitudinal arch.

Following the loading response phase single limb (SS1) support begins with contralateral toe-off. As body weight is loading onto the ipsilateral limb the knee joint experiences an adduction moment (Perry 1992). The medial position of the ground reaction vector, as the body drops onto the ipsilateral limb, places high-stress on the knee joint. Participants with higher %FM demonstrated greater knee adduction moments after the loading response phase. It is unclear whether this is due to greater body mass from excess adiposity or an increase in thigh girth. Regression analysis showed that BMI Z-Score was not associated with greater adduction moments of the knee suggesting that body mass is not a factor. A larger thigh girth would place the knee in a greater varus position due to abduction of the hip. This would place the ground reaction vector in a more medial position compared to a smaller thigh girth. The lower limb morphological characteristics of obese children may have a large impact of biomechanics and warrants further investigation.

At the end of the stance phase is terminal stance and pre-swing phases (approximately 30-60% of the gait cycle). Terminal stance begins when the ipsilateral heel rises until contralateral initial contact and pre-swing occurs during the second double support phase (DS2). At ipsilateral toe-off the hip joint is in maximal external rotation as the knee flexes to initial the swing phase (Perry 1992). Participants with greater %FM demonstrated greater hip joint internal rotation moments as well as greater knee flexion at ipsilateral toe-off. These two findings may be linked to greater inertia of the lower limb and a relative weakness of the knee flexors particularly the sartorius (due its combined action of knee flexion and hip external rotation). Greater knee flexion in participants with higher %FM was also related to a longer stance phase period. This maybe a compensatory mechanism to increase stability at ipsilateral toe-off, which is a relatively unstable period of the gait cycle.

The position of the ground reaction vector moves evermore anteriorly within the foot through the stance phase. As the heel rises during terminal stance the ground reaction vector is directly through the forefoot inducing dorsiflexion at the midtarsal and metatarsal-phalangeal joints (Perry 1992). Participants with greater %FM demonstrated greater midfoot dorsiflexion at contralateral initial contact and ipsilateral toe-off. This finding may be linked to the finding of greater midfoot eversion indicating a pronatory foot position and potential flat foot. Ligamentous laxity is the most commonly ascribed aetiology for the flexible flatfoot in the developing child (D'Amico 2001). At 2-3 years old ligament laxity peak in the growing child and

diminishes by the age of 8-10 years old (Valmassey, 1996). However, if the foot is put under excessive pronation in infancy the load may permanently deform and elongate the medial longitudinal arch ligaments. Since the ligamentous structure can no longer secure the osseous framework instability results and a flexible flatfoot may be present.

The findings described above indicate that excessive adiposity can have deleterious consequences on lower limb and foot motion at points of the gait cycle. Two more biomechanical findings were consistent across the gait cycle; the first was greater hip flexion and the second was greater hindfoot external rotation in participants with higher %FM. Excessive hip flexion through the stance phase can be related to postural positions of the body including forward trunk lean and knee flexion (Perry 1992). Forward tilt of the pelvis could have lead to greater hip flexion moments seen at the start of the stance phase. Forward tilting of the pelvis could be the result of an anterior displacement of the centre of mass from greater adiposity (particularly in the abdominal region). This increases the demand on the hip extensors which may not provide the necessary strength to extend the hip and prevent the pelvis and trunk from leaning forward. Greater external rotation of the hindfoot in participants with higher %FM across the gait cycle may relate to relative motion about the subtalar joint. Inman et al., (1981) suggested the subtalar joint acts like a mitered hinge, whereby supination and pronation of the foot is transferred respectively into external and internal rotation of the shank. Body weight and potentially %FM is one of the most powerful pronatory forces (D'Amico 2001). A medial displacement of the centre of gravity, caused by compensatory joint mechanisms proximal to the foot, produces subtalar joint pronation. Continuation of medially aligned body weight, through childhood development, can overstretch and weaken the medial ligamentous structures of the foot. Osseous structures on the lateral aspect of the foot can become compressed while the medial structures and put under strain. All these pathological consequences of medial displacement of the centre of the gravity make it very difficult for the underdeveloped and malleable foot to function efficiently (D'Amico 2001).

9.4 Clinical Implications

The findings of altered lower limb and foot biomechanics in boys with higher adiposity indicate the need to reduce the level of adiposity to prevent damage to the developing joints. In order to reduce or prevent increases in childhood adiposity physical activity is recommended and in

particular walking is encouraged (Shultz et al., 2011). However, excessive forces at the hip and knee joints and malalignments of the foot joints indicate that walking may cause discomfort for boys with higher adiposity. Therefore, clinical interventions such as orthotics to support and realign the midfoot would reduce further maladaptation to the foot. Furthermore, strengthening the musculature of the lower limbs may prevent misplaced motions in the frontal and transverse planes and reduce forces required to move relatively larger limbs.

9.5 Future Research

An outline for future research in this section begins with studies based on the data collected in the current study. This is followed by studies that should seek to understand the factors that influence the relationships between altered foot and lower limb gait biomechanics and higher fat in children. Finally longitudinal intervention studies should determine the causality between possible factors over time.

The current study demonstrated that participants with higher %FM have altered lower limb and foot biomechanics during the gait cycle. Further analyses into the associations between the timing of peak lower limb and foot angles and moments with body fat mass should be carried out. Furthermore, the range of motion of each lower limb and foot joint during the sub phases of gait and levels of adiposity should be examined. The culminated results from lower limb and foot angular and moment associations with body fat mass at event values, peaks values, timing of peak, and range of motion could then be analysed together. Principle component analysis and multiple regression analysis techniques could be used to explore the relationships between the significant findings. This would determine if joint angular associations with adiposity are due to a temporal offset or an alteration to the range of motion to the joint. Furthermore, combining multiple lower limb and foot joints into the analysis would uncover any relationships between the joints associated with higher levels of adiposity in children. One possible relationship could be between knee adduction moments and external foot rotation which has been reported in previous studies (Teichtahl et al., 2006).

Future research is required to determine why altered foot and lower limb biomechanics take place in children with higher adiposity. A comprehensive analysis of a child's level obesity/adiposity, physical activity levels, strength assessment, and joint alignment of the lower limb should be undertaken. Previous studies have shown that, compared to non-obese children, obese children have higher absolute muscle strength, but lower muscle strength

relative to body weight (Tsiros et al., 2011). Of particular interest is the relationship between muscular strength of the hip extensors with the amount of hip flexor moments during the early part of gait. Understanding the associations between physical activity with foot and lower limb gait biomechanics may provide an understanding of the apparent reciprocal relationship between the two factors. A lack of physical activity can lead to increased body fat and potentially to obesity due to lower energy expenditure compared to energy intake. However, a lack of physical activity can also affect the development of a healthy musculoskeletal system. Future research should consider examining the relationships between physical activity and foot and lower gait biomechanics in children over a range of adiposity levels. Previous research has demonstrated the links between lower limb musculoskeletal co-morbidities such as slipped capital femoral epiphysis, Blount's disease and flatfeet. However, a consideration of the lower limb skeletal structure and joint alignments in obese children may provide insight into co-morbidity risk before the pathology is reached. The relationship between joint alignment and foot and lower limb gait biomechanics could provide information on why children with higher fat demonstrate altered kinematics.

The discovery of the relationships between altered foot and lower limb biomechanics, physical activity, muscle strength and joint alignment in children with higher fat mass would lead to longitudinal assessments of the causal links between these variables. A muscle strength training intervention study would provide details on the causality between relatively weaker hip extensors and larger hip flexion moments during gait. A factor to control for in this study would be the possible reduction in body fat due to strength training, which may also reduce hip flexion moments. The effects of weight-loss on foot and lower limb gait biomechanics should be considered separately. Level of physical activity could be the cause of, or caused by altered foot and lower limb gait biomechanics. Therefore, longitudinal assessment of these factors would require study groups in which changes in physical activity and level of obesity were controlled over time. A possible cause of reduced physical activity in obese children is pain and discomfort which should be measured before and after interventions.

An intervention that targets foot and lower limb alignment is the use of orthotic devices. Orthotic devices such as wedges can be placed into participant's shoes to change the magnitude and position of forces during gait and alter foot and alignment. Of particular interest would be the use of orthotic to reduce pronation and knee adduction moments in children with higher fat mass. The results of the current study show a possible collapsing of the medial longitudinal arch from foot pronation and greater medial compartment stress from

greater knee adduction moments. However, the orthotic wedges required to reduce pronation are placed medially and to reduce knee adduction moments are laterally placed. This may indicate that foot pronation and knee adduction moments are related and longitudinal intervention studies could determine the associations.

Further longitudinal studies could focus on the relationships between knee adduction moments during gait in children with higher fat mass and medial knee osteoarthritis in adults which has also been linked with obesity. Preventing risk factors for medial knee osteoarthritis such as knee adduction moments, varus knee alignment and obesity could allow individuals to be more active and reduce body fat. The final intervention study could focus on weight loss programmes to understand if altered foot and lower limb gait biomechanics are reduced. The controlling factors would be physical activity, muscular strength and joint alignment which may change as a result of weight loss. The aim of future studies should be to determine the factors that can prevent children from becoming obese or manage children who are obese to prevent them becoming obese adolescents or adults. The multifaceted causes and effects of childhood obesity mean much research is required. Discovering relationships between foot and lower limb gait biomechanics and body fat in the current study may lead to future research understanding the complex nature of childhood obesity.

9.6 Conclusion

This study established protocols to reliably determine the body composition and gait biomechanics of boys between the age of 7 to 11 years old. Levels of body fat mass were related to altered lower limb and foot joint angular displacements and moments during gait. Key relationships included greater hip flexion, knee adduction moments and a pronated foot in boys with higher fat mass. These findings indicate that higher fat mass may decrease mobility and induce greater musculoskeletal demands reducing the potential for physical activity. This underpins the need for further longitudinal research looking at the prevention and management of musculoskeletal complications associated with childhood obesity.

References

Adoración Villarroya, M., Manuel Esquivel, J., Tomás, C., Buenafé, A. and Moreno, L. (2007) 'Foot structure in overweight and obese children'. *Int J Pediatr Obes,* 3(1), pp. 39-45.

Alonso-Vázquez, A., Villarroya, M. A., Franco, M. A., Asín, J. and Calvo, B. (2009) 'Kinematic assessment of paediatric forefoot varus'. *Gait Posture,* 29(2), pp. 214-219.

Azcona, C., Köek, N. and Frühbeck, G. (2006) 'Fat mass by air-displacement plethysmography and impedance in obese/non-obese children and adolescents'. *Int J Pediatr Obes,* 1(3), pp. 176-182.

Baker, R., Finney, L. and Orr, J. (1999) 'A new approach to determine the hip joint profile from clinical gait analysis data'. *Human Movement Science,* 18, pp. 655-667.

Baker, R. and Robb, J. (2006) 'Foot models for clinical gait analysis.'. *Gait Posture,* 23(4), pp. 399-400.

Barlow, S. E. and Dietz, W. H. (1998) 'Obesity evaluation and treatment: Expert committee recommendations. The maternal and child health bureau, health resources and services administration and the department of health and human services'. *Pediatrics,* 102(3), p. E29.

Beck, R. J., Andriacchi, T. P., Kuo, K. N., Fermier, R. W. and Galante, J. O. (1981) 'Changes in the gait patterns of growing children'. *J Bone Joint Surg Am,* 63(9), pp. 1452-1457.

Beechy, L., Galpern, J., Petrone, A. and Das, S. K. (2012) 'Assessment tools in obesity - psychological measures, diet, activity, and body composition'. *Physiol Behav,* 107(1), pp. 154-171.

Bell AL, Pedersen DR and RA., B. (1990) 'A comparison of the accuracy of several hip centre location prediction methods'. *Journal of Biomechanics,* 23, pp. 617–621.

Bell, L. M., Byrne, S., Thompson, A., Ratnam, N., Blair, E., Bulsara, M., Jones, T. W. and Davis, E. A. (2007) 'Increasing body mass index z-score is continuously associated with complications of overweight in children, even in the healthy weight range'. *J Clin Endocrinol Metab,* 92(2), pp. 517-522.

Benedetti, M., Merlo, A., Boschi, M. and Leardini, A. (2012) 'Inter-laboratory consistency of gait analysis measurements'. *Gait & Posture,* 36(S1), p. S44.

Benedetti, M. G., Catani, F., Leardini, A., Pignotti, E. and Giannini, S. (1998) 'Data management in gait analysis for clinical applications'. *Clin Biomech (Bristol, Avon),* 13(3), pp. 204-215.

Bernhardt, D. B. (1988) 'Prenatal and postnatal growth and development of the foot and ankle'. *Phys Ther,* 68(12), pp. 1831-1839.

Bishop, C., Paul, G. and Thewlis, D. (2012) 'Recommendations for the reporting of foot and ankle models'. *J Biomech,* 45(13), pp. 2185-2194.

Bland, J. M. and Altman, D. G. (1986) 'Statistical methods for assessing agreement between two methods of clinical measurement'. *Lancet,* 1(8476), pp. 307-310.

Board, W., J., Haight, D., J. and Browning, R., C. (2012) 'The issue of tissue: A comparison of kinematic models in obese adults'. *ASB conference*.

Bordin, D., De Giorgi, G., Mazzocco, G. and Rigon, F. (2001) 'Flat and cavus foot, indexes of obesity and overweight in a population of primary-school children'. *Minerva Pediatr,* 53(1), pp. 7-13.

Bosy-Westphal, A., Danielzik, S., Becker, C., Geisler, C., Onur, S., Korth, O., Bührens, F. and Müller, M. J. (2005) 'Need for optimal body composition data analysis using air-displacement plethysmography in children and adolescents'. *J Nutr,* 135(9), pp. 2257-2262.

Bouchard, C. (2010) 'Defining the genetic architecture of the predisposition to obesity: A challenging but not insurmountable task'. *Am J Clin Nutr,* 91(1), pp. 5-6.

Braune, W and, Fischer, O. (1987) *The human gait*. Berlin: Springer.

Bruening DA, Cooney KM and FL., B. (2012) 'Analysis of a kinetic multi-segment foot model. Part i: Model repeatability and kinematic validty'. *Gait & Posture,* 35, pp. 529-534.

Bruton, A., Conway, J., H, and Holgate, S., T. (2000) 'Reliability: What is it, and how is it measured?'. *Physiotherapy,* 86(2), pp. 94-99.

Buczek, F. L., Walker, M. R., Rainbow, M. J., Cooney, K. M. and Sanders, J. O. (2006) 'Impact of mediolateral segmentation on a multi-segment foot model'. *Gait Posture,* 23(4), pp. 519-522.

Burt Solorzano, C. M. and McCartney, C. R. (2010) 'Obesity and the pubertal transition in girls and boys'. *Reproduction,* 140(3), pp. 399-410.

Cappozzo, A., Catani, F., Croce, U. D. and Leardini, A. (1995) 'Position and orientation in space of bones during movement: Anatomical frame definition and determination'. *Clin Biomech (Bristol, Avon),* 10(4), pp. 171-178.

Cappozzo, A., Della Croce, U., Leardini, A. and Chiari, L. (2005) 'Human movement analysis using stereophotogrammetry. Part 1: Theoretical background'. *Gait Posture,* 21(2), pp. 186-196.

Caravaggi, P., Benedetti, M. G., Berti, L. and Leardini, A. (2011) 'Repeatability of a multi-segment foot protocol in adult subjects'. *Gait Posture,* 33(1), pp. 133-135.

Carriero, A., Zavatsky, A., Stebbins, J., Theologis, T. and Shefelbine, S. J. (2009) 'Correlation between lower limb bone morphology and gait characteristics in children with spastic diplegic cerebral palsy'. *J Pediatr Orthop,* 29(1), pp. 73-79.

Carson, M. C., Harrington, M. E., Thompson, N., O'Connor, J. J. and Theologis, T. N. (2001) 'Kinematic analysis of a multi-segment foot model for research and clinical applications: A repeatability analysis.'. *J Biomech,* 34(10), pp. 1299-1307.

Cavanagh, P. R., Morag, E., Boulton, A. J., Young, M. J., Deffner, K. T. and Pammer, S. E. (1997) 'The relationship of static foot structure to dynamic foot function'. *J Biomech,* 30(3), pp. 243-250.

Cavanagh, P. R. and Rodgers, M. M. (1987) 'The arch index: A useful measure from footprints'. *J Biomech,* 20(5), pp. 547-551.

Chan, G. and Chen, C. T. (2009) 'Musculoskeletal effects of obesity'. *Curr Opin Pediatr,* 21(1), pp. 65-70.

Chao, E. Y., Laughman, R. K., Schneider, E. and Stauffer, R. N. (1983) 'Normative data of knee joint motion and ground reaction forces in adult level walking'. *J Biomech,* 16(3), pp. 219-233.

Charlton, I. W., Tate, P., Smyth, P. and Roren, L. (2004) 'Repeatability of an optimised lower body model'. *Gait Posture,* 20(2), pp. 213-221.

Chester, V. L., Tingley, M. and Biden, E. N. (2006) 'A comparison of kinetic gait parameters for 3-13 year olds'. *Clin Biomech (Bristol, Avon),* 21(7), pp. 726-732.

Chester, V. L. and Wrigley, A. T. (2008) 'The identification of age-related differences in kinetic gait parameters using principal component analysis'. *Clin Biomech (Bristol, Avon),* 23(2), pp. 212-220.

Chiari, L., Della Croce, U., Leardini, A. and Cappozzo, A. (2005) 'Human movement analysis using stereophotogrammetry. Part 2: Instrumental errors'. *Gait Posture,* 21(2), pp. 197-211.

Chinn, S. (1991) 'Statistics in respiratory medicine. 2. Repeatability and method comparison'. *Thorax,* 46(6), pp. 454-456.

Cohen, J. (1992) 'A power primer'. *Psychol Bull,* 112(1), pp. 155-159.

Cole, T. J. (1991) 'Weight-stature indices to measure underweight, overweight and obesity.', in Himes, J. H. (ed.), *Anthropometric assessment of nutritional status*. New York: Wiley-Liss, pp. 83-111.

Cole, T. J., Bellizzi, M. C., Flegal, K. M. and Dietz, W. H. (2000) 'Establishing a standard definition for child overweight and obesity worldwide: International survey'. *BMJ,* 320(7244), pp. 1240-1243.

Cole, T. J., Freeman, J. V. and Preece, M. A. (1995) 'Body mass index reference curves for the uk, 1990'. *Arch Dis Child,* 73(1), pp. 25-29.

Cole, T. J., Freeman, J. V. and Preece, M. A. (1998) 'British 1990 growth reference centiles for weight, height, body mass index and head circumference fitted by maximum penalized likelihood'. *Stat Med,* 17(4), pp. 407-429.

Cook, S. D., Lavernia, C. J., Burke, S. W., Skinner, H. B. and Haddad, R. J. (1983) 'A biomechanical analysis of the etiology of tibia vara'. *J Pediatr Orthop,* 3(4), pp. 449-454.

Cornwall, M. W. and McPoil, T. G. (1999) 'Three-dimensional movement of the foot during the stance phase of walking'. *J Am Podiatr Med Assoc,* 89(2), pp. 56-66.

Cowgill, L. W., Warrener, A., Pontzer, H. and Ocobock, C. (2010) 'Waddling and toddling: The biomechanical effects of an immature gait'. *Am J Phys Anthropol,* 143(1), pp. 52-61.

Crapo, R. O., Morris, A. H., Clayton, P. D. and Nixon, C. R. (1982) 'Lung volumes in healthy nonsmoking adults'. *Bull Eur Physiopathol Respir,* 18(3), pp. 419-425.

Curtis, D. J., Bencke, J., Stebbins, J. A. and Stansfield, B. (2009) 'Intra-rater repeatability of the oxford foot model in healthy children in different stages of the foot roll over process during gait.'. *Gait Posture,* 30(1), pp. 118-121.

D'Amico, JC, (2001) 'Developmental flatfoot', in Thomson P and Volpe, R. (eds.) *Introduction to podopaediatrics*. Eastbourne: Churchill Livingstone, pp.

Das, S. K. (2005) 'Body composition measurement in severe obesity'. *Curr Opin Clin Nutr Metab Care,* 8(6), pp. 602-606.

Das, S. K., Roberts, S. B., Kehayias, J. J., Wang, J., Hsu, L. K., Shikora, S. A., Saltzman, E. and McCrory, M. A. (2003) 'Body composition assessment in extreme obesity and after massive weight loss induced by gastric bypass surgery'. *Am J Physiol Endocrinol Metab,* 284(6), pp. E1080-1088.

Davis III RB, Õunpuu S, Tyburski D and JR., G. (1991) 'A gait analysis data collection and reduction technique.'. *Human Movement Science,* 10, pp. 575–587.

de Onis, M., Onyango, A. W., Borghi, E., Siyam, A., Nishida, C. and Siekmann, J. (2007) 'Development of a who growth reference for school-aged children and adolescents'. *Bull World Health Organ,* 85(9), pp. 660-667.

de Sá Pinto, A. L., de Barros Holanda, P. M., Radu, A. S., Villares, S. M. and Lima, F. R. (2006) 'Musculoskeletal findings in obese children'. *J Paediatr Child Health,* 42(6), pp. 341-344.

Dehghan, M., Akhtar-Danesh, N. and Merchant, A. T. (2005) 'Childhood obesity, prevalence and prevention'. *Nutr J,* 4, p. 24.

della Croce, U., Cappozzo, A. and Kerrigan, D. C. (1999) 'Pelvis and lower limb anatomical landmark calibration precision and its propagation to bone geometry and joint angles'. *Med Biol Eng Comput,* 37(2), pp. 155-161.

Dempster, P. and Aitkens, S. (1995) 'A new air displacement method for the determination of human body composition'. *Med Sci Sports Exerc,* 27(12), pp. 1692-1697.

Dempster, W., T, Gabel, W., C and Felts W, J., L. (1959) 'The anthropometry of the manual workspace for the seated subject'. *American Jounral of Physiological Anthropometry,* 17, p. 289.

Deschamps, K., Staes, F., Bruyninckx, H., Busschots, E., Jaspers, E., Atre, A. and Desloovere, K. (2011a) 'Repeatability in the assessment of multi-segment foot kinematics.'. *Gait Posture*.

Deschamps, K., Staes, F., Roosen, P., Nobels, F., Desloovere, K., Bruyninckx, H. and Matricali, G. A. (2011b) 'Body of evidence supporting the clinical use of 3d multisegment foot models: A systematic review.'. *Gait Posture,* 33(3), pp. 338-349.

Deurenberg, P. (1996) 'Limitations of the bioelectrical impedance method for the assessment of body fat mass in severe obesity'. *Am J Clin Nutr,* 64(3 Suppl), pp. 449S-452S.

Deurenberg, P. and Yap, M. (1999) 'The assessment of obesity: Methods for measuring body fat mass and global prevalence of obesity'. *Baillieres Best Pract Res Clin Endocrinol Metab,* 13(1), pp. 1-11.

DeVita, P. and Hortobágyi, T. (2003) 'Obesity is not associated with increased knee joint torque and power during level walking'. *J Biomech,* 36(9), pp. 1355-1362.

Dewit, O., Fuller, N. J., Fewtrell, M. S., Elia, M. and Wells, J. C. (2000) 'Whole body air displacement plethysmography compared with hydrodensitometry for body composition analysis'. *Arch Dis Child,* 82(2), pp. 159-164.

Dietz, W. H. (1998) 'Health consequences of obesity in youth: Childhood predictors of adult disease'. *Pediatrics,* 101(3 Pt 2), pp. 518-525.

Ding, C., Cicuttini, F., Scott, F., Cooley, H. and Jones, G. (2005) 'Knee structural alteration and bmi: A cross-sectional study'. *Obes Res,* 13(2), pp. 350-361.

Donati, M., Camomilla, V., Vannozzi, G. and Cappozzo, A. (2008) 'Anatomical frame identification and reconstruction for repeatable lower limb joint kinematics estimates'. *J Biomech,* 41(10), pp. 2219-2226.

Dowling, A. M., Steele, J. R. and Baur, L. A. (2001) 'Does obesity influence foot structure and plantar pressure patterns in prepubescent children?'. *Int J Obes Relat Metab Disord,* 25(6), pp. 845-852.

Dowling, A. M., Steele, J. R. and Baur, L. A. (2004) 'What are the effects of obesity in children on plantar pressure distributions?'. *Int J Obes Relat Metab Disord,* 28(11), pp. 1514-1519.

Dubois, D. and Dbois, E., F. (1916) 'A formula to estimate the approximate surface area if height be known'. *Archives of International Medicine,* 17, pp. 863-871.

Duren, D. L., Sherwood, R. J., Czerwinski, S. A., Lee, M., Choh, A. C., Siervogel, R. M. and Cameron Chumlea, W. (2008) 'Body composition methods: Comparisons and interpretation'. *J Diabetes Sci Technol,* 2(6), pp. 1139-1146.

Dwyer, T. and Blizzard, C. L. (1996) 'Defining obesity in children by biological endpoint rather than population distribution'. *Int J Obes Relat Metab Disord,* 20(5), pp. 472-480.

Ebbeling, C. B., Pawlak, D. B. and Ludwig, D. S. (2002) 'Childhood obesity: Public-health crisis, common sense cure'. *Lancet,* 360(9331), pp. 473-482.

Egger, G. and Swinburn, B. (1997) 'An "Ecological" Approach to the obesity pandemic'. *BMJ,* 315(7106), pp. 477-480.

Ehtisham, S., Crabtree, N., Clark, P., Shaw, N. and Barrett, T. (2005) 'Ethnic differences in insulin resistance and body composition in united kingdom adolescents'. *J Clin Endocrinol Metab,* 90(7), pp. 3963-3969.

Epstein, L. H. and Roemmich, J. N. (2001) 'Reducing sedentary behavior: Role in modifying physical activity'. *Exerc Sport Sci Rev,* 29(3), pp. 103-108.

Esposito, P. W., Caskey, P., Heaton, L. E. and Otsuka, N. (2013) 'Childhood obesity case statement'. *Semin Arthritis Rheum*.

Farooqi, I. S. and O'Rahilly, S. (2000) 'Recent advances in the genetics of severe childhood obesity'. *Arch Dis Child,* 83(1), pp. 31-34.

Federico, B., D'Aliesio, F., Pane, F., Capelli, G. and Rodio, A. (2011) 'Body mass index has a curvilinear relationship with the percentage of body fat mass among children'. *BMC Res Notes,* 4, p. 301.

Ferrari, A., Benedetti, M. G., Pavan, E., Frigo, C., Bettinelli, D., Rabuffetti, M., Crenna, P. and Leardini, A. (2008) 'Quantitative comparison of five current protocols in gait analysis'. *Gait Posture,* 28(2), pp. 207-216.

Field, A. (2009) *Discovering statistics using spss*. London: Sage.

Fields, D. A. and Goran, M. I. (2000) 'Body composition techniques and the four-compartment model in children'. *J Appl Physiol,* 89(2), pp. 613-620.

Fields, D. A., Goran, M. I. and McCrory, M. A. (2002) 'Body-composition assessment via air-displacement plethysmography in adults and children: A review'. *Am J Clin Nutr,* 75(3), pp. 453-467.

Fields, D. A., Hull, H. R., Cheline, A. J., Yao, M. and Higgins, P. B. (2004) 'Child-specific thoracic gas volume prediction equations for air-displacement plethysmography'. *Obes Res,* 12(11), pp. 1797-1804.

Flegal, K. M. and Ogden, C. L. (2011) 'Childhood obesity: Are we all speaking the same language?'. *Adv Nutr,* 2(2), pp. 159S-166S.

Fleiss, J. (1986) *The design and analysis of clinical experiments*. New York: Wiley.

Fogelholm, M. (2010) 'Physical activity, fitness and fatness: Relations to mortality, morbidity and disease risk factors. A systematic review'. *Obes Rev,* 11(3), pp. 202-221.

Fogelholm, M., Sievänen, H., Kukkonen-Harjula, K., Oja, P. and Vuori, I. (1993) 'Effects of meal and its electrolytes on bioelectrical impedance'. *Basic Life Sci,* 60, pp. 331-332.

Forner-Cordero, A., Koopman, H. J. and van der Helm, F. C. (2006) 'Describing gait as a sequence of states'. *J Biomech,* 39(5), pp. 948-957.

Fortin, C., Nadeau, S. and Labelle, H. (2008) 'Inter-trial and test-retest reliability of kinematic and kinetic gait parameters among subjects with adolescent idiopathic scoliosis'. *Eur Spine J,* 17(2), pp. 204-216.

Fortuño, A., Rodríguez, A., Gómez-Ambrosi, J., Frühbeck, G. and Díez, J. (2003) 'Adipose tissue as an endocrine organ: Role of leptin and adiponectin in the pathogenesis of cardiovascular diseases'. *J Physiol Biochem,* 59(1), pp. 51-60.

Freedman, D. S., Dietz, W. H., Srinivasan, S. R. and Berenson, G. S. (1999) 'The relation of overweight to cardiovascular risk factors among children and adolescents: The bogalusa heart study'. *Pediatrics,* 103(6 Pt 1), pp. 1175-1182.

Freedman, D. S., Mei, Z., Srinivasan, S. R., Berenson, G. S. and Dietz, W. H. (2007) 'Cardiovascular risk factors and excess adiposity among overweight children and adolescents: The bogalusa heart study'. *J Pediatr,* 150(1), pp. 12-17.e12.

Freedman, D. S. and Sherry, B. (2009) 'The validity of bmi as an indicator of body fat massness and risk among children'. *Pediatrics,* 124 Suppl 1, pp. S23-34.

Freedman, D. S., Wang, J., Maynard, L. M., Thornton, J. C., Mei, Z., Pierson, R. N., Dietz, W. H. and Horlick, M. (2005) 'Relation of bmi to fat and fat-free mass among children and adolescents'. *Int J Obes (Lond),* 29(1), pp. 1-8.

Freedman, D. S., Wang, J., Thornton, J. C., Mei, Z., Pierson, R. N., Dietz, W. H. and Horlick, M. (2008) 'Racial/ethnic differences in body fat massness among children and adolescents'. *Obesity (Silver Spring),* 16(5), pp. 1105-1111.

Frigo, C., Rabuffetti, M., Kerrigan, D. C., Deming, L. C. and Pedotti, A. (1998) 'Functionally oriented and clinically feasible quantitative gait analysis method'. *Med Biol Eng Comput,* 36(2), pp. 179-185.

Fuller, N. J., Jebb, S. A., Laskey, M. A., Coward, W. A. and Elia, M. (1992) 'Four-component model for the assessment of body composition in humans: Comparison with alternative methods, and evaluation of the density and hydration of fat-free mass'. *Clin Sci (Lond),* 82(6), pp. 687-693.

Galbraith, R. T., Gelberman, R. H., Hajek, P. C., Baker, L. A., Sartoris, D. J., Rab, G. T., Cohen, M. S. and Griffin, P. P. (1987) 'Obesity and decreased femoral anteversion in adolescence'. *J Orthop Res,* 5(4), pp. 523-528.

Ganley, K. J. and Powers, C. M. (2005) 'Gait kinematics and kinetics of 7-year-old children: A comparison to adults using age-specific anthropometric data'. *Gait Posture,* 21(2), pp. 141-145.

Gately, P. J., Radley, D., Cooke, C. B., Carroll, S., Oldroyd, B., Truscott, J. G., Coward, W. A. and Wright, A. (2003) 'Comparison of body composition methods in overweight and obese children'. *J Appl Physiol,* 95(5), pp. 2039-2046.

Gidding, S. S., Bao, W., Srinivasan, S. R. and Berenson, G. S. (1995) 'Effects of secular trends in obesity on coronary risk factors in children: The bogalusa heart study'. *J Pediatr,* 127(6), pp. 868-874.

Gilmour, J. C. and Burns, Y. (2001) 'The measurement of the medial longitudinal arch in children'. *Foot Ankle Int,* 22(6), pp. 493-498.

Goran, M. I. and Gower, B. A. (1999) 'Relation between visceral fat and disease risk in children and adolescents'. *Am J Clin Nutr,* 70(1), pp. 149S-156S.

Goran, M. I., Gower, B. A., Treuth, M. and Nagy, T. R. (1998) 'Prediction of intra-abdominal and subcutaneous abdominal adipose tissue in healthy pre-pubertal children'. *Int J Obes Relat Metab Disord,* 22(6), pp. 549-558.

Gorton G.E, Stevens C.M, Masso P.D, Vannah W.M. (1997) 'Repeatability of the walking patterns of normal children'. *Gait & Posture,* 5(2), pp. 155-155.

Gorton, G., Herbert, D. and Goode, B. (2001) 'Assessment of the kinematic variability between twelve shriners motion analysis laboratories'. *Gait & Posture,* 13, p. 247.

Gorton, G., Herbert, D. and Goode, B. (2002) 'Assessment of the kinematic variability between 12 shriners motion analysis laboratories. Part 2. short term follow up'. *Gait & Posture,* 16(S1), p. S65.

Gorton, G. E., Hebert, D. A. and Gannotti, M. E. (2009) 'Assessment of the kinematic variability among 12 motion analysis laboratories'. *Gait Posture,* 29(3), pp. 398-402.

Gray, D. S., Bray, G. A., Bauer, M., Kaplan, K., Gemayel, N., Wood, R., Greenway, F. and Kirk, S. (1990) 'Skinfold thickness measurements in obese subjects'. *Am J Clin Nutr,* 51(4), pp. 571-577.

Green, J. S., Parfrey, P. S., Harnett, J. D., Farid, N. R., Cramer, B. C., Johnson, G., Heath, O., McManamon, P. J., O'Leary, E. and Pryse-Phillips, W. (1989) 'The cardinal manifestations of bardet-biedl syndrome, a form of laurence-moon-biedl syndrome'. *N Engl J Med,* 321(15), pp. 1002-1009.

Gregory, J. R., Lowe, S., Bates, C. J., Prentice, A., Jackson, L. V., Smithers, G., Wenlock, R. and Farron, M. (2000) *National diet and nutrition survey: Young people aged 4 to 18 years: Report of the diet and nutrition survey*. London: The Stationary Office.

Grood, E. S. and Suntay, W. J. (1983) 'A joint coordinate system for the clinical description of three-dimensional motions: Application to the knee'. *J Biomech Eng,* 105(2), pp. 136-144.

Gunther, K.-P. (2004) 'Musculoskeletal consequences of obesity in youth', in Keiss, W., Marcus, C. and Wabitsch, M. (eds.) *Obesity in childhood and adolescence. Pediatric adolesc med*. Basel: Karger, pp. 137-147.

Gurrici, S., Hartriyanti, Y., Hautvast, J. G. and Deurenberg, P. (1999) 'Differences in the relationship between body fat mass and body mass index between two different indonesian ethnic groups: The effect of body build'. *Eur J Clin Nutr,* 53(6), pp. 468-472.

Gushue, D. L., Houck, J. and Lerner, A. L. (2005) 'Effects of childhood obesity on three-dimensional knee joint biomechanics during walking'. *J Pediatr Orthop,* 25(6), pp. 763-768.

Hamacher, D., Singh, N. B., Van Dieën, J. H., Heller, M. O. and Taylor, W. R. (2011) 'Kinematic measures for assessing gait stability in elderly individuals: a systematic review', *J R Soc Interface*, 8(65), pp. 1682-1698.

Hamer, M. and O'Donovan, G. (2010) 'Cardiorespiratory fitness and metabolic risk factors in obesity'. *Curr Opin Lipidol,* 21(1), pp. 1-7.

Haroun, D., Croker, H., Viner, R. M., Williams, J. E., Darch, T. S., Fewtrell, M. S., Eaton, S. and Wells, J. C. (2009) 'Validation of bia in obese children and adolescents and re-evaluation in a longitudinal study'. *Obesity (Silver Spring),* 17(12), pp. 2245-2250.

Haycock, G. B., Schwartz, G. J. and Wisotsky, D. H. (1978) 'Geometric method for measuring body surface area: A height-weight formula validated in infants, children, and adults'. *J Pediatr,* 93(1), pp. 62-66.

Henley, J., Richards, J., Hudson, D., Church, C., Coleman, S., Kersetter, L. and Miller, F. (2008) 'Reliability of a clinically practical multisegment foot marker set/model', in Harris, G. F., Smith, P. A. and Marks, R., M. (ed.), *Foot and ankle motion analysis clinical. Treatment and technology*: Taylor & Francis, pp. 445-464.

Heyward, V. and Wagner, D. (2004) *Applied body composition assessment* (2nd edn.). Champaign, IL: Human Kinetic.

Higgins, P. B., Gower, B. A., Hunter, G. R. and Goran, M. I. (2001) 'Defining health-related obesity in prepubertal children'. *Obes Res,* 9(4), pp. 233-240.

Hills, A. P., Andersen, L. B. and Byrne, N. M. (2011) 'Physical activity and obesity in children'. *Br J Sports Med,* 45(11), pp. 866-870.

Hills, A. P., King, N. A. and Armstrong, T. P. (2007) 'The contribution of physical activity and sedentary behaviours to the growth and development of children and adolescents: Implications for overweight and obesity'. *Sports Med,* 37(6), pp. 533-545.

Hills, A. P. and Parker, A. W. (1991) 'Gait characteristics of obese children'. *Arch Phys Med Rehabil,* 72(6), pp. 403-407.

Hof, A., L. (1996) 'Scaling gait data to body size'. *Gait & Posture,* 4, pp. 222-223.

Horlick, M., Arpadi, S. M., Bethel, J., Wang, J., Moye, J., Cuff, P., Pierson, R. N. and Kotler, D. (2002) 'Bioelectrical impedance analysis models for prediction of total body water and fat-free mass in healthy and hiv-infected children and adolescents'. *Am J Clin Nutr,* 76(5), pp. 991-999.

Hortobágyi, T., Herring, C., Pories, W. J., Rider, P. and Devita, P. (2011) 'Massive weight loss-induced mechanical plasticity in obese gait'. *J Appl Physiol,* 111(5), pp. 1391-1399.

Houtkooper, L. B., Going, S. B., Lohman, T. G., Roche, A. F. and Van Loan, M. (1992) 'Bioelectrical impedance estimation of fat-free body mass in children and youth: A cross-validation study'. *J Appl Physiol,* 72(1), pp. 366-373.

Houtkooper, L. B., Lohman, T. G., Going, S. B. and Hall, M. C. (1989) 'Validity of bioelectric impedance for body composition assessment in children'. *J Appl Physiol,* 66(2), pp. 814-821.

Inman, V., Ralston, H. J. and Todd, F. (1981) *Human walking*. Baltimore: Williams & Watkins.

Ivanenko, Y. P., Dominici, N. and Lacquaniti, F. (2007) 'Development of independent walking in toddlers'. *Exerc Sport Sci Rev,* 35(2), pp. 67-73.

Perry, J., (1992) *Gait analysis: Normal and pathological function.* NJ: Slack International.

Jenkins SEM, Harrington ME, Elliot M, Theologis TN and JJ., O. C. (2000) The customisation of a three dimensional locomotor model to children*. Proceedings of sixth international symposium on 3-D*
analysis of human movement., Cape Town, South Africa.

Jenkyn, T. R. and Nicol, A. C. (2007) 'A multi-segment kinematic model of the foot with a novel definition of forefoot motion for use in clinical gait analysis during walking.'. *J Biomech,* 40(14), pp. 3271-3278.

Kadaba, M. P., Ramakrishnan, H. K. and Wootten, M. E. (1990) 'Measurement of lower extremity kinematics during level walking'. *J Orthop Res,* 8(3), pp. 383-392.

Kadaba, M. P., Ramakrishnan, H. K., Wootten, M. E., Gainey, J., Gorton, G. and Cochran, G. V. (1989) 'Repeatability of kinematic, kinetic, and electromyographic data in normal adult gait'. *J Orthop Res,* 7(6), pp. 849-860.

Katz, J. N., Larson, M. G., Phillips, C. B., Fossel, A. H. & Liang, M. H. (1992). 'Comparative measurement sensitivity of short and longer health status instruments'. *Med Care,* 30**,** 917-25.

Kelsey, J. L., Acheson, R. M. and Keggi, K. J. (1972) 'The body build of patients with slipped capital femoral epiphysis'. *Am J Dis Child,* 124(2), pp. 276-281.

Kidder, S. M., Abuzzahab, F. S., Harris, G. F. and Johnson, J. E. (1996) 'A system for the analysis of foot and ankle kinematics during gait.'. *IEEE Trans Rehabil Eng,* 4(1), pp. 25-32.

Kim, H. W. and Weinstein, S. L. (2000) 'Flatfoot in children: Differential diagnosis and management'. *Current Orthopaedics,* 14(6), pp. 441-447.

Kirtley, C. (2002) Sensitivity of the modified helen hayes model to marker placement errors. *Seventh International Symposium on the 3-D Analysis of Human Movement*, Newcastle, UK.

Kisho Fukuchi, R., Arakaki, C., Veras Orselli, M. I. and Duarte, M. (2010) 'Evaluation of alternative technical markers for the pelvic coordinate system'. *J Biomech,* 43(3), pp. 592-594.

Klejman, S., Andrysek, J., Dupuis, A. and Wright, V. (2010) 'Test-retest reliability of discrete gait parameters in children with cerebral palsy'. *Arch Phys Med Rehabil,* 91(5), pp. 781-787.

Kotchen, J. M., Kotchen, T. A., Guthrie, G. P., Cottrill, C. M. and McKean, H. E. (1980) 'Correlates of adolescent blood pressure at five-year follow-up'. *Hypertension,* 2(4 Pt 2), pp. 124-129.

Kuczmarski, R. J., Ogden, C. L., Grummer-Strawn, L. M., Flegal, K. M., Guo, S. S., Wei, R., Mei, Z., Curtin, L. R., Roche, A. F. and Johnson, C. L. (2000) 'Cdc growth charts: United states'. *Adv Data*(314), pp. 1-27.

Kullberg, J., Brandberg, J., Angelhed, J. E., Frimmel, H., Bergelin, E., Strid, L., Ahlström, H., Johansson, L. and Lönn, L. (2009) 'Whole-body adipose tissue analysis: Comparison of mri, ct and dual energy x-ray absorptiometry'. *Br J Radiol,* 82(974), pp. 123-130.

Kyle, U. G., Bosaeus, I., De Lorenzo, A. D., Deurenberg, P., Elia, M., Gómez, J. M., Heitmann, B. L., Kent-Smith, L., Melchior, J. C., Pirlich, M., Scharfetter, H., Schols, A. M., Pichard, C. and Group, C. o. t. E. W. (2004a) 'Bioelectrical impedance analysis--part i: Review of principles and methods'. *Clin Nutr,* 23(5), pp. 1226-1243.

Kyle, U. G., Bosaeus, I., De Lorenzo, A. D., Deurenberg, P., Elia, M., Manuel Gómez, J., Lilienthal Heitmann, B., Kent-Smith, L., Melchior, J. C., Pirlich, M., Scharfetter, H., M W J Schols, A., Pichard, C. and ESPEN. (2004b) 'Bioelectrical impedance analysis-part ii: Utilization in clinical practice'. *Clin Nutr,* 23(6), pp. 1430-1453.

l'Allemand-Jander, D. (2010) 'Clinical diagnosis of metabolic and cardiovascular risks in overweight children: Early development of chronic diseases in the obese child'. *Int J Obes (Lond),* 34 Suppl 2, pp. S32-36.

Lai, P. P., Leung, A. K., Li, A. N. and Zhang, M. (2008) 'Three-dimensional gait analysis of obese adults'. *Clin Biomech (Bristol, Avon),* 23 Suppl 1, pp. S2-6.

Lang, T. and Rayner, G. (2005) 'Obesity: A growing issue for european policy?'. *Journal of European Social Policy,* 15(4), pp. 301-327.

Lazarus, R., Baur, L., Webb, K. and Blyth, F. (1996) 'Body mass index in screening for adiposity in children and adolescents: Systematic evaluation using receiver operating characteristic curves'. *Am J Clin Nutr,* 63(4), pp. 500-506.

Lazzer, S., Bedogni, G., Agosti, F., De Col, A., Mornati, D. and Sartorio, A. (2008) 'Comparison of dual-energy x-ray absorptiometry, air displacement plethysmography and bioelectrical impedance analysis for the assessment of body composition in severely obese caucasian children and adolescents'. *Br J Nutr,* 100(4), pp. 918-924.

Le Carvennec, M., Fagour, C., Adenis-Lamarre, E., Perlemoine, C., Gin, H. and Rigalleau, V. (2007) 'Body composition of obese subjects by air displacement plethysmography: The influence of hydration'. *Obesity (Silver Spring),* 15(1), pp. 78-84.

Leardini A, Cappozzo A, Catani F, Toksvig-Larsen S, Petitto A, Sforza V, Cassanelli G and S., G. (1999) 'Validation of a functional method for the estimation of the hip joint centre location'. *Journal of Biomechanics,* 32, pp. 99–103.

Leardini, A., Benedetti, M. G., Catani, F., Simoncini, L. and Giannini, S. (1999) 'An anatomically based protocol for the description of foot segment kinematics during gait.'. *Clin Biomech (Bristol, Avon),* 14(8), pp. 528-536.

Leardini, A., Chiari, L., Della Croce, U. and Cappozzo, A. (2005) 'Human movement analysis using stereophotogrammetry. Part 3. Soft tissue artifact assessment and compensation'. *Gait Posture,* 21(2), pp. 212-225.

Leardini, A., Benedetti, M. G., Berti, L., Bettinelli, D., Nativo, R. and Giannini, S. (2007a) 'Rear-foot, mid-foot and fore-foot motion during the stance phase of gait.'. *Gait Posture,* 25(3), pp. 453-462.

Leardini, A., Sawacha, Z., Paolini, G., Ingrosso, S., Nativo, R. and Benedetti, M. G. (2007b) 'A new anatomically based protocol for gait analysis in children'. *Gait Posture,* 26(4), pp. 560-571.

Levinger, P., Murley, G. S., Barton, C. J., Cotchett, M. P., McSweeney, S. R. and Menz, H. B. (2010) 'A comparison of foot kinematics in people with normal- and flat-arched feet using the oxford foot model'. *Gait Posture,* 32(4), pp. 519-523.

Link, K., Moëll, C., Garwicz, S., Cavallin-Ståhl, E., Björk, J., Thilén, U., Ahrén, B. and Erfurth, E. M. (2004) 'Growth hormone deficiency predicts cardiovascular risk in young adults treated for acute lymphoblastic leukemia in childhood'. *J Clin Endocrinol Metab,* 89(10), pp. 5003-5012.

Lissau, I., Burniat, W., Poskitt, E. M. E. and Cole, T. (2002) 'Prevention.', in Burniat, W., Cole, T., Lissau, I. and Poskitt, E. M. E. (eds.) *Child and adolescent obesity. Causes and consequences; prevention and management*. Cambridge: Cambridge University Press, pp. 243–269.

Liu, W., Siegler, S. and Hillstrom HJ. (1997) 'Three-dimensional, six-degree of freedom kinematics of the human hindfoot during the stance phase of level walking'. *Human Movement Science,* 16, pp. 283-298.

Lobstein, T., Baur, L., Uauy, R. and TaskForce, I. I. O. (2004) 'Obesity in children and young people: A crisis in public health'. *Obes Rev,* 5 Suppl 1, pp. 4-104.

Lockner, D. W., Heyward, V. H., Baumgartner, R. N. and Jenkins, K. A. (2000) 'Comparison of air-displacement plethysmography, hydrodensitometry, and dual x-ray absorptiometry for assessing body composition of children 10 to 18 years of age'. *Ann N Y Acad Sci,* 904, pp. 72-78.

Lohman, T. G. (1989) 'Assessment of body composition in children'. *Pediatric Exercise Science,* 1, pp. 19-30.

Lundberg, A., Goldie, I., Kalin, B. and Selvik, G. (1989) 'Kinematics of the ankle/foot complex: Plantarflexion and dorsiflexion'. *Foot Ankle,* 9(4), pp. 194-200.

Lundgren, P., Nester, C., Liu, A., Arndt, A., Jones, R., Stacoff, A., Wolf, P. and Lundberg, A. (2008) 'Invasive in vivo measurement of rear-, mid- and forefoot motion during walking'. *Gait Posture,* 28(1), pp. 93-100.

MacWilliams, B. A., Cowley, M. and Nicholson, D. E. (2003) 'Foot kinematics and kinetics during adolescent gait.'. *Gait Posture,* 17(3), pp. 214-224.

Malt, M., A., Fevang, J., M., Aarli, A., Madujano, A., M. and Jansen, K. (2012) 'Adjustment of the thigh rotation offset results in reduced variability in the hip rotation curve'. *Gait & Posture,* 36(S1), pp. S46–S47.

Marquez-Vidal P, Marcelino G, Ravasco P, Ermelinda CM and JM., O. (2008) 'Body fat mass levels in children and adolescents: Effects on prevalence of obesity'. *The European e-journal of Clinical Nutrition and Metabolism,* 3, pp. e321-e327.

Marshall, S. J., Biddle, S. J., Gorely, T., Cameron, N. and Murdey, I. (2004) 'Relationships between media use, body fat massness and physical activity in children and youth: A meta-analysis'. *Int J Obes Relat Metab Disord,* 28(10), pp. 1238-1246.

Matheison, I., Upton, D. and Birchenough, A. (1999) 'Comparison of footprint parameters calculated from static and dynamic footprints'. *The Foot,* 9.

Mauch, M., Grau, S., Krauss, I., Maiwald, C. and Horstmann, T. (2008) 'Foot morphology of normal, underweight and overweight children'. *Int J Obes (Lond),* 32(7), pp. 1068-1075.

Maynard, L. M., Wisemandle, W., Roche, A. F., Chumlea, W. C., Guo, S. S. and Siervogel, R. M. (2001) 'Childhood body composition in relation to body mass index'. *Pediatrics,* 107(2), pp. 344-350.

Maynard, V., Bakheit, A. M., Oldham, J. and Freeman, J. (2003) 'Intra-rater and inter-rater reliability of gait measurements with coda mpx30 motion analysis system'. *Gait Posture,* 17(1), pp. 59-67.

McCarthy, H. D., Cole, T. J., Fry, T., Jebb, S. A. and Prentice, A. M. (2006) 'Body fat mass reference curves for children'. *Int J Obes (Lond),* 30(4), pp. 598-602.

McGinley, J. L., Baker, R., Wolfe, R. and Morris, M. E. (2009) 'The reliability of three-dimensional kinematic gait measurements: A systematic review.'. *Gait Posture,* 29(3), pp. 360-369.

McGraw, B., McClenaghan, B. A., Williams, H. G., Dickerson, J. and Ward, D. S. (2000) 'Gait and postural stability in obese and nonobese prepubertal boys'. *Arch Phys Med Rehabil,* 81(4), pp. 484-489.

McMillan, A. G., Auman, N. L., Collier, D. N. and Blaise Williams, D. S. (2009) 'Frontal plane lower extremity biomechanics during walking in boys who are overweight versus healthy weight'. *Pediatr Phys Ther,* 21(2), pp. 187-193.

McMillan, A. G., Pulver, A. M., Collier, D. N. and Williams, D. S. (2010) 'Sagittal and frontal plane joint mechanics throughout the stance phase of walking in adolescents who are obese'. *Gait Posture,* 32(2), pp. 263-268.

Mei, Z., Grummer-Strawn, L. M., Pietrobelli, A., Goulding, A., Goran, M. I. and Dietz, W. H. (2002) 'Validity of body mass index compared with other body-composition screening indexes for the assessment of body fat massness in children and adolescents'. *Am J Clin Nutr,* 75(6), pp. 978-985.

Menz, H. B. (2005) 'Analysis of paired data in physical therapy research: Time to stop double-dipping?'. *J Orthop Sports Phys Ther,* 35(8), pp. 477-478.

Messier, S. P., Davies, A. B., Moore, D. T., Davis, S. E., Pack, R. J. and Kazmar, S. C. (1994) 'Severe obesity: Effects on foot mechanics during walking'. *Foot Ankle Int,* 15(1), pp. 29-34.

Metcalf, B. S., Hosking, J., Jeffery, A. N., Voss, L. D., Henley, W. and Wilkin, T. J. (2011) 'Fatness leads to inactivity, but inactivity does not lead to fatness: A longitudinal study in children (earlybird 45)'. *Arch Dis Child,* 96(10), pp. 942-947.

Mickle, K. J., Steele, J. R. and Munro, B. J. (2006) 'Does excess mass affect plantar pressure in young children?'. *Int J Pediatr Obes,* 1(3), pp. 183-188.

Miller, F., Castagno, M., S,, Richards, J., Lennon, N., Quigley, M., S, and Njiler, M., S. (1996) 'Reliability of kinematics during clinical gait analsyis: A comparison between normal and children with cerebal palsy'. *Gait & Posture,* 4, pp. 167-208.

Miyazaki, T., Wada, M., Kawahara, H., Sato, M., Baba, H. and Shimada, S. (2002) 'Dynamic load at baseline can predict radiographic disease progression in medial compartment knee osteoarthritis'. *Ann Rheum Dis,* 61(7), pp. 617-622.

Moisio, K. C., Sumner, D. R., Shott, S. and Hurwitz, D. E. (2003) 'Normalization of joint moments during gait: A comparison of two techniques'. *J Biomech,* 36(4), pp. 599-603.

Monaghan, K., Delahunt, E. and Caulfield, B. (2007) 'Increasing the number of gait trial recordings maximises intra-rater reliability of the coda motion analysis system'. *Gait Posture,* 25(2), pp. 303-315.

Morris, E., A. and Hsiao-Wecksler, E, T. (2010) *Time normalizing gait data based on gait events. ASB Conference*, Providence, RI,

Morrison, S. C., Durward, B. R., Watt, G. F. and Donaldson, M. D. (2007) 'Anthropometric foot structure of peripubescent children with excessive versus normal body mass: A cross-sectional study'. *J Am Podiatr Med Assoc,* 97(5), pp. 366-370.

Morrison, S. C., Durward, B. R., Watt, G. F. and Donaldson, M. D. (2008) 'The influence of body mass on the temporal parameters of peripubescent gait'. *Gait Posture,* 27(4), pp. 719-721.

Moseley, L., Smith, R., Hunt, A. and Gant, R. (1996) 'Three-dimensional kinematics of the hindfoot during the stance phase of walking in normal young adult males'. *Clin Biomech (Bristol, Avon),* 11(1), pp. 39-45.

Mueller, W. H. and Kaplowitz, H. J. (1994) 'The precision of anthropometric assessment of body fat mass distribution in children'. *Ann Hum Biol,* 21(3), pp. 267-274.

Must, A., Dallal, G. E. and Dietz, W. H. (1991) 'Reference data for obesity: 85th and 95th percentiles of body mass index (wt/ht2) and triceps skinfold thickness'. *Am J Clin Nutr,* 53(4), pp. 839-846.

Must, A., Jacques, P. F., Dallal, G. E., Bajema, C. J. and Dietz, W. H. (1992) 'Long-term morbidity and mortality of overweight adolescents. A follow-up of the harvard growth study of 1922 to 1935'. *N Engl J Med,* 327(19), pp. 1350-1355.

Myers, K. A., Wang, M., Marks, R. M. and Harris, G. F. (2004) 'Validation of a multisegment foot and ankle kinematic model for pediatric gait.'. *IEEE Trans Neural Syst Rehabil Eng,* 12(1), pp. 122-130.

Nair, S. P., Gibbs, S., Arnold, G., Abboud, R. and Wang, W. (2010) 'A method to calculate the centre of the ankle joint: A comparison with the vicon plug-in-gait model'. *Clin Biomech (Bristol, Avon),* 25(6), pp. 582-587.

Nantel, J., Brochu, M. and Prince, F. (2006) 'Locomotor strategies in obese and non-obese children'. *Obesity (Silver Spring),* 14(10), pp. 1789-1794.

National Child Measurement Program. (2012). National child measurement program (NCMP) 2012/13. *http://www.dh.gov.uk* Retrieved August 2012.

National Institute for Health, (1996) 'NIH consensus statement. Bioelectrical impedance analysis in body composition measurement. National institutes of health technology assessment conference statement. December 12-14, 1994'. *Nutrition,* 12(11-12), pp. 749-762.

Nester, C., Jones, R. K., Liu, A., Howard, D., Lundberg, A., Arndt, A., Lundgren, P., Stacoff, A. and Wolf, P. (2007) 'Foot kinematics during walking measured using bone and surface mounted markers'. *J Biomech,* 40(15), pp. 3412-3423.

Nester, C. J. (2009) 'Lessons from dynamic cadaver and invasive bone pin studies: Do we know how the foot really moves during gait?'. *J Foot Ankle Res,* 2, p. 18.

Nester, C. J., Liu, A. M., Ward, E., Howard, D., Cocheba, J. and Derrick, T. (2010) 'Error in the description of foot kinematics due to violation of rigid body assumptions'. *J Biomech,* 43(4), pp. 666-672.

North, C., Patton, M. A., Baraitser, M. and Winter, R. M. (1985) 'The clinical features of the cohen syndrome: Further case reports'. *J Med Genet,* 22(2), pp. 131-134.

Okita, N., Meyers, S. A., Challis, J. H. and Sharkey, N. A. (2009) 'An objective evaluation of a segmented foot model'. *Gait Posture,* 30(1), pp. 27-34.

Ounpuu, S., Gage, J. R. and Davis, R. B. (1991) 'Three-dimensional lower extremity joint kinetics in normal pediatric gait'. *J Pediatr Orthop,* 11(3), pp. 341-349.

Owen, C. G., Nightingale, C. M., Rudnicka, A. R., Sattar, N., Cook, D. G., Ekelund, U. and Whincup, P. H. (2010) 'Physical activity, obesity and cardiometabolic risk factors in 9- to 10-year-old uk children of white european, south asian and black african-caribbean origin: The child heart and health study in england (chase)'. *Diabetologia,* 53(8), pp. 1620-1630.

Peters, A., Galna, B., Sangeux, M., Morris, M. and Baker, R. (2010) 'Quantification of soft tissue artifact in lower limb human motion analysis: A systematic review'. *Gait Posture,* 31(1), pp. 1-8.

Pfeiffer, M., Kotz, R., Ledl, T., Hauser, G. and Sluga, M. (2006) 'Prevalence of flat foot in preschool-aged children'. *Pediatrics,* 118(2), pp. 634-639.

Piazza, S. J. and Cavanagh, P. R. (2000) 'Measurement of the screw-home motion of the knee is sensitive to errors in axis alignment'. *J Biomech,* 33(8), pp. 1029-1034.

Pietrobelli, A., Faith, M. S., Allison, D. B., Gallagher, D., Chiumello, G. and Heymsfield, S. B. (1998) 'Body mass index as a measure of adiposity among children and adolescents: A validation study'. *J Pediatr,* 132(2), pp. 204-210.

Pietrobelli, A., Malavolti, M., Battistini, N. C. and Fuiano, N. (2008) 'Metabolic syndrome: A child is not a small adult'. *Int J Pediatr Obes,* 3 Suppl 1, pp. 67-71.

Portney L G and P., W. M. (2000) *Foundations of clinical research application to practice* (Vol. 1). NewJersey: Prentice-Hall.

Powell, D. W., Hanson, N. J., Long, B. and Williams, D. S. (2012) 'Frontal plane landing mechanics in high-arched compared with low-arched female athletes'. *Clin J Sport Med,* 22(5), pp. 430-435.

Power, C., Lake, J. K. and Cole, T. J. (1997) 'Body mass index and height from childhood to adulthood in the 1958 british born cohort'. *Am J Clin Nutr,* 66(5), pp. 1094-1101.

Pritchett, J. W. and Perdue, K. D. (1988) 'Mechanical factors in slipped capital femoral epiphysis'. *J Pediatr Orthop,* 8(4), pp. 385-388.

Pupil Level Annual School Census (2009) 'Http://www.Education.Gov.Uk/rsgateway/db/sfr/s001012/index.Shtml'. *accessed February 2013*.

Quigley, E., Miller, F., Castagno, P., Richar and Edward Quigley, M. S., Freeman Miller, M.D., Patrick Castagno, M.S., James Richards, Ph.D., Nancy Lennon, P.T. (1997) 'Reliability of kinetics during clinical gait analysis: A comparison between normal and children with cerebral palsy'. *Gait & Posture,* 5(2), p. 143.

Quigley, E., Miller, F., Castagno, P., Richards, J. and Lennon, N. (1999) 'Variability of gait measurements for typically developing children and children with cerebral palsy'. *Gait & Posture,* 10(3), pp. 187-286.

Rabuffetti, M. and Crenna, P. (2004) 'A modular protocol for the analysis of movement in children'. *Gait & Posture,* 20, pp. S77–S78.

Ramakrishnan, H. K. and Kadaba, M. P. (1991) 'On the estimation of joint kinematics during gait'. *J Biomech,* 24(10), pp. 969-977.

Rankin, G. and Stokes, M. (1998) 'Reliability of assessment tools in rehabilitation: An illustration of appropriate statistical analyses'. *Clin Rehabil,* 12(3), pp. 187-199.

Rankine, L., Long, J., Canseco, K. and Harris, G. F. (2008) 'Multisegmental foot modeling: A review'. *Crit Rev Biomed Eng,* 36(2-3), pp. 127-181.

Rash, G., Quesada, P., Roberts, C. and Herringshaw, C. (1999) 'An investigation of alternate asis marker placement on the kinematics & kinetics of gait: A simulation of analysis on obese subjects'. *ASB Proceedings*.

Razeghi, M. and Batt, M. E. (2002) 'Foot type classification: A critical review of current methods'. *Gait Posture,* 15(3), pp. 282-291.

Reilly, J. J., Dorosty, A. R., Emmett, P. M. and Team, A. L. S. o. P. a. C. S. (2000) 'Identification of the obese child: Adequacy of the body mass index for clinical practice and epidemiology'. *Int J Obes Relat Metab Disord,* 24(12), pp. 1623-1627.

Reinschmidt C, van den Bogert AJ, Lundberg A, Nigg BM, Murphy N, Stacoff A and A., S. (1997) 'Tibiofemoral and tibiocalcaneal motion during walking: External vs. Skeletal markers'. *Gait Posture,* 6(2), pp. 98–109.

Rennie, K. L. and Jebb, S. A. (2005) 'Prevalence of obesity in great britain'. *Obes Rev,* 6(1), pp. 11-12.

Richards, J. (2008) *Biomechanics in clinic and research*. Philadelphia: Churchill Livingstone.

Riddiford-Harland, D. L., Steele, J. R. and Baur, L. A. (2011) 'Are the feet of obese children fat or flat? Revisiting the debate'. *Int J Obes (Lond),* 35(1), pp. 115-120.

Riddiford-Harland, D. L., Steele, J. R. and Storlien, L. H. (2000) 'Does obesity influence foot structure in prepubescent children?'. *Int J Obes Relat Metab Disord,* 24(5), pp. 541-544.

Riddoch, C. J., Leary, S. D., Ness, A. R., Blair, S. N., Deere, K., Mattocks, C., Griffiths, A., Davey Smith, G. and Tilling, K. (2009) 'Prospective associations between objective measures of physical activity and fat mass in 12-14 year old children: The avon longitudinal study of parents and children (alspac)'. *BMJ,* 339, p. b4544.

Robinson, T. N. (2001) 'Television viewing and childhood obesity'. *Pediatr Clin North Am,* 48(4), pp. 1017-1025.

Rolland-Cachera, M. F. (2011) 'Childhood obesity: Current definitions and recommendations for their use'. *Int J Pediatr Obes,* 6(5-6), pp. 325-331.

Rosenthal, M., Cramer, D., Bain, S. H., Denison, D., Bush, A. and Warner, J. O. (1993) 'Lung function in white children aged 4 to 19 years: Ii--single breath analysis and plethysmography'. *Thorax,* 48(8), pp. 803-808.

Røislien, J., Skare, O., Opheim, A. and Rennie, L. (2012) 'Evaluating the properties of the coefficient of multiple correlation (cmc) for kinematic gait data'. *J Biomech,* 45(11), pp. 2014-2018.

Sadeghi, H., Allard, P., Shafie, K., Mathieu, P. A., Sadeghi, S., Prince, F. and Ramsay, J. (2000) 'Reduction of gait data variability using curve registration'. *Gait Posture,* 12(3), pp. 257-264.

Saraswat, P., MacWilliams, B. A. and Davis, R. B. (2012) 'A multi-segment foot model based on anatomically registered technical coordinate systems: Method repeatability in pediatric feet'. *Gait Posture,* 35(4), pp. 547-555.

Sardinha, L. B., Going, S. B., Teixeira, P. J. and Lohman, T. G. (1999) 'Receiver operating characteristic analysis of body mass index, triceps skinfold thickness, and arm girth for obesity screening in children and adolescents'. *Am J Clin Nutr,* 70(6), pp. 1090-1095.

Saxena, S., Ambler, G., Cole, T. J. and Majeed, A. (2004) 'Ethnic group differences in overweight and obese children and young people in england: Cross sectional survey'. *Arch Dis Child,* 89(1), pp. 30-36.

Schaefer, F., Georgi, M., Wühl, E. and Schärer, K. (1998) 'Body mass index and percentage fat mass in healthy german schoolchildren and adolescents'. *Int J Obes Relat Metab Disord,* 22(5), pp. 461-469.

Schwartz, M. H., Trost, J. P. and Wervey, R. A. (2004) 'Measurement and management of errors in quantitative gait data'. *Gait Posture,* 20(2), pp. 196-203.

Scott, S. and Winter, D. (1991) 'Talocrural and talocalcaneal joint kinematics and kinetics during the stance phase of gait'. *Journal of Biomechanics,* 24(8), p. 743.

Seidel, G. K., Marchinda, D. M., Dijkers, M. and Soutas-Little, R. W. (1995) 'Hip joint center location from palpable bony landmarks--a cadaver study'. *J Biomech,* 28(8), pp. 995-998.

Shafer, K. J., Siders, W. A., Johnson, L. K. and Lukaski, H. C. (2009) 'Validity of segmental multiple-frequency bioelectrical impedance analysis to estimate body composition of adults across a range of body mass indexes'. *Nutrition,* 25(1), pp. 25-32.

Sheehan, K. J. and Gormley, J. (2013) 'The influence of excess body mass on adult gait'. *Clin Biomech (Bristol, Avon)*.

Shrout, P. E. and Fleiss, J. L. (1979) 'Intraclass correlations: Uses in assessing rater reliability'. *Psychol Bull,* 86(2), pp. 420-428.

Shultz, S. P., Sitler, M. R., Tierney, R. T., Hillstrom, H. J. and Song, J. (2009) 'Effects of pediatric obesity on joint kinematics and kinetics during 2 walking cadences'. *Arch Phys Med Rehabil,* 90(12), pp. 2146-2154.

Shultz, S. P., Anner, J. and Hills, A. P. (2009) 'Paediatric obesity, physical activity and the musculoskeletal system'. *Obes Rev,* 10(5), pp. 576-582.

Shultz, S. P., Hills, A. P., Sitler, M. R. and Hillstrom, H. J. (2010) 'Body size and walking cadence affect lower extremity joint power in children's gait'. *Gait Posture,* 32(2), pp. 248-252.

Shultz, S. P., Browning, R. C., Schutz, Y., Maffeis, C. and Hills, A. P. (2011) 'Childhood obesity and walking: Guidelines and challenges'. *Int J Pediatr Obes,* 6(5-6), pp. 332-341.

Siegel, K., Kepple, T. and O'Connell, P. (1995) 'A technique to evaluate foot function during the stance phase of gait'. *Foot and ankle international,* 16(12), p. 764.

Simon, J., Doederlein, L., McIntosh, A. S., Metaxiotis, D., Bock, H. G. and Wolf, S. I. (2006) 'The heidelberg foot measurement method: Development, description and assessment'. *Gait Posture,* 23(4), pp. 411-424.

Siri, W., E. (1961) 'Body composition from fluid spaces and density: Analysis of methods', in Brozek, J. and Henschel, A. (eds.) *Techniques for measuring body composition*. Washington DC: National Academy of Sciences, National Research Council, pp. 223-224.

Skaaret, I., Fosdahl, M., A., Huse, A., B., Beyer, K., K. and Roislien, J. (2012) 'The reliability of three-dimensional gait kinematics in healthy children'. *Gait & Posture,* 36(S1), pp. S43-S44.

Skinner, S. (1996) 'Orthopedic disorders', in Rudolph, A. M. (ed.), *Rudolph's pediatrics*. Standford: Appleton and Lange, pp. 2145-2146.

Smith, P. A., Hassani, S., Graf, A. N. and Harris, G., F. (2008) 'Clinical applications of foot and ankle motion analysis in children', in Harris, G. F., Smith, P. A. and Marks, R., M. (eds.) *Foot and ankle motion analysis clinical. Treatment and technology*: Taylor & Francis, pp. 21-46.

Speiser, P. W., Rudolf, M. C., Anhalt, H., Camacho-Hubner, C., Chiarelli, F., Eliakim, A., Freemark, M., Gruters, A., Hershkovitz, E., Iughetti, L., Krude, H., Latzer, Y., Lustig, R. H., Pescovitz, O. H., Pinhas-Hamiel, O., Rogol, A. D., Shalitin, S., Sultan, C., Stein, D., Vardi, P., Werther, G. A., Zadik, Z., Zuckerman-Levin, N., Hochberg, Z. and Group, O. C. W. (2005) 'Childhood obesity'. *J Clin Endocrinol Metab,* 90(3), pp. 1871-1887.

Spyropoulos, P., Pisciotta, J. C., Pavlou, K. N., Cairns, M. A. and Simon, S. R. (1991) 'Biomechanical gait analysis in obese men'. *Arch Phys Med Rehabil,* 72(13), pp. 1065-1070.

Stagni, R., Fantozzi, S., Cappello, A. and Leardini, A. (2005) 'Quantification of soft tissue artefact in motion analysis by combining 3d fluoroscopy and stereophotogrammetry: A study on two subjects'. *Clin Biomech (Bristol, Avon),* 20(3), pp. 320-329.

Stansfield, B. W., Hillman, S. J., Hazlewood, M. E., Lawson, A. A., Mann, A. M., Loudon, I. R. and Robb, J. E. (2001) 'Sagittal joint kinematics, moments, and powers are predominantly characterized by speed of progression, not age, in normal children'. *J Pediatr Orthop,* 21(3), pp. 403-411.

Stebbins, J. A., Harrington, M. E., Giacomozzi, C., Thompson, N., Zavatsky, A. and Theologis, T. N. (2005) 'Assessment of sub-division of plantar pressure measurement in children'. *Gait Posture,* 22(4), pp. 372-376.

Stebbins, J., Harrington, M., Thompson, N., Zavatsky, A. and Theologis, T. (2006) 'Repeatability of a model for measuring multi-segment foot kinematics in children.'. *Gait Posture,* 23(4), pp. 401-410.

Steinwender, G., Saraph, V., Scheiber, S., Zwick, E. B., Uitz, C. and Hackl, K. (2000) 'Intrasubject repeatability of gait analysis data in normal and spastic children'. *Clin Biomech (Bristol, Avon),* 15(2), pp. 134-139.

Stolze, H., Kuhtz-Buschbeck, J. P., Mondwurf, C., Jöhnk, K. and Friege, L. (1998) 'Retest reliability of spatiotemporal gait parameters in children and adults.'. *Gait Posture,* 7(2), pp. 125-130.

Styne, D. M. (2001) 'Childhood and adolescent obesity. Prevalence and significance'. *Pediatr Clin North Am,* 48(4), pp. 823-854, vii.

Sun, S. S., Chumlea, W. C., Heymsfield, S. B., Lukaski, H. C., Schoeller, D., Friedl, K., Kuczmarski, R. J., Flegal, K. M., Johnson, C. L. and Hubbard, V. S. (2003) 'Development of bioelectrical impedance analysis prediction equations for body composition with the use of a multicomponent model for use in epidemiologic surveys'. *Am J Clin Nutr,* 77(2), pp. 331-340.

Sutherland, D. H., Olshen, R., Cooper, L. and Woo, S. L. (1980) 'The development of mature gait'. *J Bone Joint Surg Am,* 62(3), pp. 336-353.

Sweeting, H. N. (2007) 'Measurement and definitions of obesity in childhood and adolescence: A field guide for the uninitiated'. *Nutr J,* 6, p. 32.

Swinburn, B. and Egger, G. (2002) 'Preventive strategies against weight gain and obesity'. *Obes Rev,* 3(4), pp. 289-301.

Taisa Filippin, N., de Almeida Bacarin, T. and Lobo da Costa, P. H. (2008) 'Comparison of static footprints and pedobarography in obese and non-obese children'. *Foot Ankle Int,* 29(11), pp. 1141-1144.

Taylor, E. D., Theim, K. R., Mirch, M. C., Ghorbani, S., Tanofsky-Kraff, M., Adler-Wailes, D. C., Brady, S., Reynolds, J. C., Calis, K. A. and Yanovski, J. A. (2006) 'Orthopedic complications of overweight in children and adolescents'. *Pediatrics,* 117(6), pp. 2167-2174.

Taylor, R. W., Jones, I. E., Williams, S. M. and Goulding, A. (2000) 'Evaluation of waist circumference, waist-to-hip ratio, and the conicity index as screening tools for high trunk fat mass, as measured by dual-energy x-ray absorptiometry, in children aged 3-19 y'. *Am J Clin Nutr,* 72(2), pp. 490-495.

Taylor, R. W., Jones, I. E., Williams, S. M. and Goulding, A. (2002) 'Body fat mass percentages measured by dual-energy x-ray absorptiometry corresponding to recently recommended body mass index cutoffs for overweight and obesity in children and adolescents aged 3-18 y'. *Am J Clin Nutr,* 76(6), pp. 1416-1421.

Teichtahl, A. J., Morris, M. E., Wluka, A. E., Baker, R., Wolfe, R., Davis, S. R. and Cicuttini, F. M. (2006) 'Foot rotation--a potential target to modify the knee adduction moment'. *J Sci Med Sport,* 9(1-2), pp. 67-71.

Theologis, T. and Stebbins, J. (2010) 'The use of gait analysis in the treatment of pediatric foot and ankle disorders'. *Foot Ankle Clin,* 15(2), pp. 365-382.

Theologis, T. N., Harrington, M. E., Thompson, N. and Benson, M. K. (2003) 'Dynamic foot movement in children treated for congenital talipes equinovarus'. *J Bone Joint Surg Br,* 85(4), pp. 572-577.

Tremblay, M. S. and Willms, J. D. (2003) 'Is the canadian childhood obesity epidemic related to physical inactivity?'. *Int J Obes Relat Metab Disord,* 27(9), pp. 1100-1105.

Troiano, R. P. and Flegal, K. M. (1999) 'Overweight prevalence among youth in the united states: Why so many different numbers?'. *Int J Obes Relat Metab Disord,* 23 Suppl 2, pp. S22-27.

Twomey, D., McIntosh, A. S., Simon, J., Lowe, K. and Wolf, S. I. (2010) 'Kinematic differences between normal and low arched feet in children using the heidelberg foot measurement method'. *Gait Posture,* 32(1), pp. 1-5.

Ulijaszek, S. J. and Kerr, D. A. (1999) 'Anthropometric measurement error and the assessment of nutritional status'. *Br J Nutr,* 82(3), pp. 165-177.

Ulijaszek, S. J. and Lourie, J. A. (1997) 'Anthropometry in health assessment: The importance of measurement error'. *Coll Antropol,* 21(2), pp. 429-438.

Valmassy, R. L. (1996) *Clinical biomechanics of the lower extremities*: Mosby.

Van Boerum, D. H. and Sangeorzan, B. J. (2003) 'Biomechanics and pathophysiology of flat foot'. *Foot Ankle Clin,* 8(3), pp. 419-430.

van der Linden, M. L., Kerr, A. M., Hazlewood, M. E., Hillman, S. J. and Robb, J. E. (2002) 'Kinematic and kinetic gait characteristics of normal children walking at a range of clinically relevant speeds'. *J Pediatr Orthop,* 22(6), pp. 800-806.

Vicente-Rodríguez, G., Rey-López, J. P., Mesana, M. I., Poortvliet, E., Ortega, F. B., Polito, A., Nagy, E., Widhalm, K., Sjöström, M., Moreno, L. A. and Group, H. S. (2012) 'Reliability and intermethod agreement for body fat mass assessment among two field and two laboratory methods in adolescents'. *Obesity (Silver Spring),* 20(1), pp. 221-228.

Vicon Manual, (2010). Vicon Motion Systems. Oxford, UK.

Villarroya, M. A., Esquivel, J. M., Tomás, C., Moreno, L. A., Buenafé, A. and Bueno, G. (2009) 'Assessment of the medial longitudinal arch in children and adolescents with obesity: Footprints and radiographic study'. *Eur J Pediatr,* 168(5), pp. 559-567.

Viner, R. M., Cole, T. J., Fry, T., Gupta, S., Kinra, S., McCarthy, D., Saxena, S., Taylor, S., Wells, J. C., Whincup, P. and Zaman, M. J. (2010) 'Insufficient evidence to support separate bmi definitions for obesity in children and adolescents from south asian ethnic groups in the uk'. *Int J Obes (Lond),* 34(4), pp. 656-658.

Wabitsch, M., Braun, U., Heinze, E., Muche, R., Mayer, H., Teller, W. and Fusch, C. (1996) 'Body composition in 5-18-y-old obese children and adolescents before and after weight reduction as assessed by deuterium dilution and bioelectrical impedance analysis'. *Am J Clin Nutr,* 64(1), pp. 1-6.

Wang, J., Gallagher, D., Thornton, J. C., Yu, W., Weil, R., Kovac, B. and Pi-Sunyer, F. X. (2007) 'Regional body volumes, bmi, waist circumference, and percentage fat in severely obese adults'. *Obesity (Silver Spring),* 15(11), pp. 2688-2698.

Wang, Z. M., Deurenberg, P., Guo, S. S., Pietrobelli, A., Wang, J., Pierson, R. N. and Heymsfield, S. B. (1998) 'Six-compartment body composition model: Inter-method comparisons of total body fat mass measurement'. *Int J Obes Relat Metab Disord,* 22(4), pp. 329-337.

Wardle, J. (1995) 'The assessment of obesity: Theoretical background and practical advice'. *Behav Res Ther,* 33(1), pp. 107-117.

Watt, G., F., Goel, K., Wilcox, D., E and Connor, J., M. (2006) 'Paediatric podiatry & genetics', in Frowen, P., O'Donnell, M., Gordon Burrow, J., G, and Lorimer, D., L. (eds.) *Neale's disorders of the foot*. Edinburgh: Churchill Livingstone, pp.

Wearing, S. C., Hennig, E. M., Byrne, N. M., Steele, J. R. and Hills, A. P. (2006) 'The impact of childhood obesity on musculoskeletal form'. *Obes Rev,* 7(2), pp. 209-218.

Wearing, S. C., Hills, A. P., Byrne, N. M., Hennig, E. M. and McDonald, M. (2004) 'The arch index: A measure of flat or fat feet?'. *Foot Ankle Int,* 25(8), pp. 575-581.

Weiss, R., Dziura, J., Burgert, T. S., Tamborlane, W. V., Taksali, S. E., Yeckel, C. W., Allen, K., Lopes, M., Savoye, M., Morrison, J., Sherwin, R. S. and Caprio, S. (2004) 'Obesity and the metabolic syndrome in children and adolescents'. *N Engl J Med,* 350(23), pp. 2362-2374.

Wells, J., C., Fuller, N., J., Dewit, O., Fewtrell, M., S., Elian, M. and Cole, T., J. (1999) 'Four-component model of body composition in children: Density and hydration of fat-free mass and comparison with simpler models'. *American Journal of Clinical Nutrition,* 69, pp. 904-912.

Wells, J. C. and Fuller, N. J. (2001) 'Precision of measurement and body size in whole-body air-displacement plethysmography'. *Int J Obes Relat Metab Disord,* 25(8), pp. 1161-1167.

Wells, J. C., Fuller, N. J., Wright, A., Fewtrell, M. S. and Cole, T. J. (2003) 'Evaluation of air-displacement plethysmography in children aged 5-7 years using a three-component model of body composition'. *Br J Nutr,* 90(3), pp. 699-707.

Westlake, C. G., Milner, C. E., Zhang, S. and Fitzhugh, E. C. (2013) 'Do thigh circumference and mass changes alter knee biomechanics during walking?'. *Gait Posture,* 37(3), pp. 359-362.

Whittle, M., W. (1997) *Gait analysis; an introduction*. Oxford: Butterworth-Heinemann.

World Health Organisation. (2000) *Obesity: Preventing and managing the global epidemic. Report of a WHO consultation. Who technical report series no. 894.* Geneva: World Health Organisation.

World Health Organisation. (2006) *WHO child growth standards: Length/height-for-age, weight for-age, weight-for-length, weight-for-height and body mass index for-age: Methods and development.* Geneva: World Health Organisation.

Williams, D. P., Going, S. B., Lohman, T. G., Harsha, D. W., Srinivasan, S. R., Webber, L. S. and Berenson, G. S. (1992) 'Body fat massness and risk for elevated blood pressure, total cholesterol, and serum lipoprotein ratios in children and adolescents'. *Am J Public Health,* 82(3), pp. 358-363.

Williams, J., Wake, M. and Campbell, M. (2007) 'Comparing estimates of body fat mass in children using published bioelectrical impedance analysis equations'. *Int J Pediatr Obes,* 2(3), pp. 174-179.

Wills, M. (2004) 'Orthopedic complications of childhood obesity'. *Pediatr Phys Ther,* 16(4), pp. 230-235.

Winter, D., A. (2004) *Biomechanics and motor control of human movement*. New Jersey: John Wiley & Sons.

Winter, D. A. (1987) *The biomechanics and motor control of human gait*. Waterloo: University of Waterloo Press.

Woltring, H., J. (1986) 'A fortran package for generalised, cross-validatory spline smoothing and differentiation'. *Advances in Engineering Software,* 8, pp. 104–113.

Woltring, H. J. (1994) '3-d attitude representation of human joints: A standardization proposal'. *J Biomech,* 27(12), pp. 1399-1414.

Woodburn, J., Turner, D., Helliwell, P. and Barker, S. (1999) 'A preliminary study determining the feasibility of electromagnetic tracking for kinematics at the ankle joint complex'. *Rheumatology,* 38(12), p. 1260.

Wright, C. J., Arnold, B. L., Coffey, T. G. and Pidcoe, P. E. (2011) 'Repeatability of the modified oxford foot model during gait in healthy adults.'. *Gait Posture,* 33(1), pp. 108-112.

Wu, G., Siegler, S., Allard, P., Kirtley, C., Leardini, A., Rosenbaum, D., Whittle, M., D'Lima, D. D., Cristofolini, L., Witte, H., Schmid, O., Stokes, I. and Biomechanics, S. a. T. C. o. t. I. S. o. (2002) 'ISB recommendation on definitions of joint coordinate system of various joints for the reporting of human joint motion--part i: Ankle, hip, and spine. International society of biomechanics'. *J Biomech,* 35(4), pp. 543-548.

Wu, G., van der Helm, F. C., Veeger, H. E., Makhsous, M., Van Roy, P., Anglin, C., Nagels, J., Karduna, A. R., McQuade, K., Wang, X., Werner, F. W., Buchholz, B. and Biomechanics, I. S. o. (2005) 'ISB recommendation on definitions of joint coordinate systems of various joints for the reporting of human joint motion--part ii: Shoulder, elbow, wrist and hand'. *J Biomech,* 38(5), pp. 981-992.

Yates, B. (2009) *Merriman's assessment of the lower limb* (3rd Edition edn.): Churchill Livingstone.

Young, T., Peppard, P. E. and Gottlieb, D. J. (2002) 'Epidemiology of obstructive sleep apnea: A population health perspective'. *Am J Respir Crit Care Med,* 165(9), pp. 1217-1239.

Zapletal, A., Paul, T. and Samánek, M. (1976) '[normal values of static pulmonary volumes and ventilation in children and adolescents]'. *Cesk Pediatr,* 31(10), pp. 532-539.

Zimmermann, M. B., Gübeli, C., Püntener, C. and Molinari, L. (2004) 'Detection of overweight and obesity in a national sample of 6-12-y-old swiss children: Accuracy and validity of reference values for body mass index from the us centers for disease control and prevention and the international obesity task force'. *Am J Clin Nutr,* 79(5), pp. 838-843.

Zwiauer, K. (2006) '[obesity in children and young adults]'. *Pharm Unserer Zeit,* 35(6), pp. 490-498.

Zwiauer, K. F. M., Caroli, M., Malecka-Tendera, E. and Poskitt, E. M. E. (2006) 'Clinical features and adverse outcomes', in Burniat, W., Cole, T., Lissau, I. and Poskitt, E. M. E. (eds.) *Child and adolescent obesity. Causes and consequences; prevention and management.* Cambridge: Cambridge university press, pp. 131-153.

Appendix I: Ethical Approval

Dr Stewart Morrison
HAB
Stratford

ETH/13/11

24 September 2013

Dear Dr Morrison,

Application to the Research Ethics Committee: Does body mass alter the dynamic function of children's feet (R Mahaffey)

I advise that Members of the Research Ethics Committee have now approved the above application on the terms previously advised to you. The Research Ethics Committee should be informed of any significant changes that take place after approval has been given. Examples of such changes include any change to the scope, methodology or composition of investigative team. These examples are not exclusive and the person responsible for the programme must exercise proper judgement in determining what should be brought to the attention of the Committee.

In accepting the terms previously advised to you I would be grateful if you could return the declaration form below, duly signed and dated, confirming that you will inform the committee of any changes to your approved programme.

Yours sincerely

Debbie Dada
Admissions and Ethics Officer
Direct Line: 0208 223 2976
Email: d.dada@uel.ac.uk

Research Ethics Committee: ETH/13/11

I hereby agree to inform the Research Ethics Committee of any changes to be made to the above approved programme and any adverse incidents that arise during the conduct of the programme.

Signed:.....Date: .....

Please Print Name:

Appendix II: Study Information Sheets

"Does Body Mass Alter the Dynamic Function of Children's Feet?"

Stratford Campus,
Water Lane, Stratford,
London, E15 4LZ

University Research Ethics Committee

If you have any queries regarding the conduct of the programme in which you are being asked to participate, please contact the Secretary of the University Research Ethics Committee, Ms Debbie Dada, Admissions and Ethics Officer, Graduate School, University of East London, Docklands Campus, London E16 2RD (Tel 020 8223 2976, Email: d.dada@uel.ac.uk

Principal Investigators
Mr Ryan Mahaffey, MSc. r.mahaffey@uel.ac.uk. 0208 223 4033
Dr Stewart Morrison, PhD. s.c.morrison@uel.ac.uk. 0208 223 2679

We would like to invite your child to participate in a research project being undertaken by the School of Health and Bioscience at the University of East London. This form provides you with the information about the study so you can make an informed decision whether your child can participate. It also informs you of how your child's privacy will be protected and what your child's involvement will be if you agree they can take part. Your child's participation is voluntary and you can withdraw your child from the research at anytime without giving any reason and this will not affect the status of your child's medical care or legal rights.

What is the study looking at?

This work is being conducted to look at how the foot moves during walking in children. There is some research to suggest that a number of factors (such as body weight) can affect the way the foot moves and this is what we want to find out.

How can my child be included?

To participate in the research your child needs to be aged between 7 - 11 years old, you will be asked to complete a pre-screening health questionnaire before testing. The research will be undertaken by one PHD student and one assistant, both from the University of East London.

What will we be measuring?

We are examining the reliability of body composition measures which tell us how much lean and fat mass a child has, this will be done in three ways;

During the testing we will measure the Body Mass Index (BMI) of your child by recording their height and weight. Data collection will take place behind a medical screen to maintain the privacy of your child. If you or your child is not happy with this procedure taking place (you/they are in no way obliged to do so) then the measurements will not be taken and your child will still be more than welcome to continue their participation in the study at no disadvantage to themselves what-so-ever. We will measure the body composition of your child using two measures; the first, called BODPOD measures the amount of air which is displaced when someone sits in a chamber. The second is called BIA and measures the amount of water in the child's body by passing a very small and unnoticeable electric current from stickers on their feet to stickers on their hands. This will take at least 30 mintues. Any travelling costs will be fully reimbursed and refreshments will also be provided. We ask that you bring a pair of shorts and swimming trunks to be worn during the tests and suggest that you bring a towel and/or dressing gown to keep your child warm in between tests. Finally please do not feed your child 4 hours before coming to the laboratory, we will provide food following the testing procedure.

Are there any possible discomforts or risks?

- **Pain is highly unlikely – they are more likely to feel uncomfortable or embarrassed because they need to wear swimsuit or shorts and vest. Getting tired or feeling bored is also more likely. Your child is in no way obliged to complete the testing procedure, if at any time you or your child wishes to stop you can do so without any reason.**

Data Protection

Information collected about your child will be stored in computers with security passwords. Only the primary researcher and his research team have access to review these research records, and they will protect the confidentiality of these records.

We hope you will give your consent for your child to participate in this valuable research. If you have any questions or would like to discuss this further please contact Ryan Mahaffey, details at the top of the letter.

Kind regards

Ryan Mahaffey

"Does Body Mass Alter the Dynamic Function of Children's Feet?"

Stratford Campus,
Water Lane, Stratford,
London, E15 4LZ

University Research Ethics Committee

If you have any queries regarding the conduct of the programme in which you are being asked to participate, please contact the Secretary of the University Research Ethics Committee, Ms Debbie Dada, Admissions and Ethics Officer, Graduate School, University of East London, Docklands Campus, London E16 2RD (Tel 020 8223 2976, Email: d.dada@uel.ac.uk)

Principal Investigators

Mr Ryan Mahaffey, MSc. r.mahaffey@uel.ac.uk. 0208 223 4033
Dr Stewart Morrison, PhD. s.c.morrison@uel.ac.uk. 0208 223 2679

We would like to invite your child to participate in a research project being undertaken by the School of Health and Bioscience at the University of East London. This form provides you with the information about the study so you can make an informed decision whether your child can participate. It also informs you of how your child's privacy will be protected and what your child's involvement will be if you agree they can take part. Your child's participation is voluntary and you can withdraw your child from the research at anytime without giving any reason and this will not affect the status of your child's medical care or legal rights.

What is the study looking at?
This work is being conducted to look at how the foot moves during walking in children. There are many methods for determining foot motion during walking; we need to examine which will be most accurate and reliable.

How can my child be included?
To participate in the research your child needs to be aged between 7 - 11 years old, you will be asked to complete a pre-screening health questionnaire before testing. The research will be undertaken by one PHD student and one assistant, both from the University of East London.

What will we be measuring?
We will also look to investigate the effects of walking on the legs of your child by using specialist equipment called the VICON Motion Analysis which will take place in the

laboratories at the University of East London. Your child will be asked to walk across a room containing ten specially designed cameras.

These cameras are designed to analyse the way an individuals walks three-dimensionally. They will also have small markers and pieces of equipment attached to their skin and muscles.

During the testing we will measure the Body Mass Index (BMI) of your child by recording their height and weight. Data collection will take place behind a medical screen to maintain the privacy of your child. If you or your child is not happy with this procedure taking place (you/they are in no way obliged to do so) then the measurements will not be taken and your child will still be more than welcome to continue their participation in the study at no disadvantage to themselves what-so-ever. This will take around 1 hour. Any travelling costs will be fully reimbursed and refreshments will also be provided. We ask that you bring a pair of shorts to be worn during the tests.

Are there any possible discomforts or risks?

- **Having the small pieces of equipment attached to the skin and muscles of your child, might feel a little odd for them, but it will not hurt and they can be removed easily.**
- **Pain is highly unlikely – getting tired or feeling bored is more likely. Your child is in no way obliged to complete the testing procedure, if at any time you or your child wishes to stop you can do so without any reason.**

Data Protection

Information collected about your child will be stored in computers with security passwords. Only the primary researcher and his research team have access to review these research records, and they will protect the confidentiality of these records.

We hope you will give your consent for your child to participate in this valuable research. If you have any questions or would like to discuss this further please contact Ryan Mahaffey, details at the top of the letter.

Kind regards

Ryan Mahaffey

Research Assistant School of Health and Bioscience
University of East London
U.H. 2.16 | Stratford Campus |
Water Lane | Stratford | London | E15 4LZ

t: +44 (0)208 223 3317 | r.mahaffey@uel.ac.uk

www.uel.ac.uk

SCHOOL OF HEALTH, SPORT AND BIOSCIENCE
Dean: Professor Neville Punchard PhD FIBMS FHEA
uel.ac.uk/hsb
School Office

"Does Body Mass Alter the Dynamic Function of Children's Feet?"

University Research Ethics Committee

If you have any queries regarding the conduct of the programme in which you are being asked to participate, please contact the Secretary of the University Research Ethics Committee, Ms Debbie Dada, Admissions and Ethics Officer, Graduate School, University of East London, Docklands Campus, London E16 2RD (Tel 020 8223 2976, Email: d.dada@uel.ac.uk)

Principal Investigators

Mr Ryan Mahaffey, MSc. r.mahaffey@uel.ac.uk. 0208 223 4110

Dr Stewart Morrison, PhD. s.c.morrison@uel.ac.uk. 0208 223 2679

We would like to invite your child to participate in a research project being undertaken by the School of Health, Sport and Bioscience at the University of East London. This form provides you with the information about the study so you can make an informed decision whether your child can participate. It also informs you of how your child's privacy will be protected and what your child's involvement will be if you agree they can take part. Your child's participation is voluntary and you can withdraw your child from the research at anytime without giving any reason and this will not affect the status of your child's medical care or legal rights.

What is the study looking at?

This work is being conducted to look at how the foot moves during walking in children. There is some research to suggest that a number of factors (such as body weight) can affect the way the foot moves and this is what we want to find out.

How can my child be included?

To participate in the research your child needs to be aged between 7 - 11 years old, you will be asked to complete a pre-screening health questionnaire before testing. The research will be undertaken by one PhD student and one assistant, both from the University of East London

What will we be measuring?

We will also look to investigate the effects of walking on the legs of your child by using specialist equipment called the VICON Motion Analysis which will take place in the laboratories at the University of East London. Your child will be asked to walk across a room containing ten specially designed cameras.

SCHOOL OF HEALTH, SPORT AND BIOSCIENCE
Dean: Professor Neville Punchard PhD FIBMS FHEA
uel.ac.uk/hsb
School Office

These cameras are designed to analyse the way an individual walks three-dimensionally. They will also have small markers attached to their skin**.** During the testing we will measure the Body Mass Index (BMI) of your child by recording their height and weight. Data collection will take place behind a medical screen to maintain the privacy of your child. If you or your child is not happy with this procedure taking place (you/they are in no way obliged to do so) then the measurements will not be taken and your child will still be more than welcome to continue their participation in the study at no disadvantage to themselves what-so-ever. We will measure the body composition of your child using two measures; the first, called BODPOD measures the amount of air which is displaced when someone sits in a chamber. The second is called BIA and measures the amount of water in the child's body by passing a very small and unnoticeable electric current from stickers on their feet to stickers on their hands. This will take at least 1 hours. Any travelling costs will be fully reimbursed and refreshments will also be provided.

Are there any possible discomforts or risks?

- Having the small pieces of equipment attached to the skin of your child, might feel a little odd for them, but it will not hurt and they can be removed easily.
- Pain is highly unlikely – they are more likely to feel uncomfortable or embarrassed because they need to wear shorts and vest. Getting tired or feeling bored is also more likely. Your child is in no way obliged to complete the testing procedure, if at any time you or your child wishes to stop you can do so without any reason.

Data Protection

Information collected about your child will be stored in computers with security passwords. Only the primary researcher and his research team have access to review these research records, and they will protect the confidentiality of these records.

We hope you will give your consent for your child to participate in this valuable research. If you have any questions or would like to discuss this further please contact Ryan Mahaffey, details at the top of the letter.

Kind regards

Ryan Mahaffey, MSc (r.mahaffey@uel.ac.uk). Office: 0208 223 4110. Mobile: 07708 258 174

Appendix III: Consent Form

CONSENT FORM
(Parent / Guardian of child)

Title of project: Does body mass alter the dynamic function of children's feet?
Name of Researcher: Ryan Mahaffey

Please Initial

1. **I have the read the information leaflet, dated_____, relating to the above programme of research in which my child has been asked to participate and have been given a copy to keep. The nature and purposes of the research have been explained to me, and I have had the opportunity to discuss the details and ask questions about this information. I understand what it being proposed and the procedures in which my child will be involved have been explained to me.** _____

2. **I understand that my child's involvement in this study, and particular data from this research, will remain strictly confidential. Only the researchers involved in the study will have access to the data. It has been explained to me what will happen once the experimental programme has been completed.** _____

3. **As my child's participation in this study is voluntary, I understand that I have the right to withdraw from the programme at any time without disadvantage to myself and without being obliged to give any reason.** _____

4. **I agree to my child's participation in the above study** _____

Name of Child (block capitals) **Parent / Guardian contact number/email**

_____ _____

Name of Parent / Guardian **Date** **Signature**

_____ _____ _____

Name of Researcher **Date** **Signature**

_____ _____ _____

Appendix IV: Assumptions of Normality and Homogeneity for ICCs for Chapters 6 and 7

In order to carry out ICC calculations in experimental chapters 2 and 3 (chapters 6 and 7) the assumptions of normality and homogeneity for parametric tests were examined. Figure A4.1 demonstrates a typical histogram of the spread of angular and moment outputs; the distribution appears to form a bell-shaped curve. The normal probability plot represents normal distribution as all points a close to the line. The scatter plot of standardised residuals against standardised predictor value shows a random dispersion of points demonstrating homogeneity.

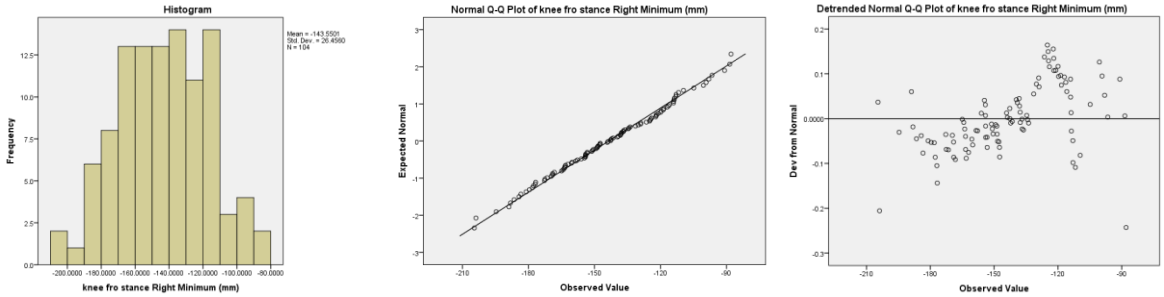

FigureA4.1 Histogram of frontal knee joint angle peak minimum during stance phase standardised regression residual, normal probability plot and plot of standardised predicted values against standard residuals.

Appendix V: Example of Normalising Gait Parameters to 100 or 50 Data Points Compared with no Normalisation.

Normalising hip joint motion to 100 or 50 data points over the gait cycle significantly changed angular outputs at gait events and peaks compared to no normalisation. The largest differences from normalisation were found in the transverse plane where peak internal rotation varied by 3.21° between 50 data points and both 100 and 183 data points. However, these differences were not significantly different due to high variation in hip transverse plane motion between the ten subjects. Frontal plane normalisation differences were generally smaller than in the transverse plane with no event or peak being greater than 1°. However, the difference was significant at contralateral initial contact and ipsilateral toe off between 50 and both 100 and 183 data points. Differences in sagittal plane hip joint motion at gait cycle events and peaks were also no greater than 1° but were significantly different at contralateral initial contact and at ipsilateral toe off between all three normalisation protocols.

Differences in joint angles at gait cycle events is a result of altered timing of the events due to normalisation to 100 or 50 data points. Ipsilateral initial contact does not alter between normalisation protocols, contralateral toe-off occurs at 7.76 ± 2.56%, 7.52 ± 2.91% and 8.59 ± 2.87% for 183, 100 and 50 data points respectively, contralateral initial contact occurs at 49.78 ± 1.99%, 49.78 ± 1.87% and 49.78 ± 2.56% for 183, 100 and 50 data points respectively, and finally ipsilateral toe-off occurs at 57.85 ± 2.23%, 57.70 ± 2.13% and 58.37 ± 2.78% for 183, 100 and 50 data points respectively. These differences were significant at contralateral toe-off between 183 and 50 data points ($p<.001$) and between 100 and 50 data points ($P<.05$) and ipsilateral toe-off between 183 and 50 data points ($p<.05$) and 100 and 50 data points ($p<.05$).

These findings suggest that in absolute terms normalising to 50 data points reduces peak angular motion compared to 100 and 183 data points, especially in the transverse plane. Small angular differences between groups may be reduced and significance lost increasing the likelihood of a type II error (false negative). The areas of the gait cycle that are most affected are the points when angular motion changes direction (transverse plane) or angular velocity is high (sagittal plane).

Table A5.1. 3D hip angles at gait cycle events and peaks during phases following; no normalisation (183 frames captured); normalising the gait cycle to 100 frames or; normalising the gait cycle to 50 frames. [1] = significant difference between 183 and 100, [2] = significant differences between 183 and 50, [3] = significant differences between 183 and 50. Significance set at p<.009 following Bonferoni adjusted for multiple t-tests. 183 represents non-normalisation (mean frames captured per gait cycle was 183 ± 18.37). N=10.

	IIC	DS 1 Max	CTO	SS1 Max	SS 1 Min	CIC	ITO	SS2 Max	SS2Min
Sag									
183	37.22 ± 10.31	37.36 ± 10.86	36.33 ± 9.25			-4.37 ± 8.93[1]	-1.93 ± 10.46[1]	38.49 ± 10.99	
100	37.22 ± 10.31	37.36 ± 10.86	36.33 ± 8.73			-4.15 ± 8.45	-1.49 ± 11.25[2]	38.46 ± 11.54	
50	37.22 ± 10.31	37.22 ± 10.86	35.36 ± 9.00			-4.15 ± 8.49[3]	-2.39 ± 11.11[3]	38.43 ± 11.54	
Fro									
183	-6.77 ± 6.24		-2.71 ± 6.17	1.55 ± 6.42		-0.82 ± 2.55	-5.67 ± 3.51	-5.28 ± 6.65	-8.24 ± 3.82
100	-6.77 ± 6.24		-2.71 ± 6.17	1.55 ± 6.40		-0.98 ± 2.51[2]	-6.07 ± 3.67[2]	-5.38 ± 6.60	-8.24 ± 3.98
50	-6.77 ± 6.24		-1.98 ± 5.78	1.55 ± 6.37		-0.69 ± 2.58[3]	-5.26 ± 3.38[3]	-5.62 ± 6.51	-8.24 ± 3.98
Tra									
183	-2.66 ± 12.64		4.51 ± 14.31	7.80 ± 14.93	0.23 ± 5.01	2.75 ± 5.01	5.98 ± 10.96	16.20 ± 11.91	-10.98 ± 8.07
100	-2.66 ± 12.64		4.51 ± 14.31	7.80 ± 14.93	0.27 ± 5.03	2.60 ± 5.07	6.28 ± 11.20	16.12 ± 11.50	-10.98 ± 8.07
50	-2.66 ± 12.64		6.70 ± 14.27	7.52 ± 14.93	0.41 ± 5.03	2.88 ± 5.03	5.62 ± 10.41	15.84 ± 11.43	-10.98 ± 8.24

Appendix VI: Sample Size Calculation for the Main Study

In order to calculate sample size for the main study (Chapter 8) three elements were required; the minimal detectable difference, the effect size statistic, statistical significance and statistical power. Based on previous clinical studies using 3D motion capture to analysis gait a minimal detectable difference of 5° is appropriate for differences in lower limb joint angles (McGinley et al., 2009). The effect size is calculated by dividing the minimal detectable difference by inter-subject standard deviation (SD). The pooled inter-subject SD is calculated from the subjects in the lower limb and foot reliability study. For a conservative estimate of effect size the joint parameter with the highest SD was chosen, 3DFoot's hallux segment (SD = 10.22°). All other joint angles and moments demonstrated lower SD and would therefore lead to a smaller sample size. By choosing the variable with the highest inter-subject variability the sample size of the main study should be large enough to detect differences of 5°. Statistical significance was set at 0.95, this means the chances of finding a type I error (false positive) is 5%. Statistical power was set at 0.80, this means the chances of finding a type II error (false negative) is 20%. The formula for calculating sample size (Eng 2003) based on these parameters is:

$$N = \frac{4\delta^2\left(Z_{crit} + Z_{pwr}\right)^2}{D^2} \quad (1)$$

Where N is the sample size, δ is the pooled SD, Z_{crit} is a value corresponding to statistical significance of 0.95, Z_{pwr} is a value corresponding to statistical power of 0.80 and D is the minimum detectable difference.

The results of the sample size calculation are that a sample of 66 participants is required to detect a difference of 5° in joint angles. Joint moments demonstrated higher SD (hip sagittal moments were highest at 10.91Nm) but the minimum detectable differences was much larger based on previous studies on obesity and gait parameters.

Appendix VII: Collinearity of Confounding Variables

Table A7.1 presents the full list of age, spatiotemporal and anthropometric measured variables to assess the confounding affect on the relationship between %FM with lower limb and foot biomechanics. Table A7.2 presents the selected confounding variables which could be entered into multiple regression analysis without violating the limits of the variance inflation factor (VIF <10) and the tolerance statistic (>0.2).

Table A7.1 Collinearity of all confounding variables with %FM

	Collinearity Statistics	
	Tolerance	VIF
Age	.523	1.913
BMI Z-Score	.262	3.824
Height	.234	4.266
Weight	.142	7.024
Stride time (s)	.002	527.367
Step time (s)	.002	526.903
Contralateral toe-off (%)	.018	85.396
Contralateral initial contact (%)	.011	90.088
Stance phase (%)	.423	2.366
Stride Distance (mm)	.088	11.337
Step Distance (mm)	.007	151.018
Velocity Right (mm)	.004	230.557
Step width (mm)	.941	1.063
Cadence	.006	165.333
Total single support	.698	1.433

Table A7.2. Collinearity of confounding variables with %FM following removal of selected variables due to high collinearity

	Collinearity Statistics	
	Tolerance	VIF
Age	.496	2.016
Height	.453	2.206
BMI Z-score	.679	1.472
Stance phase (%)	.707	1.415
Step distance	.395	2.532
Velocity	.484	2.064
Step width	.951	1.051
Total single support (%)	.871	1.148

Appendix VIII: Example of PC and Multiple Regression Analysis.

This example is for the hip joint. Nineteen points of the gait cycle were extracted for analysis including 5 peaks and events in the sagittal plane, 7 in the frontal and 7 in the transverse plane. These were entered into PCA and scree plot was created in order to distinguish the components for further analysis. The first three components were extracted for further investigation these had eigenvalues of 34.80%, 25.99% and 19.47% explaining 80.26% of the variance in 3D hip joint angles.

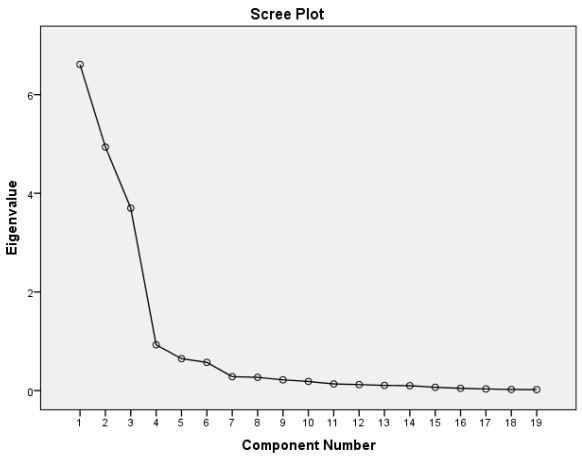

Figure A8.1. Scree plot of PCA components based on variance across %FM of hip joint angles.

A transformation matrix of the first three components was created with variables >0.722 or less than <0.722 indicted as contributing to that component. The components were saved as an output score which was taken forward into multiple regression.

Table A8.1. Rotated Component Matrix and loading magnitudes

	Component		
	1	2	3
SS 2 sag Max (deg.)	-.040	.943*	-.075
SS 1 fro Max (deg.)	.047	.130	.755*
SS 2 fro Min (deg.)	-.197	-.235	.774*
SS 2 fro Max (deg.)	-.017	-.221	.834*
SS 1 tra Min (deg.)	.957*	-.170	-.003
SS 2 tra Min (deg.)	.899*	-.055	-.195
SS 2 tra Max (deg.)	.919*	-.022	.095
Sag IIC (deg.)	-.078	.946*	-.051
Sag CTO (deg.)	-.047	.906*	-.082
Sag CIC (deg.)	-.159	.909*	-.027
Sag ITO (deg.)	-.160	.887*	-.017
Fro IIC (deg.)	.117	-.221	.810*
Fro CTO (deg.)	.073	-.030	.826*
Fro CIC (deg.)	.028	.256	.751*
Fro ITO (deg.)	-.159	-.037	.815*
Tra IIC (deg.)	.903*	.014	-.184
Tra CTO (deg.)	.947*	-.006	.003
Tra CIC (deg.)	.934*	-.214	.048
Tra ITO (deg.)	.914*	-.167	.148

Component 1 relates to hip joint angles in the transverse plane, component 2 to the sagittal plane and component to the frontal plane. At this stage the initial nineteen hip joint variables are represented by 3 components based on the angles in the three cardinal planes. The first stage of multiple regression involves linear regression of the dependent variables with the 3 output scores for each component. Table A8.2 is the output from linear regression on component 1 (hip transverse plane angles). This shows that height, age BMI Z-Score, body fat mass, velocity and step width are associated ($P<.05$) with component 1. These dependent variables are therefore taken forward to mixed model regression with component 1. Table A8.3 shows the outputs of mixed model regression analysis only BMI Z-Score is significantly associated with the output score of component 1 (hip transverse plane angles). Therefore, because no significant associations with body fat mass were found no further exploration of hip joint transverse plane angles is undertaken.

Table A8.2. Linear regression of component score 1 with dependent variables

Model		Unstandardized Coefficients		Standardized Coefficients	t	Sig.
		B	Std. Error	Beta		
1	(Constant)	-2.615	.842		-3.107	.002
	Height	.022	.006	.164	3.471	.001
	age	-.146	.042	-.150	-3.507	.000
	BMI Z-Score	-.071	.012	-.233	-5.754	.000
	%FM	.000	.000	.221	4.988	.000
	Stance phase (%)	-5.179E-005	.000	-.013	-.358	.720
	Step Distance (mm)	.000	.001	-.007	-.140	.889
	Velocity (mm)	.001	.000	.190	4.194	.000
	Step width (mm)	-8.751E-006	.000	-.078	-2.418	.016
	Total single support	.000	.000	-.036	-1.075	.283

Table A8.3. Mixed model regression of component score 1 with dependent variables

Source	Numerator df	Denominator df	F	Sig.
Intercept	1	14.850	.459	.508
Height	1	14.696	.007	.935
age	1	14.839	.309	.586
BMI Z-Score	1	301.505	4.976	.026
%FM	1	15.766	1.880	.189
Velocity	1	831.980	.148	.701
Step width	1	313.116	2.430	.120

Component 2 (hip sagittal plane angles) output score was then entered into linear regression analysis. Height, age, BMI Z-Score, %FM, step distance and velocity were significantly ($p<.05$, Table A8.4) associated with component 2. These dependent variables were taken forward into mixed model regression analysis. Table A8.5 shows that height and body fat mass remain significantly associated with component 2 (hip joint sagittal angles) when adjusted for the dependent variables.

Table A8.4. inear regression of component score 2 with dependent variables

Model		Unstandardized Coefficients		Standardized Coefficients	t	Sig.
		B	Std. Error	Beta		
1	(Constant)	-2.176	.738		-2.947	.003
	Height	7.966E-005	.000	.171	4.606	.000
	age	-.007	.002	-.145	-4.299	.000
	BMI Z-Score	-.025	.010	-.082	-2.535	.011
	%FM	.001	.000	.603	17.076	.000
	Stance phase (%)	5.703E-005	.000	.015	.498	.619
	Step Distance (mm)	3.959E-006	.000	.294	7.416	.000
	Velocity (mm)	.000	.000	-.213	-5.983	.000
	Step width (mm)	-2.364E-006	.000	-.021	-.820	.412
	Total single support	-.002	.015	-.005	-.171	.865

Table A8.5. Mixed model regression of component score 2 with dependent variables

Source	Numerator df	Denominator df	F	Sig.
Intercept	1	152.187	24.336	.000
Height	1	141.441	5.697	.018
age	1	156.679	.468	.495
BMI Z-Score	1	598.205	.038	.846
%FM	1	172.744	36.966	.000
Velocity (mm)	1	895.519	.333	.564
Step Distance (mm)	1	341.578	1.763	.185

At this point the results of linear regression analysis indicate that there is a significant association between body fat mass and height and hip joint sagittal angles at peaks and events during the gait cycle. In order to determine whether all or only some of the hip sagittal joint angles are associated with body fat mass linear and mixed model regression analysis was run on each of the 5 data points comprising component 2. Linear regression outputs determined the dependent variables entered in to mixed model regression analysis. The output of mixed model regression on the five data points for hip sagittal plane angles are shown in tables A8.6 to A8.10. The findings indicate that body fat mass is significantly associated with hip sagittal joint angles at ipsilateral initial contact, contralateral initial contact and ipsilateral toe-off. In order interpret the association between body fat mass and hip joint sagittal plane joint angles scatter plots were produced. The linear relationship between the variables determines the regression range across levels of body fat mass with-in this sample of boys.

Table A8.6. Mixed model regression of Hip Angle Sag at IIC with dependent variables

Source	Numerator df	Denominator df	F	Sig.
Intercept	1	71.931	193.487	.000
BMI Z-Score	1	3.536	1.095	.362
%FM	1	30.269	10.346	.003
Step Length	1	1535.522	2.817	.093
Velocity	1	913.725	.081	.775

Table A8.7. Mixed model regression of Hip Angle Sag at CTO with dependent variables

Source	Numerator df	Denominator df	F	Sig.
Intercept	1	57.216	32.591	.000
Age	1	56.131	.945	.335
BMI Z-Score	1	238.056	.811	.369
%FM	1	28.756	4.075	.053
Step Length	1	895.812	8.808	.003
Velocity	1	120.157	.041	.841

Table A8.8. Mixed model regression of SS 2 Hip sag Max with dependent variables

Source	Numerator df	Denominator df	F	Sig.
Intercept	1	47.732	83.953	.000
BMI Z-Score	1	921.740	.888	.346
%FM	1	32.500	3.327	.077
Step Length	1	2424.774	7.965	.005
Velocity	1	911.212	4.702	.030

Table A8.9. Mixed model regression of Hip Angle Sag at CIC with dependent variables

Source	Numerator df	Denominator df	F	Sig.
Intercept	1	2808.439	14.984	.000
Height	1	2789.206	6.388	.012
BMI Z-Score	1	1003.503	2.038	.154
%FM	1	3850.631	21.019	.000
Velocity	1	47.726	4.993	.030

Table A8.10. Mixed model regression of Hip Angle Sag at ITO with dependent variables

Source	Numerator df	Denominator df	F	Sig.
Intercept	1	45.253	6.050	.018
Height	1	45.017	3.224	.079
Age	1	45.731	.084	.774
BMI Z-Score	1	285.874	.000	.986
%FM	1	56.131	18.232	.000
Velocity	1	32.474	2.112	.156

Appendix IX: Regression Model Assumptions of Normality and Homoscedasticity for the Main Study

In order to carry out regression analysis in the main study (chapter 8) the assumptions of normality and homoscedasticity must be explored. Figure A9.1 demonstrates a typical histogram of the standardised residuals; the distribution appears to form a bell-shaped curve. The normal probability plot represents normal distribution as all points a close to the line. The scatter plot of standardised residuals against standardised predictor value shows a random dispersion of points demonstrating homoscedasticity.

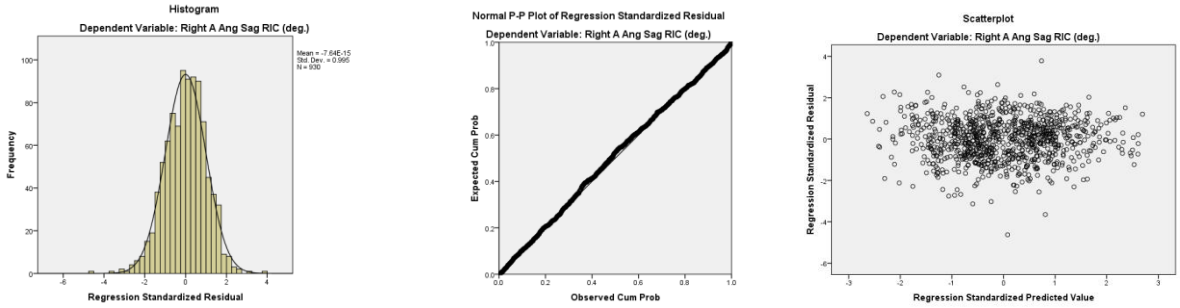

Figure A9.1. Histogram of standardised regression residual, normal probability plot and plot of standardised predicted values against standard residuals for right ankle angle in the sagittal plane and %FM.

Appendix X: Linear and Mixed Regression Analysis Coefficients and Significance from Chapter 8.

Tables A10.1 to A10.33 present the results of linear and mixed regression analysis outputs for each lower limb and foot joint.

Table A10.1. Hip joint component linear regression coefficients for regression score model and predictors

Model		Unstandardized Coefficients		Standardized Coefficients	t	Sig.
		B	Std. Error	Beta		
1	(Constant)	-2.615	.842		-3.107	.002
	Height	.122	.043	.101	2.837	.005
	age	.022	.006	.164	3.471	.001
	BMI Z-score	-.146	.042	-.150	-3.507	.000
	%FM	-.071	.012	-.233	-5.754	.000
	Stance phase duration	.000	.000	.221	4.988	.000
	Step length	-5.179E-005	.000	-.013	-.358	.720
	Velocity	.000	.001	-.007	-.140	.889
	Step width	.001	.000	.190	4.194	.000
	Total single support duration	-8.751E-006	.000	-.078	-2.418	.016
2	(Constant)	-2.176	.738		-2.947	.003
	Height	-.099	.034	-.083	-2.899	.004
	age	7.966E-005	.000	.171	4.606	.000
	BMI Z-score	-.007	.002	-.145	-4.299	.000
	%FM	-.025	.010	-.082	-2.535	.011
	Stance phase duration	.001	.000	.603	17.076	.000
	Step length	5.703E-005	.000	.015	.498	.619
	Velocity	3.959E-006	.000	.294	7.416	.000
	Step width	.000	.000	-.213	-5.983	.000
	Total single support duration	-2.364E-006	.000	-.021	-.820	.412
3	(Constant)	-4.306	1.041		-4.137	.000
	Height	.044	.006	.338	7.368	.000
	age	-.212	.044	-.217	-4.814	.000
	BMI Z-score	-.236	.037	-.383	-6.387	.000
	%FM	.002	.006	.021	.375	.708
	Stance phase duration	.000	.000	.046	1.259	.208
	Step length	-6.850E-007	.000	-.051	-1.047	.295
	Velocity	.000	.000	-.074	-1.701	.089
	Step width	-5.356E-006	.000	-.048	-1.507	.132
	Total single support duration	-.002	.018	-.004	-.111	.911

Table A10.2. Hip joint component Mixed model regression of regression scores with significant predictors from linear regression

Model	Source	Numerator df	Denominator df	F	Sig.
1	Intercept	1	14.850	.459	.508
	Height	1	14.696	.007	.935
	Age	1	14.839	.309	.586
	BMI Z-Score	1	301.505	4.976	.026
	%FM	1	15.766	1.880	.189
	Velocity	1	831.980	.148	.701
	Step width	1	313.116	2.430	.120
2	Intercept	1	152.187	24.336	.000
	Height	1	141.441	5.697	.018
	Age	1	156.679	.468	.495
	BMI Z-Score	1	598.205	.038	.846
	%FM	1	172.744	36.966	.000
	Velocity	1	895.519	.333	.564
	Step length	1	341.578	1.763	.185
3	Intercept	1	26.837	1.452	.239
	Height	1	33.217	2.512	.122
	Age	1	37.838	2.379	.131
	BMI Z-Score	1	30.568	5.605	.024

Table A10.3. Hip joint individual variables linear regression coefficients for sagittal hip angles at gait cycle events and peaks and predictors

Model		Unstandardized Coefficients		Standardized Coefficients	t	Sig.
		B	Std. Error	Beta		
SS 2 sag Max (deg.)	(Constant)	28.635	8.164		3.508	.000
	Height	.008	.048	.006	.159	.874
	age	-.231	.339	-.026	-.681	.496
	BMI Z-score	1.506	.283	.269	5.315	.000
	%FM	.007	.001	.347	7.061	.000
	Stance phase duration	-.001	.001	-.035	-1.108	.268
	Step length	3.982E-005	.000	.324	7.711	.000
	Velocity	-.003	.001	-.152	-4.080	.000
	Step width	3.485E-006	.000	.003	.126	.900
	Total single support duration	.103	.140	.021	.732	.464
Sag IIC (deg.)	(Constant)	20.039	8.781		2.282	.023
	Height	.015	.049	.012	.301	.764
	age	-.026	.018	-.055	-1.424	.155
	BMI Z-score	.992	.291	.175	3.403	.001
	%FM	.008	.001	.376	7.569	.000
	Stance phase duration	.110	.130	.027	.849	.396
	Step length	5.300E-005	.000	.426	10.007	.000
	Velocity	-.005	.001	-.243	-6.466	.000
	Step width	1.146E-006	.000	.001	.040	.968
	Total single support duration	-.001	.001	-.014	-.475	.635
Sag CTO (deg.)	(Constant)	23.403	10.132		2.310	.021
	Height	-.040	.050	-.034	-.805	.421
	age	-.042	.018	-.090	-2.369	.018
	BMI Z-score	-.301	.101	-.108	-2.986	.003
	%FM	.010	.001	.528	13.352	.000
	Stance phase duration	.090	.133	.022	.673	.501
	Step length	5.998E-005	.000	.491	11.059	.000
	Velocity	-.005	.001	-.249	-6.271	.000
	Step width	-1.240E-005	.000	-.012	-.423	.672
	Total single support duration	.015	.149	.003	.100	.920
Sag CIC (deg.)	(Constant)	-18.580	6.570		-2.828	.005
	Height	.001	.000	.262	7.574	.000
	age	-.026	.016	-.053	-1.589	.112
	BMI Z-score	1.369	.263	.231	5.204	.000
	%FM	.007	.001	.341	7.923	.000
	Stance phase duration	-.001	.001	-.038	-1.387	.166
	Step length	6.172E-006	.000	.047	1.286	.199
	Velocity	-.005	.001	-.247	-7.571	.000
	Step width	-8.270E-006	.000	-.008	-.321	.748
	Total single support duration	.015	.130	.003	.113	.910
Sag ITO (deg.)	(Constant)	-27.774	7.036		-3.947	.000
	Height	.001	.000	.306	8.565	.000
	age	-.052	.016	-.103	-3.155	.002
	BMI Z-score	-.364	.094	-.120	-3.864	.000
	%FM	.012	.001	.549	16.139	.000
	Stance phase duration	.002	.001	.044	1.548	.122
	Step length	4.121E-007	.000	.003	.081	.935
	Velocity	-.004	.001	-.171	-4.991	.000
	Step width	-5.736E-006	.000	-.005	-.209	.835
	Total single support duration	.001	.139	.000	.008	.994

Table A10.4. Hip joint individual variables mixed model regression of sagittal hip angles at gait cycle events and peaks with significant predictors from linear regression

Model	Source	Numerator df	Denominator df	F	Sig.
SS 2 sag Max (deg.)	Intercept	1	47.732	83.953	.000
	BMI Z-score	1	921.740	.888	.346
	%FM	1	32.500	3.327	.077
	Step length	1	2424.774	7.965	.005
	Velocity	1	911.212	4.702	.030
Sag IIC (deg.)	Intercept	1	71.931	193.487	.000
	BMI Z-score	1	3.536	1.095	.362
	%FM	1	30.269	10.346	.003
	Step length	1	1535.522	2.817	.093
	Velocity	1	913.725	.081	.775
Sag CTO (deg.)	Intercept	1	57.216	32.591	.000
	Age	1	56.131	.945	.335
	BMI Z-Score	1	238.056	.811	.369
	FM%	1	28.756	4.075	.053
	Step Length	1	895.812	8.808	.003
	Velocity	1	120.157	.041	.841
Sag CIC (deg.)	Intercept	1	2808.439	14.984	.000
	Height	1	2789.206	6.388	.012
	BMI Z-Score	1	1003.503	2.038	.154
	FM%	1	3850.631	21.019	.000
	Velocity	1	47.726	4.993	.030
Sag ITO (deg.)	Intercept	1	45.253	6.050	.018
	Height	1	45.017	3.224	.079
	Age	1	45.731	.084	.774
	BMI Z-Score	1	285.874	.000	.986
	FM%	1	56.131	18.232	.000
	Velocity	1	32.474	2.112	.156

Table A10.5. Knee joint component linear regression coefficients for regression score model and predictors

Model		Unstandardized Coefficients		Standardized Coefficients	t	Sig.
		B	Std. Error	Beta		
1	(Constant)	2.288	.769		2.977	.003
	Height	-.055	.006	-.423	-9.474	.000
	age	.441	.042	.455	10.593	.000
	BMI Z-score	.151	.035	.247	4.335	.000
	%FM	-8.856E-005	.000	-.041	-.743	.458
	Stance phase duration	.000	.000	-.030	-.861	.389
	Step length	1.333E-006	.000	.100	2.102	.036
	Velocity	2.833E-005	.000	.014	.326	.745
	Step width	9.167E-006	.000	.082	2.690	.007
	Total single support duration	.001	.000	.134	4.206	.000
2	(Constant)	-.153	.711		-.215	.830
	Height	-1.975E-005	.000	-.043	-.899	.369
	age	-.041	.042	-.043	-.990	.323
	BMI Z-score	-.063	.012	-.209	-5.085	.000
	%FM	.001	.000	.271	6.016	.000
	Stance phase duration	-8.984E-005	.000	-.023	-.618	.537
	Step length	.000	.001	.025	.481	.631
	Velocity	.001	.000	.190	4.112	.000
	Step width	-2.253E-006	.000	-.020	-.620	.536
	Total single support duration	.000	.000	-.035	-1.025	.306
3	(Constant)	1.266	.558		2.270	.023
	Height	.000	.000	-.372	-8.837	.000
	Age	-.007	.002	-.135	-3.338	.001
	BMI Z-score	-.151	.033	-.245	-4.537	.000
	%FM	.001	.000	.338	6.430	.000
	Stance phase duration	.000	.000	.113	3.370	.001
	Step length	1.034E-005	.000	.768	17.069	.000
	Velocity	-.001	.000	-.391	-9.811	.000
	Step width	7.328E-006	.000	.065	2.256	.024
	Total single support duration	.000	.000	-.080	-2.668	.008
4	(Constant)	-.767	.669		-1.147	.252
	Height	.000	.000	.251	5.667	.000
	Age	-.003	.002	-.053	-1.212	.226
	BMI Z-score	.051	.036	.083	1.431	.153
	%FM	.018	.006	.159	2.920	.004
	Stance phase duration	.000	.000	.071	1.997	.046
	Step length	-.003	.001	-.178	-3.700	.000
	Velocity	-4.299E-005	.000	-.021	-.485	.628
	Step width	-2.582E-006	.000	-.023	-.751	.453
	Total single support duration	.000	.000	-.068	-2.141	.033

Table A10.6. Knee joint component mixed model regression of regression scores with significant predictors from linear regression

Model	Source	Numerator df	Denominator df	F	Sig.
1	Intercept	1	14.051	1.079	.316
	Height	1	14.055	.222	.645
	age	1	14.099	1.503	.240
	BMI Z-score	1	321.203	.128	.721
	Total single support duration	1	308.329	2.984	.085
	Step length	1	309.228	.996	.319
	Step width	1	308.235	.038	.846
2	Intercept	1	56.444	.795	.376
	BMI Z-score	1	4.429	.968	.376
	%FM	1	37.128	.045	.833
	Velocity	1	1341.279	.067	.796
3	Intercept	1	32.063	.000	.992
	Height	1	22.681	.010	.923
	Age	1	22.930	.899	.353
	BMI Z-score	1	188.461	1.954	.164
	%FM	1	34.898	2.065	.160
	Stance phase duration	1	316.549	.067	.795
	Velocity	1	318.715	1.227	.269
	Step width	1	309.420	.244	.622
	Total single support duration	1	312.073	.992	.320
	Step length	1	185.848	1.318	.252
4	Intercept	1	99.028	3.384	.069
	Height	1	61.938	1.786	.186
	%FM	1	57.718	6.951	.011
	Stance phase duration	1	904.572	1.627	.202
	Step length	1	817.940	2.630	.105
	Total single support duration	1	893.097	.028	.867

Table A10.7. Knee joint individual variables linear regression coefficients for sagittal hip angles at gait cycle events and peaks and predictors

Model		Unstandardized Coefficients		Standardized Coefficients	t	Sig.
		B	Std. Error	Beta		
Sag CIC (deg.)	(Constant)	17.169	4.188		4.100	.000
	Height	9.615E-005	.000	.035	.743	.458
	age	.173	.264	.030	.656	.512
	BMI Z-score	-.590	.223	-.165	-2.645	.008
	%FM	.169	.038	.259	4.420	.000
	Stance phase duration	-.001	.001	-.022	-.583	.560
	Step length	-.003	.005	-.031	-.609	.542
	Velocity	-.001	.001	-.101	-2.213	.027
	Step width	.006	.005	.046	1.390	.165
	Total single support duration	-.001	.001	-.027	-.783	.434
Sag ITO (deg.)	(Constant)	10.708	4.374		2.448	.015
	Height	.000	.000	.120	2.710	.007
	age	-.018	.016	-.049	-1.133	.257
	BMI Z-score	.493	.263	.109	1.876	.061
	%FM	.124	.045	.151	2.767	.006
	Stance phase duration	.006	.001	.194	5.464	.000
	Step length	7.019E-006	.000	.071	1.505	.133
	Velocity	-.002	.001	-.126	-2.987	.003
	Step width	-1.195E-005	.000	-.015	-.473	.637
	Total single support duration	-.001	.001	-.035	-1.102	.271

Table A10.8. Knee joint individual variables mixed model regression of sagittal Knee angles at gait cycle events and peaks with significant predictors from linear regression

Model	Source	Numerator df	Denominator df	F	Sig.
Sag CIC (deg.)	Intercept	1	59.272	29.638	.000
	BMI Z-score	1	362.099	3.509	.062
	%FM	1	79.886	3.428	.062
	Velocity	1	85.880	1.544	.217
Sag ITO (deg.)	Intercept	1	42257.264	4.821	.028
	Height	1	299833.453	1.040	.308
	%FM	1	631793.630	7.296	.007
	Stance phase duration	1	925.385	5.601	.018
	Velocity	1	988.776	.004	.951

Table A10.9. Ankle joint component linear regression coefficients for regression score model and predictors

Model		Unstandardized Coefficients		Standardized Coefficients	t	Sig.
		B	Std. Error	Beta		
1	(Constant)	-1.958	1.181		-1.657	.098
	Height	.004	.002	.083	1.937	.053
	age	-1.314E-005	.000	-.028	-.594	.553
	BMI Z-score	-.027	.013	-.087	-2.112	.035
	%FM	.000	.000	.214	4.763	.000
	Stance phase duration	.002	.017	.004	.101	.920
	Step length	.000	.001	-.013	-.256	.798
	Velocity	.000	.000	.176	3.871	.000
	Step width	-1.493E-005	.000	-.133	-4.084	.000
	Total single support duration	.034	.019	.061	1.808	.071
2	(Constant)	2.284	1.145		1.995	.046
	Height	-.023	.040	-.024	-.577	.564
	age	-.056	.006	-.424	-10.034	.000
	BMI Z-score	-.039	.033	-.064	-1.184	.237
	%FM	.048	.006	.428	8.576	.000
	Stance phase duration	.048	.015	.109	3.180	.002
	Step length	.009	.001	.542	11.683	.000
	Velocity	-.002	.000	-.301	-7.298	.000
	Step width	-.001	.001	-.030	-1.017	.309
	Total single support duration	-.025	.017	-.046	-1.496	.135
3	(Constant)	-1.989	1.139		-1.746	.081
	Height	-.220	.040	-.225	-5.473	.000
	Age	.022	.006	.166	3.942	.000
	BMI Z-score	.100	.033	.163	3.040	.002
	%FM	.017	.006	.156	3.135	.002
	Stance phase duration	.032	.015	.071	2.087	.037
	Step length	.003	.001	.184	3.980	.000
	Velocity	-.002	.000	-.265	-6.457	.000
	Step width	.000	.001	-.011	-.370	.712
	Total single support duration	-.021	.017	-.039	-1.262	.207

Table A10.10. Ankle joint component mixed model regression of regression scores with significant predictors from linear regression

Model	Source	Numerator df	Denominator df	F	Sig.
1	Intercept	1	46.536	.016	.898
	BMI Z-score	1	2.685	.983	.402
	%FM	1	30.717	4.395	.047
	Velocity	1	1393.222	.002	.960
	Step width	1	1220.068	.676	.411
2	Intercept	1	55.314	5.102	.028
	Height	1	50.399	7.849	.007
	%FM	1	47.312	7.449	.009
	Stance phase duration	1	896.396	.012	.912
	Step length	1	691.927	1.085	.298
	Velocity	1	918.081	.186	.666
3	Intercept	1	74.409	3.199	.078
	age	1	62.958	5.786	.019
	Height	1	63.442	4.359	.041
	BMI Z-score	1	6.688	.026	.878
	%FM	1	31.605	4.458	.043
	Stance phase duration	1	944.546	2.375	.124
	Step length	1	1004.502	.055	.815
	Velocity	1	968.698	2.506	.114

Table A10.11. Ankle joint individual variable linear regression coefficients for sagittal Ankle angles at gait cycle events and peaks and predictors

Model		Unstandardized Coefficients		Standardized Coefficients	t	Sig.
		B	Std. Error	Beta		
SS 2 fro Min (deg.)	(Constant)	-9.560	3.217		-2.972	.003
	Height	.008	.006	.056	1.333	.183
	age	.000	.000	-.198	-4.281	.000
	BMI Z-score	-.052	.035	-.060	-1.492	.136
	%FM	.002	.000	.260	5.909	.000
	Stance phase duration	.111	.046	.088	2.393	.017
	Step length	2.163E-06	.000	.057	1.149	.251
	Velocity	.002	.001	.135	3.034	.002
	Step width	-3.996E-05	.000	-.126	-3.937	.000
	Total single support duration	.051	.051	.033	.987	.324
SS 2 fro Max (deg.)	(Constant)	-4.556	2.354		-1.935	.053
	Height	.133	.098	.059	1.364	.173
	age	.023	.014	.077	1.707	.088
	BMI Z-score	-.748	.082	-.525	-9.148	.000
	%FM	.002	.000	.439	7.894	.000
	Stance phase duration	-.001	.000	-.127	-3.569	.000
	Step length	-2.774E-06	.000	-.089	-1.863	.063
	Velocity	.001	.000	.203	4.814	.000
	Step width	-1.364E-05	.000	-.052	-1.704	.089
	Total single support duration	.146	.040	.115	3.610	.000
SS 2 tra Min (deg.)	(Constant)	18.601	12.233		1.521	.129
	Height	-.242	.509	-.021	-.476	.634
	age	-.021	.072	-.014	-.297	.766
	BMI Z-score	3.388	.425	.473	7.963	.000
	%FM	-.010	.001	-.391	-6.779	.000
	Stance phase duration	.003	.002	.070	1.894	.059
	Step length	-.001	.010	-.007	-.138	.890
	Velocity	-.002	.001	-.077	-1.752	.080
	Step width	.000	.000	.090	2.836	.005
	Total single support duration	-.831	.210	-.130	-3.948	.000
SS 2 tra Max (deg.)	(Constant)	23.571	15.391		1.531	.126
	Height	-.083	.030	-.120	-2.744	.006
	age	.001	.000	.178	3.878	.000
	BMI Z-score	.186	.488	.022	.382	.703
	%FM	-.011	.002	-.376	-6.594	.000
	Stance phase duration	-.105	.219	-.017	-.481	.630
	Step length	-.004	.011	-.019	-.383	.702
	Velocity	-.003	.001	-.101	-2.323	.020
	Step width	.000	.000	.103	3.290	.001
	Total single support duration	-.248	.242	-.033	-1.024	.306
Fro IIC (deg.)	(Constant)	-4.380	3.312		-1.322	.186
	Height	.010	.007	.064	1.438	.151
	Age	.000	.000	-.205	-4.408	.000
	BMI Z-score	-.280	.107	-.156	-2.602	.009
	%FM	.002	.000	.380	6.564	.000
	Stance phase duration	.066	.048	.051	1.380	.168
	Step length	9.260E-06	.000	.235	4.723	.000
	Velocity	.000	.001	.023	.511	.609
	Step width	-3.284E-05	.000	-.100	-3.127	.002
	Total single support duration	.021	.053	.013	.403	.687
Fro CTO (deg.)	(Constant)	-1.460	3.263		-.447	.655
	Height	.020	.006	.152	3.562	.000
	age	-.037	.016	-.109	-2.305	.021
	BMI Z-score	-.096	.032	-.122	-2.999	.003

	%FM	.002	.000	.300	6.773	.000
	Stance phase duration	.030	.043	.026	.710	.478
	Step length	.008	.002	.177	3.504	.000
	Velocity	.000	.000	.080	1.790	.074
	Step width	-3.649E-05	.000	-.126	-3.914	.000
	Total single support duration	.007	.047	.005	.154	.878
	(Constant)	-8.246	4.089		-2.017	.044
	Height	-.138	.136	-.044	-1.014	.311
	age	.010	.020	.024	.502	.616
	BMI Z-score	.078	.041	.080	1.921	.055
Fro CIC (deg.)	%FM	.000	.000	-.020	-.448	.654
	Stance phase duration	.064	.054	.045	1.181	.238
	Step length	.000	.003	.006	.111	.912
	Velocity	.001	.001	.059	1.264	.207
	Step width	-.006	.002	-.078	-2.356	.019
	Total single support duration	.055	.060	.032	.920	.358
	(Constant)	-4.380	3.312		-1.322	.186
	Height	.010	.007	.064	1.438	.151
	age	.000	.000	-.205	-4.408	.000
	BMI Z-score	-.280	.107	-.156	-2.602	.009
Fro ITO (deg.)	%FM	.002	.000	.380	6.564	.000
	Stance phase duration	.066	.048	.051	1.380	.168
	Step length	9.260E-06	.000	.235	4.723	.000
	Velocity	.000	.001	.023	.511	.609
	Step width	-3.284E-05	.000	-.100	-3.127	.002
	Total single support duration	.021	.053	.013	.403	.687
	(Constant)	34.559	16.540		2.089	.037
	Height	-.095	.031	-.129	-3.127	.002
	age	.002	.000	.235	5.162	.000
	BMI Z-score	.672	.176	.151	3.821	.000
tra IIC (deg.)	%FM	-.014	.001	-.456	-10.597	.000
	Stance phase duration	-.086	.234	-.013	-.370	.712
	Step length	-.057	.012	-.236	-4.801	.000
	Velocity	.000	.001	.008	.181	.856
	Step width	.000	.000	.102	3.263	.001
	Total single support duration	-.296	.260	-.037	-1.142	.254
	(Constant)	31.899	14.069		2.267	.024
	Height	-.069	.029	-.099	-2.325	.020
	age	.001	.000	.135	2.865	.004
	BMI Z-score	.676	.169	.162	3.989	.000
tra CTO (deg.)	%FM	-.009	.001	-.321	-7.219	.000
	Stance phase duration	-.396	.226	-.065	-1.751	.080
	Step length	-.054	.011	-.238	-4.665	.000
	Velocity	.000	.004	-.003	-.070	.944
	Step width	.000	.000	.132	4.087	.000
	Total single support duration	.000	.003	-.003	-.075	.940
	(Constant)	41.463	16.581		2.501	.013
	Height	-.008	.032	-.010	-.237	.813
	age	-.143	.092	-.073	-1.553	.121
	BMI Z-score	.120	.186	.026	.645	.519
tra CIC (deg.)	%FM	-.004	.001	-.132	-2.943	.003
	Stance phase duration	.001	.002	.013	.357	.721
	Step length	2.272E-05	.000	.114	2.269	.024
	Velocity	-.004	.001	-.118	-2.618	.009
	Step width	.000	.000	.106	3.241	.001
	Total single support duration	-.427	.274	-.053	-1.560	.119
tra ITO (deg.)	(Constant)	93.284	16.536		5.641	.000

	Height	-.072	.566	-.005	-.128	.898
	age	-.397	.084	-.221	-4.741	.000
	BMI Z-score	.119	.169	.028	.706	.480
	%FM	-.003	.001	-.084	-1.920	.055
	Stance phase duration	-.099	.224	-.016	-.441	.659
	Step length	4.230E-05	.000	.230	4.650	.000
	Velocity	-.009	.001	-.319	-7.205	.000
	Step width	.000	.000	.118	3.680	.000
	Total single support duration	-.627	.249	-.084	-2.518	.012
	(Constant)	-16.033	3.613		-4.437	.000
	Height	.008	.008	.038	.954	.340
	age	-.001	.000	-.320	-7.405	.000
	BMI Z-score	.139	.044	.112	3.140	.002
DS 1 sag Min	%FM	.139	.017	.307	8.191	.000
(deg.)	Stance phase duration	.249	.063	.138	3.958	.000
	Step length	2.540E-005	.000	.466	9.967	.000
	Velocity	-.002	.000	-.213	-5.055	.000
	Step width	-.008	.003	-.081	-2.652	.008
	Total single support duration	.000	.001	-.016	-.510	.610
	(Constant)	-1.507	5.593		-.269	.788
	Height	-.134	.197	-.029	-.678	.498
	age	-.192	.027	-.305	-7.055	.000
	BMI Z-score	.193	.162	.066	1.193	.233
Sag IIC (deg.)	%FM	.171	.027	.321	6.282	.000
	Stance phase duration	.307	.074	.145	4.125	.000
	Step length	.026	.004	.331	6.972	.000
	Velocity	-.006	.001	-.227	-5.366	.000
	Step width	-.008	.003	-.070	-2.305	.021
	Total single support duration	-.059	.082	-.022	-.710	.478
	(Constant)	7.070	4.565		1.549	.122
	Height	-.662	.161	-.175	-4.111	.000
	age	-.117	.022	-.230	-5.283	.000
	BMI Z-score	-.039	.132	-.016	-.295	.768
	%FM	.139	.022	.321	6.252	.000
Sag CTO (deg.)	Stance phase duration	.173	.061	.100	2.849	.004
	Step length	.029	.003	.456	9.537	.000
	Velocity	-.006	.001	-.280	-6.596	.000
	Step width	-.002	.003	-.018	-.596	.551
	Total single support duration	-.193	.067	-.091	-2.871	.004
	(Constant)	-61.983	8.403		-7.377	.000
	Height	-.109	.017	-.276	-6.437	.000
	age	.244	.045	.238	5.475	.000
	BMI Z-score	-.413	.273	-.087	-1.513	.131
SS 2 sag Min	%FM	.304	.046	.350	6.553	.000
(deg.)	Stance phase duration	.335	.120	.097	2.791	.005
	Step length	9.976E-006	.000	.095	2.060	.040
	Velocity	.000	.002	.003	.082	.934
	Step width	-.008	.006	-.046	-1.516	.130
	Total single support duration	-.002	.001	-.055	-1.745	.081
	(Constant)	3.240	8.185		.396	.692
	Height	-.783	.289	-.103	-2.713	.007
	age	-.036	.040	-.035	-.899	.369
	BMI Z-score	1.027	.237	.216	4.338	.000
Sag CIC (deg.)	%FM	.156	.040	.180	3.918	.000
	Stance phase duration	.321	.109	.093	2.945	.003
	Step length	.057	.005	.447	10.451	.000
	Velocity	-.024	.002	-.547	-14.407	.000
	Step width	.003	.005	.017	.628	.530

	Total single support duration	-.197	.121	-.047	-1.635	.102
Sag ITO (deg.)	(Constant)	-9.624	8.609		-1.118	.264
	Height	-1.702	.304	-.237	-5.607	.000
	age	.148	.042	.153	3.527	.000
	BMI Z-score	.495	.249	.110	1.988	.047
	%FM	.153	.042	.187	3.654	.000
	Stance phase duration	.096	.115	.029	.836	.403
	Step length	.022	.006	.185	3.892	.000
	Velocity	-.010	.002	-.232	-5.492	.000
	Step width	-.006	.005	-.036	-1.184	.237
	Total single support duration	-.324	.127	-.081	-2.555	.011

Table. A10.12. Ankle joint individual variables mixed model regression of sagittal Ankle angles at gait cycle events and peaks with significant predictors from linear regression

Model	Source	Numerator df	Denominator df	F	Sig.
SS 2 fro Min (deg.)	Intercept	1	76.842	.073	.788
	Height	1	63.515	2.618	.111
	%FM	1	67.303	4.967	.029
	Stance Phase Duration	1	737.949	1.561	.212
	Velocity	1	887.121	.974	.324
	Step Width	1	877.603	.023	.879
SS 2 fro Max (deg.)	Intercept	1	121.567	9.032	.003
	BMI Z-Score	1	914.401	.790	.374
	%FM	1	22.010	.510	.483
	Stance phase duration	1	210.806	1.296	.256
	Velocity	1	884.070	.073	.787
	Total Single Support Phase	1	874.316	.450	.503
SS 2 tra Min (deg.)	Intercept	1	78.485	7.495	.008
	BMI Z-Score	1	.879	1.611	.446
	%FM	1	19.539	.130	.722
	Step Width	1	860.688	.402	.526
	Total Single Support Phase	1	598.445	.493	.483
SS 2 tra Max (deg.)	Intercept	1	46.079	.472	.496
	Age	1	45.933	.468	.497
	Height	1	45.968	.333	.566
	%FM	1	45.979	5.777	.020
	Velocity	1	889.190	.089	.766
	Step Width	1	879.554	.023	.880
Fro IIC (deg.)	Intercept	1	54.203	.220	.641
	Height	1	49.283	.053	.819
	BMI Z-Score	1	316.756	.794	.374
	%FM	1	108.392	26.366	.000
	Step Width	1	309.507	.599	.439
	Step Length	1	36.838	3.231	.080
Fro CTO (deg.)	Intercept	1	48.450	1.155	.288
	Age	1	56.187	5.345	.024
	Height	1	50.816	1.880	.176
	BMI Z-Score	1	15.698	.002	.968
	%FM	1	40.553	2.093	.156
	Step Length	1	379.633	.364	.547
	Step Width	1	874.043	.422	.516
Fro CIC (deg.)	Intercept	1	49.499	.679	.414
	Step Width	1	881.760	.030	.863
Fro ITO (deg.)	Intercept	1	51.294	2.495	.120
	Height	1	46.116	1.903	.174
	BMI Z-Score	1	14.781	.487	.496
	%FM	1	38.924	.324	.573
	Step Length	1	903.865	1.074	.300
	Velocity	1	905.474	.821	.365
	Step Width	1	879.991	1.150	.284
	Total Single Support Phase	1	855.756	.141	.708
tra IIC (deg.)	Intercept	1	44.245	.020	.887
	Age	1	43.102	.605	.441
	Height	1	43.010	.765	.387
	BMI Z-Score	1	199.285	.575	.449
	%FM	1	57.142	5.521	.022

	Step Length	1	194.955	2.591	.109
	Step Width	1	878.097	.332	.565
	Intercept	1	38.264	.127	.723
	Age	1	35.597	2.212	.146
	Height	1	37.155	.620	.436
Tra CTO (deg.)	BMI Z-Score	1	20.369	.047	.831
	%FM	1	39.531	1.653	.206
	Step Length	1	232.601	.706	.402
	Step Width	1	865.602	.734	.392
	Intercept	1	63.448	.868	.355
	%FM	1	38.121	.021	.885
Tra CIC (deg.)	Step Length	1	900.777	3.657	.056
	Velocity	1	104.043	.759	.386
	Step Width	1	870.474	.309	.579
	Intercept	1	61.320	6.105	.016
	Height	1	57.001	5.485	.023
Tra ITO (deg.)	Step Length	1	908.268	3.369	.067
	Velocity	1	907.168	2.597	.107
	Step Width	1	881.331	1.357	.244
	Total Single Support Phase	1	907.579	.699	.403
	Intercept	1	3548.748	.730	.393
	Height	1	3364.478	3.235	.072
	BMI Z-Score	1	4200.604	.043	.835
DS 1 sag Min	%FM	1	4252.119	6.601	.010
(deg.)	Stance Phase Duration	1	929.341	1.020	.313
	Step Length	1	1105.640	.124	.725
	Velocity	1	1211.770	.000	.992
	Step Width	1	56.013	3.559	.064
	Intercept	1	62.138	1.973	.165
	Height	1	54.898	4.556	.037
	%FM	1	52.674	3.096	.052
Sag IIC (deg.)	Stance Phase Duration	1	901.994	.043	.835
	Step Length	1	511.779	.462	.497
	Velocity	1	931.136	.276	.599
	Step Width	1	889.405	2.840	.092
	Intercept	1	80.242	.007	.932
	age	1	40.795	1.868	.179
	BMI Z-Score	1	355.736	.903	.343
Sag CTO (deg.)	%FM	1	68.084	3.060	.068
	Stance Phase Duration	1	917.540	2.600	.107
	Step Length	1	904.603	12.544	.000
	Velocity	1	566.807	16.541	.000
	Intercept	1	56.421	11.741	.001
	age	1	47.281	3.872	.055
SS 2 sag Min	Height	1	48.829	5.717	.021
(deg.)	%FM	1	48.674	3.560	.064
	Stance Phase Duration	1	921.452	.384	.536
	Step Length	1	922.997	3.097	.079
	Intercept	1	80.242	.007	.932
	age	1	40.795	1.868	.179
	BMI Z-Score	1	355.736	.903	.343
Sag CIC (deg.)	%FM	1	68.084	5.060	.028
	Stance Phase Duration	1	917.540	2.600	.107
	Step Length	1	904.603	12.544	.000
	Velocity	1	566.807	16.541	.000

Sag ITO (deg.)	Intercept	1	59.888	4.367	.041
	age	1	50.724	5.724	.020
	Height	1	47.213	4.635	.036
	BMI Z-Score	1	285.811	.273	.602
	%FM	1	81.789	4.985	.026
	Step Length	1	572.279	.516	.473
	Velocity	1	276.237	.760	.384
	Total Single Support Phase	1	884.409	.227	.634

Table A10.13. Hip joint moment component linear regression coefficients for regression score model and predictors

Model		Unstandardized Coefficients		Standardized Coefficients	t	Sig.
		B	Std. Error	Beta		
Sagittal						
1	(Constant)	-7.653	1.638		-4.671	.000
	age	-.075	.059	-.079	-1.266	.206
	BMI Z-score	-.020	.018	-.064	-1.155	.249
	Height	.062	.009	.475	7.143	.000
	%FM	.000	.000	.132	2.162	.031
	Stance phase duration	-.046	.027	-.094	-1.717	.087
	Step length)	-.004	.001	-.242	-3.041	.003
	Velocity	.002	.000	.382	5.392	.000
	Step width	.000	.001	.010	.224	.823
	Total single support duration	.001	.000	.093	1.782	.076
2	(Constant)	2.952	1.788		1.651	.100
	age	.053	.066	.056	.813	.416
	BMI Z-score	-.066	.020	-.206	-3.332	.001
	Height	-7.030E-005	.000	-.152	-2.067	.039
	%FM	-9.399E-005	.000	-.042	-.618	.537
	Stance phase duration	-.033	.030	-.068	-1.117	.265
	Step length)	1.056E-006	.000	.082	.932	.352
	Velocity	.000	.000	-.147	-1.860	.064
	Step width	-.001	.001	-.040	-.771	.441
	Total single support duration	.003	.032	.005	.091	.928
3	(Constant)	-6.289	1.437		-4.375	.000
	age	-.016	.004	-.316	-4.321	.000
	BMI Z-score	-.231	.061	-.377	-3.777	.000
	Height	.049	.010	.372	5.013	.000
	%FM	.000	.000	.169	1.836	.067
	Stance phase duration	.000	.000	.100	1.649	.100
	Step length)	-.001	.001	-.059	-.681	.497
	Velocity	.001	.000	.243	3.144	.002
	Step width	.000	.001	.014	.280	.780
	Total single support duration	-.001	.000	-.099	-1.745	.082
Frontal						
1	(Constant)	-2.990	.928		-3.221	.001
	age	-.186	.065	-.196	-2.840	.005
	BMI Z-score	-.128	.058	-.209	-2.211	.028
	Height	.000	.000	.512	7.300	.000
	%FM	.001	.000	.256	2.935	.004
	Stance phase duration	.000	.000	-.078	-1.362	.174
	Step length)	-1.510E-006	.000	-.117	-1.431	.153
	Velocity	.000	.000	.107	1.451	.148
	Step width	.001	.001	.021	.430	.667
	Total single support duration	.000	.000	.040	.748	.455
2	(Constant)	-1.343	1.085		-1.238	.216
	age	.030	.069	.031	.425	.671
	BMI Z-score	.254	.063	.414	4.055	.000
	Height	.000	.000	.282	3.825	.000
	%FM	-.030	.010	-.265	-2.889	.004
	Stance phase duration	.000	.000	.029	.487	.627
	Step length)	-.004	.001	-.261	-3.042	.003
	Velocity	.001	.000	.153	1.993	.047
	Step width	5.999E-006	.000	.042	.845	.399
	Total single support duration	.000	.000	-.021	-.381	.703
3	(Constant)	-2.698	1.590		-1.696	.091
	age	.280	.062	.295	4.517	.000
	BMI Z-score	.114	.055	.185	2.080	.038

	Height	-.013	.009	-.097	-1.461	.145
	%FM	.000	.000	.171	2.074	.039
	Stance phase duration	.037	.026	.075	1.395	.164
	Step length)	.003	.001	.163	2.101	.036
	Velocity	-.001	.000	-.438	-6.383	.000
	Step width	-1.382E-005	.000	-.098	-2.155	.032
	Total single support duration	.000	.000	-.020	-.403	.687
Transverse						
1	(Constant)	.003	.003	.059	.871	.384
	age	.069	.057	.112	1.197	.232
	BMI Z-score	8.718E-005	.000	.188	2.710	.007
	Height	.001	.000	.286	3.305	.001
	%FM	.000	.000	.024	.418	.676
	Stance phase duration	-.001	.001	-.076	-.933	.352
	Step length)	.000	.000	.198	2.739	.006
	Velocity	7.233E-006	.001	.000	.005	.996
	Step width	3.101E-006	.000	.001	.010	.992
	Total single support duration	.003	.003	.059	.871	.384
2	(Constant)	.045	.061	.047	.732	.464
	age	-.192	.054	-.312	-3.537	.000
	BMI Z-score	-9.123E-005	.000	-.197	-3.008	.003
	Height	5.578E-005	.000	.025	.305	.760
	%FM	-4.668E-005	.026	.000	-.002	.999
	Stance phase duration	-5.627E-006	.000	-.436	-5.725	.000
	Step length)	.000	.000	.196	2.863	.004
	Velocity	-1.926E-005	.000	-.136	-3.029	.003
	Step width	-.021	.028	-.038	-.757	.449
	Total single support duration	.045	.061	.047	.732	.464
3	(Constant)	-3.161	1.859		-1.701	.090
	age	-.016	.003	-.328	-4.801	.000
	BMI Z-score	.042	.018	.133	2.320	.021
	Height	.038	.009	.289	4.040	.000
	%FM	-.001	.007	-.012	-.197	.844
	Stance phase duration	-.048	.029	-.098	-1.615	.107
	Step length)	-1.473E-006	.000	-.114	-1.337	.182
	Velocity	.001	.000	.221	2.854	.005
	Step width	-.001	.001	-.045	-.884	.377
	Total single support duration	.000	.000	.052	.912	.362

Table A10.14. Hip joint moment component mixed model regression of regression scores with significant predictors from linear regression

Model	Source	Numerator df	Denominator df	F	Sig.
Sagittal					
	Intercept	1	341.256	20.099	.000
	Height	1	411.440	9.606	.002
1	%FM	1	80.861	4.667	.040
	Step Length	1	438.340	.156	.693
	Velocity	1	417.568	3.549	.060
	Intercept	1	2028.154	8.164	.004
2	BMI Z-Score	1	369	26.063	.000
	Height	1	369.000	5.701	.017
	Intercept	1	26.837	1.452	.239
	age	1	2680.626	4.352	.037
3	BMI Z-Score	1	2293.896	3.642	.056
	Height	1	2227.718	7.148	.008
	Velocity	1	604.852	4.927	.027
Frontal					
	Intercept	1	12520.839	13.094	.000
	age	1	7281.548	1.318	.251
1	BMI Z-Score	1	19078.348	.584	.445
	Height	1	4941.367	11.211	.001
	%FM	1	27404.724	.969	.325
	Intercept	1	2453.866	6.617	.010
	BMI Z-Score	1	5615.525	8.971	.003
2	Height	1	2544.458	9.460	.002
	%FM	1	5405.064	2.515	.113
	Step distance	1	508.325	2.236	.135
	Velocity	1	522.788	5.803	.016
	Intercept	1	365	10.746	.001
	age	1	365	20.483	.000
	BMI Z-Score	1	365	9.789	.002
3	%FM	1	365	2.253	.134
	Step distance	1	365	2.637	.105
	Velocity	1	365	45.250	.000
	Step width	1	365	5.473	.020
Transverse					
	Intercept	1	5952.389	14.901	.000
1	Height	1	7101.523	7.149	.008
	%FM	1	18431.539	13.059	.000
	Velocity	1	452.888	3.802	.052
	Intercept	1	71.387	19.331	.000
	BMI Z-Score	1	47.313	9.482	.003
2	Height	1	60.891	3.674	.060
	Velocity	1	359.309	.002	.961
	Step distance	1	349.074	.578	.448
	Step width	1	352.398	5.687	.018
	Intercept	1	3024.541	6.307	.012
	age	1	4615.782	5.803	.016
3	BMI Z-Score	1	3285.854	1.891	.169
	Height	1	3586.808	5.079	.024
	Velocity	1	585.083	2.841	.092

Table A10.15. Hip joint moment individual variables linear regression coefficients for sagittal hip angles at gait cycle events and peaks and predictors

Model		Unstandardized Coefficients		Standardized Coefficients	t	Sig.
		B	Std. Error	Beta		
DS1 sag Max (Nm)	(Constant)	-430558.140	78894.758		-5.457	.000
	age	-142.567	151.219	-.062	-.943	.346
	BMI Z-score	-5199.295	2554.600	-.183	-2.035	.043
	Height	3003.978	405.094	.496	7.416	.000
	%FM	16.660	8.602	.161	1.937	.054
	Stance phase duration	699.053	1226.563	.031	.570	.569
	Step length)	-130.125	58.838	-.173	-2.212	.028
	Velocity	78.363	17.401	.313	4.503	.000
	Step width	129.710	59.773	.099	2.170	.031
	Total single support duration	-.413	13.492	-.002	-.031	.976
SS1 sag Max (Nm)	(Constant)	-3275.179	2355.156	-.091	-1.391	.165
	age	-1004.257	702.720	-.083	-1.429	.154
	BMI Z-score	1921.380	343.625	.387	5.592	.000
	Height	11.888	5.410	.140	2.197	.029
	%FM	-1838.868	1059.782	-.100	-1.735	.084
	Stance phase duration	-.128	.040	-.262	-3.194	.002
	Step length)	31.201	5.397	.427	5.781	.000
	Velocity	-.183	.258	-.034	-.712	.477
	Step width	20.165	11.789	.093	1.711	.088
	Total single support duration	-3275.179	2355.156	-.091	-1.391	.165
Sag CTO (Nm)	(Constant)	7.070	4.565		1.549	.122
	age	-.662	.161	-.175	-4.111	.000
	BMI Z-score	-.117	.022	-.230	-5.283	.000
	Height	-.039	.132	-.016	-.295	.768
	%FM	.139	.022	.321	6.252	.000
	Stance phase duration	.173	.061	.100	2.849	.004
	Step length)	.029	.003	.456	9.537	.000
	Velocity	-.006	.001	-.280	-6.596	.000
	Step width	-.002	.003	-.018	-.596	.551
	Total single support duration	-.193	.067	-.091	-2.871	.004
SS1 tra Max (Nm)	(Constant)	-3747.395	1625.541		-2.305	.022
	age	11.300	5.282	.143	2.139	.033
	BMI Z-score	339.483	91.527	.346	3.709	.000
	Height	.199	.050	.269	4.026	.000
	%FM	2.221	15.258	.012	.146	.884
	Stance phase duration	.085	.369	.013	.229	.819
	Step length)	-3.074	2.023	-.118	-1.520	.129
	Velocity	1.772	.602	.205	2.945	.003
	Step width	.007	.010	.033	.722	.471
	Total single support duration	-.093	.465	-.010	-.199	.843
Tra CIC (Nm)	(Constant)	-2989.558	1567.332		-1.907	.057
	age	4.522	5.342	.062	.846	.398
	BMI Z-score	233.225	92.482	.260	2.522	.012
	Height	.081	.050	.119	1.620	.106
	%FM	11.667	15.404	.070	.757	.449
	Stance phase duration	.286	.373	.046	.767	.444
	Step length)	-8.110E-005	.002	-.004	-.051	.959
	Velocity	.768	.605	.097	1.269	.205
	Step width	-1.029	2.088	-.025	-.493	.623
	Total single support duration	-.086	.472	-.010	-.182	.855
Tra ITO (Nm)	(Constant)	-1318.589	2078.137		-.635	.526

	age	-154.940	126.970	-.083	-1.220	.223
	BMI Z-score	87.946	38.084	.140	2.309	.021
	Height	.043	.066	.048	.661	.509
	%FM	1.040	.294	.236	3.540	.000
	Stance phase duration	.063	.502	.008	.125	.901
	Step length)	-.002	.002	-.094	-1.102	.271
	Velocity	1.545	.818	.146	1.888	.060
	Step width	-.003	.014	-.009	-.188	.851
	Total single support duration	.157	.638	.014	.247	.805

Table A10.16. Hip joint moment individual variables mixed model regression of sagittal hip angles at gait cycle events and peaks with significant predictors from linear regression

Model	Source	Numerator df	Denominator df	F	Sig.
DS1 sag Max (Nm)	Intercept	1	51.986	12.104	.001
	BMI Z-Score	1	33.427	.938	.340
	Height	1	62.281	11.245	.001
	Step length	1	353.111	.002	.964
	Velocity	1	333.429	6.099	.014
	Step Width	1	60.244	.159	.691
SS1 sag Max (Nm)	Intercept	1	74.537	4.227	.043
	Height	1	81.367	4.519	.037
	Step length	1	358.449	.173	.677
	Velocity	1	364.570	4.529	.034
Sag CTO (Nm)	Intercept	1	80.217	1.772	.187
	age	1	60.045	.919	.341
	Height	1	59.817	.786	.379
	%FM	1	57.981	6.256	.015
	Stance phase	1	903.216	.032	.858
	Step length	1	877.720	1.162	.281
	Velocity	1	921.991	2.822	.093
	Total single support phase	1	895.307	1.597	.207
SS1 tra Max (Nm)	Intercept	1	69.717	6.089	.016
	age	1	58.775	.613	.437
	BMI Z-Score	1	49.808	9.310	.004
	Height	1	69.986	3.719	.058
	Velocity	1	365.643	4.010	.046
Tra CIC (Nm	Intercept	1	36.972	64.309	.000
	BMI Z-Score	1	38.696	5.599	.023
Tra ITO (Nm)	Intercept	1	180.960	1.482	.225
	BMI Z-Score	1	103.689	4.632	.034
	%FM	1	73.007	11.278	.001

Table A10.17. Knee joint moments component linear regression coefficients for regression score model and predictors

Model		Unstandardized Coefficients		Standardized Coefficients	t	Sig.
		B	Std. Error	Beta		
Sagittal						
1	(Constant)	-5.887	1.538		-3.828	.000
	age	-.105	.062	-.111	-1.696	.091
	BMI Z-score	.072	.019	.225	3.858	.000
	Height	7.672E-005	.000	.166	2.372	.018
	%FM	.000	.000	.054	.844	.399
	Stance phase duration	.000	.000	.063	1.093	.275
	Step length)	.005	.001	.308	3.679	.000
	Velocity	.000	.000	-.083	-1.108	.269
	Step width	1.745E-005	.000	.123	2.557	.011
	Total single support duration	.023	.031	.041	.756	.450
2	(Constant)	4.174	1.655		2.522	.012
	age	.024	.061	.025	.392	.695
	BMI Z-score	-.008	.017	-.025	-.462	.644
	Height	-.056	.009	-.432	-6.347	.000
	%FM	.008	.007	.069	1.199	.231
	Stance phase duration	.054	.028	.110	1.933	.054
	Step length)	.004	.001	.272	3.318	.001
	Velocity	-.001	.000	-.335	-4.567	.000
	Step width	-.002	.001	-.055	-1.147	.252
	Total single support duration	.000	.000	-.037	-.695	.488
3	(Constant)	-2.420	1.874		-1.291	.197
	age	-.053	.067	-.055	-.783	.434
	BMI Z-score	.018	.020	.055	.871	.384
	Height	9.473E-005	.000	.204	2.725	.007
	%FM	7.807E-005	.000	.035	.503	.615
	Stance phase duration	.021	.030	.044	.697	.486
	Step length)	-2.853E-006	.000	-.221	-2.489	.013
	Velocity	.001	.000	.217	2.702	.007
	Step width	-1.451E-006	.000	-.010	-.196	.844
	Total single support duration	-.010	.033	-.018	-.306	.760
Frontal						
1	(Constant)	-4.040	.938		-4.305	.000
	age	-.047	.057	-.049	-.818	.414
	BMI Z-score	-.038	.017	-.118	-2.181	.030
	Height	.000	.000	.225	3.513	.000
	%FM	.001	.000	.354	5.976	.000
	Stance phase duration	.000	.000	-.060	-1.116	.265
	Step length)	3.811E-006	.000	.295	3.897	.000
	Velocity	.000	.000	.041	.594	.553
	Step width	.003	.001	.122	2.718	.007
	Total single support duration	.000	.000	.054	1.065	.288
2	(Constant)	1.531	1.281		1.195	.233
	age	.319	.064	.336	4.991	.000
	BMI Z-score	-.048	.019	-.150	-2.518	.012
	Height	-.034	.009	-.263	-3.667	.000
	%FM	.000	.000	.151	2.296	.022
	Stance phase duration	.000	.000	.083	1.399	.163
	Step length)	-.001	.001	-.087	-1.013	.312
	Velocity	.000	.000	-.142	-1.867	.063
	Step width	-1.101E-006	.000	-.008	-.158	.875
	Total single support duration	.000	.000	.058	1.038	.300
3	(Constant)	-.750	1.326		-.566	.572
	age	-.111	.072	-.117	-1.558	.120
	BMI Z-score	-.090	.063	-.147	-1.432	.153

	Height	.023	.010	.180	2.349	.019
	%FM	.000	.000	-.161	-1.695	.091
	Stance phase duration	-9.777E-006	.000	-.002	-.037	.970
	Step length)	-1.749E-006	.000	-.136	-1.534	.126
	Velocity	.000	.000	.161	2.023	.044
	Step width	.001	.001	.042	.812	.417
	Total single support duration	.000	.000	-.067	-1.140	.255
Transverse						
1	(Constant)	.008	.003	.155	2.466	.014
	age	.263	.054	.428	4.871	.000
	BMI Z-score	6.765E-005	.000	.146	2.332	.020
	Height	.014	.009	.121	1.543	.124
	%FM	.000	.000	-.027	-.530	.597
	Stance phase duration	-8.015E-008	.000	-.006	-.087	.931
	Step length)	.000	.000	.026	.405	.686
	Velocity	1.219E-005	.000	.086	2.005	.046
	Step width	.001	.000	.096	2.004	.046
	Total single support duration	.008	.003	.155	2.466	.014
2	(Constant)	5.256	1.646		3.192	.002
	age	.048	.066	.051	.728	.467
	BMI Z-score	-.039	.020	-.122	-1.946	.052
	Height	-1.105E-005	.000	-.024	-.319	.750
	%FM	.000	.000	.087	1.265	.207
	Stance phase duration	-.001	.000	-.128	-2.068	.039
	Step length)	-.003	.001	-.194	-2.163	.031
	Velocity	.000	.000	.231	2.896	.004
	Step width	-2.143E-006	.000	-.015	-.293	.770
	Total single support duration	-.042	.033	-.075	-1.289	.198

Table. A10.18. Knee joint moments component mixed model regression of regression scores with significant predictors from linear regression

Model	Source	Numerator df	Denominator df	F	Sig.
Sagittal					
1	Intercept	1	640.057	18.661	.000
	BMI Z-Score	1	29.044	3.594	.068
	Step Length	1	428.622	4.400	.037
	Step width	1	342.521	.754	.386
	Height	1	433.606	8.721	.003
2	Intercept	1	68.252	13.227	.001
	Height	1	72.390	8.700	.004
	Step Length	1	366.635	.310	.578
	Velocity	1	359.611	1.040	.309
3	Intercept	1	513.622	8.313	.004
	Height	1	524.102	11.274	.001
	Step Length	1	498.175	8.010	.005
	Velocity	1	497.004	4.621	.032
Frontal					
1	Intercept	1	4359.636	26.428	.000
	BMI Z-Score	1	57510.885	1.664	.197
	Height	1	6708.222	12.210	.000
	%FM	1	48306.052	5.814	.016
	Step width	1	345.646	.096	.757
	Step Length	1	394.208	5.476	.020
2	Intercept	1	48.550	5.609	.022
	age	1	33.491	2.388	.132
	BMI Z-Score	1	38.218	1.578	.217
	Height	1	42.739	5.987	.019
	%FM	1	56.277	1.228	.273
3	Intercept	1	50.146	.068	.796
	Height	1	46.617	.112	.739
	Velocity	1	98.668	.099	.753
Transverse					
1	Intercept	1	593.062	6.242	.013
	age	1	464.808	.750	.387
	BMI Z-Score	1	80.643	17.289	.000
	Height	1	385.622	.887	.347
	Step width	1	387.616	.857	.355
	Total single support duration	1	362.431	1.115	.292
2	Intercept	1	574.591	2.517	.113
	Stance phase duration	1	412.474	1.879	.171
	Step Length	1	666.465	.478	.490
	Velocity	1	582.222	.514	.474

Table A10.19. Knee joint moments individual variables linear regression coefficients for sagittal hip angles at gait cycle events and peaks and predictors

Model		Unstandardized Coefficients		Standardized Coefficients	t	Sig.
		B	Std. Error	Beta		
SS1 fro Max (Nm)	(Constant)	-15865.019	14610.337		-1.086	.278
	age	-87.678	30.098	-.169	-2.913	.004
	BMI Z-score	-452.662	174.059	-.136	-2.601	.010
	Height	1.299	.298	.269	4.353	.000
	%FM	8.412	1.341	.360	6.275	.000
	Stance phase duration	-550.651	262.431	-.108	-2.098	.037
	Step length)	.043	.010	.319	4.340	.000
	Velocity	5.944	3.737	.105	1.591	.113
	Step width	27.863	12.776	.095	2.181	.030
	Total single support duration	5.940	2.911	.100	2.041	.042
Fro CTO (Nm)	(Constant)	-32617.963	13865.624		-2.352	.019
	age	-55.479	613.958	-.006	-.090	.928
	BMI Z-score	1054.467	542.103	.175	1.945	.053
	Height	.824	.306	.181	2.690	.007
	%FM	.865	1.835	.039	.472	.638
	Stance phase duration	1.735	2.277	.042	.762	.447
	Step length)	48.510	12.607	.305	3.848	.000
	Velocity	3.186	3.730	.060	.854	.394
	Step width	36.596	12.760	.132	2.868	.004
	Total single support duration	-381.909	282.471	-.070	-1.352	.177

Table. A10.20. Knee joint moments individual variables mixed model regression of sagittal hip angles at gait cycle events and peaks with significant predictors from linear regression

Model	Source	Numerator df	Denominator df	F	Sig.
SS1 fro Max (Nm)	Intercept	1	213.545	.502	.479
	age	1	49.664	.560	.458
	BMI Z-Score	1	42.353	.946	.336
	Height	1	63.662	8.662	.005
	%FM	1	43.907	7.906	.007
	Stance phase	1	342.279	9.149	.003
	Step length	1	206.233	3.417	.066
	Step width	1	338.531	.292	.589
	Total single support duration	1	342.826	.638	.425
Fro CTO (Nm)	Intercept	1	79.941	16.064	.000
	Height	1	63.435	14.843	.000
	Step length	1	325.191	5.243	.023
	Step width	1	358.247	2.248	.135

Table A10.21. Ankle joint moments component linear regression coefficients for regression score model and predictors

Model		Unstandardized Coefficients		Standardized Coefficients	t	Sig.
		B	Std. Error	Beta		
Sagittal						
1	Constant)	-7.206	.997		-7.227	.000
	age	.002	.002	.041	1.066	.287
	BMI Z-score	.312	.033	.509	9.377	.000
	Height	.000	.000	.531	13.621	.000
	%FM	.004	.006	.038	.784	.433
	Stance phase duration	.057	.015	.117	3.701	.000
	Step length)	.000	.001	.024	.535	.593
	Velocity	.000	.000	.032	.781	.435
	Step width	-.001	.001	-.048	-1.800	.073
	Total single support duration	-.038	.017	-.067	-2.268	.024
2	Constant)	.354	2.126		.167	.868
	age	.000	.003	.006	.084	.933
	BMI Z-score	-.015	.020	-.047	-.743	.458
	Height	-.030	.010	-.227	-3.034	.003
	%FM	.000	.000	.153	2.211	.028
	Stance phase duration	.086	.030	.178	2.884	.004
	Step length)	.001	.001	.043	.478	.633
	Velocity	.000	.000	.075	.936	.350
	Step width	-7.678E-006	.000	-.054	-1.047	.296
	Total single support duration	-.033	.033	-.059	-1.002	.317
Frontal						
1	Constant)	2.017	1.385		1.457	.146
	age	.201	.068	.211	2.942	.003
	BMI Z-score	-.027	.020	-.086	-1.350	.178
	Height	-.017	.010	-.131	-1.711	.088
	%FM	.000	.000	.082	1.168	.243
	Stance phase duration	.000	.000	-.107	-1.684	.093
	Step length)	-.002	.001	-.098	-1.076	.283
	Velocity	.000	.000	.091	1.115	.266
	Step width	-.001	.001	-.047	-.886	.376
	Total single support duration	.000	.000	.034	.562	.575
2	Constant)	3.276	1.365		2.399	.017
	age	.009	.003	.180	2.627	.009
	BMI Z-score	-.041	.018	-.127	-2.211	.028
	Height	-.045	.009	-.344	-4.791	.000
	%FM	-.004	.007	-.036	-.584	.560
	Stance phase duration	.001	.000	.126	2.070	.039
	Step length)	-5.502E-008	.000	-.004	-.049	.961
	Velocity	8.099E-005	.000	.042	.537	.591
	Step width	.003	.001	.093	1.815	.070
	Total single support duration	.000	.000	.034	.599	.550
Transverse						
1	Constant)	-3.526	1.466		-2.405	.017
	age	.151	.061	.159	2.458	.014
	BMI Z-score	.246	.055	.401	4.440	.000
	Height	.000	.000	.225	3.456	.001
	%FM	.005	.009	.040	.492	.623
	Stance phase duration	-.016	.026	-.034	-.640	.522
	Step length)	-.002	.001	-.132	-1.735	.084
	Velocity	.001	.000	.127	1.878	.061
	Step width	7.936E-006	.000	.056	1.263	.208
	Total single support duration	.000	.000	.030	.599	.549
2	Constant)	2.781	1.992		1.396	.164
	age	.038	.065	.040	.578	.564

	BMI Z-score	-.034	.019	-.108	-1.766	.078
	Height	.006	.010	.047	.647	.518
	%FM	.000	.000	.152	2.267	.024
	Stance phase duration	-.034	.029	-.070	-1.160	.247
	Step length)	-.003	.001	-.189	-2.158	.032
	Velocity	.002	.000	.410	5.267	.000
	Step width	-.002	.001	-.063	-1.236	.217
	Total single support duration	-.053	.032	-.095	-1.674	.095
3	Constant)	-.248	1.433		-.173	.863
	age	.001	.004	.023	.328	.743
	BMI Z-score	.054	.020	.170	2.670	.008
	Height	.003	.010	.023	.308	.758
	%FM	-1.764E-005	.000	-.008	-.113	.910
	Stance phase duration	.000	.000	.043	.691	.490
	Step length)	7.621E-007	.000	.059	.657	.512
	Velocity	-5.092E-005	.000	-.026	-.327	.744
	Step width	-.005	.001	-.161	-3.048	.002
	Total single support duration	.000	.000	-.057	-.949	.343

Table. A10.22. Ankle joint moments component mixed model regression of regression scores with significant predictors from linear regression

Model	Source	Numerator df	Denominator df	F	Sig.
Sagittal					
1	Intercept	1	261.041	50.723	.000
	BMI Z-score	1	34.159	67.534	.000
	Height	1	44.414	116.027	.000
	Stance phase duration	1	351.804	2.559	.111
	Total single support duration	1	348.588	.694	.405
2	Intercept	1	104.901	.620	.433
	Height	1	48.010	3.683	.061
	%FM	1	74.987	.080	.777
	Stance phase duration	1	349.199	16.303	.000
Frontal					
1	Intercept	1	59.535	.910	.344
	age	1	57.352	.906	.345
2	Intercept	1	367.000	8.638	.003
	age	1	367	6.147	.014
	BMI Z-score	1	367	8.313	.004
	Height	1	367	25.828	.000
	Stance phase duration	1	367	6.268	.013
Transverse					
1	Intercept	1	29010.246	15.988	.000
	age	1	7983.027	1.325	.250
	BMI Z-score	1	41712.450	11.797	.001
	Height	1	3216.567	2.194	.139
2	Intercept	1	791.695	2.014	.156
	%FM	1	1960.201	1.365	.243
	Step length	1	744.065	.617	.432
	Velocity	1	650.625	9.146	.003
3	Intercept	1	168.729	1.359	.245
	BMI Z-score	1	13.325	6.067	.028
	Step width	1	359.978	7.621	.006

Table A10.23. Shank-calcaneus component linear regression coefficients for regression score model and predictors

Model		Unstandardized Coefficients		Standardized Coefficients	t	Sig.
		B	Std. Error	Beta		
1	(Constant)	-.114	.925		-.123	.902
	age	-.027	.044	-.029	-.605	.545
	BMI Z-Score	.070	.015	.223	4.771	.000
	Height	-.006	.007	-.049	-.934	.350
	%FM	-.001	.000	-.261	-5.053	.000
	Stance phase duration	.000	.000	.096	2.386	.017
	Step length	.002	.001	.124	2.401	.017
	Velocity	2.680E-005	.000	.005	.103	.918
	Step width	.004	.001	.158	4.568	.000
	Total single support duration	.000	.000	-.080	-2.176	.030
2	(Constant)	-2.885	1.187		-2.430	.015
	age	-.386	.046	-.416	-8.477	.000
	BMI Z-Score	-.353	.041	-.559	-8.567	.000
	Height	.050	.007	.381	7.488	.000
	%FM	.001	.000	.375	5.877	.000
	Stance phase duration	-.008	.018	-.017	-.423	.673
	Step length	.002	.001	.132	2.608	.009
	Velocity	-.001	.000	-.113	-2.628	.009
	Step width	-.001	.001	-.028	-.843	.400
	Total single support duration	.000	.000	-.056	-1.549	.122
3	(Constant)	-1.246	.913		-1.364	.173
	age	-.006	.002	-.114	-2.800	.005
	BMI Z-Score	-.087	.012	-.280	-7.003	.000
	Height	.000	.000	.305	6.875	.000
	%FM	.001	.000	.443	10.054	.000
	Stance phase duration	.000	.000	-.067	-1.939	.053
	Step length	-.004	.001	-.213	-4.796	.000
	Velocity	.001	.000	.112	2.948	.003
	Step width	-3.264E-006	.000	-.026	-.885	.376
	Total single support duration	.038	.017	.068	2.171	.030

Table A10.24. Shank-Calcaneus component mixed model regression of regression scores with significant predictors from linear regression

Model	Source	Numerator df	Denominator df	F	Sig.
1	Intercept	1	99.568	1.927	.168
	BMI Z-Score	1	50.995	2.649	.110
	%FM	1	24.930	.001	.978
	Stance phase duration	1	736.970	.144	.704
	Step length	1	122.373	.047	.829
	Step width	1	718.416	.002	.961
	Total single support duration	1	736.953	.608	.436
2	Intercept	1	47.062	2.595	.114
	age	1	47.045	1.991	.165
	BMI Z-Score	1	47.021	5.374	.025
	Height	1	47.046	3.095	.085
	%FM	1	47.010	2.674	.109
	Step length	1	736.319	.406	.524
	Velocity	1	736.732	1.651	.199
3	Intercept	1	77.350	.141	.709
	age	1	72.508	.105	.747
	BMI Z-Score	1	64.933	5.140	.027
	Height	1	69.070	.620	.434
	%FM	1	66.495	10.621	.002
	Step length	1	743.842	.002	.968
	Velocity	1	747.425	.631	.427
	Total single support duration	1	605.213	.768	.381

Table A10.25. Shank-Calcaneus individual variables linear regression coefficients for sagittal hip angles at gait cycle events and peaks and predictors

Model		Unstandardized Coefficients		Standardized Coefficients	t	Sig.
		B	Std. Error	Beta		
SS 1 tra Min (deg.)	(Constant)	-34.955	8.894		-3.930	.000
	age	-1.603	.306	-.247	-5.231	.000
	BMI Z-score	-.134	.269	-.030	-.497	.619
	Height	.436	.044	.475	9.857	.000
	%FM	.158	.045	.198	3.497	.000
	Stance phase duration	-.305	.121	-.097	-2.531	.012
	Step length	-.034	.006	-.270	-5.613	.000
	Velocity	.003	.002	.073	1.753	.080
	Step width	-.003	.006	-.018	-.552	.581
	Total single support duration	.193	.134	.050	1.446	.149
SS 2 tra Min (deg.)	(Constant)	-28.000	8.770		-3.193	.001
	age	-1.801	.302	-.281	-5.962	.000
	BMI Z-score	.273	.265	.063	1.031	.303
	Height	.438	.044	.483	10.057	.000
	%FM	.076	.045	.096	1.707	.088
	Stance phase duration	-.286	.119	-.092	-2.402	.017
	Step length	-.033	.006	-.260	-5.445	.000
	Velocity	.002	.002	.050	1.209	.227
	Step width	-.002	.006	-.012	-.360	.719
	Total single support duration	.118	.132	.031	.894	.371
Tra IIC (deg.)	(Constant)	-16.587	6.774		-2.449	.015
	age	-.064	.015	-.175	-4.320	.000
	BMI Z-score	-.542	.093	-.233	-5.852	.000
	Height	.001	.000	.393	8.866	.000
	%FM	.006	.001	.392	8.912	.000
	Stance phase duration	-.003	.001	-.088	-2.574	.010
	Step length	-.033	.006	-.244	-5.522	.000
	Velocity	.007	.002	.155	4.087	.000
	Step width	-2.730E-005	.000	-.029	-.998	.319
	Total single support duration	.256	.128	.063	1.995	.046
Tra CTO (deg.)	(Constant)	-17.139	6.701		-2.558	.011
	age	-.042	.015	-.121	-2.867	.004
	BMI Z-score	-.520	.092	-.235	-5.646	.000
	Height	.001	.000	.389	8.403	.000
	%FM	.006	.001	.379	8.262	.000
	Stance phase duration	-.003	.001	-.100	-2.784	.006
	Step length	-.029	.006	-.229	-4.995	.000
	Velocity	2.359E-006	.000	.153	3.881	.000
	Step width	-3.837E-005	.000	-.043	-1.411	.159
	Total single support duration	.258	.128	.066	2.023	.043
Tra CIC (deg.)	(Constant)	-6.323	6.733		-.939	.348
	age	-.034	.015	-.094	-2.295	.022
	BMI Z-score	-.704	.092	-.309	-7.657	.000
	Height	.001	.000	.186	4.143	.000
	%FM	.008	.001	.519	11.661	.000
	Stance phase duration	-.002	.001	-.078	-2.258	.024
	Step length	-.025	.006	-.189	-4.213	.000
	Velocity	.003	.002	.073	1.884	.060
	Step width	-3.187E-005	.000	-.035	-1.172	.241
	Total single support duration	.359	.128	.090	2.812	.005
Tra ITO (deg.)	(Constant)	2.111	7.143		.295	.768
	age	-1.191	.296	-.165	-4.028	.000
	BMI Z-score	-.771	.099	-.317	-7.793	.000
	Height	.001	.000	.266	5.898	.000

%FM	.007	.001	.448	10.000	.000
Stance phase duration	-.003	.001	-.088	-2.525	.012
Step length	-.022	.006	-.159	-3.531	.000
Velocity	-3.355E-007	.000	-.020	-.514	.607
Step width	-2.565E-005	.000	-.026	-.878	.380
Total single support duration	.332	.137	.078	2.425	.016

Table. A10.26. Shank-Calcaneus individual variables mixed model regression of sagittal hip angles at gait cycle events and peaks with significant predictors from linear regression

Model	Source	Numerator df	Denominator df	F	Sig.
SS 1 tra Min (deg.)	Intercept	1	94.097	6.702	.011
	age	1	89.617	3.354	.070
	Height	1	91.903	3.745	.056
	%FM	1	92.528	3.802	.054
	Step length	1	383.745	.182	.670
SS 2 tra Min (deg.)	Intercept	1	59.078	9.915	.003
	age	1	57.302	5.357	.024
	Height	1	57.072	8.788	.004
	Stance phase duration	1	653.105	.982	.322
	Step length	1	265.428	.102	.749
Tra IIC (deg.)	Intercept	1	49295.262	2.849	.091
	age	1	3744886.161	1.394	.238
	BMI Z-Score	1	4279774.544	2.400	.121
	Height	1	2503649.484	3.686	.055
	%FM	1	3609843.984	5.243	.022
	Stance phase duration	1	758.856	6.011	.014
	Step length	1	759.738	.938	.333
	Velocity	1	768.226	.101	.751
	Total single support duration	1	757.187	1.445	.230
Tra CTO (deg.)	Intercept	1	48986.486	7.207	.007
	age	1	3568367.149	.432	.511
	BMI Z-Score	1	3966371.518	2.251	.134
	Height	1	2351058.439	3.123	.077
	%FM	1	3433969.968	4.771	.029
	Stance phase durations	1	755.821	.844	.359
	Step length	1	762.527	.198	.656
	Total single support duration	1	759.157	.023	.880
	Velocity	1	804.033	.231	.631
Tra CIC (deg.)	Intercept	1	103.450	.053	.819
	age	1	76.657	.183	.670
	BMI Z-Score	1	75.543	2.991	.088
	Height	1	71.212	.002	.966
	%FM	1	75.889	14.185	.000
	Stance phase duration	1	525.379	.834	.361
	Step length	1	752.742	.006	.940
	Total single support duration	1	740.982	1.214	.271
Tra ITO (deg.)	Intercept	1	123.980	.015	.903
	age	1	80.232	1.196	.277
	BMI Z-Score	1	78.903	8.492	.005
	Height	1	76.774	.806	.372
	%FM	1	79.788	14.033	.000
	Stance phase duration	1	666.940	1.345	.247
	Step length	1	764.200	.105	.746
	Total single support duration	1	748.048	.396	.529

Table A10.26. Calcaneus-Midfoot component linear regression Regression coefficients for regression score model and predictors

Model		Unstandardized Coefficients		Standardized Coefficients	t	Sig.
		B	Std. Error	Beta		
1	(Constant)	-1.920	1.365		-1.407	.160
	age	.011	.002	.221	4.463	.000
	BMI Z-score	-.255	.041	-.403	-6.160	.000
	Height	.002	.007	.019	.369	.712
	%FM	.000	.000	.186	2.909	.004
	Stance phase duration	.015	.018	.034	.856	.392
	Step Length	-.002	.001	-.115	-2.277	.023
	Velocity	.000	.000	.058	1.348	.178
	Step width	-1.109E-005	.000	-.089	-2.655	.008
	Total single support duration	.027	.020	.048	1.355	.176
2	(Constant)	-1.923	.807		-2.384	.017
	age	.247	.041	.266	6.023	.000
	BMI Z-score	.239	.037	.377	6.425	.000
	Height	-.010	.006	-.078	-1.704	.089
	%FM	.000	.000	.194	3.369	.001
	Stance phase duration	.000	.000	-.040	-1.113	.266
	Step Length	.003	.001	.180	3.965	.000
	Velocity	-.001	.000	-.164	-4.229	.000
	Step width	-8.195E-007	.000	-.007	-.218	.828
	Total single support duration	-7.588E-007	.000	.000	-.004	.997
3	(Constant)	-.901	.693		-1.301	.194
	age	.176	.045	.189	3.881	.000
	BMI Z-score	-.238	.042	-.376	-5.685	.000
	Height	5.643E-005	.000	.121	2.463	.014
	%FM	.020	.007	.172	2.743	.006
	Stance phase duration	.000	.000	-.117	-2.972	.003
	Step Length	-2.789E-007	.000	-.019	-.388	.698
	Velocity	-.001	.000	-.120	-2.848	.005
	Step width	9.113E-005	.001	.004	.108	.914
	Total single support duration	.000	.000	.038	1.068	.286

Table. A10.27. Calcaneus-midfoot component mixed model regression of regression scores with significant predictors from linear regression

Model	Source	Numerator df	Denominator df	F	Sig.
1	Intercept	1	47.675	.014	.905
	age	1	47.019	.392	.535
	BMI Z-score	1	46.978	2.009	.163
	%FM	1	46.976	.377	.542
	Step Length	1	736.510	1.233	.267
	Step width	1	735.263	.021	.884
2	Intercept	1	47.737	8.044	.007
	age	1	47.357	3.682	.061
	BMI Z-score	1	48.267	28.384	.000
	%FM	1	47.149	5.469	.024
	Step Length	1	739.394	1.419	.234
	Velocity	1	740.894	3.520	.061
3	Intercept	1	536.308	8.642	.003
	age	1	543.404	1.588	.208
	BMI Z-score	1	543.653	4.294	.039
	Height	1	551.086	2.833	.093
	%FM	1	587.886	3.679	.041
	Stance phase duration	1	733.644	.355	.552
	Velocity	1	77.570	2.341	.130

Table A10.28. Calcaneus-midfoot individual variables linear regression coefficients for sagittal hip angles at gait cycle events and peaks and predictors

Model		Unstandardized Coefficients		Standardized Coefficients	t	Sig.
		B	Std. Error	Beta		
DS 1 sagMin (deg.)	(Constant)	-11.446	8.198		-1.396	.163
	age	1.295	.314	.186	4.123	.000
	BMI Z-Score	2.256	.284	.476	7.949	.000
	Height	-.064	.046	-.065	-1.405	.160
	%FM	.001	.001	.064	1.103	.270
	Stance phase duration	.100	.123	.030	.813	.416
	Step length	2.221E-005	.000	.199	4.382	.000
	Velocity	-.008	.002	-.179	-4.603	.000
	Step width	-.004	.006	-.019	-.628	.530
	Total single support duration	-.001	.001	-.035	-1.066	.287
SS 1 sagMin (deg.)	(Constant)	-11.446	8.198		-1.396	.163
	age	1.295	.314	.186	4.123	.000
	BMI Z-Score	2.256	.284	.476	7.949	.000
	Height	-.064	.046	-.065	-1.405	.160
	%FM	.001	.001	.064	1.103	.270
	Stance phase duration	.100	.123	.030	.813	.416
	Step length	2.221E-005	.000	.199	4.382	.000
	Velocity	-.008	.002	-.179	-4.603	.000
	Step width	-.004	.006	-.019	-.628	.530
	Total single support duration	-.001	.001	-.035	-1.066	.287
SS 2 sagMin (deg.)	(Constant)	-14.480	6.652		-2.177	.030
	age	1.921	.327	.267	5.869	.000
	BMI Z-Score	1.876	.296	.383	6.349	.000
	Height	-.036	.048	-.036	-.762	.446
	%FM	.002	.001	.147	2.496	.013
	Stance phase duration	-.002	.001	-.059	-1.614	.107
	Step length	8.758E-006	.000	.076	1.658	.098
	Velocity	-.005	.002	-.106	-2.689	.007
	Step width	-.005	.006	-.026	-.825	.410
	Total single support duration	-.001	.001	-.015	-.455	.650
SS 2 sagMax (deg.)	(Constant)	1.035	7.697		.134	.893
	age	1.085	.279	.168	3.888	.000
	BMI Z-Score	-.378	.092	-.175	-4.092	.000
	Height	-.040	.043	-.044	-.922	.357
	%FM	.008	.001	.567	12.040	.000
	Stance phase duration	6.777E-005	.001	.002	.068	.946
	Step length	1.192E-005	.000	.116	2.490	.013
	Velocity	-.007	.002	-.171	-4.273	.000
	Step width	-.006	.006	-.033	-1.027	.305
	Total single support duration	-.073	.128	-.019	-.567	.571
Sag IIC (deg.)	(Constant)	-9.670	7.351		-1.316	.189
	age	1.796	.286	.283	6.274	.000
	BMI Z-Score	1.972	.258	.457	7.633	.000
	Height	-.127	.042	-.142	-3.050	.002
	%FM	.001	.001	.100	1.709	.088
	Stance phase duration	-.001	.001	-.036	-.982	.326
	Step length	1.933E-005	.000	.191	4.185	.000
	Velocity	-.004	.002	-.101	-2.593	.010
	Step width	.005	.005	.030	.973	.331
	Total single support duration	.127	.123	.034	1.028	.304
Sag CTO (deg.)	(Constant)	-4.251	5.862		-.725	.469
	age	1.890	.288	.298	6.552	.000
	BMI Z-Score	2.132	.260	.494	8.186	.000
	Height	-.156	.042	-.174	-3.707	.000

	%FM	.001	.001	.043	.732	.464
	Stance phase duration	-.001	.001	-.041	-1.121	.263
	Step length	2.013E-005	.000	.199	4.326	.000
	Velocity	-.003	.002	-.087	-2.204	.028
	Step width	.003	.005	.016	.512	.609
	Total single support duration	.001	.001	.040	1.197	.231
Sag CIC (deg.)	(Constant)	-24.188	8.937		-2.706	.007
	age	.554	.299	.078	1.856	.064
	BMI Z-Score	-.545	.099	-.227	-5.493	.000
	Height	-.024	.046	-.024	-.525	.600
	%FM	.011	.001	.648	14.264	.000
	Stance phase duration	.223	.122	.065	1.825	.068
	Step length	2.712E-005	.000	.238	5.309	.000
	Velocity	-2.398E-006	.000	-.144	-3.724	.000
	Step width	.001	.006	.006	.201	.841
	Total single support duration	.049	.137	.012	.356	.722
Sag ITO (deg.)	(Constant)	-20.930	6.246		-3.351	.001
	age	.459	.286	.068	1.609	.108
	BMI Z-Score	-.615	.094	-.269	-6.507	.000
	Height	.027	.044	.028	.610	.542
	%FM	.010	.001	.670	14.677	.000
	Stance phase duration	.001	.001	.025	.688	.492
	Step length	2.380E-005	.000	.219	4.857	.000
	Velocity	-.004	.002	-.086	-2.214	.027
	Step width	-1.916E-005	.000	-.021	-.685	.494
	Total single support duration	-6.239E-005	.001	-.002	-.047	.962
DS 1 froMax (deg.)	(Constant)	2.014	4.646		.433	.665
	age	2.242	.277	.355	8.109	.000
	BMI Z-Score	.775	.086	.365	8.991	.000
	Height	7.727E-005	.000	.024	.517	.606
	%FM	-.293	.034	-.376	-8.676	.000
	Stance phase duration	-.004	.001	-.166	-4.411	.000
	Step length	-6.098E-006	.000	-.060	-1.287	.199
	Velocity	-.004	.002	-.111	-2.709	.007
	Step width	.004	.006	.020	.623	.533
	Total single support duration	.001	.001	.024	.704	.482
SS 2 froMin (deg.)	(Constant)	-13.122	4.600		-2.853	.004
	age	1.207	.300	.190	4.026	.000
	BMI Z-Score	-2.218	.278	-.513	-7.986	.000
	Height	.000	.000	.137	2.869	.004
	%FM	.177	.048	.226	3.730	.000
	Stance phase duration	-.003	.001	-.103	-2.699	.007
	Step length	-6.778E-006	.000	-.067	-1.422	.155
	Velocity	-.003	.002	-.063	-1.532	.126
	Step width	-3.734E-005	.000	-.044	-1.362	.174
	Total single support duration	.002	.001	.054	1.575	.116
SS 2 froMax (deg.)	(Constant)	-3.908	4.948		-.790	.430
	age	.728	.323	.110	2.257	.024
	BMI Z-Score	-2.290	.299	-.507	-7.667	.000
	Height	.000	.000	.126	2.575	.010
	%FM	.177	.051	.216	3.458	.001
	Stance phase duration	-.003	.001	-.090	-2.294	.022
	Step length	-2.637E-006	.000	-.025	-.514	.607
	Velocity	-.004	.002	-.092	-2.199	.028
	Step width	-3.032E-005	.000	-.034	-1.028	.304
	Total single support duration	.001	.001	.036	1.016	.310
Fro IIC (deg.)	(Constant)	-6.909	4.891		-1.413	.158

	age	1.243	.313	.186	3.970	.000
	BMI Z-Score	-2.135	.285	-.470	-7.482	.000
	Height	.000	.000	.135	2.794	.005
	%FM	.003	.001	.177	2.883	.004
	Stance phase duration	-.003	.001	-.108	-2.815	.005
	Step length	-6.761E-006	.000	-.063	-1.324	.186
	Velocity	-.004	.002	-.090	-2.182	.029
	Step width	-.003	.006	-.014	-.437	.662
	Total single support duration	.002	.001	.049	1.422	.155
Fro CTO (deg.)	(Constant)	-14.013	4.531		-3.093	.002
	age	1.080	.296	.171	3.646	.000
	BMI Z-Score	-1.920	.274	-.448	-7.010	.000
	Height	.001	.000	.207	4.375	.000
	%FM	.095	.047	.122	2.018	.044
	Stance phase duration	-.003	.001	-.122	-3.218	.001
	Step length	-1.191E-005	.000	-.118	-2.536	.011
	Velocity	-.002	.002	-.057	-1.411	.159
	Step width	-.004	.006	-.026	-.807	.420
	Total single support duration	.003	.001	.073	2.133	.033
Fro CIC (deg.)	(Constant)	-9.968	4.590		-2.172	.030
	age	1.619	.300	.251	5.399	.000
	BMI Z-Score	-2.029	.277	-.463	-7.312	.000
	Height	.000	.000	.085	1.814	.070
	%FM	.108	.048	.136	2.280	.023
	Stance phase duration	-.003	.001	-.113	-3.006	.003
	Step length	-1.002E-005	.000	-.097	-2.105	.036
	Velocity	-.001	.002	-.036	-.899	.369
	Step width	9.836E-005	.006	.001	.018	.986
	Total single support duration	.002	.001	.041	1.216	.225
Fro ITO (deg.)	(Constant)	-2.386	4.937		-.483	.629
	age	1.356	.323	.200	4.202	.000
	BMI Z-Score	-2.136	.298	-.462	-7.158	.000
	Height	.000	.000	.080	1.667	.096
	%FM	.140	.051	.167	2.734	.006
	Stance phase duration	-.003	.001	-.121	-3.147	.002
	Step length	-3.881E-006	.000	-.036	-.758	.449
	Velocity	-.005	.002	-.117	-2.846	.005
	Step width	.001	.006	.007	.221	.825
	Total single support duration	.002	.001	.042	1.214	.225

Table. A10.29. Calcaneus-midfoot individual variables mixed model regression of sagittal hip angles at gait cycle events and peaks with significant predictors from linear regression

Model	Source	Numerator df	Denominator df	F	Sig.
DS 1 sagMin (deg.)	Intercept	1	134.476	18.888	.000
	age	1	122.033	11.362	.001
	BMI Z-Score	1	143.331	13.940	.000
	Step Length	1	754.140	.000	.990
SS 1 sagMin (deg.)	Intercept	1	134.476	18.888	.000
	age	1	122.033	11.362	.001
	BMI Z-Score	1	143.331	13.940	.000
	Step Length	1	754.140	.000	.990
	Velocity	1	342.640	.874	.351
SS 2 sagMin (deg.)	Intercept	1	47.987	12.919	.001
	age	1	47.226	4.845	.033
	BMI Z-Score	1	47.033	2.079	.156
	%FM	1	46.997	.258	.614
	Velocity	1	745.873	2.304	.129
SS 2 sagMax (deg.)	Intercept	1	49.246	3.152	.082
	age	1	48.404	2.445	.124
	BMI Z-Score	1	48.035	1.468	.232
	%FM	1	48.050	10.153	.003
	Step Length	1	749.883	2.744	.098
	Velocity	1	750.554	4.219	.040
Sag IIC (deg.)	Intercept	1	47.453	1.150	.289
	age	1	47.069	2.392	.129
	BMI Z-Score	1	47.109	11.117	.002
	Height	1	47.210	.043	.836
	Step Length	1	742.743	.419	.518
	Velocity	1	744.705	.315	.575
Sag CTO (deg.)	Intercept	1	250.072	1.292	.257
	age	1	259.414	1.966	.162
	BMI Z-Score	1	238.371	12.064	.001
	Height	1	267.667	.110	.740
	Step Length	1	742.110	.400	.527
	Velocity	1	195.911	.184	.668
Sag CIC (deg.)	Intercept	1	47.600	.954	.334
	BMI Z-Score	1	48.631	3.258	.077
	Height	1	47.815	.914	.344
	%FM	1	48.476	12.710	.001
	Step Length	1	737.153	.063	.802
	Velocity	1	76.019	.663	.418
Sag ITO (deg.)	Intercept	1	72.706	24.487	.000
	BMI Z-Score	1	49.043	4.751	.034
	%FM	1	49.046	20.593	.000
	Step Length	1	760.689	.202	.653
	Velocity	1	759.160	.172	.678
DS 1 froMax (deg.)	Intercept	1	53.837	7.889	.007
	age	1	47.628	12.641	.001
	BMI Z-Score	1	55.931	12.685	.001
	%FM	1	53.303	7.062	.010
	Stance phase duration	1	738.930	.258	.612
	Velocity	1	85.714	2.283	.134
SS 2 froMin (deg.)	Intercept	1	1338918.595	12.175	.000
	age	1	13161314.617	2.075	.150

	BMI Z-Score	1	21646510.435	4.351	.037
	Height	1	36283207.555	.332	.565
	%FM	1	32145877.229	1.036	.309
	Stance phase duration	1	742.300	.586	.444
SS 2 froMax (deg.)	Intercept	1	48.330	2.019	.162
	age	1	61.903	2.168	.146
	BMI Z-Score	1	57.028	1.604	.210
	Height	1	60.426	.231	.632
	%FM	1	61.224	.066	.799
	Stance phase duration	1	906.013	.001	.971
	Velocity	1	62.100	.832	.365
Fro IIC (deg.)	Intercept	1	319.137	7.280	.007
	age	1	310.203	1.660	.199
	BMI Z-Score	1	333.730	3.873	.050
	Height	1	464.149	.483	.488
	%FM	1	447.255	.888	.347
	Stance phase duration	1	737.454	1.486	.223
	Velocity	1	59.610	4.822	.032
Fro CTO (deg.)	Intercept	1	1501.347	31.848	.000
	age	1	1744.653	5.434	.020
	BMI Z-Score	1	1381.074	14.037	.000
	Height	1	1575.606	3.713	.054
	%FM	1	1402.115	1.110	.292
	Stance phase duration	1	760.471	.028	.867
	Step Length	1	7880.479	.974	.324
Fro CIC (deg.)	Intercept	1	47.794	12.367	.001
	age	1	41.659	10.106	.003
	BMI Z-Score	1	38.198	1.379	.248
	%FM	1	33.524	.064	.802
	Stance phase duration	1	737.004	1.674	.196
	Step Length	1	741.931	.646	.422
Fro ITO (deg.)	Intercept	1	65.592	8.446	.005
	age	1	58.751	7.601	.008
	BMI Z-Score	1	50.061	.755	.389
	%FM	1	75.653	.071	.791
	Stance phase duration	1	149.662	.355	.552
	Velocity	1	87.165	.260	.611

Table A10.30. Midfoot-metatarsal component linear regression coefficients for regression score model and predictors

Model		Unstandardized Coefficients		Standardized Coefficients	t	Sig.
		B	Std. Error	Beta		
1	(Constant)	-3.678	.982		-3.745	.000
	age	.014	.002	.289	6.422	.000
	BMI Z-Score	-.109	.014	-.350	-7.854	.000
	Height	-2.298E-005	.000	-.049	-1.004	.316
	%FM	.001	.000	.238	4.866	.000
	Stance phase duration	.056	.017	.125	3.285	.001
	Step length	1.520E-006	.000	.102	2.119	.034
	Velocity	-2.066E-007	.000	-.095	-2.275	.023
	Step width	-1.659E-005	.000	-.133	-4.048	.000
	Total single support duration	.000	.000	.020	.565	.572
2	(Constant)	2.456	1.161		2.115	.035
	age	.230	.046	.248	4.967	.000
	BMI Z-Score	.248	.042	.392	5.912	.000
	Height	-.049	.007	-.377	-7.274	.000
	%FM	-.001	.000	-.343	-5.282	.000
	Stance phase duration	-4.172E-005	.000	-.011	-.262	.793
	Step length	.000	.001	.013	.245	.807
	Velocity	.000	.000	.078	1.779	.076
	Step width	.004	.001	.146	4.294	.000
	Total single support duration	.033	.020	.060	1.656	.098
3	(Constant)	-1.555	1.041		-1.493	.136
	age	.001	.002	.014	.295	.768
	BMI Z-Score	.039	.015	.124	2.659	.008
	Height	.000	.000	.251	4.890	.000
	%FM	-.001	.000	-.337	-6.552	.000
	Stance phase duration	.000	.000	-.035	-.865	.387
	Step length	-2.110E-006	.000	-.142	-2.795	.005
	Velocity	.001	.000	.218	4.957	.000
	Step width	-.001	.001	-.045	-1.286	.199
	Total single support duration	-.012	.020	-.022	-.600	.549

Table A10.31. Midfoot-metatarsal component mixed model regression of regression scores with significant predictors from linear regression

Model	Source	Numerator df	Denominator df	F	Sig.
1	Intercept	1	52.738	.031	.862
	age	1	48.123	.651	.424
	BMI Z-Score	1	48.784	3.477	.068
	%FM	1	48.797	.789	.379
	Stance phase duration	1	776.051	.541	.462
	Step length	1	784.393	.821	.365
	Velocity	1	1143.866	.004	.949
	Step width	1	838.696	.176	.675
2	Intercept	1	47.062	2.595	.114
	age	1	47.045	1.991	.165
	BMI Z-Score	1	47.021	5.374	.025
	Height	1	47.046	3.095	.085
	%FM	1	47.010	2.674	.109
	Step length	1	736.319	.406	.524
	Velocity	1	736.732	1.651	.199
3	Intercept	1	103000.090	4.075	.044
	BMI Z-Score	1	158424.225	2.217	.136
	Height	1	113901.315	5.894	.015
	%FM	1	193243.217	3.915	.052
	Step length	1	8291284357.248	.002	.969
	Velocity	1	766.070	1.164	.281

Table A10.32. First metatarsal-hallux component linear regression coefficients for regression score model and predictors

Model		Unstandardized Coefficients		Standardized Coefficients	t	Sig.
		B	Std. Error	Beta		
1	(Constant)	-.576	.869		-.663	.508
	age	.048	.042	.051	1.147	.252
	BMI Z-Score	.141	.013	.450	10.940	.000
	Height	-.006	.006	-.048	-.993	.321
	%FM	-.043	.005	-.374	-8.513	.000
	Stance phase duration	.000	.000	.124	3.256	.001
	Step length	-.003	.001	-.148	-3.068	.002
	Velocity	.001	.000	.178	4.255	.000
	Step width	-.002	.001	-.072	-2.180	.030
	Total single support duration	8.495E-005	.000	.015	.442	.658
2	(Constant)	3.160	1.010		3.129	.002
	age	-.100	.042	-.108	-2.369	.018
	BMI Z-Score	.059	.013	.190	4.487	.000
	Height	-5.979E-005	.000	-.128	-2.612	.009
	%FM	.025	.005	.221	4.920	.000
	Stance phase duration	.000	.000	-.038	-.985	.325
	Step length	-4.264E-007	.000	-.029	-.588	.557
	Velocity	.000	.000	.061	1.428	.154
	Step width	.001	.001	.046	1.354	.176
	Total single support duration	-.032	.020	-.058	-1.622	.105

Table. A10.33. First metatarsal-hallux component mixed model regression of regression scores with significant predictors from linear regression

Model	Source	Numerator df	Denominator df	F	Sig.
	Intercept	1	57.647	.000	.984
	BMI Z-Score	1	42.920	9.882	.003
	%FM	1	49.260	3.243	.056
1	Stance phase duration	1	746.543	.467	.494
	Step length	1	292.314	.663	.416
	Velocity	1	761.125	.272	.602
	Step width	1	728.723	1.798	.180
	Intercept	1	4817232.500	.285	.593
	age	1	12291175.642	.033	.855
2	BMI Z-Score	1	19530432.718	1.331	.249
	Height	1	24776309.105	.564	.453
	%FM	1	23532381.625	1.915	.166

Appendix XI: Publications and Presentations

Conference Presentations Abstract:

Mahaffey, R., Morrison, S.C., Cramp, M., Drechsler, W.I. (2011) Three-dimensional analysis of the paediatric foot during gait. Annual Conference of the Society of Chiropodists and Podiatrists. Harrogate, United Kingdom.

Published Conference Proceedings Abstract:

Mahaffey, R., Morrison, S.C., Drechsler, W., Cramp, M (2012) Reliability of three foot models to examine paediatric gait. *Journal of Foot and Ankle Research*, 5 (Suppl1): O18

Published Manuscript:

Morrison, S.C., Mahaffey, R.D., Cousins, S.D. and Drechsler, W.I. (2012). Current understanding of the impact of childhood obesity on the foot and lower limb. *Journal of the Association of Paediatric Physiotherapists.* 3 (2), 5 – 11.

Annual Conference of the Society of Chiropodists and Podiatrists. Harrogate, United Kingdom.

Three-dimensional analysis of the paediatric foot during gait

Mahaffey, R.[1], Morrison, S.C. [1], Cramp, M. [1], Drechsler, W.I. [1]

[1]School of Health, Sport & Bioscience, University of East London

During 3-D gait analysis foot and ankle segments have typically been presented as a single rigid mass. This not only excludes frontal plane motions but also negates 3-D movements that occur between the toes and the ankle. However, over the last decade, a variety of multi-segmental foot models have been produced to examine, in detail, the movement of the foot during gait. The aims of this study is to evaluate available foot models to determine the most appropriate for comparing biomechanical gait characteristics in children. Twenty one children were recruited to the University of East London gait lab where marker sets for three foot models were applied to their right feet. Each foot model was examined for intra- and inter-session reliability. All models demonstrated acceptable intra session reliability for the hindfoot and forefoot but not the hallux segment. Inter session reliability was lower in foot models that divide the foot up into more segments and in foot models that don't normalise to a static pose. The application of 3-D modelling techniques to measure paediatric foot motion over the gait cycle is reliable both within and between testing sessions however caution must be taken with hallux segments.

Mahaffey et al. Journal of Foot and Ankle Research 2012, 5(Suppl 1):O18
http://www.jfootankleres.com/content/5/S1/O18

JOURNAL OF FOOT AND ANKLE RESEARCH

ORAL PRESENTATION Open Access

Reliability of three foot models to examine paediatric gait

Ryan Mahaffey*, Stewart Morrison, Wendy Drechsler, Mary Cramp

From 3rd Congress of the International Foot and Ankle Biomechanics Community
Sydney, Australia. 11-13 March 2012

Background

A variety of multi-segmental foot models have been produced to examine patterns of foot segmental movement during gait cycle to identify biomechanical differences between normal and pathological foot function[1-3]. The reliability of foot models to accurately describe motion of the foot joints is dependent on the ability of the examiner to repeatedly apply markers to specific landmarks and the relevance of models' segmental descriptions to underlying anatomy. The aim of this study was to test the reliability of segmental angles measured by three published foot models during paediatric gait.

Materials and methods

Sixteen children, aged 6 to 12 years old, were recruited to the study. Marker sets for three foot models 3DFoot [1], Oxford Foot Model (OFM)[2], and Kinfoot[3] were applied to their right feet simultaneously which to the authors knowledge, is the first direct comparison of the three models during gait. Each foot model was assessed for repeatability of maximal joint angle and range of motion during the gait cycle between two testing occasions. Absolute angular differences and standard error of measurement (SEM) are reported.

Results

Repeatability of all maximal segmental angles and range of motions were higher in 3DFoot compared to OFM and Kinfoot (Table 1).

Table 1 Inter-session repeatability of foot model's 3D maximal segmental angles over the gait cycle.

Model	Segments	Maximal joint angle		Range of joint angle	
		° Difference	SEM °	° Difference	SEM °
OFM	Hindfoot to Shank	2.1 ± 15.1	10.9	1.2 ± 8.0	5.7
3DFoot	Hindfoot to Shank	1.0 ± 5.2	3.6	1.0 ± 4.6	3.3
Kinfoot	Hindfoot to Shank	1.0 ± 5.1	3.6	1.4 ± 6.3	4.3
3DFoot	Midfoot to Hindfoot	0.8 ± 3.5	2.2	0.3 ± 2.7	1.9
Kinfoot	Midfoot to Hindfoot	3.0 ± 11.1	6.7	3.7 ± 11.3	6.6
OFM	Metatarsals to Hindfoot	0.8 ± 8.5	5.3	1.3 ± 5.7	5.4
3DFoot	Metatarsals to Midfoot	0.7 ± 4.0	2.9	0.6 ± 3.6	2.5
Kinfoot	Metatarsals to Midfoot	2.8 ± 7.8	4.8	2.6 ± 6.6	3.7
OFM	Hallux to Metatarsals	2.3 ± 15.6	11.2	0.4 ± 13.7	9.1
3DFoot	Hallux to Metatarsals	1.5 ± 10.0	6.2	0.4 ± 12.6	8.8
Kinfoot	Hallux to Metatarsals	4.4 ± 21.8	15.1	2.1 ± 11.8	7.2

Conclusion

Decreased measurement error observed in 3DFoot and Kinfoot models may be attributable to normalisation of kinematics data to subject standing position. In the OFM, non-normalisation of gait data resulted in variable segmental offsets, particularly in the frontal plane. Greater measurement error was observed for several foot segments in the Kinfoot model. This may be due to discrepancies in model segment definitions in relation to the underlying joint anatomy, especially around the midfoot to hindfoot segments. 3Dfoot model consistently showed the least measurement error in the segment motions examined and thus is appropriate for use to examine foot biomechanics in gait.

Published: 10 April 2012

References

1. Leardini A, Benedetti M, Berti L, Bettinelli D, Nativo R, Giannini S: **Rear-foot, mid-foot and fore-foot motion during the stance phase of gait.** *Gait Posture* 2007, 25:453-462.

* Correspondence: r.mahaffey@uel.ac.uk
School of Health, Sport & Bioscience, University of East London, UK

2. Carson M, Harrington M, Thompson N, O'Connor J, Theologis T: **Kinematic analysis of a multi-segment foot model for research and clinical applications: a repeatability analysis.** *J Biomech* 2001, 34:1299-2307.
3. MacWilliams B, Cowley M, Nicholson D: **Foot kinematics and kinetics during adolescent gait.** *Gait Posture* 2003, 17:214-224.

doi:10.1186/1757-1146-5-S1-O18
Cite this article as: *Mahaffey et al.*: **Reliability of three foot models to examine paediatric gait.** *Journal of Foot and Ankle Research* 2012 5(Suppl 1):O18.

Current Understanding of the Impact of Childhood Obesity on the Foot and Lower Limb

Stewart C Morrison PhD MChS [a*], Ryan D Mahaffey MRes [a], Stephen D Cousins [a,b], Wendy I Drechsler [a]

[a] School of Health, Sport and Bioscience, University of East London, Water Lane, London, E15 4LZ

[b] School of Education and Health Sciences, Faculty of Engineering, Health Science and Environment, Charles Darwin University, Darwin, Northern Territory 0909, Australia

*Corresponding author email: s.c.morrison@uel.ac.uk

ABSTRACT

Childhood obesity has emerged in recent years as a major public health problem. As this continues to concern across local, national and international populations, and as our understanding of obesity advances, access to multi-disciplinary care and understanding of the complications is warranted. Recent findings have suggested that the musculoskeletal system is one of the multiple body systems compromised by obesity and that aberrant biomechanical function may be a precursor to the onset of musculoskeletal symptoms. This review will consider childhood obesity and its impact on the paediatric foot and lower limb through examination of literature on foot structure and biomechanics of gait. An overview of evidence-based management is out with the context of this review, however some recommendations for clinical practice will be proposed.

Introduction

Childhood obesity is a major public health concern with recent figures from the National Child Measurement Programme (2010/11) reporting the proportion of overweight and obese in reception year to be 22.6%, rising to 33.4% in year 6 (The NHS Information Centre, 2011). There is evidence emerging of the association between socio-economic status and obesity with variable rates of obesity being linked to the socio-demographic mix of local populations (Dinsdale and Ridler, 2010). The escalation of childhood obesity over the previous decade is even more of a concern when it is considered that obesity in childhood tends to persist into adulthood and is associated with an increase in adult mortality and morbidity (Reilly et al, 2003). Associated with obesity in children are co-morbidities affecting multiple body systems including cardiovascular disease, liver disease, diabetes mellitus, respiratory disease and various musculoskeletal disorders, particularly affecting the feet and lower limbs (Hills et al, 2001). This review will consider the impact of obesity on the musculoskeletal system in children, with a particular focus on the foot and biomechanics of gait.

Persistent and abnormal loading of the musculoskeletal system has been implicated in the predisposition to aberrant gait patterns in children, loss of mobility (Messier et al, 1994) and to a range of long-term orthopaedic conditions including Blount's Disease (Dietz, 1998) and Slipped Capital Femoral Epiphysis (Murray and Wilson, 2008). Nevertheless, the implications of childhood obesity on the lower limb musculoskeletal and locomotor systems, particularly during weight-bearing tasks, are poorly understood (Wearing et al, 2006). Past research in children with obesity has revealed changes in foot structure (Riddiford-Harland et al, 2000), aberrant mechanics of foot loading (Messier et al, 1994), altered gait characteristics (Hills and Parker, 1991; McGraw et al, 2000; Morrison et al, 2008) and reduced muscle strength and power (Riddiford-Harland et al, 2006) when compared with non-obese individuals. Futher problems commonly reported among obese children include general discomfort in simple activities of daily living such as walking and stair climbing and pains in the joints of the lower extremities (Hills et al, 2001). Hills et al, (2001) reported that these pains might be due to the increased stresses placed upon the feet and the greater absolute loads experienced at joints by the need to bear excessive mass.

To date, the consequences of childhood obesity on the development and function of the musculoskeletal system and the musculoskeletal injuries that result from altered lower limb/foot mechanics has received little attention. A greater understanding of these areas will have implications for the prevention, treatment and management of pathological gait patterns, loss of mobility and other mal-adaptations in the lower extremities of obese children. Thus, the aim of this review is to consider current literature pertaining to the influence of obesity on the structure and function of the foot and lower limb.

Discussion

Foot Structure in the Obese Child

The foot is a complex biomechanical structure, which acts as a shock absorber, force transducer and stabiliser through progression of gait (Perry, 1992). Throughout stages of growth and development, the posture of the foot adapts in response to the demands placed upon it and, as a consequence of aberrant mechanics, the foot is susceptible to deformity due to its distal location, flexibility and late ossification (LeVeau and Bernhardt, 1984).

A common musculoskeletal co-morbidity associated with childhood obesity is pes planus (flat feet) (Bordin et al, 2001; Chen et al, 2011; Pfeiffer et al, 2006; Riddiford-Harland et al, 2011; Villarroya et al, 2009). The link between the development of pes planus and obesity is yet to be elucidated, but is thought to be a result of excessive mass disrupting the immature musculoskeletal structure of the child's foot and consequently, altering foot function (Dowling et al, 2001; Dowling et al, 2004; Morrison et al, 2007; Morrison et al, 2008; Nantel et al, 2006; Riddiford-Harland, et al2000; Villaroya et al, 2008). The suggestion that structural foot differences are associated with obesity emerged from early studies utilising static footprint assessment to characterise the weight bearing foot and also to identify contact area of the midfoot; the view being that the greater the mid-foot contact the more planus (flatter) the foot type. Riddiford-Harland et al, (2000) explored the association between obesity and foot structure. This research utilised the Footprint Angle and the Chippaux-Smirak Index (CSI) as ratio measures of the narrowest and widest part of the foot, purported to indicate flattening of medial longitudinal arch. Static footprints were collected from 62 obese and 62 non-obese children (mean age: 8.5 ± 0.5 years) and the results reported a lower mean arch height, suggestive of the pes planus foot type. Following this study Dowling et al, (2004) utilised both static and dynamic measures to evaluate foot structure in obese children. A smaller sample size was recruited (n=13 obese children and n=13 non-obese children) and similar findings emerged with the obese subjects demonstrating a flatter foot type. Changes in foot structure identified by static footprint analysis have also been reported in more recent studies (Mickle et al, 2006; Villarroya et al, 2008), but the validity of the conclusions from this body of work are limited. It can be asserted that the static footprint may offer an indirect measure of arch height but provides little or no information with regards to three-dimensional structure or foot function. Further to this, a recent study looking at arch structure in adults with obesity suggested that footprint based measures should be interpreted with caution as they were not reflective of the actual osseous changes of the foot (Wearing et al, 2012).

The evaluation of discrete changes in anthropometric characteristics of the foot in childhood obesity may offer further understanding of the structural changes underpinning the development of pathology, and on the wider demands placed upon the foot structure. Mauch et al, (2004) evaluated the influence of age, gender and body mass index (BMI) on the 3-dimensional foot shape in 1,996 children, aged 3–10 years and concluded that BMI influenced all foot measures. Emerging from this study was the suggestion that footwear modifications may be needed for obese children and thus, clinical assessment by appropriate Allied Health Professionals was warranted. A later study by Mauch et al, (2008) evaluated the static morphology of the feet in normal, underweight and overweight children. In keeping with the previous study, this work concluded that increased body mass resulted in larger foot dimensions (indicated by higher than normal foot volume and length), but associations between BMI and flat feet were weak. Findings from this work identified 5 foot types - *flat feet, slender feet, robust feet, short feet and long feet* - where children with a higher BMI had robust feet (normal arch, higher volume and length) and children with lower BMI had slender feet (higher arch, lower volume and length). Changes in anthropometric foot characteristics are further echoed in recent work by Morrison et al, (2007) where obese children were reported to have larger and wider feet. Reasons underpinning these changes are not clear but, could be related to a number of factors such as biomechanical deformity, excess of adipose tissue and/or increased bone formation and sub-periosteal expansion resulting from increased plantar forces experienced during gait.

Whether obesity leads to the clinical presentation of flat feet is yet to be elucidated and it has been proposed that the flat feet in obese children may be due to the existence of a thicker plantar fat pad underneath the midfoot, giving the appearance of a flatter foot due to greater ground contact. This was investigated by Riddiford-Harland et al, (2011) who compared 75 obese children to 75 age and sex-matched non-obese children and reported that the obese group had both a significantly greater medial midfoot fat pad thickness (4.7 and 4.3mm respectively, $p<0.001$) and a lower medial

longitudinal arch (23.5 and 24.5mm respectively, p< 0.006) when compared to their leaner counterparts.

With the increasing evidence of changes to the foot structure in children with obesity there is an additional need to understand the impact of the structural changes observed and to further understand the functional impact, particularly in relation to biomechanical function and the development of musculoskeletal pathology. It is important that approaches to evaluating foot structure are both valid and reliable in order to further inform the evidence base. It must be recognised that measures of static foot structure offer little information about dynamic function and thus the links between obesity, foot pathology and foot structure are yet to be determined. In light of this, further studies looking at the dynamic function of the foot are required.

Characteristics of Foot Loading in Obese Children

The clinical evaluation of the dynamic foot is challenging, particularly when attempting to classify foot structure and establish relationships to pathology. In clinical practice and in research, plantar pressure assessment can be employed to determine the dynamic loading of the foot, as well as providing specific loading information at each region of the foot to determine loading characteristics (Stebbins et al, 2005; Mickle et al, 2006). Several authors have commented upon the clinical relevance of plantar pressure assessment in not only describing the overall loading effects on structures of the foot but also having the potential to express the damage that may occur in the tissues of the foot as a result of these loads, making them meaningful and effective in the management of patients with a wide variety of foot and lower-extremity disorders (Cavanagh and Ulbrecht, 1994; Hennig, 2002). When compared with other assessment devices typically used in clinical gait analysis, plantar pressure assessment is easier to implement, less time consuming and cumbersome for the patient and less expensive than complex gait analysis equipment (Giacommozzi, 2011).

In a study utilising a pressure platform (Mini E-med system, Novel, Munich) Dowling et al, (2001) investigated the effects of obesity on plantar pressures generated by 13 obese and 13 non-obese peripubescent children, matched by gender, age and height. The obese children generated significantly higher pressures under the forefoot during walking (39.3 ± 15.7 N.cm-2) when compared to the non-obese children (32.3 ± 9.2 N.cm-2). These results were re-iterated in 2004 by Dowling et al, who identified that during standing, obese children generated significantly higher forces over a larger foot area and experienced significantly higher plantar pressures compared to their non-obese counterparts. During walking, the obese children generated significantly greater forces over all areas of their feet, except the toes. In addition the obese children experienced significantly higher plantar pressures in the midfoot, heel and metatarsal heads compared to non-obese children. An increased loading at the midfoot may be indicative of a pes planus foot type with increased loading at the metatarsal heads predisposing to soft-tissue and osseous pathology.

Other studies investigating the effects of childhood obesity on plantar pressure distributions during standing and walking have also reported significantly higher pressures and forces across different regions of the foot (Gravante et al, 2003; Kellis, 2001; Mickle et al, 2006). Mickle et al, (2006) compared the dynamic plantar pressures generated in 17 overweight/obese children (4.4 ± 0.8 years) and 17 age, gender and height matched non-obese peers (4.4 ± 0.7 years). The authors reported that when walking, the overweight/obese children displayed significantly larger contact areas and generated significantly larger forces on the plantar surface of their total foot, heel, midfoot and forefoot compared to the non-obese children.

A study investigating the effects of obesity on plantar pressure distributions in young adults reported an increase in contact area of the midfoot and significantly higher peak and mean pressures (P< 0.0001) in the foot (Gravante et al, 2003). Gravante et al, (2003) compared the plantar contact area and peak plantar pressures in 38 obese young adults and 34 health controls (mean age 23 years) during standing on a pressure platform. The authors reported that obesity was associated with significantly larger plantar contact areas (+ 10.6%) and peak pressures (+ 43.0 %) in both the rearfoot and forefoot. These increased pressures exerted on the foot contribute to the view that assessment of biomechanics and gait in the clinical evaluation of the obese patient is warranted.

The findings from the literature are consistent with the view that obese children are at an increased risk of developing foot discomfort and/or foot pathologies, including stress fractures as a result of the increased pressure acting upon the immature musculoskeletal structure of the foot. Furthermore,

foot discomfort associated with these increased plantar pressures in obese children may hinder their participation in physical activity; weight-bearing activities can become difficult if not appropriately designed to account for these structural characteristics. Recently, Mickle et al, (2011) explored the relationships between obesity, physical activity and sedentary behaviour in a sample of 95 children aged 3–5 years. Findings from the study confirmed that increased peak pressures negatively correlated with physical activity and sedentary behaviour. Emerging from this research was the suggestion that raised foot pressures may influence engagement with activity and thus, interventions to reduce pressures under the foot are required. In light of these findings further research is required to understand the impact of obesity on the foot to ensure that foot pathologies in obese children are identified and managed appropriately.

The findings reported in the aforementioned studies must be interpreted with some caution as methodological differences with regards to the classification of childhood obesity, different methodological protocols, sample sizes and lack of control for ethnicity all affect the external validity of the work. As the long-term consequences of the increased planter pressure distributions are unknown, it is recommended that the effects of obesity on the potential alterations of foot function characteristics between obese and non-obese children be further investigated. Furthermore, this body of literature has tended to view the foot in isolation and it must be appreciated that the foot forms part of the lower limb kinetic chain and therefore, the foot should be assessed as part of this. Further work on the impact of obesity on the gait patterns of children with obesity will be discussed.

Gait Analysis in Childhood Obesity

Clinical gait analysis allows the measurement and assessment of walking biomechanics but is limited in that the clinician cannot capture movement in three planes or appreciate the kinetics of the movements taking place. Clinical analysis facilitates the identification of abnormal characteristics and can guide clinical management strategies but detailed analysis is required to characterise the impact of disease processes. Changes to gait patterns can be identified in many pathological conditions and recent findings have suggested changes to the gait pattern in children with obesity.

Changes in the gait pattern of children with obesity were first documented by Hills and Parker (1991a,b,c,d). Conclusions from this body of work were that obese children displayed greater asymmetry with their gait, along with increased double-limb and shorter single-limb support period when compared with non-obese children (Hills and Parker, 1991b). Other temporal differences included a longer cycle duration, lower cadence, lower relative velocity and greater stride width (Hills and Parker, 1991c); all pointing to a slower, safer and more tentative walking gait in obese children relative to normal weight children. Additionally, the findings from this work indicated that obese children displayed a more flat-footed weight acceptance pattern in early stance and a greater external rotation of the foot at all phases of the gait cycle (Hills and Parker, 1991a).

A later study by McGraw et al, (2000) also reported that instability during gait in children was linked to excessive body mass. In this study 20 male participants were recruited (10 obese, 10 non-obese, aged between 8 and 10 years) and gait and postural stability was evaluated with two-dimensional video and a force platform. The authors concluded that the obese subjects displayed increased double-stance duration ($p<0.02$), and significantly greater sway areas ($p<0.01$) in the medial-lateral direction. Changes in spatio-temporal gait parameters have been echoed by recent studies where the temporal gait parameters of decreased preferred walking speed, reduction in step length and lower step frequency have been reported in obese compared to normal weight children (DeVita and Hortobágyi, 2003; Morrison et al, 2008; Nantel et al, 2006).

Differences in preferred walking speed between obese and non-obese individuals might account for the reported alterations in spatiotemporal measures. DeVita and Hortobágyi (2003) reported that spatiotemporal stride characteristics were comparable when 21 obese and 18 non-obese adults walked at a standard speed (1.50m·s-1) compared to self selected speed (1.29m·s-1). DeVita and Hortobágyi (2003), observed, however, that joint kinematics varied with body weight in the obese group irrespective of walking speed; obese adults demonstrated approximately 5° greater hip extension, approximately 4° less of knee flexion and approximately 6° greater ankle plantar flexion compared to the non-obese adults. Results from this work also presented kinetic differences revealing that when walking at a standardised speed only ankle joint torque and powers were higher (both $p<0.000$) in obese adults by 88% and 61%, respectively.

Frontal plane kinematics of the lower limbs during gait in male children (aged 10 to 12 years) has been examined (McMillan et al, 2009). The overweight subjects (BMI 40.5 ± 10.0 kg/m2) produced a significantly greater rearfoot eversion range of motion and later timing of peak eversion motion relative to the healthy weight subjects (BMI 17.0 ± 3.3 kg/m2). Peak knee adduction motion in early and late stance was of greater amplitude and the timing of peak hip adduction motion was significantly later in the healthy weight group. These findings suggest that overweight males may redistribute forces in the medial-lateral direction during gait. Shultz et al, (2009) reported no significant differences for joint kinematics between 10 overweight (BMI 30.47 ± 5.54 kg/m2) and normal weight (BMI 16.85 ± 1.31 kg/m2) children during swing and stance phase. The study did reveal that overweight children had significantly greater sagittal, frontal and transverse plane absolute peak joint moments at the hip, knee and ankle regardless of walking cadence. The authors surmise that because body mass is not proportional to joint articulating surfaces, higher absolute peak joint moments will increase the risk of malalignment and injury in overweight children. In particular, the ankle dorsiflexor moments were significantly greater in the overweight compared to normal weight group. This suggests a greater muscular force is needed when carrying excess mass to implement a braking mechanism during stance phase.

Gushue et al, (2005) investigated the effects of excessive body mass on 3-D knee joint biomechanics during walking. Ten overweight children (BMI 29.9kg/m2) were compared to 13 normal weight subjects (BMI 18 kg/m2) using an ethnically diverse sample of children. It was reported that overweight participants demonstrated significantly lower peak knee flexion angle (14.5° ± 5.5°) compared to normal weight subjects (21.1° ± 5.0°), but no significant differences in peak internal knee extension moment were found (22.5° ± 10.5° and 10.8° ± 5.5°). The overweight group, however, showed a significantly higher peak internal knee abduction moment (22.5° ± 10.5° and 10.8° ± 5.5°) suggesting that overweight children may not be able to compensate for increased force through the knee in the frontal plane. In a study by Nantel et al, (2006) looking at the locomotor lower limb strategies of obese and non-obese children, it was reported that only the hip joint kinetics were modified in the obese compared to non-obese children during walking. The obese subjects demonstrated decreased energy generation from the hip extensors and increased energy absorption from the hip flexors. In addition, obese children were less efficient at transferring energy between the eccentric and concentric phases at the hip. The work suggests that obese children develop a gait adaptation to maintain a similar knee extensor load and take advantage of a passive hip strategy to achieve forward progression during gait.

Recently Shultz et al, (2009) reported that obese children (n=10) demonstrated greater absolute peak joint moments of flexion and extension at the hip, knee and the ankle joints in the sagittal plane of motion in comparison to normal weight children (n=10). It was thought that this increased joint loading might result in cumulative stress, which has been associated with the development of varus angular deformities of the knee joint (i.e. Blounts Disease). Increased joint moments (particularly at the knee), may compromise the structures that control joint stability and this could explain the slower more tentative walking pattern displayed in obese children (Hills and Parker, 1991a; McGraw et al, 2000). These findings, however, require further investigation to determine the impact of excessive body weight on joint forces and the influence this has on the biomechanics of the lower limb and foot of young children.

Conclusion

Biomechanical changes impacting upon the foot and lower limb in children with obesity have been documented in the literature. Changes to foot structure and foot loading characteristics can predispose to the development of musculoskeletal pathology, however the links between these changes and the manifestation of pathology are lacking. Changes in the gait pattern and joint loading have also been proposed which may also be linked to the development of musculoskeletal problems. Further exploration of the impact of the biomechanics of adiposity is required, utilising robust and rigorous protocols, along with a uniform approach to defining obesity. The long-term implications of obesity in childhood are yet to be determined. In light of the trends identified in the literature further work is required to inform the multidisciplinary care of children with obesity.

Recommendations for Clinical Practice

1. Clinicians involved in the management of children with obesity should consider the biomechanics of the lower limb and consider the impact upon the foot.

2. Access to specialist foot care and footwear services is needed for children with obesity reporting foot and/or lower limb musculoskeletal pathology.

3. The application of appropriate technology can enhance the assessment of children with obesity and inform the clinical management.
4. Clinical management of childhood obesity should utilise weight management services as a fundamental part of multi-disciplinary care

References

Bordin B, De Giorgi G, Mazzocco G, and Rigon F. (2001). Flat and cavus foot, indexes of obesity and overweight in a population of primary-school children. *Minerva Pediatrics*, 53, 7-13.

Cavanagh P and Ulbrecht J. (1994). Clinical plantar pressure measurements in diabetes. The Foot, 4, 123-135.

Chen K-C, Yeh C-J, Tung L-C, Yang J-F, Yang, S-F, and Wang C-H. (2011). Relevant factors influencing flatfoot in preschool-aged children. *European Journal of Pediatrics*, 170, 931-936.

DeVita P, and Hortobágyi T. (2003). Obesity is not associated with increased knee joint torque and power during level walking. *Journal of Biomechanics*. 36: 1355–1362.

Dietz W. (1998). Health consequences of obesity in youth: Childhood predictors of adult disease. *Paediatrics*, 101(3pt2), 518-525.

Dinsdale, H and Ridler C. (2010). National Child Measurement Programme: Changes in children's body mass index between 2006/07 and 2008/09. Oxford: National Obesity Observatory.

Dowling A.M, Steele J.R. & Baur L.A. (2001). Does obesity influence foot structure and plantar pressure patterns in prepubescent children? *International Journal of Obesity*. 25, 845-852.

Dowling A.M, Steele J.R, & Baur L.A. (2004). What are the effects of obesity in children on plantar pressure distributions? *International Journal of Obesity*. 28, 11. 1514 – 1519.

Giacomozzi C. (2011). Potentialities and Criticalities of Plantar Pressure Measurements in the Study of Foot Biomechanics: Devices, Methodologies and Applications, Biomechanics in Applications, Vaclav Klika (Ed.), ISBN: 978-953-307-969-1, InTech, Available from: http://www.intechopen.com/articles/show/title/potentialities-and-criticalities-of-plantar-pressure-measurements-in-the-study-of-foot-biomechanics

Gravante G, Russo G, Pomara F, and Ridola C. (2003). Comparison of ground reaction forces between obese and control young adults during quiet standing on a baropodometric platform. *Clinical Biomechanics*, 18, 780-782.

Gushue D, Houck J, and Lerner A. (2005). Effects of childhood obesity on the three-dimensional knee joint biomechanics during walking. *Journal of Pediatric Orthopaedics*. 25(6), 763-768.

Hennig, E. (2002). Pedobarograph assessment in gait analysis. *Physical Medicine and Rehabilitation*, 16(2), 215-229.

Hills A and Parker A. (1991a). Gait characteristics of obese children. *Archives of Physical Medicine and Rehabilitation*, 72, 403,407.

Hills A and Parker A. (1991b). Gait Asymmetry in Obese Children. *Neuro-Orthopedics*, 12, 29-33.

Hills A and Parker A. (1991c). Gait Characteristics of Pre-Pubertal Children: Effects of Diet and Exercise on Parameters. *International Journal of Rehabilitation Research*, 14, 348-349.

Hills A and Parker A. (1991d). Locomotor characteristics of obese children. *Child Care Health and Development*, 18, 29-34.

Hills A, Hennig E, McDonald M, and Bar-Or O. (2001) 'Plantar pressure differences between obese and non-obese adults: a biomechanical analysis'. *International Journal of Obesity*, 25(11), 1674-9.

Kellis, E. (2001). Plantar pressure distribution during barefoot standing, walking and landing in pre-school boys. *Gait and Posture*, 14, 92-97.

LeVeau BF, Bernhardt DB. (1984). Developmental Biomechanics. *Physical Therapy*, 64 (12), 1874-1882.

Mauch M, Grau S, Krauss I, Maiwald C, and Horstmann T. (2004). Influence of Age, Gender and Body-Mass-Index on 3-D Foot Shape In Children. *Gait and Posture*. 20 (1001), pp. s91.

Mauch M, Grau S, Krass I, Maiwald C, and Horstmann T. (2008). Foot morphology of normal, underweight and overweight children. *International Journal of Obesity*, 32, 1068-1075.

McGraw B, McClenaghan B, Williams H, Dickerson J, and Ward D. (2000). Gait and postural stability in obese and nonobese prepubertal boys. *Archives of Physical Medicine and Rehabilitation*. 81, 484-489.

McMillan AG, Auman NL, Collier DN, Williams B. (2009). Frontal plane lower extremity biomechanics during walking in boys who are overweight versus healthy weight. *Pediatric Physical Therapy*. 21, pp. 187–193

Messier S, Davies A, Moore D, Davis S, Pack R, and Kazmar S. (1994). Severe obesity: effects on foot mechanics during walking. *Foot Ankle International*, 15 (1), 29-34.

Mickle K.J, Cliff D.P, Munro B.J, Okely A.D, and Steele J.R. (2011). Relationship between plantar pressures, physical activity and sedentariness among preschool children. *Journal of Science and Medicine in Sport*. 14 (1), pp. 36 - 41.

Mickle K, Steele J, and Munro, B. (2006). The feet of overweight and obese children: Are they flat or fat? *Obesity*. 14, 1949-1953.

Morrison SC, Durward BR, Watt GF and Donaldson MDC (2007). Anthropometric foot structure of peripubescent children with excessive body mass versus normal body mass. *Journal of the American Podiatric Medicial Association*. 97, 366-370.

Morrison SC, Durward BR, Watt GF and Donaldson MDC. (2008). The influence of body mass on the temporal parameters of peripubescent gait. *Gait & Posture*. 27, 719 – 721.

Murray A, and Wilson N. (2008). Changing incidence of slipped capital femoral epiphysis: A relationship with obesity? *The Journal of Bone and Joint Surgery*, 90 (1), 92-94.

Nantel J, Brochu M, and Prince F. (2006). Locomotor strategies in Obese and Non-obese Children. *Obesity*. 14 (10), 1789 – 1794.

Perry, J. (1992). Gait analysis: normal and pathological function. NJ: Slack.

Pfeiffer M, Kotz R, Ledl T, Hauser G, and Sluga M. (2006). Prevalence of flat foot in preschool-aged children. *Pediatrics*, 118(2), 634-639.

Reilly J, Methven E, McDowell Z, Hacking B, Alexander D, Stewart L, and Kelnar C. (2003). Health consequences of obesity. *Archives of the Disease in Childhood*, 88(9), 748-752.

Riddiford-Harland DL, Steele JR, and Storlein LH. (2000). Does obesity influence foot structure in prepubescent children? *International Journal of Obesity*. 54, 541-544.

Riddiford-Harland D, Steele J, and Baur L. (2011). Are the feet of obese children fat or flat? Revisiting the debate. *International Journal of Obesity*, 35, 115-120.

Schultz S, Sitler M, Tierney R, Hillstrom H, and Song J. (2009). Effects of paediatric obesity on joint kinematics and kinetics during 2 walking cadences. *Achieves of Physical Medicine and Rehabilitation*, 90, 2146-2154.

Stebbins J, Harrington M, Giacommozzi C, Thompson N, Zavatsky A, and Theologis T. (2005). Assessment of sub-division of plantar pressure measurement in children. Gait and Posture, 22, 372-376.

The NHS Information Centre, Lifestyle Statistics. (2011) National Child Measurement Programme: 2010/2011 school year. Available Online: http://www.ic.nhs.uk/webfiles/publications/003_Health_Lifestyles/ncmp%202010-11/NCMP_2010_11_Report.pdf (Accessed 22nd December, 2011)

Villarroya M, Esquivel J, Tomas C, Buenafe A, and Moreno L. (2008). Foot Structure in Overweight and Obese Children. *International Journal of Pediatric Obesity*. 3 (1), pp. 39 - 45

Wearing S.C, Hennig E, Byrne N, Steel, J, and Hill, A. (2006). Musculoskeletal disorders associated with obesity: a biomechanical perspective. *Obesity Reviews*, 7(3), 239-50.

Wearing SC, Grigg NL, Lau HC, Smeathers JE. (2012). Footprint-based estimates of arch structure are confounded by body composition in adults. *Journal of Orthopaedic Research*. Available online: http://onlinelibrary.wiley.com/doi/10.1002/jor.22058/abstract;jsessionid=CC5A3F2D9F4BEED4403E8F294D5617DA.d03t01 [Accessed: 20th April, 2012]